Integration of wound-induced calcium signals to transcriptional activation and regulation of cutaneous wound healing responses.

Laura E. M. Hudson

Thesis submitted in fulfilment of the requirements of the regulations for the degree of Doctor of Philosophy

Institute of Cellular Medicine

Faculty of Medical Sciences

Newcastle University

Abstract.

Wounding is a major clinical problem. Calcium is a common secondary messenger eliciting a range of responses through spatial/temporal regulation. In keratinocytes, intracellular calcium (Ca^{2+}_i) plays a key role in growth and differentiation. An epidermal calcium gradient exists in skin which is disrupted post-wounding and wounding of monolayer human keratinocytes results in an intercellular calcium wave. Additionally, regulation of the calcium wave is known to be dependent on purinergic signalling and/or gap-junctions. However, their relative contribution in mediating the calcium flux post-wounding in primary human keratinocytes have not been well characterised. Furthermore, the importance of this calcium flux to downstream transcriptional and functional responses is not fully understood. To address this knowledge gap, the effect of store-operated calcium entry (SOCE), gap-junctions and extracellular ATP was investigated using primary human keratinocyte monolayers loaded with the calcium dye Fluo4-AM. Scratch wounding was performed in 0.06mM and 1.2mM $[Ca^{2+}]_o$ and images captured using confocal microscopy. Calcium add-back experiments and the use of specific inhibitors were used to characterise the calcium responses. Results showed that, as expected, wounding caused an increase in Ca^{2+}_i within cells at the wound edge, which then travelled back as a wave. Both gap-junction inhibition (18αGA) and the removal of extracellular ATP (hexokinase) reduced Ca^{2+}_i flux and prevented the spread of the calcium wave following wounding. Nuclear factor of activated T-cells (NFAT) is a transcription factor activated by an increase in Ca^{2+}_i and known to be involved in keratinocyte differentiation. NFAT firefly luciferase was used to investigate activation in response to wounding. Results show NFAT transcriptional activation post-wounding in 1.2mM but not 0.06mM $[Ca^{2+}]_o$. Additionally, 18αGA, and the SOCE inhibitor GSK-7975A significantly reduced wound-induced NFAT activation. Perhaps surprisingly, hexokinase had no effect. Finally, the functional consequence of these signalling pathways were investigated using scratch wound migration assays. Wounds closed at a faster rate when wounding was performed in 1.2mM $[Ca^{2+}]_o$ compared to 0.06mM. Manipulation of all three signalling pathways inhibited wound closure. However, gap-junction blockade completely prevented wound closure. Together these data indicate that, whilst purinergic and gap-junction signalling regulate the Ca^{2+}_i flux and wave post-wounding, there is a dominant effect of gap-junctions in the activation of NFAT and cell migration.

Acknowledgments.

I would like to thank my supervisors Professor Nick Reynolds, Professor Colin Jahoda and Dr Fiona Oakley for their help and support throughout my PhD. Thank you to Dr Malcolm Begg at GlaxoSmithKline for providing the GSK compound used throughout this project and your advice with this. I would like to acknowledge Dr Anna Brown who optimised the calcium-dye loading protocol prior to the commencement of this PhD. This project was funded by the MRC.

Preliminary results which formed the basis of experimental design and concept for some results were obtained during my preceding MRes project to this PhD (awarded September 2011). However, all data generated for the analysis presented herein was obtained during the three year PhD period.

Thank you to Dr Penny Lovat for proof reading this thesis; your comments and kindness were greatly appreciated as was the emergency M&S picnic! Additional thanks to Dr Alex Laude in the Bioimaging unit at Newcastle University for your help and patience with the calcium imaging.

I would like to thank all the members of dermatological sciences both past and present who have made this an unforgettable experience! Team NJR (Carole, Keith, Martina, Emma and Darren) - your help and support both inside and out of the lab have been amazing! Thank you for always being there with chocolate, cake, tissues or anything else required! I honestly couldn't have wished for a better office to work in!

I would additionally like to acknowledge the support of my friends outside of the lab; there are too many to individually name but you have all been amazing, provided great distractions from the stresses of the lab/experiments and have helped keep me sane throughout these past few months. A big thanks to my family and in particular my parents for your ongoing love and support through everything I do (especially my mum for her years of proof reading, I promise this is the last one!). Finally, to my husband Alex, without your amazing support and patience these past four years, none of this would have been possible, from the bottom of my heart, thank you.

Declaration.

This thesis is submitted for the degree of Doctor of Philosophy at Newcastle University. The research was performed in the Dermatological Sciences department in the Institute of Cellular Medicine under the supervision of Professor Nick J. Reynolds. This thesis is my own work. I certify that none of the data offered in this thesis has previously been submitted by me for a degree or any other qualification at this, or any other university.

Table of Contents

List of figures

List of tables

Abbreviations

- $[ATP]_i$ – Intracellular ATP concentration
- $[ATP]_o$ – Extracellular ATP concentration
- $[Ca^{2+}]_i$ – Intracellular calcium concentration
- $[Ca^{2+}]_o$ – Extracellular calcium concentration
- µg - microgram
- µL – microliter
- µm - micrometre
- µM – micromolar
- 18αGA - 18α-Glycyrrhetinic Acid
- 2-APB – 2-Aminoethoxydiphenyl borate
- 2D – Two dimensional
- 3D – Three dimensional
- ABC – ATP-Binding Cassette
- ADP – Adenosine Diphosphate
- AM – Acetoxymethyl
- AP1 –Activator Protein 1
- ATP – Adenosine Triphosphate
- AUC – Area Under the Curve
- CaM – Calmodulin
- CFTR - Cystic Fibrosis Transmembrane Conductance Regulator
- cm – centimetre
- CM – Conditioned Media
- CMH – Conditioned Media + Hexokinase
- CsA – Cyclosporine A
- Cx - Connexin
- DAG - diacylglycerol
- DES – Diethylstilbestrol
- DMSO – Dimethyl Sulfoxide
- *E. coli – Escherichia coli*
- ER – Endoplasmic Reticulum
- FCS – Fetal Calf Serum

- fps – frames per second
- Ft/F0 – temporal fluorescence over initial fluorescence
- GPCR – G-Protein Coupled Receptor
- GSK – GlaxoSmithKline
- HaCaT – immortalised keratinocyte cell line
- HKGS - Human Keratinocyte Growth Supplement
- HUVEC – Human Umbilical Vein Endothelial Cell
- IL - Interleukin
- IP_3 - Inositol 1,4,5-trisphosphate
- IP_3R - Inositol 1,4,5-trisphosphate Receptor
- kDA – kilodalton
- KSC – Keratinocyte Stem Cells
- LPA – Lysophosphatidic Acid
- MDR – Multidrug Resistance
- mg - milligram
- mL – millilitre
- mm – millimetre
- mM – millimolar
- MMC – mitomycin C
- MTT - Thiazolyl Blue Tetrazolium Bromide
- NEM – N-ethylmaleimide
- NFAT - Nuclear Factor of Activated T cells
- NFκB - Nuclear Factor kappa-light-chain-enhancer of activated B cells
- NHS – National Health Service
- nm – nanometres
- nM - nanomolar
- PBS - Phosphate Buffered Saline
- P-gp – P- glycoprotein
- PIP_2 - Phosphatidylinositol 4,5-bisphosphate
- PKA – Protein Kinase A
- PKC – Protein Kinase C
- PLC – Phospholipase C

- PM – Plasma Membrane
- PSA – Penicillin Streptomycin Amphotericin B
- Px - Pannexin
- QoL – Quality of Life
- RM – Repeated Measure
- ROC – Receptor operated calcium entry
- ROI – Region of Interest
- SERCA – sarco/endoplasmic reticulum calcium ATPase
- SEM – Standard Error of the Mean
- SOCE – Store-Operated Calcium Entry
- SRB - Sulphorhodamine B
- STIM – Stromal Interaction Molecule
- TE - Trypsin Ethylene iamine tetraacetic acid
- Tg – Thapsigargin
- TRPC – Transient Receptor Potential Channel
- U - Units
- UTP – Uridine Triphosphate

Chapter 1.

Introduction

1 Chapter 1. Introduction.

1.1 Structure and function of skin.

The skin, covering the entire body surface, has a variety of important roles including physical protection, maintenance of barrier function, immunological protection and prevention of water loss. Therefore, there is great evolutionary pressure for wounds to heal quickly. Insults resulting in disruption of the skin require immediate attention to protect the internal environment of the body from the potentially dangerous external environment. Structurally the skin consists of two main layers; the outermost epidermis and the thicker underlying dermis (Proksch *et al.*, 2008). The dermis is usually 2mm thick, increasing to 4.5mm on locations such as the back. It is made up of fibroblasts, collagen and connective tissue providing a tough elastic layer central to maintaining the structure of the skin (Tobin, 2006). The epidermis is a multi-layered stratified structure composed of four layers of keratinocytes in different stages of differentiation. A constant balance between proliferation and differentiation exists to maintain the epidermis. As shown in figure 1.1, highly proliferative keratinocytes are found in the stratum basale and as they undergo differentiation they form the stratum spinosum and the stratum granulosum, progressively losing their mitotic ability. Finally, as keratinocytes reach terminal differentiation, proteolytic and nucleolytic activity is initiated whereby cellular organelles and DNA is degraded leading to the formation of the outermost cell layer; the stratum corneum (SC). Corneocytes, the cells found in the SC, are flattened, enucleated and surrounded by a lipid matrix. Corneocytes are eventually shed from the skin surface (Proksch *et al.*, 2008). Keratinocyte differentiation is a calcium-dependent process mediated by the altering expression and modification of structural proteins, enzymes and lipids (Candi *et al.*, 2005). These changes in expression facilitate the use of such proteins as differentiation markers in laboratory investigations. For example, keratins are structural proteins that make up the majority of epidermal proteins. They function to form monomeric intracellular networks of keratin intermediate filaments to enhance epidermal integrity and link neighbouring cells via desmosomes. The majority of the cytoskeleton of cells located in the basal layers of the epidermis contains keratin 5 (K5) and K14 heterodimers. During differentiation, K5 becomes replaced by K1 and K14 by K10; in the upper layers of the epidermis, K1/K10 are predominant (Candi *et al.*, 2005). Therefore, expression of these

keratins can be used to determine keratinocyte differentiation state. Furthermore, corneocytes are surrounded by a strong cornified envelope consisting of a lipid layer and a protein layer. Structural proteins within this layer include involucrin and loricrin. Again, these antibodies specific to these proteins can be used to decipher keratinocyte differentiation status (Proksch *et al.*, 2008). Moreover, proteins like involucrin and loricrin are covalently cross-linked by the calcium-dependent transglutaminase which is activated in response to increased intracellular calcium. Keratinocyte differentiation is believed to be mediated by three MAP kinase pathways which are activated by calcium influx, epidermal growth factor (EGF) and tumour necrosis factor (TNF) (Jost *et al.*, 2001). The epidermis is usually 75-150μm thick, however on sites such as the palm of the hands and the soles of the feet, an additional fifth layer, the stratum lucidum, can increase in thickness to 600μm (MacNeil, 2007). Keratinocytes make up 90-95% of the total cell population in the epidermis and are the primary cell type within this layer of the skin (McGrath and Uitto, 2010). The remaining cells are mainly langerhan cells and melanocytes. The epidermis provides the functional barrier against chemical and mechanical stress and therefore is central to wound healing responses.

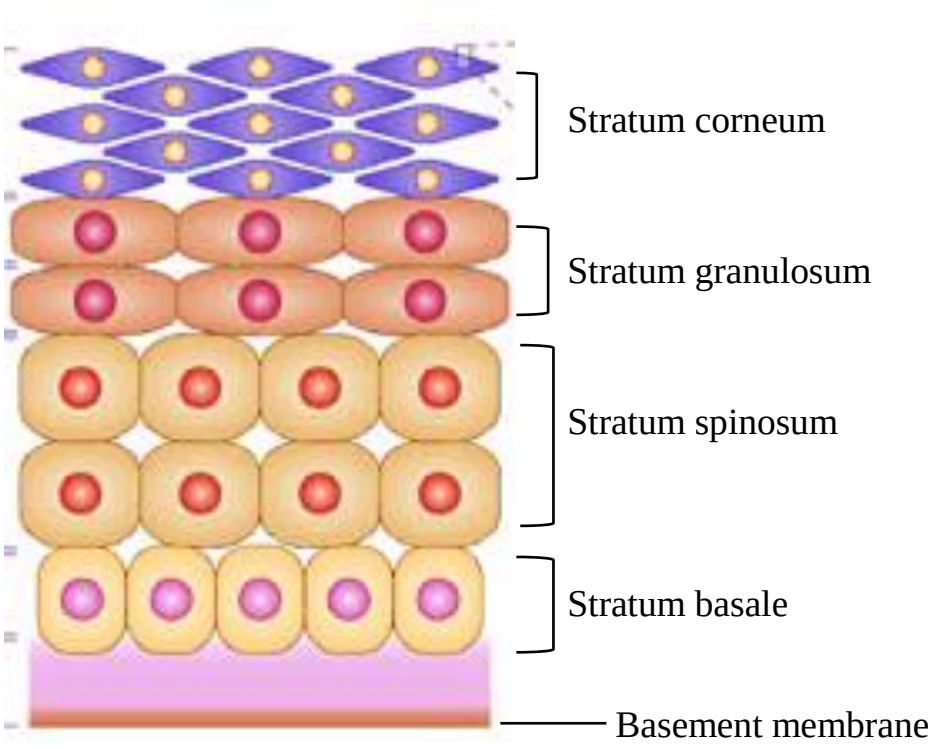

Figure 1.1 Diagram of the epidermal layers of the skin.

The basal layer of the epidermis consists of highly proliferative keratinocytes. As cells differentiate they form the stratum spinosum, stratum granulosum and finally, the terminally differentiate, outmost layer of the skin is termed the stratum corneum. Adapted from (Candi *et al.*, 2005).

1.2 Cutaneous wound healing.

1.2.1 Acute versus chronic wounding healing.

The many crucial functions of the skin mean that any insult or injury can be extremely detrimental and wounds require a rapid signalling cascade to ensure appropriate wound closure. Cutaneous wound healing can be classified into acute and chronic. Li *et al.* described acute wounds as typically being caused by a sudden occurring surgical incision or a trauma to the skin and underlying tissue such as lacerations, abrasions and burns. Acute wounds can occur at any location on the body and range from superficial to deep. The latter causes damage to underlying tissues including nerve and muscle. Post-injury, the wound undergoes normal wound healing processes in an appropriate and predicted time frame resulting in complete wound closure, with minimal

complications (Jie Li *et al.*, 2007). In humans, adults fail to achieve the desirable outcome of complete regeneration and wound healing results in a tissue that is similar in structure and function to the original skin but not identical. In particular, epidermal appendages do not regenerate and scar formation occurs due to collagen matrix deposition (Paul Martin, 1997). In contrast, some eukaryotic organisms as well as pre-natal injury in humans result in complete regeneration without scar formation. This difference has mainly been attributed to a decreased inflammatory response in the first two trimesters of development compared to the third trimester and post-natally (Wilgus *et al.*, 2004). Recently, it has been suggested that mast cell maturation and degranulation causes scar formation in later stages of development (Wulff *et al.*, 2012). However, pathways involved in complete regeneration are poorly understood.

When an acute wound does not heal within the predicted time frame, the wound is said to be chronic (Moreo, 2005). Chronic wounds are difficult to define and the aetiology is complex and poorly understood. However, it is accepted that these wounds develop due to a delay during one of the phases of wound healing, preventing the continuation through the normal wound healing processes (Kamolz and Wild, 2013). These wounds may take months or years to fully heal and require specialist clinical intervention. Examples of chronic wounds include infectious and diabetic leg ulcers, venous ulcers, pressure ulcers and radiation poisoning wounds (James *et al.*, 2008). People at risk of developing chronic wounds include the elderly, diabetics and the obese. Additionally, chronic wounds such as pressure sores are common in those with limited mobility including the elderly and patients' requiring long-term hospital stays. Unlike acute wounds, chronic wounds are normally found on the lower leg, foot and pelvic regions of the body. Whilst exact mechanisms are incompletely understood, there are many reported factor involved in non-healing wounds. Appropriate oxygenation is required for all phases of the wound healing process including reepithelialisation in order supply the cell with adequate energy in the form of ATP to drive keratinocyte proliferation, migration and differentiation. In general wounds are initially depleted of oxygen which is thought to be important in the initiation of wound healing responses; however, prolonged hypoxic conditions can be detrimental in wound closure and are detected in chronic wounds. Other associated risks of impaired wound healing are sex hormones, stress, smoking, diabetes and age as well as certain medications for other disorders such as chemotherapeutic drugs (Guo and DiPietro, 2010).

The complexity and time frame associated with the development of chronic wounds make them challenging to study in the laboratory. For these reasons laboratory-based investigations normally focus on phases of acute wound healing. However, as chronic wounds are known to develop from acute wounds, findings from these studies could be applicable to exploring how and why chronic wounds develop as well as novel therapies that could promote wound closure. Additionally, there is a need to investigate normal physiological wound healing to develop therapeutic agents to promote wound closure of both traumatic and surgical acute wounds. For example, surgical procedures to excise tumours result in a substantial acute wound (figure 1.2). Wounds akin to the one shown may take weeks to heal. During this time several dressing changes and visits to specialist health care professionals may be required, causing a significant cost to the NHS. The wound may also be painful and unsightly having a detrimental effect on patient quality of life (QoL) and causing a significant cost to the NHS.

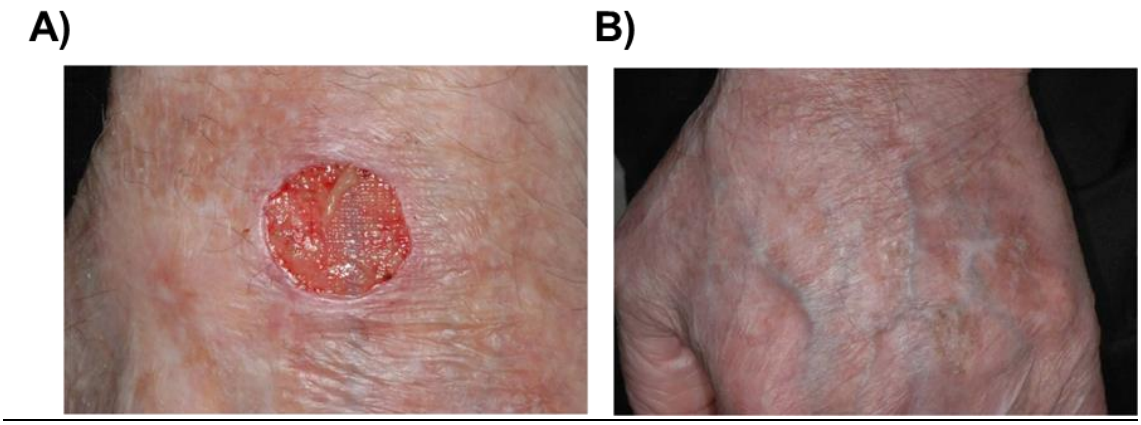

Figure 1.2 Photographic representation of acute wound healing.

The dorsum of the hand following surgery to remove a squamous cell carcinoma as a representation of the acute wound healing process. The wound was allowed to heal by secondary intention. **A)** Wound caused by surgical excision, day 0. **B)** Wound closure by 9 weeks. Images courtesy of Dr J. A. A. Langtry.

1.2.2 Clinical and socioeconomic implications of cutaneous wound healing abnormalities.

Cutaneous wound healing is a major socioeconomic and clinical problem resulting in a significant burden on the patient's QoL and as well as being time-consuming and costly to the National Health Service (NHS) in the UK. It has been estimated that £2.3-3.1 billion per year is spent on wound care, 3% of the NHS total expenditure (based on 2006-2007 audit and costs) (Posnett and Franks, 2008). The majority of these costs are due to in-patient hospital care, wound dressings and nursing time. In western countries there is an estimated life time prevalence of 1-2% for chronic wounds and almost every person will experience acute wounding, albeit minor in the majority of cases (Augustin and Maier, 2003). Studies have shown that patients facing wound healing abnormalities also suffer from reduced QoL reporting problems with mobility, sleep, malodour and pain as well as a range of negative emotions, affecting psychological wellbeing. A study has shown that the majority of healthcare professionals believe that 50–75% of chronic and 25% of acute wound patients suffered mood problems related to their wounds (Upton *et al.,* 2012). These include lack of self-worth, despair, stress and anxiety due to prolonged exposure to pain and malodour as well as reduced mobility affecting social activities, contact with family and friends and in some cases loss of income due to inability to work. The cost to the NHS of these psychological consequences can be overlooked; however it has been estimated to be £750 per patient or a total of £85.5 million per year (Upton *et al.,* 2012).

The financial, physiological and psychological burden of chronic wound healing is expected to increase exponentially over coming decades. This is primarily due to the population of the UK set to increase by 5.6% by 2025, with a rise of 36% in the over 65 age group as well as a dramatic increase in the incidence of type two diabetes (Posnett and Franks, 2008). As the elderly and diabetics are high risk groups for non-healing and chronic wounds this remains and important issue.

1.2.3 Biology of cutaneous wound healing.

Cutaneous wound healing has been accepted as one of the most complex biological processes that occurs post-embryonic development. Its complexity arises from the involvement of many cell types and lineages simultaneously over an extended time

period which requires activation and coordination of multiple intracellular, intercellular and extracellular pathways (Braiman-Wiksman *et al.*, 2007; Jie Li *et al.*, 2007). As with other signalling pathways, the stages involved in wound healing responses cannot be easily classified into sequential events; rather accepted simplified categories have been assigned to each phase.

As shown in figure 1.3, several cell types are involved at each stage of wound healing with each conducting a different role, all of which contribute to normal wound closure. Although the timing and order of these stages is highly debated within the literature, they allow investigations into understanding the physiological processes that are occurring. An added difficulty is that wound healing responses vary patient to patient depending on medical history, aetiology of the wound and wound location. Additionally, within a specific wound on an individual patient, several stages may be occurring simultaneously. The primary stage of haemostasis and inflammation occurs immediately post-wounding and usually lasts for 24-48 hours, extending to two weeks in some circumstances (Guo and DiPietro, 2010). Tissue injury causing disruption to blood vessels results in platelet aggregation forming a clot. The clot acts as a scaffold matrix to recruit cells such as macrophages and neutrophils to the wound site to begin the cleaning processes of removing damaged tissue and pathogens from the wound (Swift *et al.*, 2001). This stage also involves the release or recruitment of cytokines and growth factors such as epidermal growth factor, fibroblast growth factor and transforming growth factor-β which aid wound healing (Barrientos *et al.*, 2008). Once the wound site has been cleansed and a fibrin clot formed, the replacement of the functional barrier can take place; this occurs during the proliferative phase. This phase involves cellular activity from three main cells types co-ordinating three different processes; keratinocytes and reepithelialisation, fibroblasts and fibroplasia and endothelial cells producing new blood vessels during angiogenesis. Reepithelialisation is an event of particular interest and is crucial to early and medium phases of wound healing. There are several stages that are required for complete reepithelialisation; keratinocyte migration, proliferation and differentiation in order to form a stratified epidermis, as well as restoration of the basal membrane connecting the epidermis to the dermis (Jie Li *et al.*, 2007). Initially post-injury, keratinocytes switch to a migratory phenotype and actively migrate across the wound bed (Hell and Lawrence, 1979). The exact mechanisms of this process have long been of interest, however, remain poorly

understood. Nevertheless, it is known that 12-24 hours post-wounding, keratinocytes at the wound edge become elongated and form lamellipodia projections. Cell-to-cell and cell-to-matrix connections are also lost, thus allowing migration across the wound bed (Parks, 1999; Santoro and Gaudino, 2005). In cultured cells, growing from sub-confluent populations to a complete monolayer involves the transition from calcium-dependent desmosomes which provide cell-to-cell junctions within epithelia to calcium-independent desmosomes. The sensitivity to calcium in sub-confluent cells means that an increase in calcium can promote desmosome formation and a reduction in extracellular calcium can disrupt formation. Interestingly, Wallis and co-workers showed that, in canine kidney cells, wounding reverses this transition, re-introducing calcium-dependent desmosome formation (Wallis *et al.,* 2000).

To ensure an adequate number of keratinocytes to restore the damaged tissue, keratinocytes at the wound margin then enter a proliferative state forming a dense hyperproliferative epithelium. Once keratinocytes have covered the wound surface, contact inhibition prevents further migration and links to basal membrane are reformed (Raja *et al.,* 2007). This attachment of the new epidermis to the dermis is crucial for skin integrity. The cells undergo terminal differentiation to form a functionally stratified epidermis similar in structure to undamaged tissue. The final stage of wound healing is the remodelling, where the extracellular matrix composition is altered. Fibroblasts produce collagen and in normal adults this is predominantly in the form of collagen I, however, for the first 2-4 weeks post-injury type III is preferentially synthesised. This switch provides a strong dermal substrate for tissue remodelling to occur. However, it is thought that several months to a year post-injury, collagen III degradation occurs and collagen I synthesis increases, restoring the balance back to normal (Jie Li *et al.*, 2007).

Chronic wounds occur by a delay in any stage of the normal wound healing process. Defects in reepithelialisation have been identified as a cause of chronic wounds; however, the causes of these defects are unknown. It has been speculated that the signalling switching keratinocytes to a migratory phenotype is absent and therefore keratinocytes do not migrate to close the wound. Additionally, it has been suggested that reepithelialisation is initiated as normal but migration occurs at a slower rate (Raja *et al.*, 2007). Therefore the wound remains open for a longer period of time, increasing susceptibility to infection. Morphological analysis of the skin present in chronic wounds

has shown that mitotically active cells are present in the suprabasal layers of the skin due to over activity of c-myc, under normal homeostatic conditions; mitotically active keratinocytes are limited to the basal layer. Combined with parakertosis, hyperkaratosis, nuclear β-catenin within cells in the SC, suppression of early differentiation markers and induction of late differentiation markers, it has been accepted that non-healing wounds display a non-migratory, hyperproliferative epidermis which fails to reepithelialise appropriately (Stojadinovic *et al.*, 2005).

Underlying mechanisms regulating keratinocyte motility in normal acute wound healing responses remain incompletely understood and still require further investigation. Wounds that do not undergo reepithelialisation are not considered to be healed. A greater understanding of processes regulating reepithelialisation may provide insights for new therapeutic targets in the treatment of both acute and chronic wounds.

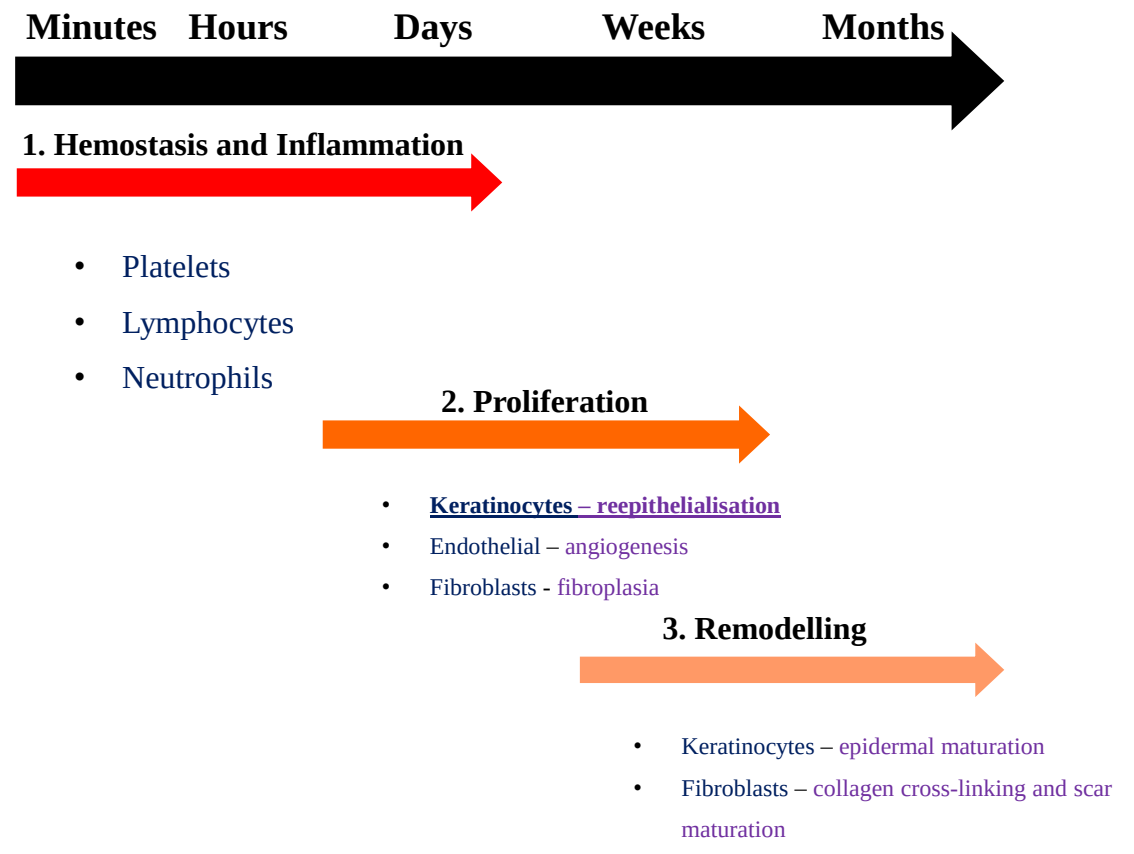

Figure 1.3 Stages of wound healing.

Wound healing is a complex biological event involving many cell types and lineages simultaneously. The first phase to occur post-wounding is the inflammatory phase, followed by the proliferative phase and finally the long-term remodelling phase. Keratinocytes play a particular role in the reepithelialisation stage of the proliferative phase. Modified from (Jie Li *et al.*, 2007)

1.2.4 Current therapies and outstanding issues.

Due to the presence of biofilms and the fact that a wound disrupts the skin barrier and therefore makes the patient vulnerable to pathogen invasion, historic treatment of both acute and chronic wounds to date has focussed on infection prevention. Debridement of the wound site may be required. This procedure aims to remove devitalised and damaged tissue, as well as the biofilm, whilst maintaining the integrity of healthy skin and underlying structures such as nerves, muscle and bone (Kamolz and Wild, 2013). Advances in this area of wound management involve optimising dressing gauze to create a favourable environment for wound healing to occur. However, there is the need for biological and cellular based therapies which aim to augment or restore the body's natural wound healing responses. Ongoing advances in these areas aim to supplement current wound treatments with factors known to be involved in wound healing *in vivo*. Cytokines are known to regulate the inflammatory stage of wound healing and several have been studied to investigate their beneficial properties in wound therapies. For example, granulocyte/macrophage colony-stimulating factor (GM-CSF) has been effective when used as a treatment of diabetic and venous leg ulcers (Cianfarani *et al.*, 2006). Growth factor-based therapies are the most investigated biological therapy in the field of wound healing and recombinant platelet-derived growth factor (RhPDGF), a growth factor which stimulates fibroblasts and keratinocytes, has been approved by the FDA as a treatment for diabetic leg ulcers. Clinical investigations involving 118 patients revealed 48% of patients achieved wound closure with exogenous application of rhPDGF compared to 25% of placebo treated patients over a 20 week period (Steed, 1995). However, the exact mechanisms involved in this remain unknown and further trials on other types of chronic wounds such as hypertensive leg ulcers proved unbeneficial.

Another emerging field of wound therapies is the use of stem cells. It is known that stem cells play a role in promoting wound closure (Ito *et al.*, 2005), although to what extent is highly debated in the literature. Within the epidermis, there are three stem cell niches a) the basal layer of the interfollicular epidermis (IFE), b) the base of the sebaceous gland and c) the bulge region of the hair follicle (Fuchs, 2008). Stem cells are believed to replenish their niche in a unipotent manner under normal homeostatic conditions. However, in response to epidermal injury, hair follicle and IFE stem cells

contribute to reepithelialisation responses (Lau *et al.*, 2009). The timing of activation is under debate. Evidence exists that suggests that HF stem cells, defined by K15 expression, are solely involved in the early stages of wound healing. Ito *et al*. showed that HF stem cells migrated into the IFE immediately following wounding, however, their presence was not detected in the weeks following wounding (Ito *et al.*, 2005). In contrast, studies utilising more recent bulge stem cell markers, such as SOX9, have indicated the presence of HF stem cells within the reepithelialised and healed skin (Nowak *et al.*, 2008). Whilst interesting research has been conducted regarding the characterisation of the role of stem cells in wound repair, investigations have predominantly utilised murine models. Further work is required to confirm the translation of these into human models (section 1.2.5). It has been suggested that stem cells support wound closure by trophic activation of keratinocytes and endothelial cells through release of growth factors (Steed, 1995). Mesenchymal stem cells (MSC) have been shown to secrete growth factors and cytokines which are known to promote wound healing processes in host tissue (Caplan, 2009), therefore making them attractive targets in the development of therapeutics. Interestingly, these MSC can be transplanted into wounds themselves or, arguably a safer method is the addition of conditioned media containing the secreted bioactive factors. However, investigations to date have demonstrated that MSC paracrine activity reduces with time in *in vitro* culture and inter-donor variability may be challenging (Kerpedijeva, 2012). Similarly, Lee and co-workers observed that application of conditioned media containing human embryonic stem cells from endothelial precursor cells (hESC-EPC) into excisional wounds in mice accelerated wound closure following topical treatment and subcutaneous injection. Comparative results were seen *in vitro* with these embryonic stem cells increasing both fibroblast and keratinocyte migration. A cytokine array system was utilised to investigate the composition of the conditioned media and revealed that hESC-EPC secreted growth factors and cytokines such as EGF, bFGF, GM-CSF, IL-6, IL-8 and VEGF which have all previously been reported to regulate wound healing responses (M. J. Lee *et al.*, 2011). Results from studies such as the two mentioned above are highly suggestive that cytokines and growth factors released by stem cells may act as key regulators of wound healing and highlight a role for stem cell therapy in chronic wounds. Additionally, several pre-clinical trials are investigating the possibility of inserting stem cells into wound beds to increase probability and speed of wound closure

but adequate survival of these exogenous cells in the hostile wound environment remains elusive.

Whilst advances in biological and cellular based wound therapies are encouraging, many investigations are conducted in small pre-clinical trials or are inconclusive in larger clinical trials. Currently a clinical trial is taking place to investigate whether viable cells within a bioengineered construct provide additional beneficial effects in the promotion of wound closure in non-healing wounds compared to matrix alone (Lev-Tov *et al.*, 2013). It is of note that, even the more successful biologic agents only prove to be 50% effective. A greater understanding of the mechanisms regulating individual stages of the normal wound healing would allow development of therapeutic agents aimed to promoting wound closure in a timely manner.

1.2.5 Models of wound healing in research

The complexity and involvement of different cell types and pathways in wound healing make it extremely challenging to study. Finding models that biologically represent the process of human epidermal wound healing is also problematic. Ethical considerations significantly limit the use of humans in wound healing investigations, especially at the pre-clinical stages of development.

The use of animal models such as mice, rats and dogs are both advantageous and disadvantageous in wound healing studies. Benefits include ease of availability, low cost, small size and relative ease of manipulation to mimic systemic complications associated with poor wound healing. Therefore, they cannot be completely overlooked as biological tools to provide insights into basic processes involved in tissue repair. However, vast differences exist between these species and humans regarding tissue architecture, immune response and physiological characteristics relating to ageing (Windsor *et al.*, 2009). For example, rat skin is described as loose due to lack of adherence between layers of skin and increased elasticity (Gottrup *et al.*, 2000). Additionally, rats have a subcutaneous panniculus carnosus muscle which has been shown to have an important contribution to wound contraction. Mediated by the deposition of a collagen rich matrix, wound contraction decreases the area of the wound site requiring replenishing and therefore promotes faster wound healing (Paul Martin, 1997).

The majority of animal model investigations are conducted in mice and rats; species covered in hair. It is thought that KSC are found in the bulge region, located in the outer root sheath of the hair follicle. Whilst firm evidence linking these KSC to vital wound healing responses is up and coming, Langton *et al*. have observed a quicker healing rate in wounds inflicted on areas containing hair follicles compared to areas lacking them (Langton *et al.*, 2007). This supports the self-experimental studies conducted in the 1940s which noted shallow wounds where the hair follicles were undamaged resulted in faster wound healing. As well as the clinical observation that wounds on the scalp, where there are a greater number of hair follicles heal faster than other body sites. However, it is of note that hair follicles are probably not the sole reason for this observation; factors such as increased vasculature on the scalp are likely to contribute. Furthermore, Ansell *et al*. assessed the role of KSC in wound healing and concluded the phase of hair cycle in which wounding occurs correlates to the speed of reepithelialisation. When stem cells are active in mid-to late anagen, wounds healed faster compared to wounds occurring in the telogen phase of the hair cycle when the majority of stem cells are quiescent (Ansell *et al.*, 2011). Although future investigations are required to fully assess the link between KSC and wound healing, these recent studies highlight two important facts. Firstly, if KSC are located in the bulge region of the hair follicle are important in reepithelialisation then using animal models with increased hair follicles, may provide misleading data when translating to humans. Secondly, if the stage of hair cycle is functionally related to reepithelialisation rates, it suggests that the stage of the hair cycle in animal studies should be documented in the literature and care should be taken to ensure both control and treated groups have synchronised hair cycle in order to make valid comparisons.

The vast number of differences that exist between animal and humans mean, whilst animals can provide useful indications regarding the biological processes occurring during wound healing and the effect of pharmacological intervention, translating findings into humans remains difficult. A study analysed all wound healing papers published between 2000 and 2003, in an attempt to compare experimental techniques and variables. The report showed that a large range of differences exist between studies which makes it difficult to compare and combine findings to further increase scientific knowledge within the field. These differences include animal model used, age of animal, delivery system utilised for pharmacological agents and time frames (Dorsett-

Martin, 2004). This suggests there is a need for a standardised model to investigate wound healing *in vivo* and *in vitro*.

A lack of reliable *in vivo* models for studying human wound healing, the complexity of the cell types involved and the many over-lapping phases of wound healing responses, makes it necessary to study wounding in a simplified model, with accepted incompleteness.

Herein, primary keratinocyte two-dimensional monolayers have been used to simulate wounding. This established method allows investigation into specific signalling pathways involved in keratinocyte's contribution to wound healing; primarily during the reepithelialisation phase.

1.3 Calcium Signalling.

1.3.1 Calcium signalling pathway.

Wound healing responses, alluded to in section 1.2.3, are known to incorporate an immediate response factor as well as longer term events. The calcium signalling cascade has been shown to function in both these manners and therefore its role in epidermal wound healing responses was hypothesised. Calcium is a common secondary messenger (Berridge *et al.*, 2003) used to elicit a vast range of highly important responses vital to organism survival. Examples include but are not limited to cell division, fertilisation, cell proliferation and gene regulation. To allow for this diverse range of responses, acute spatial and temporal regulation of intra-inter-and extra-cellular calcium signalling is required. The first record of calcium requirement in a physiological process came about by a reported serendipitous experiment conducted over 130 years ago. Ringer observed that, only in the presence of calcium in the perfusion media did the isolated heart contract (Ringer, 1883). This idea was taken further with Heilbrunn *et al.* confirming calcium was crucial for frog leg muscle contraction; only injection of calcium resulted in contraction, no contraction was observed by injection of other ions (Heilbrunn and Wiercinski, 1947). Further research using calcium injections highlighted an important role in a range of cellular processes including neurotransmitter release

(Miledi, 1973) and activation of mast cells (Cochrane and Douglas, 1974), oocytes (Rose and Loewenstein, 1975) and salivary glands.

Spatial and temporal regulation of calcium signalling allows for these responses and cells possess an intrinsic calcium "tool kit", fundamental to these regulations. Components of this "toolkit" are cell specific and allow for calcium "on" and "off" mechanisms to regulate amplitude, frequency, temporal and spatial profiles within a signalling cascade. For example, at the synaptic junction calcium leads to neurotransmitter release within microseconds, whereas activation of gene transcription and cell proliferation occurs over a longer time period (Berridge *et al.*, 2003). In a resting cell the intracellular calcium concentration ($[Ca^{2+}]_i$) is 70-100nM, 10,000 fold lower than the external environment $[Ca^{2+}]_i$. Cytosolic increases of calcium can arise from extracellular influx or intracellular calcium release. Extracellular calcium enters the cell through plasma membrane (PM) ion channels, intracellular calcium can be released from intracellular stores (Csernoch *et al.*, 2000). The latter is primarily conducted through the endoplasmic reticulum (ER), although the golgi apparatus (Xue *et al.*, 1994) and the mitochondria (De Stefani *et al.*, 2011) have been reported to be major calcium stores. Calcium release from the ER is primarily conducted through the cellular mediator inositol 1,4,5-trisphosphate (IP_3). When an agonist binds to a cell surface receptor family such as GPCR or tyrosine-kinase-coupled receptors, phospholipase C (PLC) is activated. Variations in agonists and the receptors to which they bind influence the isoform of PLC activated and subsequent downstream pathways. To illustrate, bradykinin binding results in a large calcium flux whereas LPA causes a smaller but more persistent flux (Van der Wal *et al.*, 2001). Once activated PLC cleaves phosphatidylinositol 4,5-bisphosphate (PIP_2) into IP_3 and diacylglycerol (DAG). Due to its hydrophobic properties, DAG remains at the PM and acts as a physiological activator of protein kinase C (PKC). On the other hand, IP_3 diffuses to the ER and binds to its receptor (IP_3R) to initiate the release of calcium from the ER down its concentration gradient into the cytosol (Berridge *et al.*, 2003) (Figure 1.4).

1.3.2 Store-operated calcium entry (SOCE).

Whilst the above mechanism to increase $[Ca^{2+}]_i$ is well established, it is also known that the ER functions to ensure newly synthesised proteins are packaged and labelled correctly. Furthermore, the ER, is involved in vesicle trafficking and the release of

stress and metabolism signals. Many of these are dependent on calcium and if the calcium concentration in the ER is below optimal for a prolonged period of time it can result in protein mis-folding, ER stress responses and apoptosis. Therefore, depletion of calcium from the ER results in an inflowing calcium current into the cell, by activation of store-operated calcium channels in the PM. This concept of calcium entry occurring when the internal stores were emptied, named store-operated calcium entry (SOCE), was first introduced in 1986. Many investigations to date have focussed on determining underlying mechanisms. Initial reports were based on observations that intracellular calcium store refilling did not require receptor activation; the same pattern of calcium flux was seen in the presence of a receptor inhibitors.

SOCE is a major calcium entry pathway in both excitable and non-excitable cells (Putney, 1986). For twenty five years after its discovery, the molecular mechanisms involved in linking ER calcium depletion to extracellular calcium entry were unknown. In 2005, the role of two proteins; stromal interaction molecule 1 (STIM1) and calcium release-activate calcium channel protein 1 (Orai1) were implicated in SOCE activation. Studies indicate that STIM1 detects calcium depletion by loss of calcium binding to its N-terminal EF hand (Ross *et al.*, 2007). Therefore, resulting in the translocation of STIM1 to the PM, activation of Orai1 and subsequent entry of external calcium (Stathopulos *et al.*, 2013) (Figure 1.4). Whilst a major contributor, it is of note that SOCE is not the only calcium influx pathway utilised in non-excitable cells. During fertilisation, a process which is known to be calcium-dependent, SOCE inhibition had no effect on the occurrence of the frequency of intracellular calcium oscillations or calcium influx rate (Takahashi *et al.*, 2013).

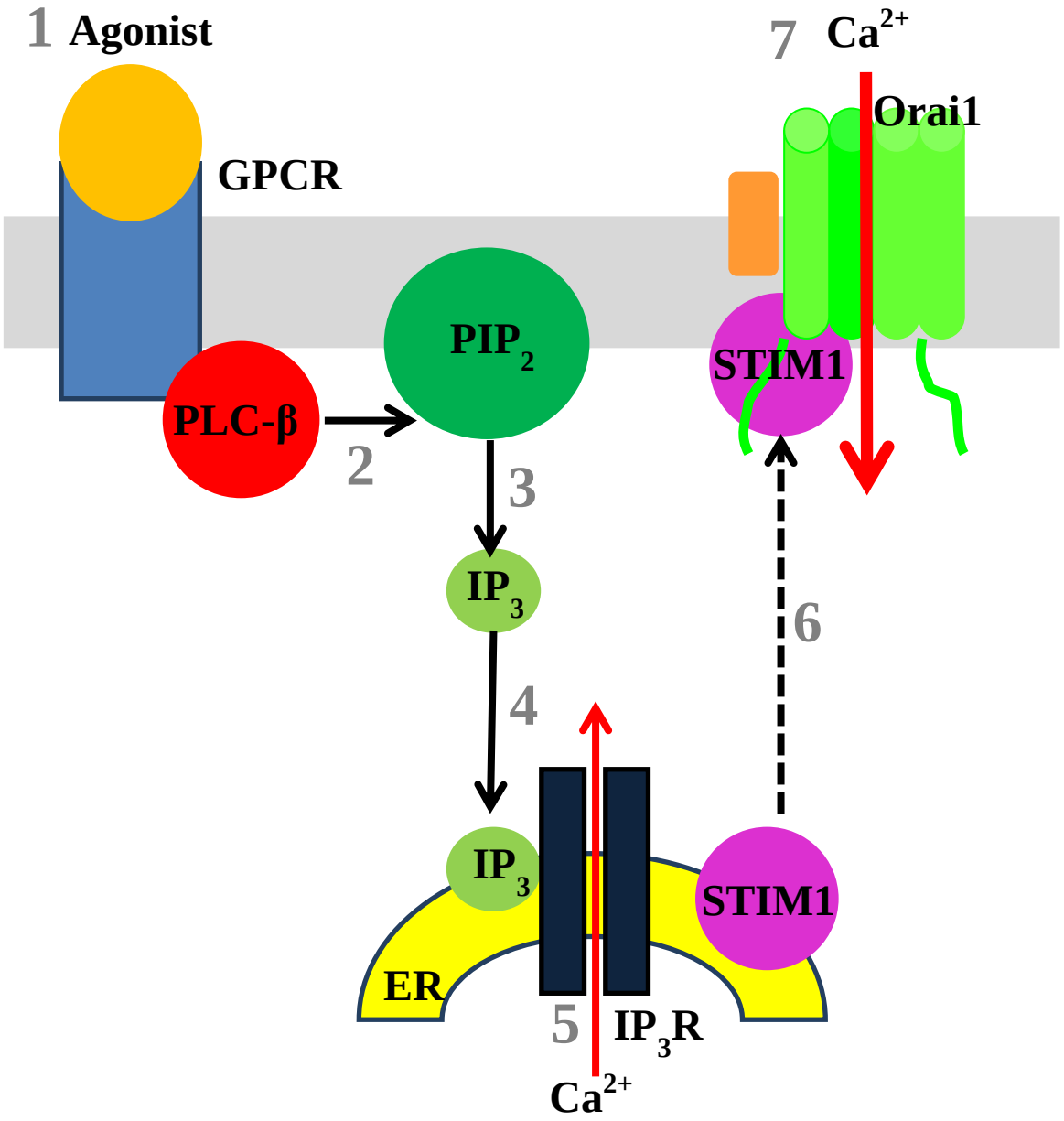

Figure 1.4 Schematic representation of IP_3-mediated calcium signalling resulting in store-operated calcium entry (SOCE).

1. Agonist binds to a GPCR on the plasma membrane. **2.** The GPCR activates PLC. **3.** PLC cleaves PIP_2 into DAG (not shown) and IP_3. **4.** IP_3 diffuses and binds to its receptor on the endoplasmic reticulum (ER). **5.** Calcium is released from the ER and increases cytosolic calcium levels. **6.** Upon ER calcium depletion, STIM1 translocates to the plasma membrane and oligomerises with Orai1. **7.** Calcium channel opens and calcium enters the cell through a process known as store-operate calcium entry (SOCE). Adapted from (Ralph Jans *et al.*, 2013)

1.3.3 Stromal interaction molecule (STIM) and calcium-release activated calcium channel protein (Orai).

There are two known STIM proteins; STIM1 and STIM2. The two homologues are identical in structure, share 65% sequence homology, both function as a ER calcium sensor and both interact with Orai on the PM (Mukherjee and Brooks, 2014). STIM is comprised of multiple domains including the EF hand which faces into the lumen and binds calcium. In the presence of calcium in the ER, STIM1 exists as an inactive monomer and resides in the ER membrane (Liou *et al.*, 2005). Following IP_3-mediated calcium depletion of the ER, the STIM1 EF hand senses a loss of calcium and rapidly induces a conformational change allowing dimerisation of STIM1 in the ER membrane. STIM1 then laterally translocates close to the PM to form punctae at the ER/PM junctions. This proximity to the PM allows for interactions between STIM and store-operated calcium channels. Experiments conducted by two groups in 2005 demonstrated that RNA-mediated STIM1 knockdown blocked thapsigargin (Tg)-induced SOCE implicating it as the regulator of the calcium entry pathway after store depletion (Liou *et al.*, 2005; Roos *et al.*, 2005).

Orai, named after the keepers of heaven's gates in Greek mythology, is a 33 kDa four-transmembrane domain protein located in the PM and has three homologues; Orai1, Orai2 and Orai3. Both the C-and N-termini are located within the cell cytosol. In the presence of calcium in the ER lumen, Orai is found in dimers in the PM. Upon calcium depletion and the subsequent STIM1 translocation to the PM, Orail dimerises to form a pore-forming tetramer unit which functions as an active and calcium-selective ion channel, allowing the entry of extracellular calcium into the cell (Prakriya *et al.*, 2006). Orai1 was identified as an essential component of SOCE in 2006. A study by Feske *et al.* demonstrated that severe combined immunodeficiency patients failed to activate SOCE after Tg-induced ER depletion. This dysfunction was attributed to a single point mutation (R91W) in Orai1. To further confirm the role of Orai1 in SOCE, transfection of wild-type Orai1 into these cells restored SOCE (Feske *et al.*, 2006).

1.3.4 Calcium signalling in disease.

Calcium functions as a ubiquitous, diverse and crucial secondary messenger in all cells and is pivotal for cell communication, responses and survival. Therefore, dysregulation

at any stage of the cascade is severely detrimental and can lead to disease states. The role calcium signalling plays in health and disease has been studied extensively and the discovery of SOCE and its regulators STIM1 and Orai1 has led to a recent acceleration of knowledge on the crucial part the SOCE pathway plays in disease pathology (Feske *et al.*, 2006). The list of diseases that have been attributed to dysfunctional calcium signalling is exhaustive and includes depression, Alzheimer's, schizophrenia, hypertension, diabetes, heart failure and polycystic kidney disease, obesity, thrombosis, infertility and stroke and are reviewed by (Berridge *et al.*, 2003; Berridge, 2014). Given the vast evidence that implicates calcium signalling in cell proliferation, growth, survival and death it is perhaps unsurprising that components of the signalling pathway, especially STIM and Orai in recent years, have been proposed to be crucial to the development and progression of cancer in many cell types. SOCE is the major calcium influx pathway in immune cells following antigen recognition and mutations in both STIM and Orai have been described in diseases of the immune system, including the aforementioned SCID as well as multiple sclerosis (Ma *et al.*, 2010) and Sjogren's syndrome (Cheng *et al.*, 2012). Increased knowledge of how calcium remodelling occurs to lead to disease has led to the hypothesis that calcium signalling could be manipulated as a therapeutic target. However, the precise functions of calcium-dependent pathways during homeostasis and how dysregulation can cause disease *in vivo* remains to be deciphered. Despite research demonstrating up-regulation or down-regulation of mediators of calcium signalling in disease, developing therapeutic targets for their treatment should be taken with caution. Calcium signalling is highly complex and required in all cell types for a range of functions, therefore the probability of disastrous side-effects is high and more detailed investigations are required to elicit specific cell-type modulation.

1.3.5 Calcium in the skin.

The role of calcium in keratinocyte growth and differentiation is well established. Indeed, calcium is thought to be a key signalling pathway regulating skin homeostasis which in part, is due to the presence of a calcium gradient in the epidermis. Ion capture cytochemistry and proton-induced X-ray emission experiments have been used to show the presence of a steep, vertical calcium ion gradient within the epidermis (G. K. Menon *et al.*, 1985). Calcium concentration is low in the proliferative basal layer and

progressively increases through the spinous layer and reaches a maximum in the granular layer, levels then fall at the outermost SC (Elias *et al.*, 2002). This attenuation in the uppermost layer of the epidermis is due to the dry lipid-rich environment which is impervious to solutes and ions. Therefore, two distinct environments are created above and below the stratum granulosum, which, through tight junctions, regulate differentiation mediated by extracellular factors (Kurasawa *et al.*, 2011). As the calcium gradient increases, keratinocytes differentiate; see section 1.1 for an overview of epidermal structure and differentiation. Factors that initiate and maintain this epidermal calcium gradient remain unknown. Evidence exists to support a role of the gradient in epidermal differentiation and function, particularly regarding the skin's hallmark role as barrier. Calcium is critical in the epidermis as it mediates the expression of cell cycle progression and apoptosis genes as well as inducing terminal differentiation (Numaga-Tomita and Putney, 2013). Coinciding with the observed relative calcium concentrations *in vivo*, studies have shown that keratinocytes cultured in low calcium (<0.1mM) are phenotypically similar to the undifferentiated cells found in the basal layer. However, when exposed to a high calcium environment (>1mM) cells change morphological and molecular characteristics in line with those of differentiated cells (Hennings *et al.*, 1980). Indeed, this pioneering work conducted by Hennings *et al.* is the fundamental basis of the culture conditions required for keratinocytes to be grown *in vitro* for experimental analysis. Despite advancing knowledge, the mechanisms regulating calcium-induced keratinocyte differentiation remain largely unknown. It has previously been shown in HaCaTs that agonist treatment induced the redistribution of STIM1 into punctae on the PM (Ross *et al.*, 2007). However, relatively few studies have investigated the role of endogenous STIM1 and Orai1 in SOCE in keratinocytes. Last year, Numaga-Tomita and James Putney demonstrated three novel roles for SOCE in keratinocyte homeostasis. Firstly, SOCE is required for the maintenance of calcium stores in undifferentiated and proliferating cells. Secondly, calcium responses underlying the induction of differentiation by calcium switch is lost following STIM1 or Orai1 knockdown. Finally, knockdown also reduced the activation of the early differentiation marker, keratin 1, in high external calcium compared to control cells. Despite these investigations being conducted in HaCaTs, which are known to have varying differentiation capabilities compared to primary human keratinocytes, these results demonstrate that STIM1 and Orai1 are responsible for the calcium entry that is required for the maintenance of stored calcium levels in undifferentiated cells as well as

the calcium signalling that induces differentiation (Numaga-Tomita and Putney, 2013). In agreement with this investigation, it has been suggested that Orai1 expression is localised to the basale proliferative layer of the epidermis, providing support for the hypothesis that SOCE is implicated in keratinocyte differentiation (Vandenberghe *et al.*, 2013). Furthermore, both Orai1 expression and epidermal proliferation are reduced in patients with skin fragility. Orai1 inhibition resulted in epidermal atrophy in mice and treatment with an Orai1 activator led to increased epidermal thickening. Together these studies are highly suggestive of a dominant role for SOCE in epidermal differentiation and stratification (Darbellay *et al.*, 2014).

1.3.6 Calcium signalling in dermatological diseases.

Having such a prominent role in the stratification of the epidermis and keratinocyte homeostasis, pathological alterations to calcium signalling in keratinocytes have severe biological repercussions. For example, mutations in the sarco/endoplasmic reticulum calcium ATPase (SERCA2) calcium pump, which are highly expressed in keratinocyte ER, results in the autosomal dominant inherited disorder Darier's disease (DD) (Ruiz-Perez *et al.*, 1999). Whereas mutations in the calcium pumps located on the golgi results in Hailey-Hailey disease. Furthermore, psoriasis is a common hyperproliferative skin disease and it has been shown that psoriatic cells have altered calcium signalling in response to agonists compared to normal keratinocytes. Together with a disturbed calcium gradient in the epidermis of psoriasis patients, this indicates calcium signalling plays a role in disease development. Fundamental work conducted by Karvonen and co-workers demonstrated that even after several passages in culture, psoriatic keratinocytes maintained their defective responses. The authors conclude that there are unknown intracellular abnormalities causing the abnormal response, rather than solely extracellular influences (Karvonen *et al.*, 2000). The first SOCE inhibitor to be used in a clinical trial is being tested as a therapeutic agent for moderate-to-severe plaque psoriasis (*CalciMedica*). Although only in Phase 1, this highlights an important advancement in the use of pharmacological inhibitor of SOCE in treating disease. In terms of this trial, the SOCE inhibitor is being investigated for the immune-suppressive benefits in psoriasis plaques, psoriasis being an immune-driven disorder. However, it is likely that results will also shed light on the effects of SOCE blockade in regulating keratinocyte proliferation and differentiation. Recently, SOCE has been implicated in

melanoma metastasis and silencing Orai1/STIM2 attenuated melanoma cell migration. This study highlights the potential of SOCE manipulation in regulating the invasiveness of human melanoma as well as increasing the beneficial effects of standard chemotherapeutics (Stanisz *et al.*, 2014).

1.4 Gap-junction communication.

1.4.1 Biology of gap-junctions.

Mechanisms regulating the spread of the intercellular calcium wave are highly debated within the literature (section 3.1.1). However, a vast amount of evidence exists for the involvement of gap-junctions in mediating the spread of small molecules between cells at the point of wounding. Therefore, the role of gap-junctional communication in both the calcium wave and downstream events was of interest within this project. It is vital that cells within a population communicate together, during both normal cell homeostasis and in response to stress. Gap-junctions represent a common, quick and direct means of intercellular communication and are widely expressed in eukaryotic organisms (Davidson and Baumgarten, 1988). Connexins are a family of transmembrane proteins encoded by different gene families and are the smallest unit of a gap-junction. Six connexins form a hemi-channel structure known as a connexon in a homo or hetero-hexameric manner. When two connexons on nearby cells come into contact a gap-junction is formed (J. Zhang *et al.*, 2011). If the two connexons are identical they form homotypic gap-junctions, if they are not identical they form heterotypic gap-junctions. Therefore the resultant gap-junction can be structured in one of four ways; heteromeric homotypic, heteromeric heterotypic, homomeric heterotypic and homomeric homotypic (Figure 1.5) (J. Zhang *et al.*, 2011). The composition of the gap-junction is thought to influence its permeability and other functional characteristics.

Communication between cells in this manner was originally thought to occur in a fixed passive manner. However, more recently it has been shown that a gating mechanism exists to regulate the opening and closing of the channels. Upon stimulation, the channels open and small molecules such as ions, secondary messengers, amino acids and nucleotides are able to freely pass from the cytosol of one cell into the cytosol of an adjacent cell (J. Z. Zhou and Jiang, 2014).

Historically, it was believed that the limiting factor for transport through a channel was its pore size; if a molecule was small enough to diffuse through it would. This idea has been contested with studies arguing that there are a range of factors regulating selectivity. These hypotheses are now being investigated. Nomenclature of gap-junctions comes from either a) the predicted molecular weight of the connexin, for example, connexin-43 (Cx43) has a molecular weight of 43 kDa or b) the Greek letter method grouping connexins in either an α or a β group depending on sequence homology. Throughout this project connexins will be addressed using the predicted molecular weight terminology.

1.4.2 Inhibition of gap-junctions.

Interestingly, despite being widely expressed across cell types and species, there remains a lack of presence in the field regarding specific and direct gap-junction inhibitors. Possible reasons for this could be the complexity of the structure of gap-junctions or the biological location of gap-junctions; located between cells they are relatively insulated from the extracellular space as reviewed by (W. H. Evans and Boitano, 2001). Thus meaning that access of pharmacological inhibitors to the required site may be restricted. Nevertheless, a range of inhibitors have been extensively assessed and shown to either directly or indirectly block or reduce gap-junction communication. However, the precise mechanisms behind this inhibition are largely unknown; with each class of inhibitor thought to act in a different manner and having varied effect depending on cell type and physiological stimulus. Classical inhibitors of gap-junction communication are aliphatic alcohols such as 1-Octanol. The proposed mechanism of action of these alcohols is thought to involve interference of function through the alteration of membrane fluidity due to the presence of the alcohol in membrane lipids. This results in the contraction of channels on the membrane (W. H. Evans and Boitano, 2001). There is much evidence to support this theory, however, it has also been noted that this contraction potentially closes other channels on the PM. Thus affecting their specificity as gap-junction blockers. Another compound that has been used as an inhibitor of gap-junction communication is 18α glycyrrhetinic acid (18αGA) (Davidson *et al.,* 1986). 18αGA is one of the stereo-isoforms of the active metabolite of glycyrrhizin; the main constituent of liquorice root. Interestingly, liquorice root is used as a herbal medicine to treat a wide range of disease and Chinese

medical practitioners believe it is beneficial in the treatment of injuries (Shetty *et al.*, 2011). Additionally, reports indicate that glycyrrhizin has anti-inflammatory, anti-viral, and anti-tumorigenic properties, although firm evidence confirming this remains elusive. It is postulated that 18αGA is a specific, reversible, inhibitor of Cx43-mediated gap-junction signalling. Unlike the aliphatic alcohols, the effect of 18αGA has been shown to occur indirectly through the altered phosphorylation of residues in the cytoplasmic tail of Cx43. This leads to changes in the assembly of connexins to form a functional gap-junction.

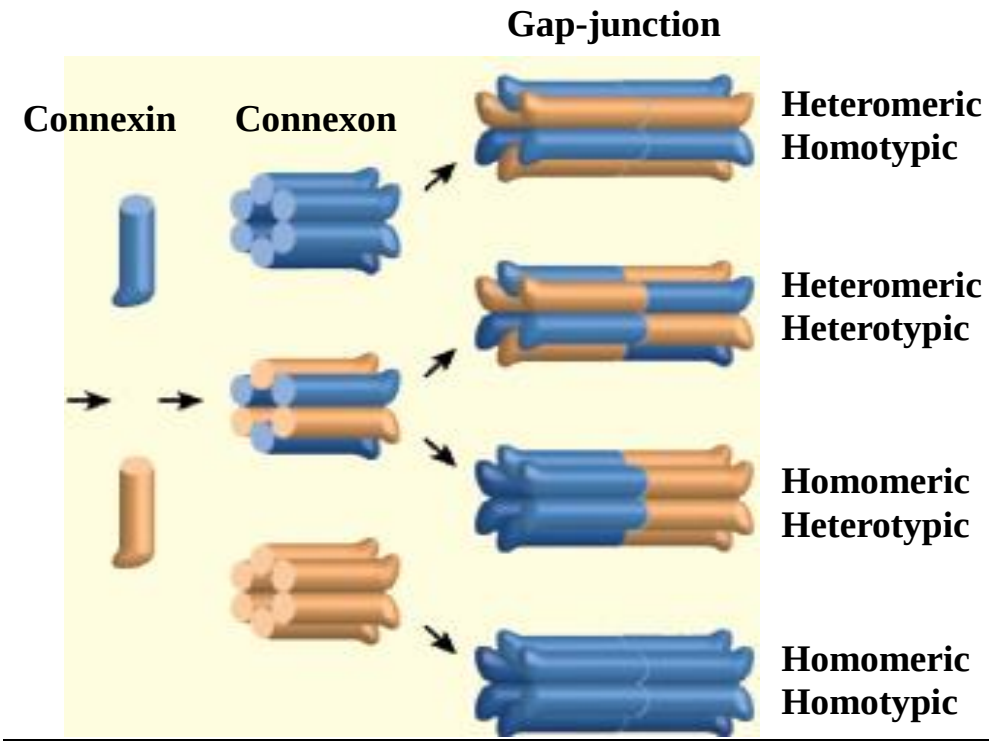

Figure 1.5 Gap-junction formation and subsequent classification.

Gap-junctions play a crucial role in cell-to-cell communication for organism survival. The smallest unit of a gap-junction is a connexin, six of which form a connexon or hemi-channel. When two hemi-channels on adjacent cells come into close proximity they form a gap-junction and a conduit connect the cytoplasm of the two cells. The hexamer of connexins can be either homomeric or heteromeric. Similarly, if the two connexons are identical they form homotypic gap-junctions, if they are non-identical they form heterotypic gap-junctions. Thus, gap-junctions can be one of four conformations; heteromeric homotypic, heteromeric heterotypic, homomeric heterotypic and homomeric homotypic. Modified from (Mese *et al.*, 2007).

1.4.3 Gap-junctions in the skin.

It is postulated that up to ten connexins are expressed within the epidermis and are found in all layers, apart from the stratum corneum. Cx43 is ubiquitous throughout the epidermis, whereas other connexins are located within a specific layer. For example, Cx26 is found in the stratum basale whereas Cx30 and Cx31 are highly expressed in more differentiated cells (P. E. Martin *et al.*, 2014). This suggests a role for connexins in epidermal stratification and keratinocyte differentiation. Aberrant connexin expression has been shown to cause epidermal disease, further supporting the role of gap-junction communication in keratinocyte homeostasis, as well as implicating their dysregulation in the development of disease states. For example, inherited palmoplanter keratodermas (PPK) are a family of skin disorders characterised by hyperkeratosis of palms and soles. Clinical presentation can occur alone or in combination with another disease; the most common of which is hearing loss (J. Zhang *et al.*, 2011). Linkage analysis and genetic studies have identified mutations in Cx26 in families with PPK. Some of these patients also suffered from hearing loss suggesting that the same mutation causes both phenotypes. However, this was contradicted by evidence presented by Kelsell *et al*. who reported that although associated, the two diseases were not mutually linked; there were some patients presenting with PPK that did not have defective hearing (Kelsell *et al.*, 1997). Additionally, there are five known Cx31 mutations that cause erythrokeratoderma variabilis (EKV), a dominant genodermatosis characterised by erythema and hyperkeratosis and two known Cx31 mutations that cause progressive hearing loss. However, there are no reports of patients presenting with both diseases. Cx30.3 mutations can also cause EKV (Macari *et al.*, 2000; Kretz *et al.*, 2003). In the context of skin research these studies provide strong evidence to implicate gap-junction communication in the development of disease, although the regulatory and molecular mechanisms leading to the phenotype of the disease require further investigation. One proposed mechanism of action linking aberrant connexin expression and hyperproliferative epidermal disorders comes from the studies conducted in HeLa cells which showed that cells transfected with Cx30 gain of function mutants, have increased extracellular ATP release (Essenfelder *et al.*, 2004). As alluded to in section 1.6.4, it is believed that ATP release from keratinocytes causes epidermal thickening, therefore it could be hypothesised that dysregulation of gap-junction signalling in keratinocytes leads to increased ATP release and therefore increased keratinocyte

proliferation. This would result in the phenotype associated with keratodermas. Intriguingly, the dermatological symptoms associated with each disease can be correlated to the position of the mutated connexin within the epidermis. For example, a mutation in Cx26, which is located in the basale layers and various appendages, tends to result in hyperproliferative disorders which also cause nail and hair dystrophy. Whereas Cx30 and Cx31 mutations cause symptoms associated with defected keratinocyte differentiation.

As described in section 1.1, a hallmark function of the skin is to act as a barrier. Research in the past decade investigating connexins and barrier function has led to the hypothesis that gap-junction communication may underlie dermatological diseases that have a strong barrier component, including psoriasis. Using the cDNA differential display technique Rivas *et al.*, first demonstrated that Cx26 was up-regulated in psoriatic plaque lesions (Rivas *et al.*, 1997); indeed, further studies have confirmed Cx26 as one of the most highly up-regulated genes in psoriasis plaques (Djalilian *et al.*, 2006). Further evidence supporting a role for connexins in epidermal barrier function comes from mouse models with a mutated C-terminal within Cx43. Cx43 is the most abundant connexin in mammals and is arguable the most studied in relation to pathogenesis of diseases. It has also been reported that phosphorylation of the C-terminus regulates gating properties of these conduits (W. H. Evans and Boitano, 2001). In order to highlight the importance of the C-terminus in Cx43-mediated gap-junction communication, mutant transgenic mice were used. These mice lacked the last 125 amino acids in the C-terminus resulting in impaired channel closure. Interestingly, these mice were not embryonic lethal, however, 97% died within two days of birth. The authors concluded that this high post-natal mortality rate was a result of defective epidermal barrier. The prolonged Cx43 expression altered the terminal differentiation pattern of keratinocytes during development compared to wild-type mice. Filaggrin is an important protein in epidermal barrier function and has been implicated in diseases such as eczema. Expression of filaggrin in the upper layers of the epidermis in the mutant mice was altered, leading therefore to the hypothesis that persistent Cx43 expression results in defective filaggrin processing causing a decrease of hygroscopic amino acids in corneocytes. This suggests that whilst not directly regulating epidermal barrier formation during development, Cx43 modulates expression of other proteins, such as filaggrin, which are crucial in barrier permeability (Maass *et al.*, 2004).

Although animal and *in vitro* models indicate a crucial role for connexins in both epidermal barrier formation and the occurrence of skin disorders, the relevance of these studies regarding human physiology and the pathogenesis of human diseases remains to be deciphered.

1.4.4 Gap-junctions in wound healing.

Given its requirement in keratinocyte growth and differentiation, there has been much interest in studying the role of gap-junction communication during wound healing. The suggestion is that cell signalling post-wounding occurs via gap-junction signalling in an on/off manner and correct initiation and cessation of these are necessary for re-epithelialisation, tissue formation and scar formation. The first report of gap-junctions having a role in wound repair came from Gabbiani *et al.* who observed that epithelial cells at the periphery of a wound had four times the surface area occupied by gap-junctions than control skin. Parallel observations showed that these areas of cells had increased actin and myosin proteins indicating that gap-junction communication was involved in the up-regulation of contractile proteins and the synchronisation of epidermal migration (Gabbiani *et al.*, 1978). Shortly afterwards, concordant results were published in epithelium of pig palate, also demonstrating a marked increase in gap-junction within sites of regeneration (Andersen, 1980). The overall mechanisms of connexins regulating reepithelialisation are incompletely understood and there remain many unanswered questions in the field. However, spatial and temporal analysis of connexin expression within the epidermis during wound healing has implicated an important role for Cx43 and Cx26 (Goliger and Paul, 1995). It has been noted that Cx43 is down-regulated at the wound edge post-wounding and this decrease is observed one to three days post-wounding. This decrease in Cx43 levels has been associated with increased cell migration and proliferation across the wound bed (Kretz *et al.*, 2003). Thus highlighting a potential mechanism in which Cx43 prevents migration and proliferation in unwounded conditions and the decrease observed in cells at the wound edge allows for the initiation of cell migration required to close the wound. Parallel to this reduction in Cx43, Cx26 levels have been shown to increase at the wound edge (C. M. Wang *et al.*, 2007). Studies into the role of Cx26 in other dermatological phenotypes have shown that gain-of-function can put the cells into a hyperproliferative state, suggesting that post-wounding, up-regulation is required for the hyperproliferative

epithelium formation needed to restore the epidermis. Although the role of other connexins during wound healing responses are less established, Cx31 is thought to follow a similar pattern to Cx43 with down-regulation post-wounding whereas, like Cx26, Cx30 expression increases (Brandner *et al.*, 2004). *In vivo* models are limited due to the lethality of connexin knockout mice either during development or soon after. However, Kretz *et al*. used a tamoxifen-induced system where Cx43 could be removed post-natally. These mice showed enhanced wound healing compared to controls through increased proliferation and migration (Kretz *et al.*, 2003). This relationship between Cx43 down-regulation and increased cell migration has been documented in other systems including the use of anti-sense oligonucleotide against Cx43 and connexin mimetics; further strengthening the potential role for Cx43 in wound healing. In addition, topical application of Cx43 antisense post-wounding increased wound closure rates, and a significant reduction in inflammation was seen in these mice, implying that connexins may have a multi-factorial role in wound healing modulation (Qiu *et al.*, 2003). The reduction in Cx43 levels is temporary and after reepithelialisation has created a continuous epithelium, Cx43 levels increase and expression returns to normal (Kretz *et al.*, 2003). Physiological relevance of Cx43 down-regulation enhancing wound healing is only partially understood, however it has been suggested that this decrease causes a lack of adhesion between keratinocytes, contributing to the switch to migratory phenotype during reepithelialisation. Despite this evidence in *in vivo* models, *in vitro* monolayer analysis has provided confounding results. Interestingly, non-confluent cell populations retain Cx43 expression and the loss is only detected after confluency has been reached (Gibson *et al.*, 1997). Additionally, investigations into mechanistic modulation of dermal fibroblast migration has illustrated that Cx43 knockdown causes a delay in wound closure in mouse cell lines. These results, shown by Churko *et al.*, analysed fibroblast from the dermis of Oculodentodigital dysplasia (ODDD) mice as well as human patient samples. ODDD is caused by a mutation in Cx43 and both these models showed decreased fibroblast migration after blockade of gap-junction communication (Churko *et al.*, 2011). It can therefore be suggested that differences exist between *in vitro* and *in vivo* models and this may be a consequence of the lack of stratification of the epidermis and the absence of a basement membrane in *in vitro* models. Kretz *et al*., suggest that responses to connexin manipulation appear to be organ-specific; their study showed increased cell migration of keratinocytes with Cx43 reduction whereas it has previously been reported that in neural crest cells, Cx43 down-

regulation results in attenuated cell migration (Kretz *et al.*, 2003). The authors concluded that their findings may be unique to the skin. However, as illustrated above, even within cell types present in the skin differences are apparent, implying that responses are not only organ-specific but also cell-specific.

1.5 NFAT signalling.

1.5.1 The NFAT family.

The nuclear factor of activated T-cells (NFAT) family of transcription factors is activated in response to a cellular increase in calcium concentration, as a result of SOCE. It therefore follows, that NFAT regulates calcium-induced keratinocyte differentiation. This highlights a potential key role for NFAT in epidermal integrity and therefore its role in epidermal wound healing responses was of interest within this project. NFAT consists of five members evolutionally related to the Rel/NFκB transcription factors. The family is split into two distinct groups based on structural and functional similarities; NFAT1-4 and NFAT5 as reviewed by (Rao *et al.*, 1997). See table 1.1 for alternative nomenclature. The proteins NFAT1-4 consist of a NFAT homology region (NHR), a DNA-binding domain which is known as a Rel-homology domain (RHD) and a carboxy-terminal domain (Figure 1.6). THE NHR is located in the N-terminus and contains an N-terminal transactivation domain (TAD), a nuclear localisation sequence (NLS) and a docking site for calcineurin. Whilst each member shares the NHR and RHD, each isoform has alternative splice isoforms that differ in the carboxy termini (Rao *et al.*, 1997). On the other hand, NFAT5, which is accepted as the primordial member of the NFAT family and as such the only member with a related gene expressed in drosophila, is distinct from the other 4 proteins with the RHD being the only conserved domain (López-Rodríguez *et al.*, 1999).

NFAT family member	Alternative nomenclature
NFAT1	NFATc2, NFATp
NFAT2	NFATc1, NFATc
NFAT3	NFATc4
NFAT4	NFATc3, NFATx
NFAT5	Tonicity enhancer binding protein (TonEBP)

Table 1-1 Members of the NFAT family.

Alternative terminology for the five NFAT proteins.

As well as being structurally different to NFAT1-4, NFAT5 is regulated by different mechanisms being primarily activated in response to hypertonicity (Miyakawa *et al.*, 1999). Alternatively, NFAT1-4 is regulated by intracellular calcium signalling mediated through calcineurin activation. Due to the calcium-dependent focus of this project, NFAT5 has not been explored further in relation to epidermal wound healing responses. Herein NFAT1-4 will collectively be referred to as NFAT.

1.5.2 NFAT signalling.

NFAT family of transcription factors was first identified in 1988 by Shaw *et al.* This original study reported that, in T-cells, NFAT1 was an inducible nuclear factor that could bind the interleukin-2 (IL-2) promoter in activated T-cells. Data showed that the time of IL-2 gene activation correlated to the time of appearance of NFAT1 (Shaw 1988). Since these original findings NFAT has been shown to have a wide role in T-cell function, being implicated in development, differentiation and self-tolerance. Additionally, NFAT is a key mediator in other cells of the immune system regulating response genes such as IL-3, IL-4, IL-5, interferon-gamma and tumour necrosis factor-α

(Macian, 2005). Complementary research and advances in technology over the past twenty-five years have confirmed the presence of all four calcium-dependent NFAT members in both immune and non-immune cells. In fact, it is believed that every mammalian cell type expresses at least one NFAT family member through which gene transcription is regulated in a wide range of developmental pathways including cardiac valve (de la Pompa *et al.*, 1998), skeletal muscle (Kegley *et al.*, 2001) and skin (Santini *et al.*, 2001). Despite upcoming research in various cell types and tissues, the role NFAT plays within the immune system remains the most explored.

The IP_3-mediated SOCE signalling cascade (as described in section 1.3.2) is fundamental to NFAT1-4 activation. The subsequent influx of calcium ions through SOCE is detected by calmodulin (CaM). CaM is expressed in all eukaryotic cells and functions as a calcium-binding protein that in turn binds to regulating proteins involved in cellular responses. Upon binding calcium (up to four ions), CaM undergoes a conformational change, which allows binding to a specific downstream protein (Klee *et al.*, 1979). In the case of NFAT, this is calcineurin. Calcineurin itself, similar to other proteins that utilise CaM, is not capable of directly binding calcium; therefore it uses CaM as a calcium sensor and signal transducer. Calcineurin is a calcium-dependent serine-threonine phosphatase. Structurally it is a heterodimer of calcineurin A; a 61kDa calmodulin-binding catalytic subunit and calcineurin B; a 19kDa calcium binding regulatory subunit (Klee *et al.*, 1979). The conformational change induced by calcium binding causes CaM to bind to the regulatory domain of calcineurin. This in turn induces a conformational change within calcineurin and the displacement of an auto-inhibitory domain from the active site leading to calcineurin activation as a phosphatase.

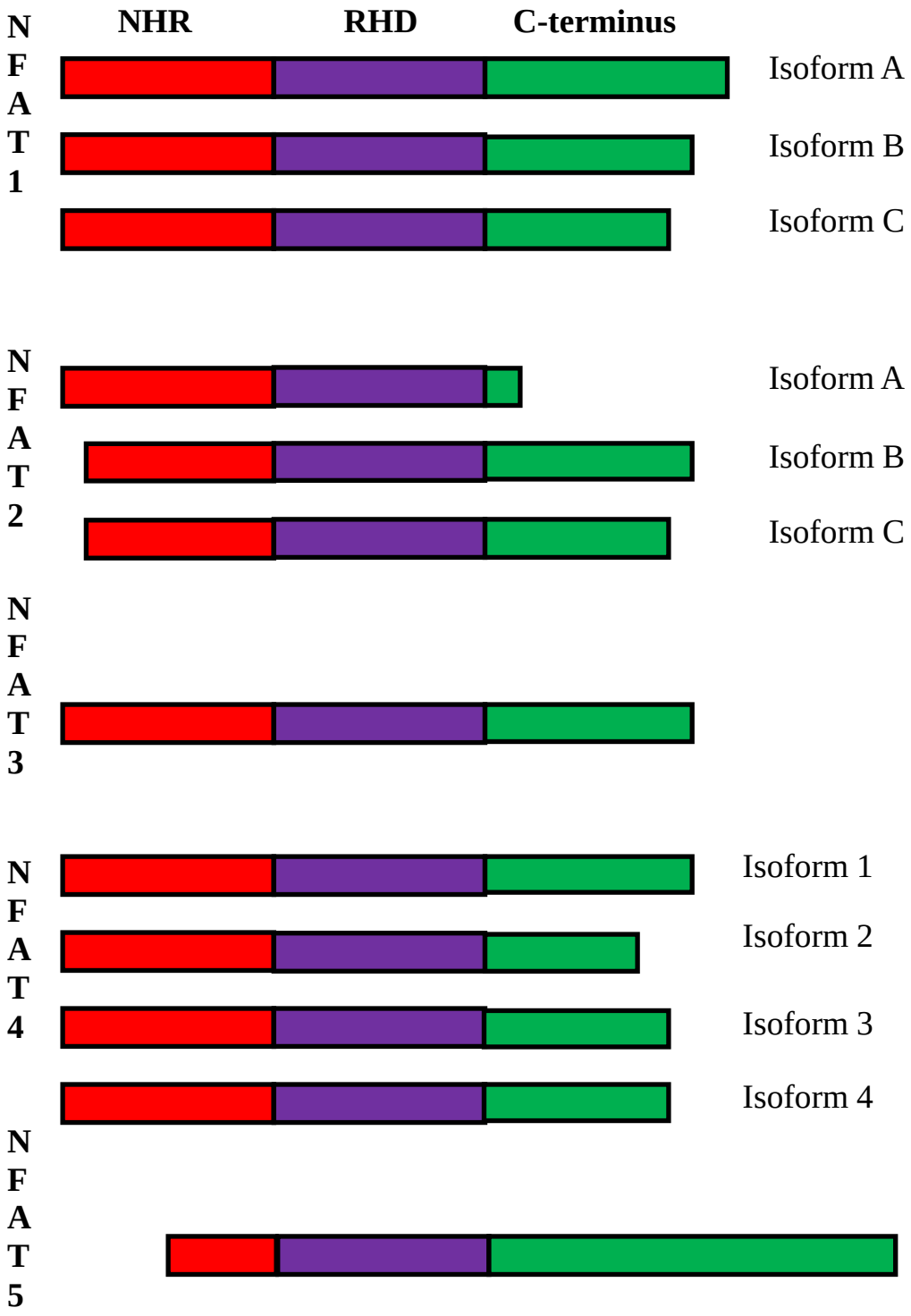

Figure 1.6 NFAT family members.

The NFAT family of transcription factors consists of five members; NFAT1-5. All proteins consist of a NFAT homology region (NHR), a Rel-homology domain (RHD) which acts as a DNA binding domain and a C-terminus. NFAT1-4 are calcium-dependent and share the NHR and RHD. Differences occur in their C-terminus and are isoform-specific. NFAT5 is not regulated by calcium and distinct from NFAT1-4 with the RHD being the only conserved domain. Adapted from (Rao *et al.*, 1997).

NFAT is primarily regulated at the level of subcellular localisation. At rest, NFAT is heavily phosphorylated and resides in the cytoplasm in an inactive conformation. Upon stimulation calcineurin is activated and dephosphorylates the NFAT regulatory domain located in the N-terminal. This then exposes a NLS and in parallel masks a nuclear export sequence, thus promoting nuclear translocation (Hogan *et al.*, 2003) (Figure 1.7). Following nuclear import, NFAT forms strong interacts with different transcription factor partners, highlighting a pivotal role for NFAT in linking calcium signalling with a dynamic range of other signalling pathways. The most common transcriptional partner of NFAT is activator protein 1 (AP1) (Fos-Jun) (Flockhart *et al.*, 2008). AP1 is comprised of Jun homodimers which bind to DNA with a low affinity and more commonly Fos-Jun heterodimers which bind with a higher affinity. Combined, these quaternary complexes drive the transcription of target genes.

Studies conducted in primary keratinocytes have shown that calcineurin accompanies NFAT1 to the nucleus where it retains NFAT in a dephosphorylated state and therefore NFAT remains nuclear (Al-Daraji *et al.*, 2002). Although this finding has not been replicated in other systems endogenously, overexpression experiments support these results. Additionally, there are several export kinases that amongst other properties function to remove NFAT from the nucleus, for example glycogen synthase 3 (GSK3). It has been suggested that GSK3 functions by preventing NFAT binding to DNA through phosphorylation of specific DNA binding sites on NFAT. Another alternative is that the phosphorylation by GSK3 masks the nuclear localisation sequence and subsequently NFAT is translocated out of the nucleus (Neal and Clipstone, 2001).

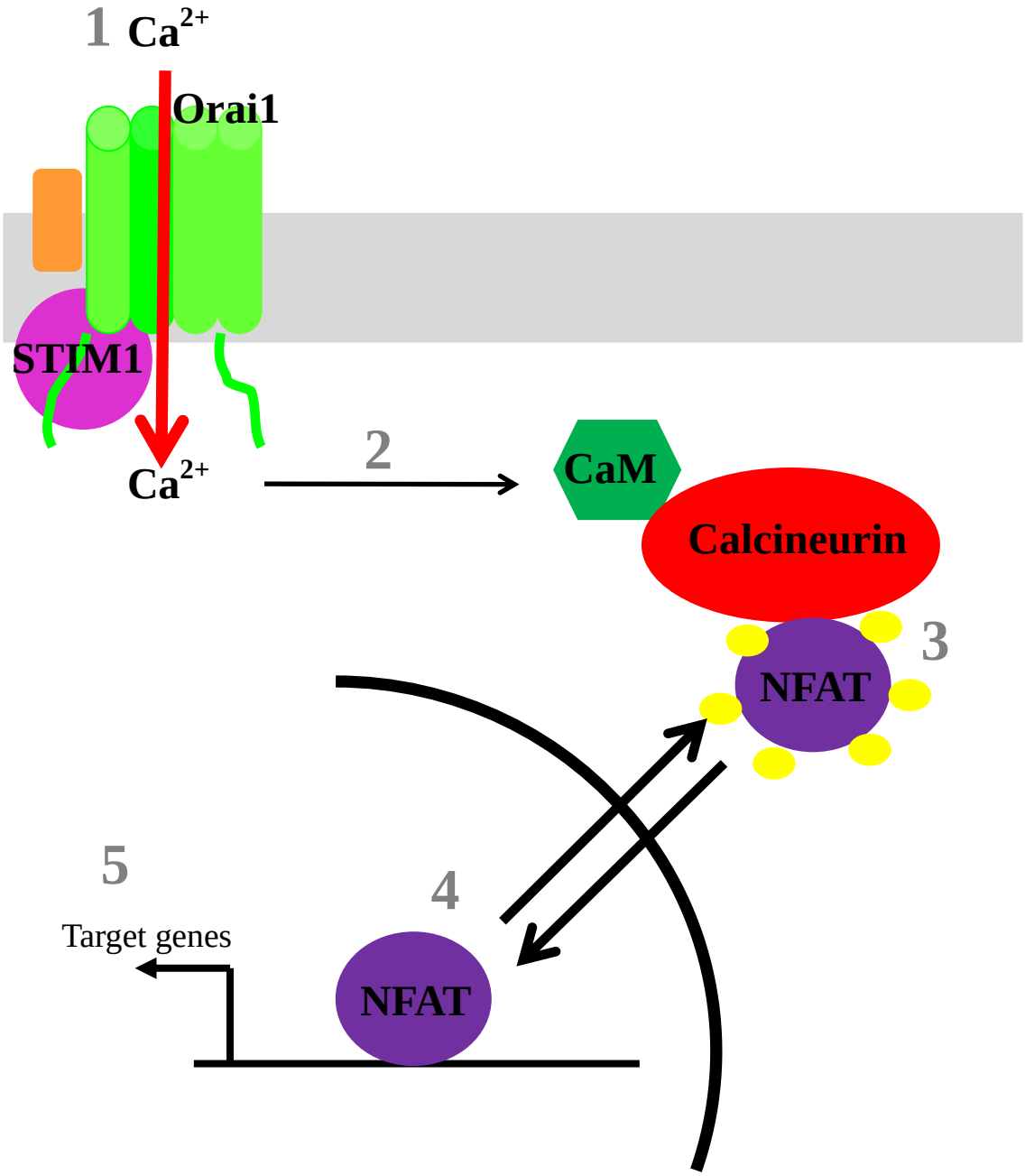

Figure 1.7 Schematic representation of NFAT activation.

1. Calcium enters the cell through SOCE (figure 1.4). **2.** The increase in cytoplasmic calcium activates calcineurin by binding a regulatory subunit and activating calmodulin (CaM) binding. **3.** At rest, NFAT is phosphorylated (yellow circles) and resides in the cytoplasm. Calcineurin activation dephosphorylates NFAT, exposing its NLS. **4.** This results in the nuclear translocation of NFAT. **5.** Once in the nucleus, NFAT forms strong interactions with other gene transcription factors (not shown) to induce expression of target genes. Adapted from (Hogan *et al.*, 2003).

1.5.3 NFAT signalling in the skin.

In addition to other tissue and cell types, NFAT has shown to be functional in the skin and it is established that all four calcium-dependent family members are expressed in keratinocytes. NFAT nuclear translocation is induced by sustained increases in $[Ca^{2+}]_i$, the role of calcium in keratinocyte differentiation is also established. Given this, it is perhaps unsurprising that NFAT has shown to be involved in keratinocyte growth and differentiation. This important study by Santini *et al.* demonstrated that CsA treatment to inhibit calcineurin and reduce NFAT activation, prevented the expression of two differentiation markers in keratinocytes. Additionally, p21 and p27 two cyclin kinases that are activated when keratinocytes undergo differentiation, where suppressed by CsA treatment. The authors link these observations to calcineurin dependent-Sp1/Sp3 transcription. Together the data shows that NFAT associates with Sp1/Sp3 to promote keratinocyte differentiation, and when required, activates p21 to inhibit cell cycle progression and promote terminal differentiation (Santini *et al.*, 2001).

Cyclosporin A (CsA) is a powerful immunosuppressant used clinically to treat a range of immune-mediated diseases. The beneficial properties of CsA in the prevention of organ rejection post-transplantation were first discovered in the 1970s on patients undergoing kidney transplants (Calne *et al.*, 1978). In 1983, CsA was approved for clinical use. Interestingly, research illustrated that CsA attenuated rejection by reducing NFAT activation. It is now known that CsA acts by inhibiting calcineurin and therefore prevents the phosphorylation of NFAT and subsequent nuclear translocation (Flanagan *et al.*, 1991). However, it highlights the fact that this compound is not NFAT specific; it is known that calcineurin regulates other transcription factors. In the past decade it has been suggested that CsA also has inhibitory effects on NFκB; another family of transcription factors with a diverse range of responses including both pro- and anti-inflammatory (Nishiyama *et al.*, 2005). Conversely, during first trimester development CsA treatment was shown to increase NFκB and cell migration rates. It is known that responses to injury during early stages of development are different to that seen post-natally and this may account for the contradictory results in this study (S. C. Wang *et al.*, 2013). Non-specificity for NFAT is thought to be responsible for the side-effects seen in patients taking CsA which include nephrotoxicity and hepatotoxicity. CsA is routinely used to treat a range of dermatological diseases including psoriasis and

eczema. Psoriasis has a strong inflammatory component and therefore it was previously assumed that the beneficial effects seen with treatment were due to a decreased NFAT-mediated inflammatory response. However, evidence presented by Al-Darajii suggested that non-immune skin cells, in particular keratinocytes, expressed calcineurin and NFAT1. Additionally, compounds known to induce keratinocyte differentiation resulted in the nuclear translocation of NFAT1. Moreover, CsA treatment prevented translocation, confirming parallel studies that NFAT1 has a role in governing keratinocyte differentiation. The authors also compared healthy skin to that of psoriasis patients and found that psoriatic keratinocytes had increased NFAT1 nuclear translocation compared to healthy skin, highlighting a potential mechanism through which the hyperproliferative disease develops and supporting the use of calcineurin inhibitors as therapeutic agents (Al-Daraji *et al.*, 2002).

Flockhart and co-workers have shown that in both 2D cell models and 3D skin equivalent models ultra violet radiation (UVR) evoked NFAT2 nuclear translocation and subsequent COX2 activation. Treatment with CsA post-UVR reduced COX2 protein induction and increased the number of apoptotic cells. This study is suggestive that NFAT regulates UVR-activation of COX2 and subsequent carcinoma development (Flockhart *et al.*, 2008). NFAT signalling in keratinocytes has also been shown to effect local immune and neuronal responses. In a study by Wilson *et al.*, Orai1-mediated NFAT activation was shown to cause TSLP release from keratinocytes. TSLP subsequently acted upon neurone receptors to evoke the classical itch behaviour associated with atopic dermatitis (Wilson *et al.*).

1.6 ATP signalling.

1.6.1 ATP as a paracrine signalling molecule.

Mechanisms regulating the spread of the intercellular calcium wave are highly debated within the literature (section 3.1.1). However, a vast amount of evidence exists for the involvement of a purinergic signalling pathway mediated by extracellular adenosine Triphosphate (ATP) in the propagation of the calcium wave through a population of cells. Therefore, the role of ATP in both the calcium wave and downstream events was of interest within this project. ATP, a molecule that comprises adenosine (a ribose sugar attached to the purine nucleotide adenine) bonded to three phosphate groups was

discovered by chemist Karl Lohmann in 1929 ('Über die Pyrophosphatfraktion im Muskel,' 1929). At the time of its discovery many scientists were trying to identify the molecule that acted as the primary "energy currency" of cells. Lohmann demonstrated that ATP was key in regulating the intracellular mechanisms that caused muscle cells to contract reviewed by (Burnstock, 2006). For many years after its discovery this was believed to be the sole role ATP played in cells (Majd and Shariatzadeh, 2004). However since then, ATP has been shown to have an important role in many physiological and biochemical processes that occur in living cells. In 1959 Pamela Holton suggested ATP may be released from sensory neurones. Subsequent investigations by Geoffrey Burnstock over the following decade proved, for the first time, that in addition to modulating intracellular activities, ATP also had a significant role in extracellular signalling (Holton, 1959). This theory was highly debated at the time due to a) scepticism that a molecule that had such a vital intracellular role could simultaneously function as an intercellular signalling molecule and b) the lack of knowledge regarding the presence of receptors on target cells. The first has since shown to be possible due to the relative extracellular ATP concentration ($[ATP]_o$) and intracellular ATP concentrations ($[ATP]_i$) in a steady-state cell. Although values vary with cell type and environment, basal $[ATP]_i$ and $[ATP]_o$ are approximately 3-10 mM and 10 nM respectively. This results in a chemical gradient favouring the ease of ATP efflux, secretion or release. Additionally, investigations have shown that only a small increase in $[ATP]_o$ are required to activate receptors. This means that extracellular autocrine/paracrine ATP signalling can occur without compromising intracellular levels, vital to maintaining energy production (Miller and Horowitz, 1986). The second challenge was met by continued research into the release of ATP from neuronal cells onto gut, bladder and muscle tissue coupled with commencement of the Human Genome Project (HGP) in the 1990s. The HGP highlighted genes regulating ATP receptors which implicated ATP as a major regulator of cellular function (Schwiebert and Zsembery, 2003). Now, it is widely accepted that these purinergic receptors exist as two broad classes of plasma membrane localised receptors termed P1 and P2 receptors. P1R are activated by adenosine, whilst P2 are activated by ATP. P2R can be further categorised into P2X and P2Y families (Abbracchio and Burnstock, 1998). There are seven P2XR present in mammalian cells which act as ion channels that are opened directly when ATP binds and causes influx of sodium and calcium. These are widely distributed in cells of the central and peripheral nervous system. P2YR and P1R both

cause intracellular changes through a cascade of indirect signalling conducted through binding of ATP or adenosine to G-protein coupled receptors (GPCR). Resulting in release of calcium from intracellular stores through the inositol 1,4,5-triphsopahte pathway. There are eight P2YR in mammals of which two are preferentially activated by ATP.

These discoveries have confirmed that ATP acts in an autocrine and paracrine manner to modulate cell function and this purinergic signalling mechanism is as widely accepted as that of other primary messengers including neurotransmitters, hormones and growth factors.

1.6.2 ATP signalling in disease.

In parallel to Burnstock's 1972 findings regarding the existence of purinergic receptors, Forrester first proposed that ATP is released in response to mechanical stimulus as a result of investigations into sustained exercise of human forearm muscle (T. Forrester, 1972). Epithelial cells, such as keratinocytes, are continually exposed to mechanical stress and therefore ATP release and autocrine/paracrine signalling plays a significant role in health and disease. Purinergic signalling has been implicated in the pathophysiology of different disease states including neurodegenerative disorders, urinary tract disease, cancer and HIV transfection (Burnstock, 2006; Séror *et al.*, 2011). Therefore highlighting ATP release, receptors and signalling as potential drug therapeutics. For example, two P2Y2 receptor agonists are in phase 3 clinical trials for dry eye and cystic fibrosis whilst antagonists of the platelet P2Y12 receptor are routinely used in cardiovascular medicine (Jacobson and Boeynaems, 2010).

1.6.3 ATP signalling in the skin.

It is known that ATP plays an important role in skin cell homeostasis and normal cell function. ATP and its receptors have been identified in almost all skin cell types including keratinocytes, fibroblasts and melanocytes and are found in a variety of skin appendages such as hair follicles and sweat glands. ATP is a key mediator in keratinocyte differentiation and proliferation contributing significantly to the formation of the stratified structure of the epidermis (Burrell *et al.*, 2005). However, conflicting data exists within the literature about the role ATP plays in keratinocyte proliferation; some studies report it functions in an anti-proliferative manner (Dixon *et al.*, 1999).

Differences may occur due to the reported variation in purinergic receptors expressed on primary keratinocytes and the cell line HaCaT (Burrell *et al.*, 2003).

Using known markers of proliferation, differentiation and apoptosis it has been determined that different ATP receptor subtypes are found at different locations within the epidermis, giving rise to speculation that each receptor has distinct functional properties (Greig *et al.*, 2003). For example, P2Y1 and P2Y2 control proliferation and are found in basal cells whereas P2X5 controls differentiation and P2X7 regulates terminal differentiation and thus cell death in suprabasal cells. Vast amounts of evidence exist that implicate ATP in keratinocyte differentiation including Celetti *et al.* who found that pannexins-1 and-3 regulated keratinocyte differentiation and epidermal integrity respectively (Celetti *et al.*, 2010). In addition to the role of ATP in differentiation, this study also speculated that ATP release is mediated through connexin and pannexins, an area that is highly debated in the literature. There are four major ways to increase $[ATP]_o$ and the mechanism through which this occurs, is almost certainly cell type and stimulus dependent (Section 4.1.3). Whilst it has been reported that keratinocytes release ATP under basal conditions as a growth regulator (Dixon *et al.*, 1999), relatively few investigations have been conducted into keratinocyte ATP release; both basal and induced. One group argue that air-exposure induces connexin-mediated ATP release from keratinocytes, showing that connexins are opened during air exposure. They confirmed this by demonstrating that Cx43 expression, the most common connexin in keratinocytes, was increased in differentiated cells compared to proliferating cells. Simultaneously, the amount of ATP released upon air-stimulation also increased supporting findings that gap junction components are involved in ATP release during keratinocyte differentiation and air exposure (Barr *et al.*, 2013). Barr *et al.* also reported that the ATP released post-air exposure caused epidermal thickening (Barr *et al.*, 2013). Similarly, direct injection of ATP into the epidermis caused thickening. This may be a potential mechanism for the development of hyperproliferative skin pathologies such as psoriasis (Dixon *et al.*, 1999). Indeed, this mechanism may be the reason epidermal equivalents are able to be cultured *in vitro*. Raising to the air-liquid-interface, a process that exposes keratinocytes to air, results in the formation of a stratified and thickened epidermis.

Inevitably, being so central to skin cell homeostasis, ATP signalling is thought to be involved in skin pathologies including the aforementioned psoriasis, Hailey-Hailey, warts and skin cancers, as well as playing a role in pain sensation and wound healing. Thus highlighting the possibility of utilising ATP signalling as a therapeutic target in dermatological diseases.

1.6.4 ATP signalling in wound healing

Having a suggested role in keratinocyte proliferation, differentiation and apoptosis, it follows that purinergic signalling could potentially mediate wound healing responses. As previously described, the epidermis is located on the outside of the body on the interface between the internal and external environments and functions as a protective barrier (section 1.1). Therefore, keratinocytes are constantly exposed to a variety of chemical, physical and mechanical injury (Yoshida *et al.*, 2006). ATP release from keratinocytes has been suggested as read-out for assessing whether chemicals have the potential to cause irritant dermatitis (Mizumoto *et al.*, 2003). Keratinocytes release ATP as a mediator signalling to neighbouring cells to activate cellular pathways. Investigations in a corneal limbal cell line highlight that ATP signalling can travel vast distances from the wound edge, highlighting its role in communication within a large cell population (E. R. Block and Klarlund, 2008). ATP is known to activate EGFR through purinergic receptors and EGFR activation was detected in cells 0.3cm from the wound edge. Diffusion to these distal cells was inhibited by scavenging ATP with apyrase, however, apyrase had no effect on cells in close proximity to the wound edge. Suggesting that, upon wounding two distinct pathways are activated for factors such as EGFR; one close to the wound which is ATP-independent and the other further back which is ATP-dependent (E. R. Block and Klarlund, 2008).

One of the first suggestions that ATP may be implicated in wound healing responses came from a study conducted by Wang *et al.* that showed that extracellular ATP synergised with other growth factors known to be released in response to wounding to cause increased DNA synthesis in fibroblast and keratinocyte cell lines. Although interesting data, the group speculated that the source of the extracellular ATP was from platelets and admitted that their findings lacked sufficient evidence at the role ATP may play following wounding (D. Wang *et al.*, 1990). Nevertheless, subsequent studies have confirmed and developed these initial ideas. Greig *et al*. used immunohistochemistry of

wounded rat skin to show that the expression pattern of purinergic receptors throughout the epidermis was changed during wound healing and that this caused keratinocytes to switch to a migratory state (Greig *et al.*, 2003). However, no link between receptor expression and functional wound healing rates were made. Whilst extracellular ATP signalling has been investigated, very little evidence exists regarding the role of intracellular ATP and wound healing. Using nude mice Chiang *et al.* optimised a fusogenic technique to deliver ATP vesicles directly into the wound of these mice and found that wound healing rates increased. Additionally, full thickness skin sections from these mice also showed improved epidermal organisation in a healing wound between ATP treated and control groups (Chiang *et al.*, 2007). Using denuded confluent monolayers of different renal tubular epithelial cell lines, Sponsel *et al.* observed that ATP stimulated wound healing. Interestingly, UTP also promoted wound closure in one cell line but had no effect on another; indicating that different subtypes of receptors may be involved in different cell types and lines (Sponsel *et al.*, 1995). Bronchial epithelial cells have also been shown to release ATP into the extracellular media upon wounding and inhibition of purinoreceptors had a functionally detrimental effect on wound closure in these cells (Yin *et al.*, 2007). It has also been suggested in astrocyte that $[ATP]_o$ is used to determine the extent of the damage in neighbouring cells. Increases in $[ATP]_o$ caused increased expression of cell cycle regulating proteins in neighbouring cells (Neary *et al.*, 2003). However, contrasting investigations suggest that increased $[ATP]_o$ significantly inhibits keratinocyte cell spreading and is detrimental wound healing (Taboubi *et al.*, 2007). This study, which used the immortalised keratinocyte cell line HaCaTs, proposed the inhibition of migration was through P2YR activation inhibiting phosphorylation of MAPK, Erk and Akt. Conversely, Pillai *et al*. used primary human keratinocytes to show that stimulation with ATP prevented terminal differentiation (Pillai and Bikle, 1992). Despite knowledge that ATP is released from a variety of cell types during wounding and evidence this plays a role in downstream functional events during wound closure, the mechanisms for stimulus-induced ATP release are difficult to characterise and conflicting theories exist within the literature. Translational studies have been conducted in human subjects with contrasting results to parallel *in vitro* and murine studies. Based on results from studies in cultured human cells and mice, Gifford *et al.* hypothesised that locally heating dermal tissue would cause an increase in ATP in the interstitial fluid; however, no increase was observed (Gifford *et al.*, 2012). This highlights differences between cultured cells *in vitro*, murine models and *in situ* human.

Importantly, it also highlights the fact that *in vitro* results may not be easily translated *in vivo*.

This project focuses on the role keratinocytes play in epidermal wound healing responses; however, as previously discussed (section 1.2.3), human dermal fibroblasts are also vital in wound healing. Although investigations into extracellular ATP in dermal fibroblasts relating to wounding are limited, in pulmonary fibroblasts, ATP has been shown to increase gene expression of collagen 1A and fibronectin 5 fold compared to basal levels (Janssen *et al.*, 2009). These two matrix proteins contribute to dermal strength and integrity during repair. Similarly, Waldman *et al.* supplemented bovine articular chondrocytes with ATP and noted an increase in collagen and proteoglycan biosynthesis. Thus suggesting that ATP released from dermal fibroblasts or keratinocytes during *in vivo* wounding could aid extracellular matrix component synthesis during the remodelling phase of wound healing (Waldman *et al.*, 2010). The role of ATP in the early intercellular communications post-wounding as well as long-term effects leading to wound healing require further investigation in human primary keratinocytes. Additionally, whilst a large number of studies have looked at ATP release from other cell types during wounding, and the effect this has on keratinocytes, relatively few have concentrated on ATP release from keratinocytes themselves post-wounding.

1.7 Aims and objectives.

The overall aim of this project was to characterise the wound-induced intercellular calcium wave and link this to downstream NFAT transcriptional activation and cell migration to close the wound.

To this, specific objectives were:

- To analyse specific parameters of the calcium wave and to determine the contribution of extracellular calcium influx in order to further understand the mechanisms of wave transmission.

- To delineate the relative contribution of gap-junctional communication and extracellular ATP to the transmission of the calcium wave following wounding.

- To analyse the occurrence of calcium oscillations induced by wounding and investigate mechanisms regulating this phenomenon.

- To establish the effects of SOCE, extracellular ATP and gap-junctional communication on both wound-induced NFAT transcriptional activation and keratinocyte migration to close the wound.

Chapter 2.

Materials and Methods

2 Chapter 2. Materials and Methods.

All compounds were purchased from Sigma-Aldrich, Gillingham, UK, unless otherwise stated

2.1 Primary keratinocyte cell culture.

2.1.1 Laboratory work.

All laboratory work during this project was carried out according to Newcastle University Health and Safety regulations and in a sterile containment level 2 safety hood where necessary.

2.1.2 Primary tissue samples.

After obtaining informed consent, normally discarded healthy adult skin samples from patients undergoing a surgical procedure were used to derive and culture primary keratinocytes (Todd and Reynolds, 1998). Immediately after surgical removal, skin samples were placed in 10mL keratinocyte growth medium (MCDB 153) supplemented with 2% penicillin streptomycin amphotericin B (PSA) (Lonza biologics, Slough, UK). Prior to transportation from theatre, samples were stored at 4^{o}C. Upon receipt, samples were stored at 4^{o}C and processed the same day. Ethical approval has been granted for this work by the Newcastle and North Tyneside Research Ethics Committee (Ref 08/H0906/95+5_Lovat) and is sponsored by The Newcastle upon Tyne Hospitals NHS Foundation Trust (trust approval for R&D project ref 4775).

2.1.3 Primary cell culture.

Prior to processing, skin samples were washed in phosphate buffered saline (PBS) supplemented with 2.5% PSA to remove any residual blood and placed in a petri-dish with PBS to keep moist. Utensils (forceps and scissors), which had previously been baked in an oven at 100^{o}C overnight, were washed in 100% ethanol and flame sterilised. Forceps and scissors were used to remove excess dermal tissue, fat and blood vessels, which were discarded. The remaining sample was firmly scored with a scalpel every 5mm to achieve a "grid" effect allowing penetration of dispase II (Roche Diagnostics Ltd, Burgess Hill, UK). Tissue was added to PBS supplemented with 10% PSA and 0.2% dispase II and stored at 4^{o}C overnight. Dispase II is a protease produced

in *Bacillus polymyxa* which hydrolyses the N-terminal peptide bonds of non-polar amino acid residues, which are found at a high frequency in collagen. This allows the separation of the epidermis from the dermis. Following an overnight incubation, flamed utensils were used to remove the epidermis which was then placed into a universal containing 0.05% trypsin ethylene diamine tetraacetic acid (TE) (Lonza biologics, Slough, UK). This was incubated in a water bath set at 37^{o}C for five minutes, shaking vigorously half way through to disaggregate keratinocytes. Fetal Calf Serum (FCS) neutralised TE and the sample was centrifuged at 3000g for five minutes to pellet the keratinocytes. The pellet was resuspended in Epilife (Life Technologies, Paisley, UK) or MCDB 153 medium supplemented with 1% PSA and 1% Human Keratinocyte Growth Supplement (HKGS) (Life Technologies, Paisley, UK) and placed into a 175cm^2 tissue culture flask. Culture medium was changed every two days to maximise keratinocyte growth until cells reached approximately 80% confluency. Cells were then passaged as required. All cells used for experiments within this project were passage 1-3. Whilst cells were growing to optimal confluency they were kept in an incubator set at 37^{o}C, 5% carbon dioxide (CO_2) and 95% humidity.

Epilife and MCDB 153 are both liquid cell culture medium, which together with HKGS, provide a complete culture environment for primary keratinocytes. The first part of this project was conducted using Epilife as the keratinocyte medium, with a change to MCDB 153 half way through due to economic savings. Parallel experiments were conducted in both mediums prior to this to ensure continuity within the project.

2.2 Calcium signalling.

2.2.1 Calcium dye loading using Fluo4-AM.

Optimisation of the calcium-dye loading protocol was conducted by Dr Anna Brown prior to the commencement of this study.

Fluo4-AM (Invitrogen, Paisley, UK) is a routinely used calcium dye which enables visualisation of whole cell calcium signalling in real-time (Ralph Jans *et al.,* 2013). Alteration of carboxylic acids with acetoxymethyl (AM) ester groups provides an uncharged molecule capable of permeating cell membrane. Lipophilic blocking groups are cleaved by non-specific esterases once the dye has entered the cell. This adds a charged group to the dye, reducing leakage rates of the dye out of the cell.

Keratinocytes were seeded into glass-bottomed Willco dishes (Intracel, Royston, UK) at a density of $5x10^5$/dish and incubated for twenty four hours. Medium was replaced with 2mL of dye solution. The dye solution was prepared immediately before use and contained 3µM Fluo4-AM, 200mM sulphinpyrazone; an anion transporter inhibitor to prevent cells exporting the dye and 0.1% pluronic acid F-127; a detergent that improves dye loading by facilitating its solubilisation in cell culture medium (Luk *et al.*, 2008). Cells were incubated at 37^{o}C for thirty minutes. Cells were washed and incubated again at 37^{o}C for forty five minutes in cell culture medium supplemented with sulphinpyrazone for de-esterification. Standard Epilife and MCDB 153 medium has a calcium concentration of 0.06mM and was classed as low calcium. High calcium keratinocyte growth medium (1.2mM or 6mM) was made using 1M calcium chloride.

2.2.2 Calcium signalling post-wounding.

Cells were prepared as described previously (section 2.2.1). Post-de-esterification, media was replaced with fresh media with a calcium concentration of either 0.06mM or 1.2mM for five minutes prior to wounding. Single scratch wounds were made approximately thirty seconds after imaging commenced using a 200µL pipette tip. After twenty minutes, 3µM thapsigargin (Tg) was added. Tg is a non-competitive inhibitor that blocks ER re-uptake of calcium, which in turn increases cytosolic calcium concentration.

In specified experiments, compounds (50 U/mL hexokinase, 10µM GSK-7975A or 20µM 18αGA) were added to the cells both during the forty five minute de-esterification period and immediately prior to wounding in the imaging media.

Hexokinase was soluble in MCDB 153 keratinocyte growth media and therefore no vehicle control was used. GSK-7975A and 18αGA were solubilised in dimethylsulfoxide (DMSO) to a final dilution of 0.001%. Throughout this project parallel experiments were conducted using DMSO without the compound of interest as a vehicle control.

Imaging was carried out using a Nikon spinning disc TIRF system (Nikon UK Limited, Surrey, UK) with 20x1.2 lens and excitation wavelength 488nm. Live images were captured at 3.7 frames per second (fps).

2.2.3 Establishing the effectiveness of the SOCE inhibitor GSK-7975A in primary human keratinocytes.

Primary human keratinocytes were cultured in 0.06mM $[Ca^{2+}]_o$ and seeded into Willco dishes as detailed previously (section 2.2.1). Once confluent, keratinocytes were loaded with Fluo4-AM and exposed to 1.2mM $[Ca^{2+}]_o$ for five minutes prior to imaging. Thirty seconds after imaging had commenced, 3µM Tg was added to induce intracellular calcium store depletion. In control experiments, imaging continued for twenty minutes. In order to establish the effectiveness of GSK-7975A (Derler *et al.*, 2013) as a SOCE inhibitor in primary human keratinocytes, 10µM GSK-7975A or 10µM diethylstilbestrol (DES) was added to cells two minutes following Tg application. DES was used as a positive control for SOCE blockade (Ralph Jans *et al.*, 2013). Imaging continued for twenty minutes.

2.2.4 Calcium add-back experiments.

For add-back experiments, keratinocytes were grown and loaded with Fluo4-AM as described previously (section 2.2.1). A single scratch wound was made in 0.06mM $[Ca^{2+}]_o$. Approximately five minutes post-wounding, 250µL of keratinocyte growth medium with a calcium concentration of 6mM was added to the dish to make a final calcium concentration of 1.2mM. Imaging continued for seventeen minutes when 3µM Tg was added.

In add-back experiments involving treatment with pharmacological inhibitors (10µM GSK-7975A or 20µM 18αGA), compounds were added to the cells both during the forty five minute de-esterification period and immediately prior to wounding in the imaging media.

2.2.5 Calcium signalling conditioned media.

For conditioned media (CM) experiments, keratinocytes were grown and loaded with Fluo4-M as described previously (section 2.2.1). For each condition, two Willco dishes were used; one contained cells that were wounded and the media removed and used as

CM and one that cells remained unwounded and were imaged whilst CM was added. Conditioned media was obtained by wounding monolayer primary human keratinocytes using a 200µL pipette tip in 0.06mM or 1.2mM $[Ca^{2+}]_o$. Five minutes post-wounding and thirty seconds after the commencement of imaging of unwounded cells, media was collected using a P1000 pipette and added to unwounded keratinocytes. Alternatively, keratinocytes were wounding in the presence of 50 U/mL hexokinase. Five minutes post-wounding, wounded media was collected and added to unwounded cells. This was referred to as conditioned media hexokinase (CMH).

2.2.6 Addition of ATP at physiologically relevant wounded concentrations.

Keratinocytes were loaded with Fluo4-AM as previously described (section 2.2.1). Thirty seconds after imaging had begun, keratinocyte growth medium, with a calcium concentration of 0.06mM or 1.2mM, supplemented with 1µM ATP was added to the dish. This was the pre-determined physiologically relevant concentration of ATP released into the extracellular space post-wounding. Imaging continued for twenty minutes.

2.2.7 Analysis of calcium signalling post-wounding.

Data from calcium signalling experiments post-wounding were analysed using Volocity software (Improvision, PerkinElmer, Cambridgeshire, UK). Figure 2.1 demonstrates the appearance of the data in this software. To facilitate the visualisation of changes in fluorescence intensity images were viewed in "rainbow" colour. To ensure continuity between experiments the black and white points were set manually on the program (Black–187 and white-13851). For each donor, 24 individual keratinocytes were analysed based on cell location from the wound edge. Cell 1 was specifically chosen due to its location at the wound edge, the terms cells 2 – 6 was then used to describe subsequent cells in a line back from cell 1 at the wound edge. This process is demonstrated in figure 2.1 and was repeated four times per experiment. This provided a total of 72 cells for each measurement, 24 from each of the 3 donors. It is of note that the four "rows" of keratinocytes described above where chosen prior to analyse on the Volocity software only taking into account the position of the wound and the location of cells at the wound edge. This was to eliminate bias analysis of cells. After keratinocytes had been selected based upon location from wound edge, regions of interest (ROI) were

manually drawn around these individual cells of interest. Creating ROI using the "free hand" tool was preferred over the "circle" tool as this ensured accurate analysis of whole cell calcium signalling. Quantification of fluorescence intensity at every time point for each ROI was then generated by Volocity in both tabular and graphical forms. Numerical data from Volocity was exported to Microsoft Excel (Microsoft Corporation, Redmond, Washington) for further analysis. This allowed for quantification of the changes in fluorescence within a cell post-wounding, comparisons between individual cells at specified locations from the wound and comparisons between various pharmacological treatments. Additionally, greyscale images were taken from Volocity and imported into ImageJ in order to create 3D surface plots of the calcium flux at specific time points.

In order to characterise the wound-induced calcium wave, as well as make comparisons between treatments, specific parameters of the $[Ca^{2+}]_i$ were assessed; maximum Ft/F0 achieved by wounding, time to reach maximum Ft/F0, area under the curve (AUC) of the $[Ca^{2+}]_i$ flux and rate of rise of the $[Ca^{2+}]_i$ flux. Ft/F0 represents temporal fluorescence/initial fluorescence. In other words Ft is the fluorescence intensity of calcium-bound Fluo4-AM at time point t and F0 is the background fluorescence intensity of calcium-bound Fluo4-AM. It was hypothesised that analysis of these parameters would also provide useful insights into mechanisms transmitting the calcium wave in primary human keratinocytes.

Each measurement was calculated as below:

- **Maximum Ft/F0** was calculated as the maximum fold increase above baseline reached during the initial calcium flux post-wounding. It was of interest whether the maximal wound-induced intracellular calcium signal was altered depending on cell location from the wound edge i.e. did cell 1 at the wound edge have a different maximal intracellular calcium response compared to cell 6. It was hypothesised that by investigating the relationship between the maximal wound-induced intracellular calcium response and the location of this cell from the wound edge, potential mechanisms regulating the transmission of the wave may be determined.

- **Time to reach maximum Ft/F0** was calculated by recording the time taken from the point of wounding for the calcium flux to reach its maximum fold change above baseline. This measurement was selected to confirm previously reported visual analysis that wounding results in a calcium wave that spreads back from the wound edge to cells located further back. For example, if wounding induced a calcium wave it would be expected that cell 1 would reach maximal Ft/F0 in a shorter time compared to cell 2, which in turn would reach maximal Ft/F0 in a shorter time to cell 3 etc.
- **AUC** of $[Ca^{2+}]_i$ flux was calculated using prism graphpad6 software; data for calcium fluorescence intensity at each time point from the start of the calcium flux until its return to baseline was imported into prism and AUC analysed. Prism calculates AUC by distinguishing a curve as a series of connected XY points with equally spaced X values. The area under each section of the curve is a trapezoid and therefore using the "trapezium" rule the area of each section is calculated. The sum of these provides a value relating to the AUC of the intracellular calcium flux. AUC was used as an integrative measure of total intracellular calcium signalling in response to wounding; combining both maximal Ft/F0 and duration of the calcium signal. It was hypothesised that the relationship between this integrative measure and cell location from the wound would provide useful insights into how the pattern of calcium signal varies at increasing distance from the wound edge.

- **Rate of rise** of the $[Ca^{2+}]_i$ flux was calculated by measuring the slope of the wound-induced calcium flux. Data provided information regarding how the rate of rise changed with increasing distance from the wound edge. It was hypothesised this would indicate the nature of the mechanisms underlying the wound-induced calcium wave propagation. For example, a reducing rate of rise in cells further back from the wound edge compared to cells at the wound edge would be indicative of a diffusion mechanism. On the other hand, a consistent rate of rise within cells regardless of location from the wound edge would suggest regeneration of the signal within each cell.

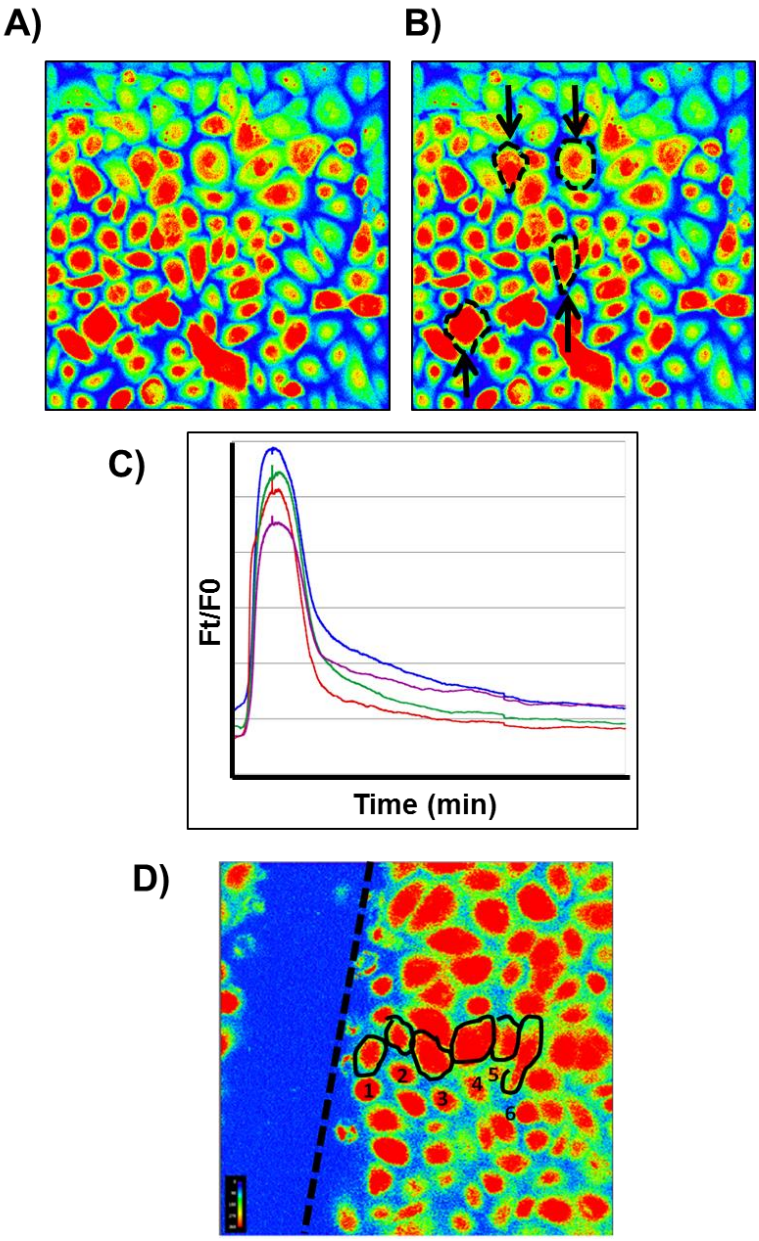

Figure 2.1 Calcium signalling analysis using Volocity software.

To quantify intracellular changes in calcium after wounding, Volocity software was used. Briefly, **A)** images generated by confocal microscopy were altered to a rainbow colour in order to facilitate visualisation of changes in fluorescence intensity over time, and then **B)** regions of interests (ROI) were manually drawn around cells of interest. Example cells are highlighted by dotted lines and arrows. **C)** Quantification of changes in fluorescence intensity within individual cells are then displayed in graphical form, as shown, whereby one trace represents one cell. **D)** In order to analyse intracellular calcium response following wounding of primary human keratinocytes, cells were labelled according to their location from the wound edge with cell 1 being located at the wound edge and cells 2-6 at subsequent locations in "rows" back from the wound edge.

2.3 Microbiology.

2.3.1 Bacterial culture.

Luria Bertani broth (LB) was used to culture One Shot® TOP 10 Chemically Competent *Escherichia coli* (*E.coli*) (Life Technologies, Paisley, UK). For the purpose of growing bacteria to isolate colonies, LB was supplemented with agar prior to autoclaving. Once cooled, ampicillin (0.1%) was added to allow for positive selection of bacteria containing the required plasmid. All plasmids used in this project were ampicillin resistant. Agar was then transferred to sterile petri-dishes to set. For the purpose of growing bacterial cultures, LB without agar was autoclaved, cooled and supplemented with 0.1% ampicillin to allow for positive selection of bacteria containing the required plasmid. All bacterial cultures were conducted using standard microbiology sterile techniques.

2.3.2 Transformation of competent E.coli.

One Shot® TOP10 Chemically competent *E.coli* (Life Technologies, Paisley, UK) were transformed with donated plasmids following manufacturer guidelines. Briefly, 50µL One Shot® TOP10 Chemically competent *E.coli* was thawed on ice with 2µL purified plasmid DNA for thirty minutes. Bacteria were then heat shocked for thirty seconds at 42^{o}C, and returned to ice for two minutes before adding S.O.C media and being shaken horizontally at 37^{o}C for one hour at 225rpm in an orbital shaker incubator. Transformed bacteria were spread on a pre-warmed selective plate and incubated at 37^{o}C overnight. Growth of plasmid-containing bacteria continued for two days in a 37^{o}C orbital shaker incubator initially in 5mL of ampicillin-supplemented LB (0.1%), then in 250mL of ampicillin-supplemented LB (0.1%).

2.3.3 Plasmid DNA extraction.

DNA extraction was carried out using High Speed® plasmid maxi kit (Qiagen, Crawley, UK), following manufacturer's instructions. Eluted DNA was stored at -80^{o}C or 4^{o}C for long and short-term storage respectively.

2.4 Measuring cell viability.

2.4.1 SRB assay to determine keratinocyte viability.

Cell density and hence assumed viability, was determined using the Sulforhodamine B (SRB) assay which measures cellular protein content based on the ability of SRB to bind to basic amino acids of cellular proteins (Voigt, 2005). Keratinocytes were seeded into 48-well plate at a density of $1.5x10^4$/well. The following day, media was removed and replaced with varying concentrations of pharmacological inhibitors. Twenty four hours post-treatment, cells were fixed using 10% trichloracetic acid (TCA) for one hour at 4^oC. After fixing, cells were washed in distilled water and 0.4% SRB dissolved in 1% glacial acetic acid was added to stain cells. Plates were incubated at room temperature for thirty minutes, then washed, dried in an oven at 60^oC and stored until required. To conduct the SRB assay, protein-bound SRB was solubilised using 10mM unbuffered Tris base using an orbital rocker for ten minutes. Analysis was carried out using a SpectraMax M250 microplate reader reading absorbance at 530nm.

2.4.2 MTT assay to determine keratinocyte viability.

Cell viability was determined using the thiazolyl blue tetrazolium bromide (MTT) assay. Yellow MTT is reduced to purple formazan when mitochondrial reductase enzymes are active; therefore if the reduction takes place the cell is assumed viable (van Meerloo *et al.*, 2011). Keratinocytes were seeded and treated as described previously for SRB assays (section 2.4.1). At specified time points post-treatment or wounding, 5mg/mL of MTT made in PBS was added to each well and incubated at 37^oC for three to four hours. After this incubation, MTT was removed and 150µL MTT solvent (4mM HCl and 0.1% Nondent P-40 in isopropanol) was added, cells agitated on an oribital shaker for fifteen minutes. Analysis was carried out using a SpectraMax M250 microplate reader reading absorbance at 620nm.

2.5 Quantification of extracellular ATP release.

2.5.1 ATP release post-wounding.

ATP release from keratinocytes post-wounding was detected using the luminescence based Cell-titre glo assay (Promega UK, Southampton, UK). The protocol supplied by the manufacturers was adapted and optimised in order to allow evaluation of

extracellular ATP. This assay works on the luciferase principle that the more ATP present in the sample, the greater the conversion of luciferin to oxyluciferin. Light is a product of this reaction, thus, an increase in ATP results in more light produced and a greater luminescence reading (Schagat). Primary human keratinocytes were seeded into a 24-well plate at a density of $1x10^5$/well. Once seeded cells had formed a complete monolayer, media was removed and replaced with 200µL media containing 0.06mM or 1.2mM $[Ca^{2+}]_o$. Cells were incubated for an hour at 37^{o}C to remove any ATP released during the process of changing the media. After an hour, a 200µL pipette tip was used to create a "cross hatch" wound, ensuring the wound extended across the entire diameter of the well. For control experiments where cells remained unwounded, all media changes were conducted in parallel to wounded cells to eliminate variables which may result in ATP release. At specified time points post-wounding, 50µL of media was carefully removed from wells containing wounded or unwounded cells and added to a blacked-out 96-well plate suitable for luminescence assays. An equal volume of cell-titre glo reagent was added to each well to make a total volume of 100µL/well. Plates were incubated at room temperature for ten minutes and read using the Glomax 96 microplate luminometer (Promega UK, Southampton, UK).

2.5.2 ATP release post-wounding in the presence of pharmacological inhibitors.

Keratinocytes were seeded, grown and media replaced as described previously (section 2.5.1). After one hour incubation, 50µL of inhibitor was added to the well at 5X the required final concentration. The following compounds were used; 2mM 1-Octanol, 100µM carbenoxolone, 20µM 18αGA, 10µM N-ethylmaleimide (NEM), 10µM monensin, 10µM cyclosporine A (CsA), 10µM verapamil or 50 U/mL hexokinase. Wounding and luciferase based assay were conducted as described above (section 2.5.1) with media sample being collected five minutes post-wounding.

2.5.3 Media replacement and conditioned media.

Keratinocytes were prepared and wounded as described previously (section 2.5.1). For media replacement experiments, one minute post-wounding, wounded media was removed and replaced with fresh media. Twenty five minutes later, 50µL samples were taken for analysis. For conditioned media experiments, five minutes post-wounding, the media was removed from wounded cells, using a P1000 pipette and added immediately

to unwounded cells. Simultaneously, media from unwounded cells was removed and added to wounded cells. Twenty five minutes later (thirty minutes post-wounding), 50µL samples were taken and assayed as described above (section 2.5.1) (figure 2.2 and figure 2.3). For double

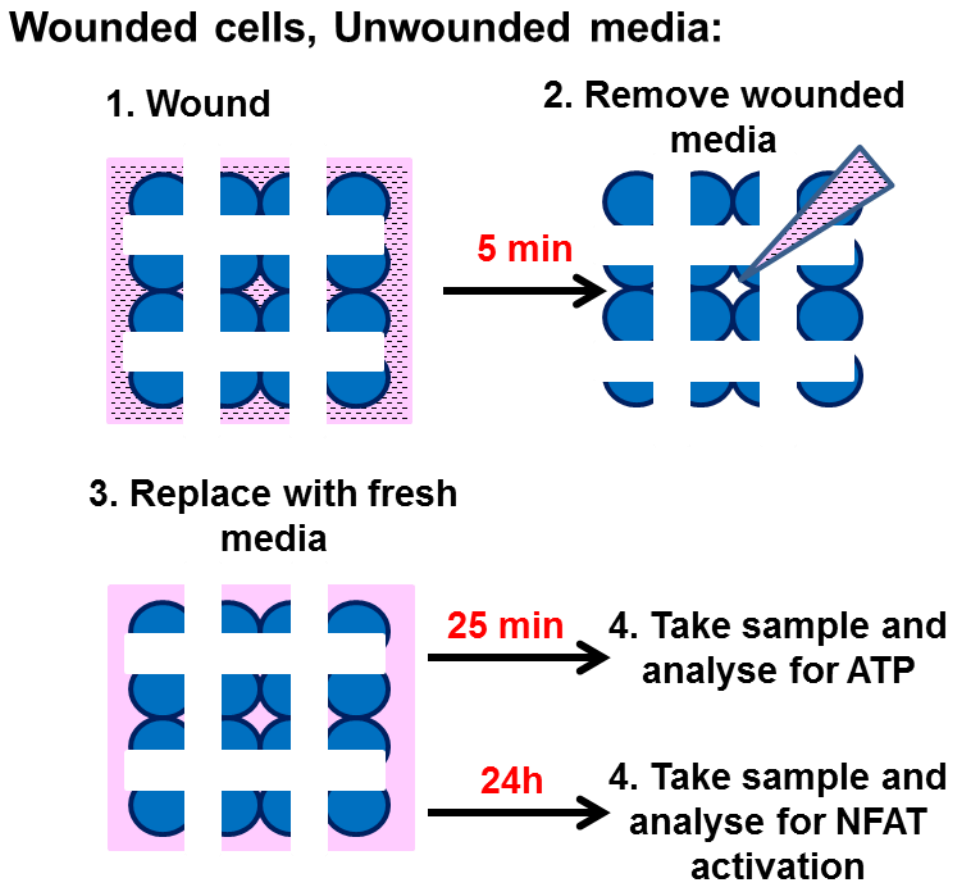

Figure 2.2 Schematic diagram of cross-hatch wounding of monolayer cells, collection of conditioned media and culture of wounded cells cultured in unwounded media.

For both ATP and NFAT luciferase-based assays a wounded conditioned media protocol was adopted within this project whereby wounded cells were exposed to unwounded media. 1) primary human keratinocytes were scratch wounded in a cross-hatch manner. 2) Five minutes post-wounding, wounded media was removed using a P1000. 3) Fresh keratinocyte growth media was immediately added to unwounded cells. 4) For ATP experiments, twenty five minutes following the media change, a 50µL sample was removed and analysed. For NFAT transcriptional experiments, twenty four hours following the media change cells were lysed and luciferase activity measured.

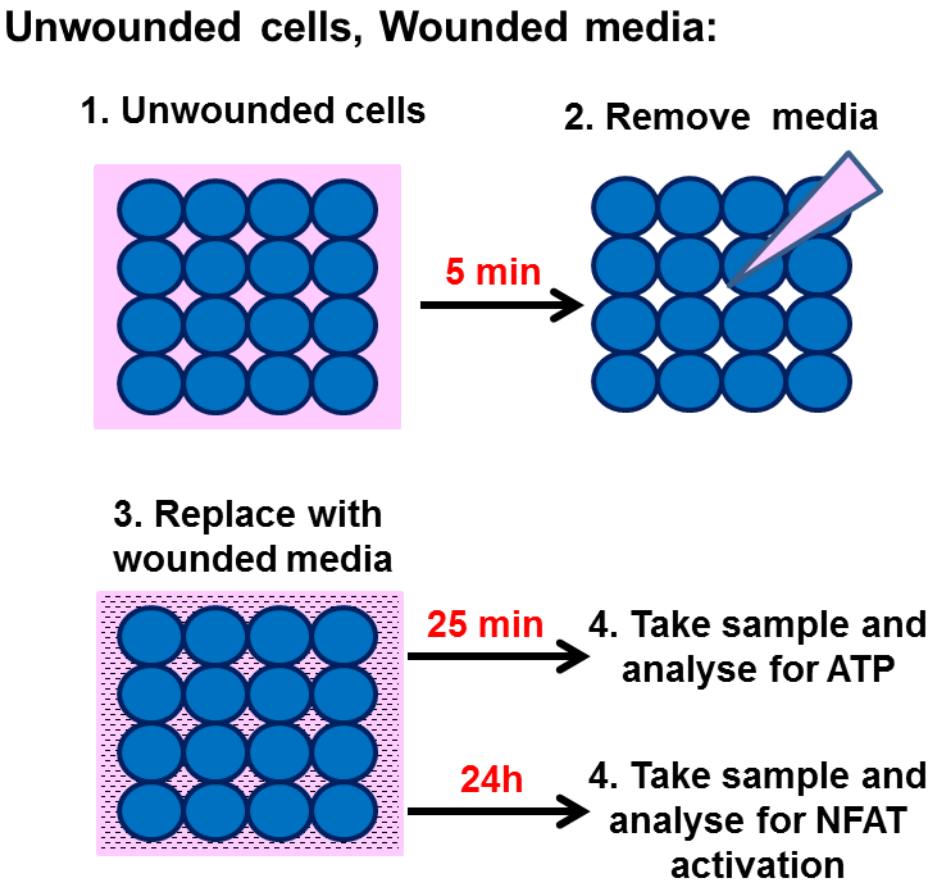

Figure 2.3 Schematic diagram of collection of conditioned media and culture of unwounded cells in wounded conditioned media.

For both ATP and NFAT luciferase-based assays a wounded conditioned media protocol was adopted within this project whereby unwounded cells were exposed to wounded media. 1) Unwounded primary human keratinocytes were cultured in media. 2) Five minutes later unwounded media was removed using a P1000. 3) Wounded media was collected from matched donor samples wounded for five minutes (see figure 2.2). 4) For ATP experiments, twenty five minutes following the media change, a 50µL sample was removed and analysed. For NFAT transcriptional experiments, twenty four hours following the media change cells were lysed and luciferase activity measured.

conditioned media experiments, cells were wounded and five minutes post-wounding, media was removed and fresh media was added. A further fifteen minutes later, media was removed and fresh media added once again, ten minutes later (thirty minutes post-wounding) 50µL samples were taken and assayed as described above (section 2.5.1). To control for the effects of removing/adding media, unwounded cells also had their media removed and replaced with fresh media.

2.5.4 Generation of an ATP standard curve.

An ATP standard curve was generated using keratinocyte growth medium supplemented with known concentrations of ATP. 50µL samples were added to a blacked-out 96-well plate suitable for luminescence assays and luminescence for each concentration measured in triplicate. A standard curve of the Log concentrations was generated on Prism Graphpad allowing the interpolation of unknown values.

2.6 Dual-luciferase receptor assays.

2.6.1 Wound-induced transcriptional activation.

NFAT activity post-wounding was measured using a NFAT firefly luciferase reporter containing three repeats of the NFAT/AP-1 binding site from the murine IL-2 promoter (a kind gift from Dr D J McKean, Mayo foundation, Rochester, MIN, USA) (Hedin *et al.*, 1997). Keratinocytes were seeded into a 24-well plate at a density of $3.5x10^4$/well. Once cells had reached approximately 60% confluency, they were transfected with 0.5µg NFAT firefly constructs and 0.0125µg renilla using the TransIT-Keratinocyte specific transfection reagent (Geneflow, Litchfield, UK). Renilla was used as an internal control vector (Flockhart *et al.*, 2008). Once a monolayer had formed, cells were exposed to keratinocyte growth medium with a calcium concentration of either 0.06mM or 1.2mM for five minutes prior to scratch wounding. A 200µL pipette tip was used to create a "cross-hatch" wound, ensuring the wound extended across the entire diameter of the well. At specified time points post-wounding, keratinocytes were harvested using passive lysis buffer and stored at -80^o until required. Luciferase activity was assessed using the Dual-luciferase reporter system following manufacturers protocol (Promega UK, Southampton, UK). Briefly, 20µL of defrosted lysate was added to a blacked-out 96-well plate suitable for luminescence assays. Luciferase assay reagent (LAR) and stop and glow (S+G) were prepared as required. Using the Glomax 96 Microplate reader,

60µL LAR and S+G was automatically added to each well using two injectors built into the luminometer. Data was exported from the luminometer and analysed using Microsoft Excel. Values were presented as a ratio of firefly to renilla.

In addition control experiments were conducted to ensure that the transfection reagent and protocol did not result in NFAT transcriptional activation. In these control experiments TE buffer was added to keratinocytes in the presence of TransIT but without the firefly plasmid.

2.6.2 Measurement of transcriptional activity after exposure to wounded conditioned media.

Confluent keratinocytes were transfected with NFAT firefly and renilla and wounded as described previously (section 2.6.1) in either 0.06mM or 1.2mM $[Ca^{2+}]_o$. Five minutes post-wounding, a P1000 was used to carefully remove the wounded media. This wounded media was termed conditioned media (CM) and added to unwounded cells. In parallel fresh media of the same calcium concentration was added to the wounded keratinocytes. Twenty four hours post-wounding, samples were lysed and analysed as detailed previously (figure 2.2 and figure 2.3).

2.6.3 Measurement of NFAT transcriptional response to ATP.

Confluent keratinocytes were transfected with NFAT firefly and renilla as described previously (section 2.6.1). Confluent cells remained unwounded and were treated with keratinocyte growth medium with a calcium concentration of either 0.06mM or 1.2mM supplement with ATP at two concentrations. The first being the pre-determined physiologically relevant wounded concentration of 1µM and the second a higher concentration of 10µM. Following twenty four hours treatment, samples were lysed and luciferase activity measured as described above (section 2.6.1).

2.6.4 Measurement of NFAT following treatment with pharmacological inhibition.

Confluent keratinocytes were transfected with NFAT firefly and renilla and wounded as described previously (section 2.6.1) in either 0.06mM or 1.2mM $[Ca^{2+}]_o$. However, in specified experiments, cells were treated with either 10µM GSK-7975A or 20µM 18αGA for one hour prior to wounding. Alternatively cells were exposed to 50 U/mL

hexokinase for five minutes prior to wounding. Twenty four hours post-wounding cells were lysed and luciferase activity measured as described above (section 2.6.1).

2.7 Migration Assay.

2.7.1 Wound closure rates.

To investigate wound closure rates post-scratch wounding, migration assays were conducted (Fullard *et al.*, 2013). Keratinocytes were seeded into a 24-well plate at a density of $1x10^5$ /well. Once seeded cells had formed a complete monolayer, media was removed and replaced with media with a calcium concentration of 0.06mM or 1.2mM for five minutes post-wounding. A 200µL pipette tip was used to create a "cross hatch" wound, ensuring the wound extended across the entire diameter of the well. Cells were then immediately transported to the Nikon Biostation CT (Nikon UK Limited, Surrey, UK) for imaging. The Biostation CT comprises a tissue culture incubator with controllable CO_2, temperature and humidity with an inbuilt microscope. For all migration assays these were set to 5%, 37^oC and 95% respectively. Movement of the plates during the imaging period was conducted via a fully automated robotic arm. Co-ordinates of wound sites were manually entered into the system for each well and images were captured every hour for twenty four hours at 4x magnification. After the imaging period, cells were removed from the Biostation and discarded. Data was exported and ImageJ was used to manually measure the initial wound area and then the subsequent wound area at specified time points within an experiment. Analysis was then conducted in Microsoft Excel. Briefly, wound area at specified time points were calculated as a percentage of the origin wound size.

2.7.2 Mitomycin C treatment to determine contribution of proliferation in wound closure.

Mitomycin C (MMC) was used to inhibit cell proliferation during wound closure experiments to analyse the contribution of cellular migration and proliferation during wound closure (Fullard *et al.*, 2013). Cells were seeded into 24-well plates as described previously (section 2.7.1), once cells had formed a complete monolayer, they were treated with 100X MMC and incubated at 37^oC for two hours. Cells were then washed

thoroughly with PBS to remove all excess MMC. Keratinocyte growth medium with a calcium concentration of either 0.06mM or 1.2mM was added to the cells for five minutes prior to wounding. Cells were immediately transferred to the Biostation and the following imaging and analysis was conducted as described previously (section 2.7.1).

2.7.3 Pharmacological inhibition to assess effects on various signalling pathways on wound closure.

Primary human keratinocytes were seeded into 24-well plates as described previously (section 2.7.1). Once cells had formed a monolayer they were treated with either 10µM GSK-7975A or 20µM 18αGA for one hour prior to wounding in either 0.06mM or 1.2mM $[Ca^{2+}]_o$. Alternatively cells were exposed to 50 U/mL hexokinase for five minutes prior to wounding. Keratinocytes were wounded and imaged using the Biostation as detailed above.

2.8 Statistical analysis.

Data was generated and analysed utilising specialised software as specified. Statistical analysis was conducted using Prism (GraphPad 5 or 6 software, San Diego, CA). Graphpad 6 was utilised during analysis of wound-induced intracellular flux between treatments as this latest version allows the input of data from an increased sample number for analysis. Within this project 72 cells from three independent donors were analysed, in previous versions of graphpad, this was limited to 52. Data presented within this project represent mean ± standard error of the mean (SEM). N depicts the number of independent donors and n indicates the total number of independent experiments (culture dishes) or number of cells analysed (as specified). For example, n=9, (N=3) would indicate 9 independent experiments using cells from 3 independent donors. Graphical representation of statistical significance utilised the "star" method of analysis whereby *** $P<0.001$, ** $P<0.01$, * $P<0.05$ and ns $P>0.05$. Specific P values were described and reported in the figure legends and main body of text.

The following statistical analysis was conducted within this project:

- In order to compare average intracellular calcium flux over time between different treatments, a repeated measure (RM) two-way ANOVA was performed. This statistical analysis is useful when one of the factors being

compared is a repeated measure. In the context of this project, the fluorescence intensity was measured from an individual cell every 270 milliseconds, thus providing a repeated measure from one cell. The analysis acknowledges that readings from each time point within the cell are not independent readings and therefore provides a more stringent statistical analysis between treatments (*Graphpad 6 Statistics Guide*). However, this analysis does not distinguish the specific time points where differences were significant. Therefore, a Bonferroni post-hoc test was conducted to determine at which time points during the intracellular calcium flux, treatments had a significant effect.

- Regression analysis was performed during specified experiments to investigate the effect of cell location from the wound edge on specific parameters of the intracellular calcium flux. Line of best fit was plotted along with the 95% confidence interval plots. Both R^2 value and P value were measured for each analysis. The null hypothesis for the P value is that there is no linear trend between cell location and parameters investigated. Therefore, a low P value suggests a significantly different slope of the line compared to zero. For maximum Ft/F0, time to reach maximum Ft/F0 and AUC linear regression analysis over other methods of analysis was chosen to determine the relationship between the parameters tested and cell location from the wound edge as there appeared to be a linear increase/decrease with increased distance from the wound edge. For example, bi-modal analysis was not conduct as when taking into account mean±SEM for each data point, there did not appear to be two clear modes in the data set. For rate of rise, a non-linear regression exponential decay analysis was conducted and deemed more appropriate than linear regression as the values from cell 1 were considerably higher than cells 2-6 which were more similar, thus suggesting a non-linear relationship for this parameter.
- An alternative method utilised to determine the effect of cell location from the wound edge, was a one-way ANOVA with Dunnett's post-hoc test. These results compared the data from cells located at specified locations from the wound edge (cell 2-6), to those obtained from cells at the wound edge (cell 1). A P value was reported for each analysis. Additionally, a post-test for linear trend was conducted whereby data was tested for an linear increase or decrease between columns from left to right, again a P value was reported to reveal the

significance of this trend. Linear analysis was deemed appropriate there appeared to be a linear relationship between parameters analysed and progressive location from the wound edge.

- Statistical analysis comparing means of two independent and random samples was performed using a unpaired, two-tailed, t-test. A P value was reported demonstrating the significance of any differences observed.
- Two-way ANOVAs were conducted when analysing the effect of two independent variables. An example within this project is the effect of drug treatment and external calcium concentration on maximum Ft/F0 achieved during the wound-induced calcium flux. When a statistical difference was revealed, a Bonferroni post-hoc test was conducted to confirm which treatments differed statistically. Results are reported as a P value.

Chapter 3.

Characterisation of the Wound-induced Intracellular Calcium Wave

3 Chapter 3. Characterisation of the Wound-induced Intracellular Calcium Wave.

3.1 Introduction.

3.1.1 Calcium wave.

Intercellular calcium waves are characterised by sequential increases in $[Ca^{2+}]_i$ in neighbouring cells that spread from the point of stimuli through the cell population depicting a wave (Charles *et al.*, 1992). They function to provide a means of communication between an individual cell and a population of cells, therefore facilitating the transmission of information for the coordination of tissue responses. The first observation that calcium signalling spread between neighbouring cells in this manner was reported in astrocytes in the presence of extracellular glutamate (Cornell-Bell *et al.*, 1990). Since these initial investigations a similar effect has been observed in a wide variety of cell types in response to locally injected or mechanical stimuli. It was originally thought that the messenger solely responsible for the wave was calcium. However, this theory was contested by demonstrating the occurrence of an intercellular calcium wave without an elevation of $[Ca^{2+}]_i$ in the initiating cell. It is now accepted that IP_3 can also act as a wave propagator and this mechanism can regulate the wave between cells by binding to IP_3R on the ER and causing intracellular store depletion (Boitano *et al.*, 1992). Mechanisms regulating both the propagation of the intercellular calcium wave and the passage of signalling messengers are debated within the literature. It was originally thought that waves propagated between cells via calcium and IP_3 movement through gap-junctions (Saez *et al.*, 1989). Structural and functional characteristics of gap-junctions are reviewed in section 1.4.1. Calcium (atomic weight 40) and IP_3 (molecular weight 486) are both small enough to pass through gap junctions highlighting a potential mechanism for transmission of the calcium signal. However, it is of note that the permeability of different connexins to IP_3 varies. Niessen *et al.* injected IP_3 into HeLa cells transfected with Cx32, Cx43 and Cx26. Their results showed that all three resulted in calcium wave spread; however spread between adjacent cells was connexin-dependent. Cx32 transfected cells resulted in intercellular calcium wave propagation that was 2.5-fold greater than Cx43 cells and 3-4-fold greater than Cx26 cells (Niessen *et al.*, 2000).

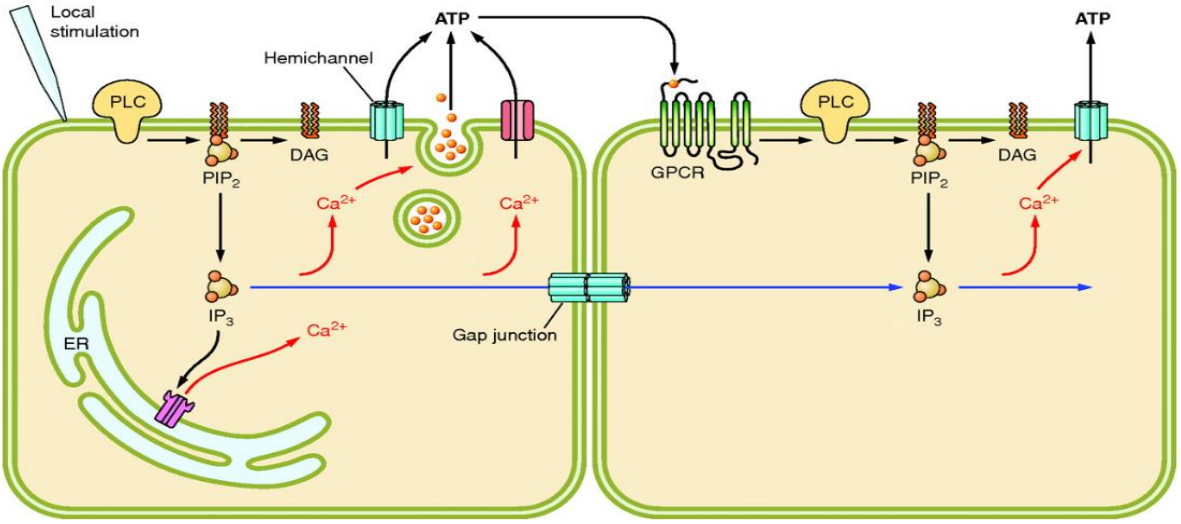

Figure 3.1 Diagram showing the two mechanisms of intercellular calcium wave propagation; gap-junction communication and ATP release.

Intercellular calcium waves are an important signalling cascade to allow transmission of information from one cell to a population of cells. This is thought to occur through one of two mechanisms. Firstly, a stimulus is applied to a cell which causes PLC to cleave PIP_2 into DAG and IP_3. IP_3 then diffuses to the ER, binds to its receptor and calcium is released from the ER. These calcium ions and/or IP3 molecules are then able to move directly between the cytoplasm of two cells via gap-junctions located on the PM. Once in the second cell, this causes either an immediate elevation of $[Ca^{2+}]_i$ or IP_3 binds to its receptor on the ER causing further release. The alternative theory is that the either through calcium-induced vesicle exocytosis or as a direct consequence of the stimulus, ATP is released into the extracellular environment. It then diffuses to a neighbouring cell and binds to a GPCR and activates PLC which through the established calcium signalling cascade causes IP_3-mediated calcium release from intracellular stores. Taken from (Leybaert and Sanderson, 2012).

3.1.2 Calcium wave propagation post-wounding.

Evidence from numerous studies has shown that, in addition to regulating keratinocyte growth and differentiation under normal physiological conditions, intracellular calcium also plays a critical role in the wound healing process. It is known that transcription factor activation is key to co-ordinating various wound healing responses to promote wound closure, thus making them important damage signals (Müller *et al.*, 2012). However, these responses occur several hours after the wound has been inflicted. It was hypothesised that early damage signals existed which were activated in response to injury and also functioned to regulate downstream transcriptional events, giving them a fundamental role in wound healing (Xu and Chisholm, 2011). Original experiments in endothelial and epithelial cells demonstrated that immediately post-wounding an intercellular calcium wave was observed from the site of injury propagating back across the monolayer (Tran *et al.*, 1999). In accordance, this pattern of wound-induced calcium signalling has been shown in many cell types including corneal epithelial (Leiper *et al.*, 2006), hepatocytes (Sung *et al.*, 2003), neurons (Antunes *et al.*, 2013) and keratinocytes (Korkiamaki *et al.*, 2005). More recently, translational studies have shown identical results in whole organisms *in vivo* including drosophila, zebra fish and *C. elegans* (Ghannad-Rezaie *et al.*, 2012; Yoo *et al.*, 2012). Investigations in *C. elegans* have shown that wounding triggers the expected rapid elevation in $[Ca^{2+}]_i$. This intercellular calcium wave was shown to be crucial for the subsequent calcium-dependent signalling pathway to promote wound closure and organism survival (Xu and Chisholm, 2011).

It is now widely accepted that inflicting injury on keratinocytes and the epidermis disrupts the epidermal calcium gradient and causes an immediate increase in $[Ca^{2+}]_i$ that spreads to neighbouring cells. As with all intercellular calcium waves, wave propagation is thought to occur through either paracrine signalling or gap-junction communication; however, the relative contribution of each pathway in facilitating calcium signal transmission remains controversial (Later discussed in section 4.1.1).

Additionally, during wounding of the skin, the epidermal barrier is breached, the dermis is damaged and the wounded tissue is exposed to serum. In the past decade it has been shown that keratinocyte migration is promoted in the presence of serum compared to plasma with factors such as TGFβ3 and p38MAPK being investigated in each condition (Bandyopadhyay *et al.*, 2006). Few studies have investigated the physiological function

and composition of wound serum; however it has been suggested that it has an altered calcium concentration than plasma. As described in section 1.3.5, a calcium gradient exists within the epidermis with calcium concentration being low in the proliferative basal layer, progressively increasing through the spinous layer reaching a maximum in the granular layer; levels then fall at the outermost stratum corneum (Elias *et al.*, 2002). Findings of such studies imply that $[Ca^{2+}]_o$ in wounding experiments could influence and determine functional outcomes, however its effect on the wound-induced calcium wave has not yet been investigated in primary human keratinocytes.

3.1.3 Pharmacological store-operated calcium entry inhibitor (SOCE) GSK7975A.

As detailed in section 1.3.4, increasing evidence exists to suggest a role for SOCE in physiological and pathological processes. Therefore, blockade of this signalling pathway would provide useful insights into both the contribution of SOCE in disease development as well as highlighting potential therapies. Lack of knowledge regarding the mechanisms involved in SOCE was extremely problematic in the development of specific pharmacological inhibitors. The discovery of the STIM and Orai families of proteins in the regulation of SOCE (section 1.3.3) allowed for the development and identification of novel compounds that specifically targetted the STIM-Orai pathway. Despite these advances, SOCE pharmacological inhibition remains a controversial topic. Inhibitors can be categorised based on whether they exert their effects directly on the channel, or are mechanism-based inhibitors. The most commonly used are the lanthanides (Gd^{3+} and La^{3+}) and 2-aminoethoxydiphenylborate (2-APB). However, like other compounds, interpretation of their potency, selectively and application remain problematic. For example, 2-APB displays a complex pharmacological profile; it blocks SOCE at concentration between 25-100µM and activates SOCE at concentrations between 1-20µM (Putney, 2010). Additionally, it has also been shown that 2-ABP treatment prevents the movement of STIM1 to the plasma membrane therefore reducing its selectivity as a SOCE channel blocker (Wayne I. DeHaven *et al.*, 2008). Gd^{3+} and La^{3+} are established SOCE inhibitors in many cell types however; application is limited due to the requirement of serum-free culture conditions (Putney, 2010).

Investigations prior to the commencement of this project highlighted that routine SOCE inhibitors, 2-ABP and Gd^{3+} did not consistently and reliably prevent Tg-induced SOCE

in primary human keratinocytes. On the other hand, it was shown that the less known diethylstilbestrol (DES) was effective in these cells (Ralph Jans *et al.*, 2013).

Whilst the aforementioned SOCE inhibitors have provided useful insights into the role of SOCE in physiological processes, the above evidence highlights an increasing need for specific and selective inhibitors especially when investigating calcium signalling pathways in dermatological diseases.

GSK-7975A (6-Difluoro-N-(1-(4-hydroxy-2-(trifluoromethyl)benzyl)-1H-pyrazol-3-yl)benzamide) is a pharmacological SOCE inhibitor developed by GlaxoSmithKline (example 36 from the GSK patent WO2010/122089). Figure 3.2 depicts the chemical structure of GSK-7975A. GSK-7975A was shown to effectively block SOCE for the first time in HEK293 and rat basophilic leukemia cells. The authors used patch clamping techniques to characterise the efficacy and action of this compound. They report that, unlike other SOCE inhibitors, GSK-7975A exerts its effect downstream of STIM1-Orai1 interactions, as demonstrated by both STIM1 oligomerisation and STIM1-Orai1 interactions being unaltered by treatment. This highlights a more selective property of the GSK compound compared to other inhibitors. Further investigations provided evidence that the target site of GSK-7975A was located within the selectivity filter of the Orai1 pore. This conclusion was drawn from two core pieces of evidence. Firstly, E106D Orai1 pore mutants required a significantly increased concentration of the compounds to produce the same inhibitory effect compared to wild-type Orai1 pores. Secondly, a decreased onset of action time was suggestive of a target site with more restricted access compared to other known compounds. Consistent with the mechanism of action of GSK-7975A being downstream of STIM1-Orai1 coupling, treatment with the inhibitor had minimal effect on other ion channels; only one (L-type calcium channel) was shown to display antagonistic effects with GSK-7975A treatment at a concentration less than the tested 10μM (Derler *et al.*, 2013). GSK-7975A has also been shown as an effective SOCE inhibitor in the following cell types lung: mast cells (human, and rat) (Ashmole *et al.*, 2012), T cells (human, rat, mouse and guinea-pig) (Rice *et al.*, 2013), platelets (mouse) (van Kruchten *et al.*, 2012), glomerular mesangial cells (human) (Chaudhari *et al.*, 2014) and pancreatic acinar cells (mouse) (Gerasimenko *et al.*, 2013). Moreover, these studies have demonstrated that in addition to blocking SOCE, GSK-7975A exerts a downstream signalling effect. For example,

GSK-7975A treatment at a concentration that effectively blocked SOCE in platelets resulted in reduced thrombus formation (van Kruchten *et al.*, 2012). Additionally, SOCE inhibition with GSK-7975A completely blocked the release of pro-inflammatory cytokines from primary human lung T cells (Rice *et al.*, 2013).

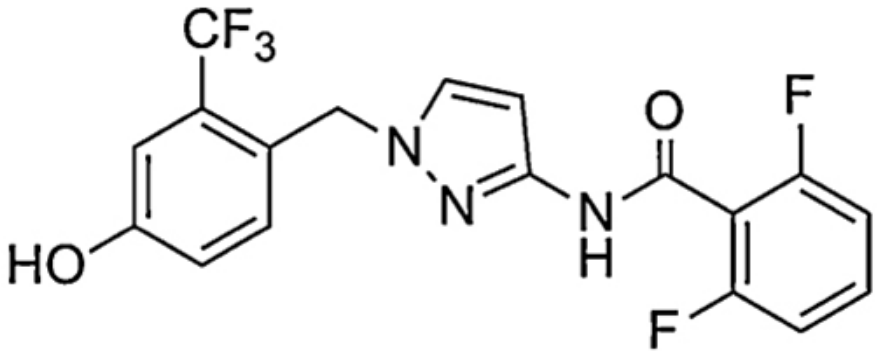

Figure 3.2 Structure of GSK-7975A.

The chemical structure of the GSK SOCE inhibitor GSK-7975A. (6-Difluoro-N-(1-(4-hydroxy-2-(trifluoromethyl)benzyl)-1H-pyrazol-3-yl)benzamide. Taken from (Derler *et al.*, 2013).

3.2 Specific aims.

- To investigate specific characteristics of the wound-induced calcium wave in order to decipher mechanism of transmission.

- To compare the calcium fluxes induced by scratch wounding in 0.06mM $[Ca^{2+}]_o$ and 1.2mM $[Ca^{2+}]_o$ to analyse the contribution of extracellular calcium in calcium wave propagation.

- To measure the effectiveness of GSK-7975A as a store-operated calcium entry (SOCE) inhibitor in primary human keratinocytes.

- To determine the role of SOCE on the spread and characteristics of the calcium wave post-wounding.

3.3 Results.

3.3.1 Characterisation of wound-induced calcium wave transmission.

As delineated in section 3.1.2, it is known that wounding keratinocytes results in a calcium signalling cascade spreading back from the site of wounding through neighbouring cells; however mechanisms regulating this transmission are not fully understood and specific parameters of the $[Ca^{2+}]_i$ flux have not previously been carefully defined in human keratinocytes. It was therefore hypothesised that analysis of a range of wave parameters would provide valuable and novel insights into mechanisms regulating the transmission of the calcium wave post-wounding.

In order to assess wave characteristics primary keratinocytes were loaded with Fluo4-AM calcium dye and wounded; images were captured at 3.7fps. As expected, immediately after wounding, there was an increase in intracellular calcium (figure 3.3 and figure 3.4). As shown by figure 3.3a it is clear that after the initial flux there was no further calcium response during the twenty minute imaging period, until the addition of thapsigargin (Tg). The trace was from a single representative cell located at wound edge. An average of 93.98±2.12% cells from the field of view in 3 independent experiments responded to wounding by displaying a similar $[Ca^{2+}]_i$ flux to that shown in figure 3.3a. No cells displayed oscillations post-wounding. As described in the material and methods (section 2.2.7), using Volocity, it was possible to draw around individual cells creating regions of interests (ROI) which generated databases providing detail on changes in fluorescence intensity over time. Wounding of keratinocytes was initially conducted in 0.06mM $[Ca^{2+}]_o$. Figure 3.3b shows that across the population of keratinocytes (n=72 from three independent donors, located up to 300µm from the wound) the $[Ca^{2+}]_i$ flux induced by wounding reached a maximum of 2.88±0.31 fold increase compared to baseline during the first three minutes post-wounding.

Initially, signalling across the whole population of cells was visually assessed. Subsequently, sub-populations were defined by their location from the wound edge and analysed to provide insights into differences between cells located at the wound edge compared to those located further back. Figure 3.4 shows representative images from one experiment taken every two seconds for twelve seconds and then three later images taken at minute intervals post-wounding, to visually depict the $[Ca^{2+}]_i$ changes triggered

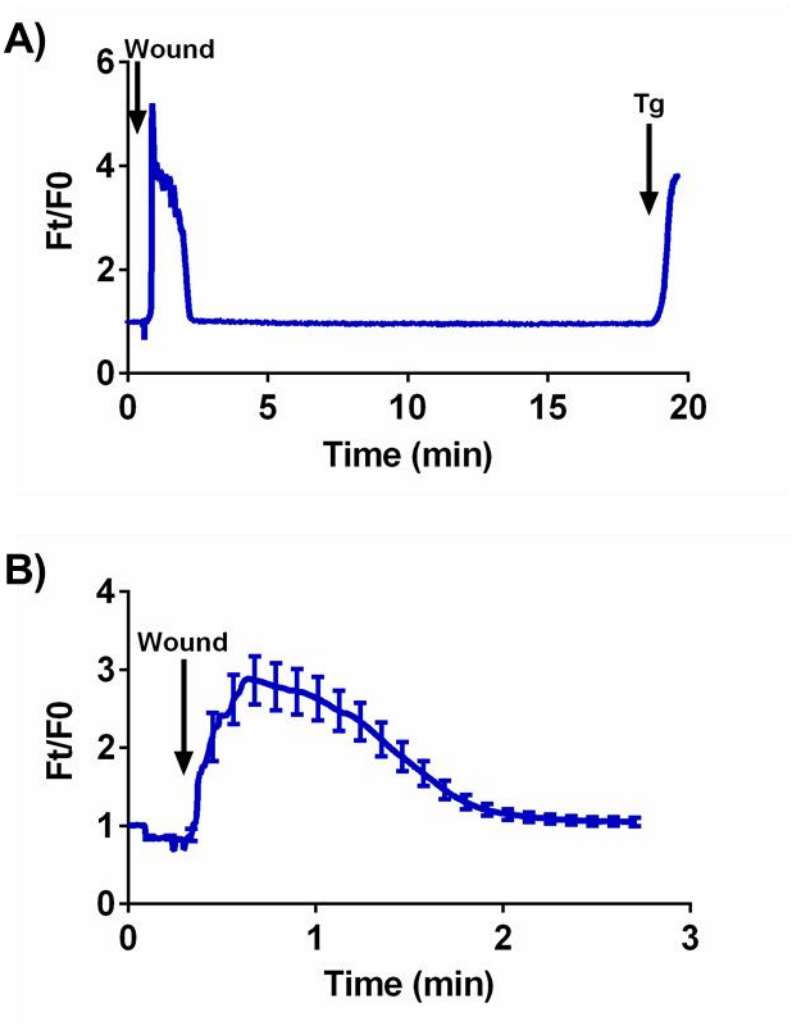

Figure 3.3 Wounding primary keratinocyte monolayer results in a calcium flux lasting up to two minutes.

Primary human keratinocytes cultured in 0.06mM $[Ca^{2+}]_o$ keratinocyte growth medium (MCDB 153) were loaded with Fluo4-AM calcium dye in 0.06mM $[Ca^{2+}]_o$ keratinocyte growth medium (MCDB 153) and wounded. Confocal images were captured at 3.7 fps. Regions of interest (ROI) were drawn around individual cells up to six cells from the wound edge for analysis. **A)** trace from a single representative cell from one donor over the twenty minute imaging period wounded in 0.06mM $[Ca^{2+}]_o$ Time of wound and addition of 3µM thapsigargin (Tg) are highlighted by arrows. **B)** Plot of the initial calcium flux triggered by wounding during the first three minutes. Data shows mean ± SEM from a total of 72 cells from three independent donors; (n=72), N=3. For clarity SEM has only been plotted every seven seconds.

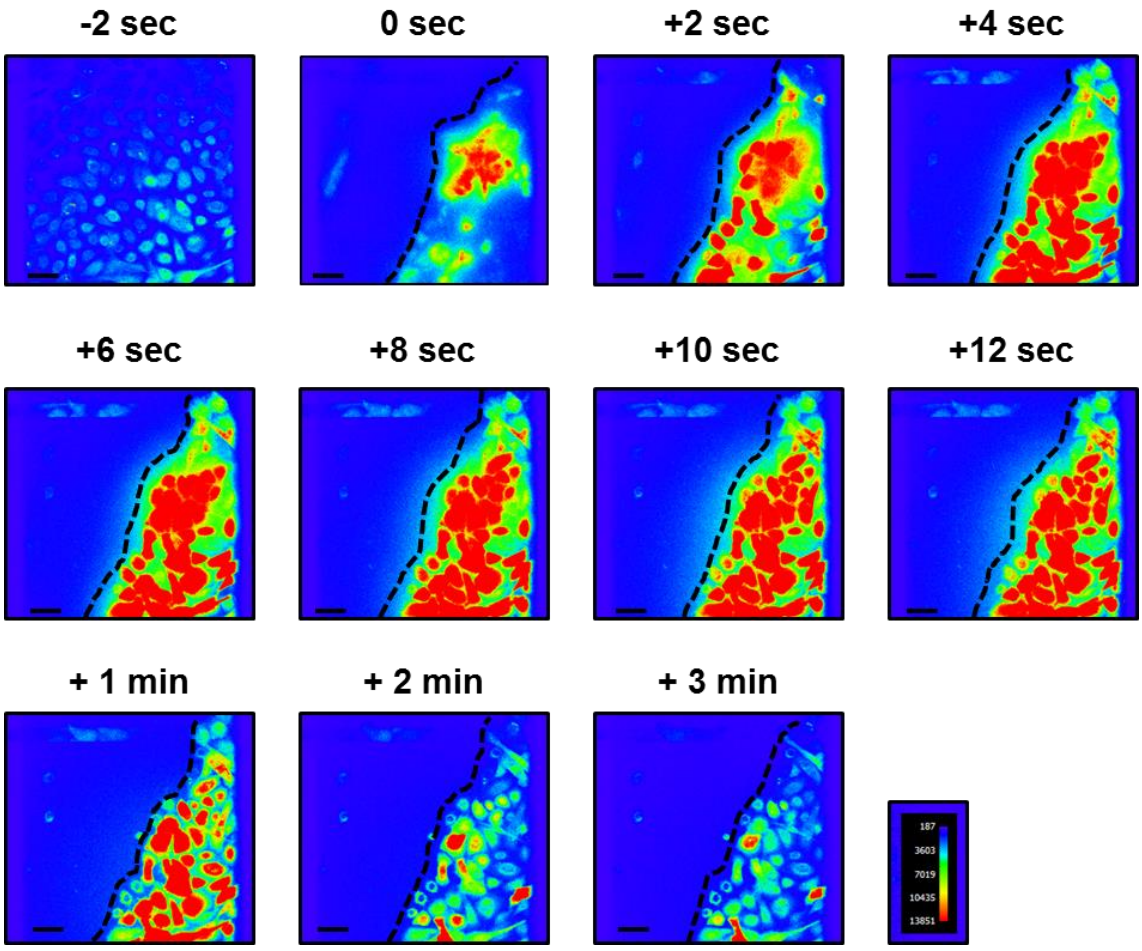

Figure 3.4 2D images demonstrating the wound-induced calcium wave.

Primary human keratinocytes cultured in 0.06mM $[Ca^{2+}]_o$ keratinocyte growth medium (MCDB 153) were loaded with Fluo4-AM calcium dye in 0.06mM $[Ca^{2+}]_o$ keratinocyte growth medium (MCDB 153) and wounded as described in figure 3.3. Pseudo colour images of confocal images were generated prior to the wound being made (-2 sec), at the point of wounding (0 sec) and then every 2 seconds for twelve seconds to demonstrate the visual appearance of the calcium signal triggered by wounding. Additionally, pseudo colour images of confocal images were generated at minute intervals for three minutes post-wounding to demonstrate calcium signal return to baseline. Scale bar=80µm. Pseudo colour reference is shown. Wound edge is highlighted by dotted line. Images are representative of three independent donors.

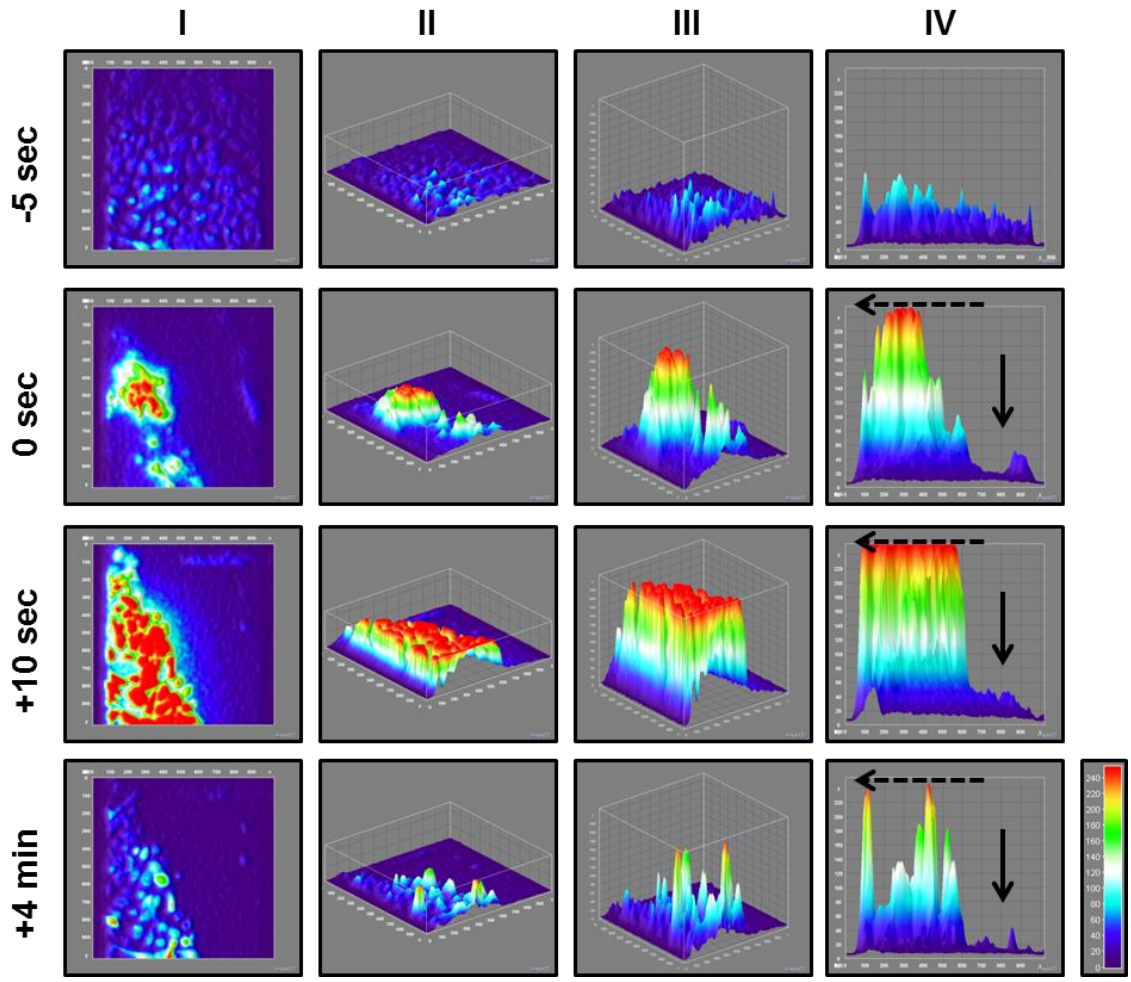

Figure 3.5 3D surface plots demonstrating the wound-induced calcium wave.

Primary human keratinocytes cultured in 0.06mM $[Ca^{2+}]_o$ keratinocyte growth medium (MCDB 153) were loaded with Fluo4-AM calcium dye in 0.06mM $[Ca^{2+}]_o$ keratinocyte growth medium (MCDB 153) and wounded. 3D surface plots of confocal images of the wound shown in figure 3.4 were created using ImageJ. Wound-induced calcium flux is shown from four view points and four specified times post-wounding. Column I shows the 2D image, column II depicts the same view as column III but with the Z-ratio equal to the XY-ratio in order to increase visual clarity of the spread of the wave, column III shows a diagonal cross section view and column IV shows the side view of the wave spreading from the wound back through cells (wound is located on the right hand side of the image (arrow), travelling left back through cells, direction highlighted by dotted arrow). Thermal LUT colour was adopted to increase visualisation of changes in fluorescence intensity. Thermal LUT scale reference is shown. Images are representative of three independent donors.

by wounding. It is clear that at the time of wounding, $[Ca^{2+}]_i$ increased at the wound edge and subsequently in neighbouring cells, appearing to travel as a wave. Using the image analysis software Volocity, the colour of the images was altered to rainbow to facilitate visualisation of changes in intensity. This can further be seen by the use of 3D surface plots, created using ImageJ (figure 3.5). These plots confirm that wounding caused an increase in calcium, initially focussed at the wound edge and spreading back through neighbouring cells during the first ten seconds.

In order to characterise the spread of the calcium wave back from the wound edge, $[Ca^{2+}]_i$ flux within individual cells were analysed according to the location of the cells away from the wound edge. Individual keratinocytes were analysed in "rows" away from the wound edge and cells were designated 1-6, with cell 1 being the cell at the wound edge, and cell 6 located six cells back from the wound. Figure 3.6 demonstrates reanalysis of the data from the flux experiments shown in figure 3.3 but with representative separate traces for each location from the wound edge (cells 1-6).

To further analyse and quantify these differences, maximum Ft/F0 post-wounding was recorded for each of the six cell locations from the wound. Maximum Ft/F0 was defined as the greatest fold change in $[Ca^{2+}]_i$ triggered by wounding. It appears that wounding caused a greater increase in maximum $[Ca^{2+}]_i$ in cells at the wound edge compared to cells further back, with a progressive decline as the wave travelled back. Regression analysis was performed and reported an R^2 value of 0.6081, which was borderline statistically significant (P=0.0674) (figure 3.7a). A one-way ANOVA with Dunnett's post-hoc revealed a statistical difference between cell location and maximum Ft/F0 ($F(2.152,23.67)=4.750$, P=0.0166) with cells 4-6 having a significantly reduced maximum Ft/F0 compared to cell 1 ($P<0.05$). A post-test for linear trend also reported a significant trend for a decreased maximum Ft/F0 the further back from the wound edge (P=0.0004) (figure 3.7b).

Visual evaluation of the wound-induced $[Ca^{2+}]_i$ flux suggested that the calcium signal travels between cells as a wave. In agreement with this, analysis of the time to reach maximum Ft/F0 showed that the further back from the wound edge a cell was located, the longer it took to reach its maximum fold change, with cells at the wound edge reaching maximum in a shorter time compared to cells six cells back. Cells at the wound edge reached their maximum increase in 3.87±0.84 seconds and those six cells

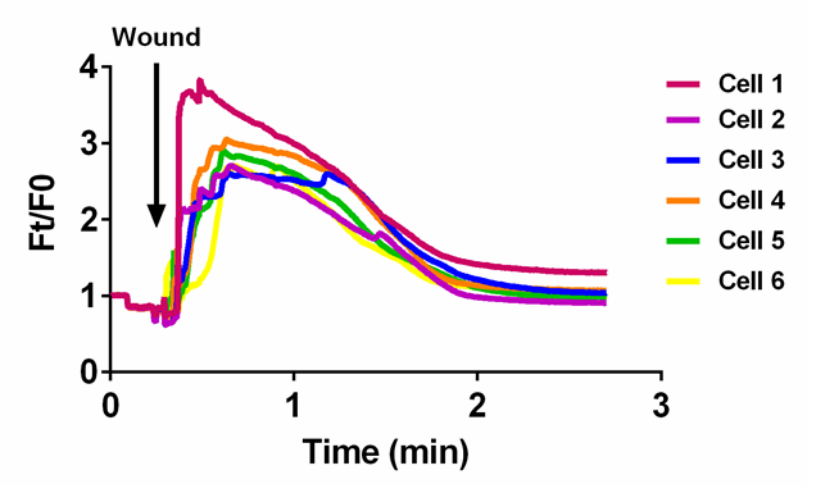

Figure 3.6 Wound-induced calcium flux occurs in cells at least six rows back from the wound.

Primary human keratinocytes cultured in 0.06mM $[Ca^{2+}]_o$ keratinocyte growth medium (MCDB 153) were loaded with Fluo4-AM calcium dye in 0.06mM $[Ca^{2+}]_o$ keratinocyte growth medium (MCDB 153) and wounded as described in figure 3.3. $[Ca^{2+}]_i$ flux within individual cells was analysed according to the location of the cells away from the wound edge. Individual keratinocytes were analysed in "rows" away from the wound edge and cells were designated 1-6, with Cell 1 being the cell at the wound edge, and Cell 6 located six cells back from the wound. Data shows mean from 12 cells from three independent donors at each location; (n=12), N=3. In order to facilitate visualisation of $[Ca^{2+}]_i$ flux at each location, error bars are not shown on the graph.

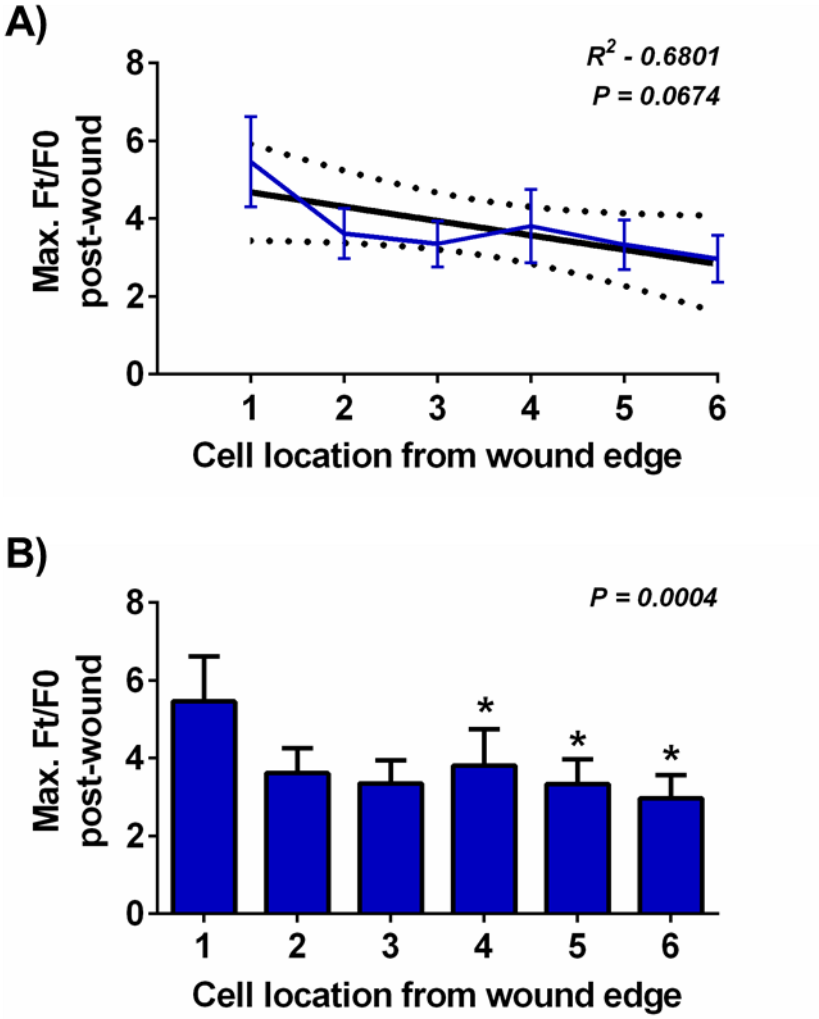

Figure 3.7 Maximum Ft/F0 calcium flux within individual keratinocytes declines as the calcium wave spreads away from the wound edge.

Primary human keratinocytes cultured in 0.06mM $[Ca^{2+}]_o$ keratinocyte growth medium (MCDB 153) were loaded with Fluo4-AM calcium dye in 0.06mM $[Ca^{2+}]_o$ keratinocyte growth medium (MCDB 153) and wounded as described in figure 3.3. The maximum fold change (Ft/F0) in calcium flux induced by wounding compared to the baseline was analysed at each location from the wound edge. **A)** Linear regression analysis was conducted and the line of best-fit plotted (black line) with the 95% confidence intervals (dotted lines). **B)** Data was plotted and a one-way ANOVA conducted with Dunnett's post-hoc test to compare maximum Ft/F0 at cell locations compared to Cell 1 (* $P<0.05$). A post-test for linear trend was also conducted (P=0.0004). Data shows mean ± SEM from 12 cells at each location from three independent donors; (n=72), N=3.

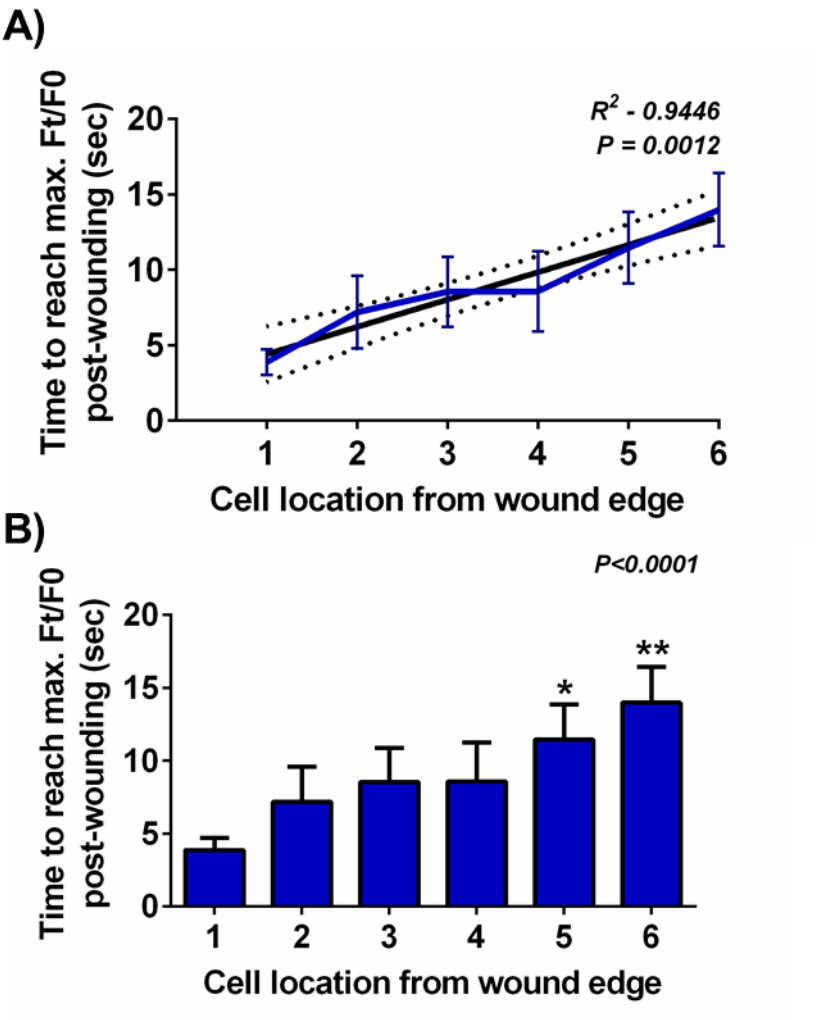

Figure 3.8 Time to reach maximum Ft/F0 calcium flux within individual keratinocytes increases as the calcium wave spreads away from the wound edge.

Primary human keratinocytes cultured in 0.06mM $[Ca^{2+}]_o$ keratinocyte growth medium (MCDB 153) were loaded with Fluo4-AM calcium dye in 0.06mM $[Ca^{2+}]_o$ keratinocyte growth medium (MCDB 153) and wounded as described in figure 3.3. The time taken to reach maximum fold change (Ft/F0) calcium flux induced by wounding was analysed at each location from the wound edge. **A)** Linear regression analysis was conducted and the line of best-fit plotted (black line) with the 95% confidence intervals (dotted lines). **B)** Data was plotted and a one-way ANOVA conducted with Dunnett's post-hoc test to compare time to reach maximum Ft/F0 at cell locations compared to Cell 1 (** $P<0.01$, * $P<0.05$). A post-test for linear trend was also conducted ($P<0.0001$). Data shows mean ± SEM from 12 cells at each location from three independent donors; (n=72), N=3.

back reached a maximum at 13.98±2.43 seconds. Linear regression revealed this line was significantly different to zero (R^2-0.9446, P=0.0012) (figure 3.8a). A one-way ANOVA with Dunnett's post-hoc also showed cell location significantly affected speed of wave (F(2.45,26.99)=4.830, P=0.0116) with cell 5 and cell 6 taking significantly longer to reach maximum Ft/F0 compared to cell 1 (** P<0.01, * P<0.05). A post-test for linear trend also reported a significant trend for a decreased maximum time to reach Ft/F0 the further back from the wound edge (P<0.0001) (figure 3.8b).

Next, the area under the curve (AUC) of the wound-induced $[Ca^{2+}]_i$ flux was calculated in individual cells at each cell location back from the wound edge. AUC was used as an integrative measure of wound-induced calcium flux. The AUC for wound-induced calcium flux in 0.06mM $[Ca^{2+}]_o$ may be considered an approximation to calcium release from the ER. From figure 3.9 is appears that the AUC decreases the further the cell is back from the wound edge; cells at the wound edge had an AUC of 3.76±1.25 whereas this value was 1.55±0.70 for cells located six rows back. Linear regression analysis reported an R^2 value of 0.5302, however this was not deemed significantly different to zero (P=0.1008) (figure 3.9a). A one-way ANOVA with a post-test for linear trend, did however, report a significant trend in the data (P=0.017) (figure 3.9b). Therefore, these data suggest a relationship between cell location from the wound and AUC. This data is consistent with that reported in figure 3.7 demonstrating the maximum Ft/F0 declining the further the wave travelled.

Finally, the rate of rise of the wound-induced $[Ca^{2+}]_i$ flux was investigated. This was measured by calculating the slope of fluorescence intensity between the time the initiation of the wound-induced $[Ca^{2+}]_i$ flux and the time maximal Ft/F0 was achieved, this value represents the gradient of wound-induced calcium increase. Figure 3.10 shows changes in the rate of rise in cells at specified locations from the wound edge. The graph shows that the rate of rise of the $[Ca^{2+}]_i$ flux decreased the further back from the wound the cell was located. Cells at the wound edge had a rate of rise of 0.67±0.23 (ΔFt/F0/second) and those six cells back from the wound had a rate of rise of 0.10±0.03 (ΔFt/F0/second). A nonlinear regression exponential decay curve was fitted to the data and an adjusted R^2 value of 0.9392 was reported highlighting a high goodness of fit (figure 3.10a). A one-way ANOVA with Dunnett's post-hoc revealed a statistical difference between the rate of rise at different cell locations (F(5,66)=2.772, P=0.0247)

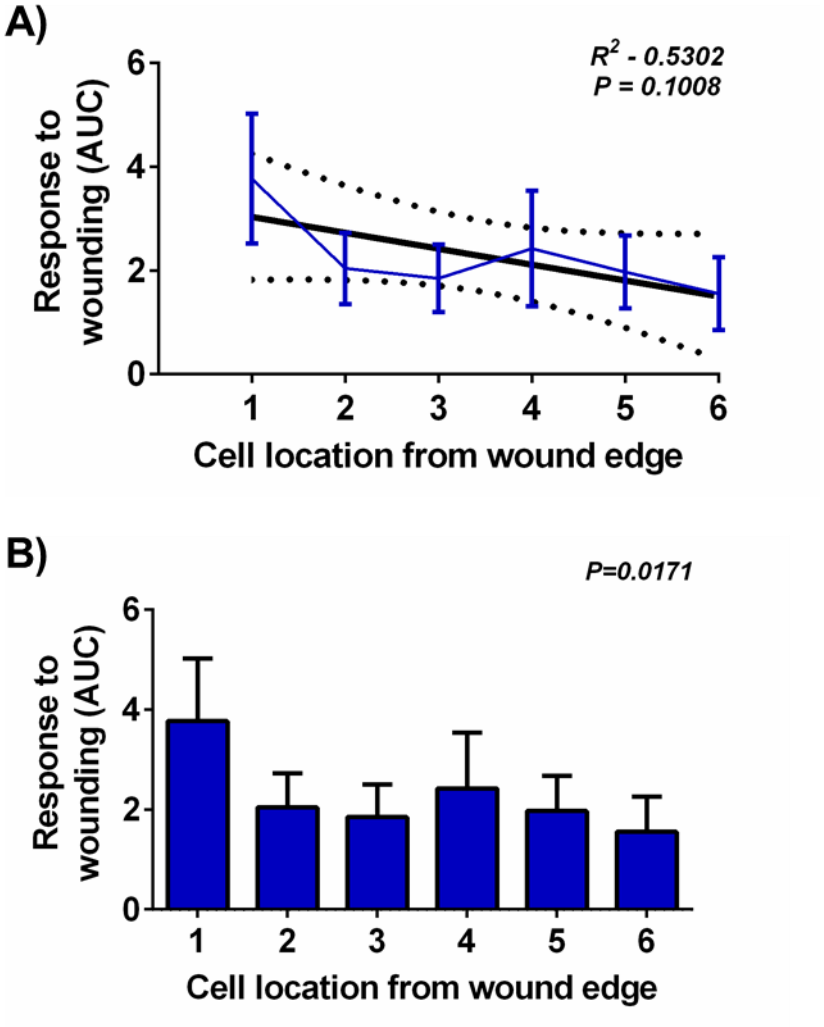

Figure 3.9 Area under the curve during wound-induced calcium flux within individual keratinocytes decreases as the calcium wave spreads away from the wound edge.

Primary human keratinocytes cultured in 0.06mM $[Ca^{2+}]_o$ keratinocyte growth medium (MCDB 153) were loaded with Fluo4-AM calcium dye in 0.06mM $[Ca^{2+}]_o$ keratinocyte growth medium (MCDB 153) and wounded as described in figure 3.3. The area under the curve AUC during the initial calcium flux was calculated at each location from the wound edge. **A)** Linear regression analysis was conducted and the line of best-fit plotted (black line) with the 95% confidence intervals (dotted lines). **B)** Data was plotted and a one-way ANOVA conducted with a post-test for linear trend was also conducted ($P<0.0001$). Data shows mean ± SEM from 12 cells at each location from three independent donors; (n=72), N=3.

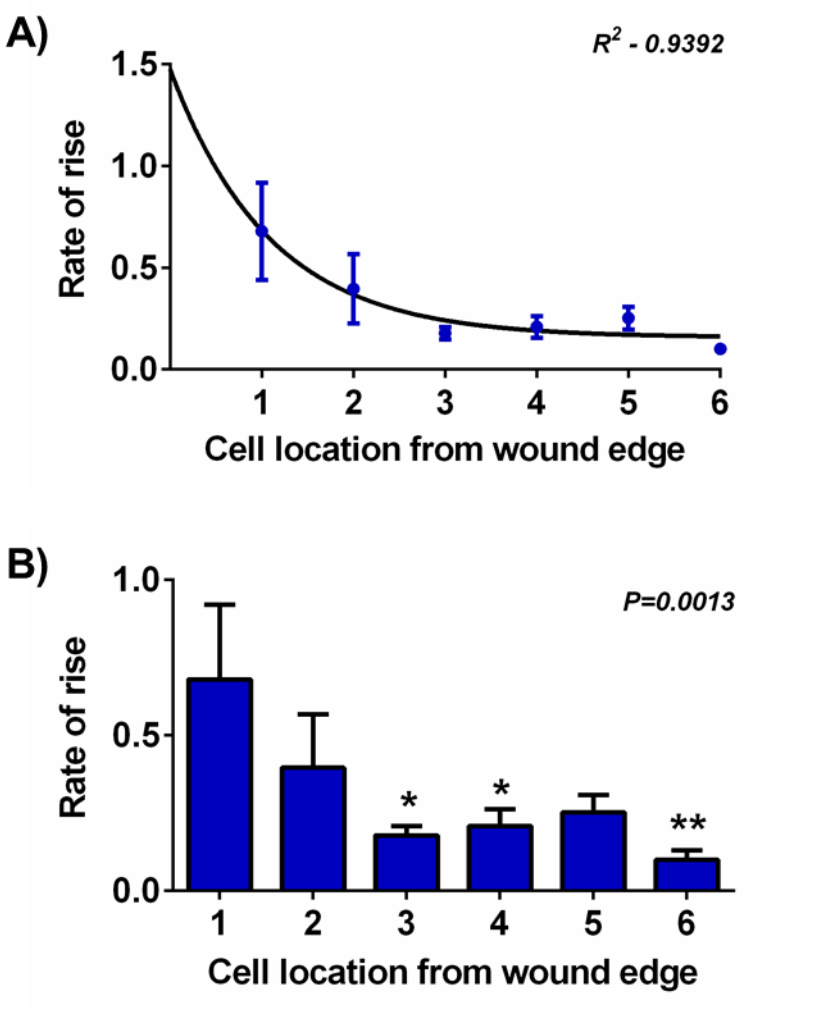

Figure 3.10 Rate of rise of calcium flux within individual keratinocytes decreases as the calcium wave spreads away from the wound edge.

Primary human keratinocytes cultured in 0.06mM $[Ca^{2+}]_o$keratinocyte growth medium (MCDB 153) were loaded with Fluo4-AM calcium dye in 0.06mM $[Ca^{2+}]_o$ keratinocyte growth medium (MCDB 153) and wounded as described in figure 3.3. The rate of rise (gradient of calcium increase) post-wounding was recorded at each location from the wound edge. **A)** A non-linear regression exponential decay graph was fitted to the data with an adjusted R^2 value of 0.9392. **B)** Data was plotted and a one-way ANOVA conducted with Dunnett's post-hoc test to compare time to reach maximum Ft/F0 at cell locations compared to Cell 1 (** P<0.01, * P<0.05). A post-test for linear trend was also conducted (P=0.0013). Data shows mean ± SEM from 12 cells at each location from three independent donors; (n=72), N=3.

with cells 3, 4 and 6 having a significantly reduced rate of rise compared to cell 1 (** $P<0.01$, * $P<0.05$). A post-test for linear trend also reported a significant trend for a decreased maximum Ft/F0 the further back from the wound edge ($P=0.0013$) (figure 3.10b). Overall, the analysis presented suggests that after wounding, the calcium wave reduces with cell location from the wound edge. This is evidenced by i) maximum Ft/F0 achieved by wounding progressively decreasing with cell location, ii) AUC diminishing further away from the wound edge and iii) declining rate of rise of calcium signal in cells located further back compared to the wound edge. Additionally, as expected for a wave, the $[Ca^{2+}]_i$ changes were delayed for keratinocytes at increasing distance from the wound. These results are indicative of an intracellular signalling mechanism through which the signal is propagated from cell to cell, potentially mediated through IP_3. It can therefore be hypothesised, that IP_3 is generated in the cell at the wound edge, and diffuses into the neighbouring cell inducing calcium-mediated regeneration of the IP_3 signal. However, as the signal travels through the population, the efflux of IP_3 into the next cell becomes progressively smaller than the influx from the preceding cell. Therefore the regeneration potential of IP_3 is partial and fails after a finite distance where the signal becomes below the threshold required to activate IP_3R preventing calcium release from the intracellular stores. A decrease in maximal Ft/F0 reached post-wounding as well as a decrease in AUC of the $[Ca^{2+}]_i$ flux in cells located further away from the wound indicates a lower intracellular calcium signal within these individual cells, supporting a reduction in IP_3-mediated calcium release from the ER. A declining rate of rise is suggestive that the IP_3 influx decreases within cells locate further from the wound, thus reducing available IP_3 to bind to IP_3R leading to the eventual failure of IP_3 regeneration.

3.3.2 Effect of increased extracellular calcium concentration on wound-induced calcium wave characteristics.

As alluded to in section 1.3.5, the existence of a calcium gradient within the epidermis is well established and it is also known that this gradient is disrupted by cutaneous wounding (Elias *et al.*, 2002). Additionally, published evidence indicates that wounding alters the calcium concentration of the extracellular wound serum which potentially influences long-term functional responses of keratinocytes such as cell migration. Moreover, it is accepted that long-term exposure to elevated extracellular calcium

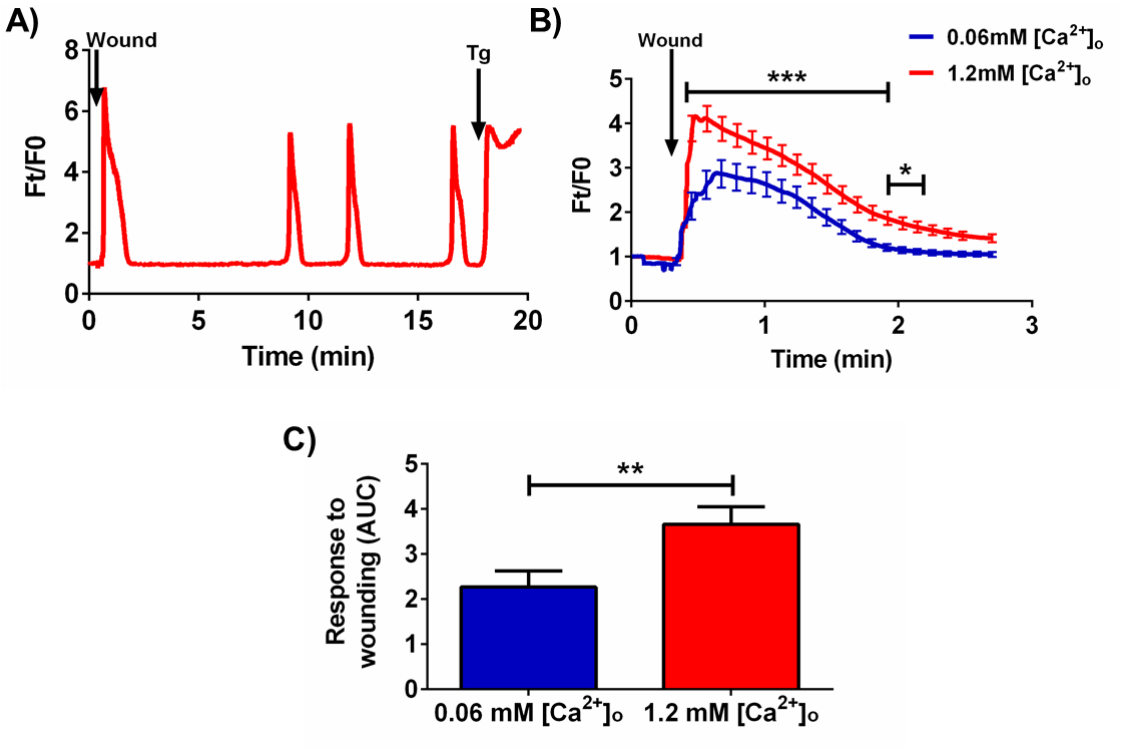

Figure 3.11 Wounding primary keratinocyte monolayer in 1.2mM $[Ca^{2+}]_o$ results in a large calcium flux compared to wounding in 0.06mM $[Ca^{2+}]_o$.

Primary human keratinocytes cultured in 0.06mM $[Ca^{2+}]_o$ keratinocyte growth medium (MCDB 153) were loaded with Fluo4-AM calcium dye. Post-de-esterification, either 0.06mM or 1.2mM $[Ca^{2+}]_o$ keratinocyte growth media (MCDB 153) was added for five minutes prior to wounding. Confocal images were captured at 3.7 fps. Regions of interest (ROI) were drawn around individual cells up to six cells from the wound edge for analysis. **A)** Trace from a single representative cell from one donor over the twenty minute imaging period wounded in 1.2mM $[Ca^{2+}]_o$. Time of wound and addition of 3µM thapsigargin (Tg) are highlighted by arrows. **B)** Plot of the average initial calcium flux triggered by wounding during the first three minutes in 0.06mM (blue) or 1.2mM (red) $[Ca^{2+}]_o$. For clarity SEM has only been plotted every seven seconds. Repeated measure (RM) two-way ANOVA with Bonferroni post-hoc test to compare 0.06mM and 1.2mM at each time point. $F(1,71)=19.36$, $P=0.9583$. *** $P<0.001$, * $P<0.05$. **C)** Average AUC for $[Ca^{2+}]_i$ fluxes performed in 0.06mM (blue bar) and 1.2mM $[Ca^{2+}]_o$. (red bar). Unpaired, two-tailed T-test (** $P=0.0097$). Data shows mean ± SEM from a total of 72 cells from three independent donors; (n=72), N=3.

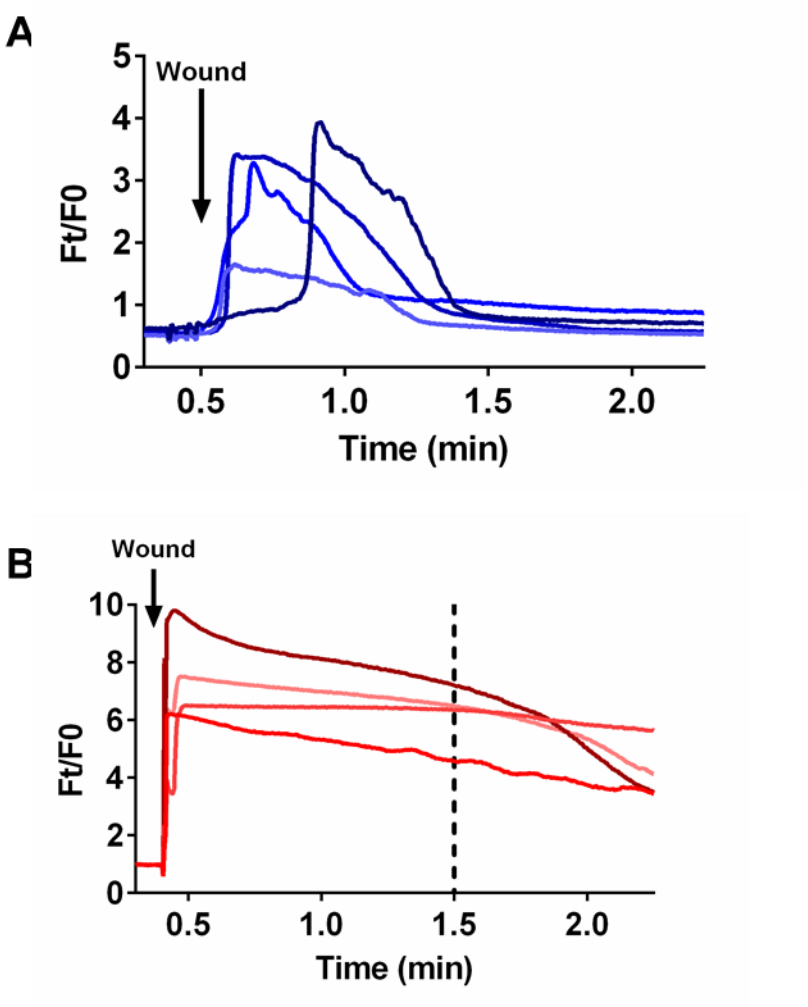

Figure 3.12 Wounding primary keratinocyte monolayer in 1.2mM $[Ca^{2+}]_o$ results in a large and prolonged calcium flux compared to wounding in 0.06mM $[Ca^{2+}]_o$.

Primary human keratinocytes cultured in 0.06mM $[Ca^{2+}]_o$ keratinocyte growth medium (MCDB 153) were loaded with Fluo4-AM calcium dye. Post-de-esterification, either 0.06mM or 1.2mM $[Ca^{2+}]_o$ keratinocyte growth media (MCDB 153) was added for five minutes prior to wounding. Confocal images were captured at 3.7 fps. Regions of interest (ROI) were drawn around individual cells up to six cells from the wound edge for analysis. Traces show four representative cells from wounds performed in **A)** 0.06mM $[Ca^{2+}]_o$ or **B)** 1.2mM $[Ca^{2+}]_o$. Time of wounding is highlighted by arrow. Four cells per condition are representative of three independent donors.

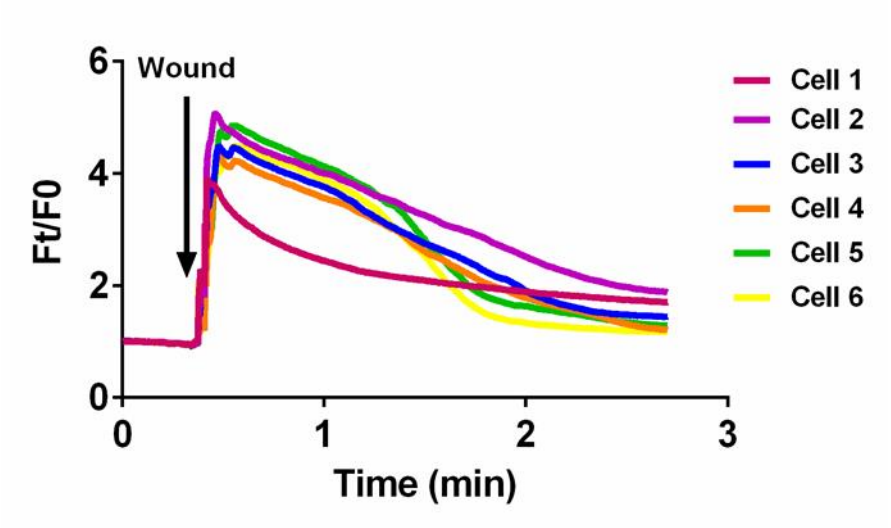

Figure 3.13 Wound-induced calcium flux occurs in cells at least six rows back from the wound in 1.2mM $[Ca^{2+}]_o$.

Primary human keratinocytes cultured in 0.06mM $[Ca^{2+}]_o$ keratinocyte growth medium (MCDB 153) were loaded with Fluo4-AM calcium dye. Post-de-esterification, 1.2mM $[Ca^{2+}]_o$ keratinocyte growth media (MCDB 153) was added for five minutes prior to wounding. $[Ca^{2+}]_i$ flux within individual cells was analysed according to the location of the cells away from the wound edge. Individual keratinocytes were analysed in "rows" away from the wound edge and cells were designated 1-6, with Cell 1 being the cell at the wound edge, and Cell 6 located six cells back from the wound. Data shows mean from 12 cells from three independent donors at each location; (n=12), N=3. In order to facilitate visualisation of $[Ca^{2+}]_i$ flux at each location, error bars are not shown on the graph.

induces phenotypic changes within keratinocytes including cellular differentiation (Numaga-Tomita and Putney, 2013). However, the effect of $[Ca^{2+}]_o$ on calcium signalling cascades that occur immediately post-wounding have not been fully deciphered.

To investigate this, primary human keratinocytes cultured in 0.06mM $[Ca^{2+}]_o$ keratinocyte growth medium (MCDB 153) were loaded with Fluo4-AM calcium dye and wounded in supplemented keratinocyte growth medium (MCDB 153) to increase the calcium concentration to 1.2mM. Cells were exposed to 1.2mM $[Ca^{2+}]_o$ for five minutes prior to wounding Experimental design and imaging parameters were identical to previous experiments conducted in 0.06mM $[Ca^{2+}]_o$. Figure 3.11a shows a trace from a single representative cell from the wound edge. Akin to wounds made in 0.06mM $[Ca^{2+}]_o$, wounding resulted in a $[Ca^{2+}]_i$ flux adjacent to the wound edge that spread outwards as a calcium wave. Interestingly, though in contrast to wounding in 0.06mM $[Ca^{2+}]_o$, further calcium fluxes in the form of repeated oscillations were detected in individual cells away from the wound edge in 1.2mM $[Ca^{2+}]_o$. The characteristics and mechanisms regulating the generation of these oscillations will be explored further in Chapter 5. This current section will focus on the calcium wave initiated by mechanical wounding in 1.2mM $[Ca^{2+}]_o$ in order to determine the effect of extracellular calcium on the propagation of the intercellular calcium wave. As shown by figure 3.11b, across the population of keratinocytes (n=72 from three independent donors, located up to 300µm from the wound) the wound-induced $[Ca^{2+}]_i$ flux reached a maximum of 4.16±0.29 fold increase compared to baseline during the first three minutes post-wounding. Although the overall pattern of the $[Ca^{2+}]_i$ fluxes appeared similar whether keratinocytes were wounded in 1.2mM or 0.06 $[Ca^{2+}]_o$, the maximal $[Ca^{2+}]_i$ flux induced by wounding, was significantly larger when wounding was performed in 1.2mM $[Ca^{2+}]_o$ ($F(1,71)=19.36$, $P<0.0001$, RM two-way ANOVA). A Bonferroni post-hoc test of the RM two-way ANOVA revealed that the average wound-induced calcium flux (Ft/F0) was greater in 1.2mM $[Ca^{2+}]_o$ compared to 0.06mM $[Ca^{2+}]_o$ between 0.41 and 2.17 minutes. This is further supported by a significantly increased AUC of $[Ca^{2+}]_i$ flux when wounding was performed in 1.2mM $[Ca^{2+}]_o$ compared to 0.06mM $[Ca^{2+}]_o$ ($P=0.0097$, unpaired, two-tailed, t-test) (figure 3.11c). Additionally, as shown by figure 3.11b, the time taken to reach maximum Ft/F0 was reduced and the calcium signal remained above baseline for a longer period of time when wounding was conducted in 1.2mM $[Ca^{2+}]_o$. Traces from

four individual cells at various locations from the wound edge in three independent donors confirmed this observation (figure 3.12). It can be seen that at ninety seconds post-wounding in 0.06mM $[Ca^{2+}]_o$ (figure 3.12a) the $[Ca^{2+}]_i$ had returned to baseline, whereas in 1.2mM $[Ca^{2+}]_o$ the $[Ca^{2+}]_i$ remained elevated at this time point (figure 3.12b).

In order to identify differences between characteristics of the spread of the calcium wave back from the wound edge in a low and high external calcium environment, $[Ca^{2+}]_i$ flux within individual cells were analysed according to the location of the cells away from the wound edge, as described previously (section 3.3.1). Figure 3.13 demonstrates reanalysis of the data from the flux experiment shown in figure 3.11b (red line) but with representative separate traces for each location from the wound edge (cells 1-6). Interestingly, in contrast to wounding in 0.06mM $[Ca^{2+}]_o$, where clear differences were seen between cells located at the wound edge and those further back, when wounding in 1.2mM $[Ca^{2+}]_o$, cells 1-6 have a similar $[Ca^{2+}]_i$ flux pattern, with minimal differences observed between those cells located at the wound edge and those cells located up to six rows back.

To test the hypothesis that calcium flux differences were cell location dependent, $[Ca^{2+}]_i$ flux was analysed taking into account the cellular location in relation to the wound edge. As shown by figure 3.14, the calcium flux in cells at the wound edge when wounding was performed in 0.06mM $[Ca^{2+}]_o$ was not significantly different to that when wounding was performed in 1.2mM$[Ca^{2+}]_o$ ($F(1,11)=0.002866$, $P=0.9583$, RM two-way ANOVA). However, at cell located two to six rows from the wound, wounding in 1.2mM $[Ca^{2+}]_o$ resulted in a significant increased mean calcium signal (Ft/F0) compared to 0.06mM $[Ca^{2+}]_o$ ($P=0.0135$, $P=0.0383$, $P=0.0198$, $P=0.0158$ respectively, RM two-way ANOVA). Analysis of data of the "cell 4" population showed no difference ($F(1,11)=1.060$, $P=0.3253$, RM two-way ANOVA). Bonferroni post-hoc tests were conducted to compare calcium intensity at each timepoint between 0.06 and 1.2mM $[Ca^{2+}]_o$. Statistical results are summarised in table 3.1.

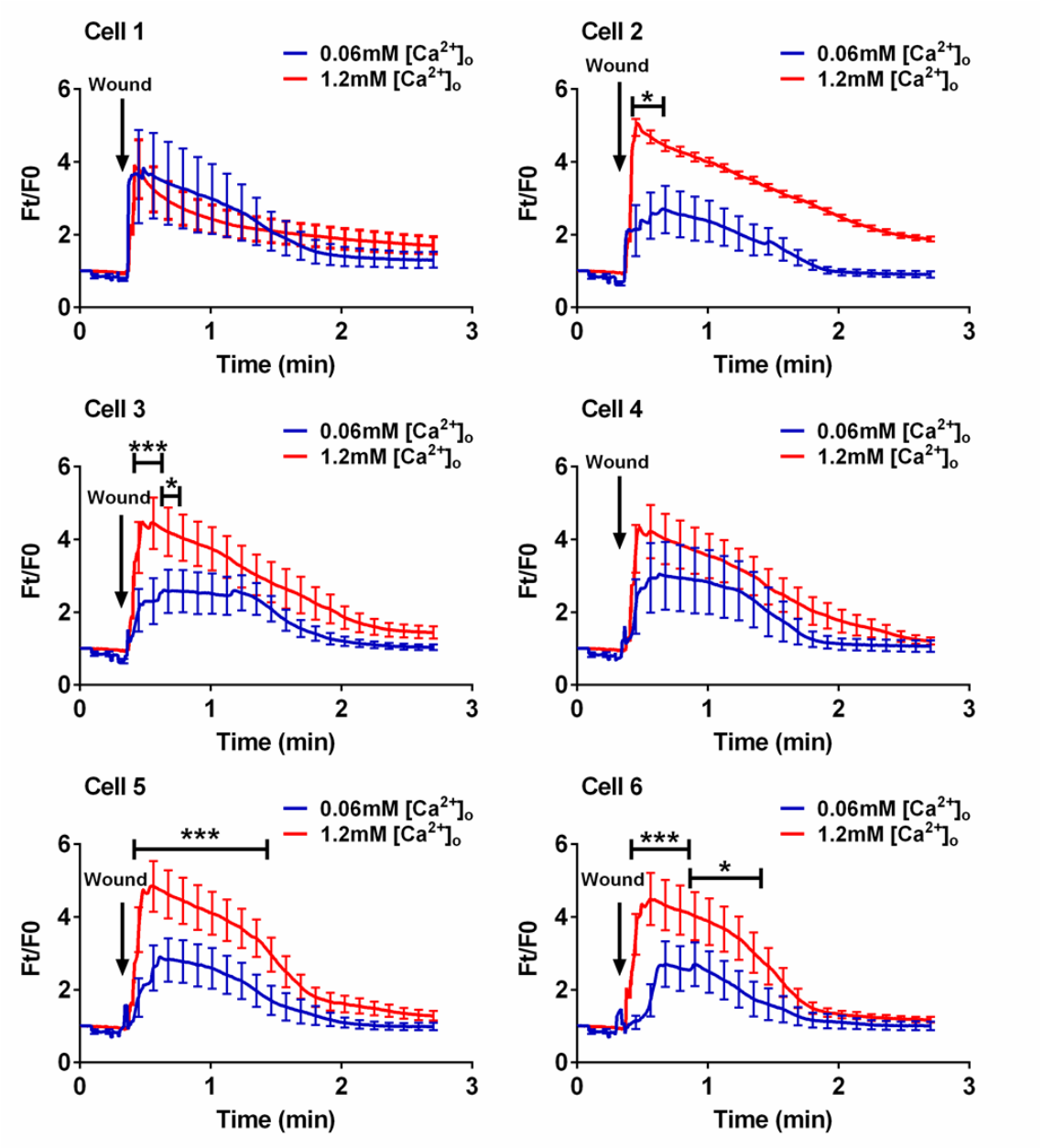

Figure 3.14 Wound-induced $[Ca^{2+}]_i$ flux is greater in 1.2mM $[Ca^{2+}]_o$ than 0.06mM $[Ca^{2+}]_o$ at cell locations back from the wound edge.

Wound-induced calcium flux in cells were analysed according to their location from the wound edge termed 1-6, with Cell 1 being at the wound edge and Cell 6 located six cells back from the wound. Each plot shows wounds made in either 0.06mM (blue) or 1.2mM (red) $[Ca^{2+}]_o$. Time of wound is highlighted by arrow. Data shows mean from 12 cells from three independent donors at each location; (n=12), N=3. For graphical clarity SEM has only been plotted every seven seconds. RM two-way ANOVA with Bonferroni post-hoc test compared calcium flux between 0.06mM and 1.2mM $[Ca^{2+}]_o$ at each timepoint, results are summaries in table 3.1. (*** P<0.001, * P<0.05).

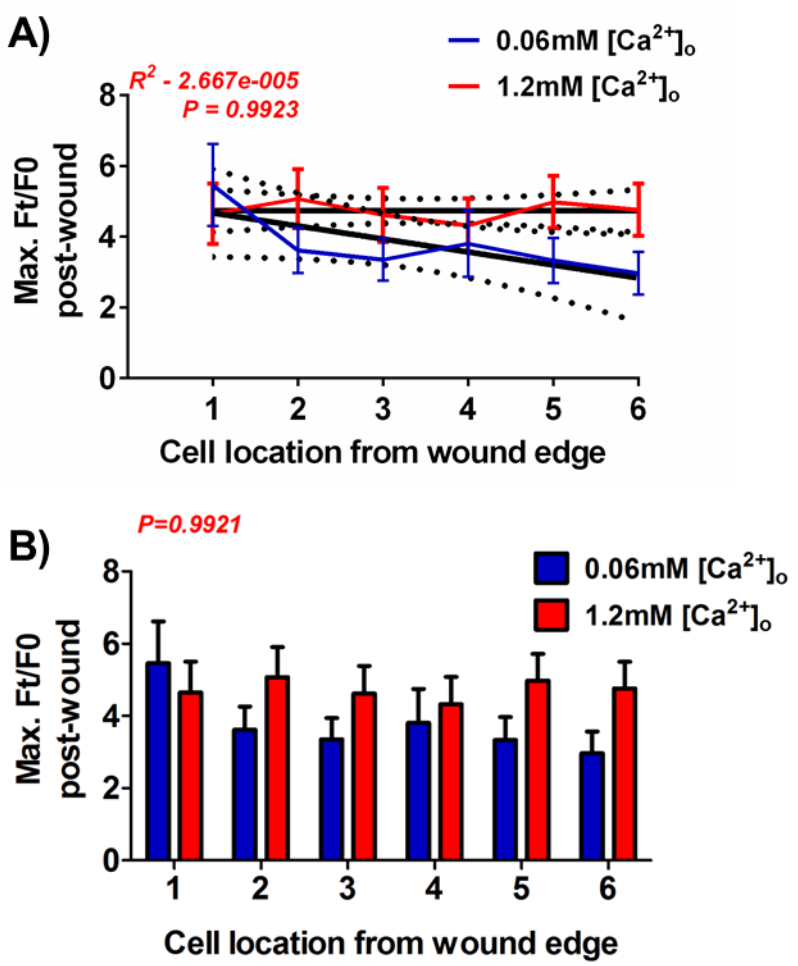

Figure 3.15 Maximum Ft/F0 calcium flux is greater in wounds made in 1.2mM compared to 0.06mM $[Ca^{2+}]_o$.

Primary human keratinocytes cultured in 0.06mM $[Ca^{2+}]_o$ keratinocyte growth medium (MCDB 153) were loaded with Fluo4-AM calcium dye. Post-de-esterification, either 0.06mM or 1.2mM $[Ca^{2+}]_o$ keratinocyte growth media (MCDB 153) was added for five minutes prior to wounding. The maximum fold change (Ft/F0) in calcium flux induced by wounding compared to the baseline was analysed at each location from the wound edge. Data is shown in two forms for clarity. **A)** Linear regression analysis was conducted and the line of best-fit plotted (black lines) with the 95% confidence intervals (dotted lines) for wounds made in 1.2mM $[Ca^{2+}]_o$ (red line). Data for wounds made in 0.06mM $[Ca^{2+}]_o$ is also shown (blue line) to visualise differences between the two external calcium concentrations. **B)** Maximal Ft/F0 in $[Ca^{2+}]_i$ flux for wounds made in 0.06mM and 1.2mM $[Ca^{2+}]_o$ were compared by two-way ANOVA ($F(1,132)=4.624$, $P=0.0334$) and a Bonferroni post-hoc test. A one-way ANOVA with a post-test for linear trend was also conducted on data from 1.2mM $[Ca^{2+}]_o$ experiments ($P=0.9921$). Data shows mean ± SEM from 12 cells at each location from three independent donors; (n=72), N=3.

To further analyse and quantify these differences, maximum Ft/F0 post-wounding was calculated for each of the six cell locations from the wound made edge (irrespective of time). As shown by figure 3.15a, when wounding in 1.2mM $[Ca^{2+}]_o$, the maximum Ft/F0 achieved remained constant irrespective of location from the wound edge. Regression analysis was performed and reported an R^2 value of 2.667e-005, which did not show statistical deviation from zero (P=0.9923). This was not the case when wounding in 0.06mM $[Ca^{2+}]_o$, where maximum Ft/F0 declined progressively through cells back from the wound (figure 3.15a). A one-way ANOVA revealed no statistical difference between cell location and maximum Ft/F0 (F(3.044,33.48)=0.742, P=0.5351). A post-test for linear trend also reported no significant trend (P=0.9921) (figure 3.15b). As shown by figure 3.15b, the intracellular calcium flux at cells located further back from the wound edge (cells 5 and 6) appeared to be increased when wounding in 1.2mM $[Ca^{2+}]_o$. While an overall statistical difference in maximum Ft/F0 between 0.06 and 1.2mM $[Ca^{2+}]_o$ was revealed (F(1,132)=4.624, P=0.0334, two-way ANOVA), a Bonferroni post-hoc test showed there were no specific locations were these differences were statistically significant. The similar maximum Ft/F0 in cells at the wound edge, regardless of external calcium concentration, implied that wound-induced calcium wave was not initiated by extracellular calcium. However, the retention of the maximum Ft/F0 $[Ca^{2+}]_i$ value (flux) across cells progressively further back from the wound edge in 1.2mM $[Ca^{2+}]_o$ suggested that as the wave travelled away from the wound, it retained the ability to initiate calcium release from ER stores and/or calcium entry from the extracellular space.

As expected for a wave, the $[Ca^{2+}]_i$ changes were delayed for keratinocytes at increasing distance from the wound edge. Thus for example, cells at the wound edge reached their maximum Ft/F0 increase in 2.13±0.48 seconds compared to 6.86±1.13 seconds for cells six rows back in 1.2mM $[Ca^{2+}]_o$. Linear regression analysis showed that this line of best fit was significantly different to zero (P=0.0007) and had an R^2 value of 0.9572 for cells wounded in 1.2mM $[Ca^{2+}]_o$. A one-way ANOVA with Dunnett's post-hoc also showed cell location significantly affected time to reach maximum Ft/F0 (F(2.091,23.00)=7.774, P=0.00024) with all cells taking significantly longer to reach maximum Ft/F0 compared to cell 1 (*** P<0.001, ** P<0.01, * P<0.05). A post-test for linear trend also reported a significant trend for a decreased maximum time to reach

Ft/F0 the further back from the wound edge (P<0.0001) (figure 3.16b). As demonstrated in figure 3.16a, the wound-induced $[Ca^{2+}]_i$ flux in 1.2mM $[Ca^{2+}]_o$, reached six cells back from the wound in a significantly reduced time compared to 0.06mM $[Ca^{2+}]_o$ (F(1,132)=1834, P<0.0001, two-way ANOVA). A Bonferroni post-hoc showed that this difference was significant six cells back from the wound edge (* P<0.05).

	RM two-way ANOVA		Bonferroni post-hoc test
Cell location from wound edge	**F value**	**P value**	**Time point of difference (min)**
1	F(1,11)=0.002866	P=0.9583	
2	F(1,11)=8.633	P=0.0135	0.42 – 0.56
3	F(1,11)=5.537	P=0.0383	0.41 – 0.62
4	F(1,11)=1.060	P=0.3253	
5	F(1,11)=7.424	P=0.0198	0.41 – 1.44
6	F(1,11)=8.130	P=0.0158	0.41 – 0.87

Table 3-1 Wounding in 1.2mM $[Ca^{2+}]_o$ results in a greater $[Ca^{2+}]_i$ flux compared to wounding in 0.06mM $[Ca^{2+}]_o$.

Summary of statistical analysis obtained from RM two-way ANOVA comparing wound-induced $[Ca^{2+}]_i$ flux in 0.06mM and 1.2mM $[Ca^{2+}]_o$. Results from two-way ANOVA are reported as well as the specific time points where a statistical difference between the two calcium concentrations were reported by Bonferroni post-hoc test.

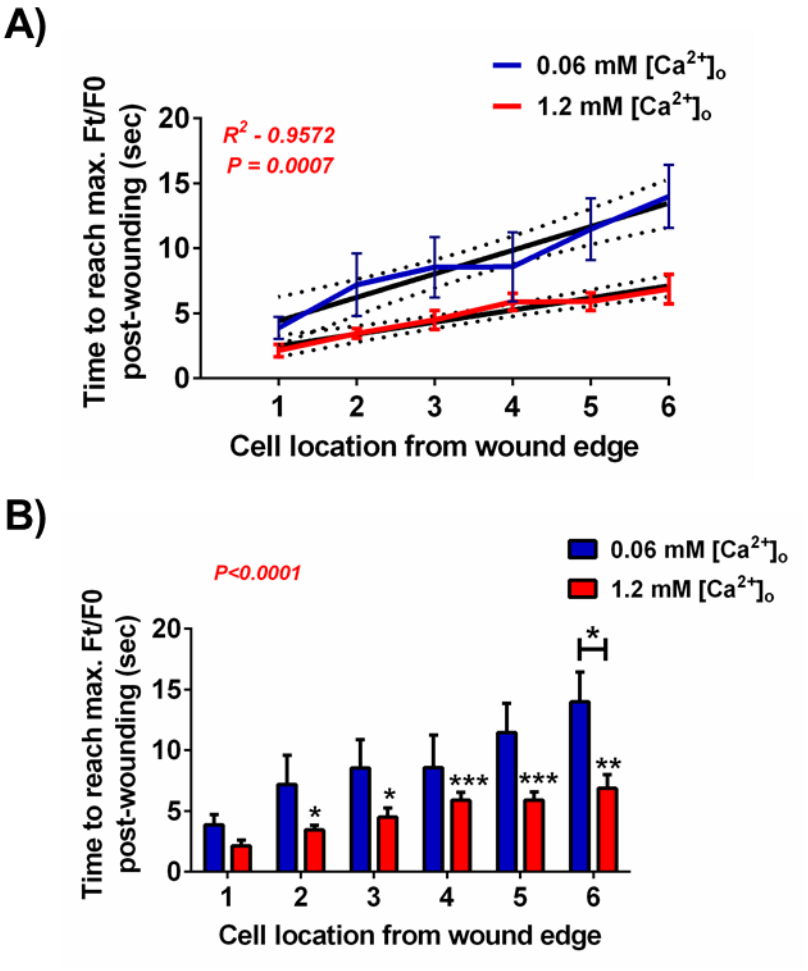

Figure 3.16 Time to reach maximum Ft/F0 calcium flux is decreased in wounds made in 1.2mM compared to 0.06mM $[Ca^{2+}]_o$.

Primary human keratinocytes cultured in 0.06mM $[Ca^{2+}]_o$ keratinocyte growth medium (MCDB 153) were loaded with Fluo4-AM calcium dye. Post-de-esterification, either 0.06mM or 1.2mM $[Ca^{2+}]_o$ keratinocyte growth media (MCDB 153) was added for five minutes prior to wounding. The time taken to reach maximum fold change (Ft/F0) calcium flux induced by wounding was analysed at each location from the wound edge. Data is shown in two forms for clarity. **A)** Linear regression analysis was conducted and the line of best-fit plotted (black line) with the 95% confidence intervals (dotted lines) for wounds made in 1.2mM $[Ca^{2+}]_o$ (red line). Data for wounds made in 0.06mM $[Ca^{2+}]_o$ is also shown (blue line) to visualise differences between the two external calcium concentrations. **B)** Time to reach maximal Ft/F0 in $[Ca^{2+}]_i$ flux for wounds made in 0.06mM and 1.2mM $[Ca^{2+}]_o$ were compared by two-way ANOVA ($F(1,132)=1834$, $P<0.0001$) and a Bonferroni post-hoc test (* $P<0.05$). A one-way ANOVA with a Dunnett's post-hoc (*** $P<0.001$, ** $P<0.01$, * $P<0.05$) and a post-test for linear trend ($P<0.0001$) was also conducted on data from 1.2mM experiments. Data shows mean ± SEM from 12 cells at each location from three independent donors; (n=72), N=3.

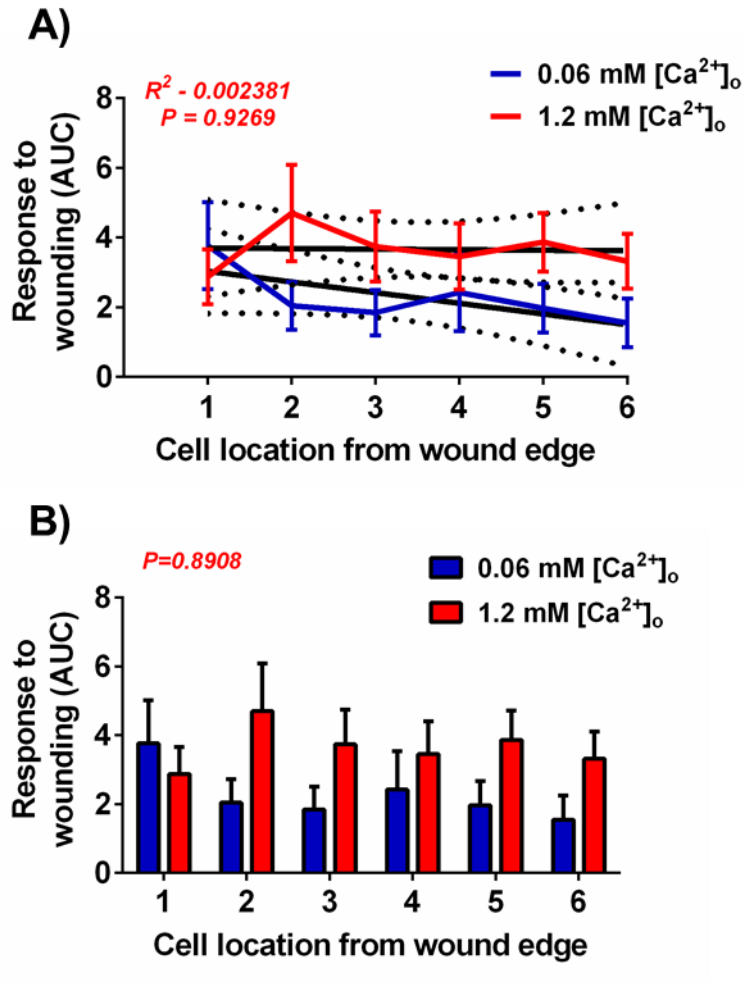

Figure 3.17 Area under the curve during wound-induced calcium flux within individual keratinocytes is greater in wounds made in 1.2mM $[Ca^{2+}]_o$.

Primary human keratinocytes cultured in 0.06mM $[Ca^{2+}]_o$ keratinocyte growth medium (MCDB 153) were loaded with Fluo4-AM calcium dye. Post-de-esterification, either 0.06mM or 1.2mM $[Ca^{2+}]_o$ keratinocyte growth media (MCDB 153) was added for five minutes prior to wounding. The area under the curve AUC during the initial calcium flux was calculated at each location from the wound edge. Data is shown in two forms for clarity. **A)** Linear regression analysis was conducted and the line of best-fit plotted (black line) with the 95% confidence intervals (dotted lines) for wounds made in 1.2mM $[Ca^{2+}]_o$ (red line). Data for wounds made in 0.06mM $[Ca^{2+}]_o$ is also shown (blue line) to visualise differences between the two external calcium concentrations. **B)** AUC of $[Ca^{2+}]_i$ flux for wounds made in 0.06mM and 1.2mM were compared by two-way ANOVA ($F(1,132)=6.671$, $P=0.0109$) A one-way ANOVA with a post-test for linear trend was also conducted on data from 1.2mM experiments ($P=0.8908$). Data shows mean ± SEM from 12 cells at each location from three independent donors; (n=72), N=3.

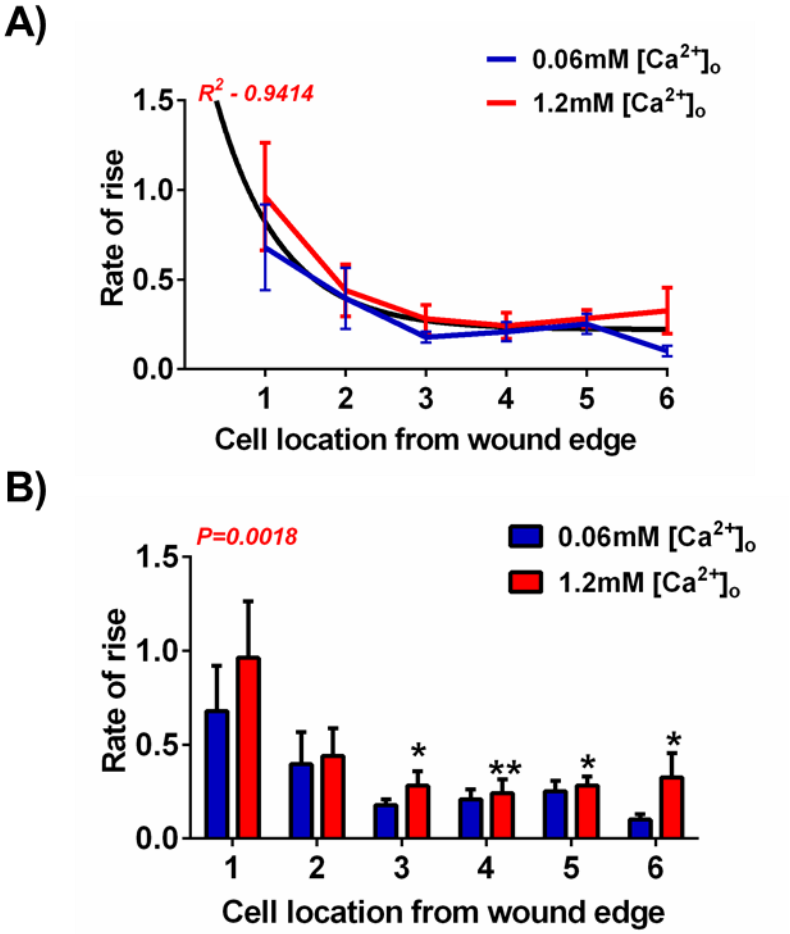

Figure 3.18 Extracellular calcium concentration has no effect on rate of rise of calcium flux within individual keratinocytes.

Primary human keratinocytes cultured in 0.06mM $[Ca^{2+}]_o$ keratinocyte growth medium (MCDB 153) were loaded with Fluo4-AM calcium dye. Post-de-esterification, either 0.06mM or 1.2mM $[Ca^{2+}]_o$ keratinocyte growth media (MCDB 153) was added for five minutes prior to wounding. The rate of rise (gradient of calcium increase) post-wounding was recorded at each location from the wound edge. Data is shown in two forms for clarity. **A)** A non-linear regression exponential decay graph was fitted to the data with an adjusted R^2 value of 0.9414 for wounds made in 1.2mM $[Ca^{2+}]_o$ (red line). Data for wounds made in 0.06mM $[Ca^{2+}]_o$ is also shown (blue line) to visualise differences between the two external calcium concentrations. **B)** Rate of rise of $[Ca^{2+}]_i$ flux for wounds made in 0.06mM and 1.2mM were compared by two-way ANOVA ($F(1,132)=2.198$, $P=0.1406$). A one-way ANOVA with a Dunnett's post-hoc (** $P<0.01$, * $P<0.05$) and a post-test for linear trend ($P=0.0018$) was also conducted on data from 1.2mM experiments. Data shows mean ± SEM from 12 cells at each location from three independent donors; (n=72), N=3.

Next, AUC of the wound-induced $[Ca^{2+}]_i$ flux was calculated in individual cells at each cell location back from the wound edge. AUC was used as an integrative quantitative measure of wound-induced calcium flux. The AUC of wound-induced calcium flux in 0.06mM calcium may be considered an approximation to calcium release from the ER (see section 3.3.1). The difference between AUC in 0.06 and 1.2mM calcium conditions may be considered to reflect calcium entry from the extracellular space. As shown by figure 3.17a, the AUC remained constant despite location from the wound edge; cells at the wound edge had an AUC of 2.87±0.78 whereas this value was 3.31±0.78 for cells located six rows back. The same analysis in 0.06mM $[Ca^{2+}]_o$ showed a trend for decreasing AUC the further away from the wound edge the cell was located. Linear regression reported an R^2 value of 0.002381 which was not deemed significantly different to zero (P=0.9269) (figure 3.17a). Similarly, a one-way ANOVA with a post-test for linear trend, did not report a significant trend in the data (P=0.8908) (figure 3.17b). The AUC of the calcium flux was significantly greater when wounding in 1.2mM $[Ca^{2+}]_o$ compared to 0.06mM $[Ca^{2+}]_o$ ($F(1,132)=6.671$, P=0.0109, two-way ANOVA), although this was not deemed significant at any specific location from the wound (P>0.05, Bonferroni post-hoc) (figure 3.17b).

Finally, the rate of rise of the wound-induced $[Ca^{2+}]_i$ flux was investigated. This was measured by calculating the slope of fluorescence intensity between the time the initiation of the wound-induced $[Ca^{2+}]_i$ flux and the time maximal Ft/F0 was achieved, this value represents the gradient of wound-induced calcium increase. As shown by figure 3.18, the rate of rise of the $[Ca^{2+}]_i$ flux when wounding in 1.2mM $[Ca^{2+}]_o$ decreased the further back from the wound the cell was located in a similar manner to that observed in 0.06mM $[Ca^{2+}]_o$. Cells at the wound edge had a rate of rise of 0.96±0.29 (ΔFt/F0/second) and those six cells back from the wound had a rate of rise of 0.32±0.12 (ΔFt/F)/second). A nonlinear regression exponential decay curve was fitted to the data and an adjusted R^2 value of 0.9414 was reported highlighting a high goodness of fit (figure 3.18a). A one-way ANOVA with Dunnett's post-hoc revealed a statistical difference between cell location and rate of rise ($F(5,66)=3.176$, P=0.0125) and cells 3, 4, 5 and 6 had a significantly reduced rate of rise compared to cell 1 (** P<0.01, * P<0.05). A post-test for linear trend also reported a significant trend for a decreased rate of rise the further back from the wound edge (P=0.0018) (figure 3.18b). A comparison of curve analysis was conducted on rate of rise from 0.06mM and 1.2mM $[Ca^{2+}]_o$ and

showed one curve fitted both data sets (F(3,138)=1.063, P=0.3672). Thus demonstrating that there was no difference in rate of rise in individual cells when wounding in 0.06mM or 1.2mM $[Ca^{2+}]_o$ (figure 3.18a), this was further supported by a two-way ANOVA (F(1,132)=2.198, P=0.1406) (figure 3.18b).

Collectively, these data suggest that a calcium entry pathway is activated in response to wounding in primary human keratinocytes as evidenced by i) elevated maximum Ft/F0 achieved by wounding, ii) increased AUC of the $[Ca^{2+}]_i$ flux and iii) reduced time to reach maximal Ft/F0 when wounding in 1.2mM $[Ca^{2+}]_o$. Compared to 0.06mM $[Ca^{2+}]_o$, interestingly, both AUC and maximum peak were unaffected by external calcium concentrations in cells located in close proximity to the wound edge. This indicates that induction of the wave at the wound edge and propagation to immediate neighbouring cells was not influenced by influx of calcium from extracellular compartments. In contrast, maximum Ft/F0 and AUC were increased in cells further back from the wound. This is indicative of a calcium entry pathway being activated by wounding causing an influx of calcium from the external environment to maintain an elevated calcium signal within these cells. Intriguingly, rate of rise was the only parameter examined that was not affected by external calcium at cell locations both close to and further back from the wound edge. If rate of rise is taken to be the rate at which calcium is released from intracellular stores, such as the ER, this decrease irrespective of external calcium concentration may indicate that the increase in $[Ca^{2+}]_i$ seen when wounding in 1.2mM $[Ca^{2+}]_o$ is due to calcium entry causing an elevated $[Ca^{2+}]_i$, rather than increased calcium release from the ER through IP_3R activation.

3.3.3 GSK-7975A as a store-operated calcium entry (SOCE) inhibitor.

GSK-7975A has been shown to be an effective store-operated calcium entry (SOCE) inhibitor, by interfering with the Orai1 selectivity pore filter (Derler *et al.*, 2013). However, its efficacy in primary keratinocytes has to date, not been investigated. To address this, primary human keratinocytes cultured in 0.06mM $[Ca^{2+}]_o$ keratinocyte growth medium (MCDB 153) were loaded with Fluo4-AM calcium dye and wounded in MCDB 153 adjusted to 1.2mM. Cells were exposed to 1.2mM $[Ca^{2+}]_o$ for five minutes prior to wounding. Prior to addition of 10µM GSK-7975A or 10µM diethylstilbestrol (DES), ER calcium stores were depleted using 3µM Tg in order to initiate SOCE. DES is a commercially available SOCE pharmacological inhibitor known to block SOCE in

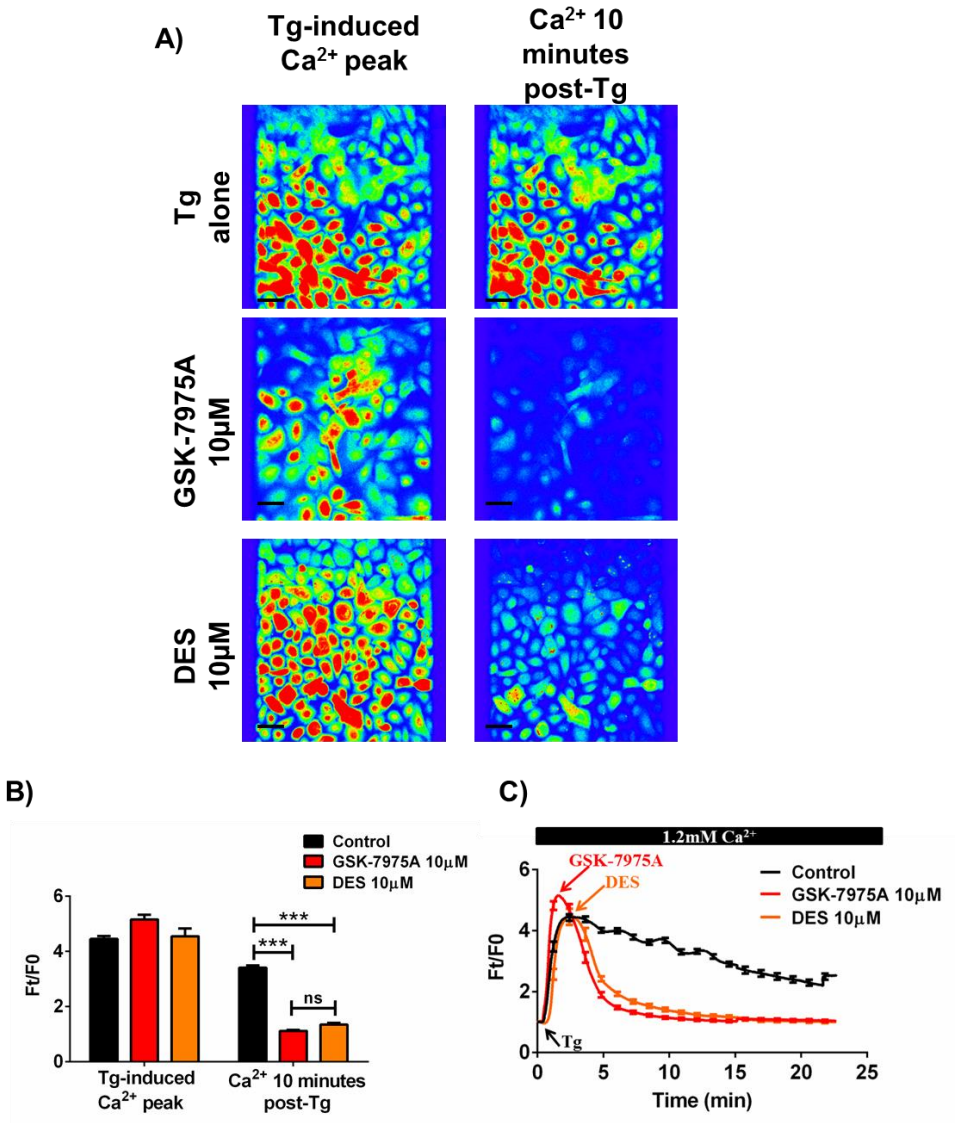

Figure 3.19 GSK-7975A effectively blocks SOCE.

Primary human keratinocytes cultured in 0.06mM $[Ca^{2+}]_o$ keratinocyte growth medium (MCDB 153) were loaded with Fluo4-AM calcium dye placed in 1.2mM $[Ca^{2+}]_o$ keratinocyte growth medium (MCDB 153) for five minutes prior to imaging. Cells were treated with Tg to induce SOCE, two minutes later 10µM GSK-7975A or 10µM DES were added. **A)** Pseudo colour images of confocal images were generated at the maximum calcium peak induced by Tg and ten minutes post-Tg application. Scale bar=80µm. Pseudo colour reference is shown. Images are representative of three independent donors. **B)** Graphical representation of data. **C)** Trace for each treatment for twenty minutes. For clarity SEM has only been plotted every hundred seconds. Arrows show addition of specified compounds. Scale bar = 80µm. Data shows mean ± SEM from a total of 72 cells from three independent donors; (n=72), N=3. Two-way ANOVA ($F(2,426)=25.63$, $P<0.0001$) with Bonferroni post-hoc (*** $P<0.001$, ns $P>0.05$).

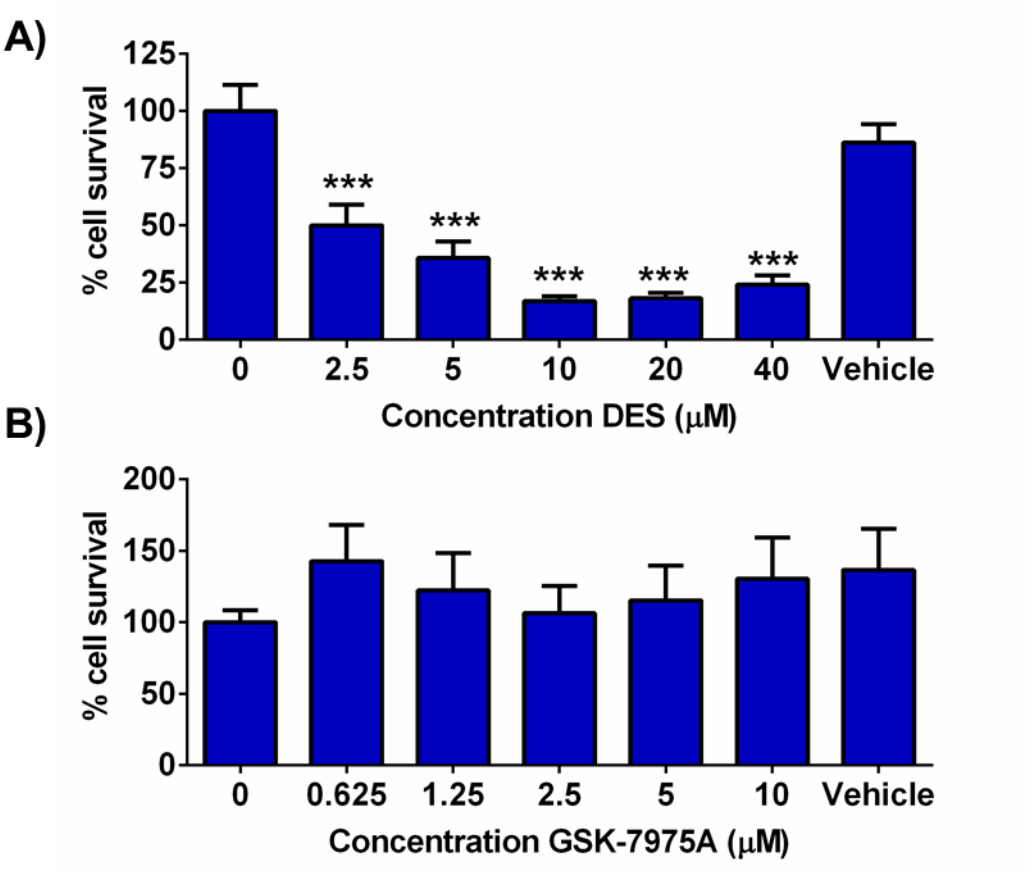

Figure 3.20 DES but not GSK-7975A is toxic to keratinocytes over twenty four hours.

Primary keratinocytes were treated with varying concentrations of **A)** DES or **B)** GSK-7975A for 24 hours. Cell viability was then analysed using SRB as described in materials and methods. Data shows mean ± SEM from 9 repeats from three independent donors (n=9), N=3. One-way ANOVA with Dunnett's post-hoc (*** $P<0.001$). MTT assays were conducted in parallel and report the same result.

primary keratinocytes at 10μM (Ralph Jans *et al.*, 2013) and was used as a positive control for SOCE inhibition. As shown by figure 3.19 the addition of GSK-7975A or DES rapidly reduced $[Ca^{2+}]_i$ to basal levels, demonstrating Tg-induced calcium entry had been blocked. In order to compare the effectiveness of the two inhibitors and the control, two time points were selected during the experiment; Tg-induced calcium peak and ten minutes post-Tg treatment. A shown by figure 3.19a, when no SOCE inhibitor was added, calcium levels ten minutes post-Tg remained elevated, consistent with Tg depleting the ER stores and initiating SOCE. The addition of DES or GSK-7975A caused a significant reduction in $[Ca^{2+}]_i$ ten minutes post-Tg treatment compared to control ($F(2,426)=25.63$, $P<0.0001$, ***$P<0.001$, two-way ANOVA with Bonferroni post-hoc). No significant difference was reported between DES and GSK-7975A ($P>0.05$) (figures 3.19b and 3.19c).

The previous experiments demonstrated that GSK-7975A and DES both effectively prevented SOCE in primary human keratinocytes, thus making them suitable candidates for exploring downstream effects of wound-induced SOCE. However, cell viability assays demonstrated that DES was highly toxic to primary human keratinocytes at twenty four hours compared to untreated cells (*** $P<0.001$, One-way ANOVA, Dunnett's post-hoc test). On the other hand, GSK-7975A did not appear to cause any significant toxic effects (figure 3.20).

3.3.4 The role of SOCE in the wound-induced calcium wave.

It was previously demonstrated in section 3.3.2, that wounding in a high external calcium environment altered parameters of the wound-induced calcium wave compared to wounding in a lower external calcium environment. Specifically, maximal Ft/F0 achieved by wounding was increased, time to reach maximum Ft/F0 after wounding was reduced and AUC of the wound-induced $[Ca^{2+}]_i$ flux was increased. Moreover, whereas the wave was shown to reduce with increasing distance from the wound edge in 0.06mM $[Ca^{2+}]_o$, calcium signalling within individual cells located further away from the wound were comparable with those at the wound edge when wounding in 1.2mM $[Ca^{2+}]_o$. It was therefore concluded that wounding activated calcium entry and subsequent influx of calcium into the cell elevated the cytosolic calcium concentration and prolonged the $[Ca^{2+}]_i$ in cells distal to the wound edge.

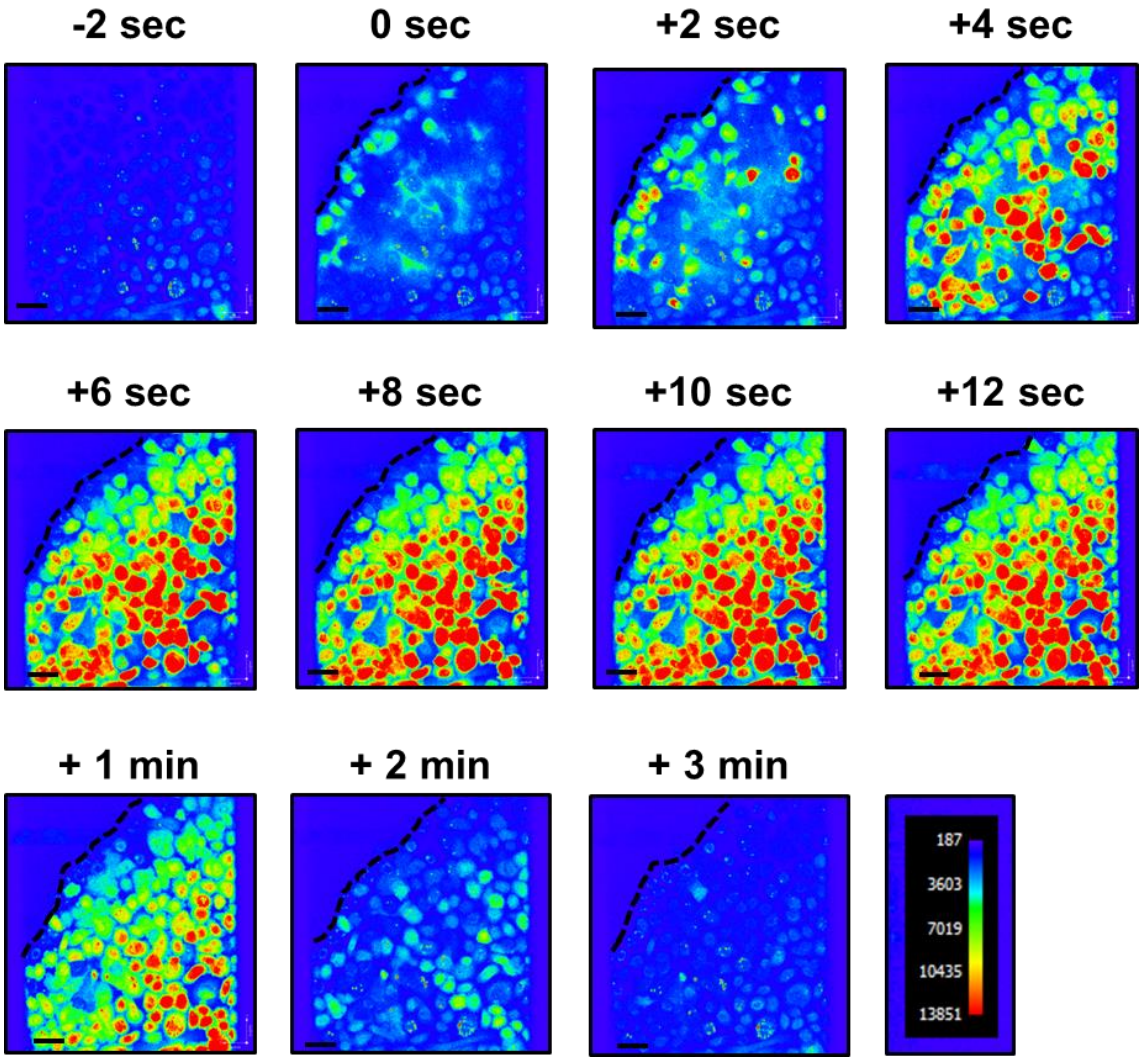

Figure 3.21 2D images demonstrating the wound-induced calcium wave post-treatment with GSK-7975A.

Primary human keratinocytes cultured in 0.06mM $[Ca^{2+}]_o$ keratinocyte growth medium (MCDB 153) were loaded with Fluo4-AM calcium dye and during the de-esterification forty five minutes cells were treated with 10µM GSK-7975A. Keratinocytes were switched 1.2mM $[Ca^{2+}]_o$ keratinocyte growth medium (MCDB 153) in the presence of 10µM GSK-7975A for five minutes prior to wounding. Pseudo colour images of confocal images were generated prior to the wound being made (-2 sec), at the point of wounding (0 sec) and then every 2 seconds for twelve seconds to demonstrate the visual appearance of the calcium signal triggered by wounding. Additionally, pseudo colour images of confocal images were generated at minute intervals for three minutes post-wounding to demonstrate calcium signal return to baseline. Scale bar=80µm. Pseudo colour reference is shown. Wound edge is highlighted by dotted line. Images are representative of three independent donors.

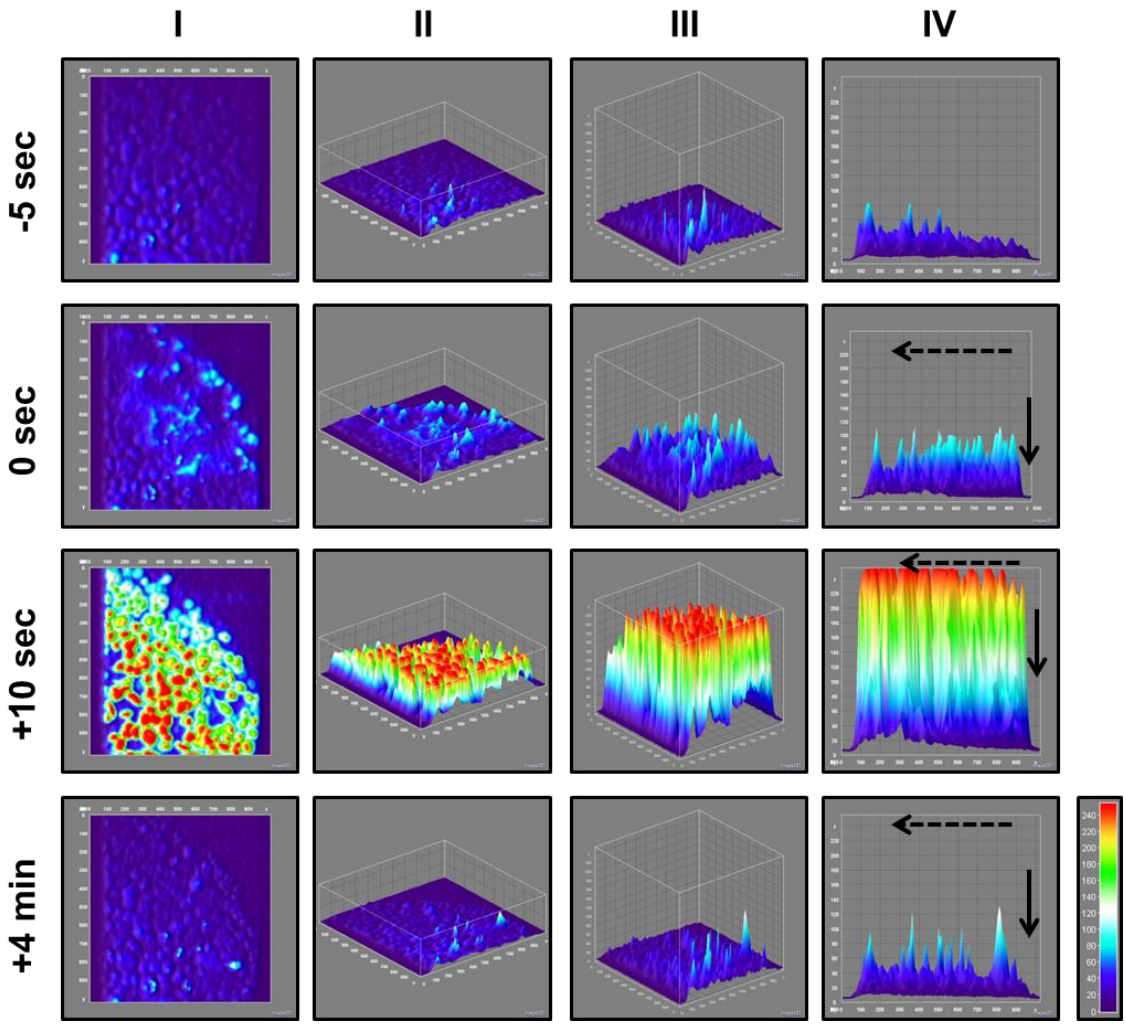

Figure 3.22 3D surface plots demonstrating the wound-induced calcium wave post-treatment with GSK-7975A.

Primary human keratinocytes cultured in 0.06mM $[Ca^{2+}]_o$ keratinocyte growth medium (MCDB 153) were loaded with Fluo4-AM calcium dye and during the de-esterification forty five minutes cells were treated with 10µM GSK-7975A. Keratinocytes were switched to 1.2mM $[Ca^{2+}]_o$ keratinocyte growth medium (MCDB 153) in the presence of 10µM GSK-7975A for five minutes prior to wounding. 3D surface plots of confocal images of the wound shown in figure 3.21 were created using ImageJ. Wound-induced calcium flux is shown from four view points and four specified times post-wounding. Column I shows the 2D image, column II depicts the same view as column III but with the Z-ratio equal to the XY-ratio in order to increase visual clarity of the spread of the wave, column III shows a diagonal cross section view and column IV shows the side view of the wave spreading from the wound back through cells (wound is located on the right hand side of the image (arrow), travelling left back through cells, direction highlighted by dotted arrow). Thermal LUT colour was adopted to increase visualisation of changes in fluorescence intensity. Thermal LUT scale reference is shown. Images are representative of three independent donors.

SOCE is a major calcium entry pathway in both excitable and non-excitable cells. Since its discovery thirty years ago, it has been implicated in many physiological and pathological processes (Feske *et al.*, 2006). However, its role in wound-induced calcium wave spread in primary keratinocytes has not yet been characterised. To address this, it was hypothesised that pharmacological inhibition of SOCE would prevent calcium influx from the extracellular compartment and reduce the elevated maximal Ft/F0 achieved by wounding and AUC observed when wounding in 1.2mM $[Ca^{2+}]_o$ compared to 0.06mM $[Ca^{2+}]_o$.

For the following experiments, primary human keratinocytes cultured in 0.06mM $[Ca^{2+}]_o$ keratinocyte growth medium (MCDB 153) were loaded with Fluo4-AM calcium dye prior to treatment with 10µM GSK-7975A or vehicle (DMSO), during the subsequent forty five minute de-esterification period. Keratinocytes were then wounded in supplemented keratinocyte growth medium (MCDB 153) to increase the calcium concentration to 1.2mM in the presence of 10µM GSK-7975A. Initially, signalling across the whole population of cells was visually assessed. Subsequently, sub-populations were defined by their location from the wound edge and analysed to provide insights into differences between cells located at the wound edge compared to those located further back. Figure 3.21 showed representative images from one experiment taken every two seconds for twelve seconds and then three later images taken at minute intervals post-wounding, visually depicting the $[Ca^{2+}]_i$ changes triggered by wounding. In a similar manner to untreated cells (figure 3.4), it was clear that at the time of wounding, $[Ca^{2+}]_i$ increased at the wound edge which spread as a wave through neighbouring cells. This can further be seen by the use of 3D surface plots, created using ImageJ (figure 3.22).

In order to identify any differences between characteristics of the spread of the calcium wave back from the wound edge with GSK-7975A treatment, $[Ca^{2+}]_i$ flux within individual cells were analysed according to the location of the cells away from the wound edge, as described previously (section 3.3.1). As demonstrated by figure 3.24, the average flux induced by wounding in 1.2mM $[Ca^{2+}]_o$ in cells located at the wound edge was significantly increased in the presence of GSK-7975A compared to vehicle ($F(1,11)=8.018$, $P=0.0163$, RM two-way ANOVA). A Bonferroni post-hoc test revealed

.

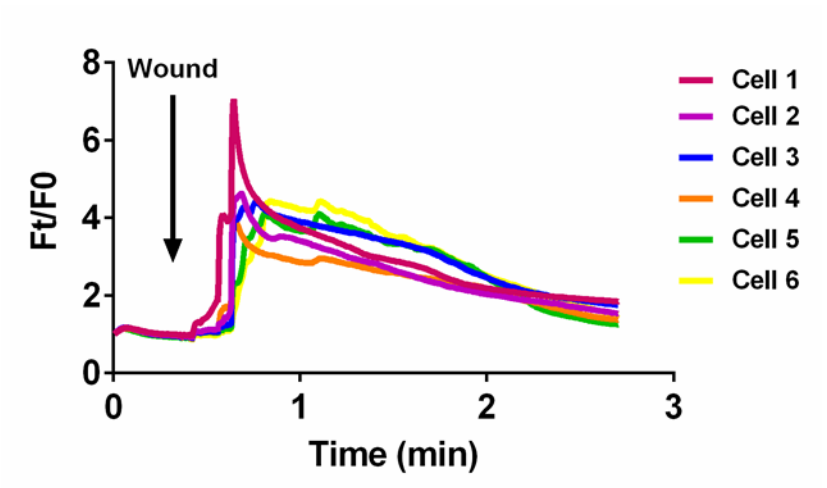

Figure 3.23 Wound-induced calcium flux occurs in cells at least six rows back from the wound in 1.2mM $[Ca^{2+}]_o$ in the presence of GSK-7975A.

Primary human keratinocytes cultured in 0.06mM $[Ca^{2+}]_o$ keratinocyte growth medium (MCDB 153) were loaded with Fluo4-AM calcium dye and during the de-esterification forty five minutes cells were treated with 10µM GSK-7975A. Keratinocytes were wounded in 1.2mM $[Ca^{2+}]_o$ keratinocyte growth medium (MCDB 153) in the presence of 10µM GSK-7975A. $[Ca^{2+}]_i$ flux within individual cells was analysed according to the location of the cells away from the wound edge. Individual keratinocytes were analysed in "rows" away from the wound edge and cells were designated 1-6, with Cell 1 being the cell at the wound edge, and Cell 6 located six cells back from the wound. Data shows mean from 12 cells from three independent donors at each location; (n=12), N=3. In order to facilitate visualisation of $[Ca^{2+}]_i$ flux at each location, error bars are not shown on the graph.

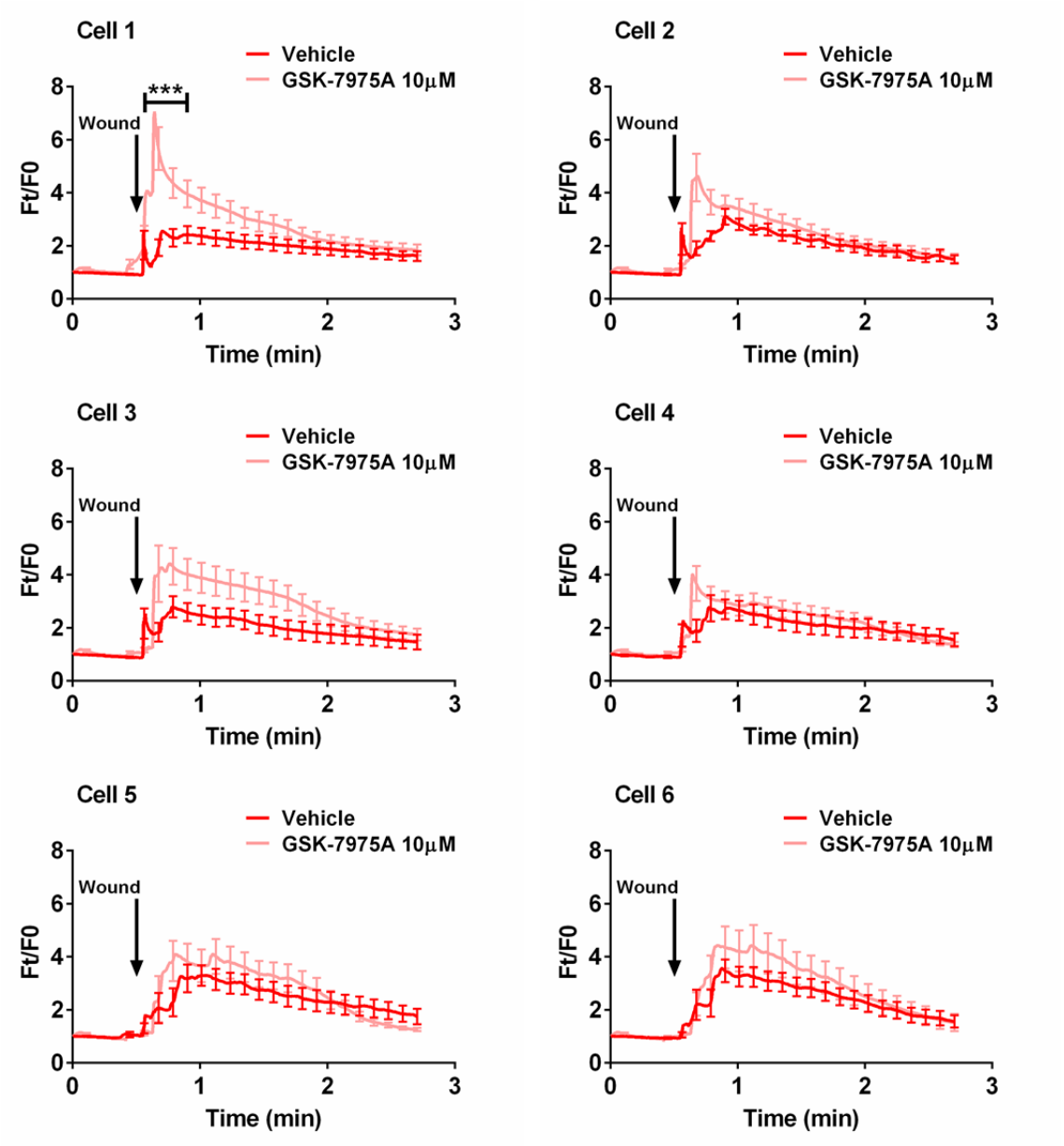

Figure 3.24 SOCE inhibition increases wound-induced $[Ca^{2+}]_i$ flux in cells located at the wound edge but cells further back are not affected by GSK-7975A.

Wound-induced calcium flux in cells were analysed according to their location from the wound edge termed 1-6, with Cell 1 being at the wound edge and Cell 6 located six cells back from the wound. Each plot shows wounds made with vehicle (DMSO) treatment or GSK-7975A 10µM treatment in 1.2mM $[Ca^{2+}]_o$. Time of wound is highlighted by arrow. Data shows mean from 12 cells from three independent donors at each location; (n=12), N=3. For graphical clarity SEM has only been plotted every seven seconds. Two-way ANOVA with Bonferroni post-hoc test compared calcium flux between 0.06mM and 1.2mM $[Ca^{2+}]_o$ at each timepoint (*** P<0.001).

that this difference was significant between 0.56 and 0.89 minutes (*** P<0.001). However, at cell located two to six rows back from the wound, blocking SOCE did not significantly affect the wound-induced $[Ca^{2+}]_i$ flux (P=0.2454, P=0.1709, P=0.6494, P=0.5981, P=0.2987 respectively, RM two-way ANOVA).

These data provide evidence that SOCE inhibition does not affect the ability of wounding to trigger an $[Ca^{2+}]_i$ flux. However, to investigate whether treatment altered characteristics of the calcium wave, maximum Ft/F0 achieved by wounding, time to reach maximum Ft/F0 post-wounding, AUC of the $[Ca^{2+}]_i$ flux and rate of rise of the $[Ca^{2+}]_i$ flux were examined compared to vehicle (DMSO).

Maximum Ft/F0 post-wounding was recorded for each of the six cell locations from the wound edge. From figure 3.25, it appears that wounding in the presence of GSK-7975A caused a greater increase in maximum $[Ca^{2+}]_i$ in cells at the wound edge (cell 1) compared to vehicle treated. No differences can be seen between GSK-7975A and vehicle treatment at all other cell locations. Regression analysis was performed and reported an R^2 value of 0.5499 (P=0.0915) (figure 3.25a). A one-way ANOVA with Dunnett's post-hoc revealed a statistical difference between cell location and maximum Ft/F0 ($F(2.816,30.97)=4.111$, P=0.00160) with cells 3, 4 and 5 having a significantly increased maximum Ft/F0 compared to cell 1 (** P<0.01, * P<0.05). A post-test for linear trend also reported a significant trend for a decreased maximum Ft/F0 the further back from the wound edge (P=0.0014) (figure 3.25b). Statistical analysis using a two-way ANOVA to compare treatments revealed that overall, GSK-7975A treatment had a significant effect on maximum Ft/F0 ($F(1,132)=7.495$, P=0.0070). However, a Bonferroni post-hoc test reported the only location relative to the wound where this difference was significant was cell 1 (** P<0.01) (figure 3.25b).

Qualitative interpretation of this data suggested that the large increase in maximum Ft/F0 with GSK-7975A treatment in cells located at the wound edge was influencing the statistical analysis, evidenced by similar values obtained from maximal Ft/F0 reached in cells 2-6 regardless of treatment condition. Therefore, it was speculated that these data was presenting a false positive trend for diminishing maximal Ft/F0 with location from the wound. To further explore this possibility, statistical analysis was repeated excluding the data from cell 1 for both treated and vehicle. A one-way ANOVA showed no relationship between cell location and treatment ($F(2.321,25.53)=0.4648$, P=0.6616).

A post-test for linear trend did not report a significant result (P=0.4678). Similarly, a two-way ANOVA did not report any significant effects of treatment on maximum Ft/F0 reached post-wounding (F(1,110)=2.453, P=0.1202). These analyses indicate that there may not be a significant trend for a diminishing maximum Ft/F0 with increased distance from the wound edge and results should be interpreted with caution.

Visual evaluation of the wound-induced $[Ca^{2+}]_i$ flux after treatment with GSK-7975A suggested that the calcium signal travelled between cells as a wave, akin to untreated experiments. As expected for a wave, the $[Ca^{2+}]_i$ changes were delayed for keratinocytes at increasing distance from the wound edge. Thus for example, cells at the wound edge reached their maximum Ft/F0 increase in 5.40±1.85 seconds compared to 16.11±2.12 seconds for cells six rows back in 1.2mM $[Ca^{2+}]_o$. A one-way ANOVA with Dunnett's post-hoc showed cell location significantly affected time to reach maximal Ft/F0 (F(2.45,26.99)=4.830, P=0.0116) with cell 5 and cell 6 taking significantly longer to reach maximum Ft/F0 compared to cell 1 (** P<0.01, * P<0.05). A post-test for linear trend also reported a significant trend for a decreased maximum time to reach Ft/F0 the further back from the wound edge (P<0.0001) (figure 3.26a). As shown by figure 3.26, the wave took a significantly longer time to reach six cells back from the wound edge when wounds were performed in the presence of GSK-7975A compared to vehicle (F(1,132)=4.511, P=0.0355, two-way ANOVA), although a Bonferroni post-hoc failed to reveal any significant differences at specific cell locations from the wound (figure 3.26b).

Next, AUC of the wound-induced $[Ca^{2+}]_i$ flux was calculated in individual cells at each cell location back from the wound edge in vehicle and GSK-7975A treated cells. AUC was used as an integrative quantitative measure of wound-induced calcium flux. Any differences between AUC in GSK-7975A and vehicle conditions may be considered to reflect calcium entry from the extracellular space. From figure 3.27 is appears that the AUC remained constant despite location from the wound edge; cells at the wound edge had an AUC of 2.18±0.63 whereas this value was 3.74±1.12 for cells located six rows back. The same analysis in 0.06mM $[Ca^{2+}]_o$ showed a trend for decreasing AUC the further away from the wound edge the cell was located. Linear regression analysis reported an R^2 value of 0.4887, which was not deemed significantly different to zero (P=0.1222) (figure 3.27a). Similarly, a one-way ANOVA with a post-test for linear

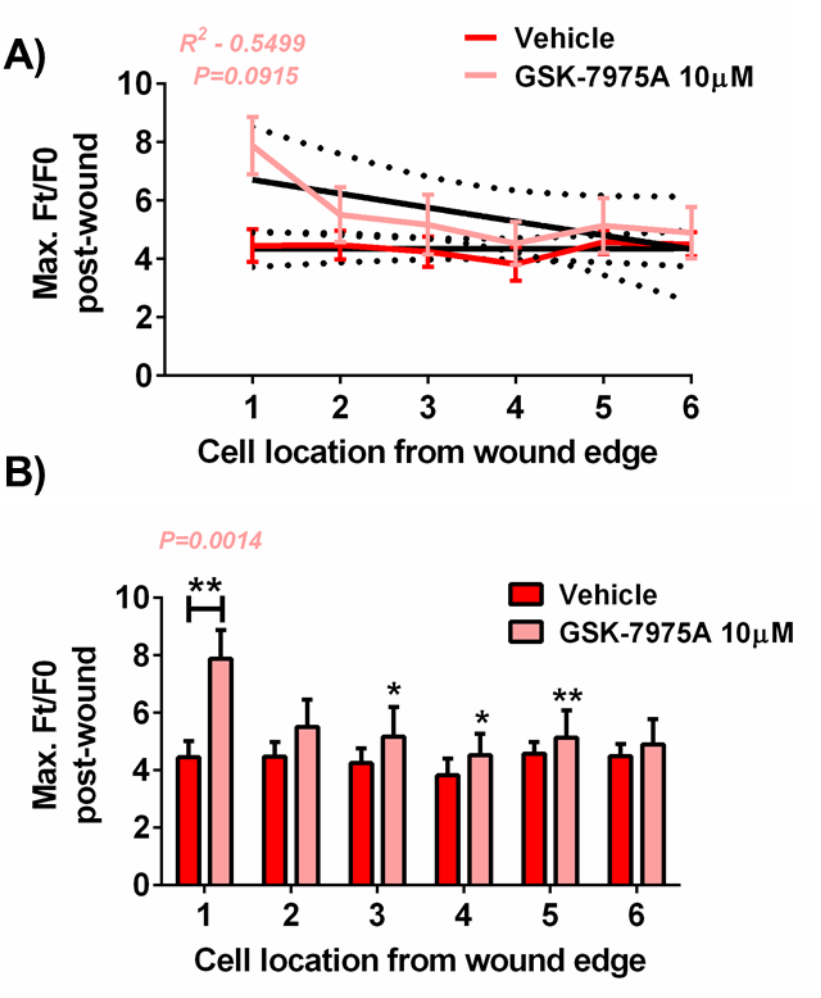

Figure 3.25 SOCE inhibition increases maximum Ft/F0 within individual cells located at the wound edge.

Primary human keratinocytes cultured in 0.06mM $[Ca^{2+}]_o$ keratinocyte growth medium (MCDB 153) were loaded with Fluo4-AM calcium dye and during the de-esterification forty five minutes cells were treated with 10µM GSK-7975A. Keratinocytes were wounded in 1.2mM $[Ca^{2+}]_o$ keratinocyte growth medium (MCDB 153) in the presence of 10µM GSK-7975A. The maximum fold change (Ft/F0) in calcium flux induced by wounding compared to the baseline was analysed at each location from the wound edge. Data is shown in two forms for clarity. **A)** Linear regression analysis was conducted and the line of best-fit plotted (black line) with the 95% confidence intervals (dotted lines). **B)** Maximal Ft/F0 in $[Ca^{2+}]_i$ flux for wounds made 1.2mM $[Ca^{2+}]_o$ in the presence or absence of GSK-7975A were compared by two-way ANOVA ($F(1,132)=7.495$, $P=0.0070$) and a Bonferroni post-hoc test (** $P<0.01$). Data shows mean ± SEM from 12 cells at each location from three independent donors; (n=72), N=3.

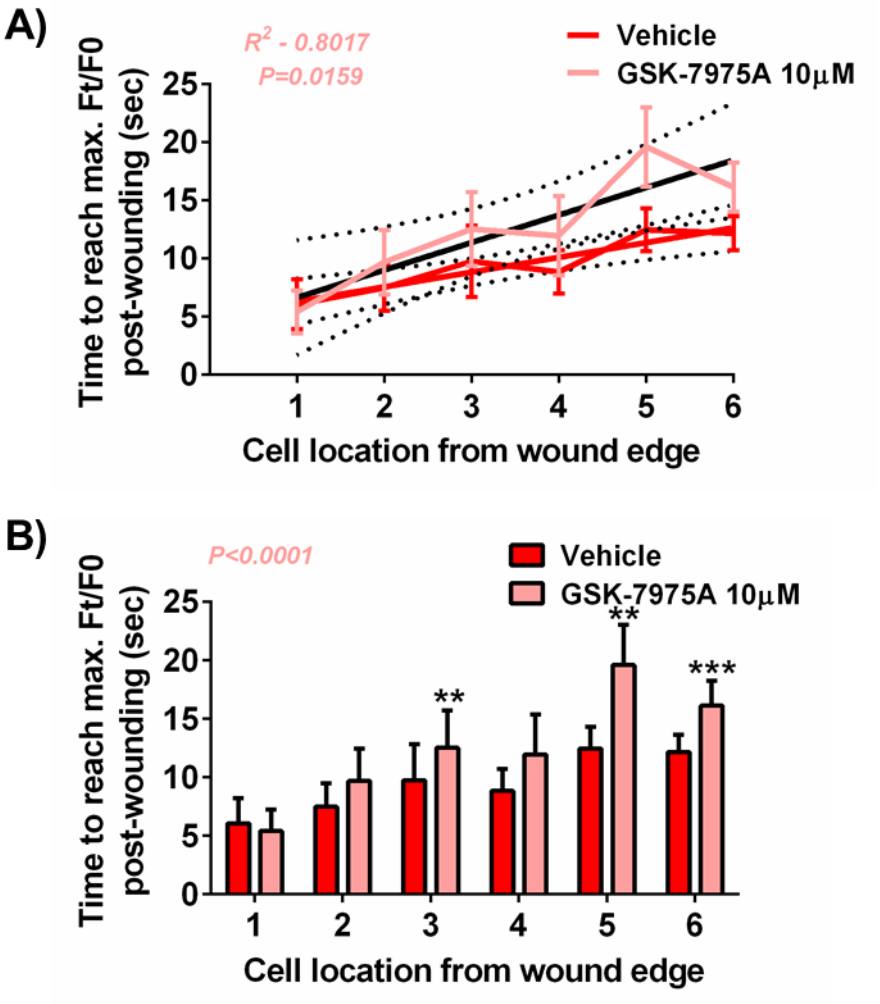

Figure 3.26 Time to reach maximum Ft/F0 calcium flux is increased in wounds made in 1.2mM $[Ca^{2+}]_o$ with GSK-7975A treatment.

Primary human keratinocytes cultured in 0.06mM $[Ca^{2+}]_o$ keratinocyte growth medium (MCDB 153) were loaded with Fluo4-AM calcium dye and during the de-esterification forty five minutes cells were treated with 10µM GSK-7975A. Keratinocytes were wounded in 1.2mM $[Ca^{2+}]_o$ keratinocyte growth medium (MCDB 153) in the presence of 10µM GSK-7975A. The time taken to reach maximum fold change (Ft/F0) calcium flux induced by wounding was analysed at each location from the wound edge. Data is shown in two forms for clarity. **A)** Linear regression analysis was conducted and the line of best-fit plotted (black line) with the 95% confidence interval (dotted lines). **B)** Data was plotted and a one-way ANOVA conducted with Dunnett's post-hoc test to compare time to reach maximum Ft/F0 at cell locations compared to Cell 1 with GSK-7975A treatment ($F(2.45,26.99)=4.830$, $P=0.0116$) (*** $P<0.001$, ** $P<0.01$, * $P<0.05$). A post-test for linear trend was also conducted ($P<0.0001$). Time to reach maximum Ft/F0 wounds made 1.2mM $[Ca^{2+}]_o$ in the presence or absence of GSK-7975A were compared by two-way ANOVA with a Bonferroni post-hoc ($F(1,132)=4.511$, $P=0.0355$). Data shows mean ± SEM from 12 cells at each location from three independent donors; (n=72), N=3.

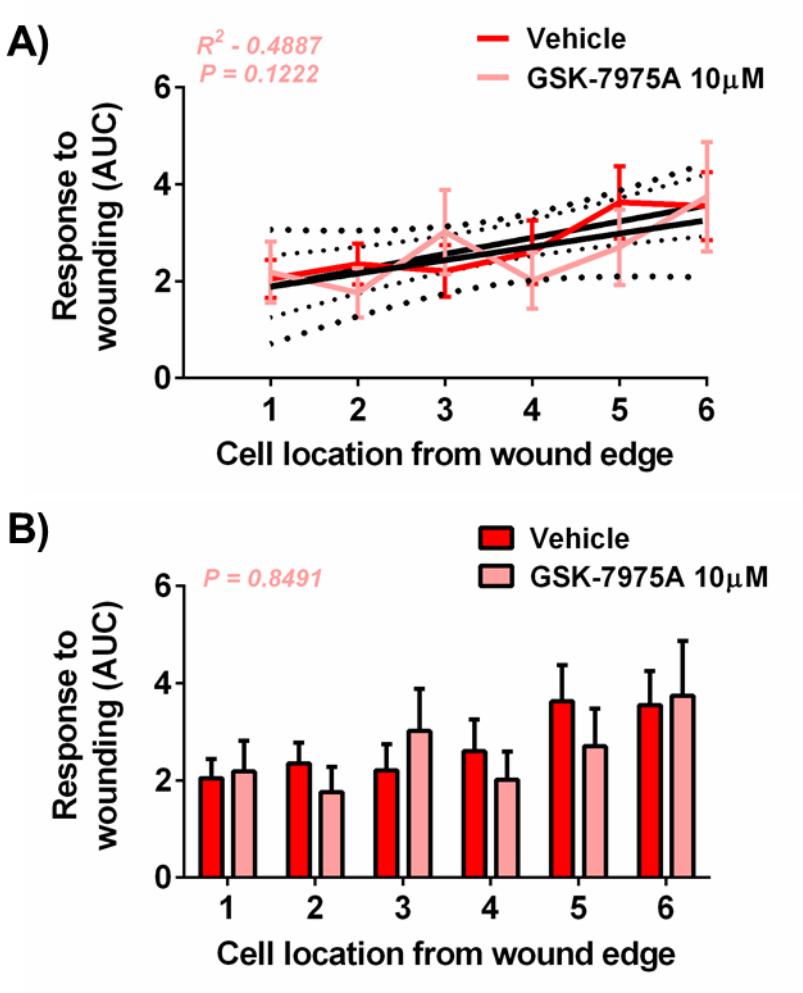

Figure 3.27 AUC of $[Ca^{2+}]_i$ flux is unaffected by SOCE inhibition.

Primary human keratinocytes cultured in 0.06mM $[Ca^{2+}]_o$ keratinocyte growth medium (MCDB 153) were loaded with Fluo4-AM calcium dye and during the de-esterification forty five minutes cells were treated with 10µM GSK-7975A. Keratinocytes were wounded in 1.2mM $[Ca^{2+}]_o$ keratinocyte growth medium (MCDB 153) in the presence of 10µM GSK-7975A. The AUC of the calcium flux induced by wounding was analysed at each location from the wound edge. Data is shown in two forms for clarity. **A)** Linear regression analysis was conducted and the line of best-fit plotted (black ine) with the 95% confidence interval (dotted lines). **B)** Data was plotted and a one-way ANOVA conducted with Dunnett's post-hoc test to compare AUC at cell locations compared to Cell 1 (P=0.8843) with GSK-7975A treatment. A post-test for linear trend was also conducted (P=0.8491). AUC for wounds made 1.2mM $[Ca^{2+}]_o$ in the presence or absence of GSK-7975A were compared by two-way ANOVA (F(1,132)=0.1591, P=0.6909). Data shows mean ± SEM from 12 cells at each location from three independent donors; (n=72), N=3.

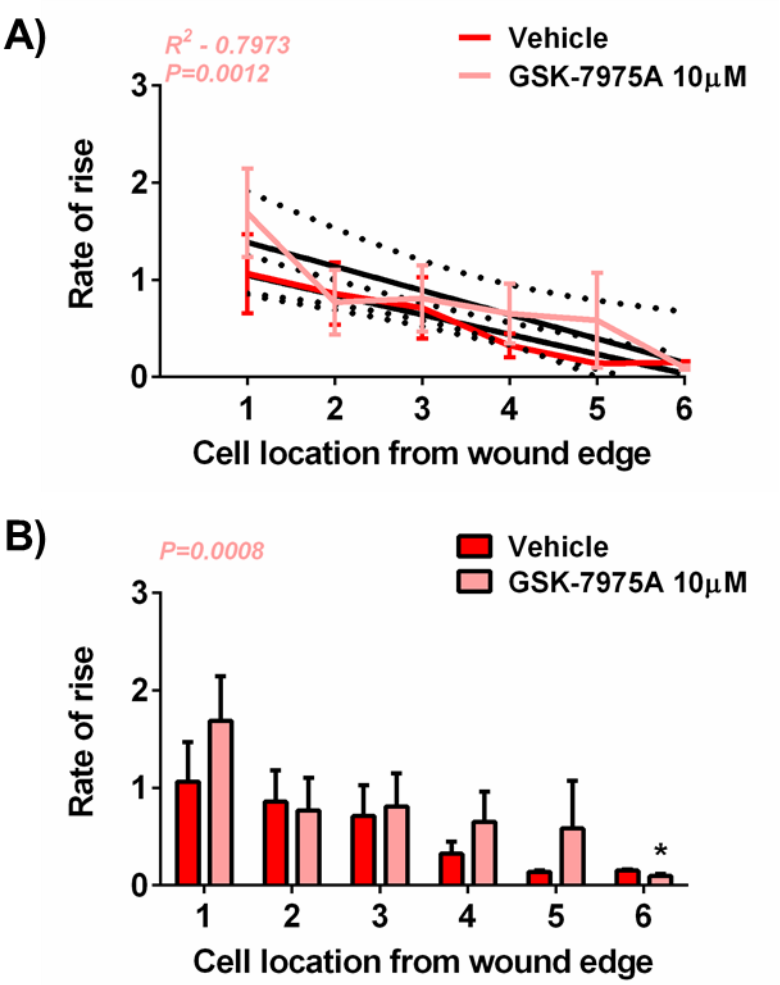

Figure 3.28 Rate of rise of $[Ca^{2+}]_i$ flux is unaffected by SOCE inhibition.

Primary human keratinocytes cultured in 0.06mM $[Ca^{2+}]_o$ keratinocyte growth medium (MCDB 153) were loaded with Fluo4-AM calcium dye and during the de-esterification forty five minutes cells were treated with 10µM GSK-7975A. Keratinocytes were wounded in 1.2mM $[Ca^{2+}]_o$ keratinocyte growth medium (MCDB 153) in the presence of 10µM GSK-7975A. The rate of rise of the calcium flux induced by wounding was analysed at each location from the wound edge. Data is shown in two forms for clarity. **A)** Linear regression analysis was conducted and the line of best-fit plotted (black line) with the 95% confidence intervals (dotted lines). **B)** Data was plotted and a one-way ANOVA conducted with Dunnett's post-hoc test to compare rate of rise at cell locations compared to Cell 1 (P=0.0615) with GSK-7975A treatment. A post-test for linear trend was also conducted (P=0.0008). Rate of rise for wounds made 1.2mM $[Ca^{2+}]_o$ in the presence or absence of GSK-7975A were compared by two-way ANOVA ($F(1,132)=1.595$, $P=0.1406$). Data shows mean ± SEM from 12 cells at each location from three independent donors; (n=72), N=3.

trend, did not report a significant trend in the data (P=0.8843). From these data it can be seen that blocking SOCE with GSK-7975A, did not significantly affect the AUC of the $[Ca^{2+}]_i$ flux (F(1,132)=0.1591, P=0.6909, two-way ANOVA) (figure 3.27b).

Finally, the rate of rise of the wound-induced $[Ca^{2+}]_i$ flux was investigated. This was measured by calculating the slope of fluorescence intensity between the time the initiation of the wound-induced $[Ca^{2+}]_i$ flux and the time maximal Ft/F0 was achieved, this value represents the gradient of wound-induced calcium increase. A shown by figure 3.28, the rate of rise of the $[Ca^{2+}]_i$ flux when wounding with GSK-7975A treatment decreased the further back from the wound the cell was located in a similar manner control. Cells at the wound edge had a rate of rise of 1.68±0.45 (ΔFt/F0/second) and those six cells back from the wound had a rate of rise of 0.096±0.02 (ΔFt/F0/second). Although a one-way ANOVA revealed no statistical difference between cell location and rate of rise (F(2.173,21.73)=3.106, P=0.0615) with GSK-7975A treatment, this was approaching significance. A post-test for linear trend reported a significant trend for a decreased rate of rise the further back from the wound edge (P=0.008). Data for both treatments were plotted simultaneously in order to assess any differences. The two data sets appear to follow the same pattern of a high rate of rise in cells located at the wound edge which then reduced as the wave travelled back from the wound edge. A two-way ANOVA statistical analysis showed no effect of GSK-7975A treatment on rate of rise (F(1,132)=1.595, P=0.1406) (figure 3.28b).

Taken together, these results suggest that SOCE regulates part of the intercellular calcium wave but not all parameters. Specifically, time to reach maximum Ft/F0 was significantly affected by SOCE inhibition. Cells located further back from the wound edge took longer to achieve maximum Ft/F0 with GSK-7975A treatment compared to cells at the same location without GSK-7975A treatment. This suggests that calcium influx from the extracellular compartment drives the transmission of the calcium wave, through SOCE mechanisms.

GSK-7975A treatment had no effect on rate of rise of the $[Ca^{2+}]_i$ flux. This result is perhaps non-surprising as increasing the calcium concentration of the extracellular environment in untreated conditions did not alter the rate of rise (section 3.3.2). In contrast, the AUC was significantly increased by extracellular calcium in untreated cells leading to the hypothesis that calcium entry was resulting in an increased $[Ca^{2+}]_i$ flux.

If this calcium entry was mediated by capacitative entry mechanisms, it would be expected that blocking SOCE in 1.2mM $[Ca^{2+}]_o$ with GSK-7975A would result in a reduced AUC in cells further back from the wound, similar to that seen when wounding in 0.06mM $[Ca^{2+}]_o$. Interestingly, GSK-7975A treatment did not affect the AUC of the wound-induced $[Ca^{2+}]_i$ flux; in 1.2mM $[Ca^{2+}]_o$ the AUC after treatment was comparable to vehicle treated cells, with both data sets displaying a constant AUC regardless of location from the wound edge. From this it can be concluded that the calcium entry mechanism causing the increased intracellular calcium flux is not SOCE mediated. The data from maximum Ft/F0 achieved by wounding was complex. Analysis of the whole data set suggested that SOCE inhibition had an overall positive effect on maximum Ft/F0 with GSK-7975A treatment resulting in an overall increased maximum Ft/F0. However, it was observed that the unexpected increase in GSK-79745A treatment within cells located at the wound edge may be influencing the statistical analysis as no differences could be seen between GSK-7975A treatment and vehicle in cells 2-6. This observation was confirmed by repeated statistical analysis on the data set excluding cell 1 i.e. cells 2-6 only. These reported no differences in maximal Ft/F0 with SOCE inhibition or any significant trends between maximum Ft/F0 and location from the wound in GSK-7975A experiments. This suggests that SOCE inhibition may not insignificantly alter the maximum Ft/F0 achieved post-wounding. The maximum Ft/F0 was significantly increased by extracellular calcium in untreated cells leading to the hypothesis that calcium entry was resulting in an increased $[Ca^{2+}]_i$ flux. If this calcium entry was mediated by capacitative entry mechanisms, it would be expected that blocking SOCE in 1.2mM $[Ca^{2+}]_o$ with GSK-7975A would result in a reduced maximum Ft/F0 in cells further back from the wound, similar to that seen when wounding in 0.06mM $[Ca^{2+}]_o$.

Combined it can be concluded from these investigations that whilst SOCE may be the calcium entry mechanism mediating the time taken to reach maximum Ft/F0 post-wounding, another non-capacitative calcium entry pathway regulates the influx of extracellular calcium resulting in increased AUC and maximal Ft/F0 in cells located further away from the wound edge in 1.2mM $[Ca^{2+}]_o$.

3.4 Discussion.

Mechanical stimulation causing an intercellular calcium wave is a common observation in many cell types. However, few studies have extensively investigated specific characteristics of the resultant calcium signalling in individual cells participating in the wave. This chapter aimed to explore specified parameters of the calcium wave induced by wounding, by assessing the time taken for the signal to travel through the cell population. Furthermore, intracellular calcium signalling was analysed within individual cells located at various distances from the wound edge in order to provide insights into intercellular calcium wave propagation in primary human keratinocytes

3.4.1 Distance travelled by the wave.

In order to ensure an adequate number of cells in the field of view post-wounding whilst still enabling both spatial and temporal analysis of signalling events, images were captured using a 20x magnification lens. Due to the restricted number of cells in the field of view, cells located up to six rows from the wound edge were analysed. It might have been beneficial to extend this to include more cells back from the wound edge, however, at 20x magnification; six was the maximum number of cells possible. Whilst reducing the magnification in future experiments would enable qualitative analysis of the distance from the wound edge the calcium wave travels, detailed analysis of intracellular calcium responses would be limited. The distance travelled by the wound-induced calcium wave in primary human keratinocytes has not been reported. Interestingly, the distance travelled by the calcium wave varies according to both cell type and stimulus. For example, Koenigsberger *et al.* showed in rat mesenteric arteries, phenylephrine triggered an intercellular calcium wave that travelled across eighty cells (Koenigsberger *et al.*, 2010). In contrast, HUVEC cells that were mechanically stimulated with a needle or force probe displayed an intercellular calcium wave that spread only 4-6 cells back (Junkin *et al.*, 2013). This was also seen in bovine aortic endothelial cells after mechanical stimulation by probing (Demer *et al.*, 1993) and more recently in human keratinocytes (Kobayashi *et al.*, 2014). Mathematical computational modelling of intercellular calcium wave propagation has been conducted using *in vitro* data from a variety of cell types. It was revealed, perhaps unsurprisingly, that the greater the stimulation the further the wave travelled. The scratch wounding technique utilised within this project represents a relatively gross stimulation method, with many cells

being damaged. Therefore, it would be hypothesised that the wave would travel a greater distance from the wound edge. As described above, images captured at a lower magnification would enable further analysis of this.

3.4.2 Characterisation of the wound-induced calcium wave.

It was hypothesised that quantitative analysis of specific parameters of the wound-induced calcium wave would provide novel insights into mechanisms transmitting the calcium wave in primary human keratinocytes. Results robustly demonstrated that wounding results in a calcium signalling cascade that travelled through the cell population as a wave. Investigations within this project did not completely decipher whether the wave was driven by calcium or IP_3 movement through cells, both of which have been reported previously (Saez *et al.*, 1989). However, data presented within this project is highly indicative of an IP_3-mediated method of transmission. Thus the pattern of calcium signalling within individual cells has also been reported to be a key factor in determining the method of transmission. The observation of all cells displaying a similar increase in Ft/F0 post-wounding regardless of cell location from the wound edge would be indicative of calcium ions mediating the wave (Leybaert and Sanderson, 2012). This is because calcium-induced calcium release (CICR) is self-limiting and would continue as long as there was calcium present in the intracellular stores. However, results from this project show that at increasing distance from the wound edge, maximum Ft/F0 reached post-wounding, AUC of the $[Ca^{2+}]_i$ flux and the rate of rise of the calcium flux were all significantly reduced. This pattern of response is highly suggestive of an IP_3-mediated calcium wave (Sneyd *et al.*, 1995). Last year, Junkin *et al.* used plasma lithography geometric confinement, to assess injury-induced calcium wave propagation in HUVEC. Characteristics of intracellular signalling such as fluorescence intensity at varying locations from the wound edge were analysed in a similar manner to those conducted within this project. Similarly, results showed that cells located further back from the wound displayed a reduced calcium flux compared to cells located closer to the wound edge (Junkin *et al.*, 2013). However, the main evidence against a calcium-mediating wave comes from add-back experiments (Chapter 5). The add-back of high calcium post-wounding resulted in a calcium flux in a sub-population of cells, however, this did not initiate calcium signalling in neighbouring

cells in the form of a wave. Thus implying that intracellular calcium elevation alone does not cause or initiate a calcium wave.

Visual analysis of data collected within this project showed a wave-like spread of calcium from the wound edge back across the cell population. It was therefore unsurprising that quantitative analysis showed that the time taken to reach maximum Ft/F0 increased the further back from the wound the cell was located, in a highly linear manner. Again, this observation has been reported to be consistent with IP_3 movement through cells by computational models (Sneyd *et al.*, 1995).

Further experiments would need to be conducted in order to confirm the dominant role of IP_3 in mediating the intercellular calcium wave post-wounding. Such experiments would involve iontophoretically injecting IP_3 into individual keratinocytes. If IP_3 was the driving force behind the calcium wave, one would expect injection to trigger an intercellular calcium wave spreading from the stimulated cell through neighbouring cells. This has been observed in other cell types including human airway epithelium (Sanderson *et al.*, 1990) and guinea pig enteric glia (W. Zhang *et al.*, 2003). Additionally, it would be of interest to treat with an IP_3R antagonist, such as heparin, to assess the effect this has on the wound-induced calcium wave. Other groups have demonstrated heparin successfully prevented the intercellular calcium wave (Boitano *et al.*, 1992). Mechanical wounding is believed to trigger an increase in IP_3 in cells at the wound edge, although exact mechanisms are still not understood. An important question that experiments conducted within this chapter has not determined is what causes the first intracellular calcium flux in the cell located at the wound edge. One argument is that the process of scratch wounding results in damage to the cell membrane and calcium enters from the extracellular space. However, evidence presented within this study does not suggest this is the case. Wounding in the presence of low or no extracellular calcium still resulted in the propagation of the calcium wave from the wound edge, thus indicating that initiation of the intracellular calcium flux in the cell at the wound edge is not dependent on extracellular calcium concentration. Additionally, an increase in calcium alone is not believed to initiate a calcium wave; calcium wave propagation requires IP_3. Therefore suggesting that mechanical stimulation activates the IP_3 signalling pathway (figure 1.4).Whilst there is no firm evidence indicating the mechanisms regulating this, possible explanations include a) if PLC is associated with

the cell membrane, mechanical stimulation could directly activate the enzyme by inducing a change in protein conformation, b) mechanical stimulation may induce a conformation change of the GPCR rather than PLC or c) mechanical stimulation may increase the accessibility of the enzyme to its substrate, PIP_2 (Hansen *et al.*, 1995). PLC functions upstream of IP_3 and it has been shown previously that treatment with the PLC inhibitor blocked the stimuli-induced intercellular calcium wave, whereas treatment with the similar control compound U73343 had no effect (Hansen *et al.*, 1995). These experiments confirm that wound-induced calcium wave propagation is initiation through activation of PLC. Similar experiments in keratinocytes in response to wounding would provide useful insights into mechanisms triggering the calcium wave. Whilst the above key experiments would confirm the role of IP_3 in mediating the calcium wave over calcium following wounding in primary human keratinocytes, further experiments are required to determine the exact mechanism through which mechanical stimulation results in an intracellular calcium peak in the cell at the wound edge. The above key experiments would confirm the role of IP_3 in mediating the calcium wave over calcium following wounding in primary human keratinocytes.

There are two proposed mechanisms through which IP_3 is believed to mediate the intercellular calcium wave. The original, IP_3-diffusion theory predicts sufficient IP_3 is generated in the initiating cell to diffuse through intercellular conduits (principally gap-junctions) and trigger a calcium response in the adjacent cells. As the concentration of IP_3 decreases as it diffuses through cells, the calcium response is reduced. Eventually, the concentration of IP_3 is sub-threshold and no response in the following cell is initiated. Snyed *et al.* generated a computational model based on *in vitro* data from airway epithelial cells. Manipulation of certain aspects of the model suggests that IP_3 diffusion in this manner drives the calcium wave post-stimulation (Sneyd *et al.*, 1995). However, this theory is highly controversial and debated within the literature. The alternative model that has been presented is that IP_3 is regenerated in each subsequent cell. This theory arose from groups stating that it was highly unlikely that sufficient levels of IP_3 were generated at the point of stimulation to drive the wave across a population of cells. For this to occur cells would have to have very high gap-junctional permeability and a very low IP_3 degradation rate (Hofer *et al.*, 2002). In the latter and arguably more likely model, IP_3 is generated in the initiating cells and diffuses into an adjacent cell by intercellular connections. In the following cell IP_3 binds to the IP_3R on

the ER and calcium is released into the cytosol. This elevation in $[Ca^{2+}]_i$ can regenerate IP_3 through PLC activation, which is then able to pass through intercellular connections to the next cell where the response is repeated. As long as the IP_3 concentration entering the cell is above the threshold for IP_3R activation, calcium will continue to be initiated and calcium wave will propagate without degradation. However, it is known that the range of the intercellular calcium wave is limited in keratinocytes (Kobayashi *et al.*, 2014); therefore it is thought that the efflux of IP_3 into the following cell must be of a lower magnitude than the influx into the current cell. Therefore, there is a progressive decline in intracellular calcium flux the further away the cell is located from the stimulus.

Whilst either of these theories would result in the decline in maximum Ft/F0, AUC and rate of rise observed post-wounding in keratinocytes, it seems unlikely that the levels of IP_3 generated by wounding would be sufficient to support the calcium wave observed. Exploring the movement of IP_3 through a cell population is highly desirable. However, changes in IP_3 are extremely difficult to visualise due to limitations of reporter dyes specific for IP_3 (Leybaert and Sanderson, 2012). The development of a dye that would allow cellular visualisation of IP_3 would prove extremely advantageous in the field.

It is known that both calcium ions and IP_3 are able to pass through gap-junctions from the initiating cell to neighbouring cells. An alternative possibility to that described above is that both molecules are required for propagation of the intercellular calcium wave post-wounding. Interestingly, it could be the case that there is a gradient for one molecule but not the other which would explain why the calcium wave is not infinite. A live cell imaging technique for IP_3 would prove beneficial for such investigations; however, currently these are not available. There are methods of globally measuring IP3, which include a) a biotinylated protein that binds to IP_3 and can be captured using beads and b) a luciferase based method whereby the IP_3 binding core of the IP_3R is fused between firefly luciferase which allows direct detection of IP_3 in the presence of luciferin. Although, these are good advances in the field, they would not provide spatial and temporal information regarding the movement of IP_3 through a cell population following wounding.

It is of note that there are another class of receptors present on the ER that may also be mediating the spread of the calcium wave and/or calcium oscillations. Ryanodine receptors are similar to IP_3R and are stimulated to transport calcium by recognising calcium in the cytoplasm. A low level of calcium near the ryanodine receptor will result in ER release of calcium, in a process known as calcium-induced calcium release. It is known that these receptors have an important role in mediating calcium signalling involved in events such as neurotransmission and section (Fill and Copello, 2002). More recently it was shown by immunohistochemistry and reverse transcription PCR that all 3 receptor proteins (RyR1, 2 and 3) were expressed in keratinocytes and expression of these subtypes was higher in differentiating keratinocytes compared to proliferative cells. The finding that keratinocytes express all receptor subtypes and their expression is altered as keratinocytes undergo differentiation suggests a potential link to wound healing responses. Moreover, it was observed that a ryanodine receptor agonist increased intracellular calcium but delay barrier recovery following tape stripping of mice skin and a ryanodine receptor antagonist blocked intracellular calcium but accelerated barrier recovery in mice following tape stripping (S. Denda *et al.*, 2012).Blockade of the ryanodine receptors prior to wounding using a compound such as DHBP would shed light on the role this class of receptors play in wound-induced intracellular calcium wave propagation and the subsequent calcium oscillations.

3.4.3 The role of calcium entry in wave propagation.

Experiments conducted prior to the commencement of this project demonstrated in primary human keratinocytes, a calcium wave was observed post-wounding even in the absence of extracellular calcium (data not shown). It can be concluded from this that the initiation and propagation of the wave does not require the presence of extracellular calcium. This result has been observed in several cell types and in response to a variety of stimuli including normal human urothelial cells (Appleby *et al.*, 2013) and human keratinocytes (Korkiamaki *et al.*, 2002). In a similar manner, increasing the concentration of extracellular calcium in the imaging media from 0.06mM to 1.2mM did not affect the occurrence of the calcium wave. However, interestingly, parameters of the wave were significantly enhanced by an increased $[Ca^{2+}]_o$; AUC and maximum Ft/F0 reached post-wounding. It has previously been shown in keratinocytes that extracellular calcium concentration exerts a differential effect on calcium-mediated

signalling depending on the disease state of the cell. It was demonstrated that cells derived from patients with neurofibromatosis-1 had decreased intracellular calcium flux in response to store depletion in high calcium compared to normal keratinocytes. The authors postulated that since elevated calcium is known to induce terminal differentiation, this attenuated response may account for the aberrant cellular junctions and differentiation seen in these patients. This study highlights a role for extracellular calcium concentration in determining cellular evidence (Korkiamaki *et al.*, 2005). Moreover, Karvonen and co-workers observed a difference between the response of normal and psoriatic keratinocytes to wounding in high and low calcium conditions. They noted that psoriatic cells showed a reduced calcium flux compared to control cells post-wounding in both a low and high external calcium environment. This provided further evidence that the disease phenotype of dermatological disorders may be a result of abnormal calcium signalling. Intriguingly, this study also shows that whilst there appeared to be an increase in intracellular calcium when wounding was performed in a high external calcium environment compared to a low environment, this was not deemed statistically significant (Karvonen *et al.*, 2000). This is in contrast to the results demonstrated within this project. However, no details were provided in the psoriasis study regarding the time point post-wounding that measurements were taken or the relative location from the wound edge. It has been shown within this project that location from the wound is important in determining the calcium flux displayed following wounding. For example, the difference in maximum Ft/F0 and AUC between 0.06mM and 1.2mM $[Ca^{2+}]_o$ is only evident at cells located distal to the wound, cells at the wound edge are comparative.

These results are indicative that a calcium entry mechanism is activated by wounding, through which extracellular calcium, enhances but does not initiate the calcium signal. Interestingly, the rate of rise of the wound-induced calcium flux was unaffected. Rate of rise is believed to indicate calcium release from the ER. A consistent measurement regardless of the extracellular calcium concentration that wounding was performed in provides further evidence that the increased maximum Ft/F0 and AUC is a result of calcium influx from the external environment rather than increased calcium release from intracellular stores.

The occurrence of the calcium wave even when wounding in 0mM $[Ca^{2+}]_o$, supports previous data that source of calcium causing the cytosolic increase is intracellular rather than extracellular. Additionally, only cells located distal to the wound displayed an elevated calcium response when wounding was performed in 1.2mM $[Ca^{2+}]_o$ compared to 0.06mM $[Ca^{2+}]_o$. Thus suggesting extracellular calcium was not affecting calcium flux within cells at the wound edge. A key experiment to determine the source of calcium which initiates and drives the wave would be to deplete intracellular calcium stores (ER) prior to wounding using Tg. Wounding the cells whilst the ER stores were empty would demonstrate whether intracellular calcium was required. If the wave persisted after ER depletion then it could be concluded that the calcium was not intracellular. On the other hand, following on from data presented thus far, it would be expected that wounding post-Tg treatment would prevent the wave from occurring. Many studies have shown this in other cell types. For example, in human urothelial cells, Tg treatment prior to wounding blocked the wound-induced calcium wave (Appleby *et al.*, 2013). Similarly, the same response was reported in HUVECs (Junkin *et al.*, 2013). These data provides, for the first time, evidence that extracellular calcium is able to alter parameters of the calcium flux within individual cells following wounding.

3.4.4 GSK-7975A as a SOCE inhibitor.

Section 3.1.3 reviewed current methods for pharmacologically inhibiting SOCE. In accordance to the literature, it was concluded that the use of these compounds are discouragingly complex. Moreover, for unknown reasons, pharmacologically blockade of SOCE in primary human keratinocytes was not possible with the commonly used 2-APB or the addition of Gd^{3+}. DES was the only effective compound (Ralph Jans *et al.*, 2013). It was therefore of interest to assess the efficacy of the GSK compound GSK-7975A which has been suggested to be highly specific. GSK-7975A has been shown over the past 18 months to effectively block SOCE in several cell types (Gerasimenko *et al.*, 2013), however, it has not previously been investigated in skin cells, in particular keratinocytes. Results show, for the first time, that 10μM GSK-7975A convincingly prevents SOCE in human keratinocytes. This concentration was initially analysed following advice from Dr Begg from GSK and is in accordance to published literature. Furthermore, no detrimental effects on cell viability were detected following twenty

four hour exposure to the compound. Therefore, GSK-7975A appears to be a suitable candidate for linking acute calcium signalling following wounding to downstream transcriptional and functional events. Importantly, Gerasimenko and co-authors observed that the GSK-7975A compound resulted in varying levels of blockade in different cell types. For example, treatment with 10μM inhibited SOCE in primary pancreatic acinar cells but had minimal effect in the pancreatic acinar cell line AR42J and isolated mouse hepatocytes (Gerasimenko *et al.*, 2013).

Further experiments are required to fully determine the mechanism of action of GSK-7975A. These would include a full dose response of the compound and a time course of pre-treatment. Additionally, investigations into the reversibility of the compound will aid future experimental design.

3.4.5 SOCE in regulation of the wound-induced calcium wave.

After confirmation that GSK-7975A consistently and reliably blocked SOCE in primary human keratinocytes, the compound was utilised to investigate the role of SOCE in mediating the elevated calcium flux when wounding was performed in 1.2mM $[Ca^{2+}]_o$. In line with previous data showing that extracellular calcium was not required for the initiation of the calcium wave, it was perhaps unsurprising that SOCE inhibition had no effect on the occurrence of the calcium wave; a calcium wave was still observed in these conditions. Intriguingly, GSK-7975A also did not affect the intracellular calcium flux within individual cells located at specified distances from the wound edge. In both GSK-7975A and vehicle treated cells, maximum Ft/F0 reached during the calcium flux and the AUC of the calcium flux remained constant. This result is in accordance with Berra-Romani *et al.*, who observed that inhibition of SOCE with the SOCE inhibitor BTP-2 did not affect the overall calcium flux triggered by wounding in rat aortic cells (Roberto Berra-Romani *et al.*, 2008).

GSK-7975A inhibits SOCE by affecting the selectivity filter of the Orai1 pore preventing calcium influx following store depletion. This initial publication described the development of the compound and noted that the compound was highly specific because it exerted its effect downstream of STIM1-Orai1 interactions, as demonstrated by both STIM1 oligomerisation and STIM1-Orai1 interactions being unaltered by

treatment (Derler *et al.*, 2013). Therefore, upon intracellular calcium store depletion and the subsequent loss of binding of calcium to the EF hand within the ER lumen, STIM1 translocation to the PM persists. A method for SOCE has been suggested that does not require either STIM1 or Orai1. Samani and co-workers demonstrated that SOCE channels were activated by a calcium influx factor (CIF) that was produced upon deletion of stores. Investigations in smooth muscle cells led to the hypothesis that intracellular calcium store depletion leads to the release of CIF which removes calcium-independent phospholipase A ($iPLA_2$) from CaM resulting in the production of lysophospholipids which in turn activate SOCE channels. $iPLA_2$ was shown to be a key mediator in this and crucial to calcium influx (Smani *et al.*, 2004). Leading on from this, the role of $iPLA_2$ was investigated in both HaCaTs and primary human keratinocytes. This study confirmed the expression of $iPLA_2$ in these cell types and reported an important role for $iPLA_2$ in the regulation of agonist-induced calcium entry (Ross *et al.*, 2008). Although not directly affirming a role for $iPLA_2$ in calcium influx post-wounding, this investigation demonstrated functional $iPLA_2$ in primary human keratinocytes. Additionally, results indicate an alternative mechanism for calcium entry that is STIM1 and Orai1independent. Thus, providing a possible reason as to why treatment with GSK-7975A did not prevent the elevated calcium flux observed when wounding was performed in 1.2mM $[Ca^{2+}]_o$.

Transient receptor potential cation channels (TRPC) are a family of non-selective ion channels that have been postulated to mediate SOCE under certain conditions. TRPC dependency on STIM1 is highly debated within the literature with conflicting data being published. For example, Dehaven *et al.* concluded from their investigation that TRPC signalling was not functionally dependent on STIM1/Orai1 signalling and the two mechanisms occurred in distinct PM locations (Wayne I. DeHaven *et al.*, 2009). In contrast, it has also been documented that the STIM1/Orai1 activating region interacted with TRPC to open TRPC channels in a STIM1-dependent manner (Kyu Pil Lee *et al.*, 2014). Clearly, further research is required to fully determine the extent the role STIM1 plays in TRPC activation, in particular in keratinocyte signalling. However, studies provide interesting viewpoints to consider regarding the effect of extracellular calcium entry on regulation of the wound-induced intercellular calcium wave.

Finally, it is possible that the calcium entry mechanism resulting in the enhanced calcium flux is non-SOCE. This may account for the enhanced intracellular calcium at the wound edge. However, due to the limited number of publications utilising the compound, this possibility has not yet been explored. Non-SOCE mechanisms of calcium influx have recently been categorised into two groups; receptor-operated calcium entry (ROCE) whereby an external ligand directly binds to a PM channel resulting in the influx of calcium ions or non-SOCE where calcium entry is activated independently of store depletion (Schubert, 2005), potentially through parallel activation of protein kinase C (PKC) (Rosado and Sage, 2000). As alluded to in section 1.6.1, purinergic receptors activated by ATP can be classified into P2XR and P2YR. P2XR are an example of ligand-gated calcium ion channels. It is known that these channels are activated by binding of extracellular ATP, resulting in channel opening and calcium entry into the cell (Egan and Khakh, 2004). The role of ATP in keratinocyte calcium signalling is explored in chapter 5.

Whilst the results presented within this chapter demonstrate that SOCE via Orai1 is not regulating parameters of the calcium wave immediately following wounding, they do not delineate which method of calcium influx is occurring. Therefore, future work would involve further pharmacological and genetic manipulation experiments to determine the relative contribution of mediating factors. For example, Jans *et al.* utilised the the Orai1 dominant negative mutant (R91W). R91W was the mutation initially described in SCID patients and provided the first link between SOCE and disease (Feske *et al.*, 2006). In keratinocytes, it was shown that transfection of this mutant effectively blocked SOCE (Ralph Jans *et al.*, 2013). It would be useful to transfect keratinocytes with the R91W mutant and conduct wounding experiments as described herein. GSK-7975A targets the Orai1 pore and therefore, similar results to GSK-7975A treatment would be expected. The Orai family has three members; Orai1, Orai2 and Orai3 (section 1.3.3). Relative contribution of each isoform in the regulation of the wound-induced calcium wave could be determined by siRNA knockdown of individual isoforms. Research to date has mainly focussed on Orai1. The role both Orai2 and Orai3 play in SOCE or indeed other calcium signalling pathways remains elusive. However, it has been illustrated in HEK293 cells that Orai2 expression induced SOCE, albeit to a lesser extent than Orai1 (Mercer *et al.*, 2006). In contrast, Orai3 expression in these cells had no effect on SOCE suggesting that Orai3 is not required for SOCE under

normal physiological conditions (W. I. DeHaven *et al.*, 2007). Although in Orai1 knockdown cells, Orai3 appeared to rescue calcium entry, indicating that Orai3 may act in a compensatory manner to induce SOCE if Orai1 is not able to. Also in non-small cell lung carcinoma (NSCLC) cells, Orai3 inhibition significantly reduced SOCE (Ay *et al.*, 2013). All together these results suggest Orai3 has varying levels on contribution to SOCE depending on cell type involved. Whilst it has now been shown that all three isoforms are expressed in human keratinocytes, further investigations are required to further explore the roles of all three homologues, especially regarding cutaneous wound healing responses.

An alternative approach would be to use siRNA targetted to STIM1, which has previously been shown to effectively reduce STIM1 expression in keratinocytes by approximately 80% (Ralph Jans *et al.*, 2013). Akin to Orai1 dominant negative, STIM1 knockdown in keratinocytes prevented SOCE. If calcium entry was occurring through a STIM1-dependent TRPC pathway such as that described above, it would be expected that STIM1 knockdown would eliminate the increase in intracellular calcium observed during the flux. On the other hand, if STIM1 knockdown had no effect, and the presence of a high external calcium environment continued to enhance parameters of the calcium wave following wounding, it would be speculated that influx was occurring through either iPLA or another non-SOCE mechanism. As described in section 1.3.3, there are two known homologues of STIM. Despite their similarities regarding structure and function, one major difference between STIM1 and STIM2 is their respective affinity for calcium. STIM1 is twice as sensitive and responds faster to alterations in ER lumen calcium levels compared to STIM2, a property thought to be attributed to a three residue difference on the calcium binding domain. Whilst STIM1 knockdown has been shown to inhibit SOCE, STIM2 knockdown had little effect. In fact it is overexpression of STIM2 that caused SOCE inhibition (Mukherjee and Brooks, 2014). Taken together, it is not surprising that STIM1 is accepted as the stronger activator of Orai channels and thus highly implicated in SOCE. However, more recently, contradictory evidence has been published suggesting that STIM1 and STIM2 are both activated in response to store depletion. After mild ER calcium depletion, STIM2 was activated and as the concentration of agonist was increased, STIM1 became preferentially activated (Thiel *et al.*, 2013). It has been established that both STIM1 and

STIM2 are expressed in human keratinocytes; however, research to date has focussed on STIM1.

Finally, in order to assess the contribution of $iPLA_2$ to wound-induced calcium entry, keratinocytes could be treated with the $iPLA_2$ inhibitor bromoenol lactone (BEL), in a similar manner to Ross *et al*. (Ross *et al.*, 2008). If this cascade was mediating calcium entry post-wounding, it would be expected that the increase in intracellular calcium flux observed when wounding in 1.2mM $[Ca^{2+}]_o$ would be reduced.

3.5 Conclusions.

- Wounding induces an increase in intracellular calcium in cells at the wound edge that spreads back across the cells.

- As determined by characterisation of specific parameters of the wound-induced wave, transmission is likely to be conducted through IP_3 movement through gap-junctions.

- Calcium entry drives the intracellular calcium flux in cells distal to the wound as shown by an elevated intracellular calcium response in these cells when wounding is performed in 1.2mM $[Ca^{2+}]_o$.

- GSK-7975A is an effective SOCE inhibitor in primary human keratinocytes.

- Calcium entry mechanism regulating the wound-induced calcium wave is not SOCE-dependent; GSK-7975A treatment has no effect on maximum Ft/F0, AUC or rate of rise of the intracellular calcium flux away from the wound edge but enhances calcium flux directly at the wound edge.

Chapter 4.

The Role of Purinergic and Gap-junctional Signalling in Wound-induced Calcium Wave Propagation

4 Chapter 4. The Role of Purinergic and Gap-junctional Signalling in Wound-induced Calcium Wave Propagation.

4.1 Introduction.

4.1.1 The role of ATP and gap-junctional communication in propagation of the wound-induced calcium wave.

As described in section 3.1.1, intercellular calcium waves are characterised by sequential increases in $[Ca^{2+}]_i$ in neighbouring cells that spread from the point of stimuli through the cell population depicting a wave (Charles *et al.*, 1992). Intercellular waves function to provide a means of communication between an individual cell and a population of cells, therefore facilitating the transmission of information for the coordination of tissue responses. There are two proposed mechanisms for the transmission of the calcium wave across a population; gap-junctions communication and extracellular purinergic signalling.

A vast amount of evidence exists to support the hypothesis that intercellular calcium waves are propagated through gap-junctions. Firstly, in airway epithelial cells, kinetic analysis showed a delay of up to one second in the wave propagation at the cell boundaries and the subsequent elevation of calcium in the neighbouring cell originated at localised points along the membrane next to the initiating cell. This is highly suggestive that the messenger is moving through conduits between cells. Secondly, airway epithelium treated with the connexin inhibitor halothane prevented the spread of the calcium wave and the calcium signal was limited to the stimulated cell (Sanderson *et al.*, 1990). Furthermore, glioma cells lacking gap-junctions were unable to propagate the wave, however when connexins were transfected into the cells, calcium spread throughout the cell population (Charles *et al.*, 1992).

Additionally, it has also been noted that an intercellular calcium wave can spread between cells either side of a cell-free zone and across a population of sub-confluent cells, suggesting that another mechanism exists by which the signal can propagate between cells lacking physical contact. ATP signalling is a strong contender and has been investigated in recent years (Hassinger *et al.*, 1996). Further evidence to support a role for ATP and paracrine signalling in calcium wave spread arose from fluid-flow

experiments. In these investigations the direction of flow of the extracellular media was dictated. Results show, that in some systems, calcium waves only spread in the direction of the movement of fluid, indicating that a signalling molecule is being released and influencing neighbouring cells downstream. In addition to this, unstimulated dorsal root ganglian sensory neurones that were co-cultured with the keratinocytes also showed an increase in intracellular calcium signalling, suggesting that ATP can mediate cross-talk between two cell types. Sensory neurones are in close proximity to basal keratinocytes within the epidermis *in vivo* and communication between different cell types within an environment is vital to whole-organism signalling (Koizumi *et al.*, 2004). In response to stimuli, ATP is released from cells into the extracellular environment. Although mechanisms of release are not completely understood, connexin and pannexins appear to be involved at least in certain cell types, such as keratinocytes and oocytes (Bao *et al.*, 2004; Barr *et al.*, 2013) . Thus, in these cell types, an accepted method for inhibiting ATP release is blocking the functioning of these channels. When investigating the contribution of gap-junction verses paracrine signalling as a regulator of intercellular calcium wave spread it is important to note that inhibitors of gap-junctional communication may also decrease ATP release and therefore caution should be taken in the interpretation of data regarding wave propagation. For example, Cotrina *et al.* demonstrated that overexpression of Cx43 increased intercellular calcium wave through increased ATP release rather than increased gap-junction signalling (Cotrina *et al.*, 1998). Released ATP from the stimulated cell(s) can bind to GPCR on the neighbouring cell's PM to activate PLC resulting in the subsequent IP_3-mediated ER calcium depletion.

Initially, the two theories of intercellular calcium wave spread stood beside each other without full integration. However, with increased knowledge, a network/systems approach is now being applied and it is highly likely that the pathways interact and work together to synergistically trigger an intercellular calcium wave. For example, Iacobus *et al*. demonstrated this by analysing the speed of the intercellular calcium wave. The authors show that wound-induced IP_3-mediated waves only travelled a short distance, about five cells. Combining ATP and IP_3 signalling mechanisms resulted in a longer propagation distance (Iacobas *et al.*, 2006).

4.1.2 Mechanisms of wound-induced calcium wave in keratinocytes.

It is now widely accepted that inflicting injury on keratinocytes and the epidermis, disrupts the epidermal calcium gradient and causes an immediate increase in $[Ca^{2+}]_i$ that spreads to neighbouring cells. As with all intercellular calcium waves, wave propagation is thought to occur through either paracrine signalling or gap-junction communication; however, the relative contribution of each pathway in facilitating calcium signal transmission in keratinocytes remains controversial.

It has been shown that in proliferating human keratinocytes that ATP has a dominant role in wound-induced intercellular wave propagation as demonstrated by apyrase treatment preventing wave spread (Tsutsumi *et al.*, 2009). However, this effect was not detected in differentiated keratinocytes where only gap-junction inhibitors blocked the intercellular calcium wave. Overall, these studies highlight that cells may use different mechanisms to regulate calcium wave spread depending on their differentiation status (Tsutsumi *et al.*, 2009).

Additionally, work by Korkiamaki *et al.* found that gap-junction blockade eliminated wound-induced intercellular calcium wave in normal human keratinocytes. However, the authors also report that keratinocytes from patients with neurofibromatosis have a dominant dependence on ATP signalling for wave spread rather than gap-junctions (Korkiamaki *et al.*, 2005). Similarly, this group also compared normal human keratinocytes to human psoriatic keratinocytes and found that, in response to wounding, psoriatic cells had a reduced intercellular calcium signal. Moreover, gap-junction blockade using heptanol had no effect in psoriatic cells but significantly reduced the calcium wave in normal keratinocytes (Karvonen *et al.*, 2000).

Together these investigations highlight a lack of consensus regarding what is mediating the intercellular wave in human keratinocytes. There appears to be many factors influencing transmission regulation which are dependent on disease and differentiation status.

4.1.3 Mechanisms of ATP release.

Section 1.6.1 describes the establishment of purinergic signalling as a mechanism through which populations of cells communicate. This signalling cascade involves the release of ATP from cells into the extracellular environment. A range of both stimuli and mechanisms results in ATP release from cells. Causes of perturbation include osmotic swelling or shrinking, pathogenic infection, air exposure, chemicals and physical damage by stretching or wounding. In fact, the disruption and cell exposure to air during routine laboratory cell culture techniques such as media replacement causes ATP release from cells and subsequent autocrine/paracrine signalling which, in the majority of situations goes undocumented (Barr *et al.*, 2013). There are four major mechanisms that result in ATP being released from non-excitable cells to increase extracellular concentrations, although these all remain poorly understood. The first is through simple lysing of cell membranes during cell damage or death; this was originally speculated to be the sole method of ATP release. However, in the ever expanding field of ATP research, three further methods have been shown to cause release of ATP in healthy cells.

The first of these is mediated through the hemi-channels connexins and pannexins. Structural and functional characteristics of gap-junctions are reviews in section 1.4.1. Connexins have been implicated for many years in ATP release. For example, Barr *et al.* showed that pre-treatment with 1-Octanol, a known connexion inhibitor and carbenoxolone, a proposed dual inhibitor of pannexins and connexins, almost entirely prevented air-stimulated ATP release from keratinocytes (Barr *et al.*, 2013). Additionally, it has been shown that poorly coupled cell lines such as HeLa and U373 glioblastoma have low basal ATP release rates, which increased 15-fold with forced connexin expression, indicating that connexins regulate ATP release (Cotrina *et al.*, 1998). In 2000, a novel family of proteins were discovered termed pannexins. Pannexins are the mammalian homologue of the invertebrate innexins and three isoforms have been identified to date. Pannexins are synthesised, packaged and inserted into the plasma membrane in a similar manner to connexins and they are structurally alike. However, they form gap-junctions on the surface of cells and allow movement of signalling molecules and secondary messengers between the internal and external environment of a cell, rather than between the two internal spaces of adjacent cells (S.

Penuela *et al.*, 2007). Additionally, in contrast to connexins, $[Ca^{2+}]_o$ is not believed to regulate the opening of pannexin channels. Primary patch-clamping experiments by Bao *et al.* in 2004 showed that the pannexin-1 channel, like connexins, is permeable to ATP (Bao *et al.*, 2004). In the past decade, this has been observed in a vast variety of cell types including astrocytes, T-cells, endothelial cells and keratinocytes. Indeed, it has been suggested that previous experiments claiming that connexin inhibition decreased ATP release involved compounds that actually inhibited pannexins and it was this manipulation that caused the resultant attenuation (Dvoriantchikova *et al.*, 2006).

ATP-binding cassette (ABC) transporters form one of the largest super-families of proteins identified in a living organism. It is well established that they act as transmembrane proteins to facilitate the active transport of molecules, including lipids and drugs, from intra- to extracellular space using energy obtained from hydrolysing ATP reviewed by (Schinkel and Jonker, 2012). However, in addition to this, the cystic fibrosis transmembrane conductance regulator (CFTR) (Reisin *et al.*, 1994) and the multidrug resistance gene product *mdr* (also termed P-glycoprotein (P-gp)) (Abraham *et al.*, 1993) have been implicated in ATP efflux from the cell, although this observation remains highly debated. The idea that P-gp functions as an ATP channel was suggested by Abraham *et al.* in 1993. Authors showed a positive correlation between the number of P-gp transporters in a cell and the $[ATP]_o$. Additionally, insertion of P-gp mutants caused a decrease in ATP release, indicating that the family of proteins were involved in ATP movement out of the cell (Abraham *et al.*, 1993). Similar experiments have been conducted investigating the CFTR transporter where it was noted that cAMP-dependent activation of CFTR caused ATP release. This was confirmed by patch-clamping where results showed that cells that did not express CFTR had no ATP release (Reisin *et al.*, 1994). More recently, ABC transport inhibitors including verapamil (Mould *et al.*, 2014) have been shown to decrease air-stimulated ATP release in keratinocytes in a similar manner to inhibition of connexins and pannexins by carbenoxolone (Barr *et al.*, 2013). Despite these investigations, there is evidence that ABC transporters do not mediate ATP release. Reddy *et al.* state that the relative sizes of the ATP molecule and the CFTR pore size makes it an impossible mediator of ATP efflux. Additionally, their investigations regarding intact human organs, human lung cell lines and stably transfected mammalian cell lines found that there was no transport of ATP through these mechanisms (Reddy *et al.*, 1996). The prospect of ABC-transporter facilitated

ATP release remains controversial. More research is needed to determine whether they are able to physically transport ATP out of the cell or, as is potentially more likely, that they facilitate the activation of other channels that are responsible for the movement of ATP. For example, in a bronchial human cell line it was shown that although not acting as an ATP conductor, the CFTR potentiates activation of a close ATP-permeable channel that is expressed in human epithelial cells, causing ATP release (Braunstein *et al.*, 2001). This may explain the original finding by Abraham *et al.* that a positive correlation existed between the number of transporters present on the membrane and the $[ATP]_o$.

The third additional mechanism is exocytosis of ATP-containing vesicles. As previously described, $[ATP]_o$ is in the range of low nanomolar, whereas vesicles within the cells have a high local concentration of ATP which can be released from the cell through fusion of these vesicles to the membrane and subsequent exocytosis. It is well established that this occurs in neuronal cells upon depolarisation, however, there is also growing evidence this method of ATP release is used in other non-neuronal cells as an alternative to channel-mediated release (Bodin and Burnstock, 2001). One of the first studies that proved this in non-neuronal cells was conducted by Bodin and Burnstock, who in 2001, showed that the previously unknown mechanism of ATP release from vascular endothelial cells experiencing shear stress was vesicle-mediated (Bodin and Burnstock, 2001). The following year Knight *et al.* showed that ureter epithelium released ATP upon distension, and again this occurred through vesicular exocytosis. Similar results have been seen in studies involving several cell types including astrocytes, HEK-293 cells, osteoblasts, fibroblasts and thrombocytes (Knight *et al.*, 2002). Methods used to demonstrate this include use of pharmacological inhibitors such as monensin which prevents vesicle formation at the golgi apparatus (Cecchelli *et al.*, 1986) and N-ethylmaleimide (NEM) which inhibits the fusion of vesicles to the plasma membrane (M. R. Block *et al.*, 1988).

The observation that ATP is released from cells both in their resting and stimulated states is well established and the three major candidates are described above. However, despite many investigations, pathways resulting in increased $[ATP]_o$, remain enigmatic and an area of controversy. Taking into account that ATP is an autocrine/paracrine signalling pathway in an enormous range of cell types, along with the fact that a wide

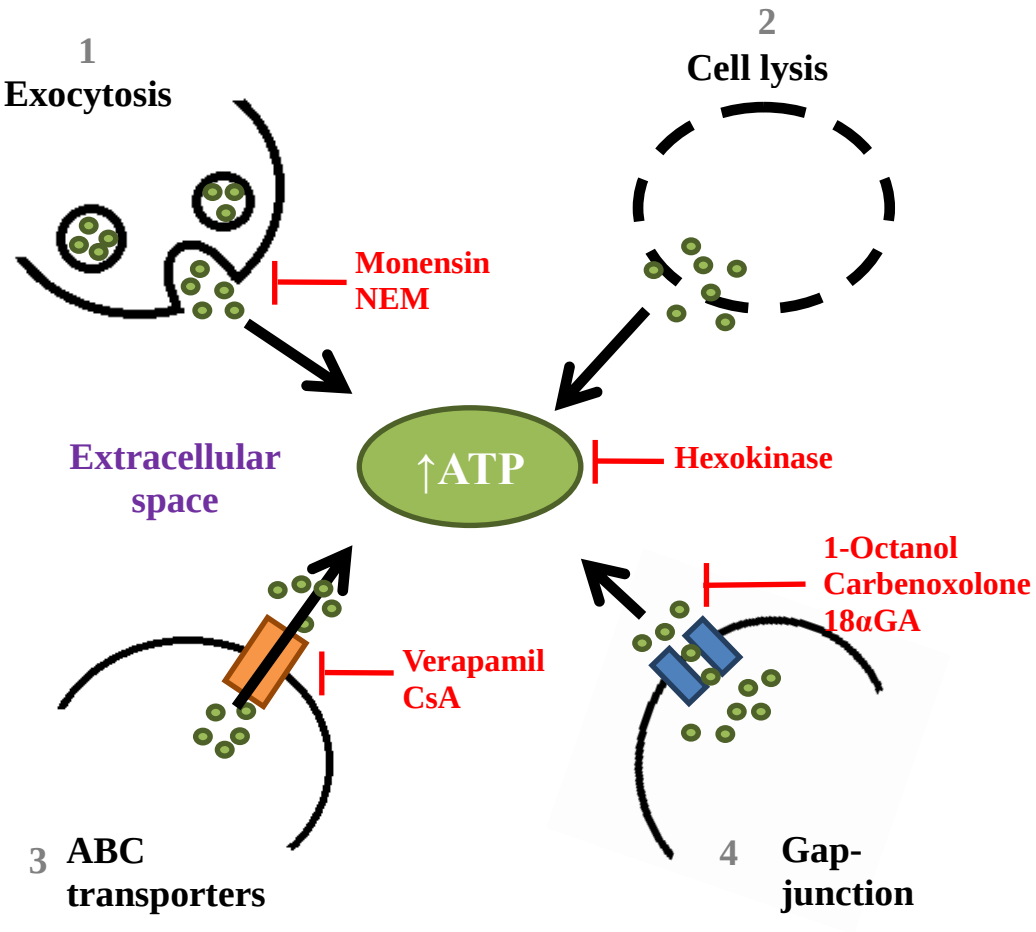

Figure 4.1 Schematic diagram of the proposed mechanisms of ATP release.

Mechanisms regulating ATP release into the extracellular environment remain controversial and evidence suggests they are stimuli and cell type dependent. However, the four suggest mechanisms are **1)** Exocytosis of ATP containing vesicles (inhibited by Monensin and N-ethylmalimide (NEM)) **2)** Cell lysis resulting in release of cellular contents including ATP **3)** ABC transporters which facilitate the active transport of molecules across the PM utilising energy from ATP hydrolysis (inhibited by verapamil and cyclosporine A (CsA)) and **4)** Gap-junction communication allowing the passage of small molecules such as ATP between adjoining cells and between cells and the extracellular environment (inhibited by 1-Octanol, Carbenoxolone and 18^{α} Glycyrrhetinic acid (18αGA)). Hexokinase can be used as an ATP scavenger to eliminate ATP from the extracellular space.

variety of stimuli cause this response, it is probable that one mechanism is not solely responsible. Rather, it is more likely to involve several different pathways which are both cell type and stimulus dependent. Additionally, there is increasing evidence that the pathways investigated may not act mutually exclusive to each other. For example, channel-mediated and vesicular-mediated ATP release may not be independent occurrences. It has been suggested that exocytosis could result in the insertion of ATP-permeable channels in the plasma membrane, although studies into this phenomenon are inconclusive and limited (Braunstein *et al.*, 2001). Similarly it has been observed in human epithelial cells that regulation of CFTR requires gap-junction communication (Scheckenbach *et al.*, 2011).

4.2 Specific aims.

- To investigate the ability of wounded conditioned media to induce a $[Ca^{2+}]_i$ flux in unwounded keratinocytes

- To measure extracellular ATP release from primary human keratinocytes post-wounding and delineate mechanisms regulating release

- To determine the contribution of ATP release post-wounding on the transmission of the intercellular calcium wave post-wounding

- To determine the contribution of gap-junction communication on the transmission of the intercellular wave post-wounding

4.3 Results.

4.3.1 The addition of wounded conditioned media to unwounded cells triggers a $[Ca^{2+}]_i$ flux.

Various investigations have shown that the wound-induced intercellular calcium wave can be driven by intercellular signalling through the cell population and/or the release of a diffusible factor into the extracellular environment (Leybaert and Sanderson, 2012). It was therefore hypothesised that wounding keratinocytes would result in the release of factors into the extracellular media that that could subsequently induce a $[Ca^{2+}]_i$ flux. To address this, primary human keratinocytes were scratch wounded in a cross-hatch manner in either 0.06mM or 1.2mM $[Ca^{2+}]_o$. Five minutes post-wounding, the extracellular media was removed and added to unwounded keratinocytes that had been loaded with the calcium dye Fluo4-AM. Images were captured at 3.7fps. The wounded media removed and added to unwounded cells was referred to as conditioned media (CM).

Signalling across the whole population was visually assessed to determine whether the CM produced an intracellular calcium response in unwounded cells. Figure 4.2 showed representative images from one experiment taken pre-CM and then ten, thirty and sixty seconds post-CM. It is clear that upon addition of the CM $[Ca^{2+}]_i$ increased within a sub-population of cells. Using the image analysis software Volocity, the colour of the images was altered to rainbow to facilitate visualisation of changes in intensity. No relationship was observed between cells that responded and their location in the field of view. Moreover, an increase in $[Ca^{2+}]_i$ after exposure to the CM did not result in an $[Ca^{2+}]_i$ increase in neighbouring cells or the induction of a intercellular calcium wave. Traces from four individual cells after the addition of either 0.06mM $[Ca^{2+}]_o$ CM or 1.2mM $[Ca^{2+}]_o$ CM showed CM caused an increase in $[Ca^{2+}]_i$ which remained elevated for a substantial period of time regardless of extracellular calcium concentration (figure 4.3). It was observed that only a sub-population of keratinocytes responded to CM with a calcium

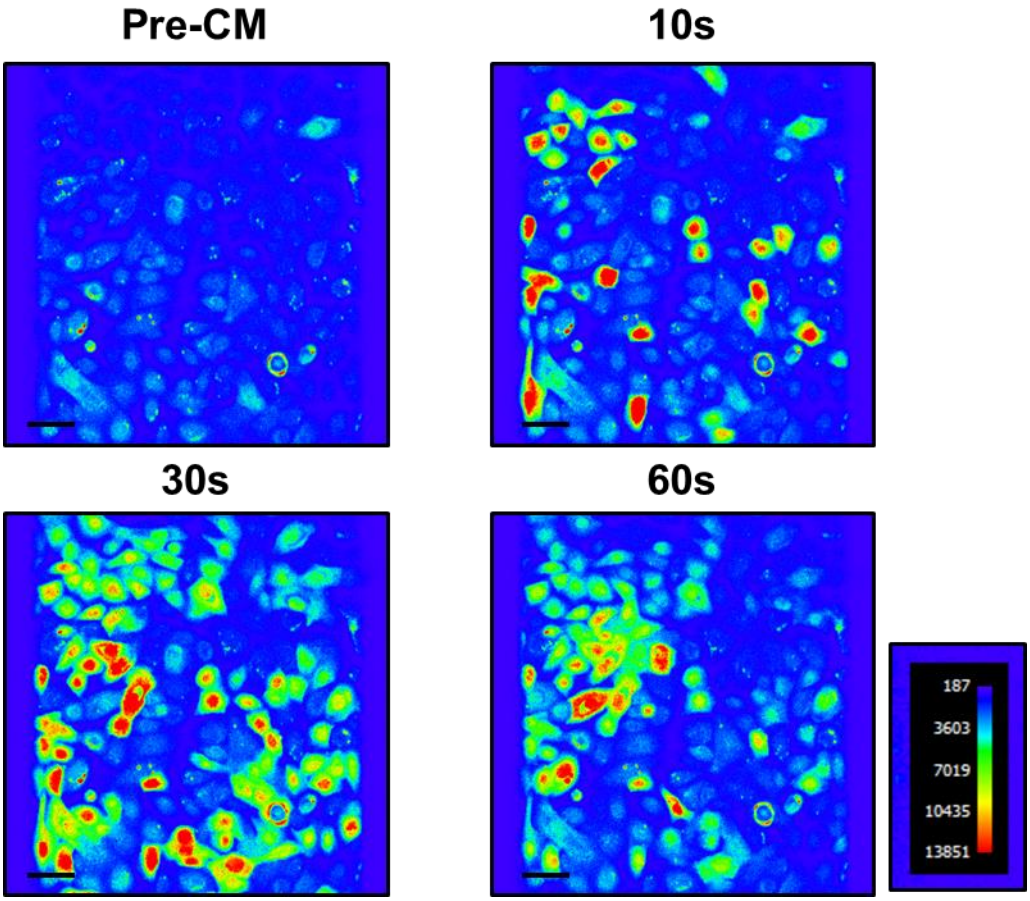

Figure 4.2 2D images demonstrating wounded conditioned-induced $[Ca^{2+}]_i$ changes in unwounded keratinocytes.

Primary human keratinocytes were scratch wounded in a cross-hatch manner or left unwounded in either 0.06mM or 1.2mM $[Ca^{2+}]_o$. Five minutes post-wounding (or control), the extracellular conditioned media (CM) was removed and added to unwounded keratinocytes that had been loaded with the calcium dye Fluo4-AM. Images were captured at 3.7fps. Pseudo colour images of confocal images were generated pre-CM in 0.06mM $[Ca^{2+}]_o$ being added and then 10, 30 and 60 seconds post-CM to demonstrate the visual appearance of the calcium signal triggered by CM. Scale bar=34µm. Pseudo colour reference is shown. Images are representative of three independent donors. No $[Ca^{2+}]_i$ flux was observed after the addition of CM collected under unwounded conditions.

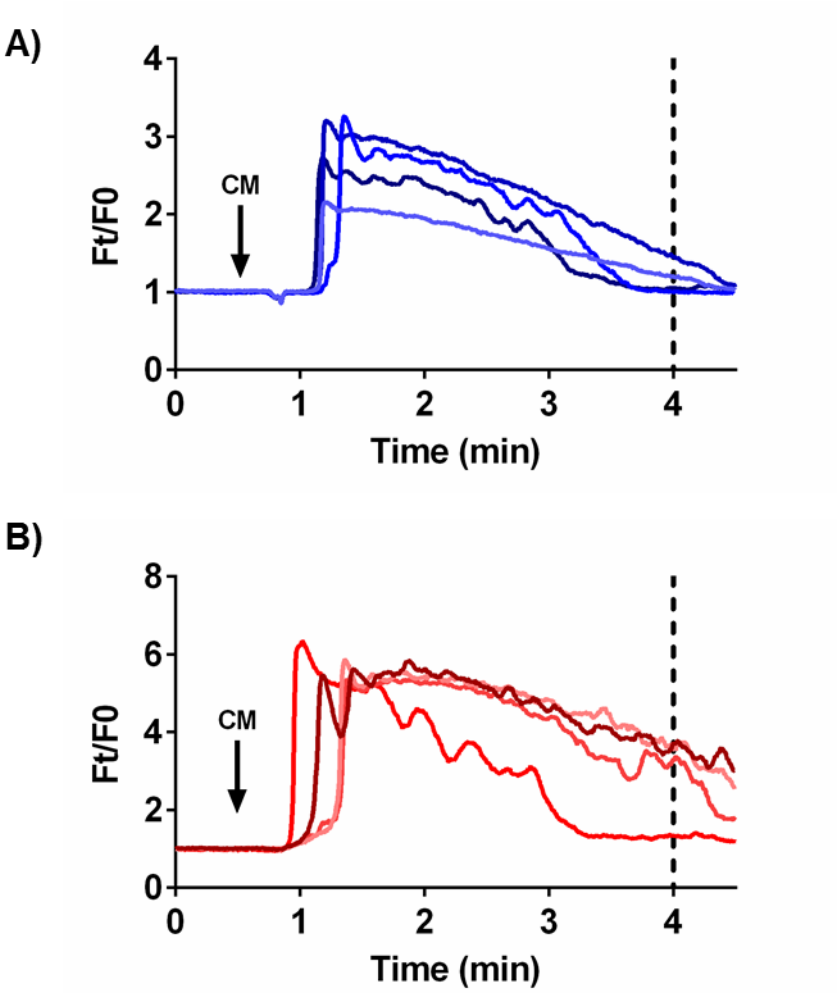

Figure 4.3 Wounded conditioned media induces a sustained and prolonged $[Ca^{2+}]_i$ in unwounded keratinocytes regardless of external calcium concentration.

Primary human keratinocytes were scratch wounded in a cross-hatch manner or left unwounded in either 0.06mM or 1.2mM $[Ca^{2+}]_o$. Five minutes post-wounding (or control), the extracellular conditioned media (CM) was removed and added to unwounded keratinocytes that had been loaded with the calcium dye Fluo4-AM. Confocal images were captured at 3.7 fps. Regions of interest (ROI) were drawn around individual cells for analysis. Traces show four representative cells from experiments performed in **A)** 0.06mM $[Ca^{2+}]_o$ or **B)** 1.2mM $[Ca^{2+}]_o$. Time of addition of CM is highlighted by arrow. Four cells per condition are representative of three independent donors. No $[Ca^{2+}]_i$ flux was observed after the addition of CM collected under sham conditions (see figure 4.5).

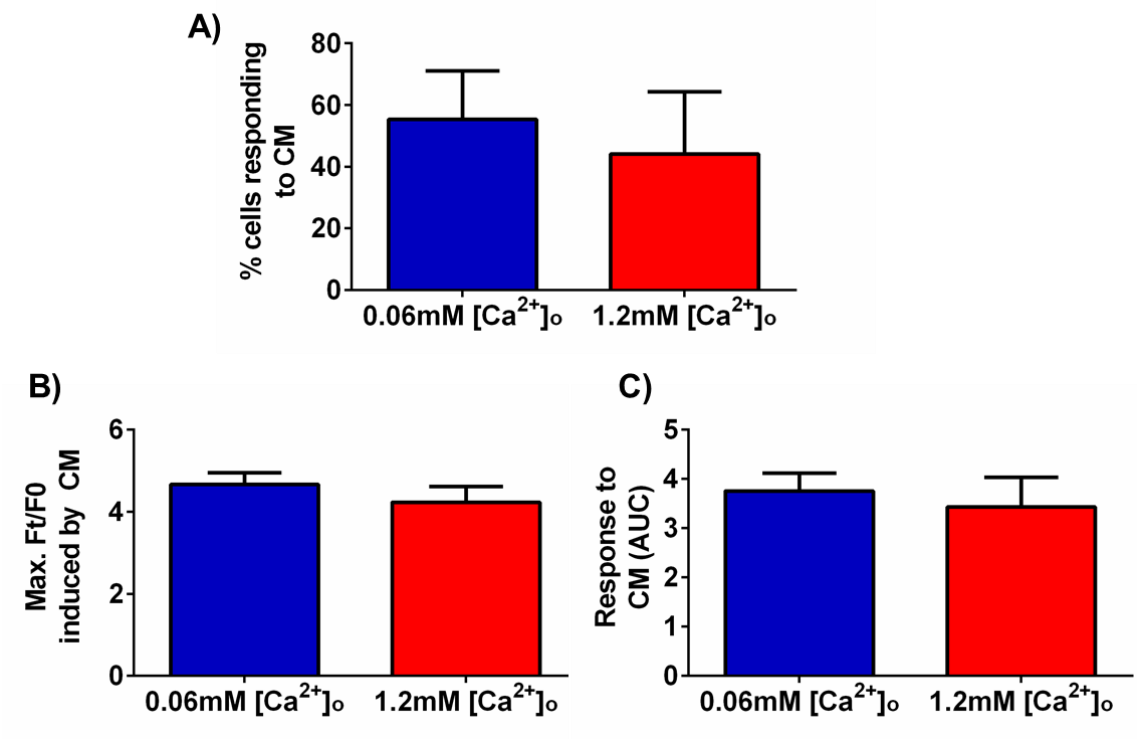

Figure 4.4 Extracellular calcium concentration does not alter parameters of wounded conditioned media-induced $[Ca^{2+}]_i$ flux in unwounded keratinocytes.

Primary human keratinocytes were scratch wounded in a cross-hatch manner or left unwounded (control) in either 0.06mM or 1.2mM $[Ca^{2+}]_o$. Five minutes post-wounding (or control), the extracellular conditioned media (CM) was removed and added to unwounded keratinocytes that had been loaded with the calcium dye Fluo4-AM. **A)** Percentage of keratinocytes responding to CM addition in 0.06mM and 1.2mM $[Ca^{2+}]_o$. P=0.2207, Chi-square. **B)** Maximum Ft/F0 reached within individual cells after addition of CM in 0.06mM and 1.2mM $[Ca^{2+}]_o$. P=0.3560, unpaired, two-tailed t-test. **C)** AUC was calculated for the $[Ca^{2+}]_i$ flux post-CM application in 0.06mM and 1.2mM $[Ca^{2+}]_o$. P=0.6219, unpaired, two-tailed t-test. No $[Ca^{2+}]_i$ flux was observed after the addition of CM collected under unwounded conditions.

signal, these were recorded as a percentage of total cell population in the field of view. As shown by figure 4.4a, 55.35±15.75% of keratinocytes in 0.06mM $[Ca^{2+}]_o$ responded to CM, this figure was 44.11±20.21% in 1.2mM $[Ca^{2+}]_o$ CM. Statistical analysis failed to report this difference as significant (P=0.2207, Chi-square test). To determine whether external calcium concentration had an effect on specific parameters of the induced $[Ca^{2+}]_i$ flux, maximum Ft/F0 post-CM was recorded for responding cells. Maximum Ft/F0 was defined as the greatest fold change in $[Ca^{2+}]_i$ within individual unwounded keratinocytes triggered by the addition of CM. There was no significant difference between the maximal Ft/F0 triggered by the CM in 0.06mM $[Ca^{2+}]_o$ (4.66±0.28) and 1.2mM $[Ca^{2+}]_o$ (4.22±0.38) (P=0.3560, unpaired, two-tailed t-test) (figure 4.4b). AUC of the CM-induced $[Ca^{2+}]_i$ flux in 0.06mM $[Ca^{2+}]_o$ was calculated as 3.75±0.36, which again was not significantly different to the AUC of the CM-induced $[Ca^{2+}]_i$ flux in 1.2mM $[Ca^{2+}]_o$ which was 3.42±0.60 (P=0.6219, unpaired, two-tailed t-test) (figure 4.4c).

Appropriate controls were conducted to ensure that the process of add-back itself did not trigger a calcium response. In these experiments, unwounded keratinocyte growth media with a concentration of 0.06mM or 1.2mM $[Ca^{2+}]_o$ was added to unwounded cells loaded with Fluo4-AM whilst images were being captured. As shown by figure 4.5a, using a P1000 pipette to gently add media into the imaging dish did not result in a calcium response. Representative images from one control experiment taken before the media was added and then ten, thirty and sixty seconds after it had been added, showed that there was no induction of $[Ca^{2+}]_i$ Traces shown from four individual cells after the addition of either 0.06mM $[Ca^{2+}]_o$ (figure 4.5b) or 1.2mM $[Ca^{2+}]_o$ media (figure 4.5c), traces are representative of three independent donors. It can be seen that media add-back did not cause an increase in $[Ca^{2+}]_i$.

These data suggest that wounding causes the release of a mediator into the extracellular environment that, through the transfer of media, is then able to trigger an increase in $[Ca^{2+}]_i$ in unwounded cells. Importantly, the addition of unwounded cell culture media did not result in a calcium response, demonstrating that the $[Ca^{2+}]_i$ changes observed were as a result of the presence of a mediator released upon wounding, rather than a response to the mechanical process of media add-back. These experiments focus solely

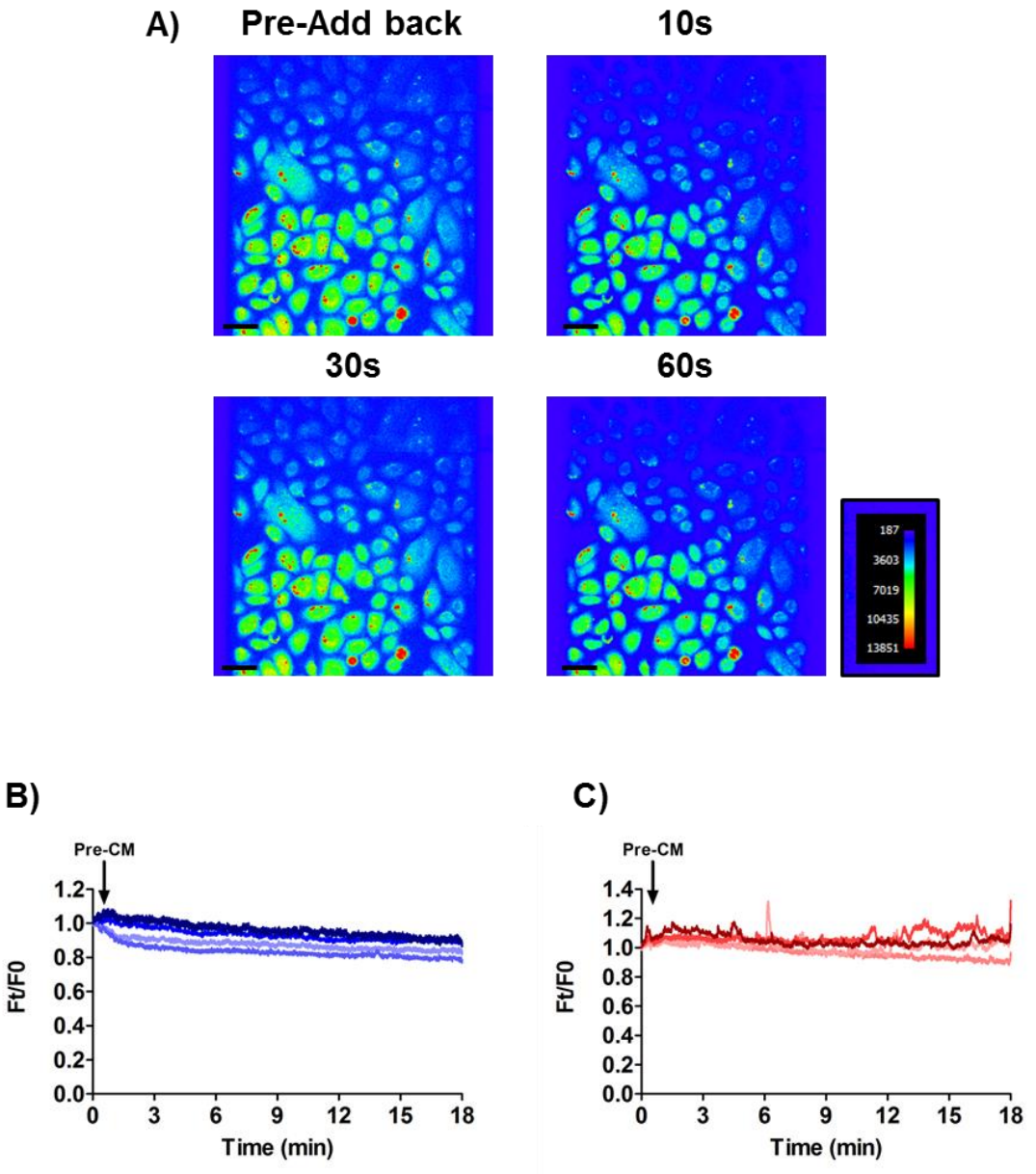

Figure 4.5 The add-back of unwounded conditioned media does not induce $[Ca^{2+}]_i$ changes.

Primary human keratinocytes were loaded with the calcium dye Fluo4-AM and images were captured at 3.7 fps. Unwounded conditioned media (CM) with a calcium concentration of 0.06mM or 1.2mM $[Ca^{2+}]_o$ was added to unwounded cells. **A)** Pseudo colour images of confocal images were generated pre-add-back of unwounded media and then 10, 30 and 60 seconds post-add-back. Scale bar=34µm. Pseudo colour reference is shown. Images are representative of three independent donors. Four representative cells exposed to media with calcium concentration of either **B**) 0.06mM $[Ca^{2+}]_o$ or **C)** 1.2mM $[Ca^{2+}]_o$. Arrows highlight the time of add-back. Traces are representative of three independent donors.

on factors released upon wounding and establish their effects on cells that have not been exposed to mechanical wounding and thus eliminate calcium responses as a result of wound-induced intercellular calcium signalling. However, they do not provide insights into what factors are being released that are capable of causing a calcium response. The lack of difference between 0.06mM and 1.2mM $[Ca^{2+}]_o$ indicates that the release of the factor initiating the subsequent calcium response is not calcium dependent.

4.3.2 ATP is released into the extracellular environment post-wounding.

Section 4.3.1 highlighted the ability of CM to induce a calcium response in a small population of cells that had not experienced mechanical wounding. Thus suggesting that keratinocytes released a mediator into the extracellular space upon wounding that consequently altered $[Ca^{2+}]_i$ in unwounded cells. It is known that ATP can be released from keratinocytes in response to stress or mechanical perturbation (Barr *et al.*, 2013). Additionally, the ability of ATP to induce $[Ca^{2+}]_i$ changes has been established through activation of both P2XR and P2YR (section 1.6.1). It was possible, therefore, based on previously published data, that ATP was released from keratinocytes as a result of wounding, and this was capable of inducing a calcium response in unwounded cells. However, the release of ATP from primary human keratinocytes in response to scratch wounding has not been quantified. Therefore, prior to commencement of these calcium imaging experiments, investigations were conducted in order to quantify ATP release from cells by scratch wounding as well as characterisation of mechanisms mediating such processes.

To address this, keratinocytes were grown to confluency and wounded in a cross hatch manner. At specific time points post-wounding, a sample of the extracellular media was obtained and analysed for ATP levels as described in materials and methods (section 2.5.1). Separate wells were used for each specific timepoint rather taking the sample from the same well at required times post-wounding. This experimental design was conducted to ensure that the volume of media remained constant throughout the time course, allowing fair comparisons between time points. Prior to commencement of experiments, appropriate control experiments were conducted and showed that the media alone did not give a positive reading and the assay was ATP-specific, as no readings were detected for various concentrations of another nucleotide, UTP (Appendix A).

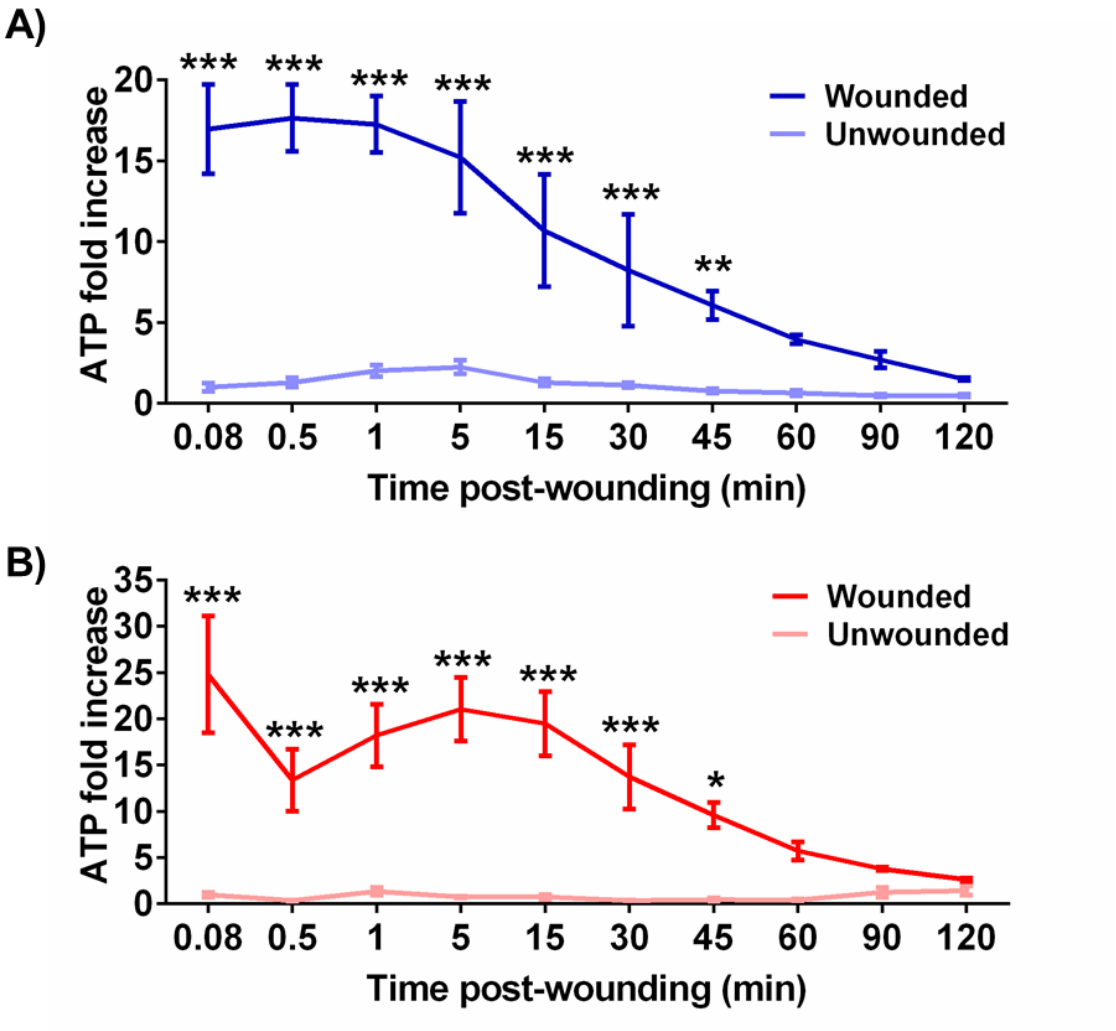

Figure 4.6 ATP is released from wounded keratinocytes in a biphasic manner and remains detectable in media for up to 60 minutes.

Primary human keratinocytes cultured in 0.06mM $[Ca^{2+}]_o$ keratinocyte growth medium (MCDB 153) were wounded in a cross-hatch manner or left unwounded (control) in either **A)** 0.06mM or **B)** 1.2mM $[Ca^{2+}]_o$. At specified time points post-wounding, a 50µL sample of the extracellular media was taken and analysed for ATP using a luminometer. Samples from unwounded controls were obtained at each timepoint for each external calcium concentration. Data shows mean ± SEM from three independent donors in triplicate; (n=9), N=3. Two-way ANOVA with Bonferroni post-hoc test (*** P<0.001, * P<0.01).

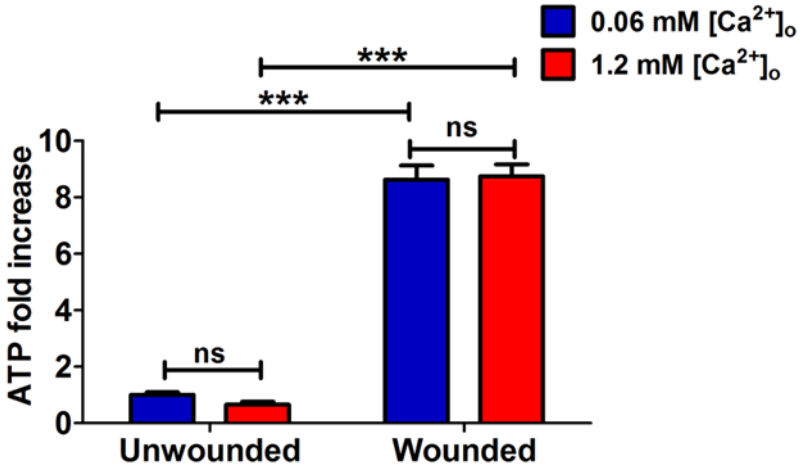

Figure 4.7 ATP is released from keratinocytes post-wounding in a calcium-independent manner.

Primary human keratinocytes cultured in 0.06mM $[Ca^{2+}]_o$ keratinocyte growth medium (MCDB 153) were wounded in a cross-hatch manner or left unwounded in either 0.06mM or 1.2mM $[Ca^{2+}]_o$ as described in figure 4.6. Five minutes post-wounding or control, samples were collected for analysis. Data shows mean ± SEM and from sixteen donors in triplicate (n=48), N=16. Two way ANOVA with Bonferroni post-hoc was conducted (*** $P<0.001$, ns = not significant $P>0.05$).

Initially, to determine an appropriate time point for collection of samples post-wounding, time course assays were conducted. From figure 4.6a it is clear that wounding in 0.06mM $[Ca^{2+}]_o$ caused an immediate release of ATP into the extracellular environment; this was detected five seconds post-wounding (the earliest time point possible for a sample to be taken). ATP levels remained elevated for five minutes post-wounding and then gradually returned to baseline over a two hour period. Unwounded samples were also obtained at each time point. Two-way ANOVA statistical analysis reported that 0.06mM $[Ca^{2+}]_o$, wounding had a significant effect on the amount of ATP in the extracellular environment ($F(1,8)=98.43$, $P<0.0001$). A Bonferroni post-hoc test to compare these differences at each time point showed that there was a significant difference between unwounded and wounded samples for forty five minutes post-wounding (*** $P<0.001$, ** $P<0.01$). Between forty five minutes and two hours no statistical difference was reported ($P>0.05$). Similarly, wounding in 1.2mM $[Ca^{2+}]_o$ (figure 4.6b) resulted in an immediate increase in ATP into the extracellular environment which was detected five seconds post-wounding. Although, in contrast to ATP released in 0.06mM $[Ca^{2+}]_o$, the pattern of release in 1.2mM $[Ca^{2+}]_o$ appeared to be biphasic. In agreement with wounding in 0.06mM $[Ca^{2+}]_o$, an immediate release was detected immediately post-wounding, however in 1.2mM $[Ca^{2+}]_o$ this decreased at thirty seconds, increased up to five minutes and then gradually decreased over the rest of the two hours. Unwounded samples were also obtained at each time point. Two-way ANOVA statistical analysis reported that in 1.2mM $[Ca^{2+}]_o$, wounding had a significant effect on the amount of ATP in the extracellular environment ($F(1,8)=63.38$, $P<0.0001$). A Bonferroni post-hoc test to compare these differences at each time point showed that there was a significant difference between unwounded and wounded samples for forty five minutes post-wounding (*** $P<0.001$, ** $P<0.01$). Between forty five minutes and two hours no statistical difference was reported ($P>0.05$). Taken together, it was decided that five minutes post-wounding was an appropriate time point to take the readings in future experiments.

To investigate whether ATP released from keratinocytes in response to wounding was dependent on the extracellular calcium environment, cells were wounded in the presence of 0.06mM or 1.2mM $[Ca^{2+}]_o$. In line with previous data (section 4.3.1), a fold increase of 8.63±0.50 and 8.74±0.42 was observed when wounding in 0.06mM and 1.2mM $[Ca^{2+}]_o$ respectively. These increases were deemed significantly different

compared to their respective unwounded conditions (*** P<0.0001). However, there was not a significant difference between ATP levels in the two extracellular environments (F1,188)=0.1130, P<0.7372, two-way ANOVA). Similarly, there was no significant difference between levels of extracellular ATP in unwounded keratinocytes in 0.06 and unwounded keratinocytes in 1.2mM $[Ca^{2+}]_o$ (ns P>0.05) (figure 4.7).

These data clearly show that wounding causes ATP release from keratinocytes. The greatest increase was detected within the first five minutes post-wounding. The comparable results between wounds made in 0.06 and 1.2mM $[Ca^{2+}]_o$ demonstrate that ATP release induced by wounding is not calcium-dependent.

4.3.3 ATP release post-wounding is an isolated one-time event

In order to determine whether the increased levels of ATP detected post-wounding was due to continued release from the cells or a one-off event, a series of "media replacement" and "conditioned media" experiments were conducted. In media replacement experiments, cells where either A) left unwounded B) wounded and a sample obtained thirty minutes post-wounding, or C) wounded and one minute post-wounding extracellular media was removed and replaced with fresh media. Media was also replaced in unwounded cells as a control to ensure that the removal process did not result in ATP release from cells as a response to air exposure, an occurrence which was previously reported (Barr *et al.*, 2013). Cells were classified as positive (+) or negative (-) for wounding; positive if they had been wounded, negative if they were left unwounded. Media replacement one minute post-wounding was classified as positive (+) or negative (-); positive if the media had been replaced, negative if the media had not been replaced.

In agreement with previous results presented, thirty minutes post-wounding in 0.06mM $[Ca^{2+}]_o$ ATP levels were raised compared to unwounded cells, as shown in figure 4.8a. Interestingly, when media was removed from wounded cells and replaced with fresh media, ATP levels detected in the extracellular media were reduced and were similar to those observed in unwounded cells. Statistical analysis was conducted to assess the effect of media replacement. Results showed that replacing the wounded media, with fresh media, had an overall significant effect on ATP levels (Two-way ANOVA,

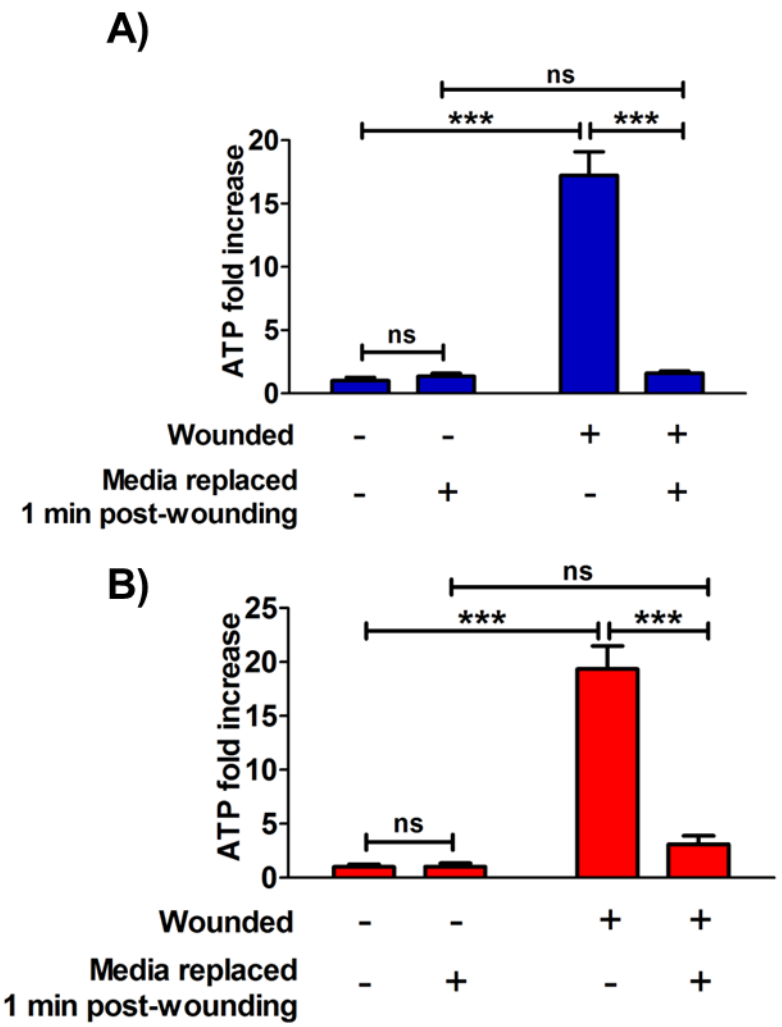

Figure 4.8 Replacing wounded media with fresh media one minute post-wounding reduced ATP levels in the extracellular conditioned media.

Primary human keratinocytes cultured in 0.06mM $[Ca^{2+}]_o$ keratinocyte growth medium (MCDB 153) were wounded in a cross-hatch manner or left unwounded in either **A)** 0.06mM or **B)** 1.2mM $[Ca^{2+}]_o$ as described in figure 4.6. Samples were collected thirty minutes post-wounding for analysis. Alternatively, in specified experiments, one minute after wounding, media was removed and replaced with fresh media and then samples collected twenty nine minutes later (total time thirty minutes post-wounding). Data shows mean ± SEM from three donors in triplicate (n=9), N=3. Two way ANOVA with Bonferroni post-hoc statistical analysis was conducted (*** $P<0.001$, ns = not significant $P>0.05$).

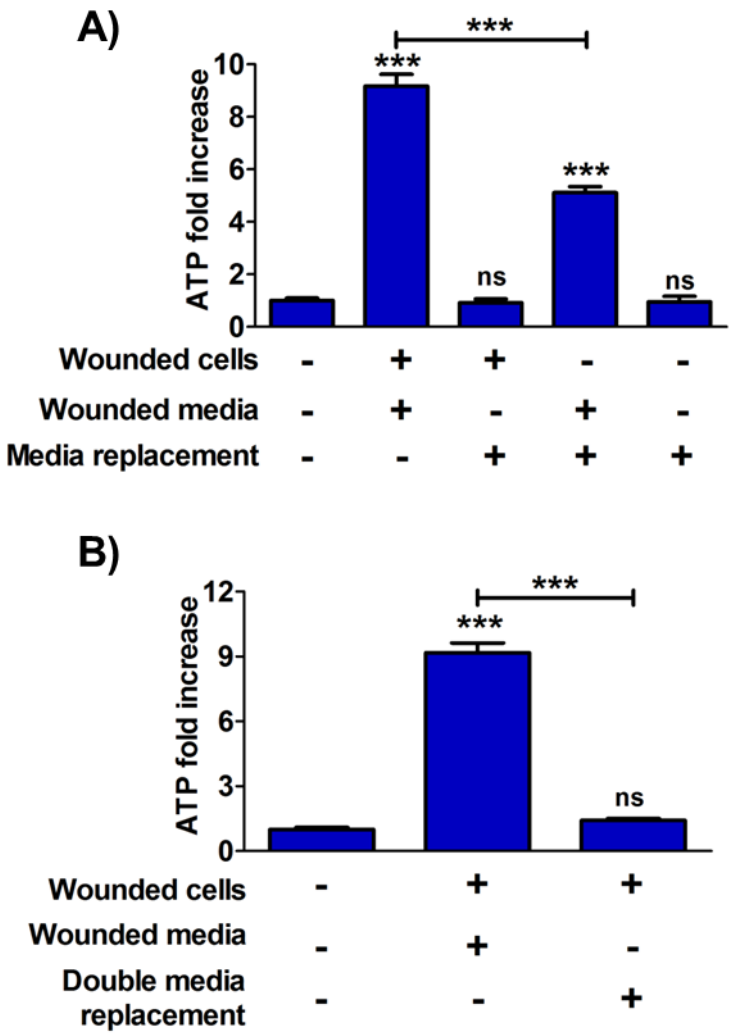

Figure 4.9 Wounded cells exposed to unwounded conditioned media do not show elevated ATP levels.

A) Primary human keratinocytes cultured in 0.06mM $[Ca^{2+}]_o$ keratinocyte growth medium (MCDB 153) were wounded and five minutes later media was removed and replaced with unwounded media, the wounded conditioned media was placed onto unwounded cells. Thirty minutes post-wounding samples were taken for analysis. **B)** Primary human keratinocytes cultured in 0.06mM $[Ca^{2+}]_o$ keratinocyte growth medium (MCDB 153) were wounded and five minutes later media was removed and replaced with unwounded media. Another media change was conducted ten minutes later and thirty minutes post-wounding samples were taken for analysis. Data shows mean ± SEM from three donors in triplicate (n=9), N=3. *** $P<0.001$, ns = not significant $P>0.05$. One way ANOVA Dunnett's post hoc.

F(F(1,32)=65.15, P<0.0001). A Bonferroni post-hoc test revealed that the process of media replacement did not affect basal ATP release in unwounded keratinocytes (P>0.05). However, there was a significant difference between wounded cells that did not have the media replaced and wounded cells that had the media replaced (*** P<0.001). Wounded cells that had the media replaced one minute post-wounding, showed no statistical difference to unwounded cells (P>0.05). Keratinocytes wounded in 1.2mM $[Ca^{2+}]_o$ displayed similar results during media replacement experiments (figure 4.8b), replacing the wounded media one minute post-wounding with fresh media appeared to decrease the ATP levels detected in the media to those similar to unwounded cells. Two-way ANOVA statistical analysis confirmed this with results showing that, akin to 0.06mM $[Ca^{2+}]_o$, media replacement had an overall significant effect on the ATP levels (F(1,32)=49.23, P<0.0001).

In conditioned media experiments cells were wounded in either 0.06 or 1.2mM $[Ca^{2+}]_o$ and five minutes post-wounding, the media was transferred to unwounded cells. Unwounded media was then added to wounded cells. Thirty minutes post-wounding, samples were obtained and ATP levels analysed. Cells were classified as positive (+) or negative (-) for wounding; positive if they had been wounded, negative if they were left unwounded. Media was classified as positive (+) or negative (-) for wounding; positive if the media originated from wounded cells, negative if the media originated from unwounded cells. A negative media replacement described cells that once wounded did not have media removed and replaced, whereas positive described experiments in which media had been removed and replaced. In experiments positive for this replacement, cells were exposed to air for a short period of time. To ensure that this air exposure did not result in ATP release appropriate controls were conducted; these cells remained unwounded and cultured in unwounded media. However after five minutes, media was removed and cells were exposed to air for an identical amount as other (wounded) conditions. It is clear that this short period of air exposure did not cause ATP release (figure 4.9a). A one-way ANOVA with Dunnett's post-hoc test confirmed this and showed no difference between unwounded cells in unwounded media that had a short period of air exposure compared to unwounded cells in unwounded media that were not air-exposed (P>0.05). As shown by figure 4.9a, exposing unwounded cells to wounded media for twenty five minutes caused an increase in $[ATP]_o$. Exposing wounded cells to unwounded media did not significantly alter ATP levels compared to unwounded cells

in unwounded media (P>0.05). Unwounded cells in wounded media had significantly elevated ATP in the media compared to unwounded cells in unwounded media (P<0.001), however, these results were significantly lower than ATP levels detected in the extracellular media as a result of wounding without media replacement (P<0.001). To support these results that there was no further release of ATP after the point of wounding, a double conditioned media experiment was conducted (figure 4.9b). Five minutes post-wounding media was replaced with fresh media. Another media change was conducted ten minutes later and then sample was obtained a further fifteen minutes later (total time post-wound of thirty minutes). Similar, to previous results, no significant increase in extracellular ATP was detected in wounded cells that had undergone media changes compared to unwounded cells (Dunnett's post-hoc test; ns P>0.05) and this level was significantly different to wounded cells that had not had the media changed (Dunnett's post-hoc test; *** P<0.001).

Collectively, these data show that ATP release post-wounding is an isolated event occurring at the point of wounding; no further release is detected.

4.3.4 Mechanisms regulating in ATP release post-wounding.

Data presented above clearly demonstrate that keratinocytes release ATP into the media upon wounding. To evaluate potential mechanisms regulating this, various pharmacological inhibitors were tested. Published results within the literature indicate that three main mechanisms exist for ATP release (section 4.1.3) i) vesicular exocytosis, ii) ABC transporters and iii) gap-junction communication. In the following experiments, keratinocyte monolayers were pre-treated with the various inhibitors or vehicle controls, for one hour prior to wounding in either 0.06 or 1.2mM $[Ca^{2+}]_o$. A cross hatch wound was performed and a sample of the extracellular media was taken five minutes post-wounding for analysis, as previously described (section 3.4.2).

The first mechanism investigated was vesicular release. N-ethylmaleimide (NEM) is an established inhibitor that blocks vesicle fusion to the PM (M. R. Block *et al.*, 1988). From figure 4.10 it can be seen the presence of 10µM NEM in either 0.06mM (figure 4.10a) or 1.2mM $[Ca^{2+}]_o$ (figure 4.10b) did not affect basal ATP release in unwounded cells. Similarly, values obtained from wounded cells remained constant regardless of NEM or vehicle (ethanol) treatment. These observations were confirmed by two-way

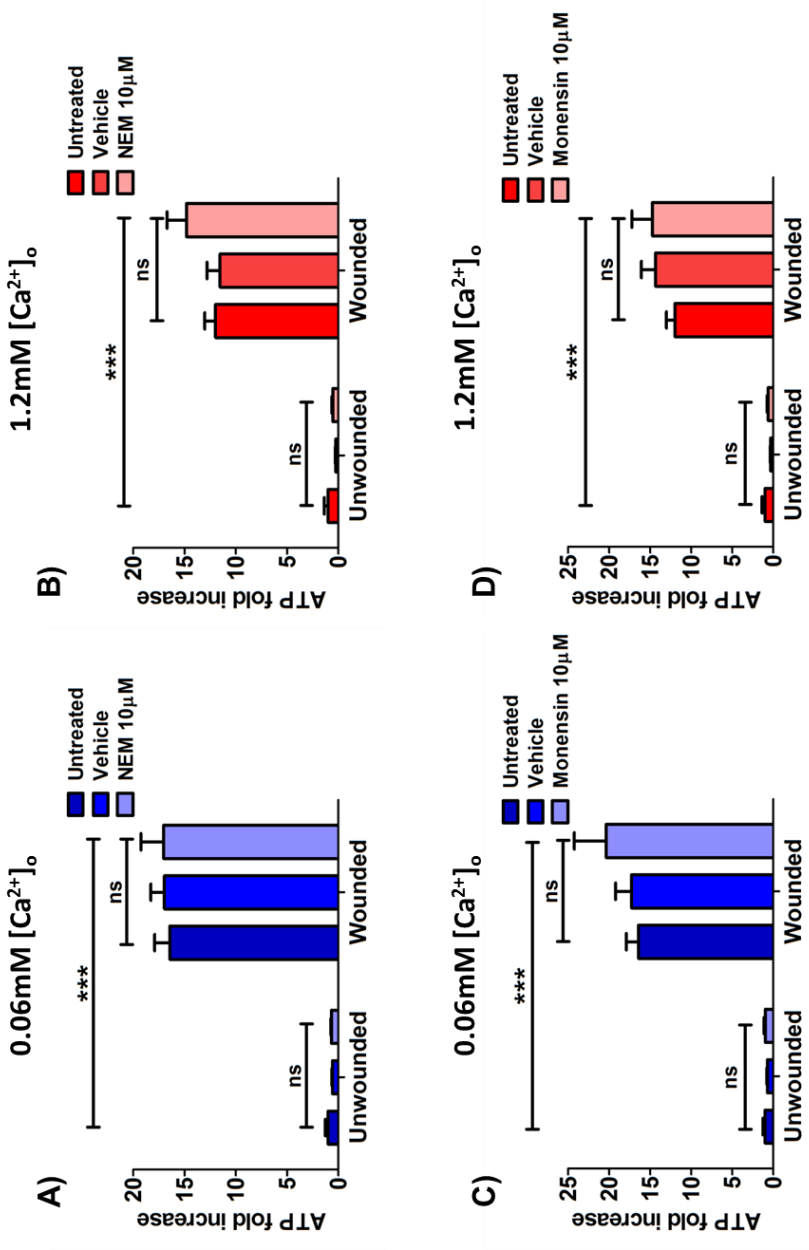

Figure 4.10 Vesicular exocytosis inhibition does not prevent ATP release from wounded keratinocytes.

Primary human keratinocytes cultured in 0.06mM $[Ca^{2+}]_o$ keratinocyte growth medium (MCDB 153) were pre-treated with either **A+B)** 10µM N-ethylmaleimide (NEM) or **C+D)** 10µM Monensin for one hour prior to wounding in **A+C)** 0.06 mM $[Ca^{2+}]_o$ or **B+D)** 1.2 $[Ca^{2+}]_o$. Vehicle controls used were monensin (DMSO) and NEM (ethanol). Samples were taken five minutes post-wounding. Data shows mean ± SEM from three donors in triplicate (n=9), N=3. Two way ANOVA with Bonferroni post-hoc was conducted (*** $P<0.001$, ns = not significant $P>0.05$).

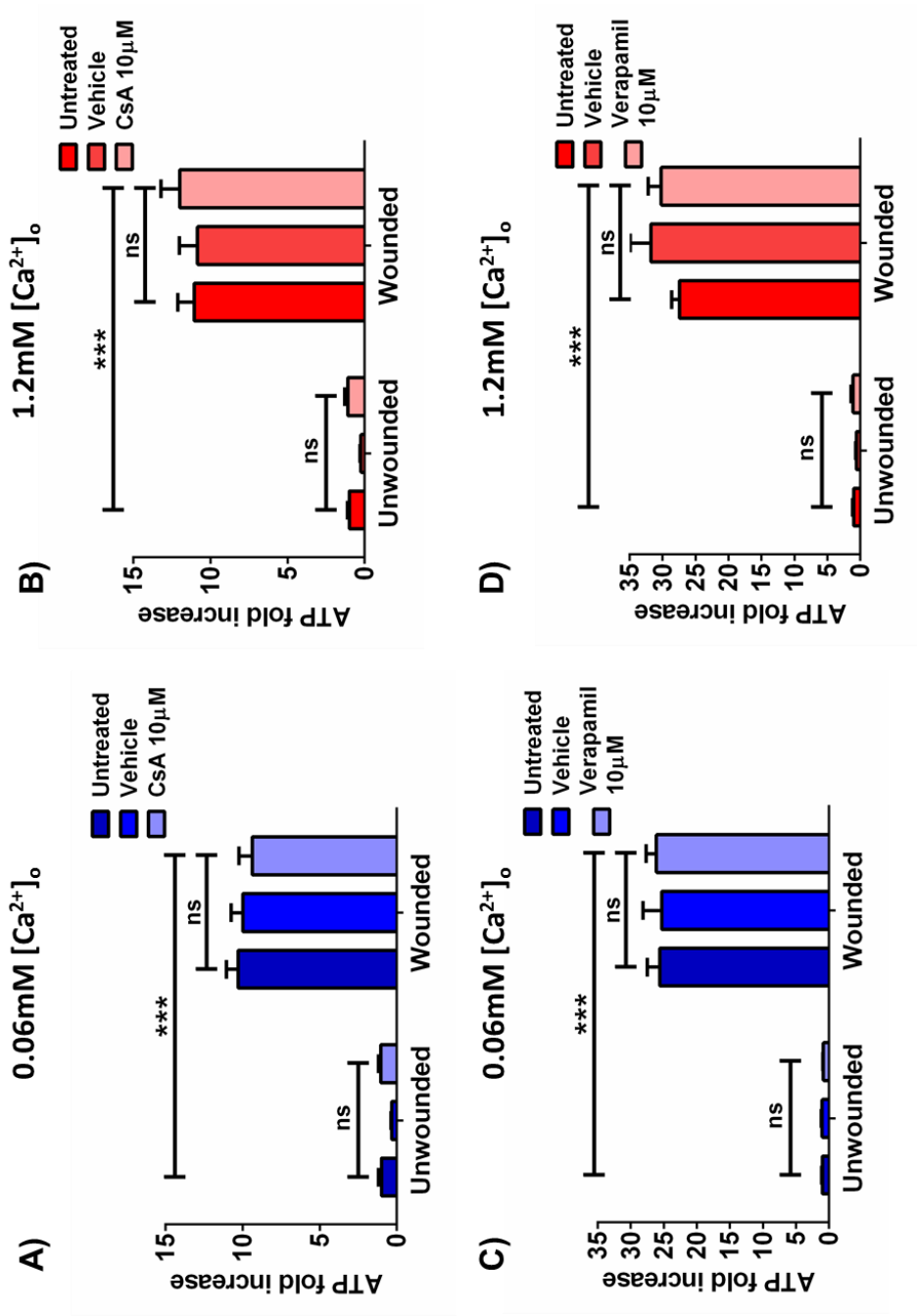

Figure 4.11 ABC transporter inhibition does not prevent ATP release from wounded keratinocytes.

Primary human keratinocytes cultured in 0.06mM $[Ca^{2+}]_o$ keratinocyte growth medium (MCDB 153) were pre-treated with either **A+B)** 10µM cyclosporin A (CsA) or **C+D)** 10µM verapamil for one hour prior to wounding in **A+C)** 0.06 mM $[Ca^{2+}]_o$ or **B+D)** 1.2 $[Ca^{2+}]_o$. Vehicle controls used were verapamil; DMSO and CsA; ethanol. Samples were taken five minutes post-wounding. Data shows mean ± SEM from three donors in triplicate (n=9), N=3. Two way ANOVA with Bonferroni post-hoc was conducted (*** $P<0.001$, ns = not significant $P>0.05$).

ANOVA statistical analysis which reported that treatment had no effect on unwounded or wounded ATP release in 0.06mM ($F(2,48)=0.007588$, $P=0.9924$) or 1.2mM $[Ca^{2+}]_o$ ($F(2,48)=0.007587$, $P=0.9924$). A Bonferroni post-hoc test demonstrated that within each treatment, wounding had a significantly positive effect on ATP levels (*** $P<0.001$). Monensin is an alternative compound that prevents vesicular-mediated release of ATP by blocking vesicle formation at the golgi apparatus (Cecchelli *et al.*, 1986). In a similar manner to NEM, 10µM monensin did not appear to affect basal or wound-induced ATP release in either 0.06mM (figure 4.10c) or 1.2mM calcium conditions (figure 4.10d). Two-way ANOVA analysis reported that keratinocytes treated with 10µM monensin showed unaltered levels of ATP compared to untreated cells and vehicle (DMSO) in 0.06mM ($F(2,48)=0.6445$, $P=0.5294$) or 1.2mM $[Ca^{2+}]_o$ ($F(2,48)=6.770$, $P=0.6505$). As expected, a Bonferroni post-hoc revealed within each treatment wounding significantly increased ATP (*** $P<0.001$).

These results indicate that vesicular exocytosis was not the mechanism by which ATP was released into the extracellular media post-wounding in a low or high external calcium environment.

ABC transporters represent an important family of transport proteins and have been implicated in ATP efflux from the cell. Verapamil and CsA are pharmacological inhibitors of p-gp, an ABC family member. It can be seen in figure 4.11a, that treatment with 10µM CsA treatment did not appear to affect basal or wound-induced ATP release with ATP levels remaining unaltered in the extracellular media regardless of treatment. Two-way ANOVA analysis failed to report a difference between treatments in 0.06mM ($F(2,48)=0.4361$, $P=0.6491$) (figure 4.11a) and 1.2mM $[Ca^{2+}]_o$ ($F(2,48)=0.7374$, $P=0.4837$) (figure 4.11b). A Bonferroni post-hoc test confirmed within each treatment, wounding had a significantly positive effect on ATP levels (*** $P<0.001$). The lack of effect of wound-induced ATP release after ABC transporter blockade was confirmed with another pharmacological inhibitor, verapamil. 10µM verapamil treatment did not cause any alterations in ATP levels detected in the media five minutes post-wounding in either calcium concentration. In agreement with CsA treatment, two-way ANOVA analysis failed to report a significant difference in 0.06mM $[Ca^{2+}]_o$ ($F(2,48)=0.02123$, $P=0.9790$) (figure 4.11c) and 1.2mM $[Ca^{2+}]_o$ ($F(2,48)=0.8301$ $P=0.4422$) (figure 4.11d).

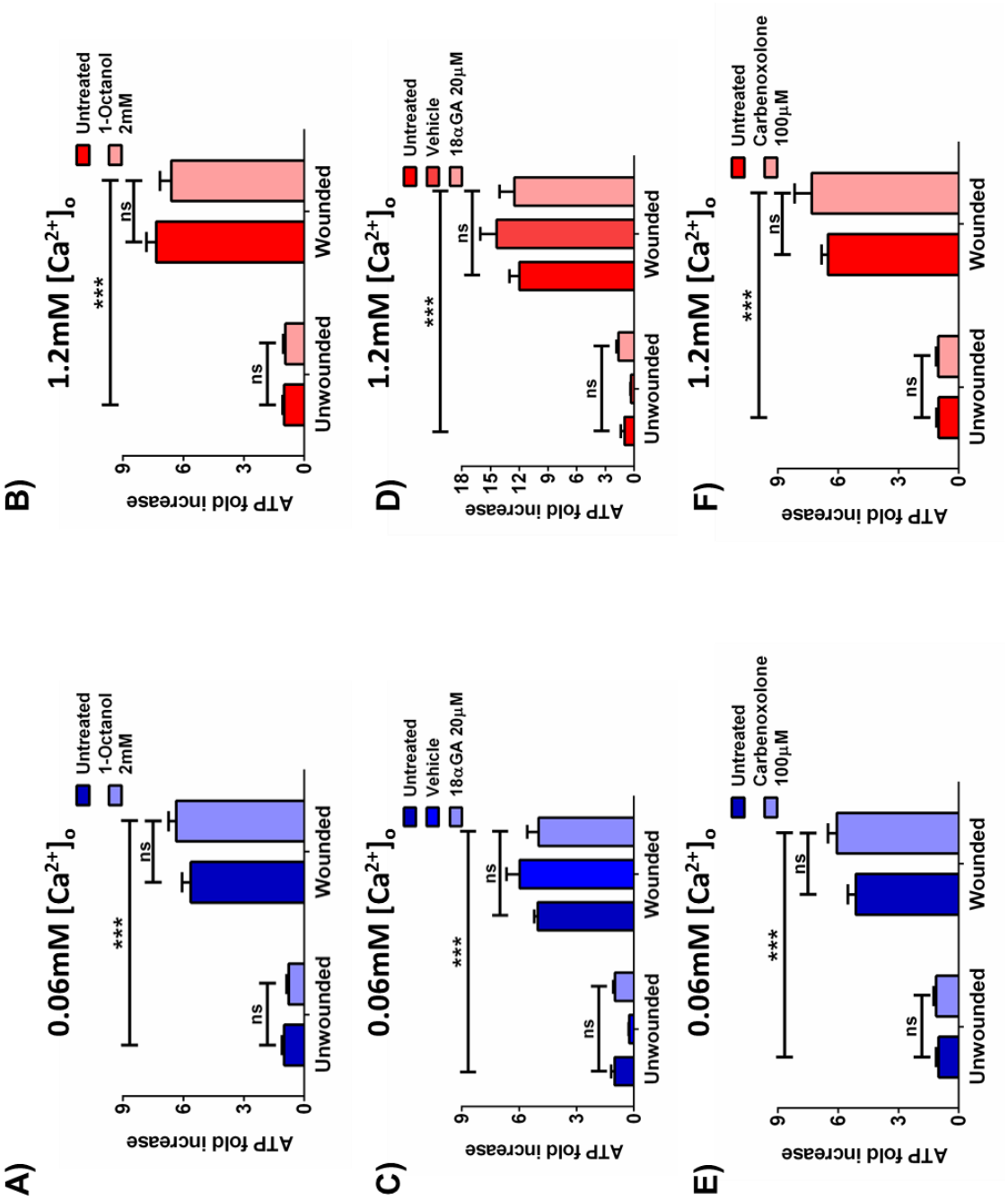

Figure 4.12 Connexin and pannexin inhibition does not prevent ATP release from wounded keratinocytes.

Primary human keratinocytes cultured in 0.06mM $[Ca^{2+}]_o$ keratinocyte growth medium (MCDB 153) were pre-treated with either **A+B)** 2mM 1-Octanol, **C+D)** 20μM 18α-glycyrrhetinic acid (18αGA) or **E+F)** 100μM carbenoxolone for one hour prior to wounding in **A,C+E)** 0.06mM $[Ca^{2+}]_o$ or **B,D+F)** 1.2mM $[Ca^{2+}]_o$. Vehicle controls used were verapamil; DMSO and CsA; ethanol. Samples were taken five minutes post-wounding. Data shows mean ± SEM from three donors in triplicate (n=9), N=3. Two way ANOVA with Bonferroni post-hoc was conducted (*** $P<0.001$, ns = not significant $P>0.05$).

A Bonferroni post-hoc test confirmed within each treatment, wounding had a significantly positive effect on ATP levels (*** P<0.001). These results indicate that ABC transporters did not mediate ATP released into the extracellular media post-wounding in a low or high external calcium environment.

The third mechanism implicated in ATP release is connexins and pannexins. Three pharmacological inhibitors were utilised to determine gap-junctional signalling involvement in wound-induced ATP release; 2mM 1-Octanol, 100µM carbenoxolone and 20µM 18αGA. Figure 4.12 shows that inhibiting gap-junction communication with 1-Octanol had no effect on ATP release compared to untreated cells in both basal unwounded keratinocytes and wounded cells. There was no statistical difference between these data in 0.06mM $[Ca^{2+}]_o$ ($F(1,76)=0.7340$, $P=0.3943$) (figure 4.12a) and 1.2mM $[Ca^{2+}]_o$ ($F(1,44)=1.149$ $P=0.2895$) (figure 4.12b), as assessed by two-way ANOVA. However, a significant difference was reported after wounding for each treatment (Bonferroni post-hoc *** P<0.001). In a similar manner, whilst a difference was detected within each treatment in response to wounding (*** P<0.001), wounding in the presence of 18αGA showed no effect on ATP in the extracellular media compared to untreated cells and vehicle (DMSO) in both 0.06mM $[Ca^{2+}]_o$ ($F(2,48)=0.05990$, $P=0.9419$) (figure 4.12c) and 1.2mM $[Ca^{2+}]_o$ ($F(2,48)=0.3470$ $P=0.7086$) (figure 4.12d), as assessed by two-way ANOVA. Finally, to ensure that connexins and pannexins had no effect on wound-induced ATP release, keratinocytes were treated with 100µM carbenoxolone. Akin to previous compounds, this treatment did not appear to have any significant effect on basal ATP release from keratinocytes or wound-induced ATP release. A two-way ANOVA was conducted and did not report any statistical differences in 0.06mM $[Ca^{2+}]_o$ ($F(1,72)=2.965$, $P=0.0894$) (figure 4.12e) and 1.2mM $[Ca^{2+}]_o$ ($F(1,32)=0.8172$ $P=0.3727$) (figure 4.12f) but within a treatment wounding had a significant effect (Bonferroni post-hoc *** P<0.001).

These results are indicative that connexin and pannexins are not involved in ATP release in response to wounding in primary human keratinocytes.

Combined, data from the above pharmacological inhibition analyses suggests that wound-induced ATP release is not conducted through any of the three well established

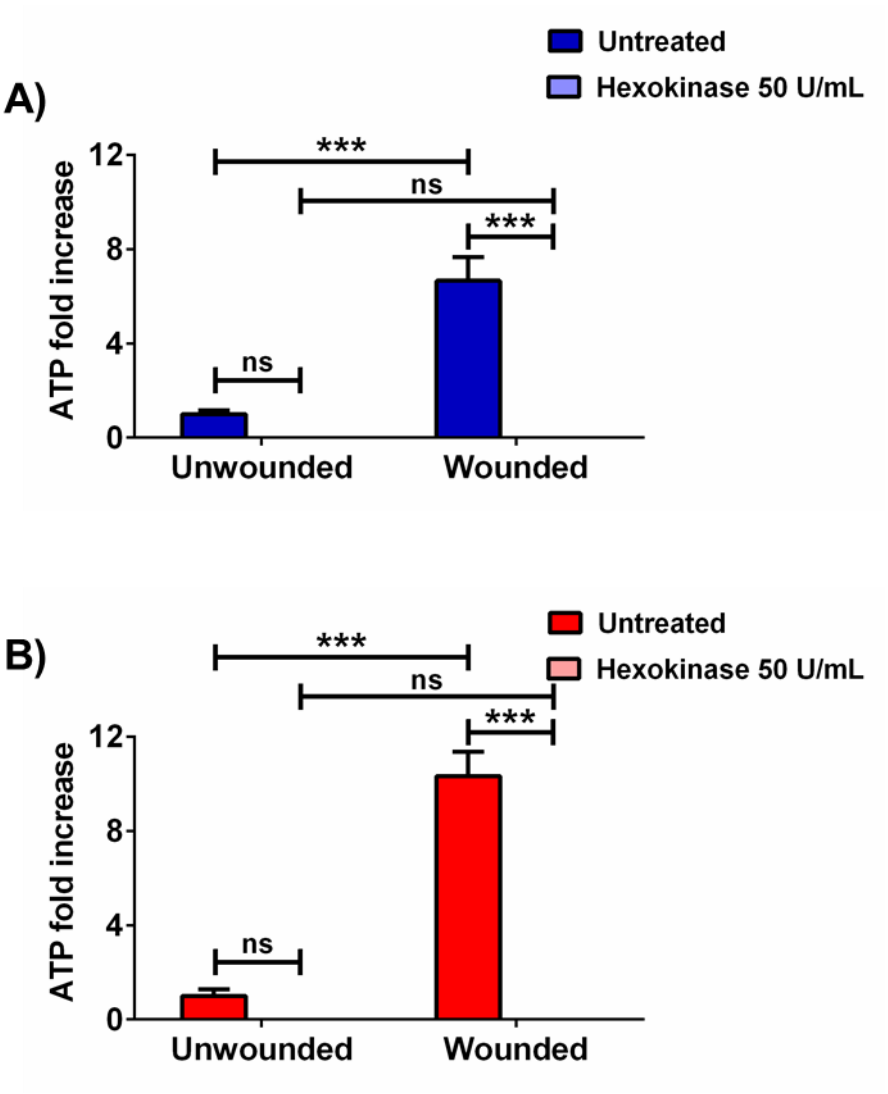

Figure 4.13 Hexokinase completely removes detectable levels of ATP in the media post-wounding of keratinocytes.

Primary human keratinocytes cultured in 0.06mM $[Ca^{2+}]_o$ keratinocyte growth medium (MCDB 153) were wounded in the presence of 50U/mL hexokinase in a cross-hatch manner in either **A)** 0.06mM $[Ca^{2+}]_o$ or **B)** 1.2mM $[Ca^{2+}]_o$. Five minutes post-wounding samples were collected for analysis. Data shows mean ± SEM from four donors in triplicate (n=12), N=4. Two way ANOVA with Bonferroni post-hoc test was conducted (*** $P<0.001$, ns $P>0.05$).

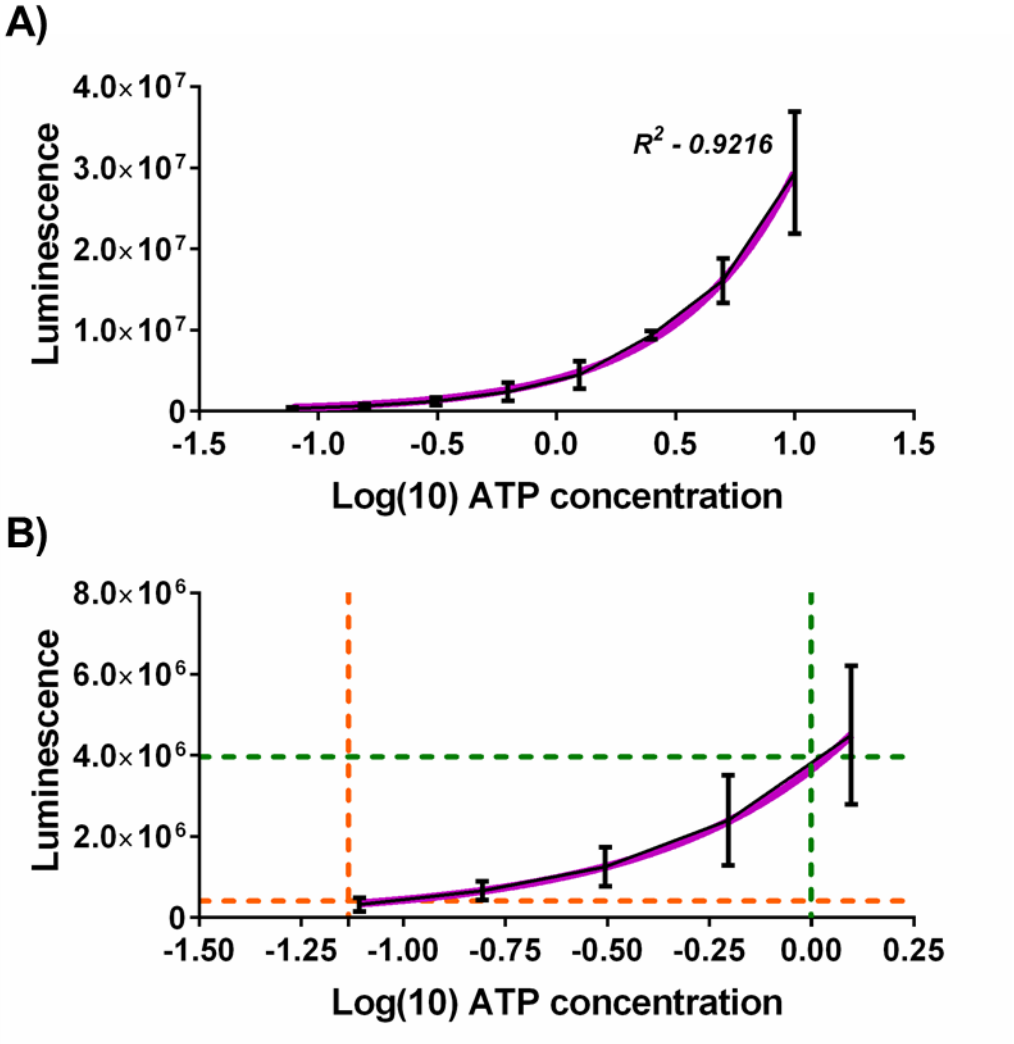

Figure 4.14 ATP standard curve to determine extracellular ATP concentration in conditioned media of wounded keratinocytes.

A) Standard curve of known ATP concentrations was generated. Purple solid line indicates curve of best fit. **B)** Data from the standard curve was used to determine the ATP concentration in unwounded and wounded conditioned media samples from keratinocytes collected as described in figure 4.6. Purple solid line indicates curve of best fit. Dotted lines allow the concentrations of ATP in unwounded (orange) and wounded (green) conditioned media to be determined. Data shows mean ± SEM and are representative of three experimental repeats.

ATP release mechanisms. It is therefore highly likely that increased ATP levels in the extracellular environment post-wounding are a direct result of the alternative mechanism of ATP release; cell lysis. Wounding disrupts the cell membrane and ATP leaks out of the cell rather than being released in a regulated manner. This is further supported by results that showed that the amount of ATP released is proportional to the number of wounds inflicted; the higher the number of scratches, the more ATP released (Appendix B).

4.3.5 Removal of released ATP from the extracellular environment by hexokinase.

As suggested previously, it appears that ATP released post-wounding did not occur through regulated mechanisms such as ABC transporters, connexins or vesicular exocytosis. Rather, increases detected were through cell lysis caused by mechanical disruption of the cell membrane. However without an effective treatment to reduce ATP release post-wounding, it would not possible to investigate the downstream consequences of wound-induced ATP release. To meet this need, hexokinase was utilised. Hexokinase is an ATP scavenger and whilst it does not prevent cellular release of ATP, it was hypothesised it would remove released ATP in the extracellular media.

As shown by figure 4.13, 50U/mL hexokinase significantly reduced detectable levels of extracellular ATP in unwounded and wounded samples exposed to both 0.06mM $[Ca^{2+}]_o$ ($F(1,4)=56.64$, $P<0.0001$, two-way ANOVA) (figure 4.13a) and 1.2mM $[Ca^{2+}]_o$ ($F(1,44)=112.0$, $P<0.0001$, two-way ANOVA)(figure 4.13b). A Bonferroni post-hoc test revealed that this result was statistically different in wounded cells (*** $P<0.01$) but not unwounded cells ($P>0.05$).

From this data it can be concluded that, hexokinase represents a robust manner in which to investigate the downstream effects of wound-induced ATP release in future experiments, by effectively removing released ATP from extracellular environment.

4.3.6 Determining the concentration of ATP released post-wounding.

In order to quantify the concentration of ATP released into the extracellular environment post-wounding, a standard curve of known ATP concentrations was established (R^2–0.9216) (figure 4.14a). Average relative luminescence for both unwounded and wounded cells was calculated and utilising the standard curve it was

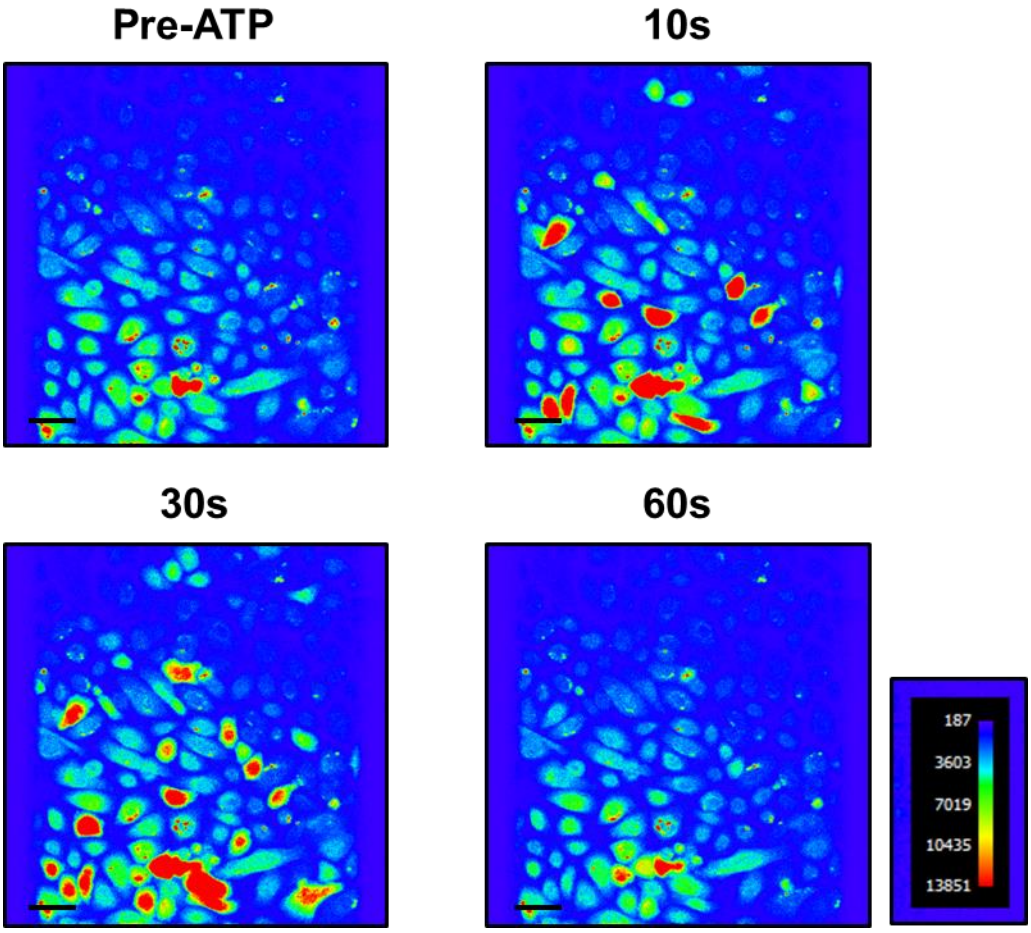

Figure 4.15 2D images demonstrating physiologically wound relevant concentrations of ATP induces $[Ca^{2+}]_i$ changes in unwounded keratinocytes.

Keratinocyte growth media (MCDB 153) with an external calcium concentration of either 0.06mM or 1.2mM was supplement with ATP. This was added to unwounded keratinocytes that had been loaded with the calcium dye Fluo4-AM, to make a final concentration of 1µM – the concentration of ATP determined to be present in conditioned media (CM). Images were captured at 3.7fps. Pseudo colour images of confocal images were generated pre-ATP being added and then 10, 30 and 60 seconds post-ATP to demonstrate the calcium signal triggered by ATP. Scale bar=80µm. Pseudo colour reference is shown. Images are representative of three independent donors in 1.2mM $[Ca^{2+}]_o$.

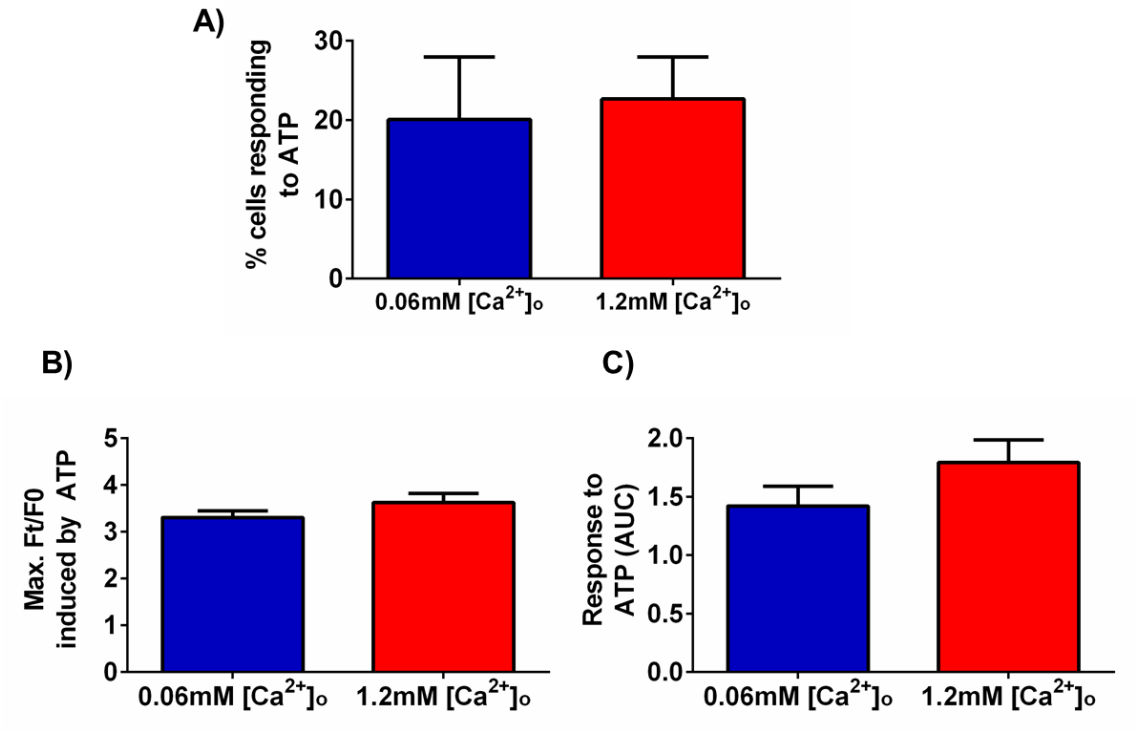

Figure 4.16 Extracellular calcium concentration does not significantly alter parameters of ATP-induced $[Ca^{2+}]_i$ flux.

Keratinocyte growth media (MCDB 153) with an external calcium concentration of either 0.06mM or 1.2mM was supplement with ATP. This was added to unwounded keratinocytes that had been loaded with the calcium dye Fluo4-AM, to make a final concentration of 1µM; the physiologically wounded relevant concentration. Images were captured at 3.7fps. **A)** percentage of keratinocytes responding to ATP in 0.06mM and 1.2mM $[Ca^{2+}]_o$. P=0.1655, Chi-square test. **B)** Maximum Ft/F0 reached within individual cells after addition of ATP in 0.06mM and 1.2mM $[Ca^{2+}]_o$. Unpaired, two-tailed t-test (P=1992). **C)** AUC was calculated for the $[Ca^{2+}]_i$ flux post-ATP in 0.06mM and 1.2mM $[Ca^{2+}]_o$. Unpaired, two-tailed t-test (P=0.1528).

determined that in unwounded conditions ATP concentration in the extracellular media was 73.5nM. Wounding then resulted in an increase to 995.8µM at five minutes post-wounding (figure 4.14b).

These values represent a concentration of ATP that is physiologically relevant to wounded primary human keratinocytes. Therefore, allowing investigation of the role of wound-induced ATP in various downstream events.

4.3.7 The addition of ATP to unwounded keratinocytes triggers a $[Ca^{2+}]_i$ flux.

Results presented above show that keratinocytes release ATP in response to mechanical wounding. It is known that purinergic signalling results in $[Ca^{2+}]_i$ changes through activation of P2XR and P2YR (section 1.6.1) (Hassinger *et al.*, 1996). Therefore, the next part of this investigation focussed on the ability of ATP to induce an $[Ca^{2+}]_i$ flux in unwounded primary human keratinocytes. Data utilising the generated ATP standard curve revealed that the concentration of ATP in the extracellular media five minutes post-wounding was approximately 1µM. Therefore, keratinocyte growth media (MCDB 153) with an external calcium concentration of either 0.06mM or 1.2mM was supplement with ATP. This was added to unwounded keratinocytes that had been loaded with the calcium dye Fluo4-AM, to make a final concentration of 1µM; the physiologically wounded relevant concentration.

Signalling across the whole population was visually assessed to determine whether 1µM ATP was able to produce an intracellular calcium response in unwounded keratinocytes. Figure 4.15 shows representative images from one experiment taken prior to ATP addition and then ten, thirty and sixty seconds after ATP was added. It is clear that upon addition of ATP, $[Ca^{2+}]_i$ increased within a small population of cells. Using the image analysis software Volocity, the colour of the images was altered to rainbow to facilitate visualisation of changes in intensity. No relationship was observed between cells that responded and their location in the field of view. Moreover, an increase in $[Ca^{2+}]_i$ after ATP application did not result in an $[Ca^{2+}]_i$ increase in neighbouring cells or the induction of a intercellular calcium wave. Additionally, it was observed that only a sub-population of keratinocytes responded to ATP with a calcium signal, these were recorded as a percentage of total cell population in the field of view. As shown by figure 4.16a, 20.1±7.8% of keratinocytes in 0.06mM $[Ca^{2+}]_o$ responded to ATP, this figure was

22.6±5.2% in 1.2mM $[Ca^{2+}]_o$. Statistical analysis failed to report this difference as significant (P=0.1655, Chi-square test). To determine whether external calcium concentration had an effect on specific parameters of the induced $[Ca^{2+}]_i$ flux, maximum Ft/F0 post-ATP was recorded for responding cells. Maximum Ft/F0 was defined as the greatest fold change in $[Ca^{2+}]_i$ within individual unwounded keratinocytes triggered by the addition of ATP. There was no significant difference between the maximal Ft/F0 triggered by the ATP in 0.06mM $[Ca^{2+}]_o$ (3.30±0.14) and 1.2mM $[Ca^{2+}]_o$ (3.62±0.19) (P=0.1992, unpaired, two-tailed t-test) (figure 4.16b). AUC of the ATP-induced $[Ca^{2+}]_i$ flux in 0.06mM was not significantly different to the AUC of the ATP-induced $[Ca^{2+}]_i$ flux in 1.2mM $[Ca^{2+}]_o$ (P=0.1520, unpaired, two-tailed t- test) (figure 4.16c).

These data show that ATP at a comparable concentration to that detected post-wounding, is capable of inducing an $[Ca^{2+}]_i$ flux within unwounded keratinocytes. Furthermore, it demonstrates that the cultures of primary human keratinocytes express functioning P2R.

4.3.8 Removal of ATP from wounded CM reduces but does not prevent CM-induced calcium response in unwounded keratinocytes.

Results presented within this chapter so far have shown that i) a diffusible factor is released upon wounding and is capable of inducing a calcium response in unwounded cells (section 4.3.2), ii) wounding causes ATP release into the media via cell lysis (section3.5), iii) wounding in the presence of 50 U/mL hexokinase eliminates detectable ATP in the media (section 3.5) and iv) ATP at physiologically wounded concentration is able to produce an $[Ca^{2+}]_i$ response (section3.7). It was therefore hypothesised that ATP was the mediator released from keratinocytes in response to wounding that was inducing the $[Ca^{2+}]_i$ flux in unwounded cells see during CM experiments. To explore this possibility, primary human keratinocytes were scratch wounded in a cross-hatch manner in either 0.06mM or 1.2mM $[Ca^{2+}]_o$ in the presence of 50U/mL hexokinase. Five minutes post-wounding, the extracellular media was removed and added to unwounded keratinocytes that had been loaded with the calcium dye Fluo4-AM and de-esterified for forty five minutes with 50 U/mL hexokinase. Images were captured at

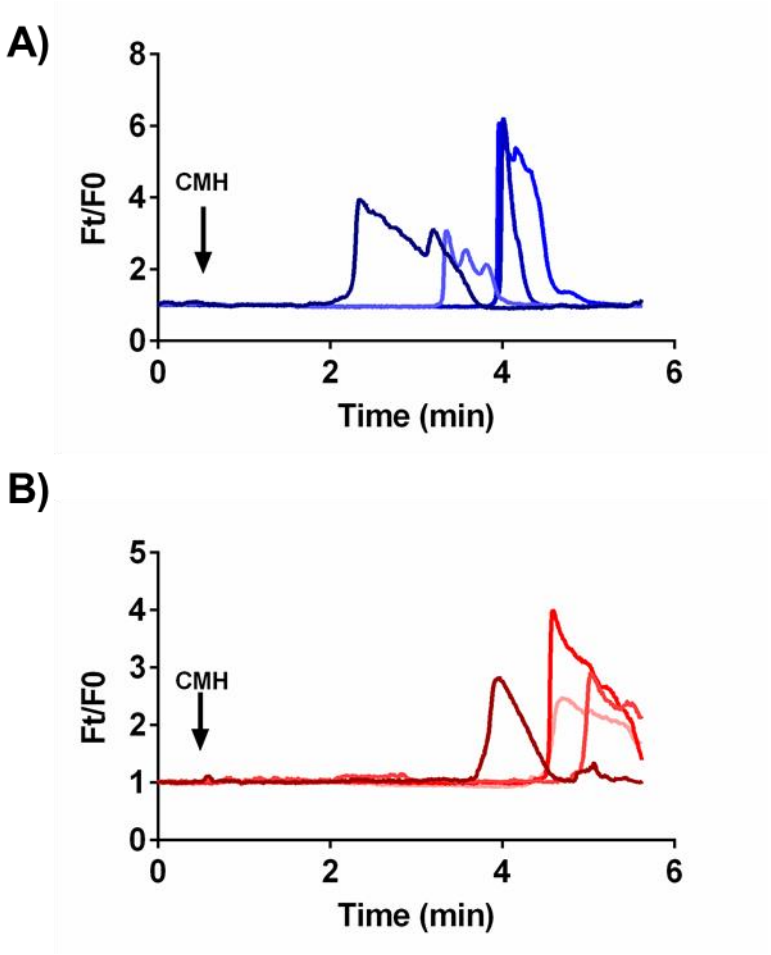

Figure 4.17 Removal of ATP from wounded conditioned media delays but does not block CM-induced increase in $[Ca^{2+}]_i$ in unwounded keratinocytes.

Primary human keratinocytes were scratch wounded in a cross-hatch manner in either A) 0.06mM $[Ca^{2+}]_o$ or B) 1.2mM $[Ca^{2+}]_o$ in the presence of 50 U/mL hexokinase. Five minutes post-wounding, the extracellular conditioned media with (CMH) or without (CM) hexokinase was removed and added to unwounded keratinocytes that had been loaded with the calcium dye Fluo4-AM. Confocal images were captured at 3.7 fps. Regions of interest (ROI) were drawn around individual cells up to six cells from the wound edge for analysis. Traces show four representative cells. Time of addition of CMH is highlighted by arrow. Four cells per condition are representative of three independent donors.

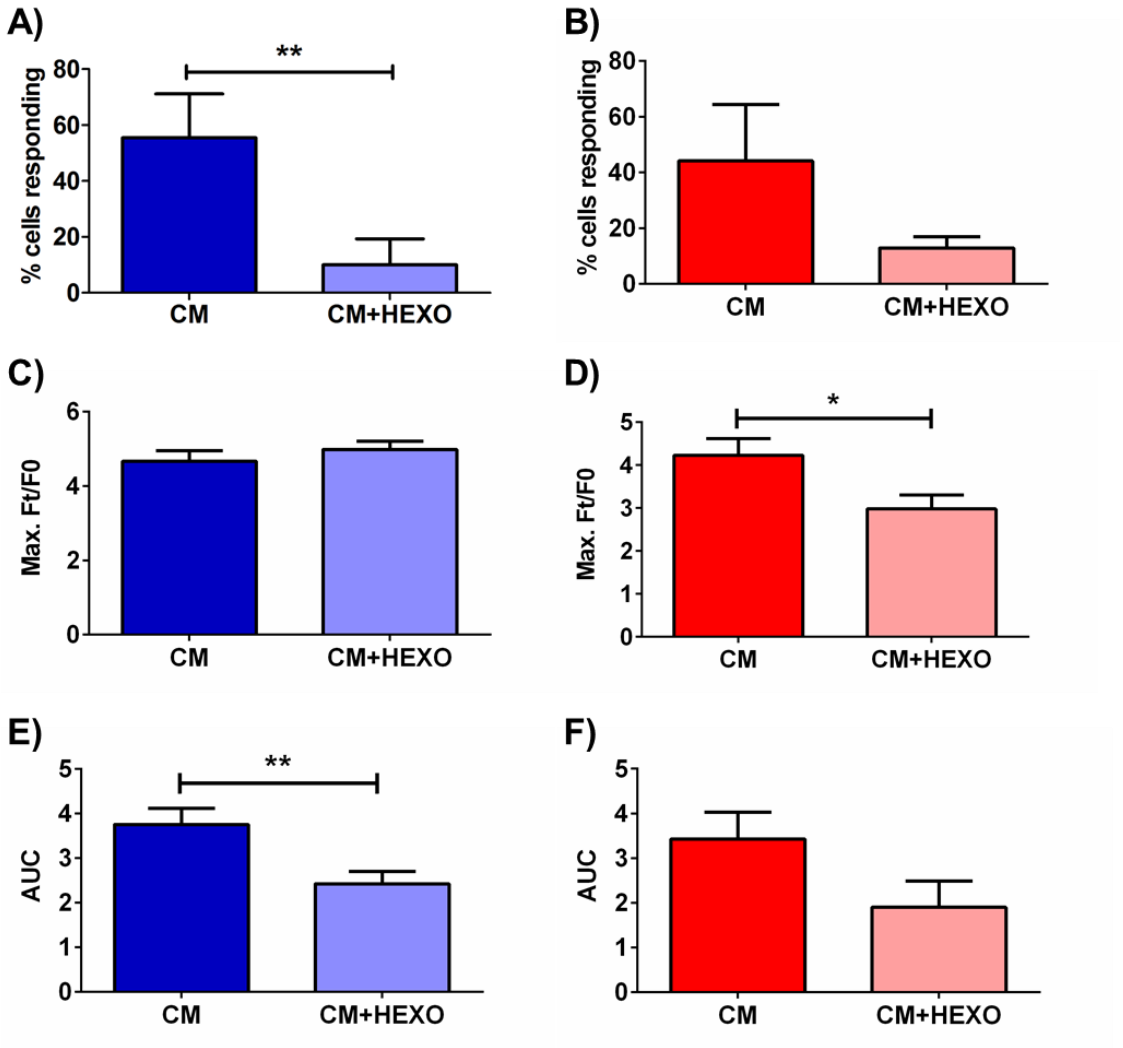

Figure 4.18 Wounding in the presence of hexokinase reduces keratinocyte intracellular calcium response to wounded conditioned media.

Primary human keratinocytes were scratch wounded in a cross-hatch manner in either **A, C and E)** 0.06mM $[Ca^{2+}]_o$ or **B, D and F)** 1.2mM $[Ca^{2+}]_o$ in the presence or absence of 50 U/mL hexokinase. Five minutes post-wounding, the extracellular conditioned media in absence (CM) or presence of hexokinase (CM+HEXO) was removed and added to unwounded keratinocytes that had been loaded with the calcium dye Fluo4-AM. Images were captured at 3.7fps. **A+B)** Percentage of keratinocytes responding; ** P=0.0024 and P=0.4985 respectively (Chi-square test) **C+D)** Maximum Ft/F0 reached within individual cells; unpaired –two tailed t-test (*** P,0.001, * P<0.05). **E+F)** AUC was calculated for the $[Ca^{2+}]_i$ flux; unpaired two-tailed t-test (* P<0.05).

3.7fps. The wounded media removed and added to unwounded cells was referred to as conditioned media hexokinase (CMH).

Signalling across the whole population was visually assessed to determine whether the CMH was able to produce an intracellular calcium response in unwounded cells. An interesting observation was that the presence of hexokinase in the CM did not eliminate the $[Ca^{2+}]_i$ response; a small population of keratinocytes still responded with intracellular calcium flux. Figure 4.17 shows traces from four individual cells after the addition of either 0.06mM $[Ca^{2+}]_o$ CMH (figure 4.17a) or 1.2mM $[Ca^{2+}]_o$ CMH (figure 4.17b), traces are representative of three independent donors. These traces confirm that CMH caused an increase in $[Ca^{2+}]_i$, however it can be seen that there was a delay between the addition of the CMH and the intracellular calcium flux in both 0.06mM and 1.2mM $[Ca^{2+}]_o$, although this delay appeared to be greater in the higher calcium environment. It was observed that only a sub-population of keratinocytes responded to CMH with a calcium signal, these were recorded as a percentage of total cell population in the field of view. As shown by figures 4.18a and 4.18b respectively, 10±9.2% of keratinocytes in 0.06mM $[Ca^{2+}]_o$ responded to CMH, this figure was 12.8±4.1% in 1.2mM $[Ca^{2+}]_o$. Statistical analysis failed to report this difference as significant in 1.2mM $[Ca^{2+}]_o$ but a significant difference was revealed in 0.06mM $[Ca^{2+}]_o$, (P=0.0024, Chi-square test). To determine whether hexokinase had an effect on specific parameters of the induced $[Ca^{2+}]_i$, maximum Ft/F0 post-CMH was recorded for responding cells. Maximum Ft/F0 was defined as the greatest fold change in $[Ca^{2+}]_i$ within individual unwounded keratinocytes triggered by the addition of CMH. Whilst there was no significant difference between the maximal Ft/F0 triggered by the CMH in 0.06mM $[Ca^{2+}]_o$ (P=0.3869, unpaired, two-tailed t-test) (figure 4.18c), CMH significantly reduced maximum Ft/F0 in 1.2mM $[Ca^{2+}]_o$ (P=0.0267, unpaired, two-tailed t-test) (figure 4.18d). AUC of the CMH-induced $[Ca^{2+}]_i$ flux was significantly reduced compared to the AUC of the CM-induced $[Ca^{2+}]_i$ flux in 0.06mM $[Ca^{2+}]_o$ (P=0.0059, unpaired, two-tailed t-test) (figure 4.18e) but CMH had no effect in 1.2mM $[Ca^{2+}]_o$ (P=0.1024, unpaired, two-tailed t-test) (figure 4.18f).

The analyses presented suggest that removing ATP from the media of wounded cells using hexokinase reduces its ability to trigger an $[Ca^{2+}]_i$ response in unwounded cells, as evidenced by i) a borderline significant reduction in the percentage of responding cells

ii) a reduced maximal Ft/F0 achieved within responding cells and iii) a reduced AUC of the $[Ca^{2+}]_i$ flux of responding cells. These findings indicate that ATP released from keratinocytes is causing a calcium response in unwounded cells. However, an interesting observation is that hexokinase treatment, which has been shown to completely eliminate ATP in the media post-wounding (section 4.3.5), does not completely prevent CM-induced intracellular calcium flux in unwounded cells. Additionally, CM causes a calcium response in a higher percentage of keratinocytes compared to the addition of ATP alone. From these data it can be concluded that whilst released ATP into the extracellular environment has a clear role in mediating $[Ca^{2+}]_i$ flux, there appears to be another factor having similar effects.

4.3.9 The role of wound-induced release of ATP in intracellular calcium wave propagation.

As described earlier, the mechanisms that regulate intercellular calcium wave propagation are an area of intensive research. Current opinion in the field concurs that both gap-junction communication and ATP are implicated (Iacobas *et al.*, 2006). Data obtained in previous sections within this chapter convincingly shows that keratinocytes release ATP into the extracellular media in response to mechanical wounding. Furthermore, the addition of ATP at physiologically wounded concentrations causes a calcium response in a subpopulation of unwounded cells. These results combined with recent literature led to the hypothesis that the ATP released at the time of wounding mediates the intercellular calcium wave. To further understand the role of extracellular ATP in regulating the wound-induced wave, primary human keratinocytes cultured in 0.06mM $[Ca^{2+}]_o$ keratinocyte growth medium (MCDB 153) were loaded with Fluo4-AM calcium dye prior to treatment with 50 U/mL hexokinase during the subsequent forty five minute de-esterification period. Keratinocytes were then exposed to 50 U/mL hexokinase in either 0.06mM or 1.2mM $[Ca^{2+}]_o$ keratinocyte growth medium (MCDB 153) for five minutes prior to wounding.

Initially, signalling across the whole population of cells was visually assessed. Subsequently, sub-populations were defined by their location from the wound edge and analysed to provide insights into differences between cells located at the wound edge compared to those located further back. Figure 4.19 shows representative images from one experiment taken every two seconds for twelve seconds and then three later images

taken at minute intervals post-wounding, to visually depict the $[Ca^{2+}]_i$ changes triggered by wounding. It can be seen that hexokinase treatment decreased the intracellular calcium flux and reduced the spread of the calcium wave. Figure 4.20 shows that across the population of keratinocytes treated with hexokinase (n=72 from three independent donors, located up to 300µm from the wound) the $[Ca^{2+}]_i$ flux induced by wounding reached a maximum 3.80±0.27 fold increase compared to baseline during the first three minutes post-wounding in 0.06mM $[Ca^{2+}]_o$ (figure 4.20a). When wounding in 1.2mM $[Ca^{2+}]_o$, the average maximum Ft/F0 reached was 2.47±0.21 (figure 4.20b). Statistical analysis using a RM two-way ANOVA of the general population of cells irrespective of location to the wound edge showed that overall, in 0.06mM $[Ca^{2+}]_o$ removing ATP had no effect on the average intracellular calcium flux (Ft/F0) ($F(1,71)=1.341$, $P=0.2507$). Conversely, RM two-way ANOVA revealed that in 1.2mM $[Ca^{2+}]_o$, hexokinase treatment significantly reduced the average intracellular calcium flux (Ft/F0) ($F(1,71)=48.16$, $P<0.0001$). A Bonferroni post-hoc test of the two-way ANOVA revealed that the average intracellular calcium flux (Ft/F0) induced by wounding in 1.2mM $[Ca^{2+}]_o$ with hexokinase was significantly decreased compared to untreated cells between 0.37 and 2.19 minutes (*** $P<0.001$, * $P<0.05$). This is further supported by a statistical difference between the average AUC of $[Ca^{2+}]_i$ flux of wounds performed without treatment and with hexokinase treatment ($F(1,284)=13.38$ $P=0.0003$, two-way ANOVA). When comparing treatment to control within each external calcium condition, a Bonferroni post-hoc test showed a significant difference in 1.2mM $[Ca^{2+}]_o$ ($P<0.0001$) but failed to report a difference in 0.06mM $[Ca^{2+}]_o$ ($P>0.05$) (figure 4.20c).

To evaluate whether the observed intracellular calcium flux differences were cell location dependent, $[Ca^{2+}]_i$ flux was analysed taking into account the cellular location in relation to the wound edge. Individual keratinocytes were analysed in “rows” away from the wound edge and cells were designated 1-6, with cell 1 being the cell at the wound edge, and cell 6 located six cells back from the wound.

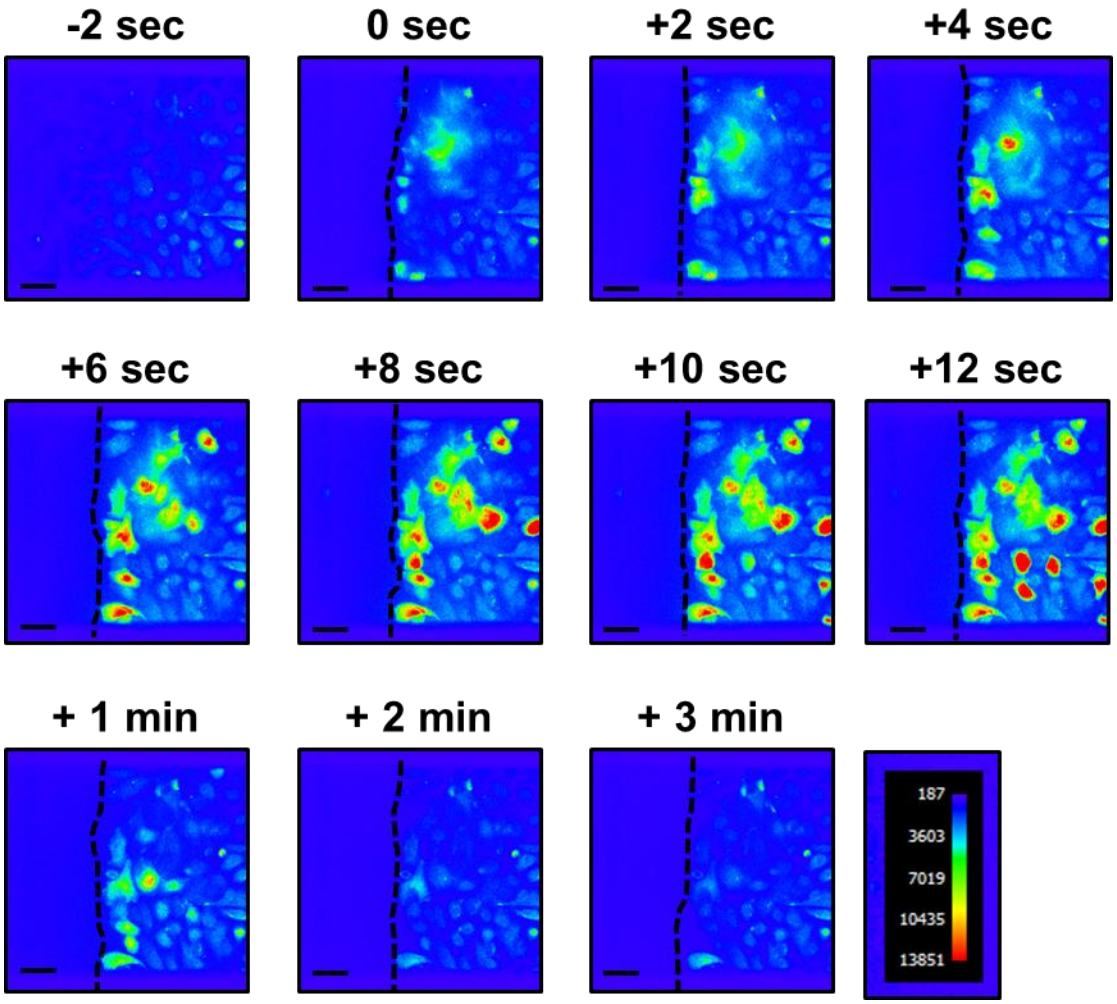

Figure 4.19 Pseudo colour images demonstrating the reduced wound-induced calcium wave in the presence of hexokinase.

Primary human keratinocytes cultured in 0.06mM $[Ca^{2+}]_o$ keratinocyte growth medium (MCDB 153) were loaded with Fluo4-AM calcium dye and during the de-esterification period of forty five minutes cells were treated with 50 U/mL hexokinase. Keratinocytes were wounded in 0.06mM or 1.2mM $[Ca^{2+}]_o$ keratinocyte growth medium (MCDB 153) in the presence of 50 U/mL hexokinase. Images were captured at 3.7fps. Pseudo colour images of confocal images were generated prior to the wound being made (-2 sec), at the point of wounding (0 sec) and then every seconds for twelve seconds to demonstrate the visual appearance of the calcium signal triggered by wounding. Images taken at minute intervals for three minutes post-wounding show the signal returning to baseline. Scale bar=80µm. Pseudo colour reference is shown. Wound edge is highlighted by dotted line. Images are representative of three independent donors wounded in 1.2mM $[Ca^{2+}]_o$. The wound-induced calcium wave in the absence of hexokinase is shown in figure 3.4.

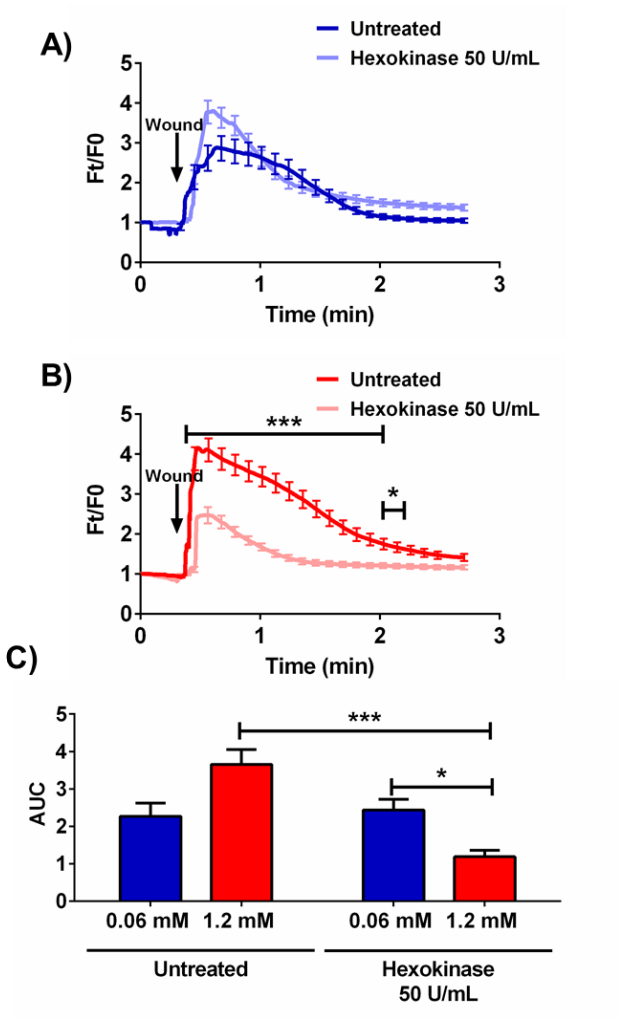

Figure 4.20 Removing extracellular ATP post-wounding results in a decreased calcium flux in 1.2mM $[Ca^{2+}]_o$ but not in 0.06mM $[Ca^{2+}]_o$.

Primary human keratinocytes cultured in 0.06mM $[Ca^{2+}]_o$ keratinocyte growth medium (MCDB 153) were loaded with Fluo4-AM calcium dye and during the de-esterification period of forty five minutes cells were treated with 50 U/mL hexokinase or left untreated. Keratinocytes were wounded in either 0.06mM or 1.2mM $[Ca^{2+}]_o$ keratinocyte growth medium (MCDB 153) in the presence of 50 U/mL hexokinase. Regions of interest (ROI) were drawn around individual cells up to six cells from the wound edge for analysis. **A)** Average initial calcium flux triggered by wounding during the first three minutes was plotted for wounds performed in 0.06mM $[Ca^{2+}]_o$. RM two-way ANOVA with Bonferroni post-hoc test to compare treated to untreated cells at each time point ($F(1,71)=1.341$, $P=0.2507$). For clarity SEM has only been plotted every seven seconds. Arrows highlight time of wounding. **B)** Average initial calcium flux triggered by wounding during the first three minutes was plotted for wounds performed in 1.2mM $[Ca^{2+}]_o$. RM two-way ANOVA with Bonferroni post-hoc test to compare treated to untreated cells at each time point ($F(1,71)=48.16$, $P<0.0001$) (*** $P<0.001$, * $P<0.05$). For clarity SEM has only been plotted every seven seconds. Arrows highlight time of wounding. **C)** Average AUC for $[Ca^{2+}]_i$ fluxes performed in 0.06mM $[Ca^{2+}]_o$ (blue bars) and 1.2mM $[Ca^{2+}]_o$. (red bars) in the presence or absence of hexokinase. Two-way ANOVA with Bonferroni post-hoc ($F(1,284)=13.38$, $P=0.0003$) (*** $P<0.001$, * $P<0.05$). Data shows mean ± SEM from a total of 72 cells from three independent donors; (n=72), N=3.

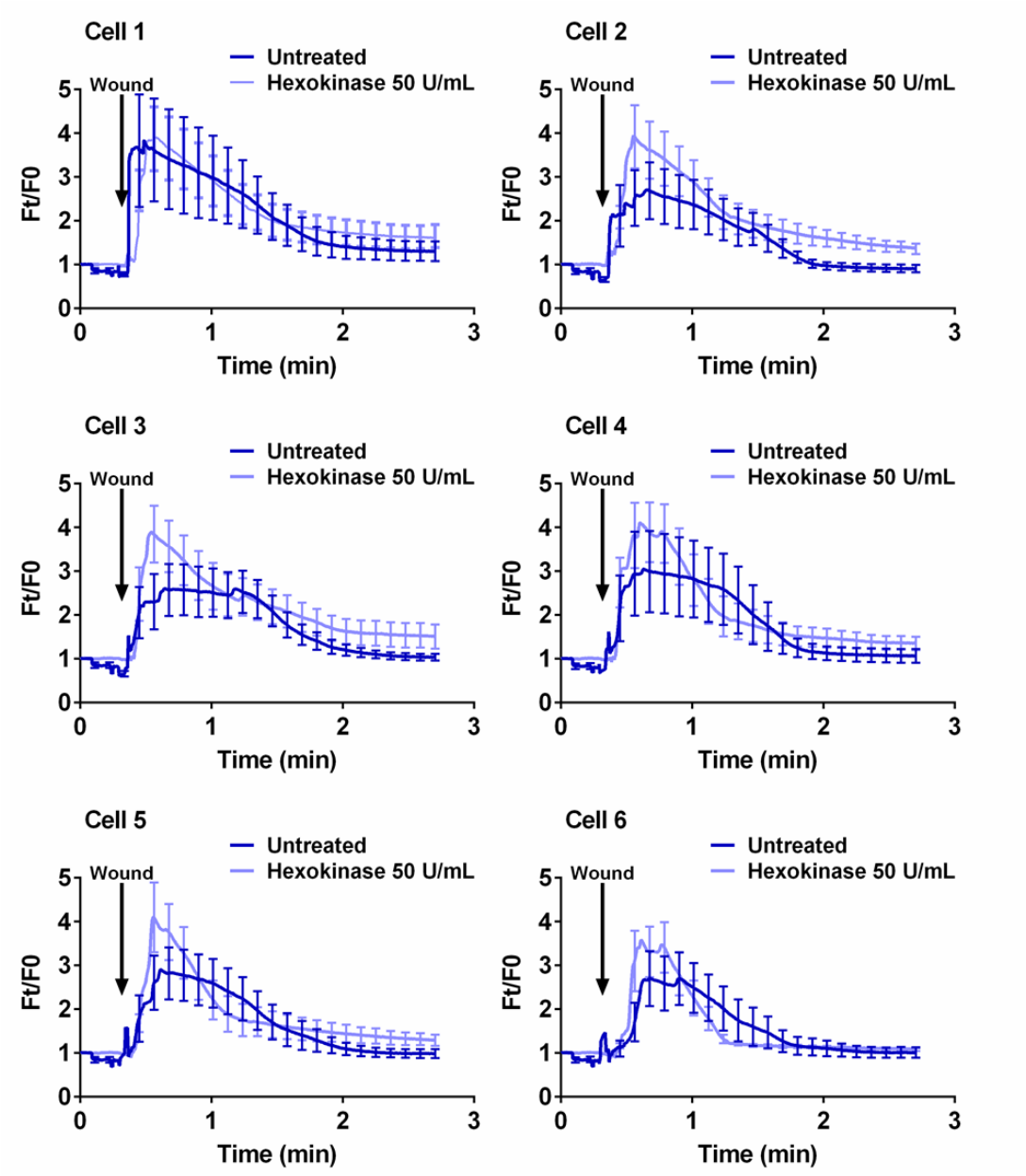

Figure 4.21 Removing extracellular ATP does not alter wound-induced $[Ca^{2+}]_I$ flux within keratinocytes at any location from the wound in 0.06mM $[Ca^{2+}]_o$.

Primary human keratinocytes cultured in 0.06mM $[Ca^{2+}]_o$ keratinocyte growth medium (MCDB 153) were loaded with Fluo4-AM calcium dye and during the de-esterification period of forty five minutes cells were treated with 50 U/mL hexokinase or left untreated. Wound-induced calcium flux in cells were analysed according to their location from the wound edge termed 1-6, with cell 1 being at the wound edge and Cell 6 located six cells back from the wound. Each plot shows wounds made in the presence or absence of 50 U/mL hexokinase in 0.06mM $[Ca^{2+}]_o$. Time of wound is highlighted by arrow. Data shows mean from 12 cells from three independent donors at each location; (n=12), N=3. For graphical clarity SEM has only been plotted every seven seconds. Two-way ANOVA with Bonferroni post-hoc test compared calcium flux between treated and untreated cells at each timepoint.

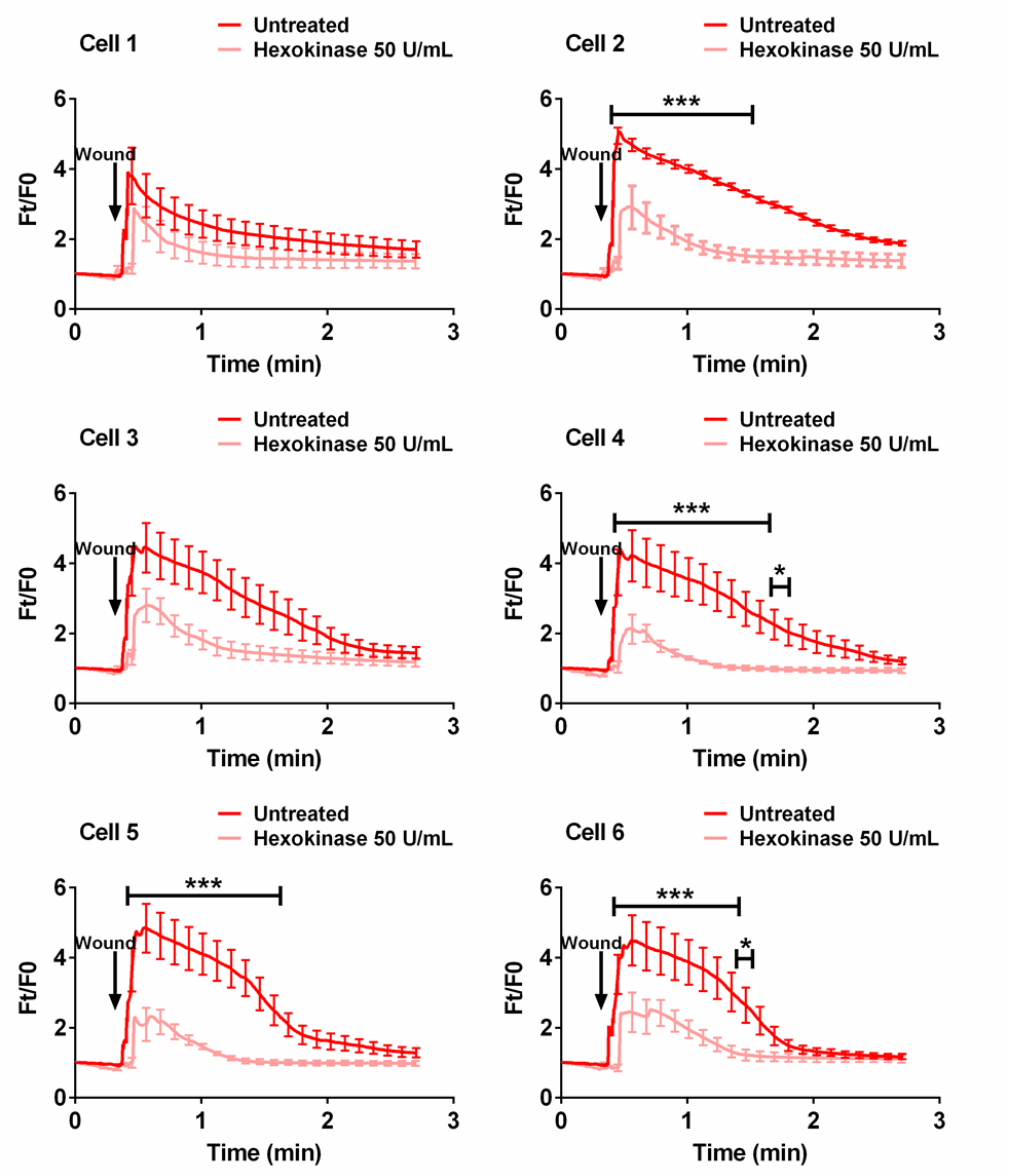

Figure 4.22 Figure 4.22. Removing extracellular ATP reduces the wound-induced $[Ca^{2+}]_i$ flux within cells located away from the wound edge in 1.2mM $[Ca^{2+}]_o$.

Primary human keratinocytes cultured in 0.06mM $[Ca^{2+}]_o$ keratinocyte growth medium (MCDB 153) were loaded with Fluo4-AM calcium dye and during the de-esterification period of forty five minutes cells were treated with 50 U/mL hexokinase or left untreated. Wound-induced calcium flux in cells were analysed according to their location from the wound edge termed 1-6, with Cell 1 being at the wound edge and Cell 6 located six cells back from the wound. Each plot shows wounds made in the presence or absence of 50 U/mL hexokinase in 1.2mM $[Ca^{2+}]_o$. Time of wound is highlighted by arrow. Data shows mean from 12 cells from three independent donors at each location; (n=12), N=3. For graphical clarity SEM has only been plotted every seven seconds. Two-way ANOVA with Bonferroni post-hoc test compared calcium flux between treated and untreated cells at each timepoint. (*** $P<0.0001$, * $P<0.05$)

As shown by figure 4.21, in 0.06mM $[Ca^{2+}]_o$, hexokinase treatment did not significantly affect the wound-induced $[Ca^{2+}]_i$ at any cell location from the wound edge (RM two-way ANOVA). In contrast, figure 4.22 showed that for wounds performed in 1.2mM $[Ca^{2+}]_o$, the calcium flux in cells at the wound edge was unaffected by the presence of hexokinase ($F(1,11)=3.771$, $P=0.0782$, RM two-way ANOVA). However, at cell locations two to six back from the wound treatment with hexokinase significantly decreased mean calcium signal (Ft/F0) compared to untreated controls ($P=0.0270$, $P=0.059$, $P=0.0020$, $P=0.0013$ respectively, RM two-way ANOVA). Analysis of data of the "cell 3" population showed no significant difference with treatment. Bonferroni post-hoc tests were conducted to compare calcium intensity at each timepoint between hexokinase and untreated. Statistical results are summarised in table 4.1.

	RM two-way ANOVA		Bonferroni post-hoc test
Cell location from wound edge	**F value**	**P value**	**Time point of difference (min)**
1	F(1,11)=3.771	P=0.782	
2	F(1,11)=6.507	P=0.0270	0.40 – 1.52
3	F(1,11)=0.3556	P=0.5630	
4	F(1,11)=11.58	P=0.059	0.41 – 1.79
5	F(1,11)=16.08	P=0.020	0.40 – 1.61
6	F(1,11)=8.692	P=0.0133	0.41 – 1.50

Table 4-1 Removing extracellular ATP reduces the wound-induced $[Ca^{2+}]_i$ flux in 1.2mM $[Ca^{2+}]_o$.

Summary of statistical analysis obtained from RM two-way ANOVA comparing wound-induced $[Ca^{2+}]_i$ flux in 0.06mM and 1.2mM $[Ca^{2+}]_o$. Results from two-way ANOVA are reported as well as the specific time points where a statistical difference between the two calcium concentrations were reported by Bonferroni post-hoc test.

To further analyse and quantify these differences seen in 1.2mM $[Ca^{2+}]_o$, maximum Ft/F0 post-wounding was recorded for each of the six cell locations from the wound. Maximum Ft/F0 was defined as the greatest fold change in $[Ca^{2+}]_i$ triggered by wounding. It can be seen that wounding with hexokinase treatment caused a decrease in maximum $[Ca^{2+}]_i$ in cells at all locations from the wound edge (figure 4.23a). Regression analysis was performed for hexokinase treated cells and reported an R^2 value

of 0.5183, which was not deemed statistically significant (P=0.1067). In order to assess whether hexokinase treatment significantly altered maximum Ft/F0 a two-way ANOVA was conducted. Result showed that overall hexokinase treatment had a significant effect on maximum Ft/F0 ($F(1,132)=10.46$, P=0.0015). Although no significant difference was reported at any specific location (Bonferroni post-hoc test, P>0.05) (figure 4.23b).

Visual evaluation of the wound-induced $[Ca^{2+}]_i$ flux after treatment with hexokinase suggested that the calcium signal travels between cells as a wave, akin to untreated experiments. As expected for a wave, the $[Ca^{2+}]_i$ changes were delayed for keratinocytes at increasing distance from the wound edge. Thus for example, cells at the wound edge reached their maximum Ft/F0 increase in 2.13±0.48 seconds compared to 6.86±1.13 seconds for cells six rows back in 1.2mM $[Ca^{2+}]_o$. Linear regression revealed this line was significantly different to zero (R^2-0.8752, P=0.0061) (figure 4.24a). When comparing time taken to achieve maximal Ft/F0, between treated and untreated cells there appeared to be a reduction in time taken to reach maximum in cells 5 and 6 back from the wound with hexokinase treatment (figure 4.24b). Whilst this difference was not reported as significant by a two-way ANOVA ($F(1,132)=3.391$, P=0.0678), the P value reported was approaching significance.

Next, the AUC of the wound-induced $[Ca^{2+}]_i$ flux was calculated in individual cells at each cell location back from the wound edge in hexokinase treated cells. AUC was used as an integrative quantitative measure of wound-induced intracellular calcium flux. Any differences between AUC in 1.2mM $[Ca^{2+}]_o$ in hexokinase and untreated conditions may be considered to reflect calcium entry from the extracellular space. From figure 4.25 is appears that the AUC in hexokinase treated cells remained constant despite location from the wound edge; cells at the wound edge had an AUC of 1.36±0.61 whereas this value was 1.26±0.41 for cells located six rows back.

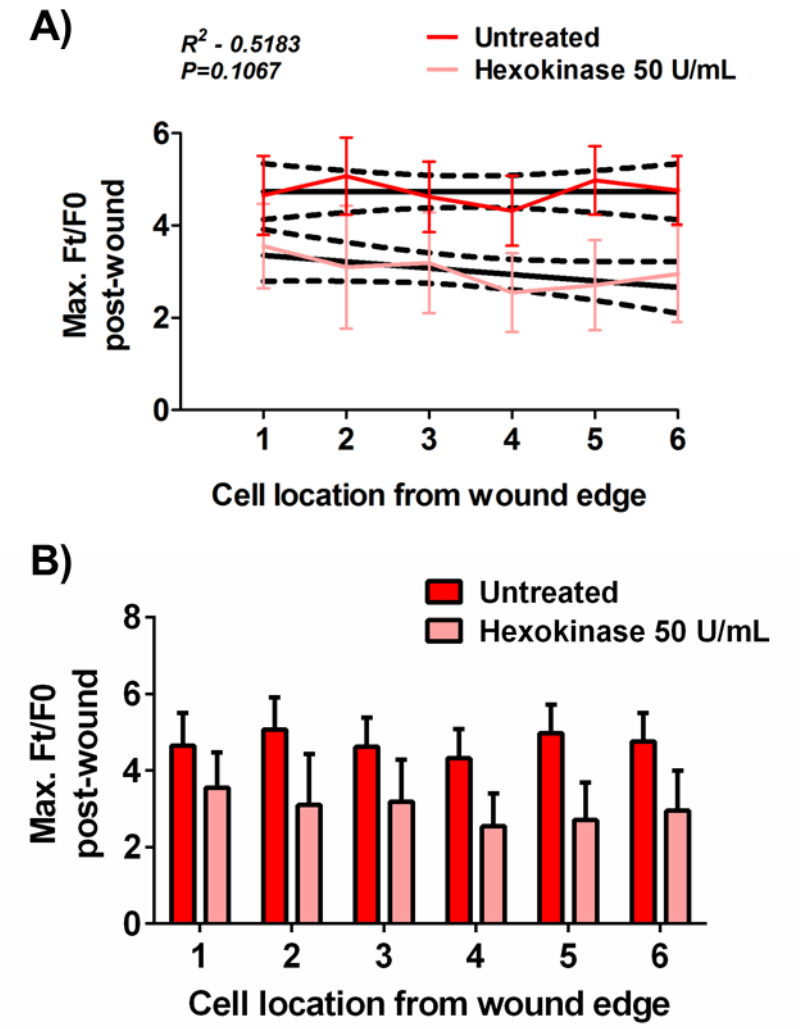

Figure 4.23 Removing extracellular ATP decreases maximum Ft/F0 of intracellular calcium flux post-wounding in 1.2mM $[Ca^{2+}]_o$.

Primary human keratinocytes cultured in 0.06mM $[Ca^{2+}]_o$ keratinocyte growth medium (MCDB 153) were loaded with Fluo4-AM calcium dye and during the de-esterification period of forty five minutes cells were treated with 50 U/mL hexokinase or left untreated. Keratinocytes were wounded in 1.2mM $[Ca^{2+}]_o$ keratinocyte growth medium (MCDB 153) in the presence of 50 U/mL hexokinase. The maximum fold change (Ft/F0) in calcium flux induced by wounding compared to the baseline was analysed at each location from the wound edge, as described in figure 4.22. Data is shown in two forms for clarity. **A)** Linear regression analysis was conducted and the line of best-fit plotted with the 95% confidence intervals (dotted lines). **B)** Maximal Ft/F0 in $[Ca^{2+}]_i$ flux for wounds made 1.2mM $[Ca^{2+}]_o$ in the presence or absence of hexokinase were compared by two-way ANOVA ($F(1,132)=10.46$, $P=0.0015$). Data shows mean ± SEM from 12 cells at each location from three independent donors; (n=72), N=3.

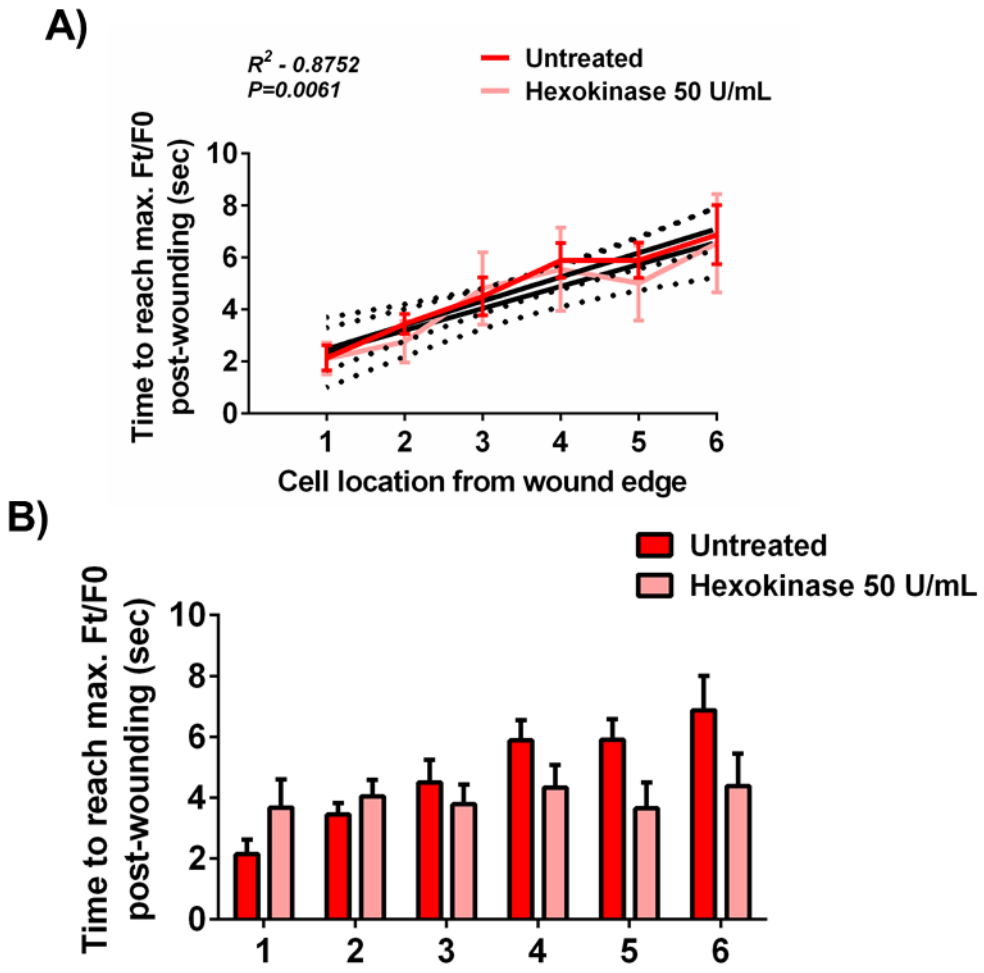

Figure 4.24 Time to reach maximum Ft/F0 intracellular calcium flux was not significantly altered by removing extracellular ATP for wounds made in 1.2mM $[Ca^{2+}]_o$.

Primary human keratinocytes cultured in 0.06mM $[Ca^{2+}]_o$ keratinocyte growth medium (MCDB 153) were loaded with Fluo4-AM calcium dye and during the de-esterification forty five minutes cells were treated with 50 U/mL hexokinase or left untreated. Keratinocytes were wounded in 1.2mM $[Ca^{2+}]_o$ keratinocyte growth medium (MCDB 153) in the presence or absence of 50 U/mL hexokinase. The time taken to reach maximum fold change (Ft/F0) intracellular calcium flux induced by wounding was analysed at each location from the wound edge, as described in figure 4.22. Data is shown in two forms for clarity. **A)** Linear regression analysis was conducted and the line of best-fit plotted with the 95% confidence intervals (dotted lines). **B)** Time to reach maximum Ft/F0 wounds made 1.2mM $[Ca^{2+}]_o$ in the presence or absence of hexokinase were compared by two-way ANOVA with a Bonferroni post-hoc ($F(1,132)=3.391$, $P=0.0678$). Data shows mean ± SEM from 12 cells at each location from three independent donors; (n=72), N=3.

Linear regression analysis reported an R^2 value of 0.2807, which was not deemed significantly different to zero (P=0.2796) (figure 4.25a). In order to compare the differences between AUC in $[Ca^{2+}]_i$ flux caused by removing extracellular ATP, a two-way ANOVA was conducted. Result showed that overall, hexokinase treatment had a statistical effect on AUC of the $[Ca^{2+}]_i$ flux ($F(1,132)=32.08$, $P<0.0001$). A Bonferroni post-hoc showed that this difference was significant at cell 2 and cell 5 back from the wound (* $P<0.05$) (figure 4.25b).

Finally, the rate of rise of the wound-induced $[Ca^{2+}]_i$ flux was investigated. This was measured by calculating the slope of fluorescence intensity between the time the initiation of the wound-induced $[Ca^{2+}]_i$ flux and the time maximal Ft/F0 was achieved, this value represents the gradient of wound-induced calcium increase. Figure 4.26 shows changes in the rate of rise in cells at specified locations from the wound edge with hexokinase treatment. The graph showed that, similar to wounding in the presence of extracellular ATP, the rate of rise of the $[Ca^{2+}]_i$ flux when wounding with hexokinase treatment decreased the further back from the wound the cell was located; cells at the wound edge had a rate of rise of 0.63±0.13 (ΔFt/F0/second) and those six cells back from the wound had a rate of rise of 0.43±0.17 (ΔFt/F0/second) (figure 4.26a). This difference was not deemed significant ($F(3,264)=1.648$, $P=0.1786$, two-way ANOVA) (figure 4.26b).

Taken together, these results suggest that ATP plays a role in intercellular calcium wave propagation as removing extracellular ATP post-wounding eliminated the $[Ca^{2+}]_i$ flux. In a lower calcium environment, extracellular ATP did not have any effect on the intercellular calcium way, suggesting that increases seen in untreated cells are a result of intercellular signalling, potentially through IP_3-mediated mechanisms rather than extracellular signalling. In contrast, raising the extracellular calcium concentration to 1.2mM whilst simultaneously removing ATP post-wounding significantly reduced aspects of the wave, namely, maximum Ft/F0 achieved post-wounding within individual cells and AUC of the $[Ca^{2+}]_i$ flux. Interestingly, these parameters were increased in untreated experiments between wounds performed in 0.06mM and 1.2mM $[Ca^{2+}]_o$ (section 3.3.2). It was concluded from these experiments that wounding activated a calcium entry mechanism resulting in calcium influx from the

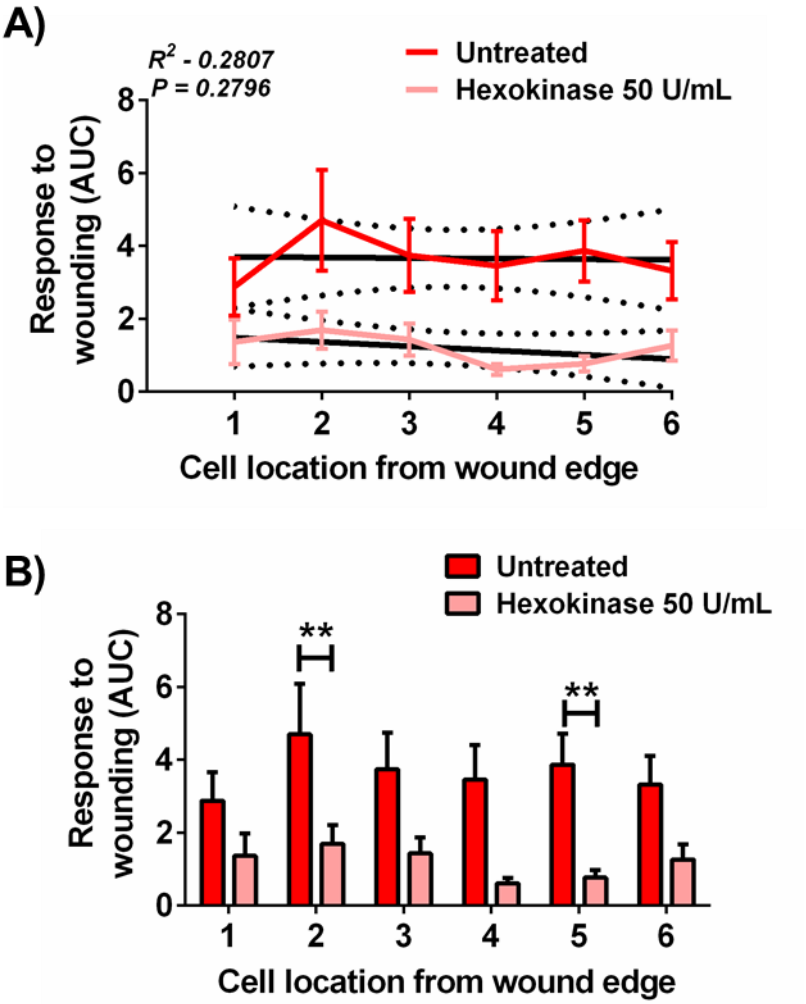

Figure 4.25 Area under the curve of wound-induced $[Ca^{2+}]_i$ flux in keratinocytes is reduced by hexokinase treatment in 1.2mM $[Ca^{2+}]_o$.

Primary human keratinocytes cultured in 0.06mM $[Ca^{2+}]_o$ keratinocyte growth medium (MCDB 153) were loaded with Fluo4-AM calcium dye and during the de-esterification period of forty five minutes cells were treated with 50 U/mL hexokinase or left untreated. Keratinocytes were wounded in 1.2mM $[Ca^{2+}]_o$ keratinocyte growth medium (MCDB 153) in the presence or absence of 50 U/mL hexokinase. The AUC of the intracellular calcium flux induced by wounding was analysed at each location from the wound edge, as described in figure 4.22. Data is shown in two forms for clarity. **A)** Linear regression analysis was conducted and the line of best-fit plotted (black line) with the 95% confidence intervals (dotted lines). **B)** AUC for wounds made 1.2mM $[Ca^{2+}]_o$ in the presence or absence of hexokinase were compared by two-way ANOVA ($F(1,132)=0.32.08$, $P<0.0001$) (** $P<0.01$). Data shows mean ± SEM from 12 cells at each location from three independent donors; (n=72), N=3

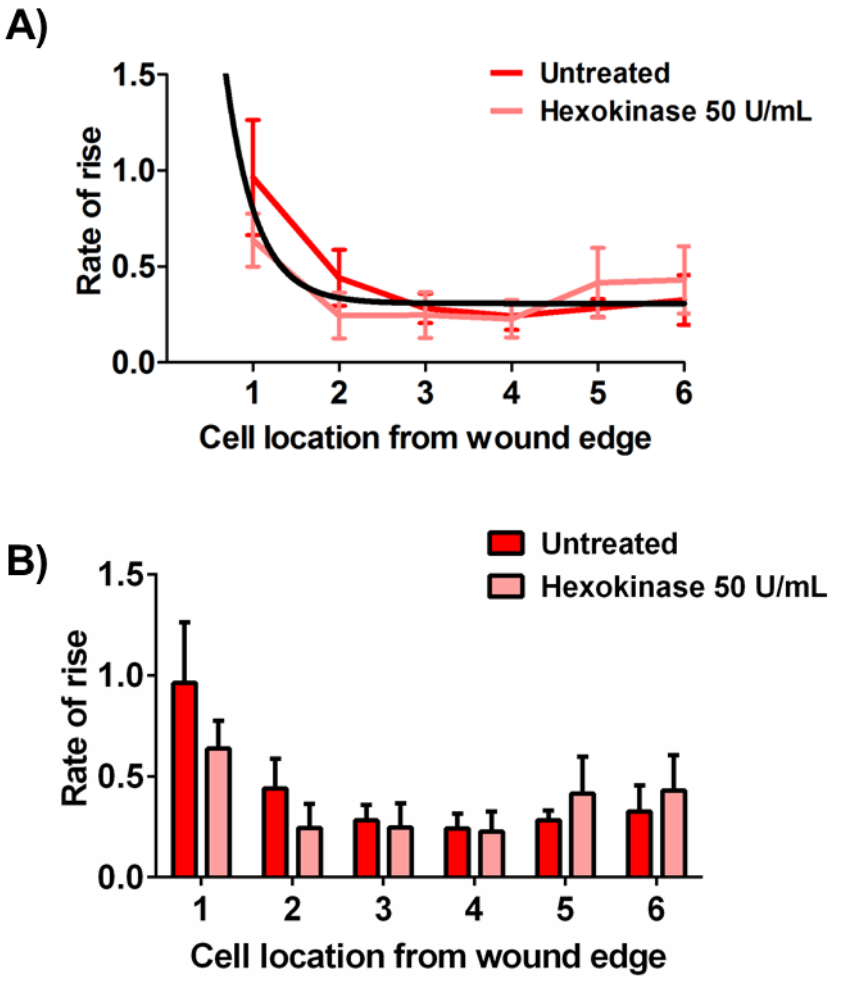

Figure 4.26 Rate of rise of wound-induced $[Ca^{2+}]_i$ flux in keratinocytes is unaffected by removal of extracellular ATP.

Primary human keratinocytes cultured in 0.06mM $[Ca^{2+}]_o$ keratinocyte growth medium (MCDB 153) were loaded with Fluo4-AM calcium dye and during the de-esterification forty five minutes cells were treated with 50 U/mL hexokinase. Keratinocytes were wounded in 1.2mM $[Ca^{2+}]_o$ keratinocyte growth medium (MCDB 153) in the presence of 50 U/mL hexokinase. The rate of rise of the calcium flux induced by wounding was analysed at each location from the wound edge. Data is shown in two forms for clarity. **A)** A non-linear regression exponential decay graph was fitted to the data for wounds made in the absence of hexokinase (dark line) and wounds made in the presence of hexokinase (pale line). **B)** Rate of rise for wounds made 1.2mM $[Ca^{2+}]_o$ in the presence or absence of hexokinase were compared by two-way ANOVA ($F(3,264)=1.648$, $P=0.1786$). Data shows mean ± SEM from 12 cells at each location from three independent donors; (n=72), N=3.

extracellular environment. Utilising hexokinase to remove ATP reduces AUC and maximum Ft/F0 in 1.2mM $[Ca^{2+}]_o$, therefore it could be suggested that the calcium entry mechanism activated by wounding is ATP-mediated through activation of purinergic receptors. Two families of receptors are activated by ATP as discussed in section 1.6.1. Activation of P2YR by ATP binding induces an IP_3-mediated release of calcium from the ER and subsequently activates SOCE. It was shown in section 3.3.5 that blocking SOCE had no effect on maximum Ft/F0 or AUC of the $[Ca^{2+}]_i$ flux, indicating that calcium entry is not occurring through this mechanism. Alternatively, P2XR are ATP-gated calcium ion channels that result in calcium influx from the extracellular space. It can therefore be hypothesised that wounding in the presence of a high external calcium environment results in increased calcium entry through ATP-gated P2XR activation.

Combined it can be concluded from these investigations that extracellular ATP is required for the intercellular calcium wave following wounding. Furthermore, it seems to mediate calcium entry mechanisms which result in an elevated maximum Ft/F0 and increased AUC of the $[Ca^{2+}]_i$ flux.

4.3.10 The role of gap-junctional communication in intracellular calcium wave propagation.

As alluded to in section 4.1.1, both gap-junctional communication and ATP have been shown to mediate intercellular calcium wave propagation (Iacobas *et al.*, 2006). This chapter so far has investigated wound-induced ATP release into the extracellular media and the effect this has on propagation of the calcium wave. It has been shown that removal of ATP from the extracellular environment with hexokinase treatment, reduced maximal Ft/F0 reached by wounding and AUC of the $[Ca^{2+}]_i$ flux induced by wounding., However, no significant difference was observed between time to reach maximum Ft/F0 in the presence or absence of extracellular ATP. Furthermore, characteristics of the wound-induced calcium wave analysed within this project are indicative of the wave travelling through the cell population via intracellular mechanisms potentially IP_3, as described in section 4.1.1. Combined, these results led to the hypothesis that the intercellular signalling cascade triggered by wounding was also mediated via gap-junctions. To address this, primary human keratinocytes cultured in

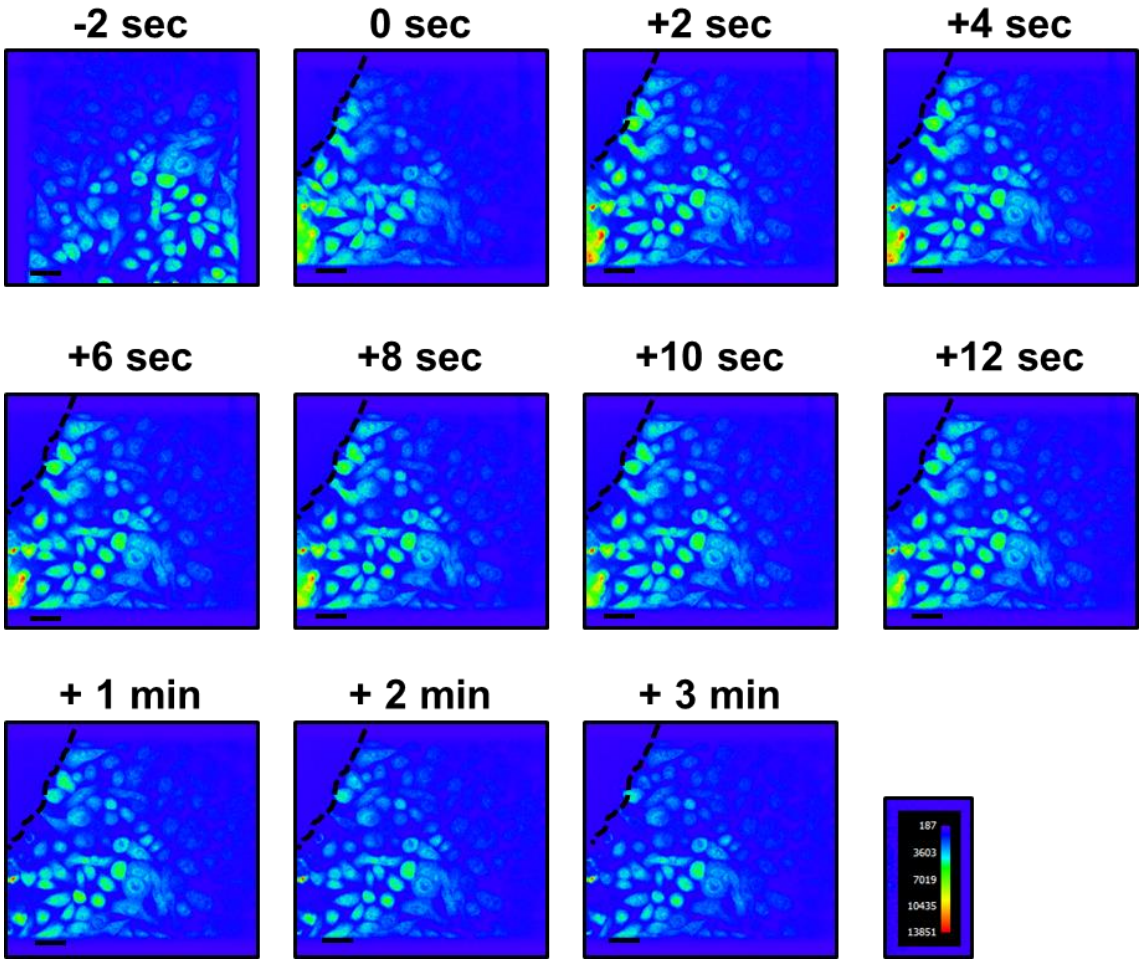

Figure 4.27 2D images demonstrating the reduced wound-induced calcium wave post-treatment with 18α-Glycyrrhetinic acid (18αGA).

Primary human keratinocytes cultured in 0.06mM $[Ca^{2+}]_o$ keratinocyte growth medium (MCDB 153) were loaded with Fluo4-AM calcium dye and during the de-esterification period of forty five minutes cells were treated with 20μM 18αGA. Keratinocytes were wounded in 0.06mM or 1.2mM $[Ca^{2+}]_o$ keratinocyte growth medium (MCDB 153) in the presence of 20μM 18αGA. Images were captured at 3.7fps. Pseudo colour images of confocal images were generated prior to the wound being made (-2 sec), at the point of wounding (0 sec) and then every seconds for twelve seconds to demonstrate the calcium signal triggered by wounding. Additionally, pseudo colour images of confocal images were generated at minute intervals for three minutes post-wounding to demonstrate calcium signal return to baseline Scale bar=80μm. Pseudo colour reference is shown. Wound edge is highlighted by dotted line. Images are representative of three independent donors. The wound-induced calcium wave in the absence of hexokinase is shown in figure 3.4.

0.06mM $[Ca^{2+}]_o$ keratinocyte growth medium (MCDB 153) were loaded with Fluo4-AM calcium dye prior to treatment with 20μM 18αGA or vehicle (DMSO) during the subsequent forty five minute de-esterification period. Keratinocytes were then wounded in supplemented keratinocyte growth medium (MCDB 153) to increase the calcium concentration to 1.2mM.

Initially, signalling across the whole population of cells was visually assessed. Subsequently, sub-populations were defined by their location from the wound edge and analysed to provide insights into differences between cells located at the wound edge compared to those located further back. Figure 4.27 shows representative images from one experiment taken every two seconds for twelve seconds and then three later images taken at minute intervals post-wounding, to visually depict the $[Ca^{2+}]_i$ changes triggered by wounding. It can be seen that at the time of wounding, $[Ca^{2+}]_i$ increased within cells located at the wound edge, however, an elevation was not observed in neighbouring cells located further back from the wound.

In order to further investigate 18αGA treatment preventing the spread of the calcium wave back from the wound edge, $[Ca^{2+}]_i$ flux within individual cells were analysed according to the location of the cells away from the wound edge. The following parameters were examined compared to vehicle (DMSO); i) maximum Ft/F0 achieved by wounding ii) time to reach maximum Ft/F0 post-wounding and iii) AUC of the $[Ca^{2+}]_i$ flux.

Maximum Ft/F0 post-wounding was recorded within individual cells that wounding resulted in a $[Ca^{2+}]_i$ flux at each of the six cell locations from the wound edge. As shown by figure 4.28a, wounding in the presence of 18αGA in 0.06mM $[Ca^{2+}]_o$ significantly decreased the maximum $[Ca^{2+}]_i$ compared to vehicle in cells at all specified locations from the wound edge. Wounding in the presence of 18αGA in 1.2mM $[Ca^{2+}]_o$ caused a reduced maximum $[Ca^{2+}]_i$ compared to vehicle in cells at all specified locations from the wound edge, although the difference was more notable at locations distal to the wound. Both these lines of best fit were revealed to be significantly different to zero by regression analysis (R^2-0.9407, P=0.0013 and R^2-0.9177, P=0.0030 respectively) (figure 4.28a and figure 4.28b). This showed that although the maximum Ft/F0 induced by wounding was reduced, a pattern for a decreased maximum Ft/F0 further back from the wound edge persisted.

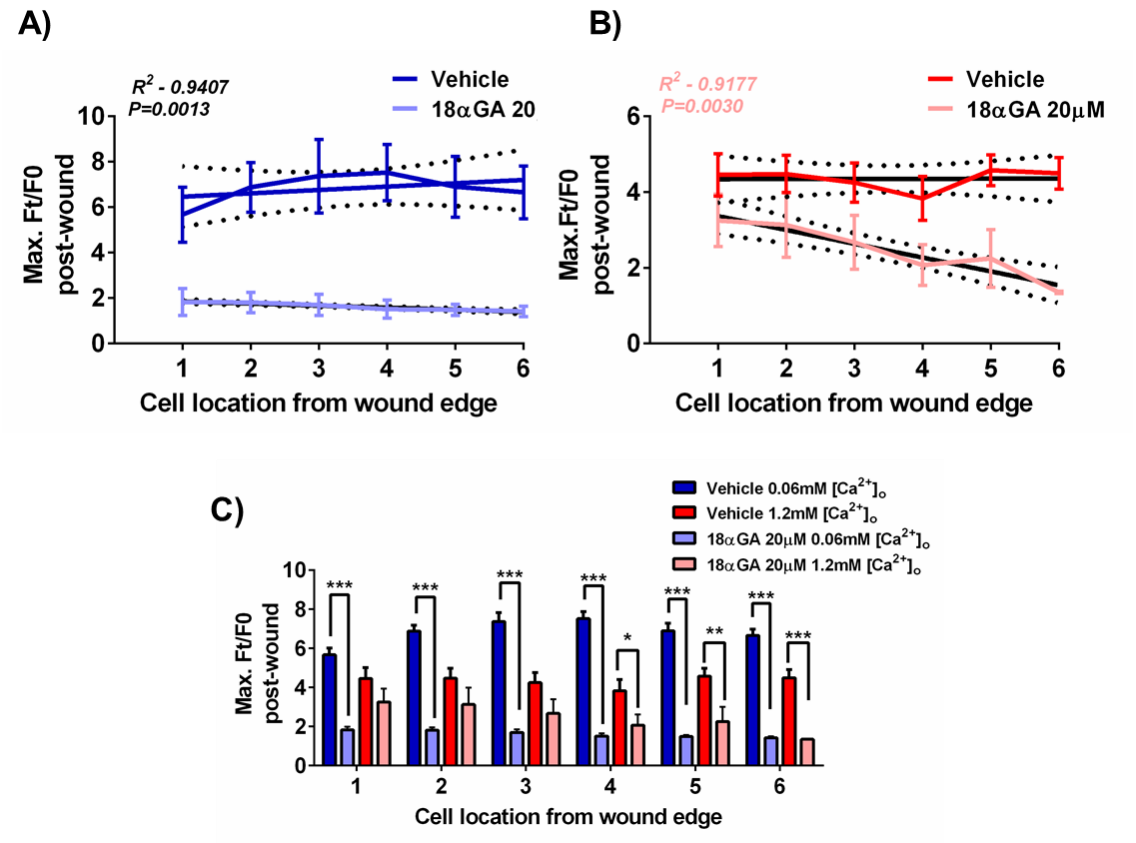

Figure 4.28 Blocking gap-junctional communication 18α-Glycyrrhetinic acid (18αGA) reduces maximum wound-induced Ft/F0 of calcium flux regardless of external calcium concentration.

Primary human keratinocytes cultured in 0.06mM $[Ca^{2+}]_o$ keratinocyte growth medium (MCDB 153) were loaded with Fluo4-AM calcium dye and during the de-esterification forty five minutes cells were treated with 20μM 18αGA or control. Keratinocytes were wounded in 0.06mM or 1.2mM $[Ca^{2+}]_o$ keratinocyte growth medium (MCDB 153) in the presence of 20μM 18αGA or vehicle control. The maximum fold change (Ft/F0) in calcium flux induced by wounding compared to the baseline was analysed at each location from the wound edge. Data is shown in two forms for clarity. Linear regression analysis was conducted for wounds made in **A)** 0.06mM $[Ca^{2+}]_o$ or **B)** 1.2mM $[Ca^{2+}]_o$ and the line of best-fit plotted (black line) with the 95% confidence interval (dotted lines) for 18αGA treatment (pale line). Data for wounds made with vehicle treatment is also shown (dark line) to visualise differences between the two treatments. **C)** Maximal Ft/F0 in $[Ca^{2+}]_i$ flux for wounds made 0.06mM or 1.2mM $[Ca^{2+}]_o$ in the presence or absence of 18αGA were compared by two-way ANOVA ($F(3,235)=152.2$, $P<0.0001$). Bonferroni post-hoc test (*** $P<0.0001$, ** $P<0.01$, * P0.05). Data shows mean ± SEM from 12 cells at each location from three independent donors; (n=72), N=3.

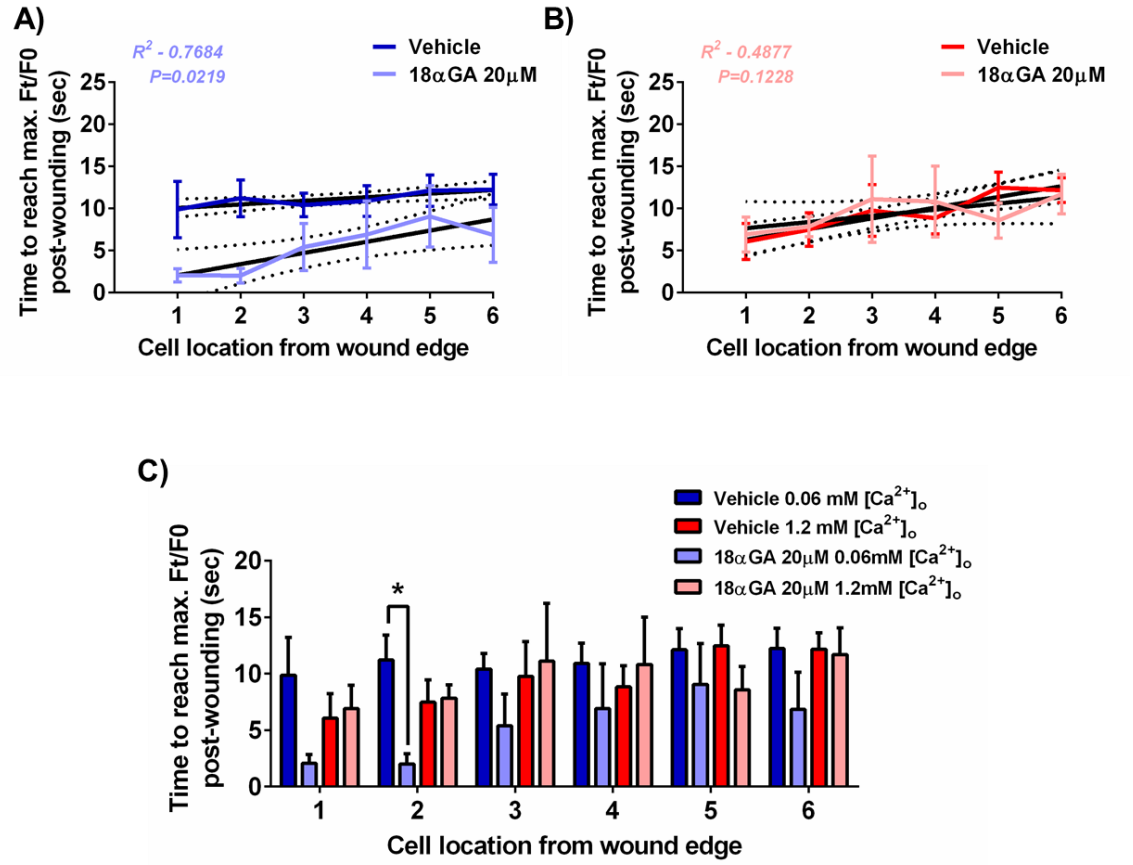

Figure 4.29 Blocking gap-junctional communication 18α-Glycyrrhetinic acid (18αGA) reduces time to reach maximum wound-induced Ft/F0 in 0.06mM $[Ca^{2+}]_o$ but had no effect in 1.2mM $[Ca^{2+}]_o$.

Primary human keratinocytes cultured in 0.06mM $[Ca^{2+}]_o$ keratinocyte growth medium (MCDB 153) were loaded with Fluo4-AM calcium dye and during the de-esterification forty five minutes cells were treated with 20μM 18αGA. Keratinocytes were wounded in 0.06mM or 1.2mM $[Ca^{2+}]_o$ keratinocyte growth medium (MCDB 153) in the presence of 20μM 18αGA. Time take to reach maximum fold change (Ft/F0) induced by wounding was analysed at each location from the wound edge. Data is shown in two forms for clarity. Linear regression analysis was conducted for wounds made in **A)** 0.06mM $[Ca^{2+}]_o$ or **B)** 1.2mM $[Ca^{2+}]_o$ and the line of best-fit plotted (black line) with the 95% confidence intervals (dotted lines) for 18αGA treatment (pale line). Data for wounds made with vehicle treatment is also shown (dark line) to visualise differences between the two treatments. **C)** Time taken to reach maximal Ft/F0 in $[Ca^{2+}]_i$ flux for wounds made 0.06mM or 1.2mM $[Ca^{2+}]_o$ in the presence or absence of 18αGA were compared by two-way ANOVA ($F(3,232)=5.833$, $P=0.0007$). Bonferroni post-hoc test (* P0.05). Data shows mean ± SEM from 12 cells at each location from three independent donors; (n=72), N=3.

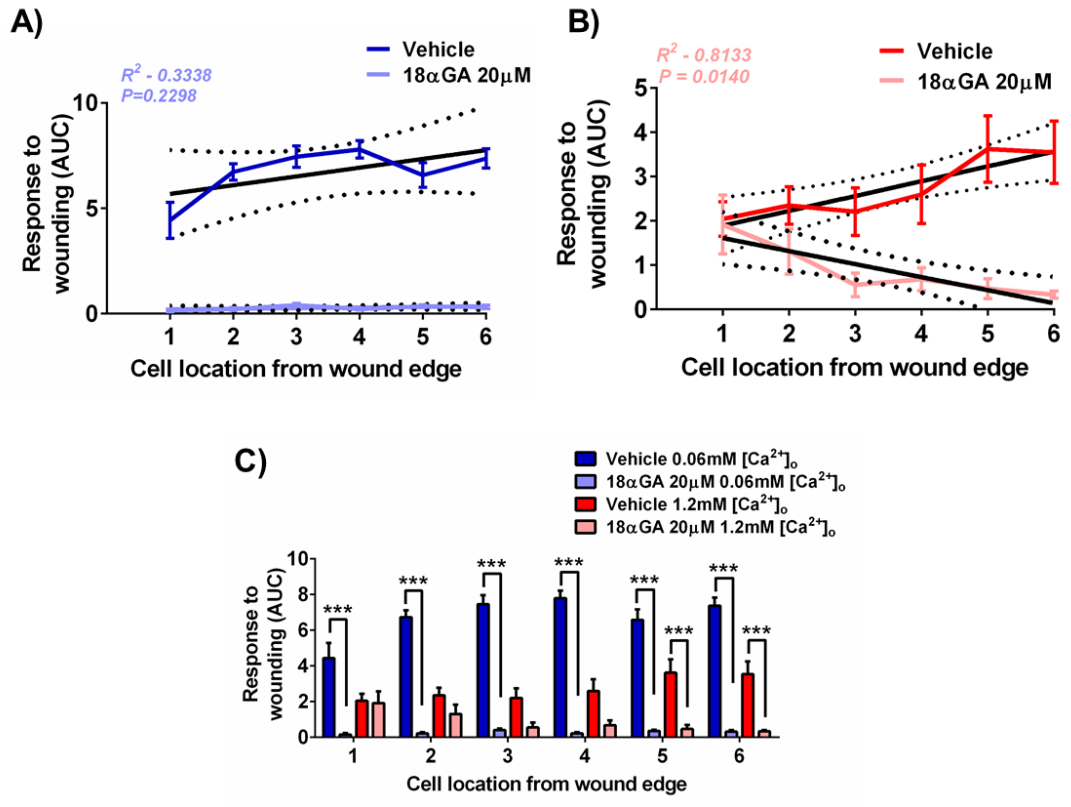

Figure 4.30 Blocking gap-junctional communication 18α-Glycyrrhetinic acid (18αGA) reduces wound-induced AUC regardless of external calcium concentration.

Primary human keratinocytes cultured in 0.06mM $[Ca^{2+}]_o$ keratinocyte growth medium (MCDB 153) were loaded with Fluo4-AM calcium dye and during the de-esterification forty five minutes cells were treated with 20μM 18αGA. Keratinocytes were wounded in 0.06mM or 1.2mM $[Ca^{2+}]_o$ keratinocyte growth medium (MCDB 153) in the presence of 20μM 18αGA. AUC of $[Ca^{2+}]_i$ flux induced by wounding was analysed at each location from the wound edge. Data is shown in two forms for clarity. Linear regression analysis was conducted for wounds made in **A)** 0.06mM $[Ca^{2+}]_o$ or **B)** 1.2mM $[Ca^{2+}]_o$ and the line of best-fit plotted (black line) with the 95% confidence interval (dotted lines) for 18αGA treatment (pale line). Data for wounds made with vehicle treatment is also shown (dark line) to visualise differences between the two treatments. **C)** AUC of $[Ca^{2+}]_i$ flux for wounds made 0.06mM or 1.2mM $[Ca^{2+}]_o$ in the presence or absence of 18αGA were compared by two-way ANOVA ($F(3,239)=213.7$, $P<0.0001$). Bonferroni post-hoc test (*** P0.001). Data shows mean ± SEM from 12 cells at each location from three independent donors; (n=72), N=3.

A two-way ANOVA revealed that overall 18αGA treatment had a significant effect on maximum Ft/F0 ($F(3,235)=152.2$, $P<0.0001$). A Bonferroni post-hoc test reported a significant difference at each cell location between vehicle and 18αGA treated cells when wounds were performed in 0.06mM $[Ca^{2+}]_o$ (*** $P<0.0001$). In line with previous observations, the difference between vehicle and 18αGA treated cells when wounds were performed in 1.2mM $[Ca^{2+}]_o$ were significantly different within cells located 4, 5 and 6 rows back from the wound (*** $P<0.001$, ** $P<0.01$, * $P<0.05$) (figure 4.28c).

As expected for a wave, the $[Ca^{2+}]_i$ changes were delayed for keratinocytes at increasing distance from the wound edge within cells that displayed a response to wounding in the presence of 18αGA in 0.06mM $[Ca^{2+}]_o$. Linear regression analysis showed that the line of best fit was significantly different to zero ($P=0.0219$) and had an R^2 value of 0.7684 (figure 4.29a). Conversely, wounds performed in the presence of 18αGA in 1.2mM $[Ca^{2+}]_o$ did not show a significantly linear pattern relating time to reach maximum Ft/F0 and cell location from the wound edge. Linear regression reported an R^2 value of 0.4877 ($P=0.1228$) (figure 4.29b). As shown by figure 4.29c, 18αGA treatment had an overall effect on the time taken to reach maximum peak ($F(3,232)=5.833$, $P=0.0007$, two-way ANOVA), a Bonferroni post-hoc reported a statistical difference within cells located two rows back from the wound edge (* $P<0.05$) in 0.06mM $[Ca^{2+}]_o$. No statistical difference was reported for wounds performed in 1.2mM $[Ca^{2+}]_o$.

The AUC of the wound-induced $[Ca^{2+}]_i$ flux was calculated in individual cells at each cell location back from the wound edge which displayed an intracellular calcium flux in response to wounding. AUC was used as an integrative quantitative measure of wound-induced intracellular calcium flux. The AUC of wound-induced intracellular calcium flux in 0.06mM $[Ca^{2+}]_o$ may be considered an approximation to calcium release from the ER (see section 3.3.1). The difference between AUC in 0.06 and 1.2mM conditions may be considered to reflect calcium entry from the extracellular space. As shown by figure 4.30a, AUC for wounds performed in 0.06mM $[Ca^{2+}]_o$ in the presence of 18αGA remained constant despite location from the wound edge (R^2-0.3338, $P=0.2298$, linear regression. In contrast, as shown in 1.2mM $[Ca^{2+}]_o$, AUC for wounds performed in 1.2mM $[Ca^{2+}]_o$ in the presence of 18αGA had a significantly decreased AUC the further back from the wound the cell was located (R^2-0.8133, $P=0.0140$, linear regression). It was clear that 18αGA reduced AUC at all cell locations in 0.06mM and at cells located

distal to the wound in 1.2mM $[Ca^{2+}]_o$ compared to vehicle. Statistical analysis reported treatment with 18αGA significantly reduced the AUC ($F(3,239)=213.7$, $P<0.0001$,two-way ANOVA). A Bonferroni post-hoc test revealed at all cell locations from the wound, this difference was significant in 0.06mM $[Ca^{2+}]_o$ (*** $P<0.001$). In 1.2mM $[Ca^{2+}]_o$ this difference was significant in cells 5 and 6 (*** $P<0.0001$).

4.4 Discussion.

4.4.1 The ability of CM to induce a calcium response.

The addition of wounded conditioned media (CM) to unwounded primary keratinocytes triggered a calcium response. CM is a useful technique to determine the downstream effect of factors released from cells upon wounding. Wounding is believed to trigger both intracellular and extracellular signalling mechanisms and CM provides a tool for the differentiation of these. This result is consistent with findings from Klepeis *et al.* who also demonstrated the ability of CM, collected from wounded human corneal epithelial cell line, to increase intracellular calcium. In contrast to the observation in keratinocytes where 55.3±15.7% cells responded to CM with an intracellular calcium flux, Klepeis *et al.* reported that an intracellular calcium flux was detected in all cells in the field of view (Klepeis *et al.*, 2001). This difference is likely to be due to a) differences between the components of the CM from each cell type and b) receptor expression being cell specific or c) the timing of the collection of the CM; within this project wounded media was collected five minutes post-wounding, in the corneal experiments wounded media was collected immediately post-wounding. Recently, it has been reported that wounded media also effected vimentin protein expression mediated by EGF in breast cancer cells; however the authors do not comment on the effect the CM had on calcium signalling in these cells (Davis *et al.*, 2014). There are a limited number of published studies that utilise conditioned media collected from wounded cell monolayers. Other CM techniques involved removal of media from cell cultures and exposing a different cell type to this media with the aim to establishing the role of secreted factors. For example, media obtained from the culture of human umbilical stem cells was added to wounded human fibroblasts. Following exposure to CM from human umbilical cord stem cells, human fibroblasts cells migrated to close the wound faster than cells exposed to control media (Lin *et al.*, 2014). Whilst this experimental design is advantageous in the exploration of the effect of factors secreted by stem cells of wound healing responses of non-stem cells, it does not allow for analysis of factors secreted by keratinocytes in response to mechanical wounding; a central aim of this project. To take this result further it would be advantageous to analyse the composition of the conditioned media to investigate what factors are secreted by keratinocytes in response to wounding using ELISA assays or mass spectrometry. The challenge with the former

approach would be the requirement for pre-determined factors prior to analysis. Additionally, pre-treatment of cells with Tg to deplete intracellular calcium stores prior to addition of CM would determine whether the source of the calcium was from intracellular stores. In a similar manner, pre-treatment with GSK-7975A, to block SOCE, would define the contribution of extracellular calcium.

4.4.2 ATP release post-wounding.

Release of ATP into the extracellular environment is a common occurrence in response to stress or mechanical injury. This has been studied in various cell types and in response to different stimuli (Section 1.6.4). Results presented herein provide further confirmation that primary human keratinocytes release ATP following wounding (Tsutsumi *et al.*, 2009). The fold increase determined by wounding appears to vary between cell types. It has been shown herein that wounding induces a maximal increase in extracellular ATP of approximately 20 fold. This is substantially higher than the increase observed in the human corneal epithelial cell line following wounding which was reported as 3.5 fold (Klepeis *et al.*, 2001) and the increase in keratinocytes upon air exposure which was 7 fold (Barr *et al.*, 2013). It was decided that the optimal time post-wounding to collect samples for further investigation into mechanisms regulating release was five minutes. This was in agreement with previously published data in fibroblasts where five minutes was also noted as the time of maximal ATP release (Jin *et al.*, 2014). In other reported studies the extracellular samples were obtained immediately post-wounding, however, it was felt this was a vague time point and may cause variation between experiments.

Previous literature has demonstrated that wounding results in both an intercellular calcium wave and ATP release, it therefore follows that the two responses may be linked. It was of interest to determine whether the calcium wave was ATP-dependent or the ATP release was calcium-dependent. Wounding keratinocytes in both 0.06mM and 1.2mM $[Ca^{2+}]_o$ resulted in similar levels of ATP in the media five minutes post-wounding. Thus implying that wound-induced ATP release is not dependent on the concentration of extracellular calcium. This is in support of Azorin and co-workers who showed that ATP was released from keratinocytes in response to hypo-osmotic, but not hyperosmotic stress, in a calcium-independent manner (Azorin *et al.*, 2011). In contrast, in astrocytes, ATP release was shown to be potentiated by a decrease in extracellular

calcium (Pangršič *et al.*, 2007). It is possible that dependency on calcium is related to cell type and stimulus; wounding is a relatively severe and gross insult and therefore increased ATP is likely to be from cell lysis rather than a signalling pathway (section 4.3.4) which may account for the lack of dependency on extracellular calcium.

An interesting but undefined observation is that ATP release induced within the first five minutes of wounding appears to occur in a biphasic manner in 1.2mM but not 0.06mM $[Ca^{2+}]_o$. This is in agreement with the pattern of ATP release caused by hyposmolality in the adrenal epithelial cell line A6 (D. Jans *et al.*, 2002). This apparent biphasic response is indicative of the involvement of two processes, at least one of which is likely to be calcium-dependent manner.

Through a series of media replacement and CM experiments it was robustly demonstrated that ATP release from keratinocytes occurred as a one off event at the time of wounding. This was an important finding and showed that the effects of ATP on the calcium wave were a result of release from a single source point rather than sequential secretion from cells participating in the wave.

There are three main signalling pathways leading to the release of ATP. The majority of studies conclude that at least one of these pathways dominantly regulates ATP release (section 4.1.3).Within the present study, pharmacological inhibition of all three pathways using a range of compounds failed to reduce wound-induced ATP release. This apparent lack of consensus may reflect cell or tissue-specific specialisation. Therefore, the data strongly suggests that the increase in ATP detected following wounding is a result of cell lysis rather than a specific signalling mechanism. In order to confirm this finding, in planned future work, visualisation of the luminescence signal will be carried out using an imaging technique whereby the luciferase signal produced by ATP release is captured in real time. We hypothesis that these experiments will show that the initial release of ATP into the extracellular media will originate from the damaged cells. This will also provide further information about the apparent biphasic manner in which ATP is released following wounding in 1.2mM $[Ca^{2+}]_o$. Whilst potentially interesting finding, it does not allow for manipulation of the pathway to analysis the contribution of elevated extracellular ATP in downstream transcriptional and functional events. To address this issue, hexokinase, an ATP scavenge was utilised

whereby ATP, released by cells into the media was removed from the extracellular environment.

It was noted prior to the commencement of this study, that previously published data investigating the effect of extracellular ATP, used an arbitrary concentration of ATP. Additionally, assessment of these publications led to the conclusion that the levels of ATP released were dependent on cell type, stimulus and timing. Therefore, it was deemed important to establish the concentration of ATP released into the media following wounding of primary human keratinocytes in order to allow application of a physiological relevant wounded concentration in subsequent experiments. A standard curve of known ATP concentrations was generated, which allowed for the interpolation of the luminescence measured following wounding. For example, Korkiamaki *et al.* demonstrated that application of ATP induced an intracellular calcium flux in primary human keratinocytes. However, the concentration added in these experiments was 100µM (Korkiamaki *et al.*, 2002). Although the data provides useful insights into the purinergic signalling in keratinocytes, the concentration is substantially higher than the now known wounded concentration of 1µM.

4.4.3 Method of measuring ATP release post-wounding.

Luciferase-based assays are a common and routine technique to determine ATP release. However, there are some limitations to this method. As highlighted by Beigi *et al.* it is possible that the removal of media for sample analysis may not be truly representative of the levels of ATP in the media, for example it does not take into account the ATP in the microenvironment of the cell surface. Moreover, ecto-ATPases on the cell surface may degrade ATP before a sample is obtained. Various advances have been made in the field of detection of ATP release including the use of a luciferase/protein A conjugated to target cell surface antigen such as ABC transporters or purinergic receptors. Whilst such a method would provide interesting further data, for the purpose of this study investigating the occurrence of ATP release following wounding and the mechanisms involved, luminescence-based assays were deemed sufficient.

4.4.4 ATP-mediated intracellular calcium flux in unwounded keratinocytes.

Previous results demonstrated the ability for wounded CM to elicit an intracellular calcium flux in unwounded keratinocytes. It was speculated that the releasable factor

mediating this response was ATP. Evidence that keratinocytes release ATP into the extracellular space supported this theory. The addition of ATP at the physiologically relevant wounded concentration, resulted in a calcium response in 22.6±5.2% of cells. This is consistent with published data in both HaCaTs and primary human keratinocytes (Korkiamaki *et al.*, 2002; Ross *et al.*, 2007; Ross *et al.*, 2008). These results are suggestive of functional purinergic receptors in the cell population. However, not all cells responded to the addition of ATP. Future work will determine whether only a sub-population of keratinocytes in the culture express the required purinergic receptors. An interesting observation is that the percentage of cells responding to ATP was similar to the percentage of cells that displayed an oscillatory behaviour post-wounding (22.6±5.2% and 23.2±2.6% respectively). The mechanisms resulting in only a sub-population of cells responding were not determined within this project, although it was speculated that this may correlate to differentiation status of the cell (Chapter 5). It would be of interest to further investigate the characteristics of the cells that respond to ATP in a similar manner. One potential avenue is that the more stem cell-like cells within the population express different purinergic receptors.

ATP was postulated to be a key mediator released from cells upon wounding and triggering a intracellular calcium flux in unwounded cells. It was therefore surprising that the percentage of cells responding to ATP was less than that responding to CM (22.6±5.2% and 55.3±15.7% respectively). This is highly suggestive that another factor is released following wounding of keratinocytes simultaneous to ATP. It was also shown that UTP was able to drive a calcium response in keratinocytes in a similar manner to ATP (Ross *et al.*, 2007). Moreover, treatment with UTP also induced STIM1 translocation to the PM implicating it in the process of SOCE which is known to drive NFAT activation (Chapter 6). UTP has been noted previously to be released from cells in response to injury, however, this has not been investigated in keratinocytes (Cordeiro and Jacinto, 2013).

In agreement with both CM calcium and ATP luminescence experiments, keratinocyte response to ATP did not appear to be calcium-dependent. This is in contrast to results presented by Appleby and co-workers who last year used a computational model based on urothelial cells to observe that the calcium transient induced by ATP differed between low and high external calcium (Appleby *et al.*, 2013).

To investigate the role of ATP further, CM experiments were repeated with the inclusion of hexokinase in the media (CMH). Results showed that the intracellular calcium flux was reduced (maximum Ft/F0) following the addition of CMH to unwounded cells in 1.2mM $[Ca^{2+}]_o$ but not 0.06mM $[Ca^{2+}]_o$. However the signal remained elevated above baseline in both 0.06mM $[Ca^{2+}]_o$ and 1.2mM $[Ca^{2+}]_o$. This is in contrast to Klepeis *et al*. who observed complete attenuation of the calcium influx when CM was added in the presence of apyrase, an alternative ATP scavenger (Klepeis et al.,2001). However, the data presented in figure 17 and figure 18, does support the theory that another factor is released by keratinocytes upon wounding that is also having an effect on intracellular calcium flux.

4.4.5 The role of extracellular ATP in regulating the intercellular calcium wave.

There are two main proposed theories for the transmission of the intercellular calcium wave after wounding. One of which involves the extracellular purinergic signalling pathway whereby ATP is released from cells following stimulation and triggers a calcium response in neighbouring cells (Section 4.1.1). Results within this chapter demonstrate that this pathway is important in the spread of the intercellular calcium wave induced by wounding in primary human keratinocytes as shown by the presence of hexokinase attenuating the wound-induced intracellular calcium flux in 1.2mM $[Ca^{2+}]_o$. This finding is consistent with reports in various cell types including glomerular endothelial cells where hexokinase treatment reduced calcium wave propagation (Lohman *et al.,* 2012). Although the authors do not comment on the effect hexokinase treatment has on parameters of the intracellular calcium flux such as AUC.

Future work to confirm the role of ATP in the spread of the calcium wave in keratinocytes should consider the use of compounds that inhibit ecto-ATPases. Inhibition using compounds such as ARL-67156 would be expected to enhance the calcium wave in 1.2mM $[Ca^{2+}]_o$ following wounding in a similar manner to that shown by D'hondt *et al*. if, as suggestive herein, ATP was involved in the calcium wave (D'hondt *et al.,* 2007). Additionally, treatment with the purinergic antagonist suramin or with Mn^{2+} to acutely inhibit ATP-dependent calcium entry would provide further support (Streifel *et al.,* 2013).

Wounding in 1.2mM $[Ca^{2+}]_o$ in the presence of hexokinase resulted in a similar intracellular calcium flux to wounding in 0.06mM $[Ca^{2+}]_o$ without hexokinase. From this is can be postulated that the increased intracellular calcium flux in high calcium conditions is mediated through ATP-dependent calcium influx. Analysis of individual cells at specified locations from the wound edge showed that hexokinase treatment had no effect on calcium signalling in cells located at the wound edge, a significant difference was only reported in distal cells. Data from chapter 3 were also suggestive of an intracellular calcium source in cells close to the wound with enhanced contribution from extracellular calcium further back from the wound. Although not focussing on calcium signalling, Block and co-workers investigated the effect of wound-induced ATP on EGFR activation in human corneal limbal epithelial cells. Using apyrase to scavenge ATP, the authors demonstrated that wounding activated two distinct signalling pathways; one close to the wound which was ATP-independent and one further back which was dependent on ATP release (E. R. Block and Klarlund, 2008). It is possible that this is occurring in human keratinocytes and further experimentation will provide insights into this.

Whilst demonstrating that ATP is necessary for the calcium wave and intracellular calcium fluxes following wounding under specific extracellular calcium conditions, delineating which purinergic receptors are involved in mediating this response was beyond the scope of this project. As described in section 1.6.1 there are two classes of purinergic receptors activated by ATP; P2XR and P2YR. P2YR are known to act as GPCR and activation results in IP_3-mediated release of calcium from the ER, which then triggers STIM1 translocation to the PM and the subsequent influx of calcium ions from the extracellular space through SOCE. In contrast, P2XR act as an ATP-gated ion channel. It has been shown that P2XR-induced calcium influx is augmented by elevated extracellular calcium (Schwiebert and Zsembery, 2003). Future work using inhibitors or knockdown of specific receptors should shed light onto the relative contribution of purinergic receptors in the propagation of the calcium wave (Appleby *et al.*, 2013).

4.4.6 The contribution of gap-junctional communication to the wound-induced calcium wave.

There are two main proposed theories for the transmission of the intercellular calcium wave. One of these involves the extracellular ATP, as mentioned above, and the other

relies on gap-junction signalling. Utilising the gap-junction inhibitor 18αGA it has been shown in the current study that intercellular communications via gap-junctions are vital for the spread of the calcium wave induced by wounding in keratinocytes. This finding has been observed in a variety of cell types in response to a range of stimuli, as reviewed in section 1.4.5. However, not all investigations have highlighted a role for gap-junctions in the spread of the calcium wave. Klepeis *et al*. showed that treatment with 20μM 18αGA, the same compound and concentration used within this study, had no effect on wound-induced calcium wave propagation in a human corneal cell line (Klepeis *et al.*, 2001). This further suggests that the differences observed between publications are cell-type and stimuli dependent. It can therefore be suggested that in primary human keratinocytes, wounding results in the movement of a mediator, potentially IP_3, through gap-junctions into adjacent cells to propagate the calcium wave from the wound edge back. In the absence of this signalling pathway the wave does not persist.

Interestingly, in the present study, gap-junctional inhibition had a different effect in 0.06mM $[Ca^{2+}]_o$ compared to 1.2mM $[Ca^{2+}]_o$. In a low external calcium environment, 18αGA treatment resulted in minimal increase above baseline compared to vehicle at all cell locations from the wound. This was supported by reduced AUC of $[Ca^{2+}]_i$ flux at all cell locations compared to vehicle. Suggesting that blockade of gap-junction communication prevents the transduction of signal initiated at the wound edge. Therefore, providing further evidence that wounding activates an intercellular calcium wave that spreads from cell to cell back from the wound edge. Interestingly, wounding in the presence of 18αGA in 1.2mM $[Ca^{2+}]_o$, reduced parameters of the wave but not to the extent observed in 0.06mM $[Ca^{2+}]_o$. Both the maximum Ft/F0 reached and AUC of the wound-induced $[Ca^{2+}]_i$ flux were comparable to vehicle within cells located at the wound edge and then decreased with increasing location from the wound edge, thus indicating that the signal was propagating through a reduced number of cells. Overall, there was an elevated calcium signal within cells when wounding was performed in 1.2mM $[Ca^{2+}]_o$. Results presented in figure 4.12 clearly show that 18αGA treatment does not affect wound-induced ATP release in these external calcium conditions. Therefore it may be concluded that the increased calcium response observed when blocking gap-junctions in 1.2mM $[Ca^{2+}]_o$ compared to 0.06mM $[Ca^{2+}]_o$, was a result of ATP-mediated calcium entry rather than propagation of a mediator through gap-

junctions. Co-treatment with both hexokinase and 18αGA would be an intriguing experiment to conduct in the future to confirm the simultaneous functioning of both these signalling pathways.

The role gap-junctions play in mediating the wound-induced calcium wave following wounding of keratinocytes, have been shown to altered in different dermatological diseases. For example, Karvonen *et al.* observed that keratinocytes derived by psoriasis patients displayed a reduced calcium wave in response to wounding compared to normal keratinocytes. The authors speculated this was a result of abnormal intercoupling between cells in the disease state. In a similar manner to the current study, it was also shown that the intracellular calcium flux in normal keratinocytes in response to wounding was almost completely prevented with the gap-junction inhibitor heptanol. In contrast, the intracellular calcium flux in the presence of heptanol was slightly increased in psoriatic keratinocytes, thus suggesting gap-junctional signalling is defective in psoriasis patients (Karvonen *et al.*, 2000). Additionally, keratinocytes derived from patients with neurofibromatosis (NF1) also showed a reduced dependency on gap-junction signalling following wounding compared to normal keratinocytes (Korkiamaki *et al.*, 2002).

Data presented in this current study shows that gap-junctional communication drives the wave and ATP mediates further calcium entry in cells distal to the wound edge, it can therefore be postulated that ATP acts as a "danger signal" released from damaged cells to communicate with cells further back that an injury has occurred. This may then "prepare" the cells for exposure to other insults such as oxidative stress as well as potentially initiating migratory responses in order to close the wound.

Whilst gap-junction and ATP signalling are the two major mechanisms for calcium wave transmission, there may be other factors regulating the wave such as growth factors (Klepeis *et al.*, 2001), $iPLA_2$ (Ross *et al.*, 2007) or CaSR (Milara *et al.*, 2010). Future work should not exclude the possibility that these or other mechanisms may be key mediators.

Both 18αGA and GSK-7975A compounds were solubilised in DMSO to a final concentration of 0.001%. In parallel experiments to these, vehicle control experiments were conducted whereby DMSO was added to the keratinocyte growth media (0.001%)

but no compound was added. Whilst 0.001% DMSO is generally accepted to be tolerated by cells, it is known that DMSO can have cytotoxic effects at higher concentration. DMSO is believed to exert these effects by inducing pores in the membrane (Notman *et al.*, 2006). Gurtovenko and co-workers report supporting evidence that at high concentrations DMSO induces water pores into the membrane and can result in individual lipid molecules being desorbed from the membrane. Moreover, this study also highlighted an effect of DMSO at low concentration, with DMSO inducing membrane thinning and increasing fluidity of the membrane (Gurtovenko and Anwar, 2007). When analysing the effect of GSK-7975A and 18αGA on wound-induced intracellular calcium flux results were compared to vehicle control (DMSO) rather than untreated to ensure that any effect reported was a result of the mechanism of action of the compound rather than DMSO itself. It is of note however, that in some cases the values reported from the vehicle control were not completely comparable with those seen in wounded untreated keratinocytes (chapter 3). This may be due to DMSO having a small, but nevertheless significant effect of cell membrane fluidity even at the low concentration used. The effect of this should not be overlooked in future investigations and further experiments are required to fully determine the effect on DMSO on intracellular calcium flux in primary human keratinocytes.

4.5 Conclusions.

- Keratinocytes release ATP, through cell lysis, in response to scratch wounding in a calcium-independent manner.

- ATP induces an intracellular calcium flux in unwounded cells, however, CMH still evokes a response suggesting non-ATP releasable factors simultaneously having an effect.

- Both gap-junctional communication and extracellular ATP are required for efficient calcium wave propagation.

Chapter 5.

Regulation of Wound-induced Calcium Oscillations

5 Chapter 5. Regulation of Wound-induced Calcium Oscillations.

5.1 Introduction.

5.1.1 Calcium oscillations.

$[Ca^{2+}]_i$ increases act as a double-edged sword in terms of cellular signalling. On one hand it is known that $[Ca^{2+}]_i$ elevations are a prerequisite for downstream signalling pathways such as transcription factor activation in order to elicit a diverse range of responses (Berridge *et al.*, 2003) (section 1.3.1). However, it is also established that prolonged increases in calcium within the cytoplasm signal for apoptosis and are toxic to the cell (Dolmetsch *et al.*, 1998). Consequently, the calcium "toolkit" described in section 1.3.1 contains a variety of "off" mechanisms to complement the "on" mechanisms ensuring that $[Ca^{2+}]_i$ does not remain high for prolonged periods of time. These "off" switches are conducted through calcium ion pumps and calcium/sodium exchangers in the PM which actively pump calcium into the extracellular environment as well as calcium ATPases located on the ER membrane which allows entry of calcium from the cytosol into the internal stores. Interestingly, the mitochondria functions as an important calcium store. When cytosolic calcium levels are high, calcium is taken up into the mitochondria rapidly; it is then released slowly during recovery. The 40kDa protein responsible for the calcium uniporter in the mitochondria was identified recently (De Stefani *et al.*, 2011) providing insights into the role the mitochondrion plays in calcium signalling. It has been noted that after SOCE in excitable cells, the mitochondria is the primary intracellular calcium store, however, in non-excitable cells the ER remains prominent (García-Sancho, 2014). Finally, within the cytoplasm there are calcium binding proteins and calcium sensors that act to lower cytosolic calcium concentration (Berridge *et al.*, 2000). Calcium sensors include calmodulin, which is expressed in all eukaryotic cells and binds calcium to provoke cellular cascades (M. Zhang *et al.*, 2012). The role of calmodulin in NFAT activation is reviewed in section 1.5.2. It has been suggested that adequate activation whilst preventing cellular toxicity is achieved through the cell temporarily reducing its $[Ca^{2+}]_i$ resulting in an oscillatory pattern of calcium signalling. The occurrence of calcium oscillations have been extensively studied and are widely accepted as a ubiquitous and diverse method for governing multiple responses within the cell. The specific oscillatory pattern a cell displays not only protects against toxicity, but also is thought to encode particular

information to modulate cell activities through altered amplitude and frequency characteristics (Berridge *et al.,* 2000). In this manner, calcium is able to discriminate among different calcium-dependent pathways and can activate the required subset of targets. Dolmetsch and co-workers demonstrated that oscillating T-cells experiencing calcium oscillations had increased NFAT, NFκB and Oct/oap compared to T cells that were exposed to continued elevated calcium concentrations, confirming an important role for oscillations in transcription factor activation. Moreover, the authors also observed that the frequency of oscillations determined which transcription factors were activated; at a high frequency all three were activated, however at a low frequency, only NFκB levels increased (Dolmetsch *et al.*, 1998).

In addition to regulating the spread of the calcium wave, extracellular ATP has been shown to induce calcium oscillations (Pillai and Bikle, 1992). Meng *et al.* demonstrated that in human umbilical cord smooth muscle cells (HUCSMC) basal oscillations only occurred in 1% of cells. This figure increased to 70% after the addition of ATP in varying concentrations from 10μM to 1mM. Interestingly, authors also showed that between 10-100μM, an increase in ATP concentration resulted in an increase in oscillations frequency and amplitude. However, concentrations greater than 100μM had the opposite effect and as the ATP concentration was increased, oscillation frequency and amplitude decreased. Pharmacological inhibition assays suggested that these ATP-induced oscillations were conducted through external calcium entry into the cell and P2R activation. Paradoxically, treatment with suramin; a P2Y antagonist increased oscillation frequency in this system rather than decreasing as perhaps would be expected. The authors conclude that the specificity of suramin for receptors expressed in HUCSMC cells affects its ability to cause inhibition (Meng *et al.*, 2007).

5.2 Specific aims.

- To investigate the occurrence of calcium oscillations following wounding of primary human keratinocytes.

- To elucidate the contribution of SOCE in wound-induced calcium oscillations.

- To determine the relative contribution of extracellular ATP and gap-junctional communication in wound-induced calcium oscillations.

5.3 Results.

5.3.1 Calcium oscillations in primary human keratinocytes.

It is well established that cells display an oscillatory pattern of signalling as a form of protection from calcium-induced apoptosis and cellular toxicity (Dolmetsch *et al.*, 1998). Moreover, calcium oscillations have been proposed to be involved in the induction and regulation of downstream transcriptional events (Berridge *et al.*, 2003). Therefore, it was of interest whether wounding primary human keratinocytes resulted in calcium oscillations. However, prior to the commencement of these investigations, it was necessary to establish basal levels of oscillations in unwounded cells. To address this, primary human keratinocytes cultured in 0.06mM $[Ca^{2+}]_o$ keratinocyte growth medium (MCDB 153) were loaded with Fluo4-AM calcium dye and were imaged in either 0.06mM or 1.2mM $[Ca^{2+}]_o$ for twenty minutes. As this was a control experiment, cells were not wounded.

Traces from unwounded cells in 0.06mM $[Ca^{2+}]_o$ showed that there were no fluctuations in calcium signalling during the twenty minute imaging period (Appendix C). However, it was noted that in 1.2mM $[Ca^{2+}]_o$, a small number of cells displayed spontaneous oscillatory calcium signalling. Quantification of the percentage of keratinocytes in which, at least one calcium oscillation was observed is presented in figure 5.1. An oscillation was characterised by a full cycle of increase and decrease in fluorescence intensity. The percentage of cells oscillating in 1.2mM $[Ca^{2+}]_o$ was 2.79±1.47%. Statistical analysis was conducted using a chi-squared test. Results did not show any significant differences between the number of spontaneous oscillations observed in 0.06mM $[Ca^{2+}]_o$ and 1.2mM $[Ca^{2+}]_o$ (P=0.0810). From this it can be concluded that in the time frame of the following investigations, there is not a significant number of basal oscillations.

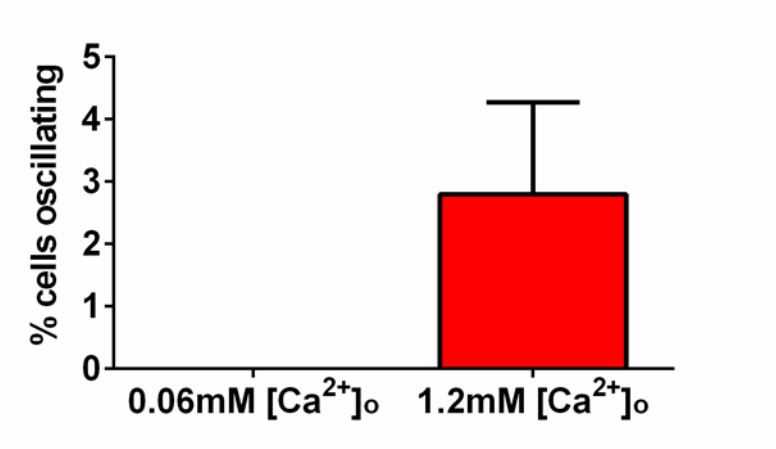

Figure 5.1 A small percentage of unwounded keratinocytes spontaneously oscillate in 1.2mM $[Ca^{2+}]_o$.

Primary human keratinocytes cultured in 0.06mM $[Ca^{2+}]_o$ keratinocyte growth medium (MCDB 153) were loaded with Fluo4-AM calcium dye and were imaged in either 0.06mM or 1.2mM $[Ca^{2+}]_o$ for twenty five minutes, these cells remained unwounded throughout the experiment. Confocal images were captured at 3.7fps and ROI were drawn around individual cells. An oscillation was characterised by a full cycle of increase and decrease in fluorescence intensity. These cells remained unwounded throughout the experiment. The percentage of cells that oscillated during the imaging period was calculated for 0.06mM and 1.2mM $[Ca^{2+}]_o$. Data shows mean ± SEM from three independent donors; N=3. All cells in the field of view were analysed. Chi-square test (P=0.0810).

5.3.2 Wound-induced calcium oscillations.

When conducting experiments to characterise the wound-induced calcium wave and determine the contribution of extracellular calcium to wave propagation (chapter 3), it was observed that after the initial $[Ca^{2+}]_i$ flux triggered by the wound, some cells displayed an oscillatory behaviour. When wounding in 0.06mM $[Ca^{2+}]_o$, no further calcium activity was seen after the spread of the calcium wave , as shown by the blue trace on figure 5.2a. However, when wounding in 1.2mM $[Ca^{2+}]_o$, a sub-population of keratinocytes oscillated. Using the image analysis software Volocity, the colour of the images was altered to rainbow to facilitate visualisation of changes in intensity. Representative images from one experiment taken at specified time points demonstrated these oscillatory $[Ca^{2+}]_i$ flux in an individual cell, highlighted by arrows (Figure 5.3). It is also of note that a) there was no relationship between location of the oscillating cell and distance from the wound edge and b) an intracellular calcium flux in the form of an oscillation did not initiate a calcium wave or signalling in neighbouring cells.

Quantification of the number of cells in each donor that oscillated post-wounding in 0.06mM and 1.2mM $[Ca^{2+}]_o$, compared to unwounded cells is shown in figure 5.2b. It is clear that wounding results in an increased percentage of cells oscillating compared to unwounded cells. Furthermore, wound-induced oscillations were only detected in 1.2mM $[Ca^{2+}]_o$. Two-way ANOVA reported a significant effect of both calcium concentration and wounding on the percentage of cells oscillating ($F(1,20)=64.95$, $P<0.0001$ and $F(1,20)=47.10$, $P<0.0001$ respectively). A Bonferroni post-hoc test showed that there was a significant difference between percentage of cells oscillating in unwounded cells in 1.2mM $[Ca^{2+}]_o$ and cells wounded in 1.2mM $[Ca^{2+}]_o$ (*** $P<0.001$). Additionally, there was a significant difference between wounded cells in 0.06mM $[Ca^{2+}]_o$ and wounded cells in 1.2mM $[Ca^{2+}]_o$ (*** $P<0.001$).

The occurrence of oscillations in 1.2mM $[Ca^{2+}]_o$ but not 0.06mM $[Ca^{2+}]_o$, suggest that an elevated external calcium environment is required for the induction of calcium oscillations post-wounding, thus indicating that oscillations are mediated by calcium influx into the cytosol.

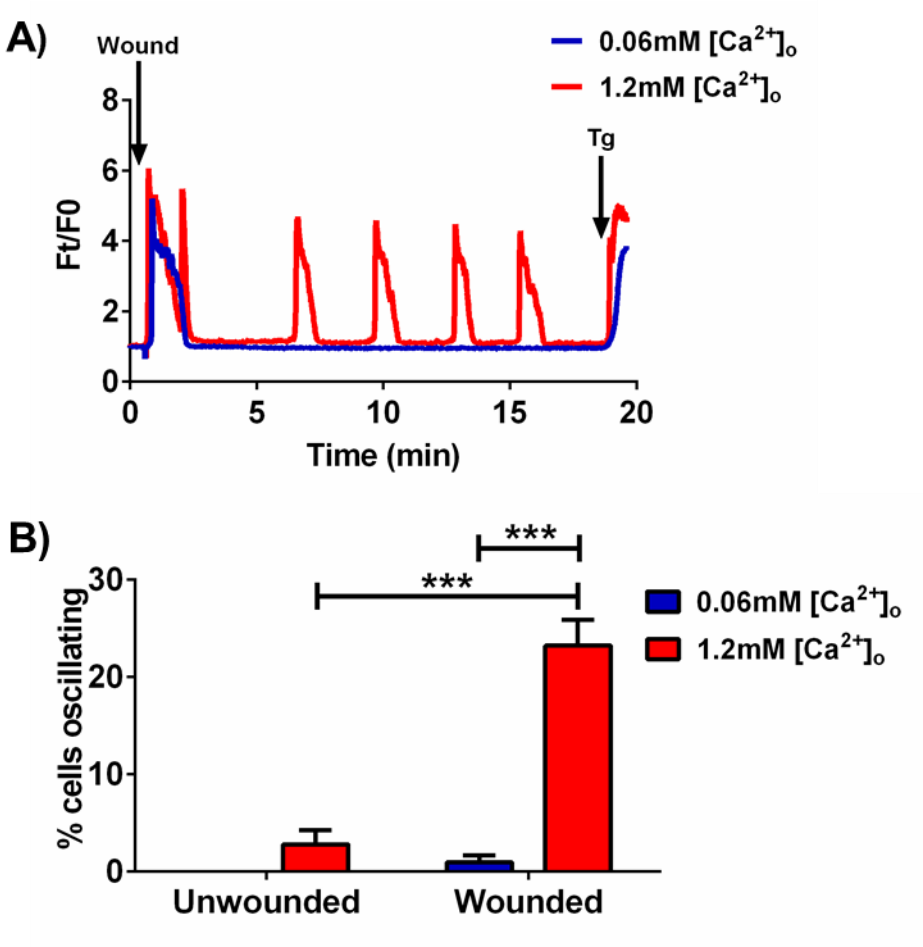

Figure 5.2 A sub-population of keratinocytes oscillate following wounding in 1.2mM $[Ca^{2+}]_o$ but not 0.06mM $[Ca^{2+}]_o$.

Primary human keratinocytes cultured in 0.06mM $[Ca^{2+}]_o$ keratinocyte growth medium (MCDB 153) were loaded with Fluo4-AM calcium dye. Post-de-esterification, either 0.06mM or 1.2mM $[Ca^{2+}]_o$ keratinocyte growth medium (MCDB 153) was added for five minutes prior to wounding. Confocal images were captured at 3.7 fps. Regions of interest (ROI) were drawn around individual cells up to six cells from the wound edge for analysis. **A)** Trace from individual cells wounded in 0.06mM (blue) or 1.2mM (red) $[Ca^{2+}]_o$. **B)** The percentage of cells that oscillated during the twenty minute imaging period, after the immediate wound-induced calcium flux, was calculated. An oscillation was characterised by a full cycle of increase and decrease in fluorescence intensity that occurred after the initial $[Ca^{2+}]_i$ flux. Following wounding in 0.06mM $[Ca^{2+}]_o$ 4 cells out of 420 in the fields of view from 6 independent donors oscillated. Following wounding in 1.2mM $[Ca^{2+}]_o$ 109 cells out of 453 in the fields of view from 6 independent donors oscillated Data shows mean ± SEM from six independent donors; N=6. Two-way ANOVA with Bonferroni post-hoc test (*** $P<0.001$).

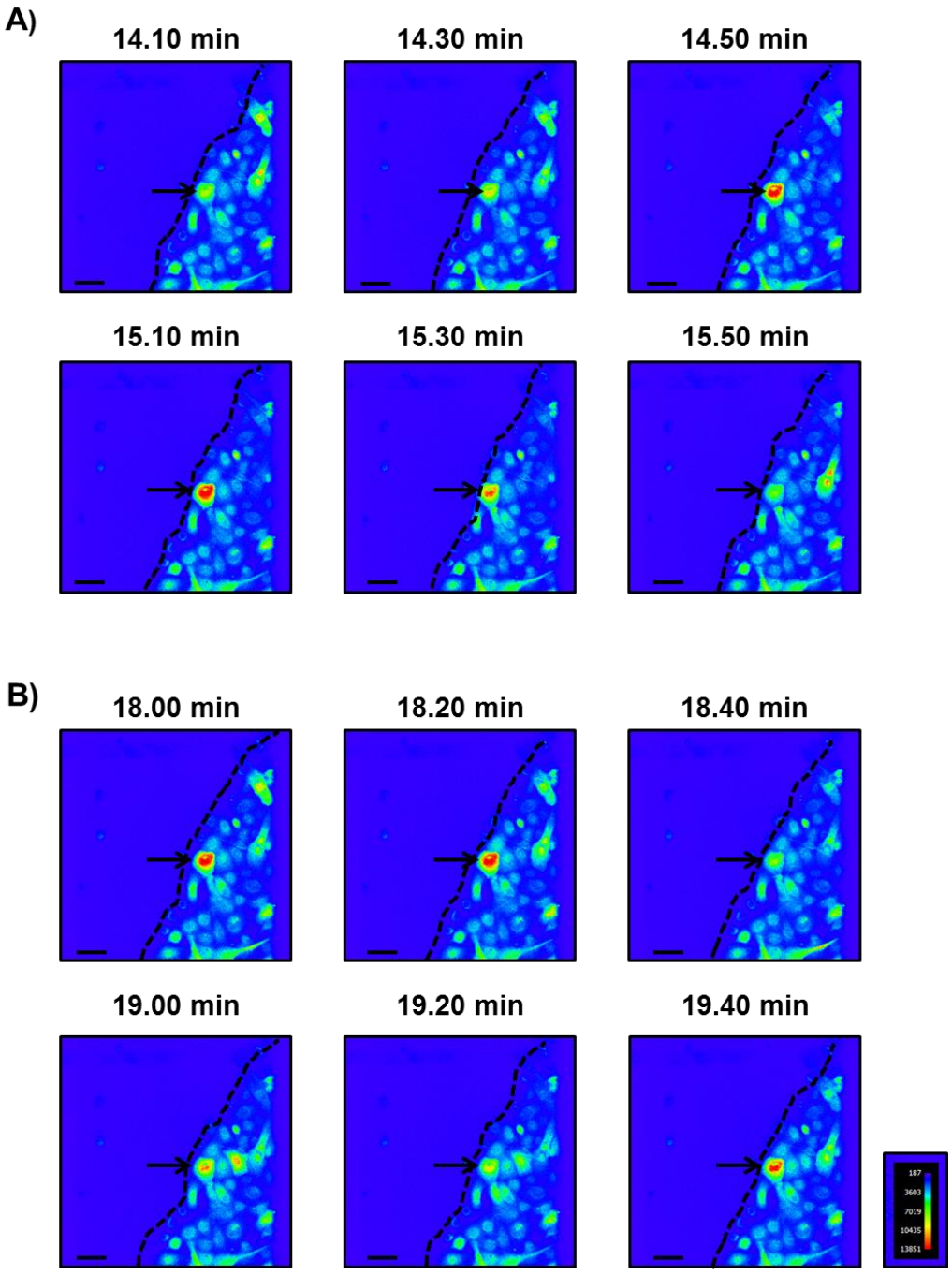

Figure 5.3 Wound-induced calcium oscillations are observed in 1.2mM $[Ca^{2+}]_o$.

Primary human keratinocytes cultured in 0.06mM $[Ca^{2+}]_o$ keratinocyte growth medium (MCDB 153) were loaded with Fluo4-AM calcium dye and switched to 1.2mM $[Ca^{2+}]_o$ five minutes prior to wounding. Pseudo colour images of confocal images were generated over two periods of time to demonstrate the oscillatory behaviour of an individual keratinocyte, as highlighted by the arrow. **A)** Oscillation 1 and **B)** Oscillation 2. Scale bar=80µm. Pseudo colour reference is shown. Wound edge is highlighted by dotted line. Images are representative of three independent donors.

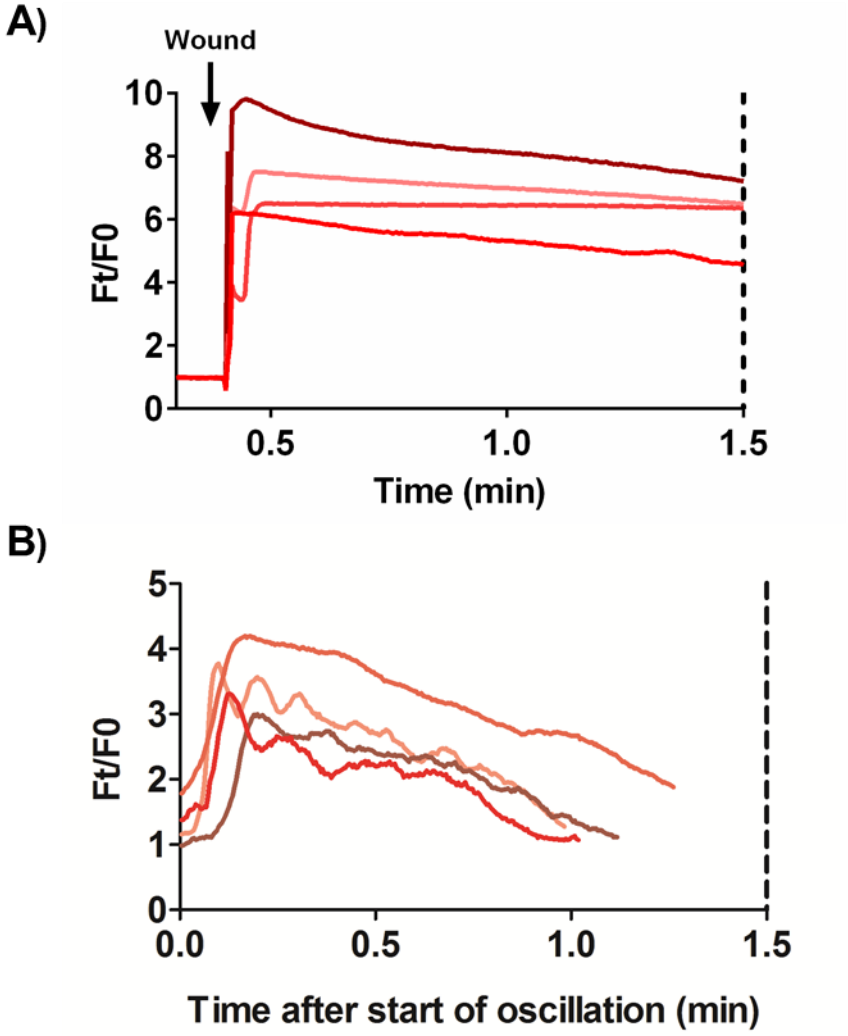

Figure 5.4 Wound-induced calcium flux is larger and more sustained compared to calcium flux during individual oscillations.

Primary human keratinocytes cultured in 0.06mM $[Ca^{2+}]_o$ keratinocyte growth medium (MCDB 153) were loaded with Fluo4-AM calcium dye. Post-de-esterification 1.2mM $[Ca^{2+}]_o$ keratinocyte growth medium (MCDB 153) was added for five minutes prior to wounding. Confocal images were captured at 3.7 fps. Regions of interest (ROI) were drawn around individual cells up to six cells from the wound edge for analysis. Traces show four representative calcium fluxes from **A)** the calcium wave initiated by wounding (time of wounding is highlighted by arrow) and **B)** individual calcium oscillations observed following the initial wound-induced flux, whereby time zero is the time point in which each individual oscillation begins. Four cells per condition are representative of three independent donors.

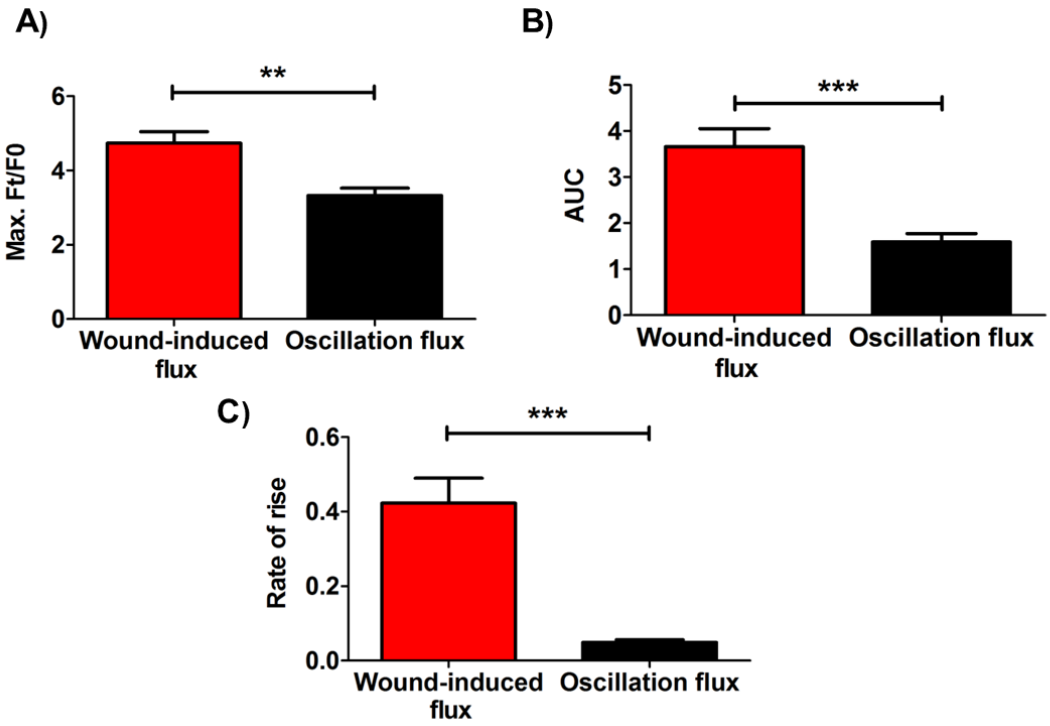

Figure 5.5 Wound-induced calcium flux shows a greater peak change and AUC and is more sustained compared to calcium flux during individual oscillations.

Primary human keratinocytes cultured in 0.06mM $[Ca^{2+}]_o$ keratinocyte growth medium (MCDB 153) were loaded with Fluo4-AM calcium dye. Post-de-esterification 1.2mM $[Ca^{2+}]_o$ keratinocyte growth medium (MCDB 153) was added for five minutes prior to wounding. **A)** Comparison between the average maximum Ft/F0 reached during the initial calcium flux post-wounding and the average maximal Ft/F0 achieved during an oscillation. **P=0.0040, unpaired, two-tailed t-test. **B)** Comparison between the average AUC of the initial calcium flux post-wounding and the average AUC of an oscillation. ***P=0.0007, unpaired, two-tailed t-test. **C)** Comparison between the rate of rise of the calcium flux during the initial calcium flux post-wounding and the average rate of rise of an oscillation. ***P=0.0003, unpaired, two-tailed t-test. Oscillation data shows mean ± SEM of 33 oscillations from 15 oscillating cells from three independent donors; (n=33), N=3.

Figure 5.4 shows four traces of individual cells. Both the initial intracellular calcium flux induced by wounding (figure 5.4a) and the calcium flux during an individual oscillation (figure 5.4b) are shown.

Studies of four representative traces from three independent donors revealed that the maximum fluorescence and the calcium signal duration were reduced in the oscillations compared to the wound-induced intracellular calcium flux. Additionally, the gradient of the intracellular calcium flux appeared to be less steep in the oscillations compared to the wound. In order to further analyse the occurrence of these oscillations and quantify the differences observed, the following parameters of the $[Ca^{2+}]_i$ flux were analysed i) maximum Ft/F0 ii) AUC of the $[Ca^{2+}]_i$ flux and iii) the rate of rise of the calcium gradient during the oscillation. Data were compared to respective data from the wound-induced intracellular calcium flux in 1.2mM $[Ca^{2+}]_o$ and expressed as mean ± SEM from thirty three oscillations occurring in fifteen oscillating cells from three independent donors. Maximum Ft/F0 was defined as the greatest fold change in $[Ca^{2+}]_i$ during the oscillation. As the oscillations detected were asynchronous, these were calculated irrespective of time. The maximum Ft/F0 reached during an oscillation was 3.32±0.19, this was statistically reduced compared to the maximum Ft/F0 achieved by wounding (4.73±0.31) (P=0.0040, Unpaired, two-tailed t-test) (figure 5.5a). AUC of the $[Ca^{2+}]_i$ observed during wounding was calculated as 1.06±0.09, again significantly lower than the AUC of the wound-induced $[Ca^{2+}]_i$ flux which was 3.65±0.39 (P<0.0001, Unpaired, two-tailed t-test) (figure 5.5b). Similarly the rate of rise of the calcium gradient during an oscillation appeared to be reduced compared to the rate of rise of the wound-induced intracellular calcium flux, 0.04±0.007 (ΔFt/F0/second) and 0.42±0.06 (ΔFt/F0/second) respectively (figure 5.5c).

Collectively, these data suggest, as expected, that a different mechanism is regulating the oscillations compared to the initial $[Ca^{2+}]_i$ flux induced by mechanical wounding.

5.3.3 The contribution of SOCE to wound-induced calcium oscillations.

The occurrence of calcium oscillations only after wounding in a high external calcium environment, implies that a calcium entry mechanism is driving the oscillations. Results from studies in section 3.3.1 show that wounding depletes the intracellular calcium

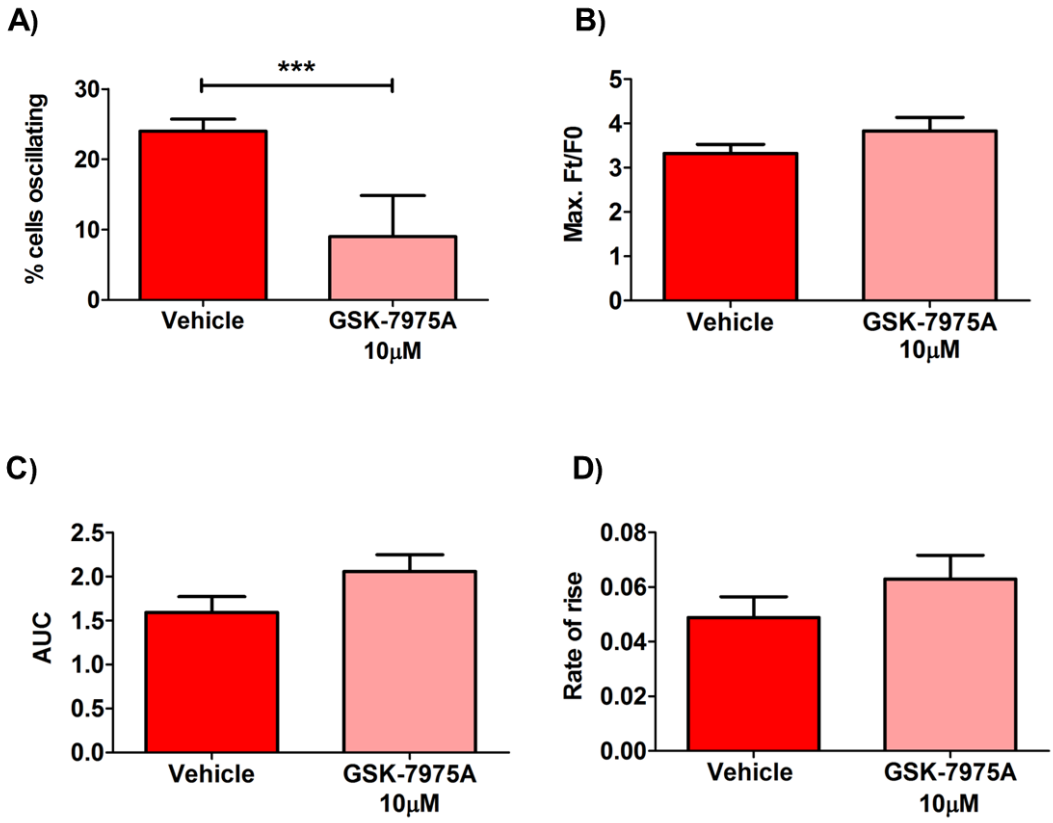

Figure 5.6 SOCE inhibition reduces the percentage of cells oscillating post-wounding.

Primary human keratinocytes cultured in 0.06mM $[Ca^{2+}]_o$ keratinocyte growth medium (MCDB 153) were loaded with Fluo4-AM calcium dye and during the de-esterification forty five minutes cells were treated with 10μM GSK-7975A or vehicle (DMSO). Keratinocytes were switched to 1.2mM $[Ca^{2+}]_o$ keratinocyte growth medium (MCDB 153) in the presence or absence of 10μM GSK-7975A for five minutes prior to wounding. **A)** The percentage of cells that oscillated during the twenty minute imaging period, after the immediate wound-induced calcium flux, was calculated. ***P=0.0007, chi-square test. Data shows mean ± SEM from three independent donors; N=3. **B)** Maximum Ft/F0 reached during an individual oscillation. Unpaired, two-tailed t-test (P=0.1648). **C)** AUC of the calcium flux during an oscillation. Unpaired, two-tailed t-test (P=0.0796). **D)** Rate of rise of the calcium flux during an oscillation. Unpaired, two-tailed t-test (P=0.2256). Data shows mean ± SEM of 31 oscillations from 17 oscillating cells from three independent donors; n=31, (N=3).

stores of the cells located at least six cells from the wound edge. It was therefore hypothesised that SOCE was the likely calcium entry mechanism initiating the oscillations. To assess the contribution of SOCE in the occurrence of calcium oscillations post-wounding, primary human keratinocytes cultured in 0.06mM $[Ca^{2+}]_o$ keratinocyte growth medium (MCDB 153) were loaded with Fluo4-AM calcium dye. During the subsequent forty five minute de-esterification period, cells were treated with the novel SOCE inhibitor 10μM GSK-7975A. Keratinocytes were then wounded in supplemented keratinocyte growth medium (MCDB 153) to increase the calcium concentration to 1.2mM in the presence of 10μM GSK-7975A prior to the calculation of the percentage of cells oscillating post-wounding in 1.2mM $[Ca^{2+}]_o$. As shown by Figure 5.6a there were significantly less oscillating cells detectable when wounding was performed following SOCE inhibition compared to untreated cells (P=0.0007, Chi-square test). Parameters of the intracellular calcium flux during individual oscillations were assessed to further delineate the effect of SOCE. As shown by figures 5.6b-d show that there were no significant differences in the maximal Ft/F0, AUC of the intracellular calcium flux or rate of rise of the intracellular calcium flux during oscillations occurring with or without SOCE inhibition by GSK-7975A (P=0.1648, P=0.0796 and P=0.2256 respectively, Unpaired, two-tailed t-tests).

These results suggest that calcium entry via SOCE mechanisms drives the occurrence of the calcium oscillations post-wounding, as supported by a statistically significant reduction in the percentage of oscillations detected in 1.2mM $[Ca^{2+}]_o$. However, it is of note that in the presence of GSK-7975A, 9.1±5.8% of cells still displayed an oscillatory behaviour. The characteristics of the remaining oscillations were similar to untreated oscillations, indicating that whilst SOCE drives the majority of oscillations, there may be another non-SOCE calcium entry mechanism occurring.

5.3.4 The effect of extracellular ATP on the occurrence of wound-induced calcium oscillations.

Results described in Chapter 4 demonstrated that ATP is released from keratinocytes into the extracellular media immediately following scratch wounding. Wounding in the presence of hexokinase, an ATP scavenger, removed all detectable levels of ATP in the extracellular media. Moreover, hexokinase treatment reduced the intracellular calcium response suggesting removal of extracellular ATP at the point of wounding, may affect

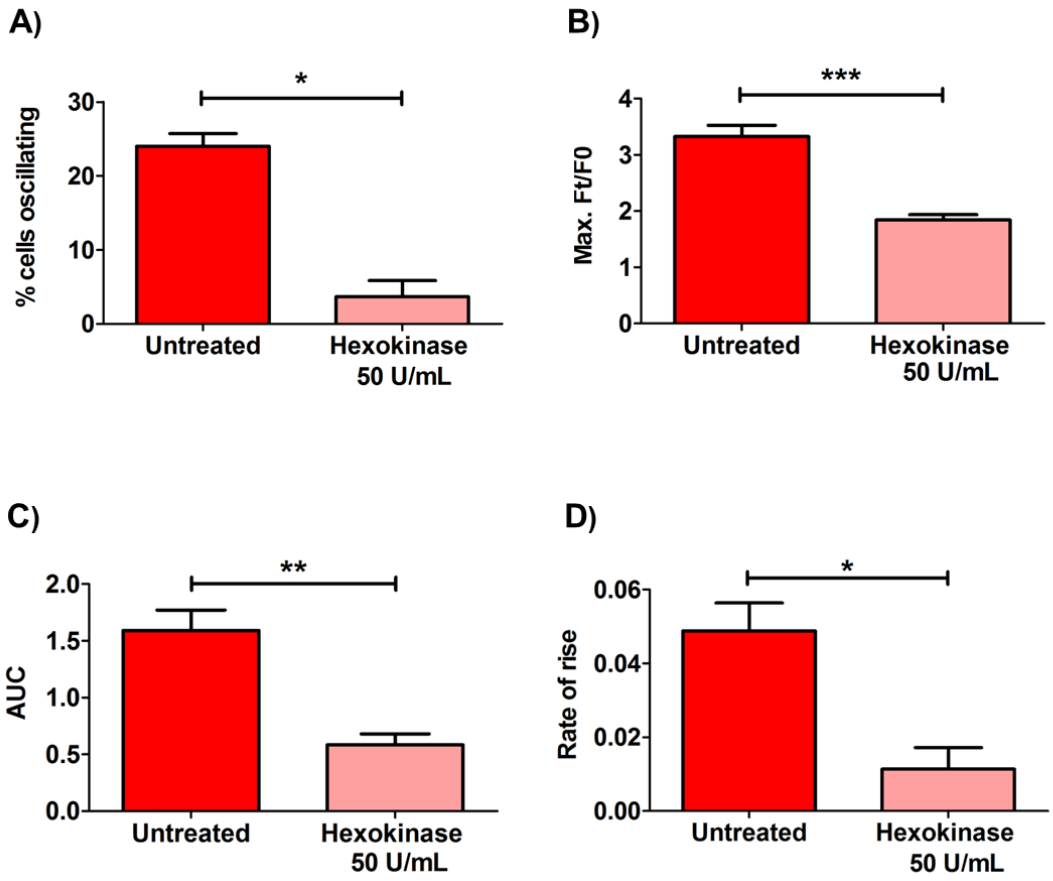

Figure 5.7 Removal of extracellular ATP reduces the percentage of cells oscillating post-wounding.

Primary human keratinocytes cultured in 0.06mM $[Ca^{2+}]_o$ keratinocyte growth medium (MCDB 153) were loaded with Fluo4-AM calcium dye and during the de-esterification forty five minutes period cells were treated with 50 U/mL hexokinase or left untreated. Keratinocytes were switched to 1.2mM $[Ca^{2+}]_o$ keratinocyte growth medium (MCDB 153) in the presence or absence of 50 U/mL hexokinase for five minutes prior to wounding. **A)** The percentage of cells that oscillated during the twenty minute imaging period, after the immediate wound-induced calcium flux, was calculated. *P=0.0380, Chi-square test. **B)** Maximum Ft/F0 reached during an individual oscillation. ***P=0.0005, unpaired, two-tailed t-test. **C)** AUC of the calcium flux during an oscillation. **P=0.0065, unpaired, two-tailed t-test. **D)** Rate of rise of the calcium flux during an oscillation. *P=0.0164, unpaired, two-tailed t-test. Data shows mean ± SEM of 9 oscillations from 8 oscillating cells from three independent donors; n=9, (N=3).

downstream oscillations. To address this point, primary human keratinocytes cultured in 0.06mM $[Ca^{2+}]_o$ keratinocyte growth medium (MCDB 153) were loaded with Fluo4-AM calcium dye prior to treatment with 50 U/mL hexokinase during the subsequent forty five minute de-esterification period. Keratinocytes were then wounded in supplemented keratinocyte growth medium (MCDB 153) to increase the calcium concentration to 1.2mM in the presence of 50 U/mL hexokinase prior to the calculation of the percentage of cells oscillating post-wounding in 1.2mM $[Ca^{2+}]_o$.

As shown by Figure 5.7a, there were significantly less oscillating cells detectable when wounding was performed following the removal of extracellular ATP compared to untreated cells (P=0.0380, Chi-square test). Parameters of the intracellular calcium flux during individual oscillations were assessed to further delineate the effect of ATP. Data presented in figure 5.7b shows that the maximum Ft/F0 reached during an oscillation in the presence of hexokinase was significantly reduced compared to the maximum Ft/F0 reached during an oscillation without hexokinase treatment (P=0.0005, Unpaired, two-tailed t-test). In a similar manner, the AUC of the intracellular calcium flux during an oscillation was also decreased in hexokinase treated cells compared to untreated, again an unpaired, two-tailed t-test revealed this as significant (P=0.0065) (figure 5.7c). Finally, the rate of rise of the intracellular calcium flux was calculated in the presence and absence of 50 U/mL hexokinase. Results showed that the rate of rise was significantly reduced with hexokinase treatment (P=0.0164, Unpaired, two-tailed t-test) (figure 5.7d).

Collectively these data indicate that extracellular ATP regulates the occurrence of the calcium oscillations post-wounding as shown by a significant decrease in the percentage of cells oscillating when wounding was performed in the presence of hexokinase. Moreover, the oscillations that did persist displayed reduced characteristics compared to oscillations from untreated cells.

5.3.5 The role of gap-junctional communication following wounding in calcium oscillations.

As shown in section 4.3.10 blockade of gap-junctional communication by 18αGA, prevented the spread of the calcium wave post-wounding, suggesting the propagation of the wave was mediated through intercellular communication. If, as preceding data

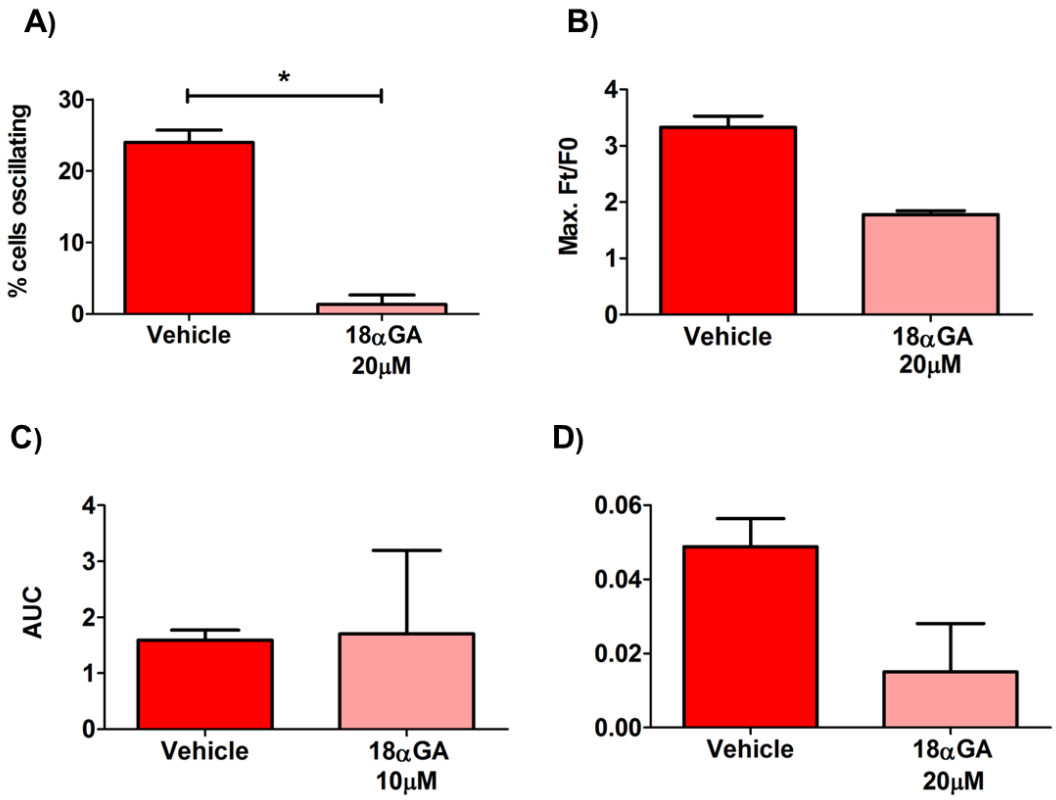

Figure 5.8 Inhibition of gap-junctional communication with 18α-Glycyrrhetinic acid (18αGA) substantially reduces the percentage of cells oscillating post-wounding.

Primary human keratinocytes cultured in 0.06mM $[Ca^{2+}]_o$ keratinocyte growth medium (MCDB 153) were loaded with Fluo4-AM calcium dye and during the de-esterification period of forty five minutes cells were pre-treated with 20μM 18αGA or control (DMSO). Keratinocytes were switched to 1.2mM $[Ca^{2+}]_o$ keratinocyte growth medium (MCDB 153) containing 20μM 18αGA and then wounded five minutes later. **A)** The percentage of cells that oscillated during the twenty minute imaging period, after the immediate wound-induced calcium flux, was calculated. Data shows mean ± SEM from three independent donors; N=3.*P=0.0467, Chi-square test. **B)** Maximum Ft/F0 reached during an individual oscillation. **C)** AUC of the calcium flux during an oscillation. **D)** Rate of rise of the calcium flux during an oscillation. Data shows mean ± SEM of 2 oscillations from 2 oscillating cells from three independent donors; n=2, (N=3). Statistical analysis was not conducted on B-D due to low sample number of oscillating cells.

indicates, the occurrences of the calcium oscillations are mediated by SOCE, it would follow that without the spread of the intercellular calcium wave post-wounding, calcium oscillations would not be detected. It was therefore hypothesised that cells wounded in the presence of 20μM 18αGA would not oscillate post-wounding. To test this hypothesis, primary human keratinocytes cultured in 0.06mM $[Ca^{2+}]_o$ keratinocyte growth medium (MCDB 153) were loaded with Fluo4-AM calcium dye and treated with 20μM 18αGA during the subsequent forty five minute de-esterification period. Keratinocytes were then wounded in supplemented keratinocyte growth medium (MCDB 153) to increase the calcium concentration to 1.2mM in the presence of 20μM 18αGA, prior to the calculation of the percentage of cells oscillating post-wounding in 1.2mM $[Ca^{2+}]_o$. As demonstrated in figure 5.8a, there were significantly less oscillating cells detected when wounding was performed following the blockade of gap-junctions compared to untreated cells (a chi-square test was conducted and this reduction was deemed significant, P=0.0467). Parameters of the intracellular calcium flux during individual oscillations were also assessed and shown by figures 5.8b-d. It was revealed that maximal Ft/F0 reached during a calcium oscillation as well as rate of rise of a calcium oscillation appeared to be reduced compared to untreated cells, whereas AUC of the intracellular calcium flux was unaltered with treatment. However, due to a low sample number of oscillating cells (n=2), statistical analysis was not conducted on this data.

These data thus highlight a requirement for the intercellular calcium wave post-wounding for the subsequent occurrence of calcium oscillations and therefore provides further evidence for the regulation of calcium oscillations by SOCE-mediated mechanisms.

5.3.6 Add-back of high calcium to keratinocytes wounded in low calcium results in calcium oscillations.

Data presented in section 5.3.2 showed that calcium oscillations were only detected when wounding was performed in 1.2mM $[Ca^{2+}]_o$, while no oscillations were observed when wounding in 0.06mM $[Ca^{2+}]_o$, therefore suggesting the presence of high calcium in the external environment is a prerequisite for oscillations. In order to confirm this point, an add-back protocol was adopted. In these experiments primary human keratinocytes cultured in 0.06mM $[Ca^{2+}]_o$ keratinocyte growth medium (MCDB153)

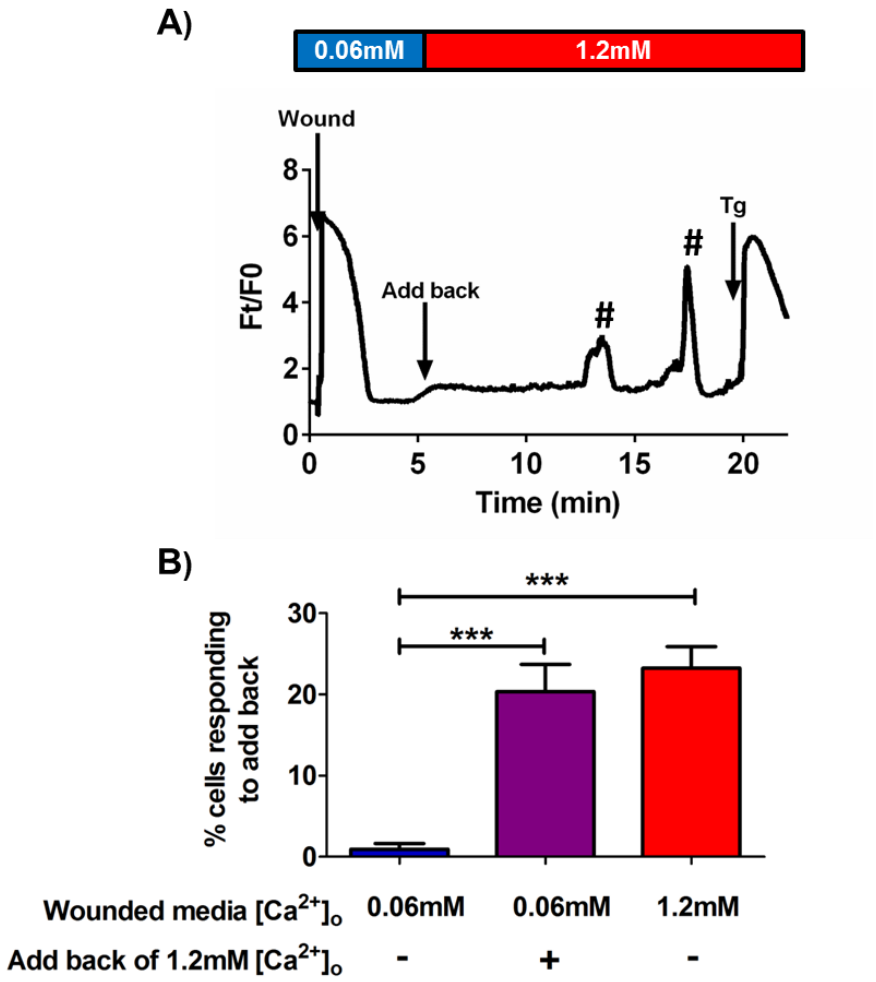

Figure 5.9 Add-back of 1.2mM $[Ca^{2+}]_o$ to wounded cells results in calcium oscillations suggesting that SOCE is involved.

Primary human keratinocytes cultured in 0.06mM $[Ca^{2+}]_o$ keratinocyte growth medium (MCDB 153) were loaded with Fluo4-AM calcium dye in 0.06mM keratinocyte growth medium (MCDB 153) and wounded. Five minutes post-wounding, MCDB 153 (adjusted to 6mM calcium) was added back to make a final extracellular calcium concentration of 1.2mM. **A)** Trace of a single representative cell post-wounding and calcium add-back. Time of wound and add-back are indicated by arrows. # mark the oscillations. Tg was added at the end of the experiment **B)** Percentage of cells that responded to calcium add-back with oscillations was calculated (purple) and compared to the percentage of oscillating cells observed when wounding in 0.06mM $[Ca^{2+}]_o$ with no add-back (blue) and when wounding in 1.2mM $[Ca^{2+}]_o$ with no add-back (red). 103 cells out of the 469 cells in the fields of view from seven independent donors responded to add-back. Data shows mean ± SEM; N=7. One-way ANOVA with Bonferroni post-hoc test (***P<0.001).

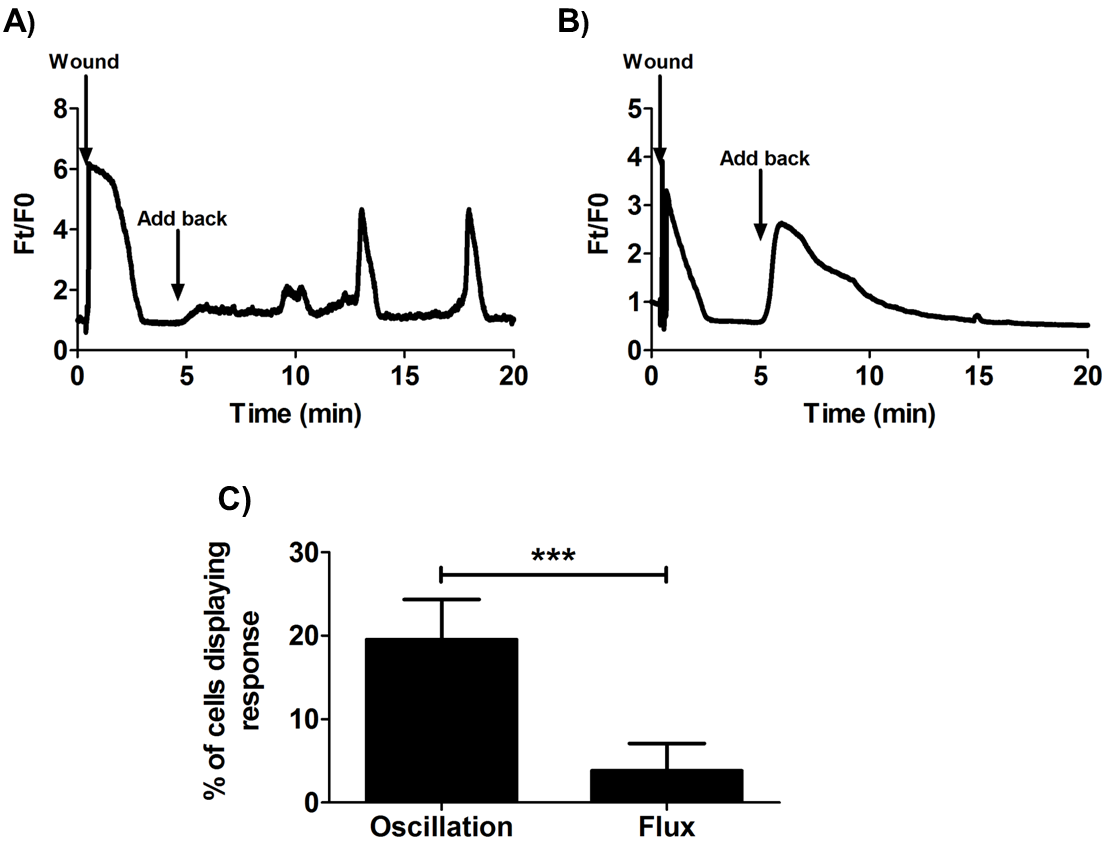

Figure 5.10 Two distinct patterns of calcium response are detected after add-back of high calcium.

Primary human keratinocytes cultured in 0.06mM $[Ca^{2+}]_o$ keratinocyte growth medium (MCDB 153) were loaded with Fluo4-AM calcium dye in 0.06mM keratinocyte growth medium (MCDB 153) and wounded. Five minutes post-wounding, MCDB 153 adjusted to 6mM calcium was added back to make a final extracellular concentration of 1.2mM. Keratinocyte response to add-back of high calcium was categorised into **A)** oscillations or **B)** prolonged flux (>3 minutes). Time of wound and add-back are highlighted by arrows. Traces are from one cell for each pattern and are representative of three independent donors. **C)** The percentage of cells responding to high calcium add-back with either oscillations or calcium flux was calculated. 8 cells out of the 353 cells in the field of view from five independent donors responded with a flux, whereas 80 out of the 353 cells responded with oscillations. ***P<0.0001, Chi-square test.

were loaded with Fluo4-AM calcium dye and wounded in 0.06mM $[Ca^{2+}]_o$ MCDB 153. Five minutes post-wounding, media adjusted to 6mM $[Ca^{2+}]_o$ was added back to make a final concentration of 1.2mM $[Ca^{2+}]_o$. As previously shown and discussed in section 3.3.1, wounding in 0.06mM $[Ca^{2+}]_o$ resulted in an $[Ca^{2+}]_i$ increase at the wound edge and subsequently in neighbouring cells, that appeared to travel as a wave. This chapter focuses on the intracellular calcium fluxes that occur after the add-back of high calcium rather than the wound-induced calcium wave. Post-add-back a sub-population of keratinocytes displayed an oscillatory behaviour, indicative that the presence of high calcium in the external media was driving the oscillations. The pattern of wound-induced intracellular calcium flux and subsequent oscillations following add-back is shown by the trace of a single cell in figure 5.9a. This cell is representative of three independent donors. Time points of wounding, calcium add-back and Tg are highlighted by arrows. Additionally, oscillations are marked by hash (#). The percentage of keratinocytes responding to high calcium add-back was calculated and compared to the percentage of cells that oscillated following wounding in 0.06mM $[Ca^{2+}]_o$ and the percentage of cells that oscillated following wounding in 1.2mM $[Ca^{2+}]_o$ (figure 5.9b). Cells were classified as positive (+) or negative (-) for add-back of 1.2mM $[Ca^{2+}]_o$; positive if they had been wounded in 0.06mM $[Ca^{2+}]_o$ and had 1.2mM $[Ca^{2+}]_o$ added back five minutes post-wounding or negative if they had been wounded in either 0.06mM or 1.2mM $[Ca^{2+}]_o$ and remained in the wounded media for the duration of the imaging period. High calcium add-back resulted in an increased percentage of responding cells compared to wounding in 0.06mM $[Ca^{2+}]_o$ without add-back of high calcium. One-way ANOVA statistical analysis was conducted with a Bonferroni post-hoc test to compare the percentage of responding cells between all treatments, demonstrating a significant increase in the percentage of responding cells with add-back compared to wounding in 0.06mM $[Ca^{2+}]_o$ alone ($P=0.001$). No statistical difference was reported between the percentage of responding cells following add-back and the percentage oscillating when wounding was conducted in 1.2mM $[Ca^{2+}]_o$ ($P>0.05$).

These data therefore provides further evidence that the presence of a high external calcium environment is required for the occurrence of calcium oscillations.

Interestingly, two forms of calcium responses were observed following add-back of high calcium to keratinocytes wounded in 0.06mM $[Ca^{2+}]_o$. The first was a typical

oscillation characterised by a full cycle of increase and decrease in fluorescence intensity that occurred after the initial $[Ca^{2+}]_i$ flux. An example of this can be seen in figure 5.10a. The other form of calcium response is shown if figure 5.10b. Upon add-back of high calcium these cells respond with a prolonged intracellular calcium flux. This flux was more sustained compared to the oscillations and occurred immediately upon add-back. Results demonstrated the majority of keratinocytes respond to add-back with an oscillatory pattern of signalling ($P<0.0001$, Chi-square test) (Figure 5.10c).

These results thus suggest calcium entry occurs via two distinct mechanisms, one dependent and one independently of SOCE.

5.3.7 The role of SOCE in add-back of calcium to wounded cells.

As alluded to previously (Section 5.3.3), SOCE inhibition reduced the percentage of cells oscillating post-wounding in 1.2mM $[Ca^{2+}]_o$, indicating that SOCE mechanisms were regulating the occurrence of the calcium oscillations. Add-back experiments further confirmed that a high external calcium environment was required for oscillations (Section 5.3.6). To further test the hypothesis that SOCE regulated calcium oscillations, the add-back protocol was performed on primary human keratinocytes were SOCE had been inhibited by 10µM GSK-7975A. In these experiments, primary human keratinocytes cultured in 0.06mM $[Ca^{2+}]_o$ keratinocyte growth medium (MCDB153) were loaded with Fluo4-AM calcium dye and during the subsequent forty five minute de-esterification period, cells were treated with 10µM GSK-7975A. Keratinocytes were then wounded in 0.06mM $[Ca^{2+}]_o$ keratinocyte growth medium (MCDB153) in the presence of 10µM GSK-7975A. Five minutes post-wounding, media adjusted to 6mM $[Ca^{2+}]_o$ was added back to make a final concentration of 1.2mM $[Ca^{2+}]_o$.

Initially, the percentage of cells responding to calcium add-back was calculated for both GSK-7975A treated cells and vehicle (DMSO) treated cells. Data shows that a significantly reduced number of keratinocytes responded to calcium add-back in GSK-7975A treated cells compared to vehicle ($P<0.0001$, Chi-square test) (figure 5.11a). The responding cells were then further categorised into those that responded with an oscillatory pattern of calcium signalling (figure 5.10a) or those that responded with a prolonged intracellular calcium flux immediately following add-back (figure 5.10b). SOCE inhibition reduced the percentage of cells oscillating following add-back;

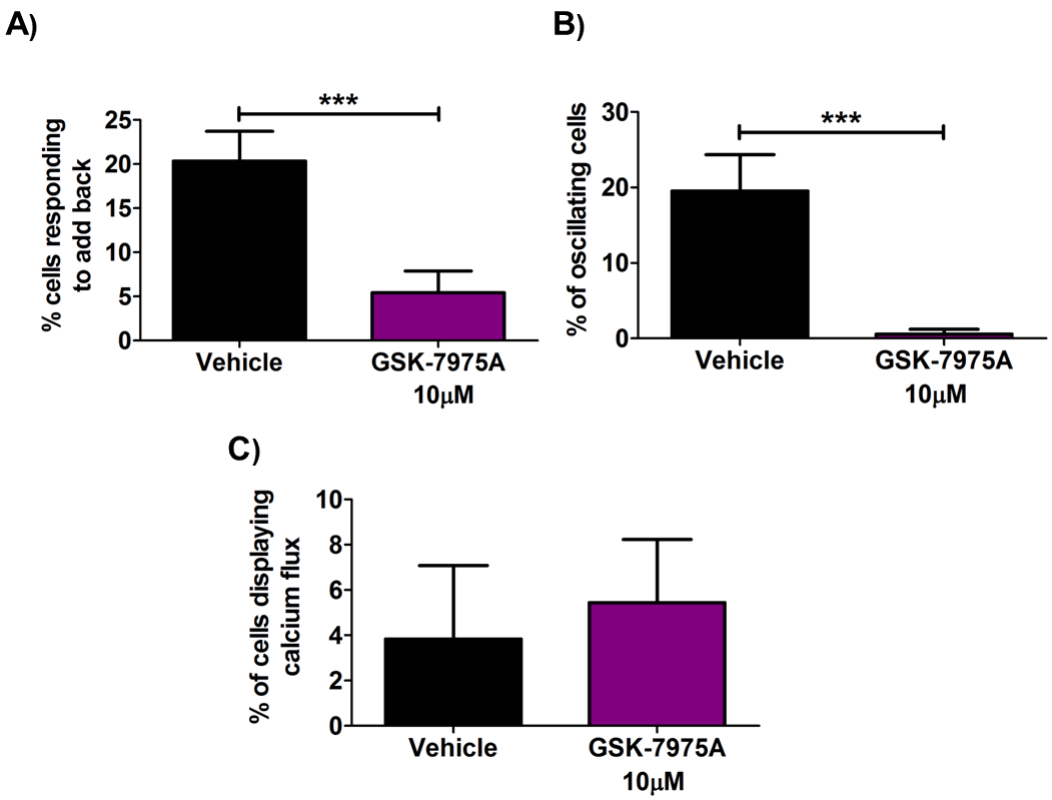

Figure 5.11 SOCE inhibition reduces the number of cells oscillating following high calcium add-back to wounded keratinocytes but does not affect cells showing prolonged calcium flux responses.

Primary human keratinocytes cultured in 0.06mM $[Ca^{2+}]_o$ keratinocyte growth medium (MCDB 153) were loaded with Fluo4-AM calcium dye and during the de-esterification period of forty five minutes, cells were pre-treated with 10μM GSK-7975A. Five minutes post-wounding, MCDB 153 (adjusted to 6mM calcium) was added back to make a final extracellular concentration of 1.2mM. **A)** The percentage of cells responding to high calcium add-back with a calcium signalling response was calculated. 18 cells out of 330 in the fields of view from six independent donors responded. ***P<0.0001, Chi-square test. **B)** The percentage of cells responding to calcium add-back by oscillating (as shown in figure 5.10a) was calculated. ***P<0.0001, Chi-square test. **C)** The percentage of cells responding to calcium add-back with a calcium flux (as shown in figure 5.10b) was calculated. P=0.1202 Chi-square test. Data shows mean ± SEM from three independent donors; N=6.

this was reported as statistically significantly different to vehicle by a chi-square test ($P<0.0001$) (figure 5.11b). Interestingly, figure 5.11c shows the percentage of cells responding to calcium add-back with an intracellular calcium flux was not affected with GSK-7975A treatment ($P=0.1202$, Chi-square test).

These results provide further supporting evidence that oscillations are mediated by calcium influx from the extracellular space via SOCE and also confirm that the two responses observed upon high calcium add-back (oscillatory and calcium flux) are regulated by different mechanisms; the oscillations via SOCE and the flux by non-SOCE calcium entry.

5.3.8 The role of gap-junctional communication in add-back of calcium to wounded cells.

Data reported in section 5.3.5 showed blocking gap-junctional communication with 18αGA significantly reduced the number of cells oscillating following wounding in 1.2mM $[Ca^{2+}]_o$, thus indicating the intercellular calcium wave is a pre-requisite for calcium oscillations. To further investigate this observation, the add-back protocol described above was applied to primary human keratinocytes treated with 20μM 18αGA during the forty five minute de-esterification period following Fluo4-AM calcium dye loading. Keratinocytes were then wounded in 0.06mM $[Ca^{2+}]_o$ keratinocyte growth medium (MCDB153) in the presence of 20μM 18αGA. Five minutes post-wounding, media adjusted to 6mM $[Ca^{2+}]_o$ was added back to make a final concentration of 1.2mM $[Ca^{2+}]_o$.

As shown by figure 5.12a demonstrates the percentage of cells responding to calcium add-back was calculated for both 18αGA treated cells and vehicle (DMSO) treated cells. Surprisingly, data showed that blocking gap-junctions resulted in a significantly increased number of cells responding to high calcium add-back compared to vehicle ($P<0.0001$, Chi-square test). Interestingly, none of the responding cells displayed an oscillatory pattern of calcium signalling following add-back, which was statistically different to vehicle ($P<0.0001$, Chi-square test) (figure 5.12b). Rather, all responding cells demonstrated a prolonged intracellular calcium flux immediately after add-back. The percentage of cells displaying this calcium flux was

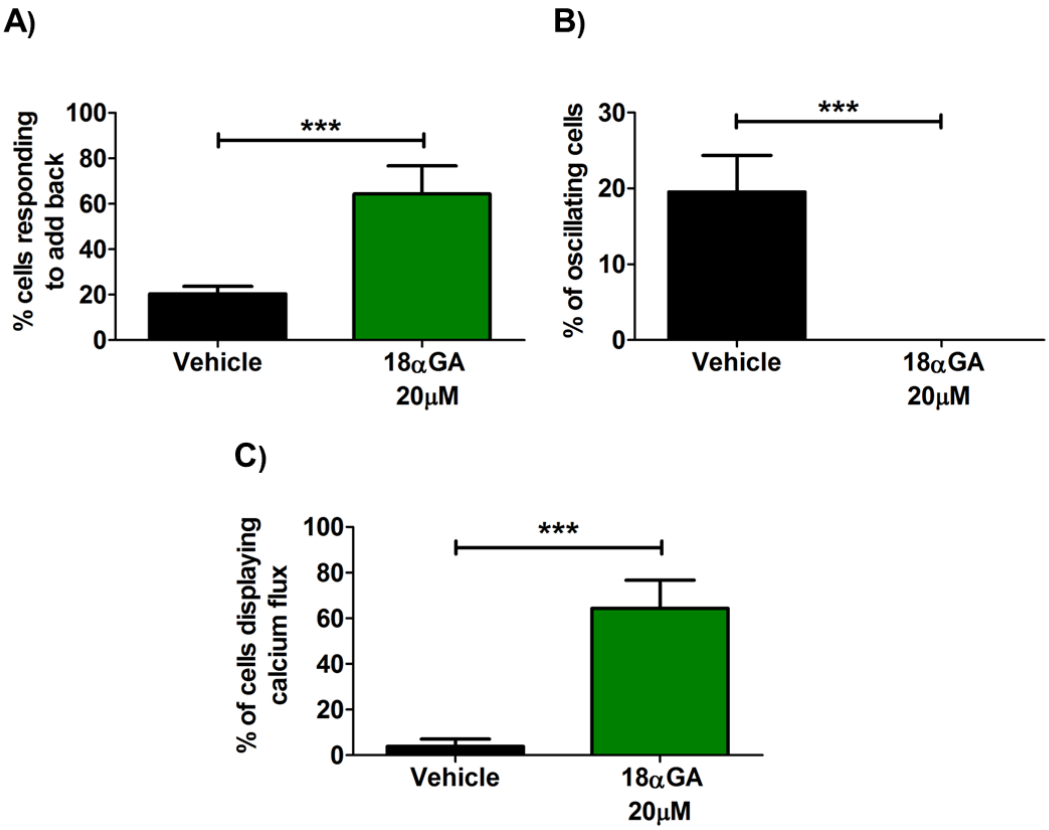

Figure 5.12 Inhibition of gap-junctional communication 18α-Glycyrrhetinic acid (18αGA) eliminates oscillations in wounded keratinocytes following high calcium add-back, but increases the percentage of cells responding with a prolonged calcium flux.

Primary human keratinocytes cultured in 0.06mM $[Ca^{2+}]_o$ keratinocyte growth medium (MCDB 153) were loaded with Fluo4-AM calcium dye and during the de-esterification period of forty five minutes cells were pre-treated with 20μM 18αGA. Five minutes post-wounding, MCDB 153 (adjusted to 6mM calcium) was added back to make a final extracellular concentration of 1.2mM. **A)** The percentage of cells responding to high calcium add-back with a calcium signalling response was calculated. ***P<0.0001, Chi-square test. 104 cells out of 207 in the fields of view from three independent donors responded **B)** The percentage of cells responding to calcium add-back by oscillating (as shown in figure 5.10a) was calculated. ***P<0.0001, Chi-square test. **C)** The percentage of cells responding to calcium add-back with a calcium flux (as shown in figure 5.10b) was calculated. ***P<0.0001, Chi-square test. Data shows mean ± SEM from three independent donors; N=3.

significantly increased compared to vehicle as revealed by a Chi-square test ($P<0.0001$) (figure 5.12c).

In summary, these data further suggest that the propagation of the calcium wave is important for the induction of oscillations. If the calcium wave is blocked at the point of wounding then oscillations are not observed, even in the presence of an increased external calcium environment.

5.4 Discussion.

5.4.1 The occurrence of wound-induced calcium oscillations post-wounding.

Data presented within this chapter highlight the novel observation of wound-induced calcium oscillations in a sub-population of primary human keratinocytes in a high external calcium environment, consistent with reports in other cell types following other stimuli. For example in bovine parathyroid cells, studies have shown oscillations only occurred in a high calcium environment (Miki *et al.*, 1995) while studies using neonatal human keratinocytes showed air exposure only induced calcium oscillations in the presence of extracellular calcium; oscillations were not detected when extracellular calcium was removed (M. Denda and Denda, 2007). However, to the best of our knowledge, wound-induced intracellular calcium oscillations have not been previously reported in keratinocytes. In the present studies in primary human keratinocytes, a small number of cells oscillated when wounding was performed in 0.06mM $[Ca^{2+}]_o$, but a significantly greater number of cells were observed to oscillate when cells were wounded in 1.2mM $[Ca^{2+}]_o$ but may have occurred due to the presence of the calcium sensing receptor (CaSR).

Calcium oscillations are a widely reported signalling behaviour within cells that are thought to occur in part to prevent cellular toxicity from excessive calcium flux (Dolmetsch *et al.*, 1998). Calcium oscillations are of particular interest following wounding as they have been shown to regulate transcriptional events that may lead to cell proliferation and migration (Berridge *et al.*, 2000). Berra-Romani *et al.* concluded from their investigations into injury-induced calcium oscillations in endothelial cells that the occurrence of these oscillations played a key role in healing damaged endothelium through the stimulation of proliferation and migration in cells distal to the wound edge. The authors concluded the oscillations were driven by both the sodium/calcium exchanger and IP_3-dependent mechanisms and also speculated this was mediated via oscillation-driven remodelling of the actin cytoskeleton and disassembly of focal adhesions (R. Berra-Romani *et al.*, 2012).

In the present study, the percentage of cells oscillating following scratch wounding in 1.2mM $[Ca^{2+}]_o$ was 23.3±2.6%. Interestingly, the reported number of cells that oscillate within a given cell population appears to be cell type and stimulus dependent. For

example, Razzell *et al.* made the observation that 40% of embryonic drosophila epidermal cells oscillated in response to wounding (Razzell *et al.*, 2013). In contrast, only 16% of rat aortic cells oscillated following EGF stimulation (Roberto Berra-Romani *et al.*, 2008). In closer agreement to data presented in this chapter, 22% of bovine parathyroid cells displayed spontaneous oscillations (Miki *et al.*, 1995). This number was 34% in primary glial cells in response to mechanical injury (Strahonja-Packard and Sanderson, 1999). In the present investigation there did not appear to be a relationship between the cells that oscillated and their location to the wound edge. This finding coincides with experiments conducted in endothelial cells that reported oscillatory cells were located both at the lesion edge and further back in the field of view (R. Berra-Romani *et al.*, 2012). However, contradictory evidence was presented by Strahonja-Packard *et al.* who reported that in primary glial cultures, initiation, frequency and duration of calcium oscillations were dependent on the distance of the cells from the wave origin (Strahonja-Packard and Sanderson, 1999)

Reasons as to why only a sub-population of keratinocytes responded to wounding with the observed oscillating pattern of signalling are unclear and experiments regarding this were beyond the scope of this project. However, possible explanations that could be explored in future include the possibility that the stage of the cell cycle that a particular cell is in can influence oscillatory behaviour or alternatively there is evidence to suggest that cells that oscillate are stem cell derived (M. Denda and Denda, 2007). Thus, Sauer *et al*. reported adipose tissue-derived mesenchymal stem cells (ASCs) displayed calcium oscillations; however, differentiated endothelial did not. This study postulated that the occurrence of oscillations could be associated with stem cell maintenance (Sauer *et al.*, 2011). Additionally, it has been suggested that ATP regulates the occurrence of calcium oscillations and that overexpression of purinergic receptors can increase oscillations (Praetorius and Leipziger, 2009). If purinergic receptor expression determines whether a cell displays an oscillatory pattern of calcium signalling, it could be speculated that keratinocyte stem cells express different receptors to non-stem cells. This may account for why not every cell in the present study oscillated. Investigations to determine defining characteristics of oscillating keratinocytes post-wounding would thus provide valuable insight.

Intriguingly, a study conducted in the immortalised keratinocyte cell line HaCaTs reported a high number of cells experiencing spontaneous oscillations. Moreover, scratch wounding diminished the number of cells oscillating (Ruzsnavszky *et al.*, 2013). This is in stark contrast to the data generated within this project where minimal spontaneous oscillations were observed in unwounded cells and wounding resulted in a significant increase. However, whilst HaCaTs are a keratinocyte cell line, it is known that significant differences exist which may account for the differences seen (Todd and Reynolds, 1998). Additionally, Ruzshavszky *et al.*, make no comment on the extracellular calcium conditions utilised within their investigation (Ruzsnavszky *et al.*, 2013). As shown herein, $[Ca^{2+}]_o$ is an important factor in regulating keratinocyte oscillations.

Detailed analysis comparing the intracellular calcium flux induced by wounding and the intracellular calcium flux during subsequent oscillations was conducted. Results showed that all three parameters; maximum Ft/F0, AUC and rate of rise were significantly reduced in oscillatory calcium patterns compared to wound-induced calcium fluxes (> three minutes). Studies conducted on endothelial cells reported a similar observation with a reduction in height of the calcium peak during an oscillation compared to the initial rise in intracellular calcium. However, this decrease was not revealed to be significant (R. Berra-Romani *et al.*, 2012).

5.4.2 Add-back experiments confirm requirement for a high external calcium environment for the occurrence of calcium oscillations.

Experiments involving the add-back of high calcium media following wounding in 0.06mM $[Ca^{2+}]_o$ provided important supporting data that a high external calcium environment was required for the occurrence of calcium oscillations. The percentage of cells oscillating after wounding in 0.06mM $[Ca^{2+}]_o$ with add-back of high calcium was comparable to the percentage observed when wounding in 1.2mM $[Ca^{2+}]_o$. To the best of our knowledge, this experimental design has not previously been reported in the context of wounding studies, however results robustly demonstrate this technique as a useful tool for dissecting the role of extracellular calcium in intracellular calcium responses. The effect of gap-junctional communication blockade and SOCE inhibition in the response of wounded keratinocytes to add-back of high calcium is discussed below.

5.4.3 The role of SOCE in wound-induced calcium oscillations.

The finding in the present study that calcium oscillations only occurred in 1.2mM $[Ca^{2+}]_o$ led to the hypothesis that SOCE mechanisms regulated the calcium influx resulting in the oscillations. This conclusion was also drawn from investigations conducted by Bird and co-workers in human embryonic kidney cells in response to the muscarinic agonist methacholine. The authors noted that calcium oscillations did not persist in a reduced extracellular calcium environment; therefore, suggesting that calcium entry across the PM played a role in the initiation or maintenance of the calcium oscillations. Additionally, an interesting point was made regarding differential regulation of oscillation initiation and oscillation maintenance. Factors regulating these distinct events were not assessed during this study; however, future investigations may provide insights into the role of oscillations in downstream signalling events during epidermal wound healing responses (Bird and Putney, 2005). The role of SOCE in mediating calcium oscillations in non-excitable cells has been suggested in a variety of cell types (Venkatachalam *et al.*, 2002). This was first demonstrated in HEK293 cells whereby both STIM1 and Orai1 genetic manipulation using RNAi resulted in a reduced frequency of calcium oscillations. However, these results were only detected in response to certain stimuli. As such, methacholine-induced calcium oscillations were diminished with STIM1 siRNA but arachidonic acid-induced calcium oscillations were unaffected (Wedel *et al.*, 2007). It has been shown in muscle cells that STIM1-dependent store-refilling was important in the maintenance of calcium oscillations in response to KCl (Stiber *et al.*, 2008). More recently, an additional role for STIM2 has emerged in the regulation of agonist-induced calcium oscillations. Thiel *et al.* concluded from their investigations in mast cells (RBL), T-cells (Jurkat) and HEK293 cells that in response to low levels of intracellular store depletion, STIM2 siRNA prevented oscillations, whereas in response to high levels of intracellular store depletion, STIM1 siRNA prevented oscillations. Thus highlighting different mechanisms of calcium entry in the initiation of calcium oscillations depending on store depletion rates (Thiel *et al.*, 2013). Akin to calcium wave propagation analysis, computational models have been utilised to facilitate understanding of pathways mediating intracellular calcium signalling. A model based on airway smooth muscle cells from lung slices also showed that SOCE was a major determinant of the frequency of agonist-induced calcium oscillations. The authors also linked effects of calcium entry to downstream events

regulating airway hyper-responsiveness, providing an interesting connection between SOCE-mediated calcium oscillations and disease states such as asthma and COPD (Croisier *et al.*, 2013).

These studies are in agreement with the findings reported within this project that treatment with GSK-7975A, to block SOCE, significantly reduced the percentage of cells oscillating post-wounding in 1.2mM $[Ca^{2+}]_{o.}$ However, it is of note that, whilst SOCE inhibition reduced the percentage of oscillating cells, it did not eliminate all oscillations, therefore indicating an additional non-SOCE mechanism. Interestingly, in the cells where oscillations persisted following blockade of SOCE, the oscillations were identical to those observed in untreated cells, with no differences observed in maximum Ft/F0, AUC or rate of rise. This suggests that SOCE initiates an "all or nothing" response in keratinocytes. Non-SOCE pathways have also been suggested in other systems such as HEK293. In these investigations, Wedel *et al*. demonstrated that TRPC3 over-expression supported calcium oscillations through non-SOCE mechanisms (Wedel *et al.*, 2007). Similarly, Bird *et al.* reported, that whilst SOCE supported oscillations, other channels mediating calcium entry were also able to regulate the oscillations (Bird et al., 2005). In contrast, it has previously been observed in C.*elegans* intestinal cells that SOCE has no role in calcium oscillations (Yan *et al.*, 2006).

Figure 3.19 shows that GSK-7975A effectively blocks the process of SOCE following treatment with thapsigargin. However, the data provided doesn't not fully determine the exact inhibition of SOCE with GSK-7975A treatment. This may explain why the percentage of cells oscillating significantly decreases when wounding in the presence of the SOCE inhibitor but in those cells that still oscillate, the parameters are similar to vehicle control.

Surprisingly, in untreated cells, two distinct forms of intracellular calcium signalling were observed in response to high calcium add-back a) oscillations and b) calcium flux. It was speculated that one of these was SOCE-mediated and one was non-SOCE. Wounding in 0.06mM $[Ca^{2+}]_o$ and adding back high calcium in the presence of GSK-7975A significantly reduced the percentage of cells responding to add-back, as was expected following from the results discussed above. Moreover, GSK-7975A treatment almost completely abrogated calcium oscillations following add-back, but, had no effect on the percentage of cells responding with a prolonged calcium flux. This provided

evidence that the oscillations triggered by add-back of high calcium were SOCE-medicated, whilst the more prolonged calcium flux was non-SOCE. In order to confirm this possibility, future experiments would need to be conducted whereby non-SOCE was inhibited both in combination with GSK-7975A treatment and alone. If the calcium flux was non-SOCE mediated, it would be expected that blockade would prevent the calcium flux detected in cells following add-back of high calcium but oscillations would persist. A similar approach was undertaken by Harper *et al.* who aimed to investigate the occurrence of two distinct calcium entry pathways in platelet calcium signalling. Utilising BTP-2, a specific SOCE inhibitor and LOE-908, a specific non-SOCE inhibitor, the authors highlighted differential roles for both calcium entry mechanisms and the regulation each had on downstream events (Harper and Poole, 2011).

As reviewed in section 3.4.5, $iPLA_2$ has been shown to mediate agonist-induced calcium entry in primary human keratinocytes and it was speculated that this may provide an alternative mechanism for SOCE which was STIM1/Orai1-independent (Ross *et al.*, 2008). In a similar manner, the contribution of $iPLA_2$ activation in response to store depletion in calcium oscillations could be assessed by utilising the pharmacological inhibitor BEL. Previous studies in astrocytes *in situ* showed a reduced number of spontaneous oscillations after inhibiting $iPLA_2$ activity and showed that BEL treatment prevented CPA-induced calcium influx (Singaravelu *et al.*, 2006). It would be of interest to co-treat keratinocytes with both BEL and GSK-7975A prior to wounding in order to assess the effect on the occurrence of calcium oscillations post-wounding.

Data generated within this study has shown that scratch wounding of primary human keratinocytes in a high external calcium environment results in calcium oscillations in a sub-population of cells. Additionally, treatment with the novel SOCE inhibitor, GSK-7975A resulted in a significant reduction in the percentage of cells that oscillated. Whilst this indicates that the process of SOCE is facilitating the occurrence of these calcium oscillations, it does not provide evidence for the source of the calcium initiating the oscillations. For example, the increase in cytosolic calcium observed during the intracellular calcium flux could be due to a plasma membrane oscillator i.e. pulsatile SOCE or a pulsatile release of calcium from intracellular stores such as the ER. In the case of the latter possibility the calcium store would be refilled between pulses by SOCE mechanisms (via translocation of STIM1 and oligomerisation with the calcium

pore Orai1, as described in figure 1.4). In both cases, inhibition of SOCE with GSK-7975A would prevent the oscillations from occurring. Therefore, it is important to note that the techniques utilised during this project do not discriminate between the possible mechanisms of calcium oscillations and future work is required to determine the source of the calcium during the oscillations. It is believed that calcium oscillations have an important role in transcription factor activation and downstream functional events and therefore a greater understanding on the mechanisms regulating these oscillations may be useful in the investigation of keratinocyte cell migration to close a wound.

5.4.4 The role of extracellular ATP in wound-induced calcium oscillations

This project has provided evidence that ATP is released from primary human keratinocytes in response to scratch wounding. It has also shown that the addition of ATP at the physiologically relevant wounded concentration triggered a calcium flux within a sub-population of cells and that wounding in the presence of the ATP scavenger, hexokinase, reduced intracellular calcium flux. Therefore, it was of interest to analysis the effect of extracellular ATP removal on the occurrence of oscillations. Results showed that not only did hexokinase treatment significantly reduce the percentage of cells oscillating, the small number of cells where oscillations persistent also displayed altered oscillatory parameters (maximum Ft/F0, AUC and rate of rise). These data thus imply that ATP released following wounding has a role in downstream calcium oscillations. In agreement with this Denda and Denda demonstrated that, in response to air exposure, neonatal human keratinocytes displayed calcium oscillations that were regulated by ATP. The authors confirmed this by treatment with the purinergic receptor antagonist suramin. Additionally, hexokinase treatment to remove extracellular ATP also abolished spontaneous calcium oscillations in hMSCs (Kawano *et al.*, 2006). To further confirm the role of released ATP in calcium oscillations post-wounding, purinergic receptors could be blocked using suramin. If ATP was mediating the oscillations, it would be expected that suramin treatment would result in a similar reduction in percentage of cells oscillating to that seen when wounding in the presence of hexokinase. It has also been demonstrated in other epithelial cells that intracellular calcium oscillations were induced by ATP (J. H. Evans and Sanderson, 1999). However, the calcium changes seen in response to air exposure in neonatal keratinocytes were only observed in pre-confluent cells, no change was reported in post-

confluent cells. This result may have arisen due to alterations in purinergic receptor expression in confluent cells or the proximity of the cells may trigger a switch to gap-junctional communication as a dominant signalling mechanism; the authors do not provide further details.

Unfortunately, due to time restraints within this project calcium add-back experiments were not conducted in the presence of hexokinase. However, following on from the results obtained, it would be expected that removal of extracellular ATP would reduce the percentage of cells responding to high calcium add-back.

In addition to this, treatment with both 18αGA and hexokinase will provide confirmation of the role of both the intercellular pathway and extracellular purinergic pathway in regulation of calcium oscillations. Within this project each pathway was investigated individual and provided interesting results, however, blockade of both pathways would highlight any signalling independent of both gap-junctions and ATP.

It was shown in figure 5.9 that calcium oscillations were observed when high calcium was added to cells wounded in low calcium 5 minutes following wounding. From this data, it was concluded that a high external calcium environment is required for calcium oscillations. Interestingly, these results may also suggest that calcium oscillations post-wounding are independent of ATP, as the calcium oscillations were promoted solely by the addition of high calcium. There are two mechanisms by which ATP can activate an intracellular calcium flux. Firstly, wound-induced ATP can activate the GPCR P2YR class of purinergic receptors. This then results in the release of calcium from the ER by PLC activation and the generation of IP_3. Add back experiment results indicate that this pathway may not be involved in the generation of calcium oscillations post-wounding as oscillations were only detected in high external calcium conditions, suggesting that this was the determining factor in oscillation promotion and not ATP. However, the second mechanism through which ATP initiates intracellular calcium flux would be dependent on the presence of calcium in the extracellular space. P2XR are ligand-gated ion channels that result in ATP-mediated calcium entry. Figure 4.7 demonstrated that wounding keratinocytes resulted in the release of ATP into the media which was detectable above unwounded baseline for at least 45 minutes following wounding. Therefore, it is possible that when wounding low calcium, the ATP released into the media had no downstream effects because the external calcium concentration is too low.

However, upon add back of high calcium, five minutes post-wounding (a time point where high levels of ATP were detected in the media), the external calcium concentration increases and therefore calcium ions enter the cell via ATP-gated ion channels resulting in a calcium oscillation. Unfortunately, data collected during this study does not provide enough evidence to delineate between these mechanisms and future work will determine the contribution of P2XR and P2YR in calcium signalling post-wounding. This should shed light as to whether ATP is necessary for the promotion of calcium oscillations, or whether the presence of high calcium following add back is sufficient.

5.4.5 The role of gap-junctional communication in wound-induced calcium oscillations.

Wounding keratinocytes after gap-junctional communication blockade prevented the spread of the calcium wave back from the wound edge across the cell population. This result demonstrated the essential role for intercellular communications in the propagation of the calcium wave. It was additionally shown that 18αGA treatment completely prevented oscillations. This observation was in accordance with Berra-Romani *et al.* who demonstrated gap-junction inhibition with 18βGA stopped calcium oscillations in endothelial cells in response to mechanical injury (R. Berra-Romani *et al.*, 2012). Similarly, in pancreatic acinar cells, inhibiting gap-junctions prevented all further calcium signalling (Deutsch *et al.*, 1995). Additionally, one study investigating neuron-astrocyte co-cultures showed that blocking gap-junctions with octanol and halothane reduced calcium oscillations in a dose-dependent manner. However, within the same cells, an alternative inhibitor, lindane, increased the amplitude and frequency of calcium oscillations (Fujita *et al.*, 1998). In contrast, previous studies in inferior olive cells showed that blocking gap-junctions with 18βGA reduced calcium wave propagation but did not completely abolish calcium oscillations (Leznik and Llinas, 2005). Combined with data generated within this project, these studies are highly suggestive that in order for oscillations to occur post-wounding, the wound has to induce an intercellular calcium wave. When this is prevented, such as is the case with treatment with 18αGA, no oscillations are seen. These data suggest that the calcium entry regulating the calcium oscillations is in response to store depletion.

It was of therefore of interest to study the calcium signalling response following add-back of high calcium when wounding had been conducted in the presence of 18αGA. Upon add-back, keratinocytes still displayed a calcium response; however this was not in the form of oscillations, as seen in untreated cells. Surprisingly, the percentage of cells responding to high calcium add-back was significantly increased compared to untreated cells. However, cells only demonstrated one prolonged calcium flux during the imaging period, rather than short repetitive calcium spikes seen in other experiments. Without the depletion of internal calcium stores caused by the initial injury it is interesting that a calcium flux was detected upon add-back. Further experiments are required in order to determine the mechanisms regulating this observation. It has been shown in this project that ATP is released post-wounding and importantly that connexins/pannexins do not regulate this release. Therefore, it could be postulated that ATP released following wounding is having a downstream effect, only highlighted upon high calcium add-back. Co-treatment with both hexokinase to remove extracellular ATP and 18αGA to block gap-junctional communication would provide evidence as to the role ATP is having in this unexpected calcium flux. If ATP was the mediating factor, it would be expected that this combined treatment would abolish all intracellular calcium signalling response upon add-back of high calcium. Blockade of P2XR would have a similar effect.

In untreated keratinocytes, the calcium oscillations were of short duration that returned to baseline between subsequent oscillations and occurred after the initial calcium wave. In 18αGA-treated cells, the oscillations detected were more gradual and occurred in the absence of a wound-induced calcium wave. Therefore, it can be speculated that the intercellular calcium wave that spreads from the wound edge back across the cell population, provides a calcium buffer to cells to provide a tight regulation of intracellular calcium signalling to prevent toxicity. Therefore, any further calcium fluxes are in the form of oscillations of a short duration. In other words, the calcium wave primes the cells. It has been demonstrated that IP_3R are also regulated by calcium ions in a biphasic manner; a moderate increase in intracellular calcium positively regulates IP_3R responses to IP_3 and cytosolic calcium is elevated. However, when $[Ca^{2+}]_i$ is higher, the effect of calcium on IP_3R is inhibitory. This is believed to occur either through direct binding of calcium ions to IP_3R on the ER or through activation of an associated protein such as CaM (Taylor and Tovey, 2010). To this end, increases in

cytosolic calcium initiate calcium-mediated inhibition of IP_3R to contribute to the termination of intracellular calcium signals. In the absence of the calcium wave to "prime" the cells in this manner, cells may respond to high calcium add-back with the increased and prolonged calcium flux observed in the presented data. Whilst this theory requires further confirmation it suggests a highly interesting intracellular protective mechanism to prevent sustained levels cytosolic calcium which has been shown to induce apoptosis.

Alternatively, a negative feedback loop has recently emerged in blowfly salivary glands. It was demonstrated that calcineurin activation acted as a negative regulator of IP_3-mediated calcium release from the ER. This was shown by CsA potentiating the 5-HT-evoked calcium signal which is known to act through cAMP/PKA activation of IP_3R. The increased calcium signal observed in the presence of calcineurin inhibition was taken to show that calcineurin and PKA may act antagonistically and calcineurin prevents further calcium release (Heindorff and Baumann, 2014). Leading on from the findings within this project, investigation of a negative feedback loop initiated by the wound-induced intercellular calcium wave would be important. Further, this may explain the appearance of an increased calcium flux upon add-back of high calcium to cells wounding in the presence of 18αGA.

5.4.6 The relevance of wound-induced oscillations.

As described previously, it is accepted that calcium oscillations regulate downstream transcriptional activation whilst preventing sustained elevations in intracellular calcium which could result in the initiation of apoptosis. Understanding the pathways mediating the occurrence of the calcium oscillations following wounding, might lead to novel therapies targetted to the promotion of reepithelialisation in the treatment of both acute and chronic wounding.

5.5 Conclusions.

- Calcium oscillations are supported by calcium influx from the extracellular space as confirmed by oscillations only occurring in 1.2mM $[Ca^{2+}]_o$.

- Two distinct calcium entry mechanisms occur following add-back of high calcium to cells wounded in 0.06mM $[Ca^{2+}]_o$; one resulting in calcium oscillations and one resulting in a more prolonged calcium flux.

- Calcium entry mediated by SOCE regulates the majority of calcium oscillations following wounding in 1.2mM $[Ca^{2+}]_o$, however, non-SOCE also occurs.

- Oscillations seen following add-back are a result of SOCE, whereas calcium flux is a result of non-SOCE as shown by GSK-7975A treatment eliminating oscillations but not affecting calcium flux.

- The wound-induced intercellular calcium wave is required for downstream calcium oscillations; no oscillations were detected with 18αGA treatment to block gap-junctional communication.

- ATP released from keratinocytes following wounding regulates the calcium oscillations.

Chapter 6.

Transcriptional and Functional Wound Healing Responses

6 Chapter 6. Transcriptional and Functional Epidermal Wound Healing Responses.

6.1 Introduction.

6.1.1 NFAT signalling in wound healing.

It is known that NFAT1-4 is expressed in keratinocytes. However, less attention has been given to the exact role of these in mediating migration, proliferation and differentiation required for epidermal wound healing responses. Jans *et al.*, demonstrated a relationship between calcium flux and NFAT activation in primary human keratinocytes. This study indicated that lysophosphatidic acid (LPA) triggered intracellular calcium signalling which led to calcineurin-mediated NFAT2 activation. This signalling pathway subsequently modulated keratinocyte migration (Ralph Jans *et al.*, 2013). Whilst not directly analysing NFAT activation post-wounding, the authors established a link between conditions mimicking wounding (LPA activation in a high external calcium environment), calcium flux and down-stream NFAT activation, therefore suggesting a potential role for NFAT activation in cutaneous wound healing. Additionally, in a macrophage cell line, it was shown that wounding caused an increase in nuclear NFAT2. Genetic silencing of NFAT2 or pharmacological inhibition with CsA resulted in decreased wound closure rates (Chow *et al.*, 2008). In contrast, it has been demonstrated that treatment of endothelial cells with the synthetic peptide VIVIT had only a small effect on wound closure rates. VIVIT specifically inhibits the calcineurin/NFAT interaction and therefore is thought to be a more specific inhibitor of NFAT signalling rather than calcineurin-mediated signalling which has alternative downstream effects (Yu *et al.*, 2006). These contradictory studies illustrate a diverse cell-specific role for NFAT activation post-wounding. Calcium-dependent NFAT activation post-wounding of keratinocytes and the subsequent proliferative and migratory responses remain unreported.

It is known that some organisms have regenerative capabilities. It has recently been shown that zebra fish fin regeneration post-amputation, is regulated by calcineurin. When cell proliferation is high, calcineurin activity is low and then as proliferation ceases, calcineurin activity increases. Inhibition of calcineurin by CsA, resulted in prolonged regrowth of the fin beyond the original dimensions. Although humans no not

have this regenerative ability, it highlights the role calcineurin plays post-injury (Kujawski *et al.*, 2014).

6.1.2 NFAT transcriptional regulation by gap-junctions.

It was originally thought that connexins modulated cell growth solely through the passage of small molecules through gap-junctions. This idea has since been contested with various studies showing that Cx43 can regulate cell growth independently of gap-junction formation. This hypothesis arose from observations that, despite having no functional effect on gap-junction communication, transfection of human Cx43 into glioblastoma cells resulted in the inhibition of cell growth in these cells (Huang *et al.*, 1998). Similarly, Moorby *et al.* demonstrated Cx43 has an inhibitory effect on the cell growth of two cell lines in the absence of gap-junction formation (Moorby and Patel, 2001). At present, there is a lack of knowledge regarding the relative contribution to each function to cellular signalling. Further investigations should provide insight into this area. Interestingly, it is thought that Cx43 influences expression of over 300 genes (Spray and Iacobas, 2007), although the mechanisms regulating connexin-induced transcriptional activation remains poorly understood, research to date suggests that mechanisms vary between different transcription factors. For example, Cx43 has been reported to interact with β-catenin at the cell membrane, preventing its nuclear translocation and therefore blocking its effects on gene expression (Ai *et al.*, 2000). Further evidence from gene array analysis on connexin-deficient mice has revealed marked alternations in gene expression. This led to the hypothesis that gap-junctions may be "hubs" in gene expression networks. The phenotypic changes observed in connexin mutants may be attributed to these changes rather than alterations in gap-junction communication. Importantly, activation of certain transcription factors is known to be a downstream effect of secondary messenger signalling such as calcium and IP_3 as demonstrated by Stains *et al*. The authors speculated that Cx43 allowed propagation of secondary messengers between cells which in turn activated ERK/PI3K cascade. With the aid of the trans-activator Sp1, ERK was converged to the promoter region to drive transcription (Stains and Civitelli, 2005). Reciprocally, Kumai *et al.* illustrated through $Cx45^{-/-}$ mice embryos, that Cx45 was important in the activation of NFATc1. In wild-type embryos NFATc1 was nuclear whereas in the knockout embryos

NFATc1 was cytoplasmic implicating Cx45 as an upstream regulator of NFAT activation. It was established that NFAT activation occurred as a result of increased cytoplasmic calcium and the subsequent activation of SOCE. The authors postulated that Cx45 was required for the rise in intracellular calcium and this was blocked in $Cx45^{-/-}$ embryos causing the observed cytoplasmic retention of NFATc1. Conversely, in wild-type embryos, calcium was able to propagate through the cell population and therefore promote the nuclear localisation of NFATc1. This study highlights the requirement of calcium signalling through gap-junctions to induce NFAT transcriptional events (Kumai *et al.*, 2000).

6.1.3 ATP and transcription factor activation.

In addition to ATP inducing calcium wave propagation and oscillations, it has been shown to be involved in transcription factor activation. Of particular interest within this project is the transcription factor NFAT. Studies directly investigating ATP and NFAT are limited. Nevertheless, it has been shown in human bone marrow-derived mesenchymal stem cells (hMSCs) that gap-junction mediated increases in extracellular ATP results in spontaneous calcium oscillations and downstream nuclear translocation of NFAT. Pharmacological inhibition of ATP release was shown to prevent induction of the calcium oscillations and block nuclear translocation of NFAT. Therefore suggesting a link between purinergic signalling, calcium oscillations and NFAT activation. However, when these stem cells differentiated into adipocytes both spontaneous oscillations and NFAT activation ceased. Thus highlighting a potential physiological mechanism involved in stem cell differentiation and proliferation (Kawano *et al.*, 2006). Similar results were seen in microglial cells; Ferrari *et al.* observed that ATP was able to activate both NFAT and NFκB. However, kinetics involved were different between the two transcription factors. Post-ATP treatment, nuclear translocation of NFAT occurred much quicker than NFκB. These results suggest that, in the nervous system, ATP is involved in the modulation of early inflammatory responses (Ferrari *et al.*, 1999). Glibenclamide, a drug used to treat type-2 diabetes, has been shown to have a wide range of anti-inflammatory effects. Additionally, it was shown by Li *et al.* that Glibenclamide reduced the ATP-induced calcium wave in macrophages and reduced the phosphorylation of the NFκB subunit p65 (D. L. Li *et al.*, 2014). Few studies have investigated ATP release from keratinocytes post-wounding and the downstream

consequences of this, for example whether transcription factor activation is observed in a similar manner to that reported in other cell types.

In summary, it is widely known that NFAT is activated by increases in cytosolic calcium concentrations through both calmodulin and calcineurin activation. Furthermore, these increases regulate processes such as proliferation, differentiation and migration which are also known to be key events in wound healing. Although in primary human keratinocytes the link between intracellular calcium increases as a result of wounding and NFAT is yet to be fully delineated. Chapter 4 defined the relative contribution of both purinergic signalling and intercellular signalling mediated by gap-junctions in the spread of the calcium wave back from the wound edge. With both signalling pathways having a significant effect on specific characteristics of the wave, their influence on NFAT transcriptional activity was of interest.

6.2 Specific aims.

- To investigate the activation of NFAT induced by wounding in 0.06mM $[Ca^{2+}]_o$ and 1.2mM $[Ca^{2+}]_o$ to analyse the contribution of extracellular calcium in wound-induced NFAT activation.

- To determine the contribution of SOCE, gap-junctional communication and extracellular ATP to wound-induced NFAT activation.

- To investigate the effect of increased extracellular calcium on keratinocyte migration and wound closure.

- To determine the contribution of SOCE, gap-junctional communication and extracellular ATP in keratinocyte migration and wound closure.

6.3 Results.

6.3.1 NFAT activity is increased post-wounding in a calcium dependent manner.

It is known that increases in cytosolic calcium results in calcium ions binding to calmodulin which in turn activates the serine phosphatase calcineurin. Calcineurin dephosphorylates NFAT, exposing its nuclear localisation domain resulting in NFAT translocation to the nucleus (Hogan *et al.*, 2003). Results within this project have demonstrated that wounding causes an increase in $[Ca^{2+}]_i$ (section 3.3.1). Therefore, it was hypothesised that wounding would activate NFAT in primary human keratinocytes. Furthermore, previous results have highlighted significant differences between wounding in 0.06mM $[Ca^{2+}]_o$ and wounding in 1.2mM $[Ca^{2+}]_o$ at the level of a) the calcium wave induced by wounding (section 3.3.2) and b) oscillatory behaviour of a sub-population of keratinocytes following wounding (section 5.3.2). It was postulated that NFAT activation post-wounding occurred in a calcium-dependent manner.

To assess wound-induced NFAT activation, primary human keratinocytes were transfected with two luciferase constructs; a NFAT firefly and a renilla. Renilla luciferase was used as an internal control. When keratinocytes had reached a complete monolayer, cells were exposed to keratinocyte growth media (MCDB 153) which had a calcium concentration of either 0.06mM or 1.2mM $[Ca^{2+}]_o$ for five minutes prior to cross-hatch wounding with a 200µL pipette tip. At specified time points post-wounding, cells were lysed and luciferase activity measured using a luminometer. From figure 6.1a it can be seen that wounding in 0.06mM $[Ca^{2+}]_o$ resulted in a maximal increase in NFAT activity six hours post-wounding, which then decreased over forty eight hours. Although, it is of note that the maximum fold increase over baseline was only 1.39±0.07. In contrast, wounding in 1.2mM $[Ca^{2+}]_o$ resulted in a steady increase in NFAT activation, which was maximal at twenty four hours post-wounding with a fold increase of 2.96±0.33. NFAT then decreased to baseline by forty eight hours post-wounding. Although statistical analysis was not conducted due to low sample number it can be suggested that wounding in high calcium conditions results in increased NFAT luciferase compared to low calcium conditions. Moreover, the optimal timepoint to further investigate these responses is twenty four hours post-wounding.

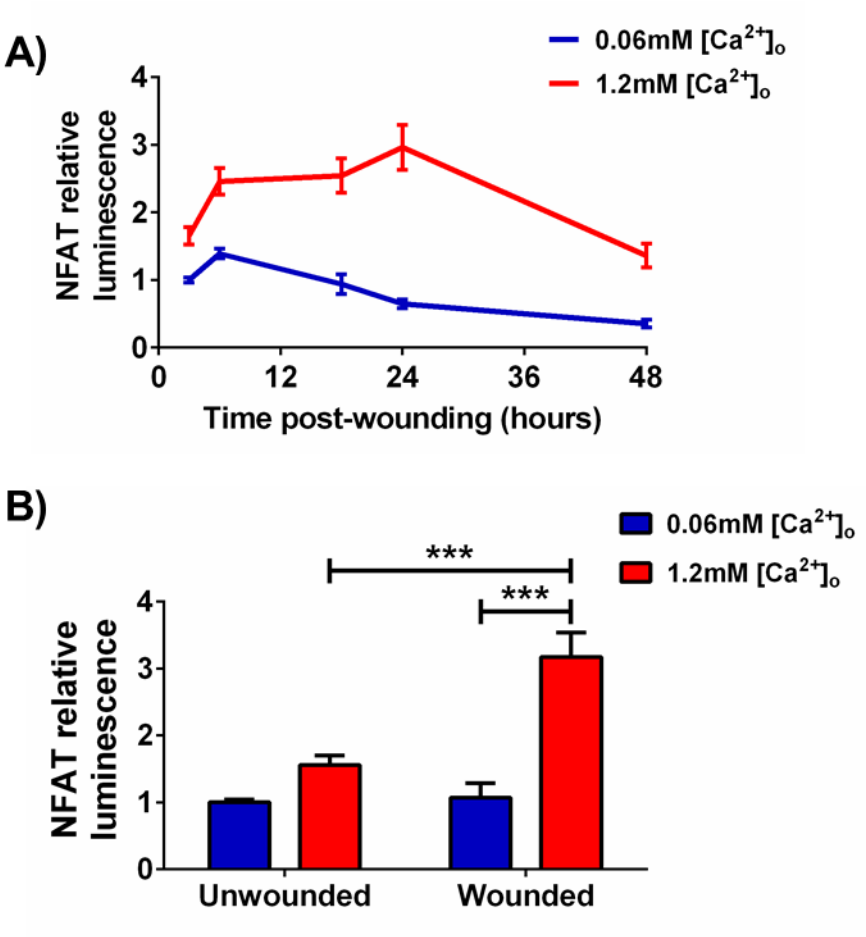

Figure 6.1 Wounding of human keratinocytes in 1.2mM $[Ca^{2+}]_o$ results in NFAT activation.

Primary human keratinocytes cultured in 0.06mM $[Ca^{2+}]_o$ keratinocyte growth medium (MCDB 153) were transfected with NFAT firefly and renilla luciferase constructs as described in materials and methods and cultured until 100% confluent. Medium was replaced with either 0.06mM or 1.2mM $[Ca^{2+}]_o$ keratinocyte growth media (MCDB 153) for five minutes prior to cross-hatch wounding. **A)** At specified time points post-wounding cells were lysed and luciferase activity measured using a luminometer. Data shows mean ± SEM from one donor in triplicate. Statistical analysis was not conducted due to low sample number. **B)** Twenty four hours post-wounding cells were lysed and luciferase activity measured using a luminometer. Results are expressed as mean firefly/renilla ratio normalised to unwounded 0.06mM $[Ca^{2+}]_o$. Graphs show mean ± SEM from 47 experiments from 17 independent donors; (n=47), N=17. Two-way ANOVA with Bonferroni post-hoc was conducted ($F(1,184)=14.04$, $P=0.0002$, *** $P<0.001$).

To further investigate these observations, primary human keratinocytes were transfected with NFAT firefly and renilla luciferase constructs and lysed twenty four hours post-wounding, a previously determined appropriate time point. Akin to preceding data wounding in 0.06mM $[Ca^{2+}]_o$ did not result in NFAT activation, with an average fold increase of 1.06±0.21 observed. However, wounding in the presence of high external calcium resulted in a 3.17±0.36 fold increase. Unwounded control experiments were conducted whereby keratinocytes were cultured in 0.06mM or 1.2mM $[Ca^{2+}]_o$ for twenty four hours but remained unwounded. Unwounded cells exposed to 1.2mM $[Ca^{2+}]_o$ showed a small increase in NFAT activation compared to unwounded cells in 0.06mM $[Ca^{2+}]_o$, with a 1.55±0.14 fold increase. This increase was not as large as that caused by wounding in 1.2mM $[Ca^{2+}]_o$. Statistical analysis was conducted using a two-way ANOVA and results showed that wounding significantly effected NFAT activation ($F(1,184)=14.04$, $P=0.0002$). Similarly, external calcium had a significant effect ($F(1,184)=34.97$, $P<0.0001$). A Bonferroni post-hoc test revealed that NFAT activation in keratinocytes wounded in 1.2mM $[Ca^{2+}]_o$ was significantly increased compared to both unwounded keratinocytes in 1.2mM $[Ca^{2+}]_o$ and wounded cells in 0.06mM $[Ca^{2+}]_o$ (*** $P< 0.001$). There was no significant difference reported between unwounded cells exposed to 0.06mM or 1.2mM $[Ca^{2+}]_o$ ($P>0.05$) (figure 6.1b).

Combined, these data suggest that a high external calcium environment and thus calcium influx from the extracellular space, is required for NFAT activation post-wounding. Importantly, the presence of 1.2mM $[Ca^{2+}]_o$ alone does not result in an increase and therefore it can be concluded that the increase detected is a direct result of wounding.

6.3.2 The role of SOCE in NFAT activation post-wounding.

Aforementioned results demonstrated that wounding in a high calcium environment resulted in NFAT activation whilst wounding in a low calcium environment did not. Therefore, it can be suggested that a calcium entry mechanism mediates NFAT activation. To determine whether this influx was a result of SOCE, cells were wounded in the presence of the novel SOCE inhibitor GSK7975A or vehicle (DMSO). Section 3.3.3 confirmed that GSK-7975A effectively blocked SOCE at a concentration of 10μM. In order to assess the effects of SOCE blockade on NFAT activation, primary human keratinocytes were transfected with NFAT firefly and renilla luciferase

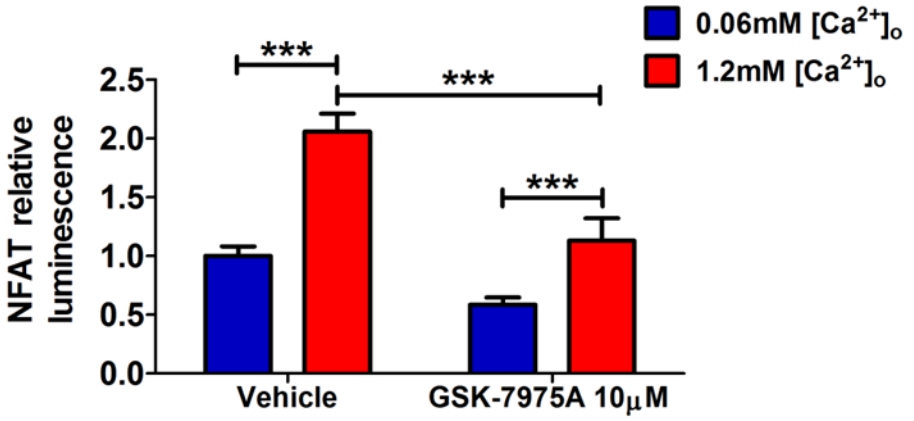

Figure 6.2 Inhibition of SOCE with GSK-7975A decreases wound-induced NFAT activation.

Primary human keratinocytes cultured in 0.06mM $[Ca^{2+}]_o$ keratinocyte growth medium (MCDB 153) were transfected with NFAT firefly and renilla luciferase constructs as described in materials and methods and cultured until 100% confluent. Medium was replaced with either 0.06mM or 1.2mM $[Ca^{2+}]_o$ keratinocyte growth media (MCDB 153) with 10μM GSK-7975A or 1:1000 vehicle (DMSO) for one hour prior to cross-hatch wounding. Twenty four hours post-wounding cells were lysed and luciferase activity measured using a luminometer. Results are expressed as mean firefly/renilla ratio normalised to unwounded 0.06mM $[Ca^{2+}]_o$. Graphs show mean ± SEM from 19 experiments from 7 independent donors; (n=19), N=7. Two-way ANOVA with Bonferroni post-hoc ($F(1,32)=25.88$, $P<0.0001$. *** $P<0.001$

constructs. Cells were grown to confluency and media was replaced with keratinocyte growth media with a calcium concentration of either 0.06mM or 1.2mM supplemented with 10μM GSK-7975A or vehicle (DMSO) for one hour prior to cross-hatch wounding. Twenty four hours post-wounding, cells were lysed and luciferase activity measured using a luminometer. Figure 6.2 shows that, in vehicle treated cells, wounding in 1.2mM $[Ca^{2+}]_o$ resulted in increased NFAT compared to wounding in 0.06mM $[Ca^{2+}]_o$, with cells showing an 2.05±0.15 fold increase. Wounding in the presence of GSK-7975A in 1.2mM $[Ca^{2+}]_o$ did not result in an increase compared to basal levels, with only a 1.12±0.19 fold change being detected. A two-way ANOVA was conducted and results revealed that GSK-7975A treatment had a significant effect on NFAT activation ($F(1,32)=25.88$, $P<0.0001$). Furthermore, a Bonferroni post-hoc test showed that a) vehicle treated cells in 1.2mM $[Ca^{2+}]_o$ had a significant increase in NFAT activation compared to vehicle treated cells wounded in 0.06mM $[Ca^{2+}]_o$ b) GSK-7975A treated cells in 1.2mM $[Ca^{2+}]_o$ had a significant increase in NFAT activation compared to GSK-7975A treated cells wounded in 0.06mM $[Ca^{2+}]_o$ and C) GSK-7975A treatment in 1.2mM $[Ca^{2+}]_o$ significantly reduced NFAT compared to vehicle treated cells in 1.2mM $[Ca^{2+}]_o$ (*** $P<0.001$).

These results indicate that calcium entry through SOCE mechanisms mediates wound-induced NFAT activation post-wounding. Further suggesting that wounding triggers SOCE through depletion of the intracellular calcium stores and it is this subsequent influx of calcium that is driving NFAT transcriptional activation, rather than passive calcium entry. Thus supporting data showing that exposure to a high external calcium environment alone i.e without mechanical stimuli is not sufficient to drive transcription.

6.3.3 NFκB transcriptional activity is not induced by wounding.

Nuclear factor kappa-light-chain-enhancer of activated B cells (NFκB) is a transcription factor that is evolutionarily similar to NFAT. At rest, NFκB is sequestered in the cytoplasm by inhibitory κB (IκB) which masks its nuclear localisation domain. Upon stimulation, these inhibitory molecules become phosphorylated by inhibitory κB kinases (IKK) and promote nuclear translocation. The role of NFκB is skin cell homeostasis has been reported (Bell *et al.*, 2003) and it has been suggested that activation is modulated by increased cytosolic calcium concentrations. Whilst the exact mechanisms by which calcium regulates NFκB remain incompletely understood, it has

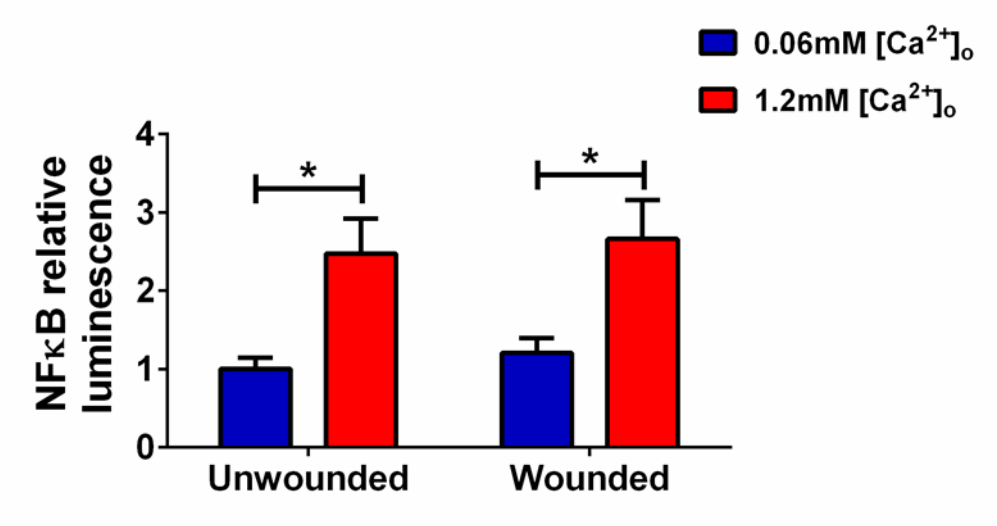

Figure 6.3 Wounding does not induced canonical NFκB.

Primary human keratinocytes cultured in 0.06mM $[Ca^{2+}]_o$ keratinocyte growth medium (MCDB 153) were transfected with NFκB firefly and renilla luciferase constructs as described in materials and methods and cultured until 100% confluent. Medium was replaced with either 0.06mM or 1.2mM $[Ca^{2+}]_o$ keratinocyte growth media (MCDB 153) for five minutes prior to cross-hatch wounding. Twenty four hours post-wounding cells were lysed and luciferase activity measured using a luminometer. Results are expressed as mean firefly/renilla ratio normalised to unwounded 0.06mM $[Ca^{2+}]_o$. Graphs show mean ± SEM from 29 experiments from 11 independent donors; (n=29), N=11. . Two-way ANOVA with Bonferroni post-hoc was conducted ($F(1,112)=16.92$, $P<0.0001$, * $P<0.05$).

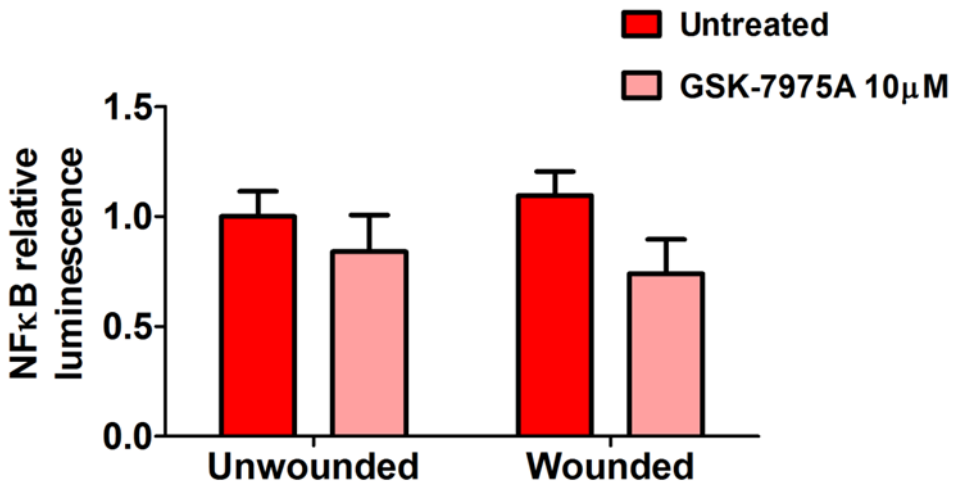

Figure 6.4 Inhibition of SOCE with GSK-7975A does not affect wound-induced NFκB activation.

Primary human keratinocytes cultured in 0.06mM $[Ca^{2+}]_o$ keratinocyte growth medium (MCDB 153) were transfected with NFAT firefly and renilla luciferase constructs as described in materials and methods and cultured until 100% confluent. Medium was replaced with either 0.06mM or 1.2mM $[Ca^{2+}]_o$ keratinocyte growth media (MCDB 153) with 10μM GSK-7975A for one hour prior to cross-hatch wounding. Twenty four hours post-wounding cells were lysed and luciferase activity measured using a luminometer. Results are expressed as mean firefly/renilla ratio normalised to unwounded untreated cells. Graphs show mean ± SEM from 9 experiments from 3 independent donors; (n=9), N=3. Two-way ANOVA was conducted ($F(1,32)=3.441$, $P=0.0728$).

been reported in T-lymphocytes that calcium activates IKK, potentially through calcineurin, thus rendering NFκB free to move to the nucleus (Trushin *et al.*, 1999). In addition, IκB is resynthesized by a reduction in calcium concentrations therefore masking the nuclear localisation domain and shuttling NFκB out of the nucleus (Fisher *et al.*, 2006). It was therefore of interest whether wounding was able to activate NFκB in a similar manner to NFAT. Primary human keratinocytes were transfected with NFκB firefly luciferase construct and a renilla luciferase as an internal control. Cells were cultured and wounded in a similar manner to NFAT investigations. In agreement with NFAT, results show wounding in 0.06mM $[Ca^{2+}]_o$ did not result in NFκB activation, with a fold increase of 1.2±0.18 observed compared to unwounded cells in the same calcium condition. Furthermore, similar to NFAT, wounding in a higher external calcium environment resulted in a marked increase in transcriptional activity; a 2.66±0.49 increase over baseline was detected. However, figure 6.3 also shows that unwounded cells cultured in 1.2mM $[Ca^{2+}]_o$ showed an increase in NFκB activity; 2.47±0.45. Two-way ANOVA was conducted and results revealed that wounding did not have a significant effect on NFκB activation ($F(1,112)=0.3112$, $P=0.5781$). The only variable that had a significant effect was external calcium concentration ($F(1,112)=16.92$, $P<0.0001$). A Bonferroni post-hoc test showed a significant increase in NFκB activation when cells were exposed to high calcium regardless of their wounded state (* $P<0.05$). No significant difference was revealed between unwounded cells in 1.2mM $[Ca^{2+}]_o$ and wounded cells in 1.2mM $[Ca^{2+}]_o$ ($P>0.05$). These results indicate that calcium entry is not as a consequence of wounding. To further investigate this, keratinocytes transfected with NFκB firefly luciferase were treated with the SOCE inhibitor GSK-7975A for one hour prior to wounding in 1.2mM $[Ca^{2+}]_o$. Twenty four hours post-wounding cells were lysed and luciferase activity measured. Figure 6.4 shows that wounding did not increase NFκB transcriptional activity, as previously described. In addition, there appears to be a slight reduction in NFκB with GSK-7975A treatment compared to untreated. A one-way ANOVA was conducted to statistically compare treated cells to untreated unwounded cells. Results revealed no significant effect of GSK-7975A treatment on NFκB activation ($P=0.2879$).

Taken together, it can be concluded that whilst the presence of high calcium in the external media and therefore calcium entry activates NFκB, wounding does not result in any further increase. Therefore, in contrast to NFAT, NFκB transcriptional activity is

not wound-dependent. Moreover, the calcium entry mechanism driving transcriptional activity of NFκB is not SOCE, further confirming a processes not linked to wounding.

6.3.4 Wounded conditioned media results in NFAT activation in unwounded cells.

Data from chapter 4 indicated that wounding caused the extracellular release of diffusible factors, such as ATP, which subsequently mediated the calcium signalling response in keratinocytes. It was therefore hypothesised that factors released into the extracellular space upon wounding would also modulate transcriptional activation. To investigate this, primary human keratinocytes were transfected with NFAT firefly and renilla luciferase constructs. In specified experiments cells were wounded in a cross-hatch manner. Five minutes post-wounding (or control) CM was collected using a P1000 pipette and placed on unwounded cells. Immediately after, fresh media was added to the wounded keratinocytes. Twenty four hours post-wounding, cells were lysed and luciferase activity measured using a luminometer as described previously. Cells were classified as positive (+) or negative (-) for wounding; positive if they had been wounded, negative if they were left unwounded. Media was classified as positive (+) or negative (-); positive if the media originated from wounded cells, negative if the media was fresh.

Figure 6.5a shows data from the above experimental design conducted in 0.06mM $[Ca^{2+}]_o$. In agreement with previous data (section 6.3.1), wounding in 0.06mM $[Ca^{2+}]_o$ did not induce NFAT activation, similarly, wounded cells cultured in unwounded media, or unwounded cells cultured in wounded media did not result in changes in NFAT activity. These observations were confirmed using a one-way ANOVA. Statistical analysis revealed no effect of wounding on NFAT activation ($F(3,32)=1.032$, $P=0.3916$). Figure 6.5b shows data from experiments conducted in 1.2mM $[Ca^{2+}]_o$. Again, in agreement with previous data (section 6.3.1), wounding caused a 2.92±0.49 fold increase in NFAT activation compared to unwounded cells. Wounded cells that had media removed five minutes post-wounding and fresh media added for the remaining twenty four hour period, appeared to have increased NFAT activation showing a 1.86±0.24 fold increase. Similarly, unwounded keratinocytes that were cultured in wounded media for twenty four hours appeared to have increased NFAT activation with a 2.23±0.35 fold increase. Neither of the increases with wounded conditioned media was as large as that caused by wounding itself. A one-way ANOVA revealed that

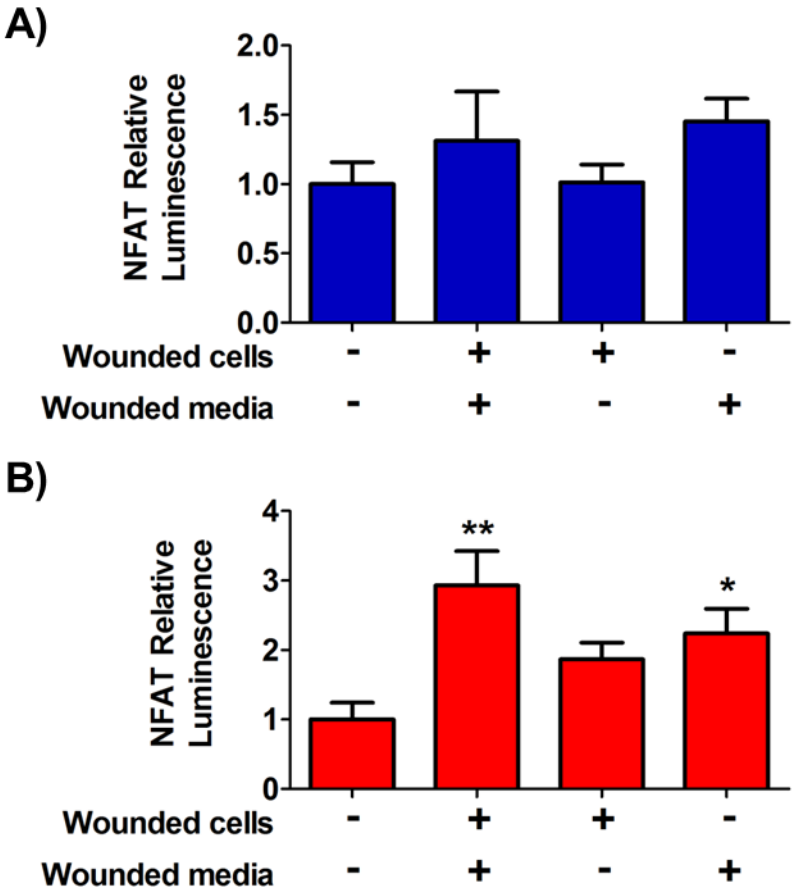

Figure 6.5 Conditioned media collected following wounding of human keratinocytes induces increased NFAT activation in unwounded cells.

Primary human keratinocytes cultured in 0.06mM $[Ca^{2+}]_o$ keratinocyte growth medium (MCDB 153) were transfected with NFAT firefly and renilla luciferase constructs as described in materials and methods and cultured until 100% confluent. Medium was replaced with either A) 0.06mM $[Ca^{2+}]_o$ or B) 1.2mM $[Ca^{2+}]_o$ keratinocyte growth media (MCDB 153) for five minutes prior to wounding or being left unwounded. Five minutes post-wounding (or unwounded control), conditioned media was collected and placed on unwounded cells. Media was replaced after removal of conditioned media. Twenty four hours post-wounding cells were lysed and luciferase activity measured using a luminometer. Cells were classified as positive (+) or negative (-) for wounding; positive if they had been wounded, negative if they were left unwounded. Media was classified as positive (+) or negative (-); positive if the media originated from wounded cells, negative if the media was fresh. Results are expressed as mean firefly/renilla ratio normalised to unwounded cells unwounded media. Graphs show mean ± SEM from 9 experiments from 3 independent donors; (n=9), N=3. One-way ANOVA with Dunnett's post-hoc were conducted A) $F(3,32)=1.032$, $P=0.3916$. B) $F(3,32)=5.270$, $P=0.0046$ (** $P<0.01$, * $P<0.05$).

wounding had a significant effect on NFAT activation ($F(3,32)=5.270$, $P=0.0046$). A Dunnett's post-hoc reported a significant increase in NFAT after wounding (** $P<0.01$), as well as a significant increase in unwounded cells cultured in wounded mediacompared to unwounded cells cultured in unwounded media (* $P<0.05$). No significant difference was reported between unwounded cells in unwounded media and wounded cells in unwounded media ($P>0.05$).

These data suggest that, in a high external calcium environment, wounding causes the release of a mediator from keratinocytes into the extracellular space. This factor subsequently activates NFAT transcriptional activity in unwounded cells, in a similar, yet not as potent manner as wounding.

6.3.5 The role of ATP signalling in wound-induced NFAT activation.

Results described above demonstrate the ability of wounded media to activate NFAT in unwounded cells, thus indicating a factor is being released from the wounded cells which can activate NFAT in unwounded cells. In previous experiments within this project it has been demonstrated that primary human keratinocytes release ATP immediately after wounding (Section 4.3.2). Moreover, ATP induced intracellular calcium signalling in a sub-population of unwounded cells (section 4.3.7). It was therefore hypothesised that keratinocytes treated with ATP would display increased NFAT activation. Through the generation of an ATP standard curve (section 4.3.6) it was determined that the concentration of ATP in the extracellular environment following wounding was 1µM, therefore this concentration plus a higher concentration of 10µM was utilised in the following experiments.

Primary human keratinocytes were transfected with NFAT firefly and renilla luciferase constructs. Once they had reach confluency, extracellular media was removed and replaced with keratinocyte growth media (MCDB 153) with a calcium concentration of either 0.06mM or 1.2mM and supplemented with either 1µM or 10µM ATP. Cells remained unwounded. Twenty four hours later, cells were lysed and luciferase activity measured using a luminometer. Data was then compared to NFAT activity induced by wounding. Cells were classified as positive (+) or negative (-) for wounding; positive if they had been wounded, negative if they were left unwounded. Result show that in 0.06mM $[Ca^{2+}]_o$ (figure 6.6a), there was no difference in NFAT activation with 1µM

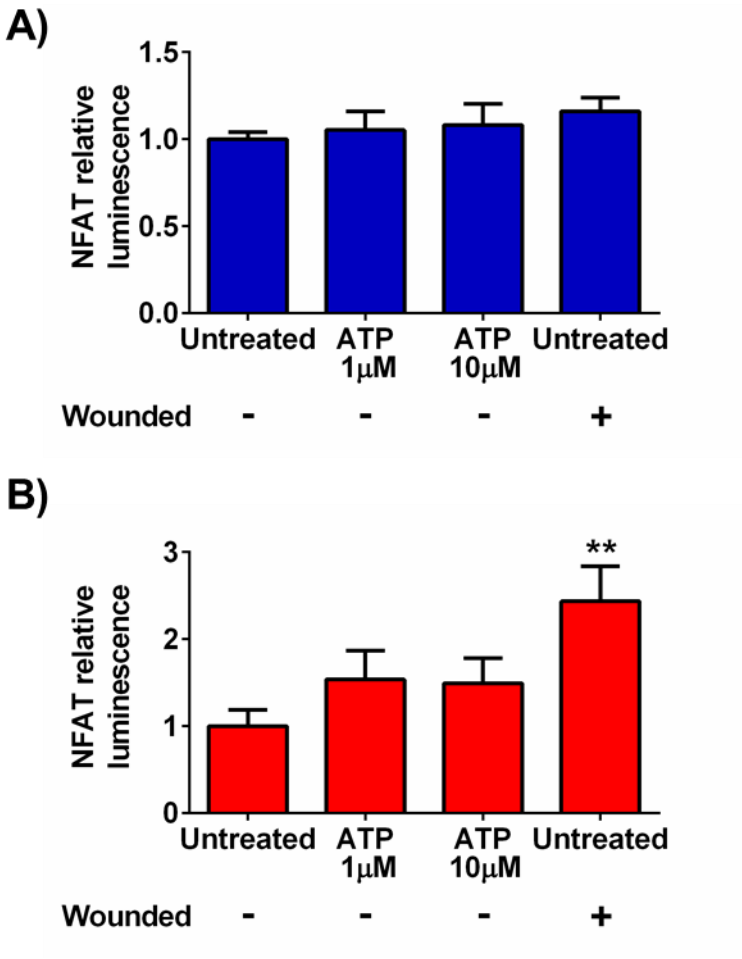

Figure 6.6 ATP does not induce NFAT activation.

Primary human keratinocytes cultured in 0.06mM $[Ca^{2+}]_o$ keratinocyte growth medium (MCDB 153) were transfected with NFAT firefly and renilla luciferase constructs as described in materials and methods and cultured until 100% confluent. Medium was replaced with either A) 0.06mM $[Ca^{2+}]_o$ or B) 1.2mM $[Ca^{2+}]_o$ keratinocyte growth media (MCDB 153) supplemented with either 1μM or 10μM ATP or cells were wounded. Twenty four hours later cells were lysed and luciferase activity measured using a luminometer. Results are expressed as mean firefly/renilla ratio normalised to untreated unwounded cells. Graphs show mean ± SEM from 21 experiments from 7 independent donors; (n=21), N=7. One-way ANOVA with Dunnett's post-hoc were conducted A) $F(3,80)=0.5289$, $P=0.6637$. B) $F(3,80)=3.691$, $P=0.0152$ (* $P<0.05$).

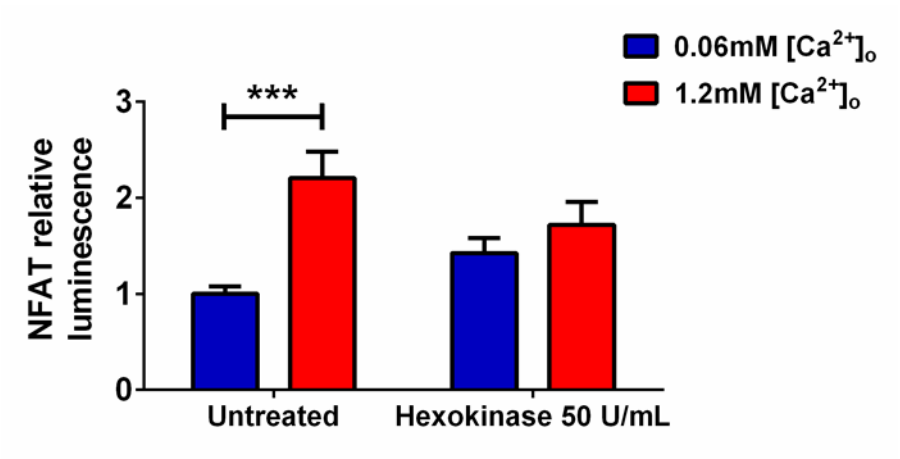

Figure 6.7 Removal of extracellular ATP with hexokinase does not reduce wound-induced NFAT activation in human keratinocytes.

Primary human keratinocytes cultured in 0.06mM $[Ca^{2+}]_o$ keratinocyte growth medium (MCDB 153) were transfected with NFAT firefly and renilla luciferase constructs as described in materials and methods and cultured until 100% confluent. Medium was replaced with either 0.06mM or 1.2mM $[Ca^{2+}]_o$ keratinocyte growth media (MCDB 153) with 50 U/mL hexokinase or left untreated for five minutes prior to cross-hatch wounding. Twenty four hours post-wounding cells were lysed and luciferase activity measured using a luminometer. Results are expressed as mean firefly/renilla ratio normalised to unwounded 0.06 mM $[Ca^{2+}]_o$. Graphs show mean ± SEM from 18 experiments from 6 independent donors; (n=18), N=6. Two-way ANOVA was conducted ($F(1,68)=0.02289$, $P=0.8802$).

ATP treatment, 10μM ATP treatment or wounding with an average fold change of 1.05±0.10, 1.08±0.12, 1.16±0.07 respectively. One-way ANOVA statistical analysis was conducted and results confirmed that ATP did not have a significant effect on NFAT activation ($F(2,60)=0.1828$, $P=0.8334$). Parallel experiments performed in 1.2mM $[Ca^{2+}]_o$ showed that wounding resulted in an increase in NFAT, as previously reported. Additionally, treatment with both 1μM and 10μM ATP appeared to slightly increase NFAT activity compared to untreated cells with a 1.53±0.33 and 1.49±0.28 fold increase respectively. Statistical analysis was conducted to compare treatments to untreated cells using a one-way ANOVA. Analysis revealed that, whilst there appeared to be an increase following ATP application, ATP had no significant effect on NFAT activation ($F(2,60)=1.170$, $P=0.3173$) (figure 6.6b).

Results from luciferase-based ATP assays presented in section 4.3.2 demonstrate that ATP was released from keratinocytes immediately post-wounding and all detectable levels of ATP were eliminated by wounding in the presence of 50 U/mL hexokinase. In order to further investigate the role of ATP signalling in wound-induced NFAT activation, primary human keratinocytes were transfected with NFAT firefly and renilla luciferase constructs as previously described and wounded in the presence of 50 U/mL hexokinase in either 0.06mM $[Ca^{2+}]_o$ or 1.2mM $[Ca^{2+}]_o$. Cells were treated with hexokinase for five minutes prior to wounding. Cells were lysed after twenty four hours treatment with hexokinase and luciferase activity measured using a luminometer.

Figure 6.7 shows data from wounded cells in both a low and high calcium conditions, with wounds being performed in the presence or absence of hexokinase. Results showed that in untreated cells wounding in 1.2mM $[Ca^{2+}]_o$ resulted in increased NFAT compared to wounding in 0.06mM $[Ca^{2+}]_o$ with cells showing an 2.20±0.27 fold increase. Cells wounded in 1.2mM $[Ca^{2+}]_o$ following hexokinase treatment showed an 1.71±0.23 fold increase. Whilst still elevated above baseline, it appears that wounding in the presence of hexokinase reduced NFAT activation compared to untreated cells. However, a two-way ANOVA failed to report a significant difference with hexokinase treatment.

Whilst preceding data revealed that a component of wounded media was able to induce NFAT transcriptional activity in unwounded cells, data present within this section suggest this factor is unlikely to be ATP, as shown by the failure of treatment of

unwounded cells with ATP at wounded (1μM) or higher (10μM) concentrations to trigger a NFAT response. Additionally, it was shown that wounding in the presence of hexokinase, to remove extracellular ATP, did not significantly affect wound-induced NFAT activation. Thus further supporting the observation that in primary human keratinocytes ATP does not mediate NFAT transcription at physiological wounded concentrations.

6.3.6 The role of gap-junctional communication in NFAT activation post-wounding.

It has been noted in the literature that connexin-43 regulates the expression of over three hundred different genes (Spray and Iacobas, 2007). It is thought that several different mechanisms mediate this regulation. One of these which is of particular interest within this project is the role of gap-junctional communication in the propagation of secondary messengers such as IP_3 and calcium. It has been shown in section 4.3.10 that blocking gap-junctional communication using 18αGA significantly reduced wound-induced intracellular calcium flux and prevented the spread of the calcium wave following scratch wounding. It was therefore of interest whether gap-junctional communication mediated NFAT activation and it was hypothesised that treatment with 18αGA prior to wounding would alter NFAT activity in 1.2mM $[Ca^{2+}]_o$. To address this, primary human keratinocytes were transfected with NFAT firefly and renilla luciferase constructs, as previously described, and wounded in the presence of 20μM 18αGA or vehicle (DMSO) in either 0.06mM $[Ca^{2+}]_o$ or 1.2mM $[Ca^{2+}]_o$. Cells were treated for one hour prior to wounding and lysed after twenty four hours of treatment, luciferase activity measured using a luminometer. Figure 6.8 shows that, as seen before, in untreated cells wounding in 1.2mM $[Ca^{2+}]_o$ resulted in increased NFAT compared to 0.06mM $[Ca^{2+}]_o$; 2.05±0.15 fold increase. Whilst wounding untreated cells in 0.06mM $[Ca^{2+}]_o$ did not induce NFAT activity, blocking gap-junctional communication prior to wounding reduced NFAT activation in low calcium conditions. Furthermore, wounding in the presence of 18αGA in 1.2mM $[Ca^{2+}]_o$ completely decreased NFAT activation to below that seen when wounding in 0.06mM $[Ca^{2+}]_o$. Two-way ANOVA statistical analysis was conducted and confirmed that treatment with 18αGA had a significant effect on NFAT activation ($F(1,32)=80.41$, $P<0.0001$). A Bonferroni post-hoc test revealed that in vehicle treated cells wounding in 1.2mM $[Ca^{2+}]_o$ resulted in increased

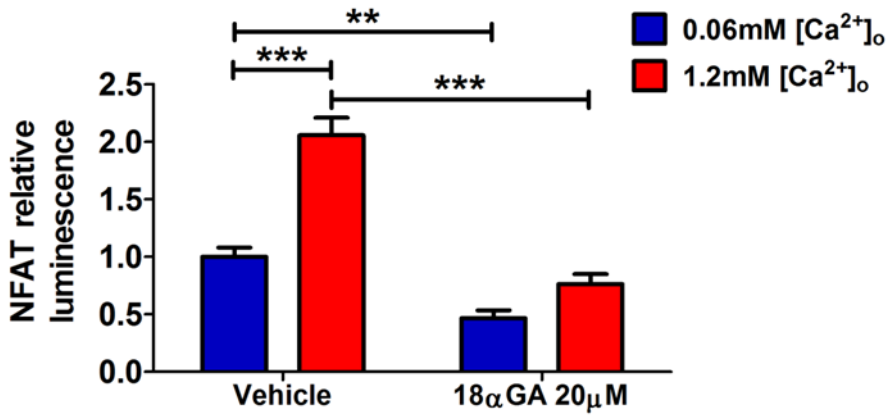

Figure 6.8 Blockade of gap-junctions with 18α-Glycyrrhetinic acid (18αGA) decreases wound-induced NFAT activation in human keratinocytes.

Primary human keratinocytes cultured in 0.06mM $[Ca^{2+}]_o$ keratinocyte growth medium (MCDB 153) were transfected with NFAT firefly and renilla luciferase constructs as described in materials and methods and cultured until 100% confluent. Medium was replaced with either 0.06mM or 1.2mM $[Ca^{2+}]_o$ keratinocyte growth media (MCDB 153) with 20μM 18αGA or 1:1000 vehicle (DMSO) for one hour prior to cross-hatch wounding. Twenty four hours post-wounding cells were lysed and luciferase activity measured using a luminometer. Results are expressed as mean firefly/renilla ratio normalised to unwounded 0.06mM $[Ca^{2+}]_o$. Graphs show mean ± SEM from 15 experiments from 5 independent donors; (n=15), N=5. Two-way ANOVA with Bonferroni post-hoc ($F(1,32)=44.02$, $P<0.0001$, *** $P<0.001$, * *$P<0.01$).

NFAT activity compared to wounding in 0.06mM $[Ca^{2+}]_o$ (*** P<0.001). Additionally, treatment with 18αGA in 0.06mM $[Ca^{2+}]_o$ significantly reduced NFAT activation (** P<0.01). Finally wounding in 1.2mM $[Ca^{2+}]_o$ in the presence of 18αGA significantly reduced NFAT activation compared to vehicle treated cells wounding in 1.2mM $[Ca^{2+}]_o$ (*** P<0.001). These data suggest that gap-junctional communication post-wounding is required for NFAT activation.

Inhibition of gap-junctions in keratinocytes prevented the calcium wave and reduced intracellular calcium fluxes post-wounding, therefore suggesting the normally occurring increases in cytosolic calcium are necessary for downstream NFAT activation following wounding.

Inhibition of gap-junctions in keratinocytes prevented the calcium wave and reduced intracellular calcium fluxes post-wounding, therefore suggesting the normally occurring increases in cytosolic calcium are necessary for downstream NFAT activation following wounding. Alternatively, it could be that calcium oscillations are required for NFAT activation and treatment with 18αGA prevented the occurrence of these oscillations and therefore transcription factor activation. This project did not delineate between the effect of the calcium wave on NFAT activation and the effect of calcium oscillations and whether one event had a dominant effect over the other.

6.3.7 Keratinocyte migration rates are dependent on extracellular calcium concentration.

Next, to further integrate signalling mechanisms that occur immediately post-wounding to long-term epidermal wound healing responses, cell migration experiments were conducted. Within this project, wounding in 1.2mM $[Ca^{2+}]_o$ has been shown to increase both immediate responses post-wounding such as the intracellular calcium flux as well as longer term transcriptional events. It was therefore postulated whether wounding in a high external calcium environment wound affect functional aspect of wound closure. To address this primary human keratinocytes cultured in keratinocyte growth media (MCDB 153) with a calcium concentration of 0.06mM were grown to confluency. Five minutes prior to wounding, media was changed and cells were exposed to either 0.06mM or 1.2mM $[Ca^{2+}]_o$. Cross-hatch wounds were performed using a 200µL pipette

tip and using the Nikon Biostation confocal images were captured every hour for twenty four hours, as described in materials and methods. Using ImageJ, the wound area was measured at specified time points and percentage wound closure was calculated compared to the original wound size.

Figure 6.9a shows images of keratinocytes wounded in 0.06mM $[Ca^{2+}]_o$ at specified time points following wounding. Images are representative of three independent donors. Percentage wound closure was calculated and quantified (figure 6.9b). As expected, it can be seen that at each progressive time point post-wounding the wound area became smaller, indicating keratinocytes were migrating to close the wound. Twenty four hours

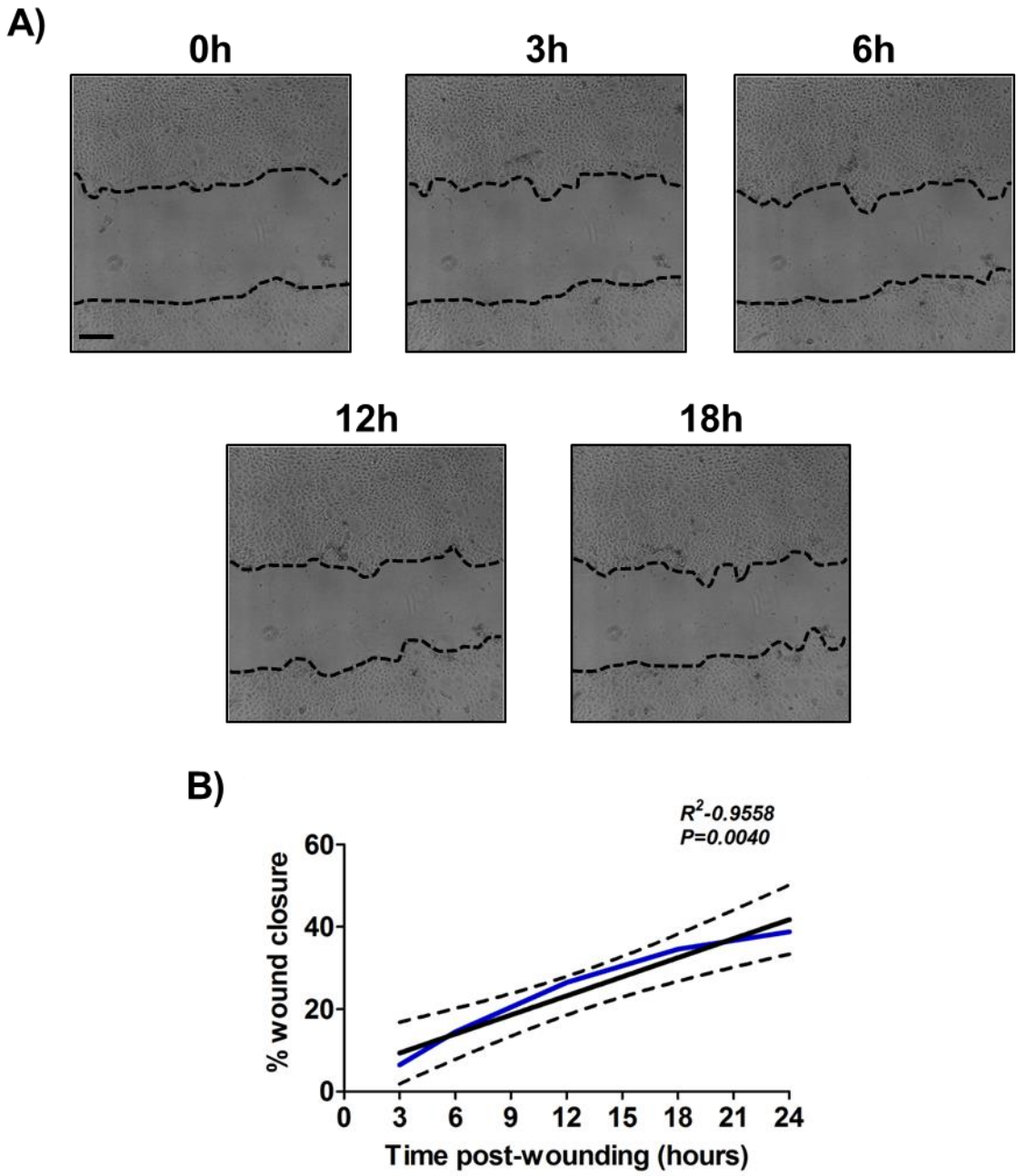

Figure 6.9 Wounding keratinocytes results in a linear temporal pattern of wound closure in 0.06mM $[Ca^{2+}]_o$.

Primary human keratinocytes cultured in 0.06mM $[Ca^{2+}]_o$ keratinocyte growth medium (MCDB 153) were grown to confluency and wounded in 0.06mM $[Ca^{2+}]_o$. Images were taken at pre-determined co-ordinates every hour for twenty four hours during the Nikon Biostation CT. **A)** Representative images of wound closure over twenty four hours at specified time points following wounding. Black lines depict wound edge. Scale bar=250µm. **B)** Wound area was measured using ImageJ and calculated as a percentage of the original wound size. Linear regression analysis was conducted and the line of best-fit plotted (black line) with the 95% confidence intervals (dotted lines) (R^2-0.9558, P=0.0040). Graphs show mean ± SEM from 18 experiments from 6 independent donors; (n=18), N=6.

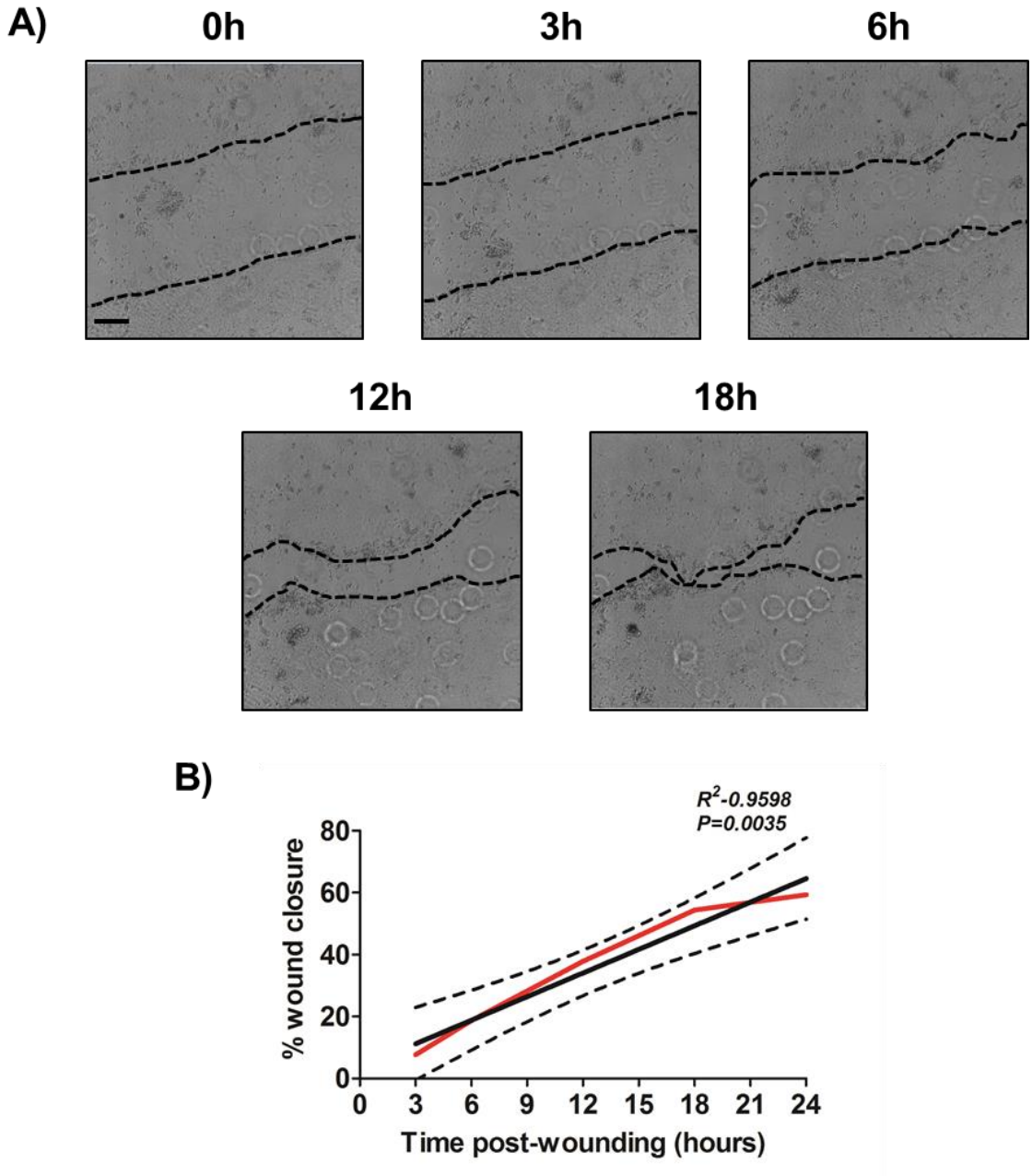

Figure 6.10 Wounding keratinocytes results in a linear temporal pattern of wound closure in 1.2mM $[Ca^{2+}]_o$.

Primary human keratinocytes cultured in 0.06mM $[Ca^{2+}]_o$ keratinocyte growth medium (MCDB 153) were grown to confluency and exposed to 1.2mM $[Ca^{2+}]_o$ for five minutes prior to wounding. Images were taken at pre-determined co-ordinates every hour for twenty four hours using the Nikon Biostation CT. **A)** Representative images of wound closure over twenty four hours at specified time points following wounding. Black lines depict wound edge. Scale bar=250µm. **B)** Wound area was measured using ImageJ and calculated as a percentage of the original wound size. Linear regression analysis was conducted and the line of best-fit (black line) plotted with the 95% confidence intervals (dotted lines) (R^2-0.9598, P=0.0035). Graphs show mean ± SEM from 18 experiments from 6 independent donors; (n=18), N=6.

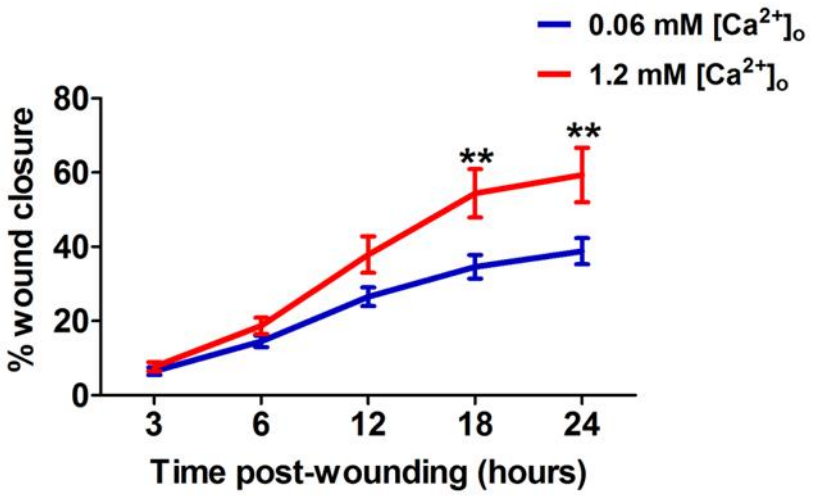

Figure 6.11 Wound closure rates are increased in 1.2mM $[Ca^{2+}]_o$ compared to 0.06mM $[Ca^{2+}]_o$.

Primary human keratinocytes cultured in 0.06mM $[Ca^{2+}]_o$ keratinocyte growth medium (MCDB 153) were grown to confluency and wounded in either 0.06mM or 1.2mM $[Ca^{2+}]_o$. Images were taken at pre-determined co-ordinates every hour for twenty four hours. Wound area was measured using ImageJ and calculated as a percentage of the original wound size. Two-way ANOVA with Bonferroni post hoc test was conducted to compare wound closure rates between the two external calcium concentrations ($F(1,170)=20.45$, $P<0.0001$, $^{**}P<0.01$). Graphs show mean ± from 18 experiments from 6 independent donors; (n=18), N=6.

post-wounding wounds had reduced by 38.7±3.5%. Linear regression analysis was conducted and reported an R^2 value of 0.9558, results also showed that this line was significantly different to zero (P=0.0040). A similar pattern of results were observed for wounds performed in 1.2mM $[Ca^{2+}]_o$ (figure 6.10a). Representative images at specified time points post-wounding show a non-surprising closure of the wound over time. Twenty four hours post-wounding wounds had reduced by 59.3±7.3% (figure 6.10b). Linear regression analysis reported an R^2 value of 0.9598 which was deemed significant different to zero (p=0.0035), indicating that percentage wound closure has a highly linear relationship to time.

Data generated from wounds conducted in 0.06mM and 1.2mM $[Ca^{2+}]_o$ were plotted together in order to compare wound closure rates in different external calcium conditions (figure 6.11). Results show that at earlier time points post-wounding, for example three and six hours, there was no difference between the percentage wound closure in high or low calcium. However, wounds performed in 1.2mM $[Ca^{2+}]_o$ appeared to have an increased wound closure at twelve hours compared to 0.06mM $[Ca^{2+}]_o$. This difference was more pronounced at eighteen and twenty four hours following wounding. Statistical analysis using a two-way ANOVA was conducted to compare wound closure rates in 0.06mM and 1.2mM $[Ca^{2+}]_o$. Results revealed a significant effect of external calcium concentration on percentage wound closure ($F(1,170)=20.45$, $P<0.0001$). A Bonferroni post-hoc test confirmed this difference was significant eighteen and twenty four hours following wounding (** $P<0.01$).

To elucidate the mechanisms behind the wound closure response seen above, the contribution of proliferation was investigated. Mitomycin C (MMC) treatment is an established method of inhibiting cellular proliferation (Fullard *et al.*, 2013). Keratinocyte monolayers were treated with MMC for two hours prior to wounding in keratinocyte growth media with a calcium concentration of 0.06mM as described in material and methods chapter. MMC was then removed and cells exposed to either 0.06mM or 1.2mM $[Ca^{2+}]_o$ keratinocyte growth media for five minutes prior to wounding. Images were captured every hour for twenty four hours. Percentage wound closure for wounds performed in 0.06mM $[Ca^{2+}]_o$ were comparable between untreated cells and MMC treated cells for the first eighteen hours following wounding, there did not appear to be any difference. However, at twenty four hours there was a reduction in

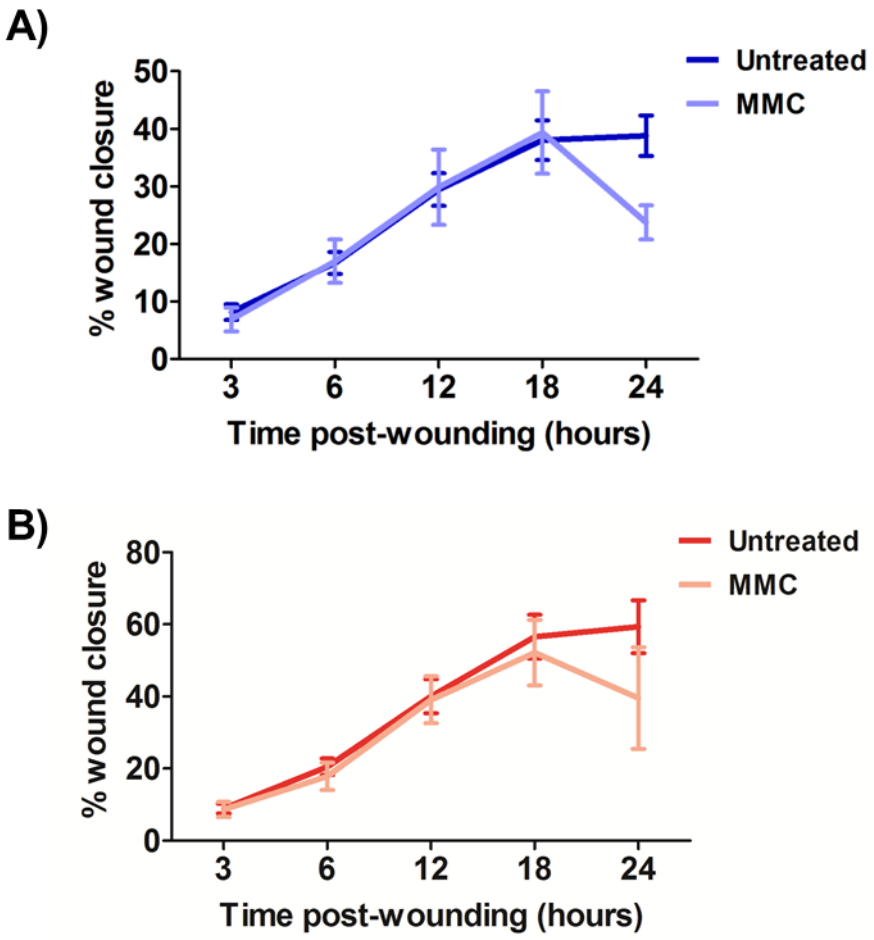

Figure 6.12 Mitomycin C treatment to prevent cell proliferation does not significantly affect wound closure suggesting migratory movement of keratinocytes is crucial for wound closure

Primary human keratinocytes cultured in 0.06mM $[Ca^{2+}]_o$ keratinocyte growth medium (MCDB 153) were grown to confluency and treated with 100X mitomycin C (MMC) for two hours. Cells were then washed with PBS and wounded. Images were taken at pre-determined co-ordinates every hour for twenty four hours. Wound area was measured using ImageJ and calculated as a percentage of the original wound size. Wounds were performed in either **A)** 0.06mM $[Ca^{2+}]_o$. Two-way ANOVA was conducted ($F(1,125)=1.516$, $P=0.2206$) or **B)** 1.2mM $[Ca^{2+}]_o$. Two-way ANOVA was conducted ($F(1,125)=1.924$, $P=0.1678$). Graphs show mean ± SEM from 9 experiments from 3 independent donors; (n=9), N=3.

wound closure in MMC treated cells which was not observed in untreated cells (figure 6.12a). A two-way ANOVA was conducted in order to compare wound closure with and without MMC treatment. Statistical analysis reported no significant difference with treatment ($F(1,125)=1.516$, $P=0.2206$). Similarly, in 1.2mM $[Ca^{2+}]_o$, MMC treatment did not appear to affect wound closure for the first eighteen hours. However, there did appear to be a slight reduction in percentage wound closure at twenty four hours in MMC treated cells (figure 6.12b). Statistical analysis with a two-way ANOVA did not report this observed difference as significant ($F(1,125)=1.924$, $P=0.1678$). These results suggest that cell movement following wounding to close the wound is cell migration rather than cell proliferation.

Combined, these data sets suggest that wounding in a high external calcium environment promotes wound closure through increased cellular migration.

6.3.8 SOCE inhibition has marginal effect on cell migration.

The results described above are indicative that cell migration during wound closure is dependent on external calcium. It was therefore speculated that calcium entry, induced by wounding, resulted in increased cell migration. To investigate whether SOCE inhibition at the point of wounding had a functional effect on wound closure, cells were pre-treated with 10µM GSK-7975A for one hour prior to wounding in 1.2mM $[Ca^{2+}]_o$. Imaging and analysis were conducted using the Nikon Biostation as previously described.

Figure 6.13a shows images of keratinocytes wounded in 1.2mM $[Ca^{2+}]_o$, at specified time points following wounding in the presence of 10µM GSK-7975A. Images are representative of three independent donors. Percentage wound closure was calculated and quantified (figure 6.13b). It can be seen that at each progressive time point post-wounding the wound area became smaller, indicating keratinocytes were migrating to close the wound. Twenty four hours post-wounding wounds had reduced by 52.2±8.6%. Linear regression analysis was conducted and reported an R^2 value of 0.9916, results also showed that this line was significantly different to zero ($P=0.0003$). Compared to untreated cells wounded in 1.2mM $[Ca^{2+}]_o$, it appears that inhibiting SOCE marginally decreased wound closure at certain time points. Although, it is of note that by twenty four hours post-wounding there does not seem to be a difference between the two

conditions. A two-way ANOVA reported a significant difference in wound closure with GSK-7975A treatment ($F(1,130)=6.692$, $P=0.0108$), although a Bonferroni post-hoc test failed to reveal a significant difference at any time point. Furthermore, an unpaired, two-tailed t-test was performed on data generated at twenty four hours post-wounding which failed to report a significant difference ($P=0.5767$).

These results indicate that increases in cytosolic calcium concentrations, through SOCE mechanisms, may play a role in keratinocyte cell migration. However, at twenty four hours following wounding there was no difference in the wound closure of cells treated with GSK-7975A and those untreated, suggesting that any effects of blocking SOCE were more prominent at earlier time points.

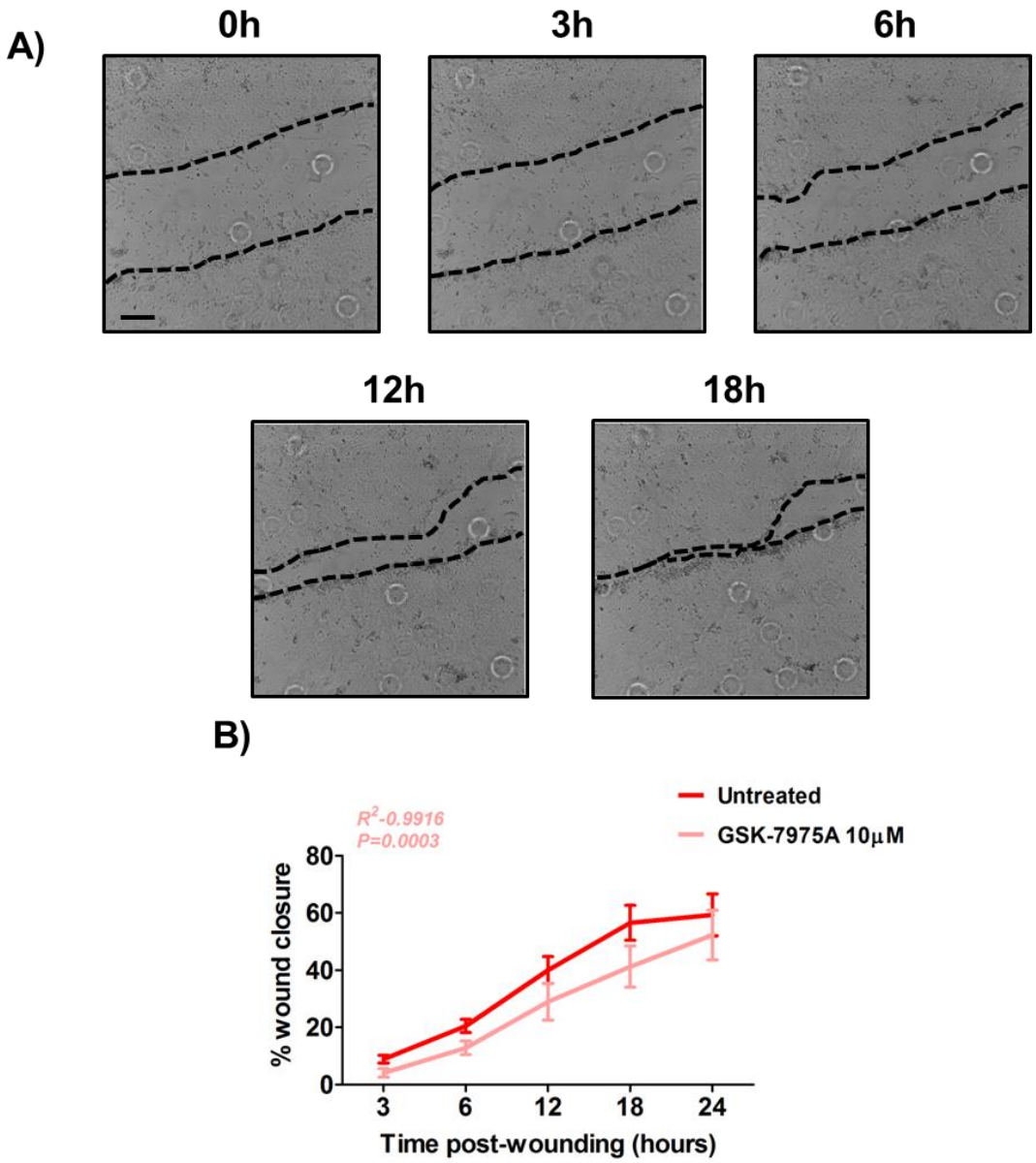

Figure 6.13 SOCE inhibition reduces rate of wound closure in 1.2mM $[Ca^{2+}]_o$.

Primary human keratinocytes cultured in 0.06mM $[Ca^{2+}]_o$ keratinocyte growth medium (MCDB 153) were grown to confluency and treated with 10µM GSK-7975A in 1.2mM $[Ca^{2+}]_o$ for one hour prior to wounding.. Images were taken at pre-determined co-ordinates every hour for twenty four hours. **A)** Representative images of wound closure over twenty four hours at specified time points following wounding. Black lines depict wound edge. Scale bar is 250µm. **B)** Wound area was measured using ImageJ and calculated as a percentage of the original wound size. Two-way ANOVA with Bonferroni post-hoc test was conducted to compare wound closure rates between untreated and GSK-7975A treated cells ($F(1,130)=6.692$, $P=0.0108$). Graphs show mean ± SEM from 10 experiments from 3 independent donors; (n=10), N=3.

6.3.9 The role of ATP signalling in keratinocyte migration post-wounding.

It was shown in section 4.3.2 that ATP is released upon wounding and hexokinase can be utilise to scavenge released ATP and eliminate the presence of ATP in the extracellular media following wounding. Additionally, it was also observed that wounding in the presence of hexokinase, significantly reduced the intracellular calcium flux post-wounding (section 4.3.5). Although, treatment with hexokinase failed to reduced wound-induced NFAT activation (section 6.3.5), it was speculated whether the removal of extracellular ATP at the point of wounding would have a functional effect on cell migration. In order to addresses this, primary human keratinocytes monolayers were wounded in either 0.06mM or 1.2mM $[Ca^{2+}]_o$ in the presence or absence of 50 U/mL hexokinase.

Figure 6.14a shows images of keratinocytes wounded in 0.06mM $[Ca^{2+}]_o$, at specified time points following wounding in the presence of 50 U/mL hexokinase. Images are representative of three independent donors. Percentage wound closure was calculated and quantified. It can be seen that at each progressive time point post-wounding the wound area became smaller, indicating keratinocytes were migrating to close the wound. Twenty four hours post-wounding wounds had reduced by 49.7±7.2%. Linear regression analysis was conducted and reported an R^2 value of 0.9753, results also showed that this line was significantly different to zero (P=0.0124). Compared to untreated cells wounded in 0.06mM $[Ca^{2+}]_o$, it appears that removal extracellular ATP increased wound closure at later time points. A two-way ANOVA reported a significant difference in wound closure with hexokinase treatment ($F(1,112)=9.588$, P=0.0025), although a Bonferroni post-hoc test failed to reveal a significant difference at any time points (figure 6.14b). Figure 6.15a shows images of keratinocytes wounded in 1.2mM $[Ca^{2+}]_o$, at specified time points following wounding in the presence of 50 U/mL hexokinase. Images are representative of three independent donors. Percentage wound closure was calculated and quantified. It can be seen that at each progressive time point post-wounding the wound area became smaller, indicating keratinocytes were migrating to close the wound. Twenty four hours post-wounding wounds had reduced by 35.2±10.5%. Linear regression analysis was conducted and reported an R^2 value of 0.9835, results also showed that this line was significantly different to zero (P=0.0083). Compared to untreated cells wounded in 1.2mM $[Ca^{2+}]_o$, it appears that removal

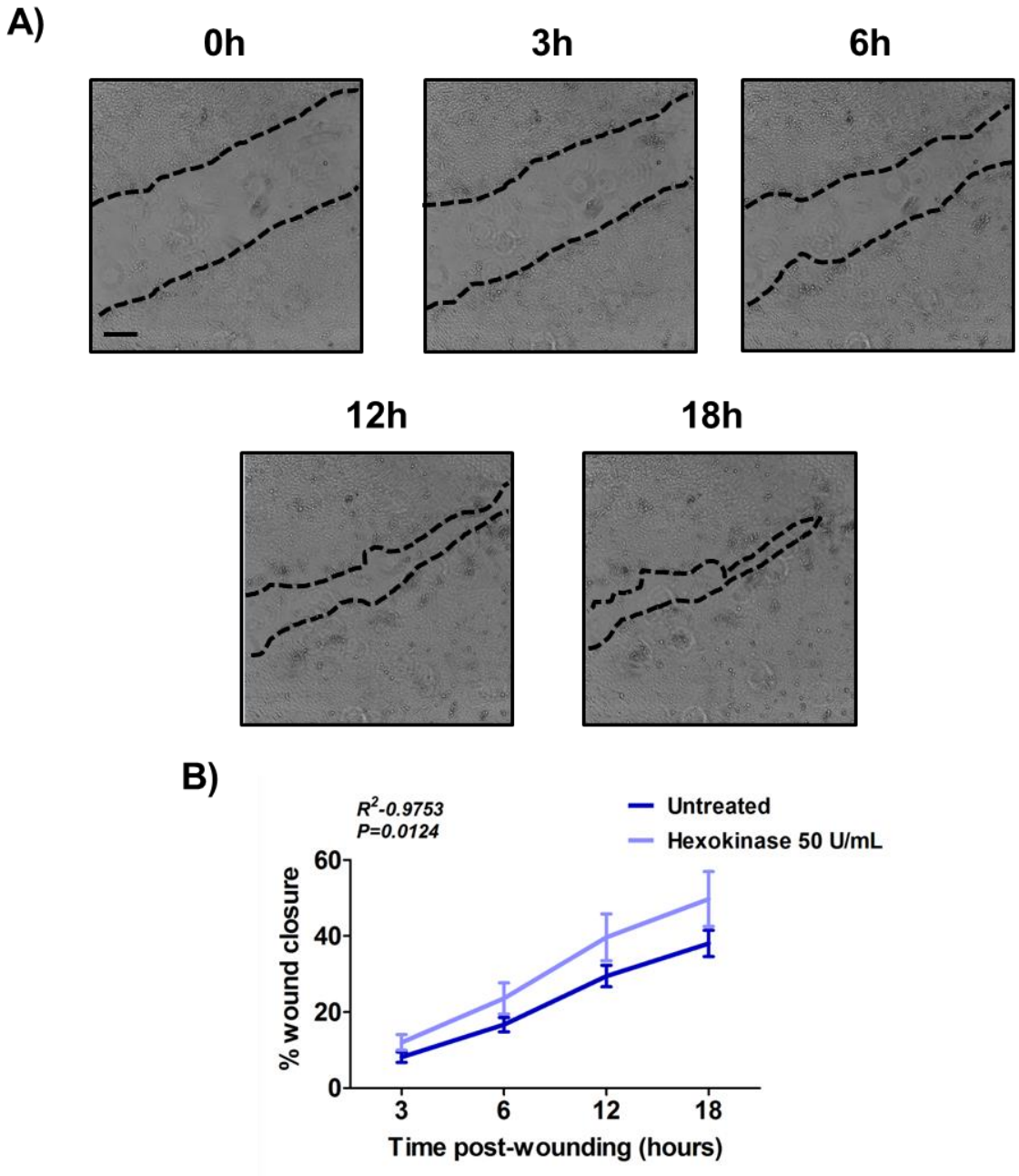

Figure 6.14 Removal of extracellular ATP post-wounding results in increased rate of wound closure in 0.06mM $[Ca^{2+}]_o$.

Primary human keratinocytes cultured in 0.06mM $[Ca^{2+}]_o$ keratinocyte growth medium (MCDB 153) were grown to confluency and treated with 50 U/mL hexokinase in 0.06mM $[Ca^{2+}]_o$ for five minutes prior to wounding.. Images were taken at pre-determined co-ordinates every hour for twenty four hours. **A)** Representative images of wound closure over twenty four hours at specified time points following wounding. Black lines depict wound edge. Scale bar=250µm. **B)** Wound area was measured using ImageJ and calculated as a percentage of the original wound size. Two-way ANOVA with Bonferroni post hoc test was conducted to compare wound closure rates between untreated and hexokinase treated cells ($F(1,112)=9.588$, $P=0.0025$). Graphs show mean ± SEM from 12 experiments from 4 independent donors; (n=12), N=4.

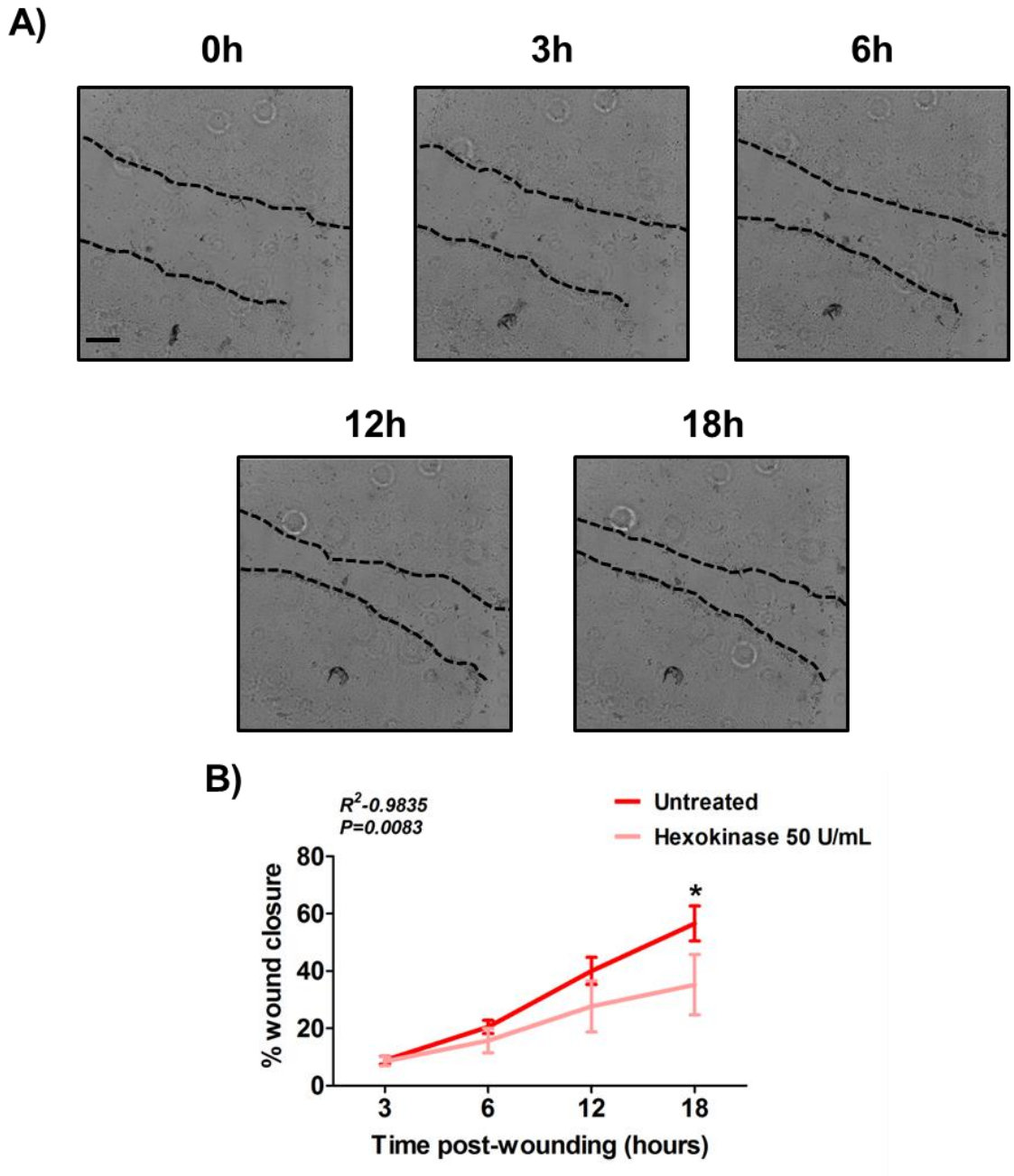

Figure 6.15 Removal of extracellular ATP post-wounding results in decreased rate of wound closure in 1.2mM $[Ca^{2+}]_o$.

Primary human keratinocytes cultured in 0.06mM $[Ca^{2+}]_o$ keratinocyte growth medium (MCDB 153) were grown to confluency and treated with 50 U/mL hexokinase in 1.2mM $[Ca^{2+}]_o$ for five minutes prior to wounding. Images were taken at pre-determined co-ordinates every hour for twenty four hours. **A)** Representative images of wound closure over twenty four hours at specified time points following wounding. Black lines depict wound edge. Scale bar=250µm. **B)** Wound area was measured using ImageJ and calculated as a percentage of the original wound size. Two-way ANOVA with Bonferroni post-hoc test was conducted to compare wound closure rates between untreated and hexokinase treated cells ($F(1,112)=6.306$, $P=0.0135$ (* $P<0.05$). Graphs show mean ± SEM from 12 experiments from 4 independent donors; (n=12), N=4.

extracellular ATP decreased wound closure at later time points. A two-way ANOVA reported a significant difference in wound closure with hexokinase treatment ($F(1,112)=6.306$, $P=0.0135$). A Bonferroni post-hoc test revealed that wound closure rates were significantly reduced at twenty four hours with hexokinase treatment (* $P<0.05$) (figure 6.15b).

These data suggest that the presence of extracellular ATP in a high external calcium environment is required for keratinocyte cell migration during wound closure.

6.3.10 Wound closure is dependent on gap-junction communication.

Gap-junction inhibition using 18αGA has been shown to prevent the spread of the calcium wave post-wounding as well as reducing wound-induced NFAT activation. It was therefore hypothesised that blockade of gap-junctional communication wound have a functional effect on wound closure. To address this, primary human keratinocytes were pre-treated with 20μM 18αGA for one hour prior to wounding in keratinocyte growth media (MCDB 153) with a calcium concentration of either 0.06mM or 1.2mM. Imaging and analysis were conducted using the Nikon Biostation as previously described.

Figure 6.16a shows images of keratinocytes wounded in 0.06mM $[Ca^{2+}]_o$, at specified time points following wounding in the presence of 20μM 18αGA. Images are representative of three independent donors. Percentage wound closure was calculated and quantified. Blocking gap-junctional communication resulted in minimal wound closure over twenty four hours, with only 10.1±1.2% observed at the final time point. Linear regression analysis was conducted and reported an R^2 value of 0.8321, results also showed that this line was significantly different to zero ($P=0.0308$), thus demonstrating that although wound closure was substantially reduced, at each progressive time point post-wounding the wound area did become smaller, indicating keratinocytes were still migrating albeit minimally. Compared to untreated cells wounded in 0.06mM $[Ca^{2+}]_o$, it appears that inhibiting gap-junctions had no effect on wound closure at three hours following wounding, however, there was a noticeable reduction at all other time points (figure 6.16b). A two-way ANOVA reported a significant difference in wound closure with 18αGA treatment ($F(1,125)=87.16$,

P<0.0001). A Bonferroni post-hoc test confirmed this difference was significant at twelve, eighteen and twenty four hours post-wounding (*** P<0.001).

Figure 6.17a shows images of keratinocytes wounded in 1.2mM $[Ca^{2+}]_o$, at specified time points following wounding in the presence of 20μM 18αGA. Images are representative of three independent donors. Percentage wound closure was calculated

and quantified. Similar to wounding in 0.06mM $[Ca^{2+}]_o$, blocking gap-junctional communication resulted in minimal wound closure over twenty four hours, with only 14.8±3.4% observed at the final time point. Linear regression analysis was conducted and reported an R^2 value of 0.9871, results also showed that this line was significantly different to zero (P=0.0006), thus demonstrating that although wound closure was reduced, at each progressive time point post-wounding the wound area did become smaller, indicating keratinocytes were still migrating. Compared to untreated cells wounded in 1.2mM $[Ca^{2+}]_o$, it appears that inhibiting gap-junctions reduced wound closure at all time points following wounding (figure 6.17b). Interestingly, the average percentage wound closure three hours post-wounding in 1.2mM $[Ca^{2+}]_o$ in the presence of 20μM 18αGA was -0.32±1.09 suggesting that in some experiments blocking gap-junctional communication initially increased the wound size. This was not observed in 0.06mM $[Ca^{2+}]_o$. A two-way ANOVA reported a significant difference in wound closure with 18αGA treatment (F(1,125)=75.03, P<0.0001). A Bonferroni post-hoc test confirmed this difference was significant at twelve, eighteen and twenty four hours post-wounding (*** P<0.001).

The results presented show that gap-junctional blockade significantly reduces wound closure in both 0.06mM and 1.2mM $[Ca^{2+}]_o$. Thus suggesting that intercellular communication via gap-junctions following wounding is necessary to promote cell migration in order to close the wound.

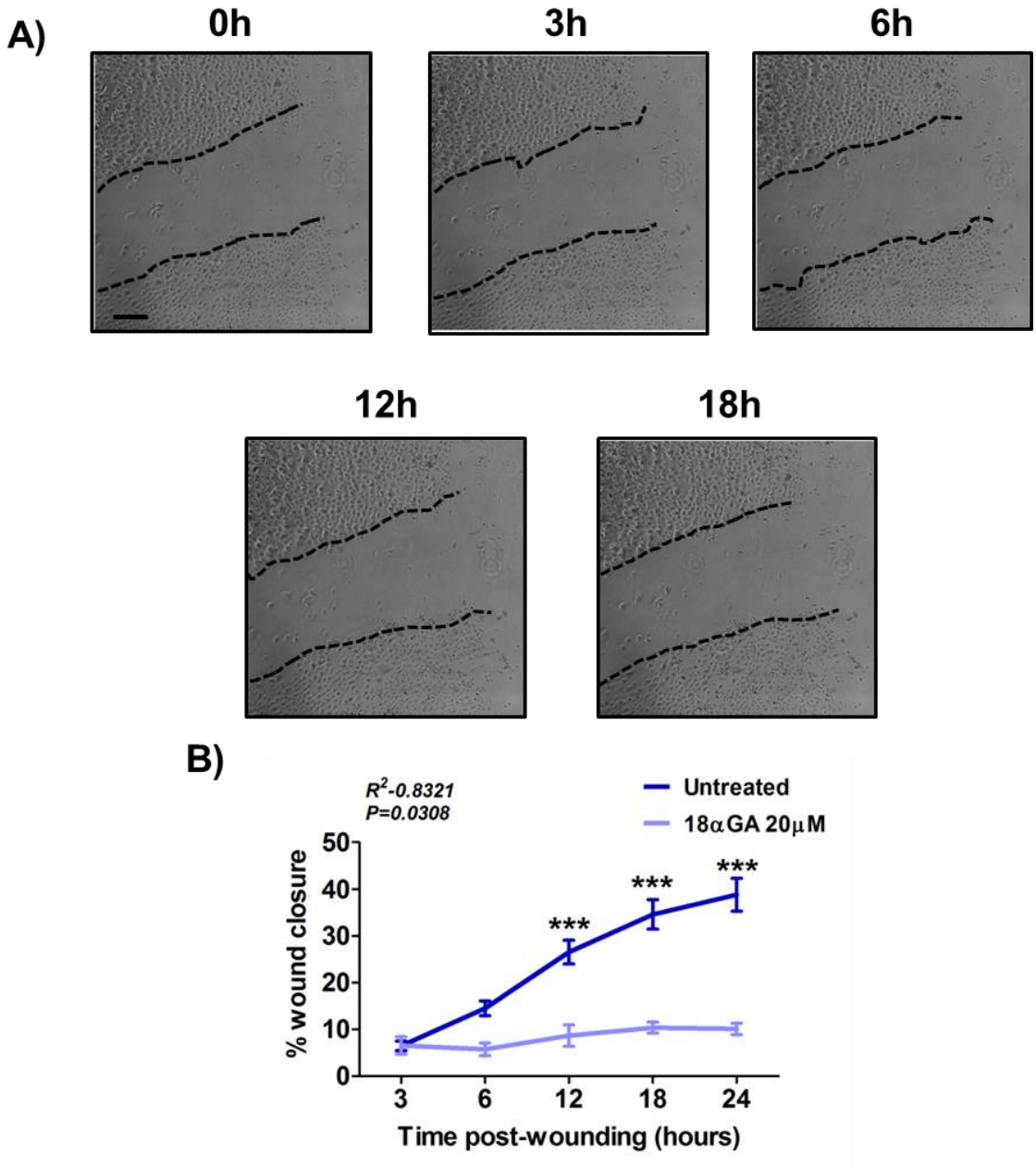

Figure 6.16 Gap-junctional communication inhibition with 18α-Glycyrrhetinic acid (18αGA) post-wounding blocks wound closure in 0.06mM $[Ca^{2+}]_o$.

Primary human keratinocytes cultured in 0.06mM $[Ca^{2+}]_o$ keratinocyte growth medium (MCDB 153) were grown to confluency and treated with 20μM 18αGA in 0.06mM $[Ca^{2+}]_o$ for one hour prior to wounding.. Images were taken at pre-determined co-ordinates every hour for twenty four hours. **A)** Representative images of wound closure over twenty four hours at specified time points following wounding. Black lines depict wound edge. Scale bar=250μm. **B)** Wound area was measured using ImageJ and calculated as a percentage of the original wound size. Two-way ANOVA with Bonferroni post hoc test was conducted to compare wound closure rates between untreated and 18αGA treated cells ($F(1,125)=87.16$, $P<0.0001$) (*** $P<0.001$). Graphs show mean ± SEM from 9 experiments from 3 independent donors; (n=9), N=3.

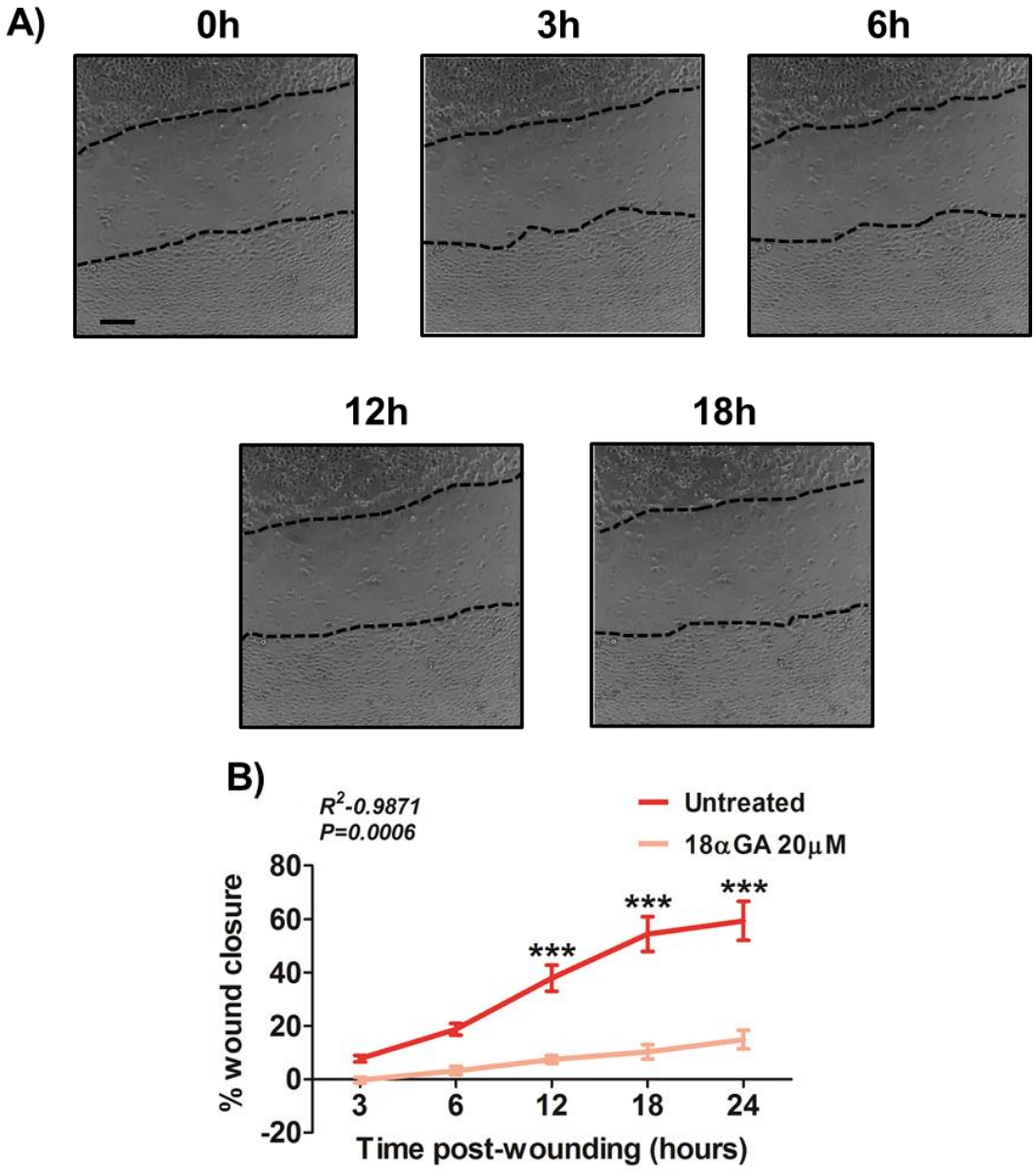

Figure 6.17 Gap-junctional communication inhibition with 18α-Glycyrrhetinic acid (18αGA) post-wounding blocks wound closure in 1.2mM $[Ca^{2+}]_o$.

Primary human keratinocytes cultured in 0.06mM $[Ca^{2+}]_o$ keratinocyte growth medium (MCDB 153) were grown to confluency and treated with 20μM 18αGA in 1.2mM $[Ca^{2+}]_o$ for one hour prior to wounding.. Images were taken at pre-determined co-ordinates every hour for twenty four hours. **A)** Representative images of wound closure over twenty four hours at specified time points following wounding. Black lines depict wound edge. Scale bar=250μm. **B)** Wound area was measured using ImageJ and calculated as a percentage of the original wound size. Two-way ANOVA with Bonferroni post hoc test was conducted to compare wound closure rates between untreated and 18αGA treated cells ($F(1,125)=75.03$, $P<0.0001$) (*** $P<0.001$). Graphs show mean ± SEM from 9 experiments from 3 independent donors; (n=9), N=3.

6.4 Discussion.

6.4.1 Transcription factor activation in response to wounding.

The NFAT family of transcription factors is regulated by increases in cytosolic calcium through activation of CaM and calcineurin. Previous studies have shown that NFAT proteins are functionally activate in human keratinocytes. Furthermore, a role for calcineurin/NFAT signalling in human keratinocyte growth and differentiation has been established (Ralph Jans *et al.*, 2013) (Al-Daraji *et al.*, 2002). However, NFAT activation of keratinocytes in response to wounding has not previously been reported. Therefore results show, for the first time, that wounding keratinocytes *in vitro* induces the transcriptional activity of NFAT in 1.2mM $[Ca^{2+}]_o$ but not 0.06mM $[Ca^{2+}]_o$. The lack of activation in a lower calcium environment is perhaps non-surprising as NFAT requires increased $[Ca^{2+}]_i$ through calcium influx from the extracellular space. In a similar manner, wounding of vascular smooth muscle cells resulted in NFATc1 activation. However, in this system NFATc1 activity was maximal four hours post-wounding, as determined by transcriptional activity and protein expression analysis (Chow *et al.*, 2008). Time course analysis herein showed that in keratinocytes, maximal activity was detected twenty four hours post-wounding. An additional difference is the fold increase induced by mechanical wounding. Chow and co-workers reported a 9-fold increases whereas herein a 3-fold increase was observed (Chow *et al.*, 2008). These differences highlight important differences in transcriptional activation between cell types.

Parallel experiments conducted on keratinocytes transfected with the NFκB luciferase showed a different response to NFAT indicating that the wounding response seen in keratinocytes is transcription factor specific. It was observed that the presence of high calcium in the extracellular environment drove NFκB transcriptional activity but wounding did not further promote this response. Whilst calcium is believed to regulate NFκB activation, results are highly suggestive that this is through non-SOCE increases in cytosolic calcium. In agreement with this hypothesis, SOCE inhibition by GSK-7975A had no significant effect on NFκB induction in 1.2mM $[Ca^{2+}]_o$. Compared to calcium-mediated NFAT activation, relatively few investigations have focussed on calcium-dependent mechanisms regulating NFκB. However, it has been recently reported that, in mast cells, STIM1 and Orai1 expression is under the transcriptional

control of NFκB (Eylenstein *et al.*, 2012). Thus highlighting that SOCE may occur downstream of NFκB and may account as to why SOCE inhibition had no effect. A possible explanation as to how elevated extracellular calcium results in increased NFκB in the absence of wounding, could involve CaSR. CaSR binds extracellular calcium to evoke intracellular signalling mechanisms. The role of CaSR in NFκB activation has been demonstrated previously in T lymphocytes where the activation of CaSR resulted in cytokine secretion through NFκB signalling (T. Li *et al.*, 2013). Further experiments investigating these observations in keratinocytes were beyond the scope of this project.

Although a preliminary time course experiment was conducted whereby samples were collected at various time points post-wounding, it is possible that the time point investigated in this project was not optimal. No unwounded control was conducted and therefore it is difficult to eliminate the possibility that the increase in luciferase with time is an effect of firefly accumulation over time rather than increased NFAT transcriptional activation. Utilising the photon camera to visualise NFAT luciferase activity in real time will shed light into the timing of NFAT activation following wounding.

It is of note that control luciferase experiments were conducted whereby TE buffer with no firefly plasmid was added to the cells with TransIT to ensure that the transfection method (TransIT) did not cause an NFAT transcriptional response (data not shown). However, this experiment does not show that the transfection method does not cause an intracellular calcium response which may have other effects within the cell. To confirm that TransIT doesn't result in a calcium flux, Fluo4-AM loaded cells would be imaged in the presence of TransIT and cytosolic calcium.

Whilst not investigated within this project, it is also possible that the increase in cytosolic calcium as a result of SOCE also activates other transcriptional pathways independent of NFAT. For example, calcium binding to calmodulin can also result in activation of the transcriptional regulator CREB in two ways. Firstly, through calmodulin-dependent kinase cascades and the secondly through Ras and ERK activation (Putney, 2012). The effects of SOCE-induced activation of these pathways on cell migration during wound closure would be interesting to study in future investigations.

6.4.2 NFAT in wound healing and downstream targets.

The wound healing process is highly complex and requires a tightly regulated sequence of events, one of which that has been of interest within this project is reepithelialisation. Reepithelialisation involves cellular events including migration, proliferation and differentiation. NFAT factors have previously been shown to be crucial in the regulation of such signalling pathways, therefore making it an interesting contender for mediating epidermal wound healing responses (Ralph Jans *et al.*, 2013). Whilst published studies have not linked NFAT to keratinocyte wound closure, investigations have confirmed a role for NFAT in events involved in wound closure in a variety of cell types. Chow *et al*. showed that knockdown of NFATc1, by RNAi in vascular smooth muscle cells or pharmacological inhibition with CsA, attenuated wound closure. Interestingly, the same effect was seen with overexpression of a constitutively activate GSK3β mutant (Chow *et al.*, 2008). It has also been suggested through analysis of genes known to be regulated by NFAT, that NFAT transcriptional activation drives cell proliferation and migration. For example, in both pancreatic carcinoma cells and fibroblasts, NFATc1 has been shown to induce cyclin D1 and c-myc, thus promoting cell cycle progression (Neal and Clipstone, 2003; Buchholz, 2006). Similarly, NFATc1 functioned alongside SP1/SP3 and egr-1 to positively regulate expression of matrix metalloproteinase which are believed to regulate cell migration (Alfonso-Jaume *et al.*, 2004). Further, IL-6 and COX2 were up-regulated by NFAT to promote cell proliferation and migration in vascular smooth muscle cells (Liu *et al.*, 2004; Liu *et al.*, 2005). More relevant to this project, the role of COX2, a downstream target gene has been explored in keratinocytes. NFAT2 inhibition in HaCaTs was detrimental to COX2 activation following UVR. Results showed that COX2 luciferase reporters that lacked a functional NFAT binding site had attenuated activity in response to stimuli, therefore indicating that the NFAT binding site in the COX2 promoter was crucial for expression (Flockhart *et al.*, 2008). COX2 is known to enhance cell migration and therefore would be an interesting downstream target of NFAT to analysis in keratinocyte migration in wound closure in future work following on from this project.

A recent observation by Koeck *et al*. was that NFAT-mediated IL-4 production occurred in an "all or nothing" manner in Th2 cells. As such, graded NFAT inhibition

decreased the frequency of IL-4 expressing cells; however the cells in which IL-4 persisted did not show reduced levels. In other words, NFAT was acting as a molecular switch which translated a graded upstream signal into an "on or off" downstream response, presumably through sub or supra threshold activation (Koeck *et al.,* 2014). This is a key finding in the physiological role of NFAT and future work will not exclude the possibility NFAT is acting in a similar manner in keratinocytes in response to wounding.

6.4.3 Wound-induced NFAT activation requires SOCE.

The role of SOCE in calcium entry leading to NFAT induction in primary keratinocytes was previously unreported until last year, where work from the Reynolds group preceding this project, showed that STIM1 and Orai1 regulated calcium entry in keratinocytes (Ralph Jans *et al.,* 2013). Although, this data was not relevant to wound healing responses, it robustly demonstrated that SOCE activated NFAT and regulated downstream migratory responses. Given that wound-induced NFAT activation only occurred in 1.2mM $[Ca^{2+}]_o$ and not in 0.06mM $[Ca^{2+}]_o$, combined with established knowledge that calcium entry drives NFAT activity, it was perhaps unsurprising that treatment with GSK-7975A significantly reduced wound-induced NFAT activation. This data provides further evidence to that presented by Jans *et al*, that SOCE leads to NFAT activation in primary human keratinocytes with wounding being a trigger for this response. Future work to confirm the role of SOCE in wound-induced NFAT activation would include genetically manipulating the STIM and Orai families of proteins. STIM1 knockdown with RNAi has recently been shown to decrease NFAT2 nuclear translocation, as visualised by NFAT2-GFP and confirmed by luciferase assays (Ralph Jans *et al.*, 2013). The importance of SOCE triggering NFAT has been shown in many cell types including lymphocyte activation. It is known that mutations in Orai1 are found in patients with SCID (Feske *et al.*, 2006). As well as preventing SOCE, this mutation resulted in defected NFAT activation and consequently decreased expression of cytokines and chemokines known to be important in immune defence. This highlighted an important physiological role for SOCE-mediated NFAT activation (Gwack *et al.,* 2007). Similarly, it has been observed that STIM1-dependent SOCE was required for NFAT-dependent gene expression in C2C12 cells, a mouse myoblast cell line. Moreover, this signalling was required for cell differentiation and muscle

development (Stiber *et al.*, 2008). More recently, gene silencing of STIM1 and Orai1 proteins prevented histamine-induced SOCE in endothelial cells which reduced NFAT activation and consequently attenuated IL-8 production (M. H. Zhou *et al.*, 2014).

In order to further delineate the temporal properties of the intracellular calcium flux which regulates NFAT, it would be of interest to perform calcium add-back experiments, similar to that used in calcium signalling investigations. This would involve wounding monolayers of primary human keratinocytes in 0.06mM $[Ca^{2+}]_o$ and a short time later, adding back high calcium. Results so far have shown that a) wounding in 0.06mM $[Ca^{2+}]_o$ does not induce NFAT and b) 1.2mM $[Ca^{2+}]_o$ does not activate NFAT in unwounded cells. Such an experiment would confirm whether add-back of calcium post-wounding resulted in NFAT activation in a similar manner to wounding in 1.2mM $[Ca^{2+}]_o$ and would determine the relative contribution of the wave and the oscillations.

The rise in cytosolic calcium initiates downstream responses over a range of time course from sub-seconds (neurotransmitter release) to hours and days (gene regulation and differentiation). The manner in which increases in cytosolic calcium can alter gene expression hours later has long been of interest. Whilst the mechanism of calcium oscillations remains undetermined in the model utilised within this project, it is accepted that oscillations provide a digital calcium signal. This digital signal functions in an all-or-nothing manner and provides check points to prevent unwanted gene expression at low levels of calcium signalling. This occurs because there is a cellular threshold for calcium concentration in the cytoplasm before downstream signalling cascades are initiated, thus small alterations in cytosolic calcium do not cause an effect, whereas repeated signals in the form of calcium oscillations do (Putney, 2012). Recently, Kar and co-workers demonstrated novel kinetic data showing that calcium-induced NFAT activation was dependent on a series of steps with long and short term memories. As such, calcium-dependent gene expression continues long after the initial calcium signal. Moreover, calcium-dependent import and export of NFAT1 to the nucleus occurred in a non-linear manner. NFAT translocation into the nucleus is quicker than export of NFAT out of the nucleus, which is relatively slow. This increases the time NFAT is in the nucleus and thus able to activate gene transcription and indicates a mechanism how gene transcription occurs long after the calcium signal has ended. Interestingly, calcium

signals that were too brief to drive transcription individually were able to synergise to activate gene expression and demonstrated a mechanism whereby agonist can reinforce one another to initiate transcriptional events, assuming that the time between signals is short. It was suggested from this study that this added level of complexity can provide additional regulation points which mediate the timings involved in gene regulation pathways (Kar *et al.*, 2012).

6.4.4 The contribution of extracellular ATP to wound-induced NFAT activation.

Purinergic signalling has been shown within this project to play an important role in mediating both the intercellular calcium wave induced by wounding, as well as the downstream calcium oscillations. It was therefore, interesting that wounding in the presence of hexokinase to remove extracellular ATP did not significantly reduce wound-induced NFAT activation in 1.2mM $[Ca^{2+}]_o$. In agreement with these results, the addition of ATP at either the physiologically relevant wounded concentration 1µM or the higher concentration of 10µM, did not lead to NFAT activation. Combined, these results are suggestive that ATP released by keratinocytes in response to wounding was not required for wound-induced NFAT activation. This is in contrast to data presented by Prasai and co-workers who showed that in PC12, a rat adrenal medulla cell line, extracellular ATP regulated neuronal gene expression through increased NFAT activation (Prasai *et al.*, 2011). A similar observation had previously been made in microglial cells (Ferrari *et al.*, 1999). However, in this study, it was shown that ATP mediated its effects rapidly, with activation occurring within one minute, whereas the experiments conducted within this project were interested in the contribution to wounding and therefore analysed results at a later time point. Nevertheless, this may account for the difference between studies. Additionally, hMSC treated with hexokinase had reduced nuclear translocation of NFAT, as shown by fluorescence staining (Kawano *et al.*, 2006).

The failure of ATP to induce NFAT transcriptional activity at the wounded concentration of 1µM was even more surprising considering the ability of ATP to induce an intracellular calcium flux in a sub-population of cells at this concentration. It is possible that the type and duration of the agonist-induced calcium flux is crucial and this may account for the failure of ATP to induce NFAT transcriptional activation (Ross *et al.*, 2007). Moreover, CM (wounded media and unwounded cells), which triggered an

intracellular calcium flux, also significantly increased NFAT activation. In order to confirm that ATP was not involved in CM-mediated NFAT activation, wounding would be performed in the presence of hexokinase to produce CMH. It would be expected that this would have no effect on CM-induced NFAT activity. These results are indicative that another factor is released from keratinocytes during wounding and it is this factor that may be inducing downstream NFAT activation in the CM. This factor may be UTP which has been shown to trigger a calcium response in keratinocytes as well as initiate STIM1 translocation to the PM (Ross *et al.*, 2007). These findings therefore make UTP a suitable candidate to investigate further for its ability to drive NFAT transcription.

6.4.5 Gap-junctional communication in NFAT transcriptional activity.

Keratinocytes monolayers treated with 18αGA did not propagate an intercellular calcium wave following wounding. It was concluded from this that gap-junctional communication is crucial for wave transmission. Further, no calcium oscillations were detected under these conditions. Gap-junctional blockade also abrogated wound-induced NFAT activation in 1.2mM $[Ca^{2+}]_o$, resulting in NFAT levels comparable to unwounded cells. Combined, these data indicate that calcium signalling post-wounding is required for longer-term transcriptional events. It could therefore be postulated that wounding induces IP_3-mediated calcium wave which spreads from the wound edge back through the cell population. This depletes calcium stores and induces further calcium flux in the form of oscillations. The presence of these oscillations provides the increased cytosolic calcium necessary to activate CaM/calcineurin/NFAT signalling. An interesting observation by Kumai *et al*. was that cardiac valve abnormalities observed in $Cx45^{-/-}$ mice where similar to those seen in NFATc1 null mice. Further analysis demonstrated an absence of nuclear NFATc1 in $Cx45^{-/-}$ mice, providing evidence that gap-junctions may regulate NFAT transcription (Kumai *et al.*, 2000). In support of the findings presented herein, the authors suggest that the lack of increase in cytosolic calcium and the subsequent failure of calcium entry through SOCE mechanisms resulted in NFATc1 being retained in the cytoplasm and the prevention of nuclear translocation.

6.4.6 Specific responses of NFAT family members.

It is widely accepted that there are five members of the NFAT family of transcription factors, with NFAT1-4 being calcium-dependent (section 1.5.1). The firefly luciferase construct utilised within the project did not delineate between NFAT members, rather it provided data relating to NFAT signalling as a whole. This was an important initial reporter to use as NFAT activation in response to wounding in primary human keratinocytes had not previously been described. However, in order to further explore the effects of wound-induced transcriptional activity it would be useful to investigate each individual members. Chow *et al*. described a potent effect of NFATc1 in wound closure rates in vascular smooth muscle cells, however failed to report the contribution of the other NFAT isoforms (Chow *et al.*, 2008). In contrast, Flockhart and co-workers demonstrated that UVR only evoked nuclear translocation of NFAT2 in keratinocytes; NFAT1, 3 and 4 were not affected (Flockhart *et al.*, 2008). This highlights an important stimulus-dependent role for NFAT in keratinocytes. It would be of interest to delineate which NFAT isoforms are activated in response to wounding. Future work would include the separation of nuclear and cytoplasmic fractions of lysates from wounded and unwounded keratinocytes. Using antibodies directed to each individual family member, western blot analysis would provide insights into differential nuclear translocation following wounding. Results from this could then be used to knockdown involved NFAT members using siRNA to assess the functional effects of this. This model could additionally be used to further understand the role of SOCE, purinergic signalling and gap-junctional communication in wound-induced NFAT activation.

6.4.7 Visualisation of NFAT activation post-wounding.

Whilst luciferase-based assays used within this project have highlighted highly interesting data, a disadvantage to this technique is that no information regarding spatial regulation of transcriptional activity is provided. It could be speculated that cells located in close proximity to the wound edge would display increased NFAT activity as these cells showed the highest maximum Ft/F0 during the intercellular calcium wave. This has previously been suggested in the mouse model of cardiac valve development, whereby the NFATc1 expression was highest within the cell stimulated and a decreasing gradient existed through neighbouring cells correlating to the reduction in IP_3 (Crabtree and Olson, 2002). On the other hand, results have suggested that the

downstream oscillations have a dominant effect at driving transcriptional activation and no relationship between the location of an oscillating cell and the wound edge was detected within this current study. Visualisation of the luminescence signal would determine if a sub-population of cells showed increased NFAT transcriptional activity in a similar manner to the sub-set of cells oscillating.

A novel method that could be utilised in future experiments is the use of microscopic luminescence camera that could capture images of cells transfected with the NFAT firefly reporter in real time. This system is routinely used to investigate calcium signalling in plant cells where calcium dyes are problematic. The technique would enable visualisation of the cells that show increased NFAT and analysis of the spatial pattern of signalling as well as providing more detailed assessment of the temporal regulation of expression. Performing add-back experiments using this equipment will provide valuable insights into the relative contribution of calcium flux post-wounding and calcium oscillations on downstream NFAT activation.

6.4.8 Wound closure rates in keratinocytes.

Scratch wound assays provide a robust method to analyse contributing factors regulating cell migration in response to mechanical stimuli. Results showed that wounding primary human keratinocytes in 0.06mM $[Ca^{2+}]_o$ resulted in an average wound closure of 26.5±2.5% by twelve hours and 38.79±3.51 by twenty four hours. Walter *et al*. observed 16±4% wound closure at twelve hours and 57±% wound closure at twenty four hours following wounding of HaCaTs (Walter *et al.*, 2010). In agreement with these results, but in contrast to data within this project, Chow *et al*. also report an approximate 50% wound closure by twenty four hours in vascular smooth muscle cells (Chow et al., 2008). Interestingly, another study utilising human epidermal keratinocytes demonstrated only a 19.6% wound closure at twenty four hours (Ojeh *et al.*, 2014). These findings suggest that even within a specific cell type, wound closure rates are highly variable. Factors such as media components, origin of cells and methods of scratch wounding could be attributed to this.

This chapter aimed to analyse the effect of extracellular calcium concentration on cell migration rates. Results showed that when wounding was performed in 1.2mM $[Ca^{2+}]_o$ wounds closed at a quicker rate compared to wounds conducted in 0.06mM $[Ca^{2+}]_o$.

This data is consistent with the role of transcription factors such as NFAT that are activated by influx of extracellular calcium as well as evidence implicating the CaSR in linking extracellular calcium and intracellular responses. On the other hand, it may be hypothesised that exposure of keratinocytes to 1.2mM $[Ca^{2+}]_o$ over twenty four hours would result in increased differentiation and suppression of migration and/or proliferation. However, it has previously been shown that an increase of extracellular calcium from 3μM to 3mM did not significantly affect migration rates in normal epidermal keratinocytes (Fang et al 2008). Whilst project did not determine the mechanism through which extracellular calcium was exerting its effects; future work using pharmacological inhibitors or RNAi of the CaSR would determine whether this was a contributing factor. A similar experimental design was adopted by Milara *et al*. who showed in human bronchial epithelial cells, knockdown of CaSR partially inhibited wound repair. Interestingly, this treatment also affected intercellular calcium wave propagation, thus proposing a link between calcium wave transmission and migration rates which could also be assessed in keratinocytes following wounding in the future (Milara *et al.*, 2010). Recently, a key role for CaSR in human keratinocyte differentiation has been revealed providing further support for future analysis of this signalling mechanism in epidermal wound healing responses (Popp *et al.*, 2014).

An interesting observation within this project was that whilst increasing the extracellular calcium concentration promoted keratinocyte migration and reduced the wound size, keratinocytes were still able to migrate in a lower calcium concentration. This suggests that extracellular calcium concentration is not involved in the initiation of cell migration. In addition, following wounding in low external calcium, calcium oscillations were not observed nor was there activation of NFAT, but as stated above, the cells still migrated. These results indicate that other pathways are activated by wounding that are not dependent on extracellular calcium that regulates NFAT activity. It is possible that adherens junctions are formed by prolonged exposure to 1.2mM $[Ca^{2+}]_o$ (section X) and these are having an effect in the promotion of keratinocyte signalling and migration compared to wounding in 0.06mM $[Ca^{2+}]_o$ where these junctions are not formed.

6.4.9 The role of SOCE in cell migration post-wounding.

The role of intracellular calcium in cell migration has been established. However, as described above, relative contribution of SOCE and receptors such as CaSR are

unknown. Scratch wound assays performed on cells treated with GSK-7975A revealed reduced wound closure rates over twenty four hours, although surprisingly the percentage wound closure at the end of the imaging period, twenty four hours, showed no difference. Therefore implying that SOCE inhibition delays short-term wound healing responses but is not significantly detrimental over the longer term. In partial agreement with these results, it has been shown using cell tracking during migration, that both STIM1 and Orai1 siRNA significantly reduced HEK293 migration. Both RNAi had a similar effect on migration. Calcium is believed to regulate a variety of events which ultimately result in appropriate wound closure, including focal adhesion assembly. Mechanisms mediating such processes were shown to be SOCE-dependent, although, it is of note that Orai1 and STIM1 exerted different effects (Schäfer *et al.*, 2012). Whilst SOCE inhibition resulted in a marginal, but still statistically significant, reduction in cell migration, wound closure still occurred in the current study. Thus implying that SOCE is not the dominant mechanism driving the increased cell migration observed in the presence of high external calcium. Although not directly linked to wound healing, it has been shown that STIM1 knockdown in primary human keratinocytes was detrimental to cell migration, indicating a role for SOCE in the migratory response (Ralph Jans *et al.*, 2013).

Intriguingly, it has recently emerged that the SOCE regulatory protein STIM1 was involved in the directionality of migrating cells. Experiments conducted in HUVEC used live cell imaging to show increased STIM1 in the front of the migrating cell and deemed this specific localisation was necessary to support cell migration (Tsai *et al.*, 2014).

Proliferation is a process known to be regulated by calcium that is involved in reepithelialisation, although not specifically investigation within this project apart from the studies reported using MMC (figure 6.12). Findings from other groups have indicated that SOCE inhibition, by both pharmacological and genetic means, resulted in decreased cell proliferation in a variety of cell types (Borowiec *et al.*, 2014).

6.4.10 Purinergic signalling and wound closure.

ATP released from keratinocytes has been shown in this present study to regulate the intercellular calcium wave and wound-induced NFAT activation. Furthermore, scratch

wounding assays conducted in the presence of hexokinase attenuated the migratory capacity of keratinocytes, with a significant reduction in percentage wound closure observed at twenty four hours in 1.2mM $[Ca^{2+}]_o$. For reasons as to yet be explained, treatment with hexokinase in 0.06mM $[Ca^{2+}]_o$ appeared to promote cell migration. Although reasons for this are unclear, it was also noted in NFAT transcriptional assays, that hexokinase treatment in 0.06mM $[Ca^{2+}]_o$ appeared to increase transcriptional activity, implying that increased NFAT may promote cell migration in this condition. Further experiments are required to fully decipher mechanisms mediating these observations and their relevance to cutaneous wound healing.

ATP is known to be a key mediator in keratinocyte differentiation and proliferation (Burrell *et al.*, 2005). Furthermore it is known that release of ATP from keratinocytes into the extracellular space regulates proliferation through activation of purinergic receptors. These findings support a role of ATP in wound closure, as observed herein. Similar results have been reported in other cell types. Wesley *et al*. showed in airway epithelial cells that purinergic receptor stimulation by extracellular ATP modulated epithelial cell migration and repair post-injury (Wesley *et al.*, 2007). Recently, an investigation aiming to investigate the role of the purinergic receptor $P2Y_2R$ demonstrated that siRNA directed to $P2Y_2R$ prevented the migration of fibroblasts in parallel activation of $P2Y_2R$ by ATP enhanced proliferation (Jin *et al.*, 2014). Future work in the model presented within this project would involve exploration of the changes in purinergic receptor expression triggered by wounding. To this end, receptors regulating ATP-mediated keratinocyte migration to close the wound would be identified and may highlight novel therapeutic targets in the treatment of chronic wounds.

It is likely that ATP released from keratinocytes post-wounding *in vivo* signals to neighbouring cells and contributes to wound closure in a regulated and efficient manner. Interestingly, it is believed that in deep wounds, epidermal replenishment is induced from the hair follicles. A large number of $P2Y_2R$ mRNA transcripts have been localised to the hair follicle, and this may account for the proliferation of basal cells within the inner root sheath of the hair follicle leading to epidermal growth in response to injury (Dixon *et al.*, 1999).

ATP was added to unwounded cells at a concentration of 1µM because this was determined to be the physiologically wound relevant concentration. An advantage of

using this concentration was that any effects observed could be linked to wound-induced ATP release from keratinocytes at a physiological concentration. Media samples taken for analysis following wounding of keratinocytes were taken from the middle of a well and care was taken not to further disrupt the keratinocytes or induce a second wound in order to ensure the ATP measurement was solely as a result of wounding. However, it is possible that this was not a true representation of the concentration of ATP on the cells extracellular surface. In other words, it is likely that there is a microenvironment at the cell surface where ATP concentration is higher. It may be the case that ATP is involved in NFAT activation in keratinocytes but the concentration of 1µM was not the true physiological concentration experienced by cells. In retrospect, dose response experiments should have been conducted to fully determine the ability of ATP to activate NFAT in unwounded keratinocytes.

6.4.11 Gap-junctional communication in cell migration during wound closure.

Data generated within this chapter showed that blockade of gap-junctional communication completely prevented wound closure in keratinocytes. From this it was concluded that intercellular communication between cells following wound was necessary for effective cell migration to close the wound. Combined with other results presented within this project, it is likely that the calcium wave triggered immediately post-wounding is an important contributing factor. In agreement with this present study, $Cx43^{-/-}$ mice fibroblast also showed reduced migration. The authors suggested this was due to dysregulation of the microtubule organisation and adverse effects on cell polarity (Francis *et al.*, 2011). However, other studies with similar findings are limited. As alluded to in section 1.4.4, it is generally accepted in the field that the down-regulation of gap-junctions, in particular Cx43, is a pre-requisite for the promotion of cell migration, such that decreased coupling between cells at the wound edge allows for the phenotypic switch to migrate across the wound bed (Kretz *et al.*, 2003). However, there are reports that Cx26 is temporally up-regulated at the wound edge (C. M. Wang *et al.*, 2007) , highlighting the various effects of different connexins in wound healing responses. Interestingly, the timing of the down-regulation of Cx43 at the wound edge post-wounding *in vivo* is controversial and reports vary between two hours and two days (Becker *et al.*, 2012). Even if the reduction in Cx43 occurred at the earliest suggested time of two hours, this would still allow for the propagation of the wave and the

occurrence of calcium oscillations. In retrospect, the additional experiment of wounding untreated keratinocytes and thus allowing calcium wave transmission, followed by the addition of 18αGA two hours post-wounding would been interesting to conduct. These results would have helped decipher contributing factors to cell migration. Furthermore, chronic inhibition of gap-junctional communication or knockdown of connexins is not realistic of *in vivo* signalling. In reality, expression occurs cyclically; therefore long-term prevention may induce a stress response. Having said this, toxicity assays conducted during this project confirmed 18αGA was not detrimental to keratinocyte cell viability at the concentrations used (Appendix D). Another possible explanation for the different results seen within is the body site from which cells were isolated. There are limited studies investigating this specifically, however, whilst there are no differences in expression of connexins between the ear and tail, it is possible that intercellular coupling may be different (Kretz *et al.*, 2003). Indeed, it is known in humans that non-healing wounds are more prominent on the lower legs compared to the rest of the body, it may be that differential connexin expression and/or intercellular communication is the reason for this clinical observation. Repeating the experimental protocols conducted herein on primary human keratinocytes isolated from body sites other than foreskin would provide insights into this.

18αGA is a routinely used compound to analyse the effect of gap-junctions in signalling cascades. Whilst it has been reported to be specific to Cx43 through a non-direct phosphorylation mechanism, general consensus within the field is that it blocks gap-junctional communication non-selectively. Future work to further confirm the role of gap-junctions in keratinocyte wound closure would include assessment of the expression patterns of Cx43 and Cx26, the connexins most commonly linked to wound healing in the epidermis (Goliger and Paul, 1995). Taking this further, knockdown of Cx26 and Cx43 using RNAi would provide insights into the specific role these connexins play in cell migration.

Research to date has focussed less on the contribution of pannexins to wound healing responses. Intriguingly, pannexin-1 has been shown recently to be up-regulated following wounding. Furthermore, pannexin-1 knockout mice showed delayed wound healing responses (Silvia Penuela *et al.*, 2014). Since connexins have been

demonstrated to play a dominant role in cutaneous wound healing responses within this project, it would be of further interest to investigate the contribution of pannexins.

It is difficult to interpret specific signalling pathways that are being affected by pharmacological inhibition of gap-junctions because they are vital to such a range of responses. For example, it is possible that expression patterns of different connexins within the skin regulate the signalling pathways of interest within this project; calcium signalling immediately post-wounding, NFAT activation and cell migration. As mentioned above, connexin-specific manipulation in the future should provide further details.

6.4.12 Differential characteristics of cells located at varying distances from the wound edge in co-ordinating wound closure.

This project has not explored wound closure beyond the effect of SOCE inhibition, extracellular ATP removal and gap-junctional blockade on scratch wounding assays. It would be highly interesting to investigate in detail cells located at varying locations from the wound edge. By imaging cells in areas of interest at higher magnifications it would be possible to assess phenotypic and morphological changes induced by wounding. It would then be possible to characterise the role played by different cells in wound closure depending on cell location from the wound edge. Studies, such as that conduct by Farooqui *et al*. aimed to analyse the movement of cells as a continuous sheet in wound closure rather than the migration of cells as single entities. Findings showed that cells located distal to the wound edge responded to wounding by extending lamellipodia underneath the cells in front, indicating that these cells actively generate a migratory machinery rather than passively following the leading row of cells. Interestingly, the authors note that manipulation of calcium signalling, extracellular ATP or gap-junctional communication had no effect on their data (Farooqui and Fenteany, 2005). This result is surprisingly considering the vast amount of evidence that implicates these signalling pathways in cell migration and proliferation. This study was conducted on canine kidney cells, which are accepted to be a readily available model for studying epithelial wound responses. However, it is probable that enormous differences exist between these cells and primary human keratinocytes, making results difficult to translate regarding reepithelialisation during cutaneous wound healing. Additionally, tracking individual cells during wound closure would enable conclusions to be drawn

relating to cell location from the wound and the role played in wound closure. In urothelial cell monolayers, such investigations have shown that cells located near the wound (3-4 rows from the wound edge) moved twice as far as those cell located further back (15-20 rows from the wound edge) suggesting cells at the wound edge migrated faster than those further back. This data confirms *in vivo* findings that during reepithelialisation keratinocytes become detached and migration across the wound bed. The following cells then proliferation to ensure there are sufficient cell numbers for repair. The authors concluded that these results may occur as the cells located near the wound experienced increased intracellular calcium responses compared to cells located further back (Stiber *et al.*, 2008). This project has shown an important role for the wound-induced intercellular calcium wave in the regulation of downstream transcriptional and functional events. Therefore, it is possible that this result may stand true in keratinocytes.

6.5 Conclusions.

- Wounding induces the activation of NFAT through SOCE-mediated calcium influx.

- Whilst intercellular calcium wave propagation is a pre-requisite for NFAT activation, extracellular ATP does not regulate transcriptional activity.

- Wound closure occurs faster in high external calcium.

- Cell migration is marginally driven by both SOCE and extracellular ATP, although there is a clear dominant effect of gap-junctional communication in wound closure.

Chapter 7.

Discussion

7 Chapter 7. Discussion.

7.1 Temporal and spatial analysis of calcium signalling following wounding.

This project aimed to characterise the propagation of the wound-induced intercellular calcium wave. As this signalling cascade occurs immediately post-wounding, the imaging period of twenty minutes was sufficient. Within such experiments, an attempt was made to spatially and temporally assess the intracellular calcium wave spreading through individual cells in order to support evidence regarding mechanisms regulating the spread of the intercellular wave. It was also of interest whether the intracellular calcium wave was affected by cell location from the wound edge. Unfortunately, it was concluded that the capture speed was not fast enough to gain maximal information to robustly investigate this. Future work would be to image for a shorter period of time (it is now known that $[Ca^{2+}]_o$ returns to baseline within three minutes) but at a faster capture rate than 3.7fps. Analysis could then be conducted by drawing ROI within a cell of interest and assessing spread of the calcium through the cell. In a similar manner, capturing at an increased rate for a longer period of time would allow the same analysis to be conducted on oscillating cells. It would be interesting to analyse whether the calcium signal within an oscillating cell originates at the membrane closest to the wound edge. Again, this would provide further information regarding mechanisms regulating the calcium wave and downstream oscillations.

An interesting observation within this investigation was that not all cells oscillated following wounding (figure 5.2) and similarly not all cells responded to CM/ATP with an intracellular calcium flux (figure 4.4 and figure 4.16 respectively). Characteristics of these responding cells were not determined within this project; however, it is likely that these sub-population of keratinocytes possess unique characteristics and represent a discrete subset of cells. It is possible that these cells are more stem cell like or progenitor cells compared to the cells that did not respond to ATP/CM or oscillate following wounding. To test this hypothesis, florescent activated cell sorting (FACS) could be conducted on the heterogeneous population of keratinocytes to split the cells into stem cells, transient amplifying cells and terminally differentiated cells based on expressed of α6-integrin and CD71. It is known that stem cells have high levels of α6-integrin and low levels of CD71, transient amplifying cells have high levels of α6-integrin and high levels of CD71 and terminal differentiating cells have low α6-integrin

levels and do not express CD71. Once the keratinocytes had been sorted, scratch wounding assays could be conducted as previously described or ATP could be added at the physiologically relevant wounded concentration of 1µM. If a specific population of keratinocytes i.e. the stem cells showed increased calcium oscillations or increased response to ATP/CM this would suggest that the differentiation status of the keratinocyte determined intracellular calcium responses. Another possible explanation is that the cell surface expression of purinergic receptors varies between sub-populations of cells. It was not determined within this project what purinergic receptors where mediating the ATP-induced intracellular calcium flux, however, it could be hypothesised that the expression of these receptors were only expressed on a sub-type of cells and therefore a response was only detected in these cells.

Imaging was only conducted for twenty minutes which was an adequate time frame to characterise the wound-induced calcium wave as well as observe calcium oscillations. However, the extension of the imaging period would provide interesting insights linking the acute calcium signalling events and downstream transcriptional and functional events. For example, it would be possible to investigate how long the oscillations continued for following wounding. Whilst, due to issues with dye leaking and photo bleaching, long term imaging may be problematic, the use of genetically encoded calcium indictors (GECI) instead of florescent dye reporters may prove advantageous in future experiments.

Chifflet *et al*. have shown that, as expected, wounding bovine corneal endothelial cells resulted in a fast calcium wave which began immediately after wounding and spread from the wound edge back across the cells lasting approximately five minutes. Intriguingly, a prolonged imaging period also demonstrated that thirty minutes following the initial fast wave, a second slower wave was detected. Again, this wave originated at the wound edge and spread back through the cells. Although the exact role of the second wave is unknown, the authors suggest the wave occurs simultaneously to plasma membrane depolarisation in cells at the wound edge which may regulate migratory responses (Chifflet *et al.,* 2012). This novel data is highly interesting and provides evidence to warrant longer imaging periods following wounding.

Calcium indicators such as Fluo4-AM are a type of calcium chelator that has florescent properties. They bind to calcium in a selective manner via carboxylic groups. The

dissociation constant (kd) of a dye describes how tightly it binds calcium ions and is measured in molar units. The molar units correspond to the concentration of calcium at which half the indicator molecules are bound with calcium at equilibrium. Fluo4-AM has a kd of 335nm and therefore demonstrates a relatively high affinity for calcium ions. An issue with calcium dyes not addressed within the experimental design of this project is saturation. There was no indication from the 2D images generated during calcium experiments that calcium saturation was a problem. However, when 3D surface plots were created using ImageJ it was noted that at 10 seconds post-wounding, the calcium signal within cells at varying distances from the wound edge appeared to be maximal and therefore this may represent saturation (figure 3.5). In other words, all the calcium indicator molecules were bound to calcium and as such no further cytosolic calcium could bind. If this was the case, then data provided for parameters such as maximum Ft/F0 may not be truly representative of the actual levels of calcium in the cytoplasm. However, analysis of the raw data generated by Volocity after quantification of individual cells did show a significant linear trend for a decreasing maximum Ft/F0 with increasing distance from the wound edge, suggesting that data generated was representative of cytosolic calcium levels. If calcium dye saturation was occurring in a manner that "capped" the quantification of the calcium signal, it would be expected that the maximal Ft/F0 reported for individual cells would be more consistent. Nevertheless, there are some important experiments that would need to be conducted in future investigations to fully conclude that calcium dye saturation is not affecting the results. These include further optimisation of the imaging settings on the confocal microscope. For example, keratinocytes could be treated with Tg to induce a large calcium response, during this period the power of the argon laser could be increased/decreased accordingly to ensure that the microscope was capturing images at a suitable level. The intensity of the argon laser would have to be adequate to capture unstimulated intracellular calcium levels as well as induced intracellular calcium flux. Alternatively, experiments could be repeated using a calcium dye with a lower kd and therefore a higher affinity for calcium. If the same results were observed it could be concluded that Fluo4-AM was not reaching saturation and that the data generated was accurate of the cytosolic calcium concentration. On the other hand, if the values for the maximum Ft/F0 were increased within individual cells, this could be indicative that Fluo4-AM was reaching saturation and therefore providing inaccurate data regarding cytosolic calcium concentration.

7.2 Methods for investigating SOCE.

As alluded to previously, routine SOCE pharmacological inhibitors are complexly discouraging especially in keratinocytes (Section 3.1.3). However, this project has provided robust data supporting the use of GSK-7975A to block SOCE in human primary keratinocytes. Thus providing a useful tool to further investigate the role of SOCE in epidermal homeostasis as well as dermatological disorders, including wound healing. STIM1 siRNA and the dominant negative R91W mutant form of Orai1 have both been used previously in keratinocytes (Ralph Jans *et al.*, 2013) and would be useful tools to utilise in further experiments following on from this project. Moreover, last year Cox *et al.* highlighted the generation of a specific anti-Orai1 monoclonal antibody. As well as being an advantageous tool in the characterisation of Orai1 expression in a variety of cells, this antibody successful reduced proliferation and pro-inflammatory cytokine production in T-cells (Cox *et al.*, 2013).

Whilst the identity of STIM and Orai families of proteins have been known for nearly a decade, mechanisms regulating translocation and interactions at the plasma membrane are only now becoming apparent. Last year a siRNA screen for NFAT activation discovered septin filaments as crucial regulators of SOCE. Septins are necessary for the organisation of Orai1 in the PM as well as the maintenance of the STIM1/Orai1 complex. Furthermore, Septin 4 siRNA reduced calcium-induced NFAT activation in HeLA cells to a similar extent to that seen with siRNA directed towards STIM1 and Orai1(Sharma *et al.*, 2013) .Whilst investigations into septins where not possible during the scope of this project, given a) the recent finding indicating the key role they play in SOCE and b) the importance of SOCE in epidermal wound healing responses presented herein, it would be of interest to assess the contribute of septin filaments in the intercellular calcium wave induced by wounding, NFAT activation and cell migration in keratinocytes.

7.3 The use 3D skin equivalent models for investigating wound healing responses.

This project utilised a widely accepted 2D keratinocyte monolayer model for the exploration of wound healing responses. Whilst extremely beneficial and necessary to dissect the relative contribution of distinct signalling pathways, it is important to

appreciate that this model does not truly represent an *in vivo* environment. However, wound healing investigations *in vivo* in humans are limited by ethics. More recently, advances have been made in the use of animal models for cutaneous wound healing research such as zebra fish (Richardson *et al.*, 2013). As discussed previously (Section 1.2.5), although animal models are advantageous, many differences exist between humans that can significantly affect wound closure, therefore results should be interpreted with caution.

Epidermal skin equivalents have been shown to be beneficial in assessing the morphological effects of both genetic manipulation and topical treatment with compounds (A. R. Forrester *et al.*, 2014). Although extremely useful, this model does not encompass a dermal layer. Fibroblasts are known to play an important role in wound healing events and therefore it would be naïve to exclude these cells in a 3D context. Although full thickness skin equivalents which incorporate a functioning epidermal and dermal layer are established, these have historically been used in melanoma and burn studies and the scaffolds used are unable to withstand a reproducible wound. One wound healing model has been proposed utilising a de-epidermised dermis (DED) as a scaffold. However, the limitations of this study are that the authors seeded keratinocytes into two steel rings and once the cells had stratified the rings were removed. Whilst providing useful insights into cell migration to close a wound, it did not actually demonstrate a wound healing response (MacNeil *et al.*, 2011). There are vast amounts of evidence both within this project and in the literature which showed that wound acquisition is important in the regulation of downstream events, examples of which are the wound-induced calcium wave and the cellular release of ATP. Therefore, there is a need for a full thickness 3D skin equivalent model that can be used in the investigations of wound healing responses. Recently, this need has been met by the development of collagen skin equivalent models (DL Johnson, 2014).

Work leading on from the data obtained within this project would involve the translation of 2D results into a 3D environment. The contribution of gap-junctional communication, extracellular ATP and SOCE as well as the role of NFAT could be investigated both through topical treatment and genetic knockdown of proteins of interest in the keratinocytes and/or fibroblasts prior to equivalent construction. For example, individual members of the NFAT family of transcription factors could be

knocked down using lentivirus to consider the effect of each isoform in reepithelialisation in more physiologically relevant environment.

Fibroblasts have been shown to play a key role in wound healing events; indeed the proximity of the physiological location of the dermis and the epidermis is highly indicative of this. *In situ*, cross-talk between keratinocytes and fibroblasts has been documented, as reviewed by Menon *et al.* (S. N. Menon *et al.*, 2012). Signalling pathways were not explored in fibroblasts within this project. However, it would be highly interesting to conduct similar CM experiments to those presented herein, whereby keratinocytes would be wounded, wounded media collected and added to unwounded fibroblasts and vice versa. These experiments would provide useful insights into the cross-talk between keratinocytes and fibroblasts during wound closure.

7.4 Use of ATP scavengers in wound healing investigations.

Hexokinase is a common scavenger used to scavenge ATP and prevent binding to P2R thus providing a useful tool for exploring the effect of ATP on signalling cascades such as those used within the current study; intercellular calcium wave propagation, NFAT activation and cell migration to close a wound. However, the product of ATP degradation by hexokinase is ADP. ADP is known to activate a subset of purinergic receptors and elicit cellular responses. Whilst this project did not aim to investigate specific receptors, future work would involve analysis of the relative contribution of different receptors activated by wound-induced ATP, therefore, forthcoming investigations into the specific receptors will need to be performed in the presence of an ADPase to eliminate both ATP and ADP from the media (Schwiebert and Zsembery, 2003).

7.5 Alternative roles for calcium in wound healing.

It is known that during the wound healing process an endogenous electric field is generated, with a maximum value at the wound edge. This electric field is believed to regulate the directionality of wound closure. Additionally, it has been shown that keratinocyte exposure to an electric field of physiological relevance induced an intracellular calcium signal mediated through calcium entry from the external space (Dubé *et al.*, 2012). In a similar manner, it has been previously shown that removal of extracellular calcium prevents the directional migration of keratinocytes in an electric

field (Fang *et al.*, 1998). Moreover, blockade of specific calcium channels significantly inhibited the directional migratory response (Trollinger *et al.*, 2002). These studies provide further evidence for a role in calcium signalling in wound healing.

Arguably the most comprehensive role for calcium signalling post-wounding is the regulation of keratinocyte migration and proliferation during reepithelialisation. This phenomenon has been studied in various cell types and data presented herein confirm a dominant role in keratinocytes. Recently, an alternative function for calcium signalling in wound healing has been proposed. Using drosophila embryos, Razzell and co-workers demonstrated for the first time that the wound-induced calcium wave also mediated the inflammatory phase of wound healing; the phase preceding reepithelialisation. Prior to this study it was known that hydrogen peroxide (H_2O_2) was involved in the recruitment of inflammatory cells to the wound within the first few minutes post-wounding, through activation of the NADPH oxidase DUOX. However, it was not known how wounding activated DUOX. This studied observed that blockade of gap-junctional communication prevented the calcium wave spreading back. Furthermore, H_2O_2 release was prevented as was subsequent migration of immune cells to the wound (Razzell *et al.*, 2013). The inflammatory phase is the first phase of the wound healing process and this publication represents a novel mechanism for calcium in regulation of wound healing in addition to reepithelialisation.

The formation of desmosomes and adherens junctions, two distinct junctional structures in the epidermis, is dependent on extracellular calcium. Keratinocytes can be cultured in vitro in a low calcium environment (0.1mM) and cells resemble those in the proliferative basal layers of the epidermis. Additionally, cells grow as small colonies, they do not express cell-to-cell connections and the borders of each individual cell are distinct as shown by phase-contrast microscopy. Interestingly, in these low calcium culture conditions keratin intermediate filaments are most dense near the nucleus and very few are detected near the cell membrane. There are no desmosome, hemidesmosomes or adherens junctions between cells. When the extracellular calcium concentration is increased to above 1.2mM a signalling cascade is initiated whereby the monolayer of individual keratinocytes is changed into a contiguous epithelial sheet of differentiated keratinocytes connected by adherens junctions. Whilst this complete process can take approximately 24 hours, the first calcium-induced changes have been

reported as early as 15 minutes following the increase in extracellular calcium. O'Keefe and co-workers showed using phase-contrast microscopy that after a 15 minute exposure to 1mM $[Ca^{2+}]_o$ cell borders had begun to fuse and cells associated more closely, 20 hours cells started to overlap and stratify. Vinculin is a membrane-cytoskeletal protein in focal adhesion plaques that is involved in linkage of integrin adhesion molecules to the actin cytoskeleton. Immunofluorescence showed that within 15 minutes of raising the extracellular calcium concentration, vinculin-containing plaques moved to the cell periphery in colonies of cells in which cell borders were close. As the cells developed contacts, vinculin was observed at high intensity at junctional areas between cells. Similarly, desmosomes are fully formed by 5 hours following exposure to medium containing 1mM $[Ca^{2+}]_o$ (Edward J. O'Keefe, 1987). It is known that keratinocytes express 2 cadherin proteins; E-cadherin and P-cadherin which are cell-to-cell adhesion proteins in adherens junctions. Moreover, blockade of cadherin activity prevents the redistribution of adherens junction and desmosome markers to the cell border even following 2 days of exposure to 1mM $[Ca^{2+}]_o$ and keratinocytes in these conditions fail to stratify (Lewis *et al.*, 1994). This study suggests that adherens junction proteins are vital to calcium-induced formation of adherens junction and desmosomes and consequently epidermal stratification.

Within this project, keratinocyte monolayers were exposed to 1.2mM $[Ca^{2+}]_o$ calcium for up to 24 hours. Experiments investigating wound-induced calcium signalling exposed keratinocytes to 1.2mM $[Ca^{2+}]_o$ for 5 minutes prior to wounding. The effect of high calcium on primary human keratinocytes for this relatively short period of time is unknown, although having a documented effect at 15 minutes following exposure suggests that redistribution of adherens proteins may already have started within the first 5 minutes. Therefore, the effect of adherens junctions and desmosomes formation on the spread of the calcium wave should not be overlooked. It is possible that the formation of these cell-to-cell connections between keratinocytes are responsible for the differences observed in intracellular calcium fluxes when wounding in high external calcium conditions compared to low.

Whilst the role of adherens junctions in intracellular calcium signalling is less known compared to other cell-to-cell communication pathways such as gap-junctions, there is evidence to suggest that adherens junctions are involved in the secondary messenger

signalling such as intracellular calcium flux. For example, it was shown in fibroblasts that stretch-induced influx of calcium was dependent on adherens junctions; treatment with antibodies against the proteins within these junctions reduced the calcium flux. Additionally, it was demonstrated that inhibition of gap-junction communication did not affect stretch-induced calcium influx in these cells; adherens junctions were more dominant (Ko *et al.*, 2001). Moreover, cadherins, the proteins which make up adherens junctions, have an extracellular calcium binding site and are dependent on calcium to function. This knowledge proposes an important link between calcium and adherens junctions in epithelial cells (Perez-Moreno *et al.*, 2003).

To analyse this further, keratinocytes could be exposed to 1.2mM $[Ca^{2+}]_o$ for a longer period of time prior to wounding and calcium imaging, for example 6 hours. During this time adherens junctions and desmosomes would form connections between cells. Monolayers could then be wounded in a similar manner to that conducted previously and the spread of the wave could then be analysed. This would provide more information regarding the importance of these connections of calcium wave propagation.

For NFAT luciferase and migration assays, keratinocyte monolayers were wounded in the presence of 0.06mM $[Ca^{2+}]_o$ or 1.2mM $[Ca^{2+}]_o$ for 24 hours. In both experiments significant differences were observed when wounding in high or low external calcium conditions. The reasons for these differences are discussed previously; however, it is also possible that the presence of adherens junctions and desmosomes induced by the increase in extracellular calcium are also influencing signalling.

Adherens junctions are fundamental in the ability of individual cells to form cohesive sheets of epithelial cells and thus function as a coordinated tissue. These junctions facilitate cell shape, polarity, spatially orientated mitotic spindle planes and actin filaments in the cytoskeleton. Thus, making them important regulators in cell movement (Perez-Moreno *et al.*, 2003).

Calcium-induced adherens junction and desmosome formation were not specifically studied within this project. In retrospect, given that keratinocytes were treated in 1.2mM $[Ca^{2+}]_o$ for a range of times from 5 minutes to 24 hours, it would have been useful to investigate the effect of adherens junctions and desmosomes on intercellular calcium

signalling following wounding in high calcium, wound-induced NFAT transcriptional activation and keratinocyte cell migration to close a wound.

7.6 The function of healed skin post-wounding.

To date, research has focused on understanding mechanisms initiating and regulating wound healing responses such as reepithelialisation. A less studied area has been the function of the healed skin. Whether recently healed skin functions in the same manner as normal skin is a highly interesting concept. Due to the fact that even the normal wound healing process can take years, it is likely that difference will exist. It would be of interest to wound keratinocyte monolayers, wait for the wound to close and then wound again, assessing factors such as the intercellular calcium wave and ATP release. A similar approach was taken by Grygorczyk *et a*l. who studied the release of ATP post-unidirectional stretch in human alveolar A549 cells. Results demonstrated that stretch induced ATP release in a dose dependent manner. Repeating these experiments on cells that had previously been wounded and allowed to heal showed a significant increase in ATP release compared to unwounded cells (Grygorczyk *et al.*, 2013).

The wound healing process can lead to the pathogenesis of skin disorders. For example, the koebner phenomenon can occur in variety of conditions including psoriasis whereby psoriatic lesions develop on the site of trauma (Djalilian *et al.*, 2006). An interesting link between cutaneous wound healing and the development of psoriasis is ATP. Results within this project have shown that wounding results in release of ATP from keratinocytes into the extracellular space. Further, it is known that purinergic signalling through ATP binding can cause keratinocyte proliferation. It would therefore be of interest to investigate the role of wound-induced ATP in the characteristic hyperproliferation of cells observed in psoriasis. Additionally, there have been reports of injury and/or chronic wounds preceding skin cancers such as basal and squamous cell carcinomas (Trent and Kirsner, 2003). It is perhaps non-surprising that wound healing can trigger carcinoma development given that the fundamental concept of wound closure is the migration and proliferation of cells. Whilst, this is necessary for efficient wound healing responses, the presence of an effective “off” switch has to be prominent in order to prevent tumour development or keloid scar formation.

7.7 Clinical relevance.

Although both acute and chronic wounds are major clinical problems resulting in a significant burden financially to the NHS and to the patients QoL (section 1.2.2), there is a lack of effective cell-based therapies to treat such conditions (section 1.2.4).

Novel data generated within this project has highlighted interesting interactions between acute signalling events that occur within seconds following wounding and downstream longer-term transcriptional and functional events. Studies investigating factors that regulate these responses may facilitate the development of targetted therapies for improved cutaneous wound healing.

The experimental design adopted in this project was to pre-treat keratinocyte monolayers with the specified compound prior to wounding. This has proved to be an extremely beneficial technique in the dissection of signalling pathways involved in wound healing. However, in retrospect, parallel experiments would have been conducted whereby untreated cells were wounded and the compound added at particular time points following wounding. This approach would be more realistic in analysis the potential of therapeutic targets.

Chapter 8.

Concluding Remarks

Chapter 8. Concluding Remarks.

This thesis aimed to characterise the spread of the wound-induced intercellular calcium wave in primary human keratinocytes and to investigate the downstream transcriptional and functions consequences of this. Whilst it is known that a calcium gradient exists within the epidermis and that calcium regulates keratinocyte growth and differentiation (events crucial to wound healing), the challenge to date has been the integration of these signalling pathways in space and time. There is an enormous unmet medical need and requirement for novel effective therapies for the treatment of both acute and chronic wounding.

There are two main current theories for the regulation of calcium waves; extracellular purinergic signalling through ATP release and intercellular propagation through gap-junctions. The relative contribution of these pathways as well as the dependence on extracellular calcium entry through SOCE was investigated on three signalling levels i) wound-induced intracellular calcium flux within cells at specified locations from the wound edge, ii) wound-induced NFAT transcriptional activation and iii) keratinocyte cell migration.

It can be concluded from these studies that calcium entry from the extracellular space is a major determinant for wound-induced responses in keratinocytes. Wounding in 1.2mM $[Ca^{2+}]_o$ resulted in an increased intracellular flux within cells located away from the wound edge; no difference was seen within cells at the immediate wound edge. This suggests that the calcium source for the initiation of the wound-induced wave in cells close to the wound was intracellular. Whereas in cells further away there was a dependency on extracellular calcium. Interestingly, this calcium entry mechanism was not shown to be regulated by SOCE mechanisms. Treatment with the novel GSK-7975A SOCE inhibitor, which was highly effective at blocking SOCE in keratinocytes, had no effect on parameters of the wound-induced intracellular calcium flux. However, removing extracellular ATP, reduced the elevated intracellular calcium flux observed in 1.2mM $[Ca^{2+}]_o$ and had no effect on intracellular calcium flux in 0.06mM $[Ca^{2+}]_o$. It can be postulated therefore, that the mechanism resulting in the influx of calcium from the extracellular space, was regulated by ATP-mediated non-SOCE dependent mechanisms. Future work will delineate site and mechanisms of ATP release, ATP receptors and ATP-initiated pathways involved following wounding. The observation that the spread

of the calcium wave near to the wound edge was not dependent on extracellular calcium was suggestive of an intracellular calcium source propagating through intercellular conduits. This was confirmed by blocking gap-junctional communication using 18αGA. Inhibiting gap-junctional communication prevented the spread of the intracellular calcium wave back from the wound edge. Collectively, data shows that in primary human keratinocytes, the wound-induced intracellular calcium flux is regulated by both extracellular ATP released from keratinocytes following wounding and the propagation of a mediator through gap-junctions. Although not specifically investigated within this project, this mediator is likely to be IP_3.

Interestingly, calcium oscillations were observed following the initial calcium flux, but only in a high calcium environment. The occurrence of these oscillations were supported by SOCE, as determined by a reduction in percentage of cells oscillating when blocking SOCE with GSK-7975A. Removal of extracellular ATP also significantly reduced the percentage of cells oscillating in 1.2mM $[Ca^{2+}]_o$ suggesting that either ATP regulates the calcium entry initiating the oscillations, or alternatively, the decreased number of cells oscillating is a consequence of reduced intracellular calcium flux during the wave leading to reduced initiation of SOCE pathways. However, the latter is more likely as blocking gap-junctional communications, which prevented the spread of the calcium wave, also abrogated oscillations. It can therefore be concluded that the intercellular calcium wave initiated by mechanical wounding, is a pre-requisite for the later occurring calcium oscillations. Experiments where high calcium was added-back to keratinocytes wounded in low calcium revealed two distinct forms of calcium response; a SOCE-dependent oscillatory pattern and a SOCE-independent prolonged flux. The transcriptional and functional consequence of these were not determined in this study, although parallel add-back experiments conducted to analyse NFAT activation would be advantageous in the future. A surprisingly finding was that add-back of high calcium to cells wounded in low calcium in the presence of 18αGA trigged a prolonged calcium flux in the majority of cells. It was therefore postulated that the intracellular calcium flux following wounding initiates a negative feedback mechanism. This has not previously been investigated in relation to wounding, however, the preliminary data presented within warrants further investigation.

The NFAT family of transcription factors is known to be regulated by SOCE in keratinocytes, however, its role in wound healing responses were unknown. It was shown in this present study that wounding activates NFAT but only in 1.2mM $[Ca^{2+}]_o$. NFAT transcriptional activity was dependent, at least in part on SOCE, as confirmed by a significant reduction when treating with GSK-7975A. Wounding in the presence of hexokinase did not attenuate transcriptional activity and the addition of ATP at a physiologically relevant concentration to unwounded keratinocytes did not induce NFAT transcriptional acrivation. Therefore it can be concluded that extracellular ATP released by keratinocytes following wounding does not have a role in NFAT activation. The propagation of the calcium wave through the population of cells appears to be important for downstream transcriptional activation, as determined by a reduction in wound-induced NFAT when wound was performed in the presence of 18αGA.

Akin to all other signalling pathways presented within this study, extracellular calcium promoted cell migration during the closure of the wound; wounds closed significantly faster in 1.2mM $[Ca^{2+}]_o$ compared to 0.06mM $[Ca^{2+}]_o$. The increased cell migration in 1.2mM $[Ca^{2+}]_o$ was marginally reduced by SOCE inhibition and removal of extracellular ATP. Therefore it can be concluded that calcium entry following wounding through SOCE-dependent mechanisms promotes keratinocyte migration. Similarly, ATP-dependent signalling also promotes keratinocyte migration, potentially through ATP-mediated calcium influx from the extracellular space. Inhibition of gap-junctions robustly prevented cell migration in both 0.06mM $[Ca^{2+}]_o$ and 1.2mM, providing further evidence that the calcium wave induced by wounding is crucial in long-term functional events.

In summary, whilst both purinergic and gap-junction signalling regulate the intracellular calcium flux, calcium wave and calcium oscillations post-wounding, there is a dominant effect of gap-junction communication in the activation of NFAT and cell migration. Studies to further determine mechanisms regulating each of these pathways in relation to epidermal wound healing and the translation of these into a 3D skin equivalent model, will hopefully lead to the development of cell-based therapies for the treatment of both acute and chronic wounds.

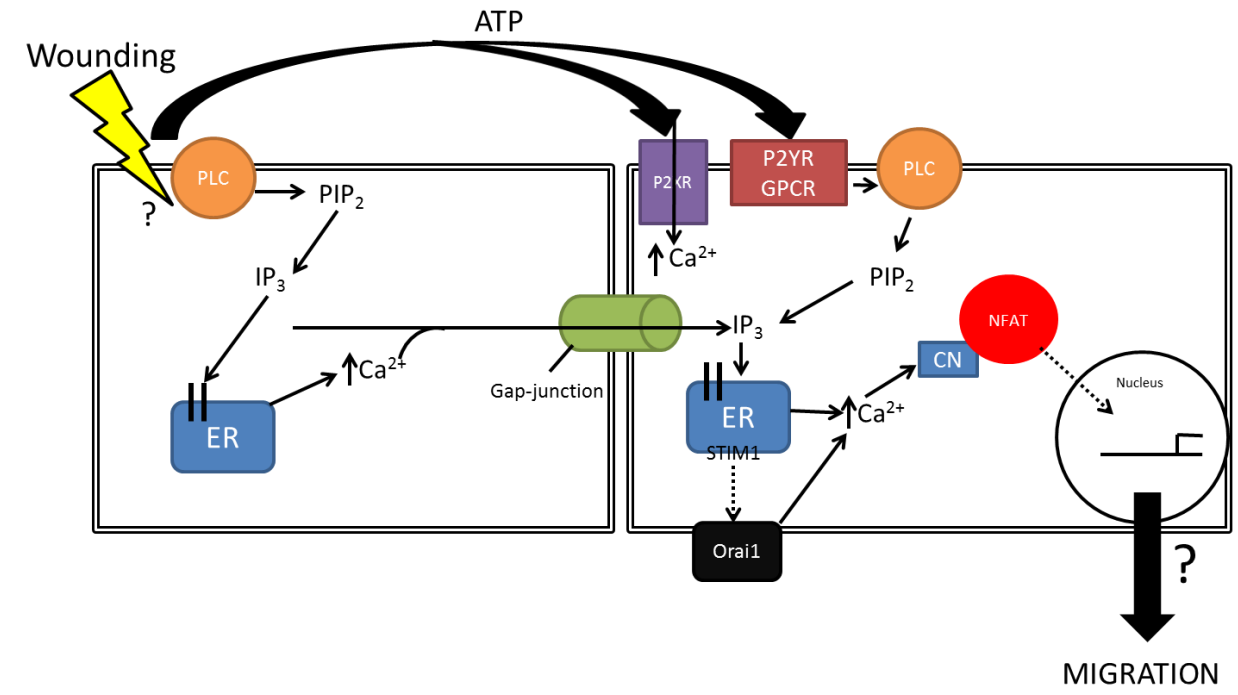

Figure 8.1. Schematic diagram of thesis findings.

The major findings from this investigation suggest that wounding activates 2 independent pathways which both contribute to calcium wave propagation. 1) ATP is released from damaged cells, probably through cell lysis and results in increased cytosolic calcium concentration through purinergic receptor signalling (P2YR and/or P2XR). 2) Through undetermined mechanisms, wounding activates the IP3 signalling pathway which results in calcium release from the ER. IP3 and/or calcium ions then move through the cell population via gap-junctions. This results in IP3-mediated release from the ER in the neighbouring cell. Depletion of calcium from the ER is detected by STIM1 which then translocates to the plasma membrane and oligomerises with Orai1, a selective calcium channel allowing entry of extracellular calcium into the cell. Increases of intracellular calcium activate the serine/threonine phosphatase calcineurin (CN), which dephosphorylates the transcription factor NFAT resulting in NFAT nuclear translocation. NFAT increases transcription of its target genes, which are currently undetermined, resulting in keratinocyte migration to close the wound. Data indicates that the extracellular ATP signalling pathway is required for wound-induced calcium wave propagation in keratinocytes, it has no effect on NFAT wound-induced NFAT activation and minimal effect on keratinocyte wound closure. Whereas the intercellular gap-junctional communication pathway appears to be required for the spread of the calcium wave following wounding, wound-induced NFAT activation and cell migration. In conclusion whilst both purinergic and gap-junctional signalling regulate the intracellular calcium flux and calcium wave post-wounding, there is a dominant effect of gap-junction communication in the activation of NFAT and cell migration.

APPENDICES

Appendices

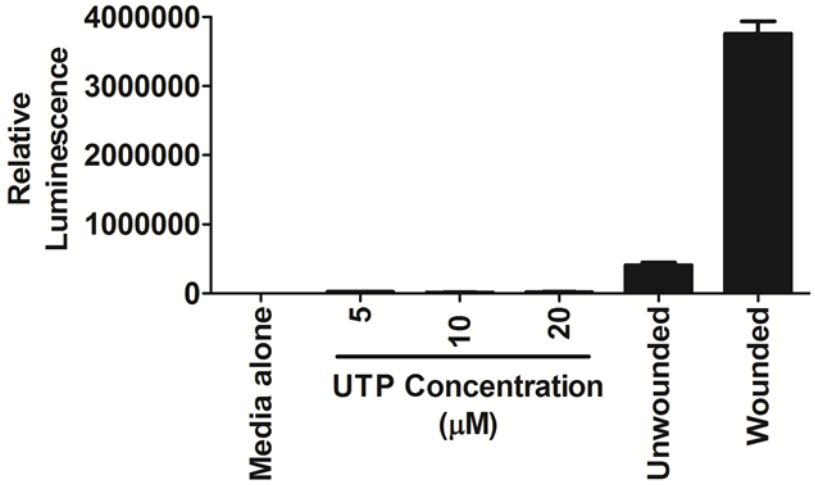

Appendix A. Luminescence assay is specific to ATP and MCDB 153 media does not auto luminesce.

MCDB 153, the media used in this project was tested using the ATP luminescence kit to ensure no positive readings due to the presence of phenol red in the media. To test for the kit's specificity to ATP, various concentrations of UTP were added to media and analysed. Unwounded and wounded samples of keratinocyte monolayers are shown as a reference to illustrate that neither media alone of UTP at any concentration resulted in a reading. It can therefore be assumed that the kit is specific to ATP. Data shows mean ± SEM and are representative of three experimental repeats.

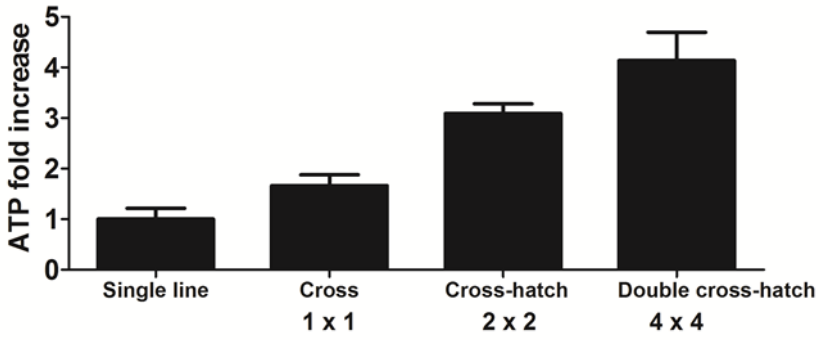

Appendix B. ATP release post-wounding correlates to amount of damage inflicted.

Primary human keratinocytes cultured in 0.06mM keratinocyte growth medium (MCDB 153) were scratch wounded with either single line, cross (1x1), cross hatch or double cross hatch (4x4). Five minutes post-wounding, 50µL sample of extracellular media was removed for analysis using the luminometer. Graphs show mean ± SEM and are representative of three donors in triplicate; N=3 (n=9).

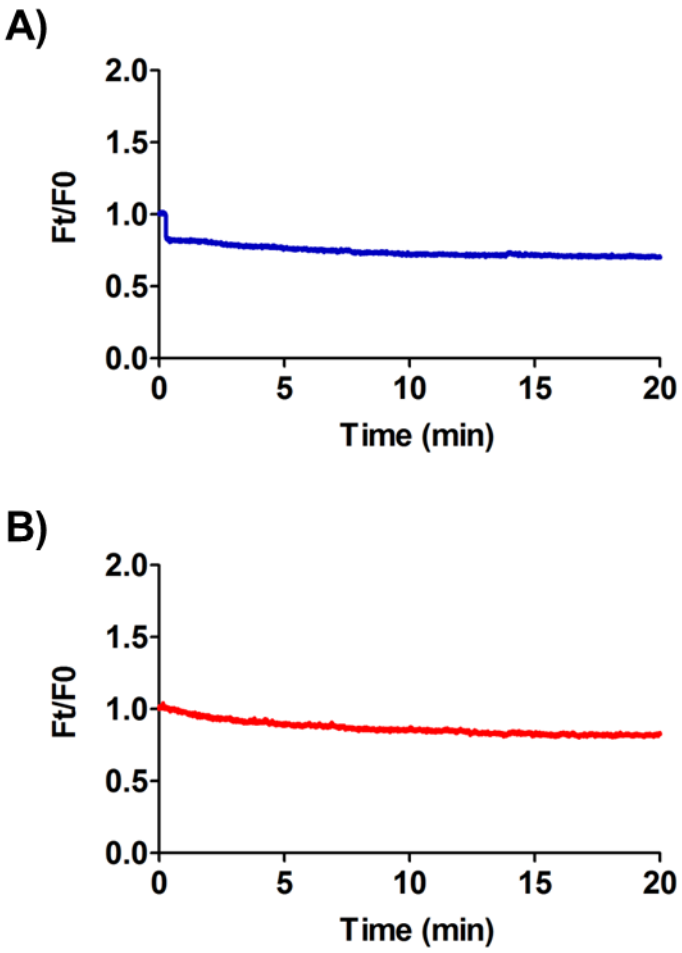

Appendix C. Unwounded cells do not display calcium fluxes.

Primary human keratinocytes cultured in 0.06mM keratinocyte growth medium (MCDB 153) were loaded with Fluo4-AM calcium dye. Post-de-esterification, either 0.06mM or 1.2mM $[Ca^{2+}]_o$ keratinocyte growth media (MCDB 153) was added for five minutes prior to imaging. Cells remained unwounded in either A) 0.06mM or B) 1.2mM $[Ca^{2+}]_o$. Traces are single cells, representative of three independent donors.

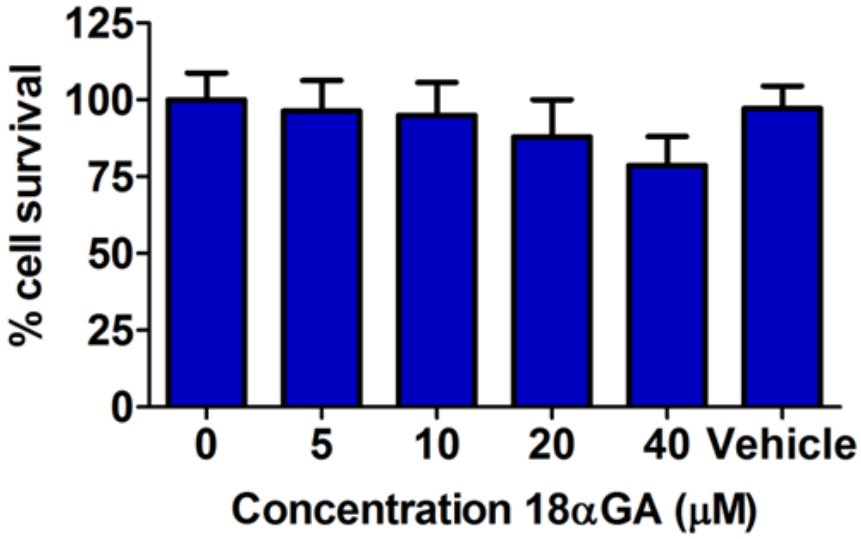

Appendix D. 18αGA is not toxic to keratinocytes at 24 hours.

Primary keratinocytes were treated with varying concentrations of 18αGA for twenty four hours. Cell viability was then analysed using SRB as described in materials and methods. Data shows mean ± SEM from 9 repeats from three independent donors (n=9), N=3. MTT assays were conducted in parallel and report the same result.

Publications, abstracts and prizes arising from this work.

Published manuscripts arising from this work:

1. Jans, R., Mottram, L., Johnson, D.L., Brown, A.M., Sikkink, S., Ross, K and Reynolds, N.J. (2013) 'Lysophosphatidic Acid Promotes Cell Migration through STIM1-and Orai1-Mediated Ca^{2+}_i Mobilization and NFAT2 Activation', *J Invest Dermatol*, 133(3), pp.793-802.

Published abstracts arising from this work:

1. European Society for Dermatology Research (ESDR), September 2014, Copenhagen, Denmark *(Oral presentation).*
   The dominant effect of gap-junction communication in mediating wound-induced calcium wave, NFAT activation, cell migration in wound closure in human keratinocytes. **Mottram L,** Begg M and Reynolds N.
2. British Society for Investigative Dermatology (BSID), April 2014, Newcastle, UK *(Oral presentation).*
   The role of store-operated calcium entry (SOCE) in epidermal wound healing responses. **Mottram L**, Begg M and Reynolds N
3. Internal Investigate Dermatology (IID), May 2013, Edinburgh, UK *(Poster presentation).*
   NFAT and NFkB activation and keratinocyte migration post-wounding is dependent on extracellular calcium concentration and SOCE. **Mottram L**, Begg M and Reynolds N
4. European Society for Dermatology Research (ESDR), September 2012, Venice, Italy *(Poster presentation).*
   Lysophosphatidic acid promotes cell migration through STIM1- and Orai1-mediated Ca^{2+}_i mobilization and NFAT2 activation. Jans R, **Mottram L,** Johnson DL, Brown AM, Sikkink S, Ross K, Reynolds, NJ

Unpublished abstracts arising from this work:

1. North East Stem Cell Institute (NESCI) Annual conference, January 2014, Newcastle: "The role of SOCE in wound-induced calcium oscillations" Oral presentation.
2. Gordon Research Seminar and Conference: Calcium Signalling, June 2013, Italy: "The role of SOCE in wound-induced calcium oscillations" Poster presentation.
3. North East Postgraduate (NEPG) Annual conference, October 2012, Newcastle: "Intracellular calcium signals, NFAT/NFκB activation and their role in epidermal wound healing responses" Oral presentation.
4. Institute of Cellular Medicine (ICM) Research Day, June 2012, Newcastle: "Intracellular calcium signals, NFAT/NFκB activation and their role in epidermal wound healing responses" Poster presentation.
5. NESCI, May 2012, Durham: Intracellular calcium signals, NFAT/NFκB activation and their role in epidermal wound healing responses" Poster presentation.

List of prizes awarded during this work:

1. Awarded best poster prize: ICM Research Day, June 2012.
2. Awarded ICM and NESCI travel grants to attend the Gordon Research Seminar and Conference in Barga, Italy. June 2013.
3. Awarded IHR/BAD research travel bursary to attend to European Society for Dermatology Research (ESDR) in Copenhagen, Denmark. September 2014.
4. Awarded ESDR travel award to attend the International Investigative Dermatology (IID) Conference in Edinburgh, Scotland. May 2013.

References

Abbracchio, M. P. and Burnstock, G. (1998) 'Purinergic signalling: Pathophysiological roles', *Japanese Journal of Pharmacology*, 78(2), pp. 113-145.

Abraham, E. H., Prat, A. G., Gerweck, L., Seneveratne, T., Arceci, R. J., Kramer, R., Guidotti, G. and Cantiello, H. F. (1993) 'The multidrug resistance (mdr1) gene product functions as an ATP channel', *Proc Natl Acad Sci U S A*, 90(1), pp. 312-6.

Ai, Z., Fischer, A., Spray, D. C., Brown, A. M. C. and Fishman, G. I. (2000) 'Wnt-1 regulation of connexin43 in cardiac myocytes', *Journal of Clinical Investigation*, 105(2), pp. 161-171.

Al-Daraji, W. I., Grant, K. R., Ryan, K., Saxton, A. and Reynolds, N. J. (2002) 'Localization of Calcineurin//NFAT in Human Skin and Psoriasis and Inhibition of Calcineurin//NFAT Activation in Human Keratinocytes by Cyclosporin A', 118(5), pp. 779-788.

Alfonso-Jaume, M. A., Mahimkar, R. and Lovett, D. H. (2004) 'Co-operative interactions between NFAT (nuclear factor of activated T cells) c1 and the zinc finger transcription factors Sp1/Sp3 and Egr-1 regulate MT1-MMP (membrane type 1 matrix metalloproteinase) transcription by glomerular mesangial cells', *Biochem J*, 380(Pt 3), pp. 735-47.

Andersen, L. I. S. (1980) 'Cell junctions in squamous epithelium during wound healing in palatal mucosa of guinea pigs', *European Journal of Oral Sciences*, 88(4), pp. 328-339.

Ansell, D. M., Kloepper, J. E., Thomason, H. A., Paus, R. and Hardman, M. J. (2011) 'Exploring the [ldquo]Hair Growth-Wound Healing Connection[rdquo]: Anagen Phase Promotes Wound Re-Epithelialization', *J Invest Dermatol*, 131(2), pp. 518-528.

Antunes, M., Pereira, T., Cordeiro, J. V., Almeida, L. and Jacinto, A. (2013) 'Coordinated waves of actomyosin flow and apical cell constriction immediately after wounding', *Journal of Cell Biology*, 202(2), pp. 365-379.

Appleby, P. A., Shabir, S., Southgate, J. and Walker, D. (2013) 'Cell-type-specific modelling of intracellular calcium signalling: a urothelial cell model', *Journal of The Royal Society Interface*, 10(86).

Ashmole, I., Duffy, S. M., Leyland, M. L., Morrison, V. S., Begg, M. and Bradding, P. (2012) 'CRACM/Orai ion channel expression and function in human lung mast cells', *J Allergy Clin Immunol*, 129(6), pp. 1628-35 e2.

Augustin, M. and Maier, K. (2003) 'Psychosomatic Aspects of Chronic Wounds', *Dermatology and Psychosomatics / Dermatologie und Psychosomatik*, 4(1), pp. 5-13.

Ay, A. S., Benzerdjerb, N., Sevestre, H., Ahidouch, A. and Ouadid-Ahidouch, H. (2013) 'Orai3 constitutes a native store-operated calcium entry that regulates non small cell lung adenocarcinoma cell proliferation', *PLoS One*, 8(9), p. e72889.

Azorin, N., Raoux, M., Rodat-Despoix, L., Merrot, T., Delmas, P. and Crest, M. (2011) 'ATP signalling is crucial for the response of human keratinocytes to mechanical stimulation by hypo-osmotic shock', *Experimental Dermatology*, 20(5), pp. 401-407.

Bandyopadhyay, B., Fan, J., Guan, S., Li, Y., Chen, M., Woodley, D. T. and Li, W. (2006) 'A "traffic control" role for TGFβ3: Orchestrating dermal and epidermal cell motility during wound healing', *Journal of Cell Biology*, 172(7), pp. 1093-1105.

Bao, L., Locovei, S. and Dahl, G. (2004) 'Pannexin membrane channels are mechanosensitive conduits for ATP', *FEBS Letters*, 572(1-3), pp. 65-68.

Barr, T. P., Albrecht, P. J., Hou, Q., Mongin, A. A., Strichartz, G. R. and Rice, F. L. (2013) 'Air-Stimulated ATP Release from Keratinocytes Occurs through Connexin Hemichannels', *PLoS ONE*, 8(2).

Barrientos, S., Stojadinovic, O., Golinko, M. S., Brem, H. and Tomic-Canic, M. (2008) 'PERSPECTIVE ARTICLE: Growth factors and cytokines in wound healing', *Wound Repair and Regeneration*, 16(5), pp. 585-601.

Becker, D. L., Thrasivoulou, C. and Phillips, A. R. J. (2012) 'Connexins in wound healing; perspectives in diabetic patients', *Biochimica et Biophysica Acta (BBA) - Biomembranes*, 1818(8), pp. 2068-2075.

Bell, S., Degitz, K., Quirling, M., Jilg, N., Page, S. and Brand, K. (2003) 'Involvement of NF-kappaB signalling in skin physiology and disease', *Cell Signal*, 15(1), pp. 1-7.

Berra-Romani, R., Raqeeb, A., Avelino-Cruz, J. E., Moccia, F., Oldani, A., Speroni, F., Taglietti, V. and Tanzi, F. (2008) 'Ca2+ signaling in injured in situ endothelium of rat aorta', *Cell Calcium*, 44(3), pp. 298-309.

Berra-Romani, R., Raqeeb, A., Torres-Jácome, J., Guzman-Silva, A., Guerra, G., Tanzi, F. and Moccia, F. (2012) 'The Mechanism of Injury-Induced Intracellular Calcium Concentration Oscillations in the Endothelium of Excised Rat Aorta', *Journal of Vascular Research*, 49(1), pp. 65-76.

Berridge, M. J. (2014) 'Calcium regulation of neural rhythms, memory and alzheimer's disease', *Journal of Physiology*, 592(2), pp. 281-293.

Berridge, M. J., Bootman, M. D. and Roderick, H. L. (2003) 'Calcium signalling: Dynamics, homeostasis and remodelling', *Nature Reviews Molecular Cell Biology*, 4(7), pp. 517-529.

Berridge, M. J., Lipp, P. and Bootman, M. D. (2000) 'The versatility and universality of calcium signalling', *Nature Reviews Molecular Cell Biology*, 1(1), pp. 11-21.

Bird, G. S. and Putney, J. W., Jr. (2005) 'Capacitative calcium entry supports calcium oscillations in human embryonic kidney cells', *J Physiol*, 562(Pt 3), pp. 697-706.

Block, E. R. and Klarlund, J. K. (2008) 'Wounding sheets of epithelial cells activates the epidermal growth factor receptor through distinct short- and long-range mechanisms', *Molecular Biology of the Cell*, 19(11), pp. 4909-4917.

Block, M. R., Glick, B. S., Wilcox, C. A., Wieland, F. T. and Rothman, J. E. (1988) 'Purification of an N-ethylmaleimide-sensitive protein catalyzing vesicular transport', *Proceedings of the National Academy of Sciences of the United States of America*, 85(21), pp. 7852-7856.

Bodin, P. and Burnstock, G. (2001) 'Evidence that release of adenosine triphosphate from endothelial cells during increased shear stress is vesicular', *Journal of Cardiovascular Pharmacology*, 38(6), pp. 900-908.

Boitano, S., Dirksen, E. and Sanderson, M. (1992) 'Intercellular propagation of calcium waves mediated by inositol trisphosphate', *Science*, 258(5080), pp. 292-295.

Borowiec, A.-S., Bidaux, G., Pigat, N., Goffin, V., Bernichtein, S. and Capiod, T. (2014) 'Calcium channels, external calcium concentration and cell proliferation', *European Journal of Pharmacology*, 739(0), pp. 19-25.

Braiman-Wiksman, L., Solomonik, I., Spira, R. and Tennenbaum, T. (2007) 'Novel Insights into Wound Healing Sequence of Events', *Toxicologic Pathology*, 35(6), pp. 767-779.

Brandner, J. M., Houdek, P., Hüsing, B., Kaiser, C. and Moll, I. (2004) 'Connexins 26, 30, and 43: Differences among spontaneous, chronic, and accelerated human wound healing', *Journal of Investigative Dermatology*, 122(5), pp. 1310-1320.

Braunstein, G. M., Roman, R. M., Clancy, J. P., Kudlow, B. A., Taylor, A. L., Shylonsky, V. G., Jovov, B., Peter, K., Jilling, T., Ismailov, I. I., Benos, D. J., Schwiebert, L. M., Fitz, J. G. and Schwiebert, E. M. (2001) 'Cystic Fibrosis Transmembrane Conductance Regulator Facilitates ATP Release by Stimulating a Separate ATP Release Channel for Autocrine Control of Cell Volume Regulation', *Journal of Biological Chemistry*, 276(9), pp. 6621-6630.

Buchholz, M. S. A. W. M. M. P. L. T. A. G. G. T. M. E. V. (2006) 'Overexpression of c-myc in pancreatic cancer caused by ectopic activation of NFATc1 and the Ca2+/calcineurin signaling pathway', *The EMBO Journal*, 25(15), pp. 3714-3724.

Burnstock, G. (2006) 'Pathophysiology and therapeutic potential of purinergic signaling', *Pharmacological Reviews*, 58(1), pp. 58-86.

Burrell, H. E., Bowler, W. B., Gallagher, J. A. and Sharpe, G. R. (2003) 'Human keratinocytes express multiple P2Y-receptors: Evidence for functional P2Y1, P2Y2, and P2Y4 receptors', *Journal of Investigative Dermatology*, 120(3), pp. 440-447.

Burrell, H. E., Wlodarski, B., Foster, B. J., Buckley, K. A., Sharpe, G. R., Quayle, J. M., Simpson, A. W. M. and Gallagher, J. A. (2005) 'Human keratinocytes release ATP and utilize three mechanisms for nucleotide interconversion at the cell surface', *Journal of Biological Chemistry*, 280(33), pp. 29667-29676.

CalciMedica. Available at: http://www.calcimedica.com.

Calne, R. Y., Thiru, S., McMaster, P., Craddock, G. N., White, D. J. G., Evans, D. B., Dunn, D. C., Pentlow, B. D. and Rolles, K. (1978) 'CYCLOSPORIN A IN PATIENTS RECEIVING RENAL ALLOGRAFTS FROM CADAVER DONORS', *The Lancet*, 312(8104), pp. 1323-1327.

Candi, E., Schmidt, R. and Melino, G. (2005) 'The cornified envelope: a model of cell death in the skin', *Nat Rev Mol Cell Biol*, 6(4), pp. 328-40.

Caplan, A. I. (2009) 'Why are MSCs therapeutic? New data: new insight', *J Pathol*, 217(2), pp. 318-24.

Cecchelli, R., Cacan, R., Porchet-Hennere, E. and Verbert, A. (1986) 'Dilatation of Golgi vesicles by monensin leads to enhanced accumulation of sugar nucleotides', *Bioscience Reports*, 6(2), pp. 227-234.

Celetti, S. J., Cowan, K. N., Penuela, S., Shao, Q., Churko, J. and Laird, D. W. (2010) 'Implications of pannexin 1 and pannexin 3 for keratinocyte differentiation', *Journal of Cell Science*, 123(8), pp. 1363-1372.

Charles, A. C., Naus, C. C. G., Zhu, D., Kidder, G. M., Dirksen, E. R. and Sanderson, M. J. (1992) 'Intercellular calcium signaling via gap junctions in glioma cells', *Journal of Cell Biology*, 118(1), pp. 195-201.

Chaudhari, S., Wu, P., Wang, Y., Ding, Y., Yuan, J., Begg, M. and Ma, R. (2014) 'High glucose and diabetes enhanced store-operated Ca(2+) entry and increased expression of its signaling proteins in mesangial cells', *Am J Physiol Renal Physiol*, 306(9), pp. F1069-80.

Cheng, K. T., Alevizos, I., Liu, X., Swaim, W. D., Yin, H., Feske, S., Oh-hora, M. and Ambudkar, I. S. (2012) 'STIM1 and STIM2 protein deficiency in T lymphocytes underlies development of the exocrine gland autoimmune disease, Sjögren's syndrome', *Proceedings of the National Academy of Sciences of the United States of America*, 109(36), pp. 14544-14549.

Chiang, B., Essick, E., Ehringer, W., Murphree, S., Hauck, M. A., Li, M. and Chien, S. (2007) 'Enhancing skin wound healing by direct delivery of intracellular adenosine triphosphate', *American Journal of Surgery*, 193(2), pp. 213-218.

Chifflet, S., Justet, C., Hernandez, J. A., Nin, V., Escande, C. and Benech, J. C. (2012) 'Early and late calcium waves during wound healing in corneal endothelial cells', *Wound Repair Regen*, 20(1), pp. 28-37.

Chow, W., Hou, G. and Bendeck, M. P. (2008) 'Glycogen synthase kinase 3beta regulation of nuclear factor of activated T-cells isoform c1 in the vascular smooth muscle cell response to injury', *Exp Cell Res*, 314(16), pp. 2919-29.

Churko, J. M., Shao, Q., Gong, X. Q., Swoboda, K. J., Bai, D., Sampson, J. and Laird, D. W. (2011) 'Human dermal fibroblasts derived from oculodentodigital dysplasia patients suggest that patients may have wound-healing defects', *Human Mutation*, 32(4), pp. 456-466.

Cianfarani, F., Tommasi, R., Failla, C. M., Viviano, M. T., Annessi, G., Papi, M., Zambruno, G. and Odorisio, T. (2006) 'Granulocyte/macrophage colony-stimulating factor treatment of human chronic ulcers promotes angiogenesis associated with de novo vascular endothelial growth factor transcription in the ulcer bed', *Br J Dermatol*, 154(1), pp. 34-41.

Cochrane, D. E. and Douglas, W. W. (1974) 'Calcium-induced extrusion of secretory granules (exocytosis) in mast cells exposed to 48-80 or the ionophores A-23187 and X-537A', *Proceedings of the National Academy of Sciences of the United States of America*, 71(2), pp. 408-412.

Cordeiro, J. V. and Jacinto, A. (2013) 'The role of transcription-independent damage signals in the initiation of epithelial wound healing', *Nat Rev Mol Cell Biol*, 14(4), pp. 249-262.

Cornell-Bell, A. H., Finkbeiner, S. M., Cooper, M. S. and Smith, S. J. (1990) 'Glutamate induces calcium waves in cultured astrocytes: Long-range glial signaling', *Science*, 247(4941), pp. 470-473.

Cotrina, M. L., Lin, J. H. C., Alves-Rodrigues, A., Liu, S., Li, J., Azmi-Ghadimi, H., Kang, J., Naus, C. C. G. and Nedergaard, M. (1998) 'Connexins regulate calcium signaling by controlling ATP release', *Proceedings of the National Academy of Sciences of the United States of America*, 95(26), pp. 15735-15740.

Cox, J. H., Hussell, S., Søndergaard, H., Roepstorff, K., Bui, J.-V., Deer, J. R., Zhang, J., Li, Z.-G., Lamberth, K., Kvist, P. H., Padkjær, S., Haase, C., Zahn, S. and Odegard, V. H. (2013) 'Antibody-Mediated Targeting of the Orai1 Calcium Channel Inhibits T Cell Function', *PLoS ONE*, 8(12), p. e82944.

Crabtree, G. R. and Olson, E. N. (2002) 'NFAT Signaling: Choreographing the Social Lives of Cells', *Cell*, 109(2, Supplement 1), pp. S67-S79.

Croisier, H., Tan, X., Perez-Zoghbi, J. F., Sanderson, M. J., Sneyd, J. and Brook, B. S. (2013) 'Activation of store-operated calcium entry in airway smooth muscle cells: insight from a mathematical model', *PLoS One*, 8(7), p. e69598.

Csernoch, L., Hunyadi, J. and Kovács, L. (2000) 'Calcium release activated calcium entry in a human skin derived cell line (HaCaT)', *Experimental Dermatology*, 9(3), pp. 200-205.

D'hondt, C., Ponsaerts, R., Srinivas, S. P., Vereecke, J. and Himpens, B. (2007) 'Thrombin Inhibits Intercellular Calcium Wave Propagation in Corneal Endothelial Cells by Modulation of Hemichannels and Gap Junctions', *Investigative Ophthalmology & Visual Science*, 48(1), pp. 120-133.

Darbellay, B., Barnes, L., Boehncke, W. H., Saurat, J. H. and Kaya, G. (2014) 'Reversal of murine epidermal atrophy by topical modulation of calcium signaling', *J Invest Dermatol*, 134(6), pp. 1599-608.

Davidson, J. S. and Baumgarten, I. M. (1988) 'Glycyrrhetinic acid derivatives: A novel class of inhibitors of gap-junctional intercellular communication. Structure-activity relationships', *Journal of Pharmacology and Experimental Therapeutics*, 246(3), pp. 1104-1107.

Davidson, J. S., Baumgarten, I. M. and Harley, E. H. (1986) 'Reversible inhibition of intercellular junctional communication by glycyrrhetinic acid', *Biochemical and Biophysical Research Communications*, 134(1), pp. 29-36.

Davis, F. M., Azimi, I., Faville, R. A., Peters, A. A., Jalink, K., Putney, J. W., Jr., Goodhill, G. J., Thompson, E. W., Roberts-Thomson, S. J. and Monteith, G. R. (2014) 'Induction of epithelial-mesenchymal transition (EMT) in breast cancer cells is calcium signal dependent', *Oncogene*, 33(18), pp. 2307-16.

de la Pompa, J. L., Timmerman, L. A., Takimoto, H., Yoshida, H., Elia, A. J., Samper, E., Potter, J., Wakeham, A., Marengere, L., Langille, B. L., Crabtree, G. R. and Mak, T. W. (1998) 'Role of the NF-ATc transcription factor in morphogenesis of cardiac valves and septum', *Nature*, 392(6672), pp. 182-6.

De Stefani, D., Raffaello, A., Teardo, E., Szabó, I. and Rizzuto, R. (2011) 'A forty-kilodalton protein of the inner membrane is the mitochondrial calcium uniporter', *Nature*, 476(7360), pp. 336-340.

DeHaven, W. I., Jones, B. F., Petranka, J. G., Smyth, J. T., Tomita, T., Bird, G. S. and Putney, J. W. (2009) 'TRPC channels function independently of STIM1 and Orai1', *The Journal of Physiology*, 587(10), pp. 2275-2298.

DeHaven, W. I., Smyth, J. T., Boyles, R. R., Bird, G. S. and Putney, J. W. (2008) 'Complex Actions of 2-Aminoethyldiphenyl Borate on Store-operated Calcium Entry', *Journal of Biological Chemistry*, 283(28), pp. 19265-19273.

DeHaven, W. I., Smyth, J. T., Boyles, R. R. and Putney Jr, J. W. (2007) 'Calcium inhibition and calcium potentiation of Orai1, Orai2, and Orai3 calcium release-activated calcium channels', *Journal of Biological Chemistry*, 282(24), pp. 17548-17556.

Demer, L. L., Wortham, C. M., Dirksen, E. R. and Sanderson, M. J. (1993) 'Mechanical stimulation induces intercellular calcium signaling in bovine aortic endothelial cells', *Am J Physiol*, 264(6 Pt 2), pp. H2094-102.

Denda, M. and Denda, S. (2007) 'Air-exposed keratinocytes exhibited intracellular calcium oscillation', *Skin Res Technol*, 13(2), pp. 195-201.

Denda, S., Kumamoto, J., Takei, K., Tsutsumi, M., Aoki, H. and Denda, M. (2012) 'Ryanodine receptors are expressed in epidermal keratinocytes and associated with keratinocyte differentiation and epidermal permeability barrier homeostasis', *J Invest Dermatol*, 132(1), pp. 69-75.

Derler, I., Schindl, R., Fritsch, R., Heftberger, P., Riedl, M. C., Begg, M., House, D. and Romanin, C. (2013) 'The action of selective CRAC channel blockers is affected by the Orai pore geometry', *Cell Calcium*, 53(2), pp. 139-51.

Deutsch, D. E., Williams, J. A. and Yule, D. I. (1995) 'Halothane and octanol block Ca2+ oscillations in pancreatic acini by multiple mechanisms', *Am J Physiol*, 269(5 Pt 1), pp. G779-88.

Dixon, C. J., Bowler, W. B., Littlewood-Evans, A., Dillon, J. P., Bilbe, G., Sharpe, G. R. and Gallagher, J. A. (1999) 'Regulation of epidermal homeostasis through P2Y2 receptors', *British Journal of Pharmacology*, 127(7), pp. 1680-1686.

Djalilian, A. R., McGaughey, D., Patel, S., Eun, Y. S., Yang, C., Cheng, J., Tomic, M., Sinha, S., Ishida-Yamamoto, A. and Segre, J. A. (2006) 'Connexin 26 regulates epidermal barrier and wound remodeling and promotes psoriasiform response', *Journal of Clinical Investigation*, 116(5), pp. 1243-1253.

DL Johnson, C. J. a. N. R. (2014) 'Lysophospholipid signalling as a therapeutic target for human skin wound healing: role of GSK-3β/β-catenin signalling', *European Society for Dermatology Research*. Copenhagen, Denmark, September 2014. Journel of Investigative Dermatology, pp. 98-102.

Dolmetsch, R. E., Xu, K. and Lewis, R. S. (1998) 'Calcium oscillations increase the efficiency and specificity of gene expression', *Nature*, 392(6679), pp. 933-936.

Dorsett-Martin, W. A. (2004) 'Rat models of skin wound healing: A review', *Wound Repair and Regeneration*, 12(6), pp. 591-599.

Dubé, J., Rochette-Drouin, O., Lévesque, P., Gauvin, R., Roberge, C. J., Auger, F. A., Goulet, D., Bourdages, M., Plante, M., Moulin, V. J. and Germain, L. (2012) 'Human keratinocytes respond

to direct current stimulation by increasing intracellular calcium: Preferential response of poorly differentiated cells', *Journal of Cellular Physiology*, 227(6), pp. 2660-2667.

Dvoriantchikova, G., Ivanov, D., Panchin, Y. and Shestopalov, V. I. (2006) 'Expression of pannexin family of proteins in the retina', *FEBS Letters*, 580(9), pp. 2178-2182.

Edward J. O'Keefe, R. A. B., * and Brian Herman (1987) 'Calcium-induced assembly of adherens junctions in keratinocytes', *The Journal of Cell Biology*, 105(2), pp. 807-817.

Egan, T. M. and Khakh, B. S. (2004) 'Contribution of calcium ions to P2X channel responses', *J Neurosci*, 24(13), pp. 3413-20.

Elias, P. M., Ahn, S. K., Denda, M., Brown, B. E., Crumrine, D., Kimutai, L. K., Kömüves, L., Lee, S. H. and Feingold, K. R. (2002) 'Modulations in epidermal calcium regulate the expression of differentiation-specific markers', *Journal of Investigative Dermatology*, 119(5), pp. 1128-1136.

Essenfelder, G. M., Bruzzone, R., Lamartine, J., Charollais, A., Blanchet-Bardon, C., Barbe, M. T., Meda, P. and Waksman, G. (2004) 'Connexin30 mutations responsible for hidrotic ectodermal dysplasia cause abnormal hemichannel activity', *Human Molecular Genetics*, 13(16), pp. 1703-1714.

Evans, J. H. and Sanderson, M. J. (1999) 'Intracellular calcium oscillations induced by ATP in airway epithelial cells', *Am J Physiol*, 277(1 Pt 1), pp. L30-41.

Evans, W. H. and Boitano, S. (2001) 'Connexin mimetic peptides: Specific inhibitors of gap-junctional intercellular communication', *Biochemical Society Transactions*, 29(4), pp. 606-612.

Eylenstein, A., Schmidt, S., Gu, S., Yang, W., Schmid, E., Schmidt, E. M., Alesutan, I., Szteyn, K., Regel, I., Shumilina, E. and Lang, F. (2012) 'Transcription factor NF-kappaB regulates expression of pore-forming Ca2+ channel unit, Orai1, and its activator, STIM1, to control Ca2+ entry and affect cellular functions', *J Biol Chem*, 287(4), pp. 2719-30.

Fang, K. S., Farboud, B., Nuccitelli, R. and Isseroff, R. R. (1998) 'Migration of Human Keratinocytes in Electric Fields Requires Growth Factors and Extracellular Calcium', *J Investig Dermatol*, 111(5), pp. 751-756.

Farooqui, R. and Fenteany, G. (2005) 'Multiple rows of cells behind an epithelial wound edge extend cryptic lamellipodia to collectively drive cell-sheet movement', *Journal of Cell Science*, 118(1), pp. 51-63.

Ferrari, D., Stroh, C. and Schulze-Osthoff, K. (1999) 'P2X7/P2Z purinoreceptor-mediated activation of transcription factor NFAT in microglial cells', *J Biol Chem*, 274(19), pp. 13205-10.

Feske, S., Gwack, Y., Prakriya, M., Srikanth, S., Puppel, S. H., Tanasa, B., Hogan, P. G., Lewis, R. S., Daly, M. and Rao, A. (2006) 'A mutation in Orai1 causes immune deficiency by abrogating CRAC channel function', *Nature*, 441(7090), pp. 179-185.

Fill, M. and Copello, J. A. (2002) 'Ryanodine receptor calcium release channels', *Physiol Rev*, 82(4), pp. 893-922.

Fisher, W. G., Yang, P. C., Medikonduri, R. K. and Jafri, M. S. (2006) 'NFAT and NFkappaB activation in T lymphocytes: a model of differential activation of gene expression', *Ann Biomed Eng*, 34(11), pp. 1712-28.

Flanagan, W. M., Corthesy, B., Bram, R. J. and Crabtree, G. R. (1991) 'Nuclear association of a T-cell transcription factor blocked by FK-506 and cyclosporin A', *Nature*, 352(6338), pp. 803-807.

Flockhart, R. J., Diffey, B. L., Farr, P. M., Lloyd, J. and Reynolds, N. J. (2008) 'NFAT regulates induction of COX-2 and apoptosis of keratinocytes in response to ultraviolet radiation exposure', *The FASEB Journal*, 22(12), pp. 4218-4227.

Forrester, A. R., Elias, M. S., Woodward, E. L., Graham, M., Williams, F. M. and Reynolds, N. J. (2014) 'Induction of a chloracne phenotype in an epidermal equivalent model by 2,3,7,8-tetrachlorodibenzo-p-dioxin (TCDD) is dependent on aryl hydrocarbon receptor activation and is not reproduced by aryl hydrocarbon receptor knock down', *Journal of Dermatological Science*, 73(1), pp. 10-22.

Forrester, T. (1972) 'An estimate of adenosine triphosphate release into the venous effluent from exercising human forearm muscle', *Journal of Physiology*, 224(3), pp. 611-628.

Francis, R., Xu, X., Park, H., Wei, C.-J., Chang, S., Chatterjee, B. and Lo, C. (2011) 'Connexin43 Modulates Cell Polarity and Directional Cell Migration by Regulating Microtubule Dynamics', *PLoS ONE*, 6(10), p. e26379.

Fuchs, E. (2008) 'Skin stem cells: rising to the surface', *J Cell Biol*, 180(2), pp. 273-84.

Fujita, K., Nakanishi, K., Sobue, K., Ueki, T., Asai, K. and Kato, T. (1998) 'Astrocytic gap junction blockage and neuronal Ca2+ oscillation in neuron-astrocyte cocultures in vitro', *Neurochem Int*, 33(1), pp. 41-9.

Fullard, N., Moles, A., O'Reilly, S., van Laar, J. M., Faini, D., Diboll, J., Reynolds, N. J., Mann, D. A., Reichelt, J. and Oakley, F. (2013) 'The c-Rel subunit of NF-kappaB regulates epidermal homeostasis and promotes skin fibrosis in mice', *Am J Pathol*, 182(6), pp. 2109-20.

Gabbiani, G., Chaponnier, C. and Huttner, I. (1978) 'Cytoplasmic filaments and gap junctions in epithelial cells and myofibroblasts during wound healing', *Journal of Cell Biology*, 76(3), pp. 561-568.

García-Sancho, J. (2014) 'The coupling of plasma membrane calcium entry to calcium uptake by endoplasmic reticulum and mitochondria', *The Journal of Physiology*, 592(2), pp. 261-268.

Gerasimenko, J. V., Gryshchenko, O., Ferdek, P. E., Stapleton, E., Hebert, T. O., Bychkova, S., Peng, S., Begg, M., Gerasimenko, O. V. and Petersen, O. H. (2013) 'Ca2+ release-activated Ca2+ channel blockade as a potential tool in antipancreatitis therapy', *Proc Natl Acad Sci U S A*, 110(32), pp. 13186-91.

Ghannad-Rezaie, M., Wang, X., Mishra, B., Collins, C. and Chronis, N. (2012) 'Microfluidic chips for in vivo imaging of cellular responses to neural injury in Drosophila larvae', *PLoS ONE*, 7(1).

Gibson, D. F. C., Bikle, D. D., Harris, J. and Goldberg, G. S. (1997) 'The expression of the gap junctional protein Cx43 is restricted to proliferating and non differentiated normal and transformed keratinocytes', *Experimental Dermatology*, 6(4), pp. 167-174.

Gifford, J. R., Heal, C., Bridges, J., Goldthorpe, S. and Mack, G. W. (2012) 'Changes in dermal interstitial ATP levels during local heating of human skin', *Journal of Physiology*, 590(24), pp. 6403-6411.

Goliger, J. A. and Paul, D. L. (1995) 'Wounding alters epidermal connexin expression and gap junction-mediated intercellular communication', *Molecular Biology of the Cell*, 6(11), pp. 1491-1501.

Gottrup, F., Ågren, M. S. and Karlsmark, T. (2000) 'Models for use in wound healing research: A survey focusing on in vitro and in vivo adult soft tissue', *Wound Repair and Regeneration*, 8(2), pp. 83-96.

Graphpad 6 Statistics Guide. Available at: http://www.graphpad.com/guides/prism/6/statistics/index.htm?stat_checklist_2wayanova_rm.htm.

Greig, A. V. H., Linge, C., Terenghi, G., McGrouther, D. A. and Burnstock, G. (2003) 'Purinergic receptors are part of a functional signaling system for proliferation and differentiation of human epidermal keratinocytes', *Journal of Investigative Dermatology*, 120(6), pp. 1007-1015.

Grygorczyk, R., Furuya, K. and Sokabe, M. (2013) 'Imaging and characterization of stretch-induced ATP release from alveolar A549 cells', *J Physiol*, 591(Pt 5), pp. 1195-215.

Guo, S. and DiPietro, L. A. (2010) 'Factors Affecting Wound Healing', *Journal of Dental Research*, 89(3), pp. 219-229.

Gurtovenko, A. A. and Anwar, J. (2007) 'Modulating the Structure and Properties of Cell Membranes: The Molecular Mechanism of Action of Dimethyl Sulfoxide', *The Journal of Physical Chemistry B*, 111(35), pp. 10453-10460.

Gwack, Y., Feske, S., Srikanth, S., Hogan, P. G. and Rao, A. (2007) 'Signalling to transcription: Store-operated Ca2+ entry and NFAT activation in lymphocytes', *Cell Calcium*, 42(2), pp. 145-156.

Hansen, M., Boitano, S., Dirksen, E. R. and Sanderson, M. J. (1995) 'A role for phospholipase C activity but not ryanodine receptors in the initiation and propagation of intercellular calcium waves', *J Cell Sci*, 108 (Pt 7), pp. 2583-90.

Harper, M. T. and Poole, A. W. (2011) 'Store-operated calcium entry and non-capacitative calcium entry have distinct roles in thrombin-induced calcium signalling in human platelets', *Cell Calcium*, 50(4), pp. 351-8.

Hassinger, T. D., Guthrie, P. B., Atkinson, P. B., Bennett, M. V. L. and Kater, S. B. (1996) 'An extracellular signaling component in propagation of astrocytic calcium waves', *Proceedings of the National Academy of Sciences of the United States of America*, 93(23), pp. 13268-13273.

Hedin, K. E., Bell, M. P., Kalli, K. R., Huntoon, C. J., Sharp, B. M. and McKean, D. J. (1997) 'Delta-opioid receptors expressed by Jurkat T cells enhance IL-2 secretion by increasing AP-1 complexes and activity of the NF-AT/AP-1-binding promoter element', *J Immunol*, 159(11), pp. 5431-40.

Heilbrunn, L. V. and Wiercinski, F. J. (1947) 'The action of various cations on muscle protoplasm', *Journal of cellular physiology*, 29(1), pp. 15-32.

Heindorff, K. and Baumann, O. (2014) 'Calcineurin is part of a negative feedback loop in the InsP3/Ca2+ signalling pathway in blowfly salivary glands', *Cell Calcium*, 56(3), pp. 215-224.

Hell, E. and Lawrence, J. C. (1979) 'The initiation of epidermal wound healing in cuts and burns', *British Journal of Experimental Pathology*, 60(2), pp. 171-179.

Hennings, H., Michael, D., Cheng, C., Steinert, P., Holbrook, K. and Yuspa, S. H. (1980) 'Calcium regulation of growth and differentiation of mouse epidermal cells in culture', *Cell*, 19(1), pp. 245-254.

Hofer, T., Venance, L. and Giaume, C. (2002) 'Control and plasticity of intercellular calcium waves in astrocytes: a modeling approach', *J Neurosci*, 22(12), pp. 4850-9.

Hogan, P. G., Chen, L., Nardone, J. and Rao, A. (2003) 'Transcriptional regulation by calcium, calcineurin, and NFAT', *Genes Dev*, 17(18), pp. 2205-32.

Holton, P. (1959) 'The liberation of adenosine triphosphate on antidromic stimulation of sensory nerves', *The Journal of Physiology*, 145(3), pp. 494-504.

Huang, R. P., Fan, Y., Hossain, M. Z., Peng, A., Zeng, Z. L. and Boynton, A. L. (1998) 'Reversion of the neoplastic phenotype of human glioblastoma cells by connexin 43 (cx43)', *Cancer Research*, 58(22), pp. 5089-5096.

Iacobas, D. A., Suadicani, S. O., Spray, D. C. and Scemes, E. (2006) 'A stochastic two-dimensional model of intercellular Ca2+ wave spread in glia', *Biophysical Journal*, 90(1), pp. 24-41.

Ito, M., Liu, Y., Yang, Z., Nguyen, J., Liang, F., Morris, R. J. and Cotsarelis, G. (2005) 'Stem cells in the hair follicle bulge contribute to wound repair but not to homeostasis of the epidermis', *Nat Med*, 11(12), pp. 1351-1354.

Jacobson, K. A. and Boeynaems, J. M. (2010) 'P2Y nucleotide receptors: Promise of therapeutic applications', *Drug Discovery Today*, 15(13-14), pp. 570-578.

James, G. A., Swogger, E., Wolcott, R., Pulcini, E., Secor, P., Sestrich, J., Costerton, J. W. and Stewart, P. S. (2008) 'Biofilms in chronic wounds', *Wound Repair Regen*, 16(1), pp. 37-44.

Jans, D., Srinivas, S. P., Waelkens, E., Segal, A., Lariviere, E., Simaels, J. and Van Driessche, W. (2002) 'Hypotonic treatment evokes biphasic ATP release across the basolateral membrane of cultured renal epithelia (A6)', *J Physiol*, 545(Pt 2), pp. 543-55.

Jans, R., Mottram, L., Johnson, D. L., Brown, A. M., Sikkink, S., Ross, K. and Reynolds, N. J. (2013) 'Lysophosphatidic Acid Promotes Cell Migration through STIM1- and Orai1-Mediated Ca2+i Mobilization and NFAT2 Activation', *J Invest Dermatol*, 133(3), pp. 793-802.

Janssen, L. J., Farkas, L., Rahman, T. and Kolb, M. R. J. (2009) 'ATP stimulates Ca2+-waves and gene expression in cultured human pulmonary fibroblasts', *International Journal of Biochemistry and Cell Biology*, 41(12), pp. 2477-2484.

Jin, H., Seo, J., Eun, S. Y., Joo, Y. N., Park, S. W., Lee, J. H., Chang, K. C. and Kim, H. J. (2014) 'P2Y2R activation by nucleotides promotes skin wound-healing process', *Experimental Dermatology*, 23(7), pp. 480-485.

Jost, M., Huggett, T. M., Kari, C. and Rodeck, U. (2001) 'Matrix-independent survival of human keratinocytes through an EGF receptor/MAPK-kinase-dependent pathway', *Mol Biol Cell*, 12(5), pp. 1519-27.

Junkin, M., Lu, Y., Long, J., Deymier, P. A., Hoying, J. B. and Wong, P. K. (2013) 'Mechanically induced intercellular calcium communication in confined endothelial structures', *Biomaterials*, 34(8), pp. 2049-56.

Kamolz, L.-P. and Wild, T. (2013) 'Wound bed preparation: The impact of debridement and wound cleansing', *Wound Medicine*, 1(0), pp. 44-50.

Kar, P., Nelson, C. and Parekh, Anant B. (2012) 'CRAC Channels Drive Digital Activation and Provide Analog Control and Synergy to Ca2+-Dependent Gene Regulation', *Current Biology*, 22(3), pp. 242-247.

Karvonen, S. L., Korkiamäki, T., Ylä-Outinen, H., Nissinen, M., Teerikangas, H., Pummi, K., Karvonen, J. and Peltonen, J. (2000) 'Psoriasis and altered calcium metabolism: Downregulated capacitative calcium influx and defective calcium-mediated cell signaling in cultured psoriatic keratinocytes', *Journal of Investigative Dermatology*, 114(4), pp. 693-700.

Kawano, S., AU - Otsu, K., AU - Kuruma, A., AU - Shoji, S., AU - Yanagida, E., AU - Muto, Y., AU - Yoshikawa, F., AU - Hirayama, Y., AU - Mikoshiba, K. and AU - Furuichi, T. (2006) 'ATP autocrine/paracrine signaling induces calcium oscillations and NFAT activation in human mesenchymal stem cells', *Cell Calcium*, 39(4), pp. 313 - 324.

Kegley, K. M., Gephart, J., Warren, G. L. and Pavlath, G. K. (2001) 'Altered primary myogenesis in NFATC3(-/-) mice leads to decreased muscle size in the adult', *Dev Biol*, 232(1), pp. 115-26.

Kelsell, D. P., Dunlop, J., Stevens, H. P., Lench, N. J., Liang, J. N., Parry, G., Mueller, R. F. and Leigh, I. M. (1997) 'Connexin 26 mutations in hereditary non-syndromic sensorineural deafness', *Nature*, 387(6628), pp. 80-83.

Kerpedijeva, K. T. a. S. S. (2012) 'Acceleration of Wound Healing by Multiple Growth Factors and Cytokines Secreted from Multipotential Stromal Cells/Mesenchymal Stem Cells', *Mary Ann Leibert*, 1(4), pp. 177 - 182.

Klee, C. B., Crouch, T. H. and Krinks, M. H. (1979) 'Calcineurin: a calcium- and calmodulin-binding protein of the nervous system', *Proc Natl Acad Sci U S A*, 76(12), pp. 6270-3.

Klepeis, V. E., Cornell-Bell, A. and Trinkaus-Randall, V. (2001) 'Growth factors but not gap junctions play a role in injury-induced Ca2+ waves in epithelial cells', *Journal of Cell Science*, 114(23), pp. 4185-4195.

Knight, G. E., Bodin, P., De Groat, W. C. and Burnstock, G. (2002) 'ATP is released from guinea pig ureter epithelium on distension', *American Journal of Physiology - Renal Physiology*, 282(2 51-2), pp. F281-F288.

Ko, K. S., Arora, P. D. and McCulloch, C. A. G. (2001) 'Cadherins Mediate Intercellular Mechanical Signaling in Fibroblasts by Activation of Stretch-sensitive Calcium-permeable Channels', *Journal of Biological Chemistry*, 276(38), pp. 35967-35977.

Kobayashi, Y., Sanno, Y., Sakai, A., Sawabu, Y., Tsutsumi, M., Goto, M., Kitahata, H., Nakata, S., Kumamoto, J., Denda, M. and Nagayama, M. (2014) 'Mathematical modeling of calcium waves induced by mechanical stimulation in keratinocytes', *PLoS ONE*, 9(3).

Koeck, J., Kreher, S., Lehmann, K., Riedel, R., Bardua, M., Lischke, T., Jargosch, M., Haftmann, C., Bendfeldt, H., Hatam, F., Mashreghi, M.-F., Baumgrass, R., Radbruch, A. and Chang, H.-D.

(2014) 'Nuclear factor of activated T cells regulates the expression of interleukin-4 in Th2 cells in an all-or-none fashion', *Journal of Biological Chemistry*.

Koenigsberger, M., Seppey, D., Bény, J.-L. and Meister, J.-J. (2010) 'Mechanisms of Propagation of Intercellular Calcium Waves in Arterial Smooth Muscle Cells', *Biophysical Journal*, 99(2), pp. 333-343.

Koizumi, S., Fujishita, K., Inoue, K., Shigemoto-Mogami, Y., Tsuda, M. and Inoue, K. (2004) 'Ca2+ waves in keratinocytes are transmitted to sensory neurons: The involvement of extracellular ATP and P2Y2 receptor activation', *Biochemical Journal*, 380(2), pp. 329-338.

Korkiamaki, T., Yla-Outinen, H., Koivunen, J., Karvonen, S. L. and Peltonen, J. (2002) 'Altered calcium-mediated cell signaling in keratinocytes cultured from patients with neurofibromatosis type 1', *Am J Pathol*, 160(6), pp. 1981-90.

Korkiamaki, T., Yla-Outinen, H., Leinonen, P., Koivunen, J. and Peltonen, J. (2005) 'The effect of extracellular calcium concentration on calcium-mediated cell signaling in NF1 tumor suppressor-deficient keratinocytes', *Arch Dermatol Res*, 296(10), pp. 465-72.

Kretz, M., Euwens, C., Hombach, S., Eckardt, D., Teubner, B., Traub, O., Willecke, K. and Ott, T. (2003) 'Altered connexin expression and wound healing in the epidermis of connexin-deficient mice', *Journal of Cell Science*, 116(16), pp. 3443-3452.

Kujawski, S., Lin, W., Kitte, F., Börmel, M., Fuchs, S., Arulmozhivarman, G., Vogt, S., Theil, D., Zhang, Y. and Antos, Christopher L. (2014) 'Calcineurin Regulates Coordinated Outgrowth of Zebrafish Regenerating Fins', *Developmental Cell*, 28(5), pp. 573-587.

Kumai, M., Nishii, K., Nakamura, K. I., Takeda, N., Suzuki, M. and Shibata, Y. (2000) 'Loss of connexin45 causes a cushion defect in early cardiogenesis', *Development*, 127(16), pp. 3501-3512.

Kurasawa, M., Maeda, T., Oba, A., Yamamoto, T. and Sasaki, H. (2011) 'Tight junction regulates epidermal calcium ion gradient and differentiation', *Biochem Biophys Res Commun*, 406(4), pp. 506-11.

Langton, A. K., Herrick, S. E. and Headon, D. J. (2007) 'An Extended Epidermal Response Heals Cutaneous Wounds in the Absence of a Hair Follicle Stem Cell Contribution', *J Invest Dermatol*, 128(5), pp. 1311-1318.

Lau, K., Paus, R., Tiede, S., Day, P. and Bayat, A. (2009) 'Exploring the role of stem cells in cutaneous wound healing', *Exp Dermatol*, 18(11), pp. 921-33.

Lee, K. P., Choi, S., Hong, J. H., Ahuja, M., Graham, S., Ma, R., So, I., Shin, D. M., Muallem, S. and Yuan, J. P. (2014) 'Molecular Determinants Mediating Gating of Transient Receptor Potential Canonical (TRPC) Channels by Stromal Interaction Molecule 1 (STIM1)', *Journal of Biological Chemistry*, 289(10), pp. 6372-6382.

Lee, M. J., Kim, J., Lee, K. I., Shin, J. M., Chae, J. I. and Chung, H. M. (2011) 'Enhancement of wound healing by secretory factors of endothelial precursor cells derived from human embryonic stem cells', *Cytotherapy*, 13(2), pp. 165-78.

Leiper, L. J., Walczysko, P., Kucerova, R., Ou, J., Shanley, L. J., Lawson, D., Forrester, J. V., McCaig, C. D., Zhao, M. and Collinson, J. M. (2006) 'The roles of calcium signaling and ERK1/2

phosphorylation in a Pax6+/- mouse model of epithelial wound-healing delay', *BMC Biol*, 4, p. 27.

Lev-Tov, H., Li, C. S., Dahle, S. and Isseroff, R. R. (2013) 'Cellular versus acellular matrix devices in treatment of diabetic foot ulcers: study protocol for a comparative efficacy randomized controlled trial', *Trials*, 14, p. 8.

Lewis, J. E., Jensen, P. J., Johnson, K. R. and Wheelock, M. J. (1994) 'E-cadherin mediates adherens junction organization through protein kinase C', *J Cell Sci*, 107 (Pt 12), pp. 3615-21.

Leybaert, L. and Sanderson, M. J. (2012) 'Intercellular Ca(2+) waves: mechanisms and function', *Physiol Rev*, 92(3), pp. 1359-92.

Leznik, E. and Llinas, R. (2005) 'Role of gap junctions in synchronized neuronal oscillations in the inferior olive', *J Neurophysiol*, 94(4), pp. 2447-56.

Li, D. L., Ma, Z. Y., Fu, Z. J., Ling, M. Y., Yan, C. Z. and Zhang, Y. (2014) 'Glibenclamide decreases ATP-induced intracellular calcium transient elevation via inhibiting reactive oxygen species and mitochondrial activity in macrophages', *PLoS One*, 9(2), p. e89083.

Li, J., Chen, J. and Kirsner, R. (2007) 'Pathophysiology of acute wound healing', *Clinics in Dermatology*, 25(1), pp. 9-18.

Li, T., Sun, M., Yin, X., Wu, C., Wu, Q., Feng, S., Li, H., Luan, Y., Wen, J., Yan, L., Zhao, B., Xu, C. and Sun, Y. (2013) 'Expression of the calcium sensing receptor in human peripheral blood T lymphocyte and its contribution to cytokine secretion through MAPKs or NF-kappaB pathways', *Mol Immunol*, 53(4), pp. 414-20.

Lin, H. D., Fong, C. Y., Biswas, A., Choolani, M. and Bongso, A. (2014) 'Human Wharton's Jelly Stem Cells, its Conditioned Medium and Cell-Free Lysate Inhibit the Growth of Human Lymphoma Cells', *Stem Cell Rev*, 10(4), pp. 573-86.

Liou, J., Kim, M. L., Won, D. H., Jones, J. T., Myers, J. W., Ferrell Jr, J. E. and Meyer, T. (2005) 'STIM is a Ca2+ sensor essential for Ca2+-store- depletion-triggered Ca2+ influx', *Current Biology*, 15(13), pp. 1235-1241.

Liu, Z., Dronadula, N. and Rao, G. N. (2004) 'A novel role for nuclear factor of activated T cells in receptor tyrosine kinase and G protein-coupled receptor agonist-induced vascular smooth muscle cell motility', *Journal of Biological Chemistry*, 279(39), pp. 41218-41226.

Liu, Z., Zhang, C., Dronadula, N., Li, Q. and Rao, G. N. (2005) 'Blockade of nuclear factor of activated T cells activation signaling suppresses balloon injury-induced neointima formation in a rat carotid artery model', *Journal of Biological Chemistry*, 280(15), pp. 14700-14708.

Lohman, A. W., Billaud, M. and Isakson, B. E. (2012) 'Mechanisms of ATP release and signalling in the blood vessel wall', *Cardiovasc Res*, 95(3), pp. 269-80.

López-Rodríguez, C., Aramburu, J., Rakeman, A. S. and Rao, A. (1999) 'NFAT5, a constitutively nuclear NFAT protein that does not cooperate with Fos and Jun', *Proceedings of the National Academy of Sciences*, 96(13), pp. 7214-7219.

Luk, V. N., Mo, G. and Wheeler, A. R. (2008) 'Pluronic additives: a solution to sticky problems in digital microfluidics', *Langmuir*, 24(12), pp. 6382-9.

Ma, J., McCarl, C. A., Khalil, S., Lüthy, K. and Feske, S. (2010) 'T-cell-specific deletion of STIM1 and STIM2 protects mice from EAE by impairing the effector functions of Th1 and Th17 cells', *European Journal of Immunology*, 40(11), pp. 3028-3042.

Maass, K., Ghanem, A., Kim, J. S., Saathoff, M., Urschel, S., Kirfel, G., Grümmer, R., Kretz, M., Lewalter, T., Tiemann, K., Winterhager, E., Herzog, V. and Willecke, K. (2004) 'Defective epidermal barrier in neonatal mice lacking the C-terminal region of connexin43', *Molecular Biology of the Cell*, 15(10), pp. 4597-4608.

Macari, F., Landau, M., Cousin, P., Mevorah, B., Brenner, S., Panizzon, R., Schorderet, D. F., Hohl, D. and Huber, M. (2000) 'Mutation in the gene for connexin 30.3 in a family with erythrokeratodermia variabilis', *American Journal of Human Genetics*, 67(5), pp. 1296-1301.

Macian, F. (2005) 'NFAT proteins: key regulators of T-cell development and function', *Nat Rev Immunol*, 5(6), pp. 472-484.

MacNeil, S. (2007) 'Progress and opportunities for tissue-engineered skin', *Nature*, 445(7130), pp. 874-80.

MacNeil, S., Shepherd, J. and Smith, L. (2011) 'Production of tissue-engineered skin and oral mucosa for clinical and experimental use', *Methods Mol Biol*, 695, pp. 129-53.

Majd, A. and Shariatzadeh, S. M. A. (2004) *"Cell and Molecular Biology", 4th edition*.

Martin, P. (1997) 'Wound Healing--Aiming for Perfect Skin Regeneration', *Science*, 276(5309), pp. 75-81.

Martin, P. E., Easton, J. A., Hodgins, M. B. and Wright, C. S. (2014) 'Connexins: Sensors of epidermal integrity that are therapeutic targets', *FEBS Letters*, 588(8), pp. 1304-1314.

McGrath, J. A. and Uitto, J. (2010) 'Anatomy and Organization of Human Skin', in *Rook's Textbook of Dermatology*. Wiley-Blackwell, pp. 1-53.

Meng, F., To, W., Kirkman-Brown, J., Kumar, P. and Gu, Y. (2007) 'Calcium oscillations induced by ATP in human umbilical cord smooth muscle cells', *Journal of Cellular Physiology*, 213(1), pp. 79-87.

Menon, G. K., Grayson, S. and Elias, P. M. (1985) 'Ionic calcium reservoirs in mammalian epidermis: Ultrastructural localization by ion-capture cytochemistry', *Journal of Investigative Dermatology*, 84(6), pp. 508-512.

Menon, S. N., Flegg, J. A., McCue, S. W., Schugart, R. C., Dawson, R. A. and McElwain, D. L. (2012) 'Modelling the interaction of keratinocytes and fibroblasts during normal and abnormal wound healing processes', *Proc Biol Sci*, 279(1741), pp. 3329-38.

Mercer, J. C., DeHaven, W. I., Smyth, J. T., Wedel, B., Boyles, R. R., Bird, G. S. and Putney Jr, J. W. (2006) 'Large store-operated calcium selective currents due to co-expression of Orai1 or Orai2 with the intracellular calcium sensor, Stim1', *Journal of Biological Chemistry*, 281(34), pp. 24979-24990.

Mese, G., Richard, G. and White, T. W. (2007) 'Gap Junctions: Basic Structure and Function', *J Invest Dermatol*, 127(11), pp. 2516-2524.

Miki, H., Maercklein, P. B. and Fitzpatrick, L. A. (1995) 'Spontaneous oscillations of intracellular calcium in single bovine parathyroid cells may be associated with the inhibition of parathyroid hormone secretion', *Endocrinology*, 136(7), pp. 2954-9.

Milara, J., Mata, M., Serrano, A., Peiró, T., Morcillo, E. J. and Cortijo, J. (2010) 'Extracellular calcium-sensing receptor mediates human bronchial epithelial wound repair', *Biochemical Pharmacology*, 80(2), pp. 236-246.

Miledi, R. (1973) 'Transmitter release induced by injection of calcium ions into nerve terminals', *Proceedings of the Royal Society of London - Biological Sciences*, 183(1073), pp. 421-425.

Miller, D. S. and Horowitz, S. B. (1986) 'Intracellular compartmentalization of adenosine triphosphate', *Journal of Biological Chemistry*, 261(30), pp. 13911-13915.

Miyakawa, H., Woo, S. K., Dahl, S. C., Handler, J. S. and Kwon, H. M. (1999) 'Tonicity-responsive enhancer binding protein, a Rel-like protein that stimulates transcription in response to hypertonicity', *Proceedings of the National Academy of Sciences*, 96(5), pp. 2538-2542.

Mizumoto, N., Mummert, M. E., Shalhevet, D. and Takashima, A. (2003) 'Keratinocyte ATP Release Assay for Testing Skin-Irritating Potentials of Structurally Diverse Chemicals', *Journal of Investigative Dermatology*, 121(5), pp. 1066-1072.

Moorby, C. and Patel, M. (2001) 'Dual functions for connexins: Cx43 regulates growth independently of gap junction formation', *Experimental Cell Research*, 271(2), pp. 238-248.

Moreo, K. (2005) 'Understanding and overcoming the challenges of effective case management for patients with chronic wounds', *The Case Manager*, 16(2), pp. 62-67.

Mould, E., Berry, P., Jamieson, D., Hill, C., Cano, C., Tan, N., Elliott, S., Durkacz, B., Newell, D. and Willmore, E. (2014) 'Identification of dual DNA-PK MDR1 inhibitors for the potentiation of cytotoxic drug activity', *Biochemical Pharmacology*, 88(1), pp. 58-65.

Mukherjee, S. and Brooks, W. H. (2014) 'Stromal interaction molecules as important therapeutic targets in diseases with dysregulated calcium flux', *Biochimica et Biophysica Acta - Molecular Cell Research*.

Müller, A. K., Meyer, M. and Werner, S. (2012) 'The roles of receptor tyrosine kinases and their ligands in the wound repair process', *Seminars in Cell and Developmental Biology*, 23(9), pp. 963-970.

Neal, J. W. and Clipstone, N. A. (2001) 'Glycogen Synthase Kinase-3 Inhibits the DNA Binding Activity of NFATc', *Journal of Biological Chemistry*, 276(5), pp. 3666-3673.

Neal, J. W. and Clipstone, N. A. (2003) 'A Constitutively Active NFATc1 Mutant Induces a Transformed Phenotype in 3T3-L1 Fibroblasts', *Journal of Biological Chemistry*, 278(19), pp. 17246-17254.

Neary, J. T., Kang, Y., Willoughby, K. A. and Ellis, E. F. (2003) 'Activation of extracellular signal-regulated kinase by stretch-induced injury in astrocytes involves extracellular ATP and P2 purinergic receptors', *J Neurosci*, 23(6), pp. 2348-56.

Niessen, H., Harz, H., Bedner, P., Krämer, K. and Willecke, K. (2000) 'Selective permeability of different connexin channels to the second messenger inositol 1,4,5-trisphosphate', *Journal of Cell Science*, 113(8), pp. 1365-1372.

Nishiyama, S., Manabe, N., Kubota, Y., Ohnishi, H., Kitanaka, A., Tokuda, M., Taminato, T., Ishida, T., Takahara, J. and Tanaka, T. (2005) 'Cyclosporin A inhibits the early phase of NF-κB/RelA activation induced by CD28 costimulatory signaling to reduce the IL-2 expression in human peripheral T cells', *International Immunopharmacology*, 5(4), pp. 699-710.

Notman, R., Noro, M., O'Malley, B. and Anwar, J. (2006) 'Molecular Basis for Dimethylsulfoxide (DMSO) Action on Lipid Membranes', *Journal of the American Chemical Society*, 128(43), pp. 13982-13983.

Nowak, J. A., Polak, L., Pasolli, H. A. and Fuchs, E. (2008) 'Hair follicle stem cells are specified and function in early skin morphogenesis', *Cell Stem Cell*, 3(1), pp. 33-43.

Numaga-Tomita, T. and Putney, J. W. (2013) 'Role of stim1-and orai1-mediated ca2+ entry in ca2+-induced epidermal keratinocyte differentiation', *Journal of Cell Science*, 126(2), pp. 605-612.

Ojeh, N., Stojadinovic, O., Pastar, I., Sawaya, A., Yin, N. and Tomic-Canic, M. (2014) 'The effects of caffeine on wound healing', *International Wound Journal*, pp. n/a-n/a.

Pangršič, T., Potokar, M., Stenovec, M., Kreft, M., Fabbretti, E., Nistri, A., Pryazhnikov, E., Khiroug, L., Giniatullin, R. and Zorec, R. (2007) 'Exocytotic Release of ATP from Cultured Astrocytes', *Journal of Biological Chemistry*, 282(39), pp. 28749-28758.

Parks, W. C. (1999) 'Matrix metalloproteinases in repair', *Wound Repair and Regeneration*, 7(6), pp. 423-432.

Penuela, S., Bhalla, R., Gong, X. Q., Cowan, K. N., Celetti, S. J., Cowan, B. J., Bai, D., Shao, Q. and Laird, D. W. (2007) 'Pannexin 1 and pannexin 3 are glycoproteins that exhibit many distinct characteristics from the connexin family of gap junction proteins', *Journal of Cell Science*, 120(21), pp. 3772-3783.

Penuela, S., Kelly, J. J., Churko, J. M., Barr, K. J., Berger, A. C. and Laird, D. W. (2014) 'Panx1 Regulates Cellular Properties of Keratinocytes and Dermal Fibroblasts in Skin Development and Wound Healing', *J Invest Dermatol*, 134(7), pp. 2026-2035.

Perez-Moreno, M., Jamora, C. and Fuchs, E. (2003) 'Sticky Business: Orchestrating Cellular Signals at Adherens Junctions', *Cell*, 112(4), pp. 535-548.

Pillai, S. and Bikle, D. D. (1992) 'Adenosine triphosphate stimulates phosphoinositide metabolism, mobilizes intracellular calcium, and inhibits terminal differentiation of human epidermal keratinocytes', *Journal of Clinical Investigation*, 90(1), pp. 42-51.

Popp, T., Steinritz, D., Breit, A., Deppe, J., Egea, V., Schmidt, A., Gudermann, T., Weber, C. and Ries, C. (2014) 'Wnt5a/beta-catenin signaling drives calcium-induced differentiation of human primary keratinocytes', *J Invest Dermatol*, 134(8), pp. 2183-91.

Posnett, J. and Franks, P. J. (2008) 'The burden of chronic wounds in the UK', *Nurs Times*, 104(3), pp. 44-5.

Praetorius, H. A. and Leipziger, J. (2009) 'ATP release from non-excitable cells', *Purinergic Signalling*, 5(4), pp. 433-446.

Prakriya, M., Feske, S., Gwack, Y., Srikanth, S., Rao, A. and Hogan, P. G. (2006) 'Orai1 is an essential pore subunit of the CRAC channel', *Nature*, 443(7108), pp. 230-233.

Prasai, P., Stefos, G. and Becker, W. (2011) 'Extracellular ATP activates NFAT-dependent gene expression in neuronal PC12 cells via P2X receptors', *BMC Neuroscience*, 12(1), p. 90.

Proksch, E., Brandner, J. M. and Jensen, J. M. (2008) 'The skin: an indispensable barrier', *Exp Dermatol*, 17(12), pp. 1063-72.

Putney Jr, J. W. (1986) 'A model for receptor-regulated calcium entry', *Cell Calcium*, 7(1), pp. 1-12.

Putney, J. W. (2010) 'Pharmacology of store-operated calcium channels', *Mol Interv*, 10(4), pp. 209-18.

Putney, James W. (2012) 'Calcium Signaling: Deciphering the Calcium–NFAT Pathway', *Current Biology*, 22(3), pp. R87-R89.

Qiu, C., Coutinho, P., Frank, S., Franke, S., Law, L. Y., Martin, P., Green, C. R. and Becker, D. L. (2003) 'Targeting Connexin43 Expression Accelerates the Rate of Wound Repair', *Current Biology*, 13(19), pp. 1697-1703.

Raja, Sivamani, K., Garcia, M. S. and Isseroff, R. R. (2007) 'Wound re-epithelialization: modulating keratinocyte migration in wound healing', *Front Biosci*, 12, pp. 2849-68.

Rao, A., Luo, C. and Hogan, P. G. (1997) 'Transcription factors of the NFAT family: regulation and function', *Annu Rev Immunol*, 15, pp. 707-47.

Razzell, W., Evans, Iwan R., Martin, P. and Wood, W. (2013) 'Calcium Flashes Orchestrate the Wound Inflammatory Response through DUOX Activation and Hydrogen Peroxide Release', *Current Biology*, 23(5), pp. 424-429.

Reddy, M. M., Quinton, P. M., Haws, C., Wine, J. J., Grygorczyk, R., Tabcharani, J. A., Hanrahan, J. W., Gunderson, K. L. and Kopito, R. R. (1996) 'Failure of the cystic fibrosis transmembrane conductance regulator to conduct ATP', *Science*, 271(5257), pp. 1876-1879.

Reisin, I. L., Prat, A. G., Abraham, E. H., Amara, J. F., Gregory, R. J., Ausiello, D. A. and Cantiello, H. F. (1994) 'The cystic fibrosis transmembrane conductance regulator is a dual ATP and chloride channel', *Journal of Biological Chemistry*, 269(32), pp. 20584-20591.

Rice, L. V., Bax, H. J., Russell, L. J., Barrett, V. J., Walton, S. E., Deakin, A. M., Thomson, S. A., Lucas, F., Solari, R., House, D. and Begg, M. (2013) 'Characterization of selective Calcium-Release Activated Calcium channel blockers in mast cells and T-cells from human, rat, mouse and guinea-pig preparations', *Eur J Pharmacol*, 704(1-3), pp. 49-57.

Richardson, R., Slanchev, K., Kraus, C., Knyphausen, P., Eming, S. and Hammerschmidt, M. (2013) 'Adult Zebrafish as a Model System for Cutaneous Wound-Healing Research', *J Invest Dermatol*, 133(6), pp. 1655-1665.

Ringer, S. (1883) 'A further Contribution regarding the influence of the different Constituents of the Blood on the Contraction of the Heart', *J Physiol*, 4(1), pp. 29-42 3.

Rivas, M. V., Jarvis, E. D., Morisaki, S., Carbonaro, H., Gottlieb, A. B. and Krueger, J. G. (1997) 'Identification of aberrantly regulated genes in diseased skin using the cDNA differential display technique', *Journal of Investigative Dermatology*, 108(2), pp. 188-194.

Roos, J., DiGregorio, P. J., Yeromin, A. V., Ohlsen, K., Lioudyno, M., Zhang, S., Safrina, O., Kozak, J. A., Wagner, S. L., Cahalan, M. D., Veliçelebi, G. and Stauderman, K. A. (2005) 'STIM1, an essential and conserved component of store-operated Ca 2+ channel function', *Journal of Cell Biology*, 169(3), pp. 435-445.

Rosado, J. A. and Sage, S. O. (2000) 'Protein kinase C activates non-capacitative calcium entry in human platelets', *The Journal of Physiology*, 529(1), pp. 159-169.

Rose, B. and Loewenstein, W. R. (1975) 'Calcium ion distribution in cytoplasm visualized by aequorin: Diffusion in cytosol restricted by energized sequestering', *Science*, 190(4220), pp. 1204-1206.

Ross, K., Parker, G., Whitaker, M. and Reynolds, N. J. (2008) 'Inhibition of calcium-independent phospholipase A impairs agonist-induced calcium entry in keratinocytes', *Br J Dermatol*, 158(1), pp. 31-7.

Ross, K., Whitaker, M. and Reynolds, N. J. (2007) 'Agonist-induced calcium entry correlates with STIM1 translocation', *Journal of Cellular Physiology*, 211(3), pp. 569-576.

Ruiz-Perez, V. L., Carter, S. A., Healy, E., Todd, C., Rees, J. L., Steijlen, P. M., Carmichael, A. J., Lewis, H. M., Hohl, D., Itin, P., Vahlquist, A., Gobello, T., Mazzanti, C., Reggazini, R., Nagy, G., Munro, C. S. and Strachan, T. (1999) 'ATP2A2 mutations in Darier's disease: Variant cutaneous phenotypes are associated with missense mutations, but neuropsychiatric features are independent of mutation class', *Human Molecular Genetics*, 8(9), pp. 1621-1630.

Ruzsnavszky, O., Dienes, B., Oláh, T., Vincze, J., Gáll, T., Balogh, E., Nagy, G., Bátori, R., Lontay, B., Erdődi, F. and Csernoch, L. (2013) 'Differential Effects of Phosphatase Inhibitors on the Calcium Homeostasis and Migration of HaCaT Keratinocytes', *PLoS ONE*, 8(4), p. e61507.

Saez, J. C., Connor, J. A., Spray, D. C. and Bennett, M. V. L. (1989) 'Hepatocyte gap junctions are permeable to the second messenger, inositol 1,4,5-trisphosphate, and to calcium ions', *Proceedings of the National Academy of Sciences of the United States of America*, 86(8), pp. 2708-2712.

Sanderson, M. J., Charles, A. C. and Dirksen, E. R. (1990) 'Mechanical stimulation and intercellular communication increases intracellular Ca2+ in epithelial cells', *Cell Regul*, 1(8), pp. 585-96.

Santini, M. P., Talora, C., Seki, T., Bolgan, L. and Dotto, G. P. (2001) 'Cross talk among calcineurin, Sp1/Sp3, and NFAT in control of p21WAF1/CIP1 expression in keratinocyte differentiation', *Proceedings of the National Academy of Sciences*, 98(17), pp. 9575-9580.

Santoro, M. M. and Gaudino, G. (2005) 'Cellular and molecular facets of keratinocyte reepithelization during wound healing', *Experimental Cell Research*, 304(1), pp. 274-286.

Sauer, H., Sharifpanah, F., Hatry, M., Steffen, P., Bartsch, C., Heller, R., Padmasekar, M., Howaldt, H. P., Bein, G. and Wartenberg, M. (2011) 'NOS inhibition synchronizes calcium oscillations in human adipose tissue-derived mesenchymal stem cells by increasing gap-junctional coupling', *J Cell Physiol*, 226(6), pp. 1642-50.

Schäfer, C., Rymarczyk, G., Ding, L., Kirber, M. T. and Bolotina, V. M. (2012) 'Role of Molecular Determinants of Store-operated Ca2+ Entry (Orai1, Phospholipase A2 Group 6, and STIM1) in Focal Adhesion Formation and Cell Migration', *Journal of Biological Chemistry*, 287(48), pp. 40745-40757.

Schagat, B. H. a. T. 'Compound Interference of CellTiter-Glo® vs PE ATPlite™ 1 Step Poster'.

Scheckenbach, K. E. L., Losa, D., Dudez, T., Bacchetta, M., O'Grady, S., Crespin, S. and Chanson, M. (2011) 'Prostaglandin E2 regulation of cystic fibrosis transmembrane conductance regulator activity and airway surface liquid volume requires gap junctional communication', *American Journal of Respiratory Cell and Molecular Biology*, 44(1), pp. 74-82.

Schinkel, A. H. and Jonker, J. W. (2012) 'Mammalian drug efflux transporters of the ATP binding cassette (ABC) family: An overview', *Advanced Drug Delivery Reviews*, 64(SUPPL.), pp. 138-153.

Schubert, R. (2005) 'Non-capacitative calcium entry–Extension of the possibilities for calcium entry in vascular tissue', *Cardiovascular Research*, 68(1), pp. 5-7.

Schwiebert, E. M. and Zsembery, A. (2003) 'Extracellular ATP as a signaling molecule for epithelial cells', *Biochimica et Biophysica Acta - Biomembranes*, 1615(1-2), pp. 7-32.

Séror, C., Melki, M. T., Subra, F., Raza, S. Q., Bras, M., Saïdi, H., Nardacci, R., Voisin, L., Paoletti, A., Law, F., Martins, I., Amendola, A., Abdul-Sater, A. A., Ciccosanti, F., Delelis, O., Niedergang, F., Thierry, S., Said-Sadier, N., Lamaze, C., Métivier, D., Estaquier, J., Fimia, G. M., Falasca, L., Casetti, R., Modjtahedi, N., Kanellopoulos, J., Mouscadet, J. F., Ojcius, D. M., Piacentini, M., Gougeon, M. L., Kroemer, G. and Perfettini, J. L. (2011) 'Extracellular ATP acts on P2Y2 purinergic receptors to facilitate HIV-1 infection', *Journal of Experimental Medicine*, 208(9), pp. 1823-1834.

Sharma, S., Quintana, A., Findlay, G. M., Mettlen, M., Baust, B., Jain, M., Nilsson, R., Rao, A. and Hogan, P. G. (2013) 'An siRNA screen for NFAT activation identifies septins as coordinators of store-operated Ca2+ entry', *Nature*, 499(7457), pp. 238-42.

Shetty, A. V., Thirugnanam, S., Dakshinamoorthy, G., Samykutty, A., Zheng, G., Chen, A., Bosland, M. C., Kajdacsy-Balla, A. and Gnanasekar, M. (2011) '18α-glycyrrhetinic acid targets prostate cancer cells by down-regulating inflammation-related genes', *International Journal of Oncology*, 39(3), pp. 635-640.

Singaravelu, K., Lohr, C. and Deitmer, J. W. (2006) 'Regulation of store-operated calcium entry by calcium-independent phospholipase A2 in rat cerebellar astrocytes', *J Neurosci*, 26(37), pp. 9579-92.

Smani, T., Zakharov, S. I., Csutora, P., Leno, E., Trepakova, E. S. and Bolotina, V. M. (2004) 'A novel mechanism for the store-operated calcium influx pathway', *Nat Cell Biol*, 6(2), pp. 113-120.

Sneyd, J., Wetton, B. T., Charles, A. C. and Sanderson, M. J. (1995) 'Intercellular calcium waves mediated by diffusion of inositol trisphosphate: a two-dimensional model', *Am J Physiol*, 268(6 Pt 1), pp. C1537-45.

Sponsel, H. T., Breckon, R. and Anderson, R. J. (1995) 'Adenine nucleotide and protein kinase C regulation of renal tubular epithelial cell wound healing', *Kidney International*, 48(1), pp. 85-92.

Spray, D. C. and Iacobas, D. A. (2007) 'Organizational principles of the connexin-related brain transcriptome', *Journal of Membrane Biology*, 218(1-3), pp. 39-47.

Stains, J. P. and Civitelli, R. (2005) 'Gap junctions regulate extracellular signal-regulated kinase signaling to affect gene transcription', *Molecular Biology of the Cell*, 16(1), pp. 64-72.

Stanisz, H., Saul, S., Muller, C. S., Kappl, R., Niemeyer, B. A., Vogt, T., Hoth, M., Roesch, A. and Bogeski, I. (2014) 'Inverse regulation of melanoma growth and migration by Orai1/STIM2-dependent calcium entry', *Pigment Cell Melanoma Res*, 27(3), pp. 442-53.

Stathopulos, P. B., Schindl, R., Fahrner, M., Zheng, L., Gasmi-Seabrook, G. M., Muik, M., Romanin, C. and Ikura, M. (2013) 'STIM1/Orai1 coiled-coil interplay in the regulation of store-operated calcium entry', *Nat Commun*, 4, p. 2963.

Steed, D. L. (1995) 'Clinical evaluation of recombinant human platelet-derived growth factor for the treatment of lower extremity diabetic ulcers. Diabetic Ulcer Study Group', *J Vasc Surg*, 21(1), pp. 71-8; discussion 79-81.

Stiber, J., Hawkins, A., Zhang, Z.-S., Wang, S., Burch, J., Graham, V., Ward, C. C., Seth, M., Finch, E., Malouf, N., Williams, R. S., Eu, J. P. and Rosenberg, P. (2008) 'STIM1 signalling controls store-operated calcium entry required for development and contractile function in skeletal muscle', *Nat Cell Biol*, 10(6), pp. 688-697.

Stojadinovic, O., Brem, H., Vouthounis, C., Lee, B., Fallon, J., Stallcup, M., Merchant, A., Galiano, R. D. and Tomic-Canic, M. (2005) 'Molecular pathogenesis of chronic wounds: the role of beta-catenin and c-myc in the inhibition of epithelialization and wound healing', *Am J Pathol*, 167(1), pp. 59-69.

Strahonja-Packard, A. and Sanderson, M. J. (1999) 'Intercellular Ca(2+) waves induce temporally and spatially distinct intracellular Ca(2+) oscillations in glia', *Glia*, 28(2), pp. 97-113.

Streifel, K. M., Miller, J., Mouneimne, R. and Tjalkens, R. B. (2013) 'Manganese inhibits ATP-induced calcium entry through the transient receptor potential channel TRPC3 in astrocytes', *NeuroToxicology*, 34(0), pp. 160-166.

Sung, Y. J., Sung, Z., Ho, C. L., Lin, M. T., Wang, J. S., Yang, S. C., Chen, Y. J. and Lin, C. H. (2003) 'Intercellular calcium waves mediate preferential cell growth toward the wound edge in polarized hepatic cells', *Experimental Cell Research*, 287(2), pp. 209-218.

Swift, M. E., Burns, A. L., Gray, K. L. and DiPietro, L. A. (2001) 'Age-Related Alterations in the Inflammatory Response to Dermal Injury', 117(5), pp. 1027-1035.

Taboubi, S., Milanini, J., Delamarre, E., Parat, F., Garrouste, F., Pommier, G., Takasaki, J., Hubaud, J. C., Kovacic, H. and Lehmann, M. (2007) 'G alpha(q/11)-coupled P2Y2 nucleotide receptor inhibits human keratinocyte spreading and migration', *FASEB J*, 21(14), pp. 4047-58.

Takahashi, T., Kikuchi, T., Kidokoro, Y. and Shirakawa, H. (2013) 'Ca(2)(+) influx-dependent refilling of intracellular Ca(2)(+) stores determines the frequency of Ca(2)(+) oscillations in fertilized mouse eggs', *Biochem Biophys Res Commun*, 430(1), pp. 60-5.

Taylor, C. W. and Tovey, S. C. (2010) 'IP3 Receptors: Toward Understanding Their Activation', *Cold Spring Harbor Perspectives in Biology*, 2(12).

Thiel, M., Lis, A. and Penner, R. (2013) 'STIM2 drives Ca2+ oscillations through store-operated Ca2+ entry caused by mild store depletion', *The Journal of Physiology*, 591(6), pp. 1433-1445.

Tobin, D. J. (2006) 'Biochemistry of human skin-our brain on the outside', *Chemical Society Reviews*, 35(1), pp. 52-67.

Todd, C. and Reynolds, N. J. (1998) 'Up-regulation of p21WAF1 by phorbol ester and calcium in human keratinocytes through a protein kinase C-dependent pathway', *Am J Pathol*, 153(1), pp. 39-45.

Tran, P. O., Hinman, L. E., Unger, G. M. and Sammak, P. J. (1999) 'A wound-induced [Ca2+]i increase and its transcriptional activation of immediate early genes is important in the regulation of motility', *Exp Cell Res*, 246(2), pp. 319-26.

Trent, J. T. and Kirsner, R. S. (2003) 'Wounds and malignancy', *Adv Skin Wound Care*, 16(1), pp. 31-4.

Trollinger, D. R., Rivkah Isseroff, R. and Nuccitelli, R. (2002) 'Calcium channel blockers inhibit galvanotaxis in human keratinocytes', *Journal of Cellular Physiology*, 193(1), pp. 1-9.

Trushin, S. A., Pennington, K. N., Algeciras-Schimnich, A. and Paya, C. V. (1999) 'Protein Kinase C and Calcineurin Synergize to Activate IκB Kinase and NF-κB in T Lymphocytes', *Journal of Biological Chemistry*, 274(33), pp. 22923-22931.

Tsai, F. C., Seki, A., Yang, H. W., Hayer, A., Carrasco, S., Malmersjö, S. and Meyer, T. (2014) 'A polarized Ca2+, diacylglycerol and STIM1 signalling system regulates directed cell migration', *Nature Cell Biology*, 16(2), pp. 133-144.

Tsutsumi, M., Inoue, K., Denda, S., Ikeyama, K., Goto, M. and Denda, M. (2009) 'Mechanical-stimulation-evoked calcium waves in proliferating and differentiated human keratinocytes', *Cell and Tissue Research*, 338(1), pp. 99-106.

'Über die Pyrophosphatfraktion im Muskel', (1929) *Die Naturwissenschaften*, 17(31), pp. 624-625.

Upton, D., Hender, C. and Solowiej, K. (2012) 'Mood disorders in patients with acute and chronic wounds: a health professional perspective', *J Wound Care*, 21(1), pp. 42-8.

Van der Wal, J., Habets, R., Várnai, P., Balla, T. and Jalink, K. (2001) 'Monitoring Agonist-induced Phospholipase C Activation in Live Cells by Fluorescence Resonance Energy Transfer', *Journal of Biological Chemistry*, 276(18), pp. 15337-15344.

van Kruchten, R., Braun, A., Feijge, M. A., Kuijpers, M. J., Rivera-Galdos, R., Kraft, P., Stoll, G., Kleinschnitz, C., Bevers, E. M., Nieswandt, B. and Heemskerk, J. W. (2012) 'Antithrombotic potential of blockers of store-operated calcium channels in platelets', *Arterioscler Thromb Vasc Biol*, 32(7), pp. 1717-23.

van Meerloo, J., Kaspers, G. J. and Cloos, J. (2011) 'Cell sensitivity assays: the MTT assay', *Methods Mol Biol*, 731, pp. 237-45.

Vandenberghe, M., Raphaël, M., Lehen'kyi, V. y., Gordienko, D., Hastie, R., Oddos, T., Rao, A., Hogan, P. G., Skryma, R. and Prevarskaya, N. (2013) 'ORAI1 calcium channel orchestrates skin homeostasis', *Proceedings of the National Academy of Sciences*, 110(50), pp. E4839-E4848.

Venkatachalam, K., van Rossum, D. B., Patterson, R. L., Ma, H.-T. and Gill, D. L. (2002) 'The cellular and molecular basis of store-operated calcium entry', *Nat Cell Biol*, 4(11), pp. E263-E272.

Voigt, W. (2005) 'Sulforhodamine B assay and chemosensitivity', *Methods Mol Med*, 110, pp. 39-48.

Waldman, S. D., Usprech, J., Flynn, L. E. and Khan, A. A. (2010) 'Harnessing the purinergic receptor pathway to develop functional engineered cartilage constructs', *Osteoarthritis and Cartilage*, 18(6), pp. 864-872.

Wallis, S., Lloyd, S., Wise, I., Ireland, G., Fleming, T. P. and Garrod, D. (2000) 'The alpha isoform of protein kinase C is involved in signaling the response of desmosomes to wounding in cultured epithelial cells', *Mol Biol Cell*, 11(3), pp. 1077-92.

Walter, M. N. M., Wright, K. T., Fuller, H. R., MacNeil, S. and Johnson, W. E. B. (2010) 'Mesenchymal stem cell-conditioned medium accelerates skin wound healing: An in vitro study of fibroblast and keratinocyte scratch assays', *Experimental Cell Research*, 316(7), pp. 1271-1281.

Wang, C. M., Lincoln, J., Cook, J. E. and Becker, D. L. (2007) 'Abnormal connexin expression underlies delayed wound healing in diabetic skin', *Diabetes*, 56(11), pp. 2809-2817.

Wang, D., Huang, N. and Heppel, L. A. (1990) 'Extracellular ATP shows synergistic enhancement of DNA synthesis when combined with agents that are active in wound healing or as neurotransmitters', *Biochemical and Biophysical Research Communications*, 166(1), pp. 251-258.

Wang, S. C., Tang, C. L., Piao, H. L., Zhu, R., Sun, C., Tao, Y., Fu, Q., Li, D. J. and Du, M. R. (2013) 'Cyclosporine A promotes in vitro migration of human first-trimester trophoblasts via MAPK/ERK1/2-mediated NF-κB and Ca2+/calcineurin/NFAT signaling', *Placenta*, 34(4), pp. 374-380.

Wedel, B., Boyles, R. R., Putney, J. W. and Bird, G. S. (2007) 'Role of the store-operated calcium entry proteins Stim1 and Orai1 in muscarinic cholinergic receptor-stimulated calcium oscillations in human embryonic kidney cells', *The Journal of Physiology*, 579(3), pp. 679-689.

Wesley, U. V., Bove, P. F., Hristova, M., McCarthy, S. and van der Vliet, A. (2007) 'Airway Epithelial Cell Migration and Wound Repair by ATP-mediated Activation of Dual Oxidase 1', *Journal of Biological Chemistry*, 282(5), pp. 3213-3220.

Wilgus, T. A., Bergdall, V. K., Tober, K. L., Hill, K. J., Mitra, S., Flavahan, N. A. and Oberyszyn, T. M. (2004) 'The impact of cyclooxygenase-2 mediated inflammation on scarless fetal wound healing', *Am J Pathol*, 165(3), pp. 753-61.

Wilson, Sarah R., Thé, L., Batia, Lyn M., Beattie, K., Katibah, George E., McClain, Shannan P., Pellegrino, M., Estandian, Daniel M. and Bautista, Diana M. 'The Epithelial Cell-Derived Atopic Dermatitis Cytokine TSLP Activates Neurons to Induce Itch', *Cell*, 155(2), pp. 285-295.

Windsor, M. L., Eisenberg, M., Gordon-Thomson, C. and Moore, G. P. M. (2009) 'A novel model of wound healing in the SCID mouse using a cultured human skin substitute', *Australasian Journal of Dermatology*, 50(1), pp. 29-35.

Wulff, B. C., Parent, A. E., Meleski, M. A., DiPietro, L. A., Schrementi, M. E. and Wilgus, T. A. (2012) 'Mast cells contribute to scar formation during fetal wound healing', *J Invest Dermatol*, 132(2), pp. 458-65.

Xu, S. and Chisholm, A. D. (2011) 'A Gαq-Ca2+ signaling pathway promotes actin-mediated epidermal wound closure in C. elegans', *Current Biology*, 21(23), pp. 1960-1967.

Xue, S., Nicoud, M. R., Cui, J. and Jovin, D. J. A. (1994) 'High concentration of calcium ions in Golgi apparatus', *Cell Res*, 4(1), pp. 97-108.

Yan, X., Xing, J., Lorin-Nebel, C., Estevez, A. Y., Nehrke, K., Lamitina, T. and Strange, K. (2006) 'Function of a STIM1 homologue in C. elegans: evidence that store-operated Ca2+ entry is not essential for oscillatory Ca2+ signaling and ER Ca2+ homeostasis', *J Gen Physiol*, 128(4), pp. 443-59.

Yin, J., Xu, K., Zhang, J., Kumar, A. and Yu, F. S. X. (2007) 'Wound-induced ATP release and EGF receptor activation in epithelial cell', *Journal of Cell Science*, 120(5), pp. 815-825.

Yoo, S. K., Freisinger, C. M., LeBert, D. C. and Huttenlocher, A. (2012) 'Early redox, Src family kinase, and calcium signaling integrate wound responses and tissue regeneration in zebrafish', *Journal of Cell Biology*, 199(2), pp. 225-234.

Yoshida, H., Kobayashi, D., Ohkubo, S. and Nakahata, N. (2006) 'ATP stimulates interleukin-6 production via P2Y receptors in human HaCaT keratinocytes', *European Journal of Pharmacology*, 540(1-3), pp. 1-9.

Yu, H., Sliedregt-Bol, K., Overkleeft, H., van der Marel, G. A., van Berkel, T. J. C. and Biessen, E. A. L. (2006) 'Therapeutic Potential of a Synthetic Peptide Inhibitor of Nuclear Factor of Activated T Cells as Antirestenotic Agent', *Arteriosclerosis, Thrombosis, and Vascular Biology*, 26(7), pp. 1531-1537.

Zhang, J., Scherer, S. S. and Yum, S. W. (2011) 'Dominant Cx26 mutants associated with hearing loss have dominant-negative effects on wild type Cx26', *Molecular and Cellular Neuroscience*, 47(2), pp. 71-78.

Zhang, M., Abrams, C., Wang, L., Gizzi, A., He, L., Lin, R., Chen, Y., Loll, P. J., Pascal, J. M. and Zhang, J. F. (2012) 'Structural basis for calmodulin as a dynamic calcium sensor', *Structure*, 20(5), pp. 911-923.

Zhang, W., Segura, B. J., Lin, T. R., Hu, Y. and Mulholland, M. W. (2003) 'Intercellular calcium waves in cultured enteric glia from neonatal guinea pig', *Glia*, 42(3), pp. 252-62.

Zhou, J. Z. and Jiang, J. X. (2014) 'Gap junction and hemichannel-independent actions of connexins on cell and tissue functions - An update', *FEBS Letters*, 588(8), pp. 1186-1192.

Zhou, M. H., Zheng, H., Si, H., Jin, Y., Peng, J. M., He, L., Zhou, Y., Munoz-Garay, C., Zawieja, D. C., Kuo, L., Peng, X. and Zhang, S. L. (2014) 'Stromal interaction molecule 1 (STIM1) and Orai1 mediate histamine-evoked calcium entry and NFAT signaling in human umbilical vein endothelial cells', *J Biol Chem*.